NATO Science for Peace and Security Series - C:
Environmental Security

Black Sea Energy Resource Development and Hydrogen Energy Problems

Edited by
Ayfer Veziroğlu
Marat Tsitskishvili

Springer

NATO OTAN

This publication is supported by:

The NATO Science for Peace and Security Programme

Black Sea Energy Resource Development and Hydrogen Energy Problems

NATO Science for Peace and Security Series

This Series presents the results of scientific meetings supported under the NATO Programme: Science for Peace and Security (SPS).

The NATO SPS Programme supports meetings in the following Key Priority areas: (1) Defence Against Terrorism; (2) Countering other Threats to Security and (3) NATO, Partner and Mediterranean Dialogue Country Priorities. The types of meeting supported are generally "Advanced Study Institutes" and "Advanced Research Workshops". The NATO SPS Series collects together the results of these meetings. The meetings are co-organized by scientists from NATO countries and scientists from NATO's "Partner" or "Mediterranean Dialogue" countries. The observations and recommendations made at the meetings, as well as the contents of the volumes in the Series, reflect those of participants and contributors only; they should not necessarily be regarded as reflecting NATO views or policy.

Advanced Study Institutes (ASI) are high-level tutorial courses to convey the latest developments in a subject to an advanced-level audience

Advanced Research Workshops (ARW) are expert meetings where an intense but informal exchange of views at the frontiers of a subject aims at identifying directions for future action

Following a transformation of the programme in 2006 the Series has been re-named and re-organised. Recent volumes on topics not related to security, which result from meetings supported under the programme earlier, may be found in the NATO Science Series.

The Series is published by IOS Press, Amsterdam, and Springer, Dordrecht, in conjunction with the NATO Emerging Security Challenges Division.

Sub-Series

A.	Chemistry and Biology	Springer
B.	Physics and Biophysics	Springer
C.	Environmental Security	Springer
D.	Information and Communication Security	IOS Press
E.	Human and Societal Dynamics	IOS Press

http://www.nato.int/science
http://www.springer.com
http://www.iospress.nl

Series C: Environmental Security

Black Sea Energy Resource Development and Hydrogen Energy Problems

edited by

Ayfer Veziroğlu
International Association for Hydrogen Energy
Miami, FL, USA

and

Marat Tsitskishvili
Academy of Ecological Sciences of Georgia
Tbilisi, Georgia

Published in Cooperation with NATO Emerging Security Challenges Division

Proceedings of the NATO Advanced Research Workshop on
The Black Sea: Strategy for Addressing its Energy Resource
Development and Hydrogen Energy Problems
Batumi, Georgia
7–10 October 2012

Library of Congress Control Number: 2013936984

ISBN 978-94-007-6157-5 (PB)
ISBN 978-94-007-6151-3 (HB)
ISBN 978-94-007-6152-0 (e-book)
DOI 10.1007/978-94-007-6152-0

Published by Springer,
P.O. Box 17, 3300 AA Dordrecht, The Netherlands.

www.springer.com
Printed on acid-free paper

Batumi Manifesto

Exactly 20 years ago – 25 June 1992 – in Istanbul, Turkey, the Black Sea Coastal Countries signed "The Bosphorus Statement". They expressed the hope that "With a shared vision of the future and through mutual cooperation, convert the Black Sea into a region of peace, freedom, stability and prosperity. They stressed that in the building of the new architecture of Europe their countries and peoples had an important and creative contribution to make and that the Black Sea Economic Cooperation constituted an effort that would facilitate the processes of European integration".

The Black Sea Region has a universal value – it is a recreational zone of Europe. Ecological well-being of this region and its energy resources are important for the entire world. Strengthening the economical potential of this region must be based on ecologically sound modern technologies. The purpose of this NATO Advanced Research Workshop is to mobilize the efforts of world scientific communities and search for new ways of development of clean energy potential of the region, while protecting its ecology.

Ecological problems of the Black Sea Region and presence of deep hydrosulphuric layers in Black Sea waters were topics that were studied by the signatories of the "Black Sea Environmental Program (BSEP)" in 1995 (Istanbul, Turkey). Since then, BSEP has been working on a policy to protect the Black Sea Region's ecology. It also provides special equipment to laboratories which work in this sphere and coordinates pertinent projects. NATO and EU are actively involved in the process of Black Sea Region's protection. They use their resources to bring investments for technical and economical development programs in this region.

The issue of energy utilization of hydrogen sulfide from the deep layers of the Black Sea has been discussed in scientific circles for a long time. After years of research, many schemes and perspectives of development and solution of this problem have been studied. The present NATO Workshop "The Black Sea: Strategy for Addressing its Energy Development and Hydrogen Energy Problems" (7–10 October 2012, Batumi, Georgia) has been a fruitful platform for the presentation and discussion of the energy development schemes from the Black Sea hydrogen sulfide.

The Workshop has invited a group of research centers and individual researchers working in the field of alternative energy to take part in the NATO ARW and has formed a working group for the development of research projects on the subject to participate in competitions for grants from NATO, the European Union and BSCBC (border cooperation Black Sea).

Taking into account the Charter of Paris for a New Europe, signed in Paris on 21 November 1990 at the Summit of the Conference on Security and Cooperation in Europe;

Considering adopted in Bonn on 11 April 1990, Document of the CSCE Conference on Economic Cooperation in Europe;

Given the accepted 17 July 1991 Statement by the London Economic Summit;

Taking into account the report of the findings and recommendations of the Sofia meeting of the CSCE to protect the environment from 3 November 1989, and its follow-up;

Desiring to make a solemn commitment to the new pan-European and global cooperation based on mutual respect and trust;

Determined to promote the development of a new model of long-term energy cooperation in Europe and globally in a market economy, and based on mutual support and the principle of non-discrimination;

Being convinced of the common interest of the workshop participants in solving the problems of energy, security, industrial plants and the environment;

Desiring to take additional measures to ensure security of supply, and effective management and use of resources, and fully realizing the potential to improve the environment, and the promotion of sustainable development;

Convinced of the primary importance of efficient energy systems in the production, conversion, transport, distribution and use of energy for energy security and environmental protection, and

Determined to establish a close, mutually beneficial relationship and to promote investment in energy.

Participants of the NATO Workshop "The Black Sea: Strategy for Addressing its Energy Development and Hydrogen Energy Problems" seek, at a reasonable cost-based view, to enhance energy security and maximize the efficiency of energy production and use, in order to raise the level of safety and minimize environmental degradation.

In full accordance with the principles of the Nordvik "integrated coastal zone management" (ICZM), and with the Strategic Plan for the Protection of the Black Sea, signed in Istanbul on 31 October 1996, will begin to develop practical technologies for the development of environmentally friendly energy of hydrogen sulfide from the deep waters of the Black Sea, we will always be guided by the Bosphorus Statement.

Regarding the scientific efforts of the leading research centers on the development of energy recovery schemes from the Black Sea hydrogen sulfide, the workshop recommends to continue intensive technology development, with a view for early implementation of environmentally safe development of hydrogen sulfide

from the deep layers of the Black Sea, and to accelerate more effective research and development recommend:

- To create Coordination Council on Energy Utilization from Hydrogen Sulfide from the Deep Layers of the Black Sea; and
- To entrust the creation of the Coordinating Council Europrojects on the subject, with the main specialized centers of the participant countries.

We the participants of the NATO Workshop "The Black Sea Strategy for Addressing its Energy Development and Hydrogen Energy Problems" consider it necessary to:

- Recommend widely used alternative schemes for heating and air conditioning, heat pumps, using as a source of cold Black Sea waters;
- Take on the development of renewable and alternative energies for the development of power in the region of the Black Sea; and
- Draw attention to the growing demand for energy caused by increased recreational pressure in the region. Sustainable and environmentally sound development of the region will be achieved only through proper planning and management of environmental pressures, development of alternative energy and environmentally friendly agriculture.

We appreciate and welcome cooperation in energy development from hydrogen sulfide from the deep waters of the Black Sea and the introduction of hydrogen energy as a priority for the Black Sea region.

We thank the Government of Georgia and the organizers of the NATO Workshop "The Black Sea: Strategy for Addressing its Energy Development and Hydrogen Energy Problems"!

Personal thanks go to the outstanding scientists and organizers, T. Nejat Veziroglu, President of the International Association for Hydrogen Energy, and Marat Tsitskishvili, President of the Academy of Ecological Sciences of Georgia.

Preface

The Black Sea and the region around it are very important economical resources for the countries of the Black Sea Region, which includes all the countries having coasts to Black Sea, as well as the countries around them which are geographically connected with the Black Sea. Potentially inexpensive hydrogen production from the hydrogen sulfide found in the deep layers of the Black Sea could provide all the Black Sea Region countries with a clean and abundant energy carrier, help speed up their economical developments, and also make the region energy independent. The purpose of the NATO Advanced Research Workshop "The Black Sea: Strategy for Addressing its Energy Resource Development and Hydrogen Energy Problems" was to evaluate the Black Sea Regions' environment, discuss the ways and means of protecting it, and to evaluate the methods of production of the energy carrier, hydrogen, from the hydrogen sulfide from the deep layers of the Black Sea.

Scientific papers have been presented at the workshop, which proposed various methods of hydrogen production from the hydrogen sulfide, from marine macro algae and other bacteria, storage and utilization of hydrogen, oil spills and pollutants in the Black Sea, degradation of the sea and the land around the region, and ways and means of protecting the environment of the Black Sea Region. The papers presented at the workshop thoroughly analyzed the region's energy potential, the current status, and future prospects. Particular attention was paid to the development opportunities in the region for alternative energies. Because of the potential positive impact on the region's economical development, special attention was paid to the theoretical and technical problems of hydrogen energy development.

In other papers, particular attention was paid to the ecological status of the region. They analyzed the main polluters of the Black Sea and its coastal zone. Some papers considered the models for the transport and elimination of major pollutants. It was unanimously agreed that there was a need for tightening of the environmental controls.

All the workshop participants unanimously expressed the need to establish close cooperation amongst the Black Sea Region countries regarding the development of its energy resources, and at the same time protecting its environment.

These recommendations have been put together in the Batumi Manifesto, which was approved in the last session of the Workshop.

This book of the Workshop Proceedings puts together the important papers presented at the workshop, starting with the Batumi Manifesto. This valuable volume should be in the libraries of all the scientists, engineers, environmentalists, economists, and decision makers involved in the development of the Black Sea Region and in the introduction of clean and abundant hydrogen energy.

T. Nejat Veziroğlu
Director, NATO ARW

Marat Tsitskishvili
Co-Director, NATO ARW

Contents

Chapter 1
Complex Investigation of Ecological State of the Black Sea and Actions for Its Protection

M. Alpenidze, R. Diasamidze, George Kordzakhia, Ramin Jomidava, and Marat Tsitskishvili

Abstract The history and development of the Black Sea are overviewed. The peculiarities of the creation of the modern structure of the Black Sea are considered. The features of the ecological conditions of the Black Sea are presented.

The individual character of the pollution of the Black Sea (hydrosulphates, main ions, organic matters etc.) is overviewed. The international efforts for the preservation of the Black Sea as well as the actions needed are pointed.

Ecological problems of the Black Sea Region and presence of deep hydro sulphuric layer in Black Sea waters are the main problems for the protection of the Black Sea. The Intentionally organized efforts with creation of necessary international organizations are discussed.

Keywords Black Sea • Environment • Ecology • Pollution • Hydrogen sulphide • Climate change • International colaboration

M. Alpenidze
Sukhumi State University of Georgia, Tbilisi, Georgia

R. Diasamidze • G. Kordzakhia (✉)
National Environmental Agency of the Ministry of Environmental Protection of Georgia, 150a, David Agmashenebeli av.,0112, Tbilisi, Georgia
e-mail: giakordzakhia@gmail.com

R. Jomidava
The expert of the Government Apparatus, 150a, David Agmashenebeli av.,0112, Tbilisi, Georgia

M. Tsitskishvili
President, Georgian Academy of Ecological Science, Nutsubidze str., 0177, Tbilisi, Georgia
e-mail: eco_marat@rambler.ru

A. Veziroğlu and M. Tsitskishvili (eds.), *Black Sea Energy Resource Development and Hydrogen Energy Problems*, NATO Science for Peace and Security Series C: Environmental Security, DOI 10.1007/978-94-007-6152-0_1,

1.1 Introduction

The present stage of civilization development is characterized by maximum aggravation of environmental problems. The most sharply these problems occur in coastal areas of inland seas that are heavily overloaded by anthropogenic impacts. The Black Sea is no exception. In this connection it would be noted that the Black Sea drainage basin collects water from an area equal almost a quarter of Europe.

1.2 The Overall Characteristic of the Black Sea

The Black Sea is surrounded on all sides by land and is connected with the Mediterranean Sea by a narrow strait of Bosporus and further with the wider one – the Dardanelles. Exchange of water with the Atlantic Ocean through these straits is difficult, therefore in the Black Sea is not observed ebb and flow. An important feature of the Black Sea, which determines most of its other unusual properties: it is almost closed, distant from the Ocean Sea, in which inflow many large rivers (the Danube, Dnieper, Dniester, Bug, Don, Kuban, Rioni). As a result of river water pressure, the level of the Black Sea is the 4–5 m above the average level of the Atlantic Ocean. The incoming water creates the water flow through the Bosporus, which is directed from the Black Sea to the Marmara Sea [1].

The origin of the sea's name, Black Sea, on one hand can be explained by the colour of the water in cloudy weather, but in the other hand by the presence at depths over 200 m of hydrogen sulphide, which causes blackening descended back items.

The salinity of the surface layer (up to 100 m deep) of the Black Sea water is equal to 17 ppm (grams of salt per litre) that makes half of the ocean one (35 ppm) [2]. This slightly reduces the biodiversity of the underwater world of the Black Sea, but it provides high productivity. Even the ancient Greek historians admired fish abundance of the Black Sea and began to build cities – colonies on its shores. The Black Sea nursed in the cradle of ancient southern European civilization.

The characteristics of the Black Sea are as follows: the volume is 550 thousand cubic km; surface area – 423 thousand sq. km; catchments area – 2.3 million sq. km; maximum depth – 2 212 m, the length of the coastline – 4 340 km; the depth of the pycnocline – 50–150 m; the boundary of oxygen-free zone – 140–200 m; runoff – 369 cubic km; rainfall – 224 cubic km; inflow of water from the Marmara Sea (low Bosporus flow) – 176 cubic km, the water flow through the Bosporus – 340 cubic km; evaporation – 395 cubic km.

The Black Sea is the world's largest meromictic pond. Generally accepted explanation of the origin of hydrogen sulphide in the Black Sea does not exist. It is obvious that hydrogen sulphide is formed as a result of the activity of sulphate-reducing bacteria, and as an output of decomposition of freshwater animals that died during the penetration of saline waters of the Mediterranean Sea during the

formation of the Bosporus and the Dardanelles. Studies of recent years suggest the Black Sea as a giant reservoir of hydrogen sulphide and methane, emitted in the process of micro-organisms, as well as from the bottom of the sea.

In recent decades, the Azov-Black Sea basin (almost one third of continental Europe) is one of the most ecologically unfavourable regions of the world. Fish catch fell sharply from 900 thousand tons in 1986 to 100 thousand tons in 1992, i.e. nine times and pollution of coastal waters is increasing [3]. The reasons of environmental degradation of the Black Sea are numerous: drainage of industrial, sewage and household waters without corresponding treatment; an oil spills emerging during transportation; removal of pollution by river runoff, increasing recreational and transit loads [4]. To abovementioned it would be added as if emerged of the deep hydrogen sulphide that was reported in the late twentieth century, with the threat of poisoning of all living things, explosion and other potential environmental disasters.

1.3 Activities for the Black Sea Protection

Since the late 1990s systematic efforts began to save the Black Sea. In 1959 was adopted Varna Convention, which established the Commission for Fisheries. Preparation of a special "Convention on Fishing and Conservation of the Black Sea" began in 1993, after the signing in Bucharest (Romania) in the 1992 "Convention on Protection of the Black Sea". This was facilitated by United Nations Recommendations on the Environment (Rio de Janeiro, 1992) and the Odessa Ministerial Declaration on the Environment (Odessa, 1993). In June 1993, GEF (Global Environmental Fund) supported the implementation of program for the protection of the Black Sea. At the same time due to the efforts of France, Netherlands, Japan, Canada, Austria, was formed "program for the protection of the Black Sea". By the concern of Black Sea countries (Bulgaria, Georgia, Romania, Russia, Turkey, Ukraine) the international body "The Black Sea Economic Cooperation" (BSEC) was founded by the Bosporus statement in 1996 [5]. The Black Sea ecology is controlled by the Standing Committee with the secretariat in Istanbul, founded in September 1993 [6]. Program collaborates extensively with donor organizations, with NATO (Programme Security through Science) and BSEC. These efforts of the official international institutions to rescue the Black Sea then were crowned with the signing by six Black Sea countries "Strategic Plan of Action for the Rehabilitation and Protection of the Black Sea" in 1996. In honour of this was established the "International Black Sea Day", which is celebrated from 1996 in October 31.

Along with the official international organizations, national academy, governmental and non-governmental organizations undertake efforts towards the development of

special national projects and international programs for environmental rehabilitation of the Black Sea. Some of important studies are listed below:

- The present state and prospects for regional development and the effectiveness of the development of recreational resources of the Azov-Black Sea basin. (Institute of Economics of the Ukrainian SSR. Odessa Branch, 1988. Executor: Zhivitsky A. V.) [7];
- A series of joint studies in Bourgas Bay by Russian, Ukrainian, Georgian and Bulgarian scientists funded by the British Embassy (leading research institute – Institute of Geochemistry, Moscow). The outputs are presented in [8];
- The program of complex oceanographic research and monitoring of the Black Sea [9];
- The complex investigation of climate change issues [10];
- NATO Programme on the Black Sea [4]. In this program were involved scientists from the former Soviet Union, including Georgia. The results of modelling of contaminants distribution from the Eastern Black Sea coast were presented. (Authors: M. Tsitskishvili, A. Shapthoshvili. "Mathematical modelling of the Pollutant Migration in the Black Sea". ISPM School & Workshop on "Scientific background and practical tools for ecological expertise", September 24–29, 2001. Tbilisi, Georgia);
- Development of scientific foundations of regional environmental problems. (Managers – G.A. Sanadze, M.S. Tsitskishvili). Resolution of the GK of Georgian SSR from 20.04.1990 № 200 and Resolution of GCST of Georgian SSR from 15.06.1990;
- In 1992 Integrated biochemical studies of ecological state of coastal zone of c. Batumi (completed by the Leningrad organization LO PO "Avtokomp" /1992/ executors: L. Bogachuk and E. Nizharadze; reviewer: M. Tsitskishvili);
- Multi-purpose monitoring of atmospheric aerosol of the Black Sea (Supervisor A. Lushnikov, Moscow; researchers: V. Zagainov, M. Tsitskishvili 1988). A unique experimental studies of full range atmospheric aerosol in the Eastern coastal zone of the Black Sea, which allowed to trace the origin and transformation of natural aerosols of marine origin, to assess the transport of pollutants from the atmosphere at the sea surface.

By the end of the last century, a range of specialized research centres and specialized, well-equipped scientific – research vessels carried out a broad program to research environmental conditions of the Black Sea. It can be noted at least one of them – the A.O. Kovalevskogo Institute of Biology of Southern Seas, who took an active part in the creation of a joint with us, "International Integrated Environmentally Safe Development of the Black Sea Basin and Provision of the Sustainable Development of the Region" (Supervisor Morozov A.L. from the IBSS). At the international level established under the International Project profile "activity centers" (five for the various aspects) performed in frames of unified programs the most advanced researches and monitoring of the Black Sea:

- Emergency Response Activity Centre – Scope, Bulgaria;
- Activity Centre for Routine Pollution Monitoring – Mersin, Turkey;

- Activity Centre for Special Monitoring Programmes, Biological and Human Health Effects, and Environmental Quality Standards – Ukraine;
- Activity Centre for the Protection of Biodiversity – Batumi, Georgia;
- Activity Centre for the Development of Common Methodologies for Integrated Coastal Zone Management – Russian Federation.

Based on positive experience in creation of the Georgian Research – Production Association "Gruzmorberegozaschita", where for the first time the research unit was equipped with the production and management functions. This allowed to increase the efficiency and effectiveness of the association. Based on resolution of the Government of the Republic of Georgia in 1993 was created "The State Commission of the Problems of the Black Sea." (Resolution of the Government of the Republic of Georgia № 140/100 from July 28, 1993). Afterwards this commission was renamed into the "State service coordination problems of the Black Sea." By this Decision, the Commission was conferred emergency powers. Later on this committee was transformed into the "Agency of the Black Sea", it changed the functions and this agency is no longer in charge of the Integrated Science and sectoral program on the Black Sea. After numerous structural changes in the governmental structures of Georgia this agency was eliminated.

Of all the above-mentioned research and development projects, almost all hydrogen sulphide was considered only as simple contaminant components. At the forefront of scientific-technical developments hydrogen sulphide – as a possible source of energy (either directly or through the production of hydrogen) appeared before the publication in the journal "Science in the USSR" (№ 5, 1990), of the journalist A. Spiridonov, "The Black Sea in danger", with extensive editorial comment "How to stop the poisoning". After this publication started the boom of publications on this topic, from journalism to pseudoscience. It should be noted that a serious efforts for the scientific – technical investigation of the hydrogen sulphide were undertaken in Russia, Ukraine and Georgia. In Georgia, in frames of the above-mentioned "State Commission on the Black Sea" were undertaken an efforts to establish the Comprehensive International Program for Development of environmentally friendly energy of hydrogen sulphide of the deep layers of the Black Sea, either through the formation of this program with the direct involvement of foreign scientific centres as well as through the "Program TASIS". The program was launched in 1997. It was financed by the state budget of Georgia from 1998. Special International Meeting of experts on the use of hydrogen sulphide of the deep layers of the Black Sea, funded by the program TASIS was hold in Batumi on September 21, 1998. Results of expert meetings have been considered at a special meeting of the Presidium of Georgian Academy of Sciences on 15 October 1998, under the chairmanship of Vice-President of Georgian Academy of Sciences, Academician Prangishvili, who was appointed as manager of the Project, by the order of the President of Georgia, Mr. Shevardnadze. In connection with the public expressed concern at the suggestion of the Academy of Ecological Sciences of Georgia, the following proposals were adopted:

- All works on the Black Sea, conducted by any country or international organization in order to use the energy of hydrogen sulphide of the deep layers of the

Black Sea, should be carried out under constant environmental control, implying a "permanent environmental support" of the projects, from concept to implementation, in addition to the usual procedures of traditional ecological control;
- Strictly centralized coordination of all these works, on both national and international levels, the inadmissibility of any private initiatives when it applies to environmentally risky action in unapproved projects;
- For the effective implementation of environmental monitoring on the basis of those provisions considered appropriate in the presence of the real perpetrators of the Project, to create a "Coordinating Council for Environmental Control of the Project", with the financing of its operation at the expenses of the project;

Background of the energy use of hydrogen sulphide of the deep layers of the Black Sea was temporarily "postponed" for a few years, due to certain political events in Georgia. This problem came back again on the initiative of the Office of the President of Georgia Mikheil Saakashvili. December 22, 2005 a special meeting was hold in the Georgian Technical University. Previously, the working group, headed by Prof. M. Tsitskishvili prepared for the meeting "An explanatory note on the problem of hydrogen sulphide in the Black Sea." The meeting was attended by almost all the leading scientists of Georgia, who has relevant relation to the problem. The meeting endorsed the working group prepared "an explanatory note on the "Challenge of the Black Sea hydrogen sulphide". The meeting recognized that this problem does not seem to the validity of the existence of an actual threat to the normal recreational use of the Eastern Black Sea coast due to a catastrophic upwelling of deep waters of the Black Sea with high concentrations of hydrogen sulphide. However, the meeting considered it expedient to continue the work on the energy use of hydrogen sulphide of the deep layers of the Black Sea, with a maximum co-ordination and concentration of efforts in this direction.

1.4 Conclusion

The Black Sea region has a universal value. It is a recreational zone of Europe. Ecological well-being of this region is important for the entire civilized world. Further development of economical potential in this region must be based on ecologically sound modern technologies. One of the purposes of this NATO Advanced Research Workshop is to mobilize the efforts of world scientific communities and to search for new ways of development of clean energy potential of the region.

References

1. Programme of Complex Research and Monitoring of the Black Sea (1990) Black Sea project., Research Manager – Academy of V. Eremeev, Hydro physical Institute of the Academy of Sciences of Ukraine, 81 p
2. Diasamidze I, Diasamidze R, Tsistskishvili M (2002) Molismologyof the Eastern part of the Black Sea. Problems of the ecology, vol 3. Publishing house of Technical University, Tbilisi

3. Buachidze N, Bilashvili K, Intskirveli L, Kordzakhia G, Kuchava G, Mchedlishvili M, Tsitskishvili M (2004) Research if the pollution by oil products and destruction dynamics of oil contamination by microorganisms in the coastal zone of the Black sea of Georgia. Problems of ecology, vol 4. Publishing house of Technical University, Tbilisi, pp 155–163
4. NATO programme on the Black Sea (2003) Creation of the Atlas pollution of the Black Sea. Scientific Manager U. Unluata. Middle-East Technical University, Ankara
5. Declaration on the Black Sea Economy Cooperation (1992) The Bosporus Declaration. J Diplomatic References 6:25–27
6. Convention about protection of the Black Sea from pollution. Bucharest, February 1992. BSEP, GEF
7. Keondzhyana VP, Kudrin AM, Terekhina Y, Tsitskishvili MS (1990) Practical ecology of marine regions. The Black Sea. Kiev, Naukova Dumka, 250 p
8. Academy V.N. Yeremeev (1980) The program of complex oceanographic research and monitoring of the Black Sea. Black Sea Project. MGI, Academy of Sciences of Ukraine, 81 p
9. The Complex Programme "Protection of Geo Biological Systems of the Black Sea in Frames of Georgian Republic and Development Methodology of Environmental Management" (1993) Research Manager – Acad. T. Mirtskulava. Commission of Biosphere and Ecological Researches of the Presidium of the Academy of Sciences of Georgia, Tbilisi
10. Kartvelishvili L, Kordzakhia G, Kutaladze N, Tsitskishvili M, Tsitskishvili L (2004) Extreme weather and climate events in Georgia on background of climate change. Problems of ecology, vol 4. Publishing house of Technical University, Tbilisi, pp 130–154

Chapter 2
Conclusions from First Black Sea Hydrogen Sulfide Workshop (BSHSW): A Review

M. Süha Yazici

Abstract Black Sea, unique in presence of H_2S and higher organic carbon levels compare to other seas and oceans, the interest to explore its energy potential. Organic and industrial wastes flowing into the Black Sea is leading to increased H_2S thickness year by year impacting sea-life. Several extraction technologies (Land Base Extraction, Off Shore Platform and Subsea Extraction) are possible to remove H_2S, while producing hydrogen, chemicals and energy. Main cost driver in the process is extracting H_2S through pumping to the surface. Extracted H_2S can be utilized through direct burning, using in H_2S Fuel Cell (H_2S Fuel Cell), electrolyzing, Claus process and wet sulphuric acid processes. Depending on the processes and associated sub-processes, cost of H_2S extraction, separation and utilization for energy purposes may or may not have economic value. During extraction and conversion, value added products and processes, i.e. H_2, H_2SO_4, S, CS_2, rare earth metals, heavy water, can impact feasibility aspect significantly. Black Sea Hydrogen Sulfide Workshop (BSHSW) has concluded that research in energy, environment and economic aspects of H_2S in different countries has to continue and a common platform including Black Sea countries should be formed to organize the actions. Moreover, establishment of a pilot plant to develop and test the proposed technologies is necessary.

Keywords Hydrogen • H_2S • Hydrogen sulfide • Black Sea

M.S. Yazici (✉)
Enerji Enstitüsü, TÜBİTAK Marmara Araştırma Merkezi,
P.K. 21, 41470 Gebze, Kocaeli, Turkey
e-mail: suha.yazici@tubitak.gov.tr

A. Veziroğlu and M. Tsitskishvili (eds.), *Black Sea Energy Resource Development and Hydrogen Energy Problems*, NATO Science for Peace and Security Series C: Environmental Security, DOI 10.1007/978-94-007-6152-0_2,

2.1 Introduction

An international workshop organized by International Centre for Hydrogen Energy Technologies (ICHET) discussed issues surrounding Hydrogen Sulfide (H_2S) extraction from Black Sea on 14–15 December 2011 in Istanbul, Turkey. The First Black Sea Hydrogen Sulfide Workshop (BSHSW) has tried to address a number of technical and economical questions including: How much hydrogen sulfide is there in the Black Sea? What is the impact of hydrogen sulfide on the Black Sea ecosystem? Can hydrogen sulfide be utilized for energy production? Is hydrogen production from hydrogen sulfide feasible? Where are the optimal places to extract hydrogen sulfide to the surface of Black Sea? What kind of facilities can be proposed to extract hydrogen sulfide from the Black Sea? A number of scientists, academicians and industrials from several Black Sea countries (Turkey, Georgia, Bulgaria, Romania, Ukraine and Russia) looked for answers for the above questions, and discussed the state of the art knowledge on the Black Sea hydrogen sulfide resources, as well as that of the diverse technologies required for its extraction and transformation into hydrogen.

Presence of H_2S zone in the Black Sea was discovered by more than 100 years ago by the Russian Geographic Society [1, 2]. Since it has been accepted that there is no life below H_2S layer and only bacteria live, there are widely accepted theories about formation of H_2S together, with range of oxygen-deficient and anoxic conditions in this highly isolated sea with rivers flowing into. A high content of organic matter, with maximum processes of bacterial sulphate reduction, is the major source of this H_2S zone. Apparently the whole H_2S issue is a consequence of insufficient environmental care along the rivers ending into the Black Sea.

Black Sea is one of the largest anoxic basins in the world, due to the lack of vertical circulation caused by the density stratification of the influx Mediterranean water. In the anoxic waters, in gas hydrates and gas saturated sediments, H_2S is produced as a result of a complex microbial sulphur cycle involving a simultaneous carbon cycle, which is replenished by the organic and inorganic carbon sources originating from the existing carbon content in the basin and that is continuously carried by the inflowing rivers. Daily production rate of H_2S is approximately 10,000 tons and the total sulphide pool in Black Sea is reported to be around 4.6×10^9 tons [3]. An oxygen-hydrogen sulphide interface starts around 150 m below and H_2S concentration starts to increase gradually until 1,000 m before reaching 9.5 mg/l concentrations [3, 4]. In the long term, the upper boundary of the H_2S containing waters may move up, while oxygen content of the top layer decreases with increasing water temperature. Hydrogen sulfide is a toxic gas, even at low concentrations. With shores in Turkey, Georgia, Bulgaria, Romania, Ukraine and Russia, Black Sea has serious environmental contamination issues.

However, it is also a potential source of hydrogen energy if a safe extraction/decomposition process can be developed. H_2S is commonly treated in natural gas industry and Clause process is used to convert it to sulfur and water for further value added products. In contrast to gas phase H2S, low concentration, liquid phase H2S is difficult to process with conventional methods. Several methods have been known for H_2S decomposition including thermal, thermochemical, electrochemical

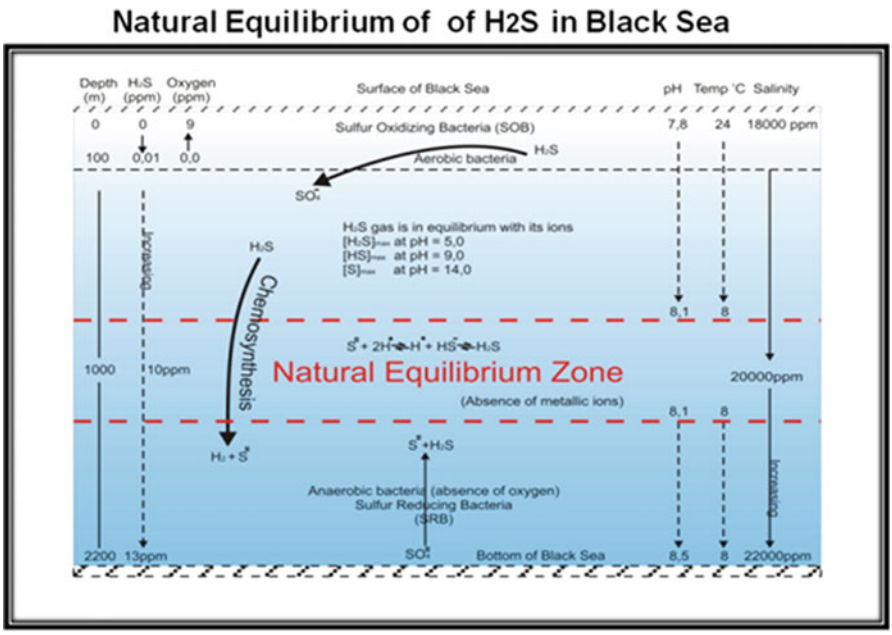

Fig. 2.1 Equilibrium schematics for H2S in the Black Sea [6] (*see color plates*)

and photochemical. All these technologies are pilot scale and their commercial feasibility has not been shown yet. Further research is required regarding effective and economic separation of H_2S from sea water. A cost-effective process addressing the harvesting of hydrogen gas from the hydrogen sulfide dissolved in the Black Sea would be a definite asset for the region's countries in their endeavor for energy self-sufficiency (Fig. 2.1).

2.2 Discussions

2.2.1 Presentations

Most of the emphasis and discussions during BSHSW focused on two aspects: Extraction of H2S for energy harvesting and economic benefits, and environmental consequences of extraction process.

Professor Sema Baykara from Yildiz Technical University made an introduction to Black Sea ecosystem in microbial sulfur cycle. Details of chemistry, pH effect, oxidation mechanism were shared with participants. She indicated that having horizontal mixing not vertically intensifies the accumulation of hydrogen sulfide (H_2S). This is partly impacted by low oxygen levels as a function of depth as expected. Redox layer, interface of hydrogen layer H_2S including water, constantly moving higher and

higher. Concentration of hydrogen sulfide is low for hydrogen production, but high for environmental issues. Equilibrium on Black Sea can be distorted by vertical diffusion of huge amounts of water removed from the deeper layer for H_2S extraction. Some financial scenarios were discussed. Her main conclusion was that the price of hydrogen (H_2) from hydrogen sulfide (H_2S) may end up being at least three times more expensive than other commercial hydrogen (H_2) production processes. She proposed efforts to continue for preparation of special regulations and even legislation pertaining to operations in Black Sea. She made emphasis on financing a pilot plant to realize all the theoretical aspects of extraction process.

Dr. Viacheslav Zgonnik presented Ukraine's perspective, representing Ukrainian Association for Hydrogen Energy in a presentation entitled "Exploring the Potential of Hydrogen Sulfide from the Black Sea: Situation in Ukraine: Past, Present, and Perspectives for the Future". Based on the scientific literature, patents and information from independent sources, exploring the Black Sea's hydrogen sulfide (BSHS) potential was analyzed. The analysis includes historic aspects, present situation and evaluation of the potential for the future. According to Dr. Zgonnik, Ex-USSR period contains only fundamental research, the idea of commercialization has started to be explored only in the late 1980s. In the end of 1990s, along with discovery of efficient methods for H_2S decomposition into hydrogen and sulfur, interest for the BSHS has grown, resulting in a series of papers and patents in the 2000s. Driven by continuously rising prices for natural gas and "gas disputes", several companies were created in the early 2010s, supported by the government or by a private sector. Some of them claim to possess a complete technological scheme and to be ready to launch it, if financially supported. The main problem in exploring the potential of the BSHS remains the energy effective extraction of the H_2S from the seawater with minimal effect on the ecosystem. Taking into account the multidisciplinary and unique nature of this project, along with its ecological aspect, Dr. Zgonnik suggested creating a large collaborative project, which will be able to unify efforts of all countries of the Black Sea region.

Prof. Eden Mamut from Ovidius University of Constantza, Romania, made a presentation on Nanostructured Materials for H_2S Decomposition and Specific Issues on the Extraction of H_2S from the Black Sea. The topic of H_2S accumulated in the Black Sea has been of interest since the beginning of the twentieth century, and developed research activities mainly in respect to mechanisms of accumulation of H_2S, the connection with different processes like eutrophication, inflow of nutrients, oxygen depletion, algae blooms and the extinction of different species. The exploitation of H_2S resources for production of energy or industrial purpose has been studied mainly from the point of view of feasibility of using different technologies. Prof. Mamut indicated that there is no commercially feasible method of hydrogen sulfide extraction that would allow utilizing hydrogen and sulphur separately. There are a number of technologies like thermal, thermo-chemical, electrochemical, photochemical and plasma-chemical methods for H_2S decomposition. The extraction of sulphur is realized mainly by the well-known Claus-process of partial oxidation, where low-quality steam is also produced, utilizing the heat of reaction. The main feature of all the methods is their high costs. His

presentation included their research using photochemical decompositions of hydrogen sulfide (H_2S) and direct utilization of H_2S at SOFC's. The direct utilization of H_2S with ceramic (solid oxide) fuel cells (SOFC) has been under study since 1987. The main obstacle of these developments is the extreme corrosion of H_2S in both types of SOFC based on oxygen or hydrogen ion conducting electrolytes. He discussed in greater detail achievements on the synthesis of sulphides of transition metals, production of porous and dense sulphide materials, nano-sized zirconia powders aiming the development of highly effective reliable ceramic fuel cells for H_2S separation. Recently, under the frame of the Black Sea Universities Network – BSUN, it has been initiated a systematic collaborative research program for addressing the complexity of the problem of H_2S from Black Sea and evaluate the possibilities of exploitation of H_2S from the Black Sea for hydrogen production as a proactive and innovative approach for sustainable development solutions in the region.

Prof. Hüseyin M. Çekirge from Prince Mohammed University, Saudi Arabia, discussed "Extraction Methodologies of H_2S Production from Black Sea Waters". Several models of extraction of H_2S from Black Sea waters were introduced including coastal installations, off-shore platforms, floating platforms and sub-sea extraction models. The feasibilities, advantages and disadvantages of each case discussed with front end engineering designs and provided cost figures. Along with the models, Prof. Cekirge discussed H_2S utilization as well. His discussion were focused on direct burning of hydrogen sulfide and/or hydrogen form, using of fuel cells via purification of H_2S to H_2 and H_2S Fuel Cell(especially SOFC's), Claus process and WSA (Wet sulfuric acid) process generating exothermic heat sufficient to fuel steam turbines for electricity. Prof. Cekirge also mentioned the absences of commercial SOFC's operable with hydrogen sulfide. WSA principles were discussed to evaluate the H_2S capacity of Black sea on H_2SO_4 production, which is the most important starting material on production of ammonium base fertilizers in agriculture. Possibility of producing gas and steam for energy production while producing H_2SO_4 from process may prove to be feasible. Direct extraction does not look feasible according to his analysis due to pumping cost. However, if electricity and H_2SO_4 prices are fixed, one model gives 6–7 years on return of investments but for any models, pumping has to be avoided.

Prof. Salah Naman from the University of Zakho, Iraq, has presented results of his research on using industrial plant to convert H2S to hydrogen. According to his research, lower energy of (H–S) bond than (H—O) bond of water molecules makes it possible to utilize H_2S as a source of clean hydrogen fuel in the future. The thermodynamic potential of H_2S oxidation is $E_{H2S} = 0.17$ V compared with $E_{H2O} = 1.23$ V for water splitting. His conclusion is that production of hydrogen from hydrogen sulfide in Black Sea should be done in two steps:

(a) Pilot plant for extraction of hydrogen sulfide gas from Black Sea water. His results shows that the stripping of this gas is increasing at low acidic pH of water and depend on temperature, pressure and salt concentration inside the sea and it should set up at maximum concentration depth of this gas inside Black sea, then continuous pumping of hydrogen sulfide to the surface is necessary.

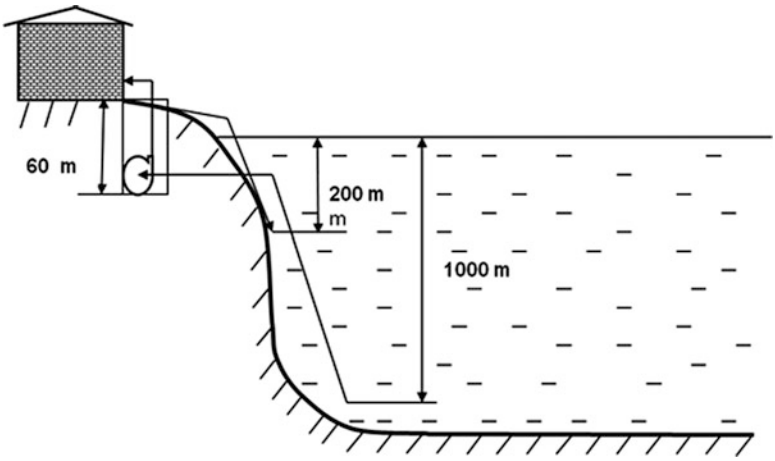

Fig. 2.2 Schematics of pumping sea water from 1,000 m depth [6]

(b) Pilot plant for production of hydrogen from decomposition of hydrogen sulfide on the surface of Black Sea. Several thermochemical methods have been well established to split this gas to clean hydrogen fuel and elemental sulfur. His group used different catalysts at temperatures between 450 and 800 °C with common industrial substitution to Claus Process.

According to his economic assessment, values of side products make process feasible. He claimed that the environmental state of Black Sea will not be affected by Hydrogen sulfide extraction according to well known LeChatelier principle of chemical equilibrium [5]. He concluded that extraction of hydrogen sulfide should be done inside the Black Sea at a maximum concentration, due to the very high expenses of pumping of Black Sea water to the surface. Hydrogen sulfide gas will naturally flow to the surface, and then storage of this gas will be by ethanolamine before thermal decomposition. He recommended, as well, setting up a pilot plant to look in to all possible methods suggested during the workshop.

Dr. Konstantin Petrov from Bulgarian Academy of Sciences, Sofia, Bulgaria, has shared results of a feasibility study his team carried out with financial support from ICHET. Technological process scheme has been proposed in a project supported by Black Sea Economic Cooperation Agency (BSEC) and UNIDO-ICHET (International Center for Hydrogen Energy Technologies), both based in Istanbul, Turkey. The processes included in the Scheme are: (i) pumping Sea water from 1,000 to 1,200 m depth; (ii) extraction of H_2S from Sea waters by absorbents and further desorption by NaOH; (iii) electrochemical production of hydrogen and polysulphides; (iv) environmental impact of the whole process is evaluated. Each process has been evaluated technically and economically, as well as the whole technology. It has been shown that the most expensive part is pumping sea water from 1,000 m depth. The feasibility of the proposed technology depends mainly on supported governments' price of renewable energy. At the present market price of Hydrogen (0.20 Euro/m^3) the process is far not profitable. This technology can be feasible at the proposed by EU price of Hydrogen from renewable energy of 3.00 Euro/m^3 [6] (Fig. 2.2).

Prof. Mehmet Aksu from Gazi University, Ankara, Turkey, presented his scientific research on electrochemical separation of hydrogen and sulfur. His study involves electrolysis of %10, %20, %30, %40 H_2S in % 3 NaCl solutions and designing a cell with suitable anode and cathode materials and dimensions. It was found that the cell designed gave a hydrogen efficacy of 0.5 kW/Nm^3 H_2. It was observed that this value was much better than the value obtainable with the conventional H_2S cell system (1.66 kW/m^3 H_2). Prof. Aksu reconfirmed in his speech that pumping water up/down to 1,000 m depth is not feasible, especially due to the required energy demand. Also production of Hydrogen (H2) at the bottom and pumping to the surface may not be feasible. Instead of these possibilities, transport of H2S from depth of Black sea may be the best solution. Defined process proposed by his team focused on a zeolite membrane H_2S separation from deep heavy water, then split in an electrolysis process.

Prof. Venko Beschkov from Bulgarian Academy of Sciences, Sofia, Bulgaria, has described H_2S Fuel Cells that his team has been working on as a BS-Era Net project. His presentation was directed towards two simultaneous goals: first, remediation of the severe environmental situation in the Black Sea and to produce "carbon-free" energy in the form of hydrogen from the deep marine water. It is based on the opportunity to recover energy from the hydrogen sulfide in the Black Sea. The thermodynamic analysis shows that the energy recovery of the latter is an energy alternative to the natural gas used in the coastal countries. The successful accomplishment of the project goals requires the composition of various chemical and physico-chemical methods into an integrated technology. The proposed technology consists of the following steps: pumping of the sea water from depths, where the sulfide concentration is relatively high; enrichment of the pumped water to attain higher concentrations of sulfide and to enhance the next step: generation of electromotive force in a new designed fuel cell operating by catalytic sulfate oxidation by oxygen; sufficiently high and required for the very hydrogen production by electrolysis; and the final step is hydrogen storage or its utilization as a complementary energy source for electrolysis, used in another traditional fuel cell. Sulfate ions are returned to the sea water, without any waste discharge. The efficiency of the technology proposed will be based on new catalysts and new fuel cell design, enabling the fast oxidation of sulfide to elemental sulfur and sulfate in order to generate high electromotive force necessary for the subsequent water splitting to hydrogen and oxygen. Dr. Beschkov indicated energy potential of H_2S (75 million ton H2S equivalent to 43 billion tons of Natural Gas)

A commercial entity, Elena Corporation, presented their commercial perspective on the extraction process. This company has patents titled "Floating complex for hydrogen sulfide deep-water extraction from sea water and the method of launching of the floating complex for hydrogen sulfide deep-water extraction from sea water", "The method of prevention of explosion-fire danger during the extraction of gaseous hydrogen sulfide from the Black Sea bed and during its transportation", "The method of extracting sodium hydrosulfide from the mixture of gases contained in hydrogen sulfide", and "The method of extraction hydrocarbon gases from solid gas-hydrates from deposits on the sea bed". Elena Corporation proposed to produce not only hydrogen, but also valuable chemical compounds, mineral

fertilizers, electricity and heat. They proposed extraction on an offshore platform at the depth of 2,000–2,200 m where hydrogen sulfide concentration is at maximum. Hydrogen sulfide transportation in liquid state to the land was proposed. Elena Corporation suggested the following action steps:

1. Development of feasibility study to establish pilot demonstration installation of hydrogen sulfide extracting and complex reprocessing.
2. Establishment of pilot installation and fine-tuning of hydrogen sulfide production and reprocessing regimes in experimental-industrial conditions.
3. Working towards industrial-scale hydrogen sulfide extraction and processing plant, and building of industrial-scale plant on the offshore platform.
4. They proposed to set up international task force for controlling the process of this project realization for economic and ecologic impact. They claim to be able to achieve three billion USD per year benefit in sea basin improvements.

2.2.2 Panel Discussions

Two different panel discussions with each comprising of 4–5 participants, took place. Participants at the first panel discussion made emphasis on utilizing not only H_2S as a H_2 source, but also products like H_2SO_4, C_2S, heavy water and other side products besides energy, and steam. Necessity for a financial and business plan mentioned to have a realistic feasibility study. Panel also agreed producing energy and preserving environment at the same time should go side by side. Collaboration with marine scientists is inevitable. Building upon the first panel, the second panel suggested not losing time on marine, oceanography, biology and chemistry of Black Sea, but taking an immediate action on setting up a pilot plant with necessary safety and environmental measures. A recommendation was also made to build this first pilot plant in Sinop, coastal city in Turkey.

2.3 Processes and Financial Considerations

Figure 2.3 summarizes possible ways to extract and utilize H2S for energy and chemical purposes. Some of the conversion processes are realistically possible and some are not. Additionally, extraction, transportation and by-product discharge seems to be as important as H_2S conversion. Since displacement of large volumes of sea water from the depths is required by the technology in consideration, thorough ecological surveillance and follow-up of the impact of such industrial activities are important. Primarily, extraction of H_2S-rich water and its discharge after processing should be carried out at levels deeper than 200 m, outside the oxygenated surface layer.

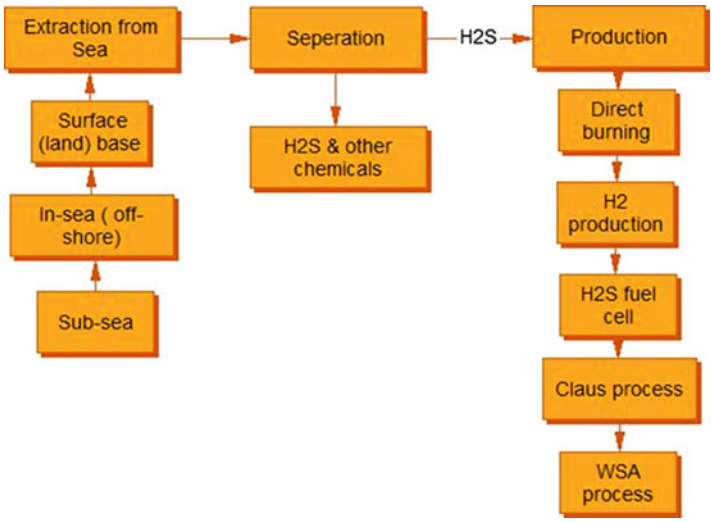

Fig. 2.3 Possible ways to extract and utilize H_2S (*see color plates*)

There was no clear financial model to encourage initial investment to be made for a pilot plant, but it was assumed that cost of hydrogen from H_2S in Black Sea was presently above the range defined by the commercial and targeted reference figures. Targeted market price of 3.00 Euro/m^3 [5] could be a more realistic benchmark presently compared to other hydrogen production methods. This is without considering other value added by-products and chemicals.

2.4 Conclusions

Scientists agree that energy and environmental concerns should be priority and the Black Sea ecosystem has to be preserved. Producing energy and preserving environment should proceed side by side. While the environmental aspect has to be under control through necessary codes and regulations, scientists should focus on making energy aspects viable. Possibility of hydrogen production from H_2S in Black Sea and industrial waste waters will continue being a challenge until a suitable technology is developed. Hydrogen production from Black Sea does not have a commercial motive currently, but it is rather an initiative which can be financed as a scientific research for future sustainability of economy in the region. Neighboring countries should make necessary investment in a pilot plant to demonstrate extraction, processing and waste management. It was observed during the workshop that what is presented and discussed were mostly ideas never experimentally tested in a laboratory scale set-up. Difficulties facing extraction and processing at this point is conceptual. Even before a business plan, a realistic scientific and technical plan for experimentation is necessary. Considering the level of

controversy and discrepancy in discussions, private investment in a pilot plant is very risky at this level of technical detail.

Acknowledgments Financial support provided by the Turkish Ministry of Energy and Natural Resources is greatly acknowledged. For further research interactions, e-mails for invited speakers are shared below:
Prof.Sema Baykara: sbaykara@gmail.com
Dr. Viacheslav Zgonnik: zgonnik@uahe.net.ua
Prof. Eden Mamut: emamut@ovidius.ro
Prof. H.M. Çekirge: hmcekirge@usa.net
Prof Salah Naman: salah.naman@yahoo.com
Prof. Konstantin Petrov: kpetrov@bas.bg
Prof. V. Beschkov: vbeschkov@yahoo.com
Elena Corporation, Ukraine: elena@infocom.ks.ua

References

1. Neretin LN (ed) (2006) Past and Present Water Column Anoxia. In: NATO advanced research workshop on past and present water column Anoxia in Sevastopol, Ukraine
2. Neretin LN, Volkov II, Böttcher ME, Grinenko V (2001) A sulfur budget for the Black Sea anoxic zone. Deep Sea Res 48:2569–2593
3. Baykara SZ, Figen EH, Kale A, Veziroglu TN (2007) Hydrogen from hydrogen sulfide in the Black Sea. Int J Hydrogen Energ 32(9):1246–1250
4. Baykara SZ (2011) Black Sea and hydrogen sulfide. In: Ryann AL, Perkins NJ (eds) The Black Sea: dynamics, ecology and conservation, Chapter 5. Nova Science Publishers, New York (ISBN: 978-1-61122-855-7)
5. Petrov K, Baykara SZ, Ebrasu D, Gulin M, Veziroglu A (2011) An assessment of electrolytic hydrogen production from H_2S in Black Sea waters. Int J Hydrogen Energ 36:8936–8942
6. Naman SA, Ture IE, Veziroglu TN (2008) Industrial extraction pilot plant for stripping H_2S gas from Black Sea water. Int J Hydrogen Energ 33(22):6577–6585

Chapter 3
Hydrogen Production with Zero Emissions Footprint: Challenges and Solutions Towards Commercialization

Nesrin Özalp

Abstract Fossil fuel economy has been under continuous criticism due to impending shortage, and environmental consequences because of heavy consumption of fossil fuels for steam, power, and commodity generation. It is unavoidable that the current fossil fuel economy will be replaced by a new economy. However, prospective alternative energy sources should conveniently replace fossil fuels and the transition from the old economy to a new one should take place smoothly. This can only happen if commonality is found between the goals of current major energy industries and the future new economy demands. Considering the significant consumption of hydrogen by the oil industry to convert crude oil into practical fuels, the most reasonable approach is to start with hydrogen as a commodity first prior to consider it as an alternative fuel. Because of the substantial emissions from the way hydrogen is produced, the best approach would be to adopt a new process which produces hydrogen with zero emissions. The use of concentrated solar energy can provide us the means to produce hydrogen with zero emissions. This would be the most appropriate first step in a transition where an alternative energy is used to produce another alternative energy source where in turn it serves in the refinement of the target fossil fuel. Once the new way of hydrogen production is fully adopted, it could be produced for consumption as a fuel as well. The main challenge, however, is to produce emission free hydrogen at a competitive cost so that it is attractive to industry. This paper presents a very promising technology for hydrogen production, which is called "solar cracking", where natural gas is decomposed into its components solar thermally with zero emissions. With this process, not only hydrogen but also another very valuable commodity is produced, namely carbon black. Emission free production of carbon black via this technique adds significant economic value and competitiveness into the process along with securing zero cost to CO_2 sequestration, transportation, and storage. The paper defines the

N. Özalp (✉)
Mechanical Engineering Program, Texas A&M University at Qatar,
P.O. Box 23874, Doha, Qatar
e-mail: Nesrin.ozalp@qatar.tamu.edu

A. Veziroğlu and M. Tsitskishvili (eds.), *Black Sea Energy Resource Development and Hydrogen Energy Problems*, NATO Science for Peace and Security Series C: Environmental Security, DOI 10.1007/978-94-007-6152-0_3,

technical details on the challenges of this process to become commercial, and presents promising solutions to the problems of hydrogen producing solar cracking reactors.

Keywords Hydrogen • Carbon black • Solar thermal • Natural gas • Reactor clogging • Iris mechanism

3.1 Introduction

This is an era in which people worldwide anxiously wait to learn of "a new energy economy" that is sustainable alternative to fossil fuel economy. There is enormous interest in seeing that this new energy economy will eliminate worries about the world's energy supply and environmental problems. Regardless of their technical knowledge or quantity of energy resources they have in their respective countries, people want to embrace this new energy era on the condition that it is environmentally friendly, easily accessible, and economically reasonable. As with any transition from an old, well-established practice into a brand new one, it will take time until a new energy economy can be fully adopted. In order to make the first transitional step, hydrogen would most likely be the best initiative because of its dual use as a fuel as well as commodity. Considering the extensive use of fossil fuels by industrial, commercial, transportation and residential sectors, the transition to a hydrogen-driven new economy can only take place if hydrogen can be produced at competitive cost compared to petroleum derivatives and without post-processing requirements, such as sequestration. A new method of hydrogen production, one with zero emissions, should be adopted by industry so the first step in transition to a new energy economy begins.

Although there is great demand for hydrogen in the chemical industry to produce commodities such as ammonia [1] and methanol [2], it is much more in demand by the petroleum industry because hydrogen is the key feedstock in the hydrotreating and hydroprocessing of hydrocarbons during crude oil processing [3, 4]. These crude oil refining processes consume such large amounts of hydrogen that it makes hydrogen one of the most important commodities in oil industry. A continuous supply of hydrogen is so important that some of the petrochemical plants and refineries are operated based on the availability of hydrogen per their policy [4]. The importance of hydrogen in the oil industry can be seen in Table 3.1, where the world's hydrotreating and hydrocracking processes are nearly half as large as the world's crude oil distillation capacity.

Considering that 139,000 barrels of hydrogen per day is needed to meet 35 % of the world's petroleum refinery capacity [6], hydrogen indeed serves as a key commodity for the refining and upgrade of crude oil. In order to meet such a large demand for hydrogen, the petroleum industry satisfies its hydrogen demand mostly via onsite manufacturing rather than purchasing and transporting from offsite. Currently, the most common technology to produce hydrogen is steam reforming of natural gas [7]

Table 3.1 Worldwide refining process units [5]

	Crude distillation	Coking and visbreaking	FCC	Catalytic reforming	Hydrotreating	Hydrocracking
Number of units	> 710	>330	360	550	1,316	168
Total world capacity	82	8	14.3	11.3	40.3	4.6
Average capacity	114,000	45,700	39,700	20,500	30,600	27,400

which produces approximately 11.9 kg of carbon dioxide equivalent per kg of hydrogen produced [8]. Therefore, an alternative hydrogen production method with zero emissions would not only reduce the emissions from oil refining but also would reshape the "environmentally unfriendly" image of the oil industry.

Ideally using feedstock that is most available in each particular region would be simplest approach to start with; for example, hydrogen sulfide (H_2S) in the Black Sea, or water and natural gas in other parts of the world. Regardless of what feedstock is used to produce hydrogen, the key is how to break the chemical bonds in that feedstock to release hydrogen. For example, electricity can be used for that purpose; however, if the electricity is produced from fossil fuels, then there are large quantities of emissions associated with hydrogen production from fossil-fuel-made electricity. To avoid this circumstance, renewable energy sources could be used to generate the necessary electrical power. Alternatively, renewable energy sources can be directly used to produce hydrogen, such as solar thermochemical processing. With concentrated solar energy, it is possible to reach temperatures as high as those achieved via fossil fuel combustion. The only difference between fossil fuel combustion and solar thermochemical processes is: no presence of air and igniter, and, therefore, no carbon-oxygen or nitrogen-oxygen based emissions. With the use of high temperature process heat obtained from concentrated solar energy, it is possible to decompose H_2S [9], H_2O [10], or CH_4 [11] to produce hydrogen. Direct solar thermal cracking of CH_4 has been shown to be a promising method of producing hydrogen because of the lower temperature requirement for decomposition compared to H_2O and H_2S [12]. Despite its attractiveness, it has not been possible to commercialize hydrogen production via solar thermal splitting of natural gas, which is also called "solar cracking" due to two major problems:

1. Reactor clogging due to carbon deposition.
2. Transient nature of solar energy.

This paper provides detailed explanation on these problems and outlines promising solutions.

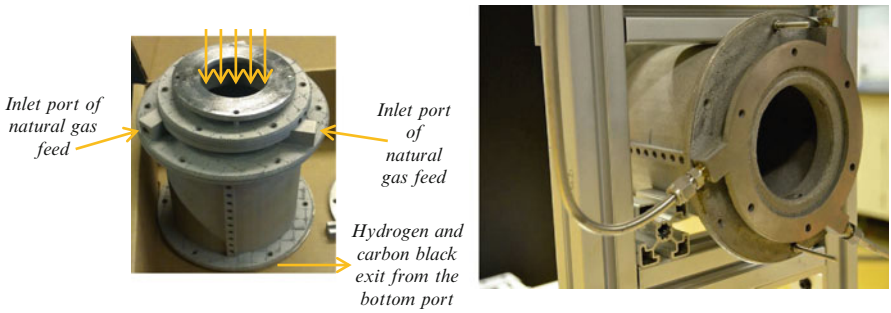

Fig. 3.1 An example solar reactor designed and manufactured at SERL of TAMU-Q (*see color plates*)

3.2 Solar Cracking of Natural Gas

Solar cracking of natural gas is a simple process which occurs via the following reaction:

$$CH_4 \rightarrow C\ (\text{solid}) + 2H_2,\ \Delta H_{298} = 75\ \text{kJ/mol} \tag{3.1}$$

As it is seen in Eq. (3.1), the process produces another commodity that is highly desired in industry: carbon black. Carbon black is an important additive for rubbers, inks, batteries and several polymers [8] and it is also used in power generation, soil amendment and environmental remediation [13, 14]. As a byproduct, it is easier to filter, store and transport carbon black as comparison to carbon dioxide which is the byproduct of steam reforming of natural gas [15]. Considering that carbon black is currently produced via the furnace process [16] which produces 5.7 kg of carbon dioxide equivalent per kg of carbon black produced [17], it is a great added value to the solar cracking process that such quality carbon is produced via no emissions. Because of these advantages, solar cracking of natural gas offers best option for the oil industry to produce hydrogen, because the carbon black can be sold to generate revenue to offset production cost.

Solar cracking of natural gas takes place in a solar reactor where concentrated solar energy enters through an aperture. An example solar reactor design and manufactured at Sustainable Energy Research Laboratory of Texas A&M University Qatar is shown in Fig. 3.1.

3.3 Problems with Solar Cracking Reactors and Promising Solutions

3.3.1 Reactor Clogging Due to Carbon Deposition

Once methane decomposes under high flux, the mechanisms present complex reaction schemes that can explain the formation of by-products and intermediates during the

decomposition reaction, such as: C_2H_6, C_2H_4, C_2H_2, C_6H_6 and polycyclic aromatic hydrocarbons with simplified steps as follows [18]:

$$2CH_4 \rightarrow C_2H_6 \rightarrow C_2H_4 \rightarrow C_2H_2 \rightarrow C + 2H_2 \tag{3.2}$$

Although the steps given above do represents the main pattern of methane decomposition, a more comprehensive mechanism accounting for thermal methane coupling using free radical mechanisms were proposed by Olsvik et al. [19], and Olsvik and Billaud [20].

Carbon particles that are produced in the last step of methane decomposition process deposit on reactor window, walls, and exit. Each of them presents a problem, however, the exit deposition clogs the reactor and the window ultimately explodes due to pressure build up. Therefore, carbon deposition is the major problem that solar cracking reactors have in common.

For example, Abanades and Flamant observed that carbon particles adhere to the walls and tapering the nozzle, which made them also to conclude that one of the major challenges in designing a solar cracking reactor is to solve the carbon deposition problem [21]. Kogan group of Weizmann Institute of Science achieved an effective way of window screening. However, although the window was kept reasonably clean from carbon deposition, carbon particles still deposited on the walls and at the exit [22].

In order to explain carbon deposition inside the solar reactor, we conducted a thorough numerical analysis based on Kogan group's experimental results presented in Ref. [23] as a reference case for "clean window" and "contaminated window" to see if we could computationally predict these results and therefore explain the physics behind this phenomenon [24]. We used Discrete Phase Model (DPM) to evaluate trajectories of carbon particles and to track them through continuous phase of gas. We got the motion of particulate phase based on force balance equating particle inertial forces on a Lagranian frame of reference with the forces acting on the particle. The governing equations used in our CFD analysis are given below:

Continuity equation:

$$\frac{\partial \rho}{\partial t} + \frac{\partial (\rho u_i)}{\partial x_i} = 0 \tag{3.3}$$

Momentum Equation:

$$\frac{\partial (\rho u_i)}{\partial t} + \frac{\partial (\rho u_i u_j)}{\partial x_j} = -\frac{\partial P_{eff}}{\partial x_i} + \frac{\partial}{\partial x_j}\left[\mu_{eff}\left(\frac{\partial u_i}{\partial x_j} + \frac{\partial u_j}{\partial x_i} - \frac{2}{3}\delta_{ij}\frac{\partial u_l}{\partial x_l}\right)\right] + S_i^M + \rho g_i \tag{3.4}$$

k – Equation:

$$\frac{\partial (\rho k)}{\partial t} + \frac{\partial (\rho k u_i)}{\partial x_i} = \frac{\partial}{\partial x_j}\left(\alpha_k \mu_{eff}\frac{\partial k}{\partial x_j}\right) + G_k + G_b - \rho\varepsilon \tag{3.5}$$

ε – Equation:

$$\frac{\partial(\rho\varepsilon)}{\partial t}+\frac{\partial(\rho\varepsilon u_i)}{\partial x_i}=\frac{\partial}{\partial x_j}\left(\alpha_\varepsilon\mu_{eff}\frac{\partial\varepsilon}{\partial x_j}\right)+C_{1\varepsilon}\frac{\varepsilon}{k}(G_k+C_{3\varepsilon}G_b)-C_{2\varepsilon}\rho\frac{\varepsilon^2}{k}-R_\varepsilon \quad (3.6)$$

Energy equation:

$$\frac{\partial(\rho E)}{\partial t}+\frac{\partial[u_i(\rho E+p]}{\partial x_i}=\frac{\partial}{\partial x_j}\left(\lambda_{eff}\frac{\partial T}{\partial x_j}+\sum_{i=1}^{N}h_iJ_{ij}+u_i\mu_{eff}\left(\frac{\partial u_j}{\partial x_i}+\frac{\partial u_i}{\partial x_j}\right)\right)+Q_{reac}+Q_{rad}+S_i^T \quad (3.7)$$

Species transport:

$$\frac{\partial(\rho Y_i)}{\partial t}+\frac{\partial(\rho u_l\,Y_i)}{\partial x_l}=\frac{\partial}{\partial x_j}\left[\left(\rho D_{i,m}+\frac{\mu_t}{Sc_t}\right)\frac{\partial Y_i}{\partial x_j}\right]+R_i \quad i=1,2,\ldots,N-1 \quad (3.8)$$

Discrete Ordinate:

$$\frac{dI_\lambda(\vec{r},\vec{s})}{dS}+(a_\lambda+\sigma_s)I_\lambda\left(\vec{r},\vec{s}\right)=a_\lambda n^2I_{b\lambda}+\frac{\sigma_s}{4\pi}\int_0^{4\pi}I_\lambda\left(\vec{r},\vec{s}\right)\Phi\left(\vec{r},\vec{s}\right)d\Omega' \quad (3.9)$$

Our simulations successfully predicted the contaminated window and clean window experiments of Kogan group as shown in Fig. 3.2, where Fig. 3.2a is the case of contaminated window, while Fig. 3.2b is the slightly contaminated window. Correct positioning of the window screening jets with the right flow rate and gas solves the window contamination problem as seen in experimental [23] and theoretical studies [24].

Although Kogan et al. studied window contamination by testing many cases; they did not give information on the reactor wall contamination during those experimental cases. Since we successfully predicted their experimental findings for the clean window case and contaminated window case, we went ahead and predicted the carbon deposition at reactor exit for those cases. As shown in Fig. 3.3a, significant carbon deposition is observed at the exit, whereas slight carbon deposition is observed in Fig. 3.3b for the case where slight carbon deposition is observed for the window as well.

Once we completed our CFD simulations for the carbon deposition at the reactor exit, we merged our simulation code with visualization tool EnSight, which gave us a three-dimensional animation of this striking process on a stereoscopic 120° curved screen showing images as large as 3,576 × 1,024 pixels. The three dimensional immersive visualization elaborated the phenomenon of solar cracking natural gas into carbon black and hydrogen molecules when solar radiation hits the natural

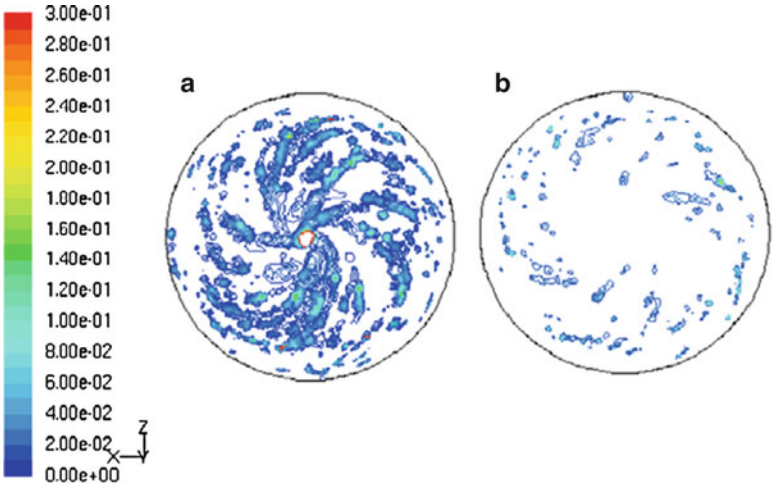

Fig. 3.2 (**a**) Significantly contaminated window, (**b**) Slightly contaminated window [24] (*see color plates*)

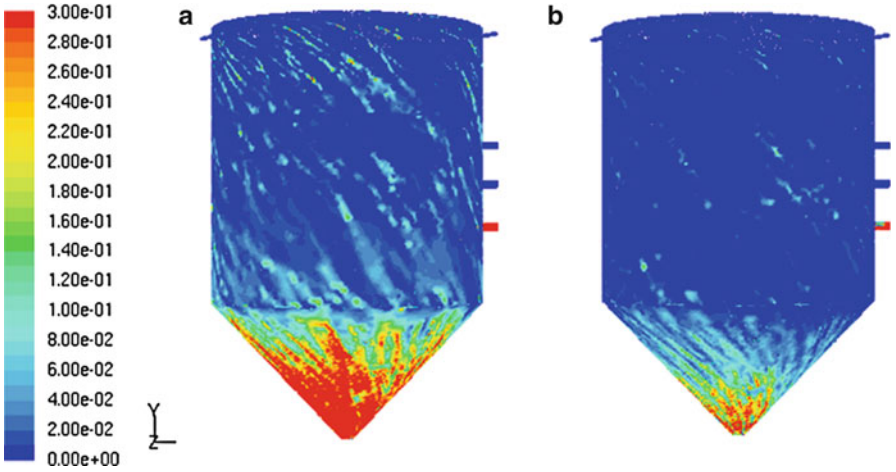

Fig. 3.3 (**a**) Significant carbon deposition at reactor exit, (**b**) Slight carbon deposition at reactor exit [24] (*see color plates*)

gas inside the reactor. With this animation, we were able visually track the carbon particles and clearly observe temperature variations inside the reactor in the three dimensional domain. We were also able to observe the changes in flow behaviour. Figure 3.4 shows the snapshots of our three dimensional video illustrating solar reactor window explosion because of carbon particles blockage at reactor exit.

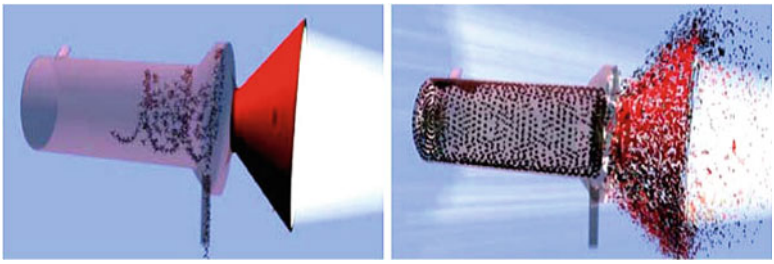

Fig. 3.4 Carbon blockage exploding the solar reactor window (*see color plates*)

3.3.2 Promising Solution to Carbon Deposition Problem: Wall Screening and Central Cyclone Flow to Regulate Carbon Move Inside the Reactor

In order to reduce carbon deposition inside the reactor, we approach this problem in three ways. First, we kept the windows screening concept just like the aforementioned solar cracking reactors. Second, we introduced a new concept where the walls are screened just like the windows. This new concept is called "wall screening", which is basically a laminar flow shield sweeping the walls of the reactor from top to bottom as shown in Fig. 3.5a. Finally, we introduced a cyclone flow in the center with a flow pattern that makes carbon particles rotate inside the reactor couple times before they move towards the exit. We found the optimum flow configuration to achieve the laminar flow shield and the turbulent flow in the center remaining without disturbing each other. Figure 3.5 shows the cyclone and laminar flows inside the proposed solar reactor concept.

3.3.3 Transient Nature of Solar Energy

Incoming solar energy is inherently transient due to variation in position of the sun throughout the day, and changing weather conditions which leads to fluctuations in available flux density. This makes it difficult to maintain a constant temperature inside a solar reactor and lowers process efficiency. In conventional industrial processes, reactor temperature can be maintained constant by changing the mass flow rate of the feedstock. However, this solution is not applicable because it disturbs the flow dynamics, crucial to prevent carbon deposition as explained above. Therefore, it is important to design a system that can solve this problem by maintaining semi-constant temperatures without disturbing the flow dynamics.

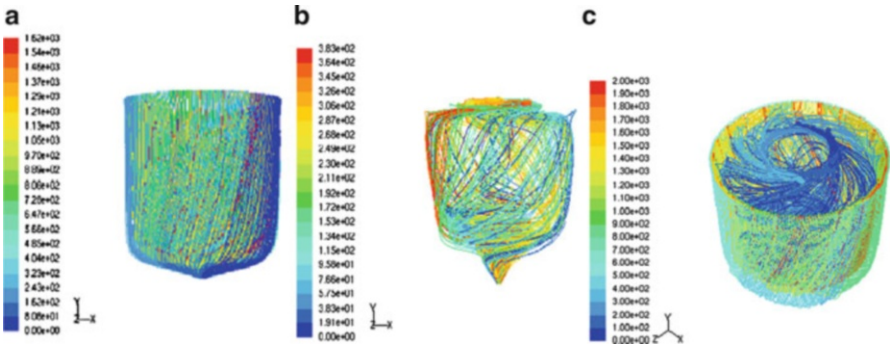

Fig. 3.5 (**a**) Laminar wall screening shield on the walls, (**b**) Cyclone flow in the center, and (**c**) Isometric view of the laminar wall screening and cyclone flow (*see color plates*)

3.3.4 Promising Solution to Problems Faced Due to Transient Nature of Solar Energy: 24/7 Operational Solar Reactor with Mechanical Human-Eye Like Aperture

We approached the problems due to transient nature of solar energy in three steps. First, one must deal with fluctuation in solar flux from sunrise to sunset. Second, one must deal with changes in weather conditions, and, finally, one must deal with the non-availability of sunlight at night time.

3.3.4.1 Throughout the Day from Sunrise to Sunset with Clear Sky

To address this problem, we developed a novel concept for a variable size aperture inspired by the human eye, where pupils enlarge in the dark and shrink when exposed to light. We have investigated the efficacy of variable size apertures to maintain semi-constant temperature in the reactor irrespective of fluctuations in incoming solar flux. We conducted an optical and heat transfer analysis of our prototype reactor concept given in Fig. 3.6 with variable size aperture exposed to changing solar flux.

The reactor shown in Fig. 3.6 has three inlet ports through which the working fluid enters, and a single exit port through which it leaves the reactor. The inlet ports are positioned in such a way that a vortex flow is formed inside the reactor. The front plate has an opening, the aperture, whose size can be varied to control the amount of incoming solar energy. In order to house the reactants inside the reactor and allow incoming radiation from the aperture into the receiver, a quartz window is fitted right behind the aperture.

We tested this solar reactor using our 5 kW solar simulator as shown in experimental setup of Fig. 3.7. The reactor is positioned such that the aperture is in the focal plane of the solar simulator.

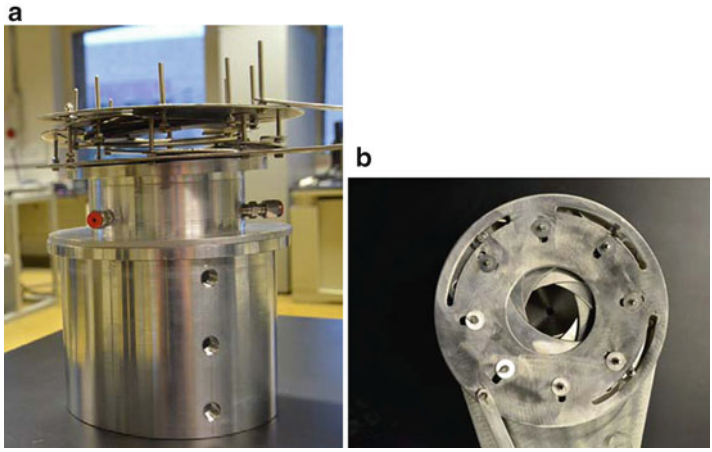

Fig. 3.6 (**a**) Solar reactor with mechanical human-eye like aperture mounted at the solar flux entry, (**b**) Mechanical human-eye like aperture (*see color plates*)

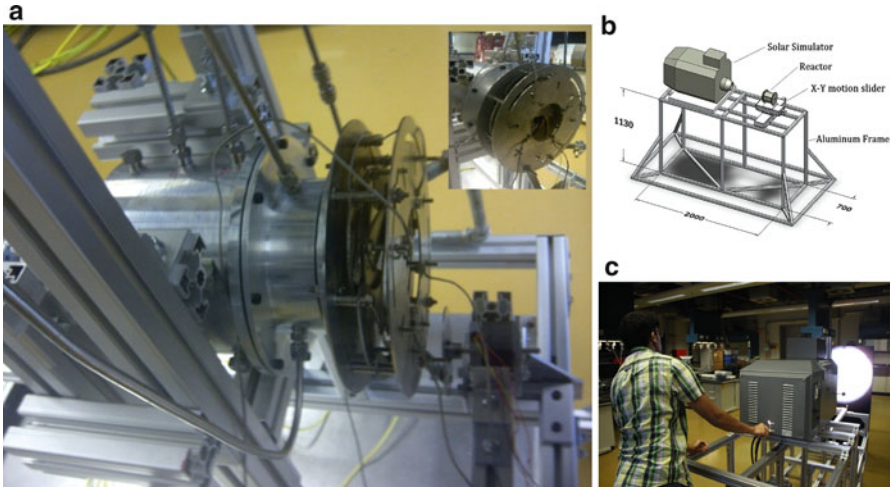

Fig. 3.7 (**a**) Solar reactor with mechanical human-eye like aperture mounted at the solar flux entry, (**b**) Schematic of the experimental setup, (**c**) Optical alignment of the 5 kW solar simulator (*see color plates*)

In order to evaluate the performance of this reactor concept under real concentrated solar energy, we have conducted a thorough heat transfer and optical analysis based on solar furnace configuration of Paul Scherrer Institute (PSI) given in [25], which is capable of delivering a peak concentration ratio, C_{peak} of approximately 5,530 suns (1 sun = 1 kW/m^2) with a distribution that is approximately Gaussian, where the mean concentration ratio, $\overline{C}$ is defined as the ratio between power intercepted by the aperture (P_{ap}) and the direct normal insolation (I) at

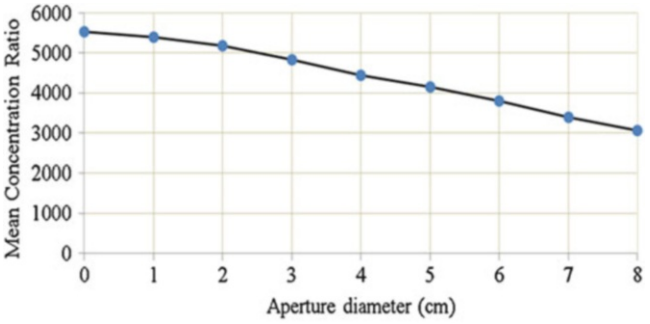

Fig. 3.8 Mean concentration ratio through a circular aperture as a function of its diameter [26] (*see color plates*)

the aperture. Due to the Gaussian distribution, the mean concentration ratio varies as a function of aperture diameter (D_{ap}) and is given by $\overline{C}(D_{ap}) = \frac{P_{ap}}{I\,\pi\left(\frac{D_{ap}^2}{4}\right)}$.

Figure 3.8 shows the mean concentration ratios $\overline{C}$ from experimental results given in [25] for different aperture diameters.

We obtained a typical daily cycle of direct normal radiation (I) from the sun referring to the National Renewable Energy Laboratory (NREL) database [27]. We calculated the normal insolation based on clear sky model by Bird et al. [28]. This corresponds to clear sky conditions on July 1, 2011, at the Solar Radiation Research Laboratory (SRRL) of NREL located at latitude $39.4\ ^{\circ}N$, longitude $105.18\ ^{\circ}W$ at an altitude of $1{,}829\ m$ above mean sea-level. Figure 3.9 shows the normal beam insolation for the entire day as position of the sun changes and the direct irradiance reaches a peak of approximately 981 W/m^2 at 1231 h. Using mean concentration ratio of the paraboloidal concentrator and the normal beam insolation we can calculate the power intercepted by the aperture (P_{ap}) as a function of its diameter.

Figure 3.10 shows $P_{ap}\left(=\frac{\overline{C}(D_{ap})\pi\, D_{ap}^2 I}{4}\right)$ calculated as a function of aperture diameter for beam normal radiation (I) equal to 200 W/m^2 (at 0449 h and 1921 h), 400 W/m^2 (at 0512 h and 1858 h), 600 W/m^2 (at 0544 h and 1826 h), 800 W/m^2 (at 0650 h and 1719 h) and 981 W/m^2 (at 1231 h).

For example, an aperture size of 4 cm intercepts a maximum of about 5.5 kW for a peak normal beam insolation of 981 W/m^2 at 1231 h. For the same aperture size, this reduces to 1.12 kW for normal insolation of 200 W/m^2 in the morning at 0449 h and evening at 1921 h. As it is seen, there is a five times decrease in the total intercepted power at the aperture between noon and the morning or evening. Therefore, in order to maintain a semi-constant temperature inside the reactor, it is necessary to use variable size apertures. It is possible to maintain desired level of temperature inside the reactor for a particular time of the day, depending on the magnitude of direct normal insolation, which is basically an optimum aperture size. For the same amount of insolation, larger aperture size implies higher P_{ap}, but this may not necessarily mean higher temperature. This is because a larger aperture size may cause higher re-radiation losses back through the aperture. This would lead to a drop in cavity receiver temperatures. For a smaller aperture, though P_{ap} is less, re-radiation losses

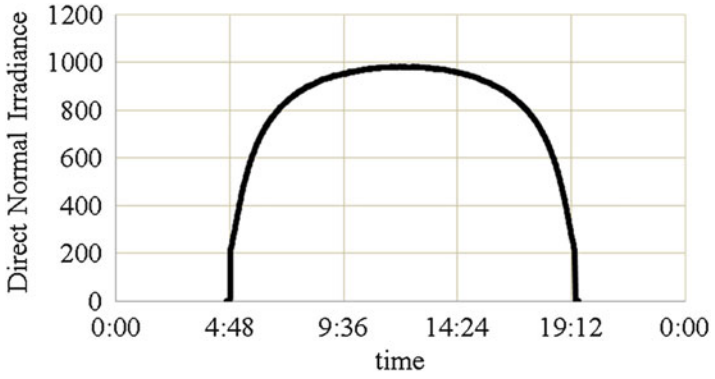

Fig. 3.9 Bird estimated direct normal insolation (*I*) [26] (*see color plates*)

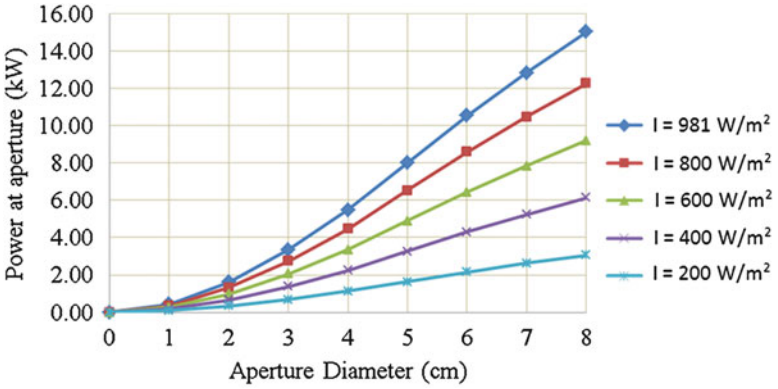

Fig. 3.10 Power intercepted at aperture (P_{ap}) as a function of diameter for different levels of normal insolation [26] (*see color plates*)

may be lower. Thus, selecting an optimum aperture size for a particular time of the day is a compromise between maximizing radiation capture and minimizing re-radiation losses as pointed out in Reference [29].

The incoming solar radiation intercepted at the aperture undergoes absorption and reflection at the receiver walls. Some of the reflected rays are further reflected or absorbed by the walls. Some escape back through the aperture as re-radiation. The power absorbed by the walls is then transferred to the working fluid by convection. Maintaining a semi-constant gas temperature inside the reactor, thus necessitates a detailed know how of the heat transfer mechanisms inside the reactor. Keeping this objective in mind, we have modeled the heat transfer characteristics of a prototype reactor manufactured in our lab. A one-dimensional steady state heat transfer model is developed which is coupled to the Monte Carlo ray tracing technique to calculate radiative heat exchange in the reactor. Details of our analysis can be found in [26], where we provide validation of in house developed MC ray tracing code results for apparent absorptivity with those provided in [30].

3.3.4.2 Changes in Weather Conditions: Cloud, Rain, Haze, Dust/Sand Storm

We approached this problem by proposing dual solar reactor use, where first reactor operates only when the sky is clear, while the second once starts only when the incoming solar flux is blocked because of any interruption including clouds, rain, haze, dust storm etc. The first reactor would operate as explained above. As for the second reactor, because the concentrated solar energy is not available during aforementioned conditions, it needs another high temperature source to conduct natural gas decomposition, which we can call as "secondary source" for this endothermic reaction. In order to make the system sustainable, the secondary source must be self-sufficient without external fuel or energy supply. Furthermore, in order to maintain the environmentally clean aspect of the whole system including both reactors, there should not be any hazardous emissions to the environment. To achieve this goal, secondary reactor can be operated via electrical heating using a direct carbon fuel to produce the electricity. In direct carbon fuel cells, the reactions take place as follows [31]:

$$\text{Cathode}: \ O_2 + 2CO_2 + 4e^- \rightarrow 2{CO_3}^{2-} \tag{3.10}$$

$$\text{Anode}: \ C + 2{CO_3}^{2-} \rightarrow 3CO_2 + 4e^- \tag{3.11}$$

$$\text{Overall}: \ C + O_2 \rightarrow \ CO_2 \tag{3.12}$$

As it is seen, the product is CO_2. However, the good thing about is that no sequestration is required because it is pure CO_2. Besides, it can be used in a cycle for CO_2 reforming of natural gas, which is commonly known as dry reforming;

$$CH_4 + CO_2 \rightarrow \ 2CO + 2H_2 \tag{3.13}$$

The product of dry reforming, syngas (CO and H_2), is a versatile feedstock for ammonia, methanol and Fischer–Tropsch synthesis processes and several other carbonization and hydrogenation or reduction processes. Alternatively, syngas can be water-shifted to produce more hydrogen.

During poor reception of sunlight due to weather changes, the secondary reactor comes into operation. As described above, with the use of secondary reactor, not only hydrogen and carbon black are produced, but also syngas is produced. This trigeneration of industrially valuable products, without emissions to the environment, is the main advantage of this combined energy system.

3.3.4.3 Night Time

The night time operation runs on exactly the same as concept described above, which can be illustrated as seen in Fig. 3.11. With a dual reactor concept, trigeneration of hydrogen, carbon black, and syngas is achieved on 24/7 basis regardless of the weather conditions, and during the night time.

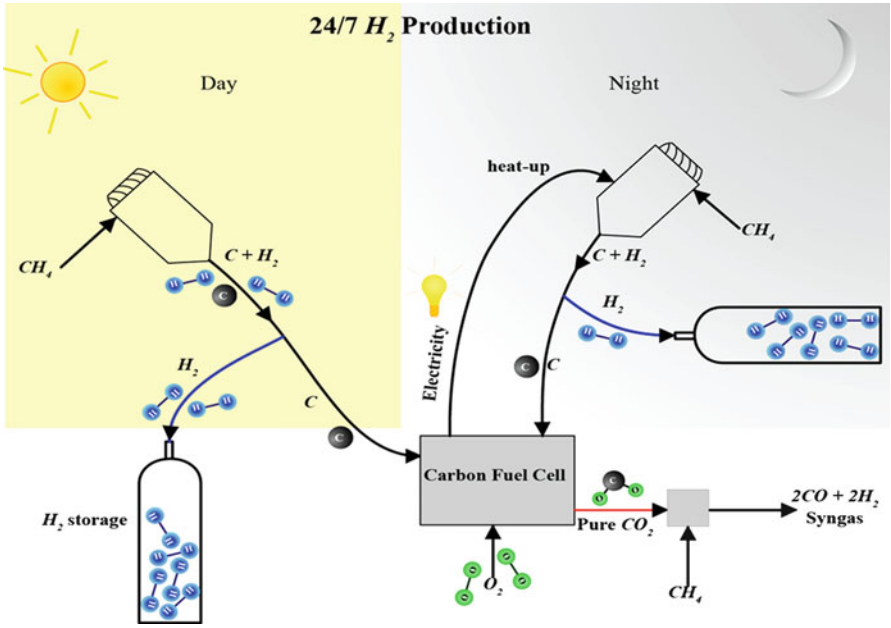

Fig. 3.11 Tri-generation of hydrogen, carbon black, and syngas on 24/7 basis (*see color plates*)

3.4 Conclusions

The importance of finding a sustainable and emission-free solution to impending fossil fuel and environmental problems of the world was reiterated. Major energy-consuming and emissions-producing industries, such as petroleum industry and chemical industry, are targeted as the potential first users of new technology. Solar thermochemical processes are the most promising alternatives to current conventional endothermic processes practiced in these industries.

Problems with solar thermochemical reactors preventing them from commercialization were outlined in the preceding discussion. An example solar reactor was described and illustrated as an alternative technology to the current technology for hydrogen production, which is mainly used by the oil industry to refine crude oil. Revenue benefits of co-production of hydrogen and carbon black were also outlined, and the advantage of selling carbon black as byproduct was emphasized to offset hydrogen production cost.

Problems with hydrogen and carbon black producing solar reactors were given as follows:

1. Carbon deposition on window, walls, and exit.
2. Reactor clogging due to blockage of the exit.

Solutions to these problems were described as a compilation of our previous work as follows:

1. Carbon deposition on window: traditional "window screening" flow can solve this problem.
2. Carbon deposition on the walls: a new method which we named "aero-shield" can sweep the walls just like the window screening flow does on the window.
3. Carbon deposition at the exit: a new flow dynamics which we named "cyclone" with specific flow pattern was described to enhance residence time and control carbon particle move inside.

In addition to solar cracking reactors, common problems to all other solar thermochemical reactors were categorized into three as follows:

1. Fluctuation of solar energy from sunrise to sunset.
2. Unavailability of concentrating sunlight due to changes in weather conditions.
3. Unavailability of sunlight during the night.

A step by step solution approach was presented addressing all three problems, which can be summarized as follows:

1. From sunrise to sunset; a human-eye like mechanism can maintain constant temperature inside the reactor as we have shown in our previously published heat transfer and optical analysis.
2. Changes in weather conditions dictate a dual reactor system, where the secondary reactor is heated up using electricity from a carbon fuel cell.
3. Night time: the same approach as described in (3.2) can be used. With this system, continuous tri-production of valuable products can be achieved with no emissions by coupling the carbon fuel cell product gas with natural gas via dry reforming of natural gas reaction.

In summary, a novel solar reactor system is proposed as a promising solution to generate valuable fuels and commodities on 24/7 basis with no emissions. An example case for tri-generation of hydrogen, carbon black and syngas was presented. The most suitable industry to adopt this system is the oil industry, where they can make tri-generation of these products to make hydrogen production cost very lower because of selling carbon black and syngas.

Acknowledgement This research has been funded by Qatar Foundation National Priorities Research Program, Qatar Foundation Research Excellence Program, and corporate agreement between Qatar Science & Technology Park and Fraunhofer Institute (IWS).

References

1. Sutton MA, Erisman JW, Dentener F, Möller D (2008) Ammonia in the environment: from ancient times to the present. Environ Pollut 156:583–604
2. Soltanieh M, Azar KM, Saber M (2012) Development of a zero emission integrated system for co-production of electricity and methanol through renewable hydrogen and CO2 capture. Int J Greenhouse Gas Control 7:145–152

3. Assabumrungrat S, Phromprasit J, Arpornwichanop A (2012) Fuel processing technologies for hydrogen production from methane. Eng J 16:2–4
4. Castaneda LC, Munoz JAD, Ancheyta J (2011) Comparison of approaches to determine hydrogen consumption during catalytic hydrotreating of oil fractions. Fuel 90:3593–3601
5. Hsu CS, Robinson PR (2006) Practical advances in petroleum processing, vol 1, Chapter 7: hydrotreating and hydrocracking: fundamentals. Springer, New York
6. Elshout R (2010) Hydrogen production by steam reforming. Chem Eng 117(5):34–38
7. Ozalp N (2008) Energy and material flow models of hydrogen production in the U.S. Chemical Industry. Int J Hydrogen Energ 33(19):5020–5034
8. Rodat S, Abanades S, Grivei E, Patrianakos G, Zygogianni A, Konstandopoulos AG, Flamant G (2011) Characterization of carbon blacks produced by solar thermal dissociation of methane. Carbon 49:3084–3091
9. Villasmil W, Steinfeld A (2010) Hydrogen production by hydrogen sulfide splitting using concentrated solar energy–thermodynamics and economic evaluation. Energ Convers Manage 51(11):2353–2361
10. Roeb M, Säck JP, Rietbrock P, Prahl C, Schreiber H, Neises M, de Oliveira L, Graf D, Ebert M, Reinalter W, Meyer-Grünefeldt M, Sattler C, Lopez A, Vidal A, Elsberg A, Stobbe P, Jones D, Steele A, Lorentzou S, Pagkoura C, Zygogianni A, Agrafiotis C, Konstandopoulos AG (2011) Test operation of a 100 kW pilot plant for solar hydrogen production from water on a solar tower. Sol Energ 85(4):634–644
11. Rodat S, Abanades S, Sans JL, Flamant G (2010) A pilot-scale solar reactor for the production of hydrogen and carbon black from methane splitting. Int J Hydrogen Energ 35(15):7748–7758
12. Ozalp N, Kogan A, Epstein M (2009) Solar decomposition of fossil fuels as an option for sustainability. Int J Hydrogen Energ 34(2):710–720
13. Wei L, Tan Y, Han Y, Zhao J, Wu J, Zhang D (2011) Hydrogen production by methane cracking over different coal chars. Fuel 90:3473–3479
14. Muradov NZ, Veziroğlu TN (2005) From hydrocarbon to hydrogen–carbon to hydrogen economy. Int J Hydrogen Energ 30:225–237
15. Trommer D, Hirsch D, Steinfeld A (2004) Kinetic investigation of the thermal decomposition of CH4 by direct irradiation of a vortex-flow laden with carbon particles. Int J Hydrogen Energ 29:627–633
16. Lockwood FC, Van Niekerk JE (1995) Parametric study of a carbon black oil furnace. Combust Flame 103:76–90
17. Rodat S, Abanades S, Flamant G (2011) Co-production of hydrogen and carbon black from solar thermal methane splitting in a tubular reactor prototype. Sol Energ 85:645–652
18. Back MH, Back RA (1983) Thermal decomposition and reactions of methane pyrolysis. Theory and Industrial Practice. Academic, New York, pp 1–24
19. Olsvik O, Rokstad OA, Holmen A (1995) Pyrolysis of methane in the presence of hydrogen. Chem Eng Technol 18:349–358
20. Olsvik O, Billaud F (1993) Modelling of the decomposition of methane at 1273 K in a plug flow reactor at low conversion. J Anal Appl Pyrolysis 25:395–405
21. Abanades S, Flamant G (2005) Production of hydrogen by thermal methane splitting in a nozzle-type scale solar reactor. Int J Hydrogen Energ 30:843–853
22. Kogan A, Israeli M, Alcobi E (2007) Production of hydrogen and carbon by solar thermal methane splitting. IV. Preliminary simulation of a confined tornado flow configuration by computational fluid dynamics. Int J Hydrogen Energ 32:4800–4810
23. Kogan A, Kogan M, Alcobi E (2004) Production of hydrogen and carbon by solar thermal methane splitting. II. Room temperature simulation tests of seeded solar reactor. Int J Hydrogen Energ 29:1227–1236
24. Ozalp N, Kanjirakat A (2010) Lagrangian characterization of multi-phase turbulent flow in a solar reactor for particle deposition prediction. Int J Hydrogen Energ 35:4496–4509
25. Haueter P, Seitz T, Steinfeld A (1999) A new high-flux solar furnace for high-temperature thermochemical research. J Sol Energ Eng 121:77–80

26. Usman S, Ozalp N (2012) Numerical and optical analysis of weather adaptable solar reactor. In: 9th international conference on heat transfer, fluid mechanics, and thermodynamics (HEFAT) proceedings, Malta
27. Retrieved from NREL database on April 2012 at http://www.nrel.gov/midc/srrl_rsp2
28. Bird RE, Hulstrom RL (1981) Simplified clear sky model for direct and diffuse insolation on horizontal surfaces, Technical report no. SERI/TR-642–761. Solar Energy Research Institute, Golden
29. Steinfeld A, Schubnell M (1993) Optimum aperture size and operating temperature of a solar cavity-receiver. Sol Energ 50:19–25
30. Kräupl S, Steinfeld A (2005) Monte Carlo radiative transfer modeling of a solar chemical reactor for the co-production of Zinc and Syngas. J Sol Energ Eng 127:102–108
31. Cherepy NJ, Krueger R, Fiet KJ, Jankowski AF, Cooper JF (2005) Direct conversion of carbon fuels in a molten carbonate fuel cell. J Electrochem Soc 152(1):A80–A87

Chapter 4
Photolysis of Hydrogen Sulfide in Gas Mixtures

S.A. Huseynova, Hokman Mahmudov, and Islam I. Mustafayev

Abstract The kinetic scheme of the processing reactions at the UV photolysis of oil refining gas products has been proposed on the basis of the experimental date. The kinetics of decomposition process of hydrogen sulfide and other components of the initial gas mixture, as well as formation of intermediate and stable products by means of the numerical simulation has been calculated. Comparative analysis of the experimental and calculation dependencies of elemental sulfur formation rates has been carried out.

Keywords Hydrogen sulfide • Gas mixture • UV photolysis • Quantum yield • "Hot" atoms • Reaction rate constant • Radicals • Molecular hydrogen

4.1 Introduction

Presence of the hydrogen sulfide impurities in composition of the natural gas, in the products of oil-refining and coal-chemical processes and of other industrial processes creates problems in their further use as a chemical row stock and a power-supplier. The hydrogen sulfide containing gases has high corrosion ability and being burnt, such products throw off sulfur dioxide and other sulfur containing compounds in the atmosphere creates unfavorable environmental situation. That is why these gas mixtures are exposed to cleaning from hydrogen sulfide. Existing methods [1, 2] of cleaning of the gas mixtures from hydrogen sulfide are multistage and power-consuming, though deep cleaning (<0.1 %) is not often achieved. Photolytic method of cleaning of the natural gas from hydrogen sulfide had been

S.A. Huseynova • H. Mahmudov (✉) • I.I. Mustafayev
Institute of Radiation Problems, National Academy of Sciences of Azerbaijan Republic,
9 Bakhtiyar Vahabzade str, Baku AZ1143, Azerbaijan
e-mail: hokman.mahmudov@gmail.com

A. Veziroğlu and M. Tsitskishvili (eds.), *Black Sea Energy Resource Development and Hydrogen Energy Problems*, NATO Science for Peace and Security Series C: Environmental Security, DOI 10.1007/978-94-007-6152-0_4,

proposed [3, 4] earlier at the Institute of Radiation Problems and it was noted availability of that method having high selectivity and simple realization.

In this work the results of mathematical modeling of the kinetics of photolytic processes of hydrogen sulfide transformations within model gas mixtures photolysis are presented.

4.2 Objects and Research Methodic

To avoid complication of kinetic description of the photolytic processes, the mathematical modeling has been performed on the example of model mixtures, containing hydrogen sulfide (Table 4.1).

Choice of such model mixture is justified by the fact that such a content of gases is maximally approximate to gas products of catalytic cracking of the oil-refining industry [5].

Numerical simulation of kinetics of the processes was carried out by means of the GEPASI (ver. 3.30) program of deterministic simulation of kinetics of the homogenous chemical and biochemical systems for MS Windows operating system. Description of this program is adduced in [6, 7]. The interface of GEPASI program simplifies significantly the task of model construction, helping a user to translate by help of program the description of the chemical system from the language of chemical reactions to the language of mathematics (matrixes and differential equations).

The program provides a choice of two methods of numerical integration: Adams method, concerning the class of the direct and explicit methods, and inverse differentiation method of Gear, concerning the class of implicit methods. The choice of this or that method is based on the reasons of rigidity degree of the integrated differential equations system. At present work we have used mainly the Gear method, as it allows to integrate either rigid or no rigid systems.

Used measurement units:

- Time – *second.*
- Volume – sm^3
- Concentration – *number of molecules*/sm^3

The following parameters were used during simulation:

- Numerical differentiation factor (Derivation factor)- +/− 0.1 %
- Stationary resolution (S.-S. resolution) – 10^{-9}
- Newton iterations – 50

Table 4.1 Initial content of investigated gas mixture

Gas mixtures	H_2	CH_4	C_2H_6	C_3H_8	C_4H_{10}	C_5H_{12}	N_2	O_2	CO_2
%, Vol.	46.7	21.1	17.2	7.8	4.2	0.6	0.5	0.3	0.1

- Gere method order (BDF order) – 5
- Adams method order (Adams order) – 12
- Absolute tolerance – 1,000 *molecules/sm*^{3}
- Relative tolerance – 10^{-8}
- In GEPASI program the formulas for calculation of constant speeds at different temperatures by Arrenius equation $k = A$*exp($-E/RT$) have been included additionally.
- The following constants were used in calculations:
- Universal gas constant R = 1,987 *cal/ (K*mole.)*
- Normal atmospheric pressure 101 *325 Pa*
- Intensity of ultraviolet radiation flux, quantum/s

4.3 Results and Their Discussion

At constructing the kinetic scheme of current processes during photolysis of the complex hydrogen sulfide containing gas mixtures the following occasions were specified:

1. Hydrogen sulfide intensively absorbs ultraviolet light $\Delta\lambda = 180 \div 250$ nm, at which other components of the mixture have very weak absorption bands.
2. Radiation source, mercury lamp at low pressure (0, 1÷100 Pa), has radiation spectrum by maximum at $\lambda = 253$ nm. Earlier had been shown that at used value of partial pressure this band was completely absorbed by hydrogen sulfide [8].
3. At absorption of radiation of mercury lamp by hydrogen sulfide, "hot" atoms of hydrogen of the excess kinetic energy are generated. The energy of particles determined by formula (4.1).

$$\varepsilon(H^*) = ((hc/\lambda) - D(H - HS)) = 5 - 3,9 = 1,1eV \tag{4.1}$$

   there hc/λ- is the energy of light quantum absorbed by hydrogen sulfide, D(H-HS)- is the energy of dissociation of hydrogen sulfide to hydrogen atoms and HS-radicals.
4. Generated "hot" atoms of hydrogen colliding with surrounding atoms during hydrogen sulfide photolysis lose kinetic energy and thermolized. Share of energy loss was calculated by formula (4.2):

$$\frac{\Delta E}{E} = \frac{4M_1M_2}{(M_1 + M_2)^2} \tag{4.2}$$

there E – is initial the energy of the "hot" atom, ΔE – is variation of atom energy at one collusion, M_1 – is weight of the "hot" atom, M_2 – is weight of the gas component. Share of energy loss calculated by this formula is presented in

Table 4.2 Calculated share of energy loss

Components	Molecular weight of the component (g/mol)	A share of energy loss during collision (α)
H_2S	34	0,111
H_2	2	0,889
CH_4	16	0,221
C_2H_6	30	0,125
C_3H_8	40	0,095
C_4H_{10}	58	0,067
C_5H_{12}	72	0,054
O_2	32	0,118
N_2	28	0,133
CO_2	44	0,087
CO	28	0,133
H_2O (vapour)	18	0,199

Table 4.2. As we see from the table, in experimental conditions the all "hot atoms" of hydrogen lose fast the energy and thermolise till entering into a reaction.

Taking into account the above stated conditions we have proposed the following scheme of elementary reactions at the photolysis of hydrogen sulfide containing gas mixtures (Table 4.3).

The calculations of kinetics of decomposition of H_2S, CH_4, C_2H_6, C_3H_8, C_4H_{10}, C_5H_{12} and generation of constant product such as SO_2, H_2O_2, $H_2S_2O_6$, O_3, SO_3, S_8, CO_2, CO and intermediate products such as H, HS, SO, HO_2, OH, hydrogen sulfide radicals and etc. according to this scheme were carried out.

As an example, kinetics of hydrogen sulfide decomposition at different temperatures (Fig. 4.1), and kinetics of generation of SO_2, S_8 is presented at T = 300 K (Fig. 4.2).

In case of generation of elementary sulfur experimental points were compared with calculation data and satisfactory fit was obtained.

4.4 Conclusion

- Kinetic model including elementary reactions at the photolysis of hydrogen sulfide in gas mixtures was developed.
- Mathematical calculations of kinetics of decomposition of initial components, as well as the generation of final and intermediate products were carried out.
- Comparison of calculated and experimental results in case of generation of elementary sulfur and sulfur dioxide was conducted and satisfactory fit was obtained between these data that testifies to reliability of the proposed model.

Table 4.3 Kinetic scheme of elementary reactions at the photolysis of hydrogen sulfide containing gas mixtures

Number	Reactions	Rate constants, sm^3/s or $sm^6/(molec^2 \cdot s)$			
		T = 300 K	T = 473 K	T = 573 K	T = 673 K
1.	$H_2S = H + SH$	3 · e-3	3 · e-3	3 · e-3	3 · e-3
2.	$H_2S + OH = HS + H_2O$	0.36 · e-11	0.57 · e-11	0.66 · e-11	0.74 · e-11
3.	$H_2S + HO_2 = H_2O + HSO$	5 · e-12	5 · e-12	5 · e-12	5 · e-12
4.	$H_2S + O = HS + OH$	2.32 · e-14	2.4 · e-13	4.9 · e-13	8 · e-13
5.	$HS + O_2 = OH + SO$	1.5 · e-17	1.5 · e-17	1.5 · e-17	1.5 · e-17
6.	$HS + HO_2 = OH + HSO$	4 · e-11	6 · e-11	4 · e-11	4 · e-11
7.	$HS + O_3 = HSO + O_2$	1.3 · e-14	4.3 · e-14	1.3 · e-14	1.3 · e-14
8.	$HSO + O_2 = SO_2 + OH$	2.0 · e-17	3 · e-17	2.0 · e-17	2.0 · e-17
9.	$H_2S + H = HS + H_2$	7.37 · e-13	2.1 · e-12	2.9 · e-12	3.6 · e-12
10.	$2HS = H_2S + S$	1.2 · e-11	1.2 · e-11	1.2 · e-11	1.2 · e-11
11.	$H_2S + S = H_2 + S_2$	2.25 · e-15	4.9 · e-14	1.20 · e-13	2.4 · e-13
12.	$H + HS = H_2 + S$	2.5 · e-11	3.5 · e-11	2.5 · e-11	2.5 · e-11
13.	$HS + S = H + S_2$	4.5 · e-10	4.5 · e-10	4.5 · e-10	4.5 · e-10
14.	$2HS = H_2 + S_2$	2.16 · e-10	2 · e-10	2.16 · e-10	2.16 · e-10
15.	$2S + M = S_2 + M$	0.22 · e-32	0.88 · e-30	0.94 · e-30	0.98 · e-30
16.	$2S_2 + M = S_4 + M$	2.5 · e-31	2.5 · e-31	2.5 · e-31	2.5 · e-31
17.	$S + O_2 = O + SO$	2.24 · e-12	3.24 · e-12	2.24 · e-12	2.24 · e-12
18.	$HS + O = H + SO$	7.5 · e-13	32.2 · e-13	7.5 · e-13	7.5 · e-13
19.	$O + S_2 = S + SO$	6.7 · e-12	7.7 · e-12	6.7 · e-12	6.7 · e-12
20.	$SO + O_2 = O + SO_2$	8.88 · e-17	1.6 · e-15	8.88 · e-17	8.88 · e-17
21.	$O + SO + M = SO_2 + M$	1.9 · e-31	1.9 · e-31	1.9 · e-31	1.9 · e-31
22.	$2SO = S + SO_2$	0.16 · e-13	1.4 · e-13	0.16 · e-13	0.16 · e-13
23.	$SO + S_2 = S + S_2O$	3.78 · e-29	1.8 · e-22	3.78 · e-29	3.78 · e-29
24.	$S_2 + O_2 = O + S_2O$	4.6 · e-32	2.55 · e-24	4.6 · e-32	4.6 · e-32
25.	$S + SO_2 = O + S_2O$	1.02 · e-43	1.02 · e-31	1.02 · e-43	1.02 · e-43
26.	$2S_4 + M = S_8 + M$	2.5 · e-31	2.5 · e-31	2.5 · e-31	2.5 · e-31

(continued)

Table 4.3 (continued)

Number	Reactions	Rate constants, sm^3/s or $sm^6/(molec^2 \cdot s)$			
		T = 300 K	T = 473 K	T = 573 K	T = 673 K
27.	$OH + SO = H + SO_2$	1 · e-10	4 · e-10	1 · e-10	1 · e-10
28.	$SO + M + O_2 = SO_3 + M$	1 · e-35	1.4 · e-35	1 · e-35	1 · e-35
29.	$2OH = O + H_2O$	1.9 · e-12	2.5 · e-12	1.9 · e-12	1.9 · e-12
30.	$HO_2 + OH = H_2O + O_2$	2.13 · e-11	2.83 · e-11	2.13 · e-11	2.13 · e-11
31.	$O_3 + OH = HO_2 + O_2$	0.07 · e-12	0.22 · e-12	0.07 · e-12	0.07 · e-12
32.	$2OH + M = H_2O_2 + M$	4.79 · e-31	4.79 · e-31	4.109 · e-31	3.62 · e-31
33.	$OH + H_2O_2 = HO_2 + H_2O$	1.69 · e-12	2.2 · e-12	1.69 · e-12	1.69 · e-12
34.	$SO_2 + OH + M = HSO_3 + M$	3 · e-30	0.68 · e-30	0.36 · e-30	0.21 · e-30
35.	$OH + HSO_3 = H_2SO_4$	8.3 · e-12	8.3 · e-12	8.3 · e-12	8.3 · e-12
36.	$OH + HSO_3 = H_2O + SO_3$	8.3 · e-12	8.3 · e-12	8.3 · e-12	8.3 · e-12
37.	$HSO_3 + O_2 = HSO_5$	6.6 · e-13	6 · e-13	6.6 · e-13	6.6 · e-13
38.	$HSO_3 + O_2 = HO_2 + SO_3$	0.43 · e-12	0.65 · e-12	0.73 · e-12	0.80 · e-12
39.	$HO_2 + HSO_3 = H_2SO_5$	8.3 · e-12	8.3 · e-12	8.3 · e-12	8.3 · e-12
40.	$2HSO_3 = H_2S_2O_6$	4.9 · e-13	4.9 · e-13	4.9 · e-13	4.9 · e-13
41.	$HSO_3 + HSO_5 = 2HSO_4$	8.3 · e-14	8.3 · e-14	8.3 · e-14	8.3 · e-14
42.	$SO_2 + HSO_5 = SO_3 + HSO_4$	1.6 · e-12	1.6 · e-12	1.6 · e-12	1.6 · e-12
43.	$O + SO_3 = SO_2 + O_2$	6.9 · e-13	6.9 · e-13	6.9 · e-13	6.9 · e-13
44.	$H_2O + SO_3 = H_2SO_4$	9 · e-13	9 · e-13	9 · e-13	9 · e-13
45.	$SO_2 + HO_2 = OH + SO_3$	1.5 · e-15	1.5 · e-15	1.5 · e-15	1.5 · e-15
46.	$O + SO_2 + M = SO_3 + M$	0.144 · e-32	0.49 · e-32	0.144 · e-32	0.144 · e-32
47.	$SO_2 + O_3 = SO_3 + O_2$	2.31 · e-22	1.12 · e-18	0.15 · e-17	0.91 · e-17
48.	$O_3 + SO = SO_2 + O_2$	0.79 · e-13	0.31 · e-12	0.47 · e-12	0.62 · e-12
49.	$S + O_3 = SO + O_2$	1.2 · e-11	2.2 · e-11	1.2 · e-11	1.2 · e-11
50.	$O + O_2 + M = O_3 + M$	6.2 · e-34	2.52 · e-34	1.7 · e-34	1.2 · e-34
51.	$O + HO_2 = OH + O_2$	1.54 · e-11	1.97 · e-11	1.54 · e-11	1.54 · e-11
52.	$O + O_3 = 2O_2$	8.3 · e-15	1.03 · e-13	8.3 · e-15	8.3 · e-15

53.	$O + OH = H + O_2$	0.69 · e-11	1.8 · e-11	0.69 · e-11	0.69 · e-11
54.	$2O + M = M + O_2$	1.6 · e-33	1.6 · e-33	1.6 · e-33	1.6 · e-33
55.	$O_3 + HO_2 = OH + 2O_2$	0.21 · e-14	0.38 · e-14	0.21 · e-14	0.21 · e-14
56.	$H + O_2 + M = HO_2 + M$	5.7 · e-32	2.75 · e-32	2.0 · e-32	1.57 · e-32
57.	$H_2 + OH = H + H_2O$	0.7 · e-14	0.8 · e-13	0.7 · e-14	0.7 · e-14
58.	$H + O_3 = OH + O_2$	0.28 · e-10	0.5 · e-10	0.28 · e-10	0.28 · e-10
59.	$HO + HO_2 = H_2 + O_2$	1.4 · e-11	1.4 · e-11	1.4 · e-11	1.4 · e-11
60.	$H + HO_2 = 2OH$	3.2 · e-11	3.2 · e-11	3.2 · e-11	3.2 · e-11
61.	$H + HO_2 = O + H_2O$	9.4 · e-13	9.4 · e-13	9.4 · e-13	9.4 · e-13
62.	$2H + M = H_2 + M$	4.8 · e-33	4.8 · e-33	4.8 · e-33	4.8 · e-33
63.	$H + OH + M = H_2O + M$	4.3 · e-31	4.3 · e-31	4.3 · e-31	4.3 · e-31
64.	$O + H_2O_2 = HO_2 + OH$	0.177 · e-14	0.2 · e-13	0.177 · e-14	0.177 · e-14
65.	$2HO_2 = H_2O_2 + O_2$	0.31 · e-13	0.65 · e-13	0.31 · e-13	0.31 · e-13
66.	$HO_2 + HSO_4 = O_2 + H_2SO_4$	4.6 · e-11	4.6 · e-11	4.6 · e-11	4.6 · e-11
67.	$HSO_5 + HSO_4 = SO_3 + O_2 + H_2SO_4$	1 · e-11	0.4 · e-11	1 · e-11	1 · e-11
68.	$O_3 + HSO = HSO_2 + O_2$	3.2 · e-12	3.2 · e-12	3.2 · e-12	3.2 · e-12
69.	$HSO_2 + O_2 = SO_2 + HO_2$	3 · e-13	3 · e-13	3 · e-13	3 · e-13
70.	$HS + HSO = H_2S + SO$	1.7 · e-12	1.7 · e-12	1.7 · e-12	1.7 · e-12
71.	$OH + CH_4 = H_2O + CH_3$	1.05 · e-14	0.4 · e-12	1.07 · e-12	2 · e-12
72.	$OH + C_2H_6 = H_2O + C_2H_5$	0.29 · e-12	0.45 · e-11	9 · e-12	14 · e-12
73.	$OH + C_3H_8 = H_2O + C_3H_7$	1.35 · e-12	13.5 · e-12		
74.	$H + CH_4 = H_2 + CH_3$	5.8 · e-18	1.68 · e-16	0.42 · e-15	0.58 · e-15
75.	$H + C_2H_6 = H_2 + C_2H_5$	2.02 · e-17	0.75 · e-14	0.01 · e-12	0.023 · e-12
76.	$H + C_3H_8 = H_2 + C_3H_7$	2.58 · e-16	2.7 · e-14	0.011 · e-12	0.32 · e-12
77.	$H + n\text{-}C_4H_{10} = H_2 + C_4H_9$	7.89 · e-16	3.9 · e-14	0.103 · e-12	0.25 · e-12
78.	$H + n\text{-}C_5H_{12} = H_2 + C_5H_{11}$	0.63 · e-16	2.63 · e-16		
79.	$O + CH_4 = OH + CH_3$	2 · e-18	6.25 · e-15	0.105 · e-12	0.25 · e-12
80.	$O + C_2H_6 = OH + C_2H_5$	3 · e-15	5.44 · e-14	0.135 · e-12	2.3 · e-12
81.	$O + C_3H_8 = OH + C_3H_7$	0.22 · e-13	0.41 · e-13	0.321 · e-12	0.52 · e-12
82.	$O + n\text{-}C_4H_{10} = OH + C_4H_9$	0.65 · e-14	6.86 · e-13	1.48 · e-12	2.6 · e-12

(continued)

Table 4.3 (continued)

Number	Reactions	Rate constants, sm^3/s or $sm^6/(molec^2 \cdot s)$			
		T = 300 K	T = 473 K	T = 573 K	T = 673 K
83.	$OH + H_2 = H_2O + H$	1.6 · e-14	1.7 · e-13		
84.	$HO_2 + CO = CO_2 + OH$	2.2 · e-14	2.75 · e-12	3 · e-12	3.3 · e-12
85.	$O + H_2 = H + OH$	0.47 · e-16	1.52 · e-15	0.77 · e-14	0.024 · e-12
86.	$CH_3 + CH_3 = C_2H_6$	6 · e-11	6 · e-11	6 · e-11	6 · e-11
87.	$C_2H_5 + C_2H_5 = C_4H_{10}$	6 · e-11	6 · e-11	6 · e-11	6 · e-11
88.	$C_3H_7 + C_3H_7 = C_6H_{14}$	6 · e-11	6 · e-11	6 · e-11	6 · e-11
89.	$C_4H_9 + C_4H_9 = C_8H_{18}$	6 · e-11	6 · e-11	6 · e-11	6 · e-11
90.	$C_5H_{11} + C_5H_{11} = C_{10}H_{22}$	6 · e-11	6 · e-11	6 · e-11	6 · e-11
91.	$CH_3 + H_2S = CH_4 + SH$	1 · e-13	1 · e-13	1 · e-13	1 · e-13

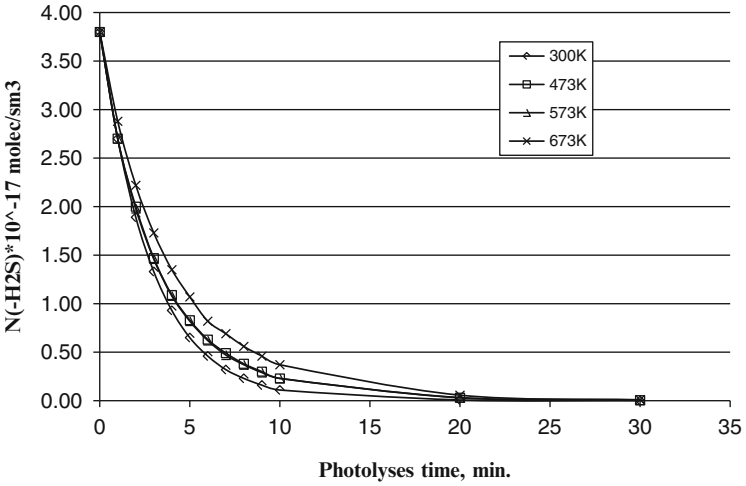

Fig. 4.1 Kinetics of hydrogen sulfide decomposition at photolysis of hydrogen sulfide

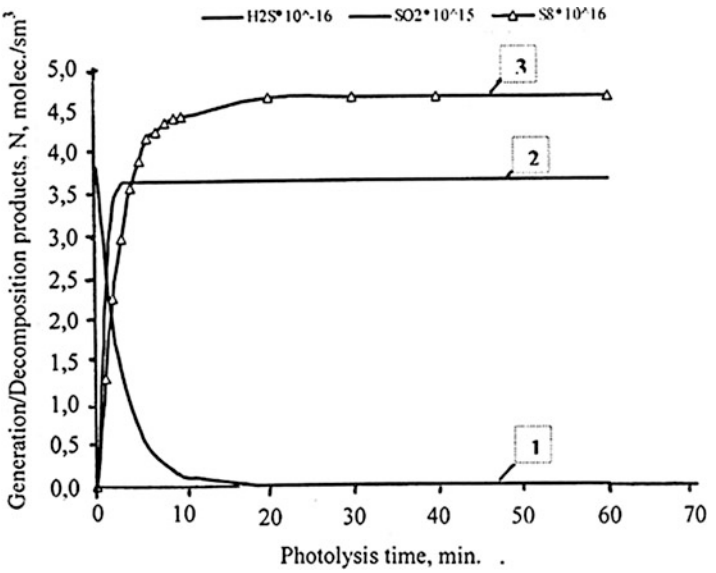

Fig. 4.2 Kinetics of hydrogen sulfide decomposition (1) and generation of SO_2 (2), S_8 (3) is presented at T = 300 K

References

1. Василевский ВВ, Гуцевич ЕИ, Потапкин БВ, Русанов ВД, Фридман АА (1991) Химия Высоких Энергия 25:283
2. Курбанов и.др МА (1986) Химия Высоких Энергия 20:554
3. Курбанов МА, Мамедов ХФ, Искендерова ЗИ, Мустафаев ИИ (1990) Способ очистки метана от сероводорода, Авторское свидетельство СССР, N1632475
4. Мустафаев ИИ, Махмудов ОМ (1988) Азербайджанский химический журнал (1):81
5. Босняцкий ГП (1998) Природный газ и сероводород, (Справ. пособие). М.: Газоил пресс
6. Mendes P (1993) Comput Appl Biosci 9:563
7. Mendes SAP (1997) Trends Biochem Sci 22:361
8. Hüseynova İİ Mustafayev, Mahmudov HM (2009) Beynəlxalq konfrans. RPİ-nin 40 illik yubleyinə həsr olunmuş. Nüvə Enerjisinin Dinc Məqsədlərlə İstifadəsi Prespeltivləri, 2–4 noyabr, Bakı, Azərbaycan: 32–33

Chapter 5
Photochemical Decomposition of Hydrogen Sulphide in the Gas Mixtures and Generation Molecular Hydrogen

S.A. Huseynova, Hokman Mahmudov, and Islam I. Mustafayev

Abstract The process of molecular hydrogen achievement during the photolysis of gas mixtures generated in the course of oil treatment processes and containing hydrogen sulfide has been studied in this work. The photochemical decomposition of hydrogen sulfide and the kinetics of hydrogen generation have been investigated in the wide range of temperature and hydrogen sulfide partial pressure variation. The role of "hot" hydrogen atoms and the mechanism of the on-going processes within the process of molecular hydrogen generation due to the photochemical decomposition of hydrogen sulfide have been discussed.

Keywords Hydrogen sulfide • Gas mixture • Photolysis • Quantum yield • "Hot" atoms • Molecular hydrogen

5.1 Introduction

Due to the refining and chemical conversions of organic fuels complex gas mixtures containing hydrogen sulfide generate as a by-product [1, 2]. In accordance with the environmental safety requirements, these gas mixtures have to be purified from hydrogen sulfide before use or discharge to the environment. As it is known because of H_2S containing combustion gases sulfide oxides emit into the atmosphere and they combine with water vapors in the air and this process consequently results in the change of pH of H_2SO_3 precipitations and acid rains. Besides the processes of hydrocarbon-containing gas mixtures purification from hydrogen sulfide are

S.A. Huseynova • H. Mahmudov (✉) • I.I. Mustafayev
Institute of Radiation Problems, Azerbaijan National Academy of Sciences, 9 Bakhtiyar Vahabzade str., Baku AZ1143, Azerbaijan
e-mail: hokman.mahmudov@gmail.com

A. Veziroğlu and M. Tsitskishvili (eds.), *Black Sea Energy Resource Development and Hydrogen Energy Problems*, NATO Science for Peace and Security Series C: Environmental Security, DOI 10.1007/978-94-007-6152-0_5,

multiphase and energy-consuming, the cleaning efficiency is low too [3]. Therefore scientific researches are intensively conducted to find out selective and low stage processes to realize such kind of processes. From this standpoint, photochemical method seems a much more reasonable one. Literature contains data [4, 5] on the investigation results on the kinetics of hydrogen sulfide selective decomposition processes during the photolysis of hydrogen-sulfide, methane-hydrogen sulfide binary gas mixtures and semicoking coal gases. The results of these studies show that though hydrogen sulfide undergoes chemical conversions by efficiently absorbing quanta at 250 nm length of light radiation, other components remain unchanged [5–7]. But the photochemical conversions in the gases, which are the products of complex component oil treatment, petrochemical processes, etc., have not been studied.

In the article, the processes of gas mixture purification being the product of oil treatment processes and mainly containing hydrocarbons from hydrogen sulfide by a photochemical method and molecular hydrogen generation have been under investigation.

5.2 Research Techniques

The model gas mixture under investigation has been prepared at a vaccum plant in the laboratory. Initially, H_2S was obtained under the impact of concentrated HCl to FeS_2. The obtained gas mixture has been air-purified being freezed by liquid nitrogen at a vacuum plant for several times. At the vacuum plant, hydrocarbon mixture (CH_4–C_4H_{10}) having different initial contents has been obtained by a manometric control and hydrogen sulfide has been added to the mixture. The initial content of hydrocarbon gas mixture has been given in Table 5.1 and this content has been approximated to that of gas compositions generated at oil treatment factories. The gas mixture with a pre-known composition has been filled into a quartz window cylindric reactor, and exposed to ultraviolet radiation. The gas pressure in the reactor has been revealed by an experimental method and the pressure has been selected as 0.13–1.33 kPa for complete radiation absorption. As a radiation source with the wave length of $\lambda = 250$–365 nm DRS and PRK lamps (P = 0.03–0.3 MPa, Hg-vapor) have been used. The irradiation has been carried out in the range of $\tau = 0$–0.5 h. The radiation intensity inside the reactor has been measured by a gas actinometer [8] and determined equal to $I = 1.5 \cdot 10^{15}$ quantum/s.

The concentration of hydrogen and hydrocarbon gas generated due to the photolysis process has been determined at “Gaschrom-3101” and “Svet-101” device by a chromatographic method. The hydrogen sensitivity of the device equals to $K(H_2) = 6.0 \cdot 10^{13}$ molecule/($cm^3 \cdot mm$) and hydrocarbon gas $K(C_xH_y) = (1.17 - 13.5)*10^{15}$ /($cm^3 \cdot mm$).

5.3 Results and Their Discussion

During the researches, the partial pressure of H_2S capable of completely absorbing the given wave-length of the radiation has been first specified. For this reason, the dependence between molecular hydrogen yield generated at the result of H_2S decomposition and hydrogen sulfide pressure (density) has been studied (Fig. 5.1). As it is obvious from the achieved diagram during $\tau = 0.5$ h period the dependence of hydrogen generation on the hydrogen sulfide pressure has a linear increase in the range of P = 0.13–1.33 kPa. At much bigger partial pressures molecular hydrogen yield is not dependent on pressure. In the gas mixture used at our experiments, the partial pressure of H_2S has changed in the range of 0–3.0 kPa which is more close to the real gas composition.

The kinetics of hydrogen sulfide decomposition and molecular hydrogen generation at different temperatures (T = 300 K, 473 K, 573 K and 673 K) at the result of photolysis process has been investigated and the results have been given in Fig. 5.2. As it becomes evident from the kinetic curves during the whole temperature range under investigation in the course of 10 min the processes of both H_2S decomposition and molecular hydrogen generation come into a stationary state. At the result of our researches it has been revealed that at all temperatures kinetic region is mainly divided into two parts: reaction rates of the speedy processes going on at the beginning of the processes, i.e., in the course of 0–5 min: $W(H_2) = 1.5*10^{15}$ molecule/(cm^3*sec), quantum yield $\varphi(H_2) = 1.2$ molecule/quantum, $W(-H_2S) = 1.63*10^{15}$ molecule/(cm^3*sec), $\varphi(-H_2S) = 1.3$ molecule/quantum, and in the course of 5–10 min these figures become equal to $-W(H_2) = 0.69*10^{15}$, $\varphi(H_2) = 0.55$, $W(-H_2S) = 0.08*10^{15}$, $\varphi(-H_2S) = 0.06$. This proves that both temperature and irradiation time have their influence on the progress rate of the processes. At the values of irradiation time more than 15 min the concentration of hydrogen sulfide

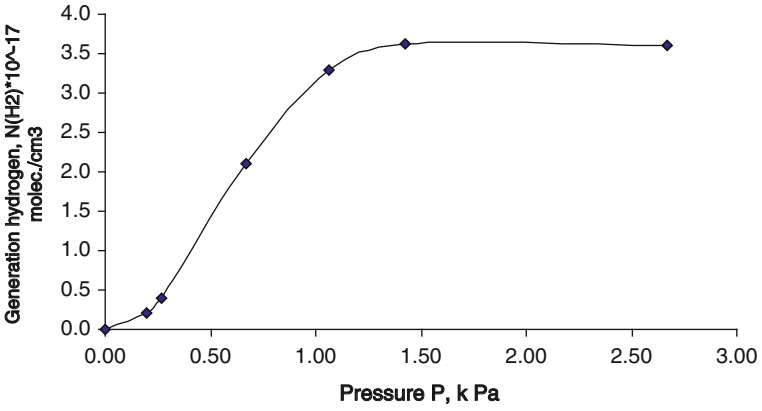

Fig. 5.1 Dependence between hydrogen concentration generated due to photolysis and the pressure of hydrogen sulfide (*see color plates*)

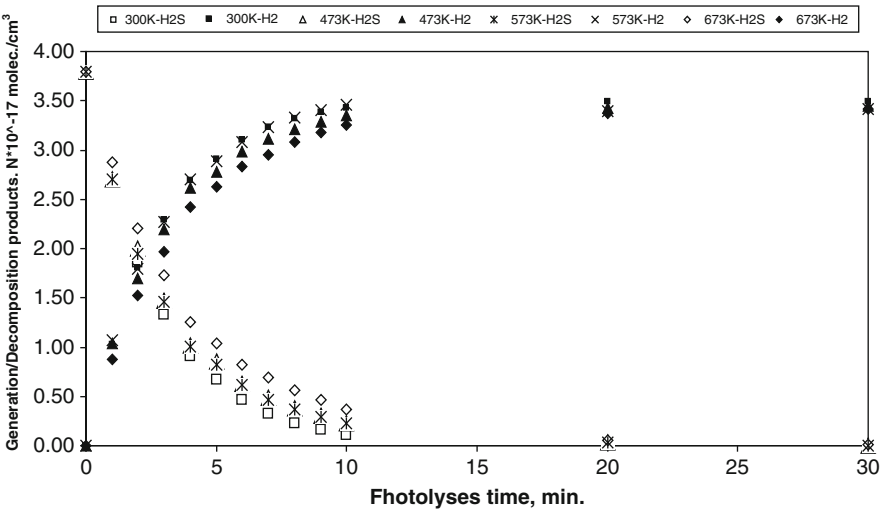

Fig. 5.2 Kinetic dependence between hydrogen sulfide decomposition by a photochemical method and molecular hydrogen generation (Δ – 300, O – 473, × – 573, ж – 673 K, $I = 1.5*10^{15}$ quantum/s)

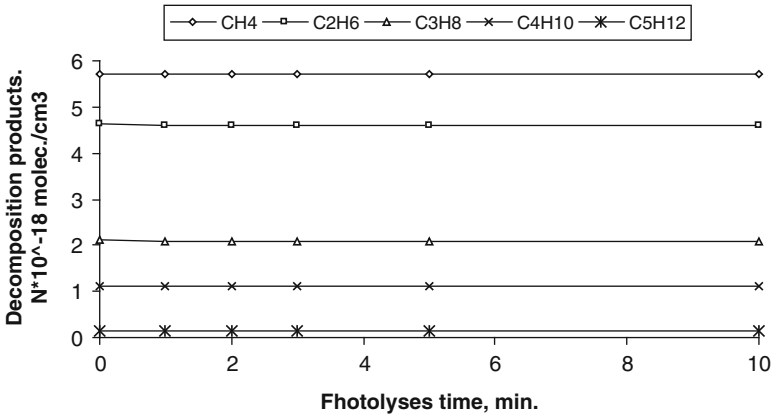

Fig. 5.3 Kinetics of photochemical decomposition of hydrocarbon gases

decreases down to 98–99 % from initial concentration and this doesn't cause serious environmental problems.

In Fig. 5.3 the impact of UV radiation on the hydrocarbon gas concentration (C_1–C_4) within 10 min has been described. As you can see from the Figure at this wave-length hydrocarbons undergo no photochemical conversions. This is manifested with the absence of excitation levels causing dissociation due to radiation absorption at the wave-length used in hydrocarbon gases [7]. The fact that

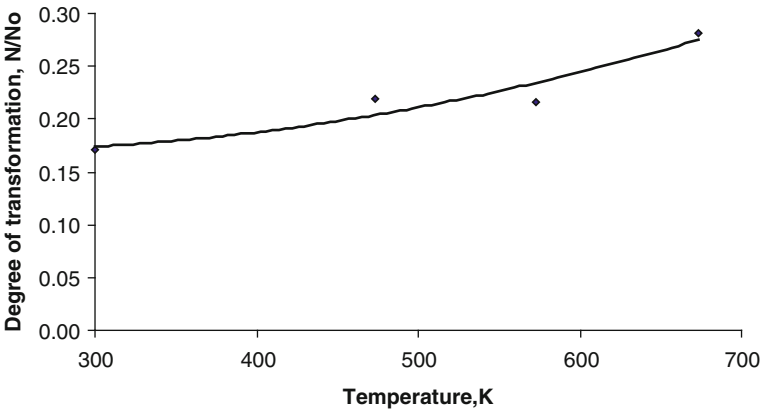

Fig. 5.4 Temperature dependence of hydrogen sulfide photochemical decomposition (*see color plates*)

these levels belong to hydrogen sulfide contained in gas mixtures has been experimentally proved.

It's evident from the experimental results given in Fig. 5.2 the rates of H_2S decomposition and molecular hydrogen generation processes are slightly dependent on temperature. During experiments with the rise in the temperature the rate of these processes are also observed to increase. The temperature dependence of hydrogen sulfide photochemical decomposition has been actually shown in Fig. 5.4.

As you can see from the diagram the progress of the process, i.e. hydrogen sulfide photochemical decomposition increases with the rise in temperature. At room temperature within 5 min the photochemical conversion rate of hydrogen sulfide is 16 %, the figure equals to 27 % at 673 K temperature, and this occurs at the expense of the reaction rate increase for $W_{673}/W_{300} = 1.6$ times. The efficient value of the activation energy calculated on the basis of these results is $E = 7.1$ kJ/mol which corresponds to diffusion processes. The temperature rise only increases the probability of collision between active particles by raising their kinetic energy and corresponding molecules, and has a weak influence on the rate of chemical processes [9].

The photolysis of hydrogen sulfide, hydrogen sulfide-ethylen and hydrogen sulfide-methane gas mixtures under the impact of UV radiation has been thoroughly investigated [4–8, 10–12]. The authors of these researches have determined that during the photolysis of hydrogen sulfide mainly "hot" hydrogen atom generates. The amount of the kinetic energy $\varepsilon(H^*)$ carried by this atom is calculated by the below formula (5.1):

$$\varepsilon(H^*) = (E_\lambda - D(H - HS)) = 5 - 3.9 = 1.1\text{eV} \tag{5.1}$$

Here E_λ-value of quantum energy absorbed by hydrogen sulfide, D(H-HS)-dissociation energy into H and OH radicals of hydrogen sulfide. It should be

Table 5.1 The initial content of hydrocarbon gas mixture and the relative amount of the energy lost during the collison of two molecules

Gas mixtures	H_2	CH_4	C_2H_6	C_3H_8	C_4H_{10}	C_5H_{12}	N_2	O_2	CO_2
Vol.%	46.7	21.1	17.2	7.8	4.2	0.6	0.5	0.3	0.1
ΔE/E,%	88.89	22.15	12.49	9.52	6.66	5.40	13.32	11.75	8.69

mentioned that the kinetic energy of gas molecules being in equilibrium at room temperature equals to 0.025 eV. Hot hydrogen atoms carrying an additional kinetic energy not depending on medium temperature go into reaction with H_2S molecule, pull out another H atom and generate molecular hydrogen. These processes going during the photolysis of pure H_2S and the hydrogen quantum yield is $\varphi(H_2) = 1–1.2$. And in the complex gas systems used by us hot hydrogen atom before the collision with H_2S molecule depending on the general pressure collides with hydrocarbon molecules for ten times and considerably loses its energy during these collisions. The relative amount of the energy lost during the collision of two molecules with preliminary kinetic energies E and 0, and molecular weights M_1 and M_2 is calculated by formula (5.2) [7].

$$\frac{\Delta E}{E} = \frac{4M_1M_2}{(M_1 + M_2)^2} \tag{5.2}$$

The amount of the energy lost during one collision between the gases contained into the gas mixture and hot hydrogen atom has been given in Table 5.1.

As you can see hot hydrogen atom loses 22.15 % of its energy during one collision with methane and 6.66 % with butane. During collision the biggest lose occurs in that case when the weights of the collided particles are equal ($M_1 = M_2$).

In this case hydrogen atom in the investigated system before the collision with hydrogen sulfide preserves much less share of its additional energy, nevertheless can participate in the following reactions:

$$H_2S \rightarrow H^* + HS \tag{5.3}$$

$$H_2S + H^* \rightarrow H_2 + HS^* \tag{5.4}$$

$$HS + HS \rightarrow H_2 + S_2 \tag{5.5}$$

$$HS + HS \rightarrow H_2S \tag{5.6}$$

$$HS + H_2S \rightarrow H_2 + S \tag{5.7}$$

$$HS + CxHy \rightarrow H_2S + CxH_{y-1} \tag{5.8}$$

At the result of these reactions molecular hydrogen generates with the quantum yield of 1.0–1.2. Due to this process the gas mixture has been purified from hydrogen sulfide and molecular hydrogen has been enriched.

5.4 Conclusion

The selective purification of hydrogen sulfide by a photochemical method in complex component gas mixture has been experimentally observed, and the process efficiency has been investigated in the wide range of temperature and pressure. It has been shown that the maximum quantum yield of hydrogen sulfide decomposition and hydrogen generation is observed at the values of H_2S partial pressure more than 1.33 kPa and the process efficiency weakly depends on temperature. Within the process hydrocarbon gases don't decompose and are enriched with molecular hydrogen, the concentration of hydrogen sulfide decreases up to 97–98 % which is not harmful for the environment.

References

1. Baykara SZ, Figen EH, Kale A, Nejat Veziroglu T (2007) Hydrogen from hydrogensulphide in Black Sea. Int J Hydrogen Energ 32(9):1246–1250
2. Zaman J, Chakma A (1995) Production of hydrogen and sulfur from hydrogen sulfide. Fuel Process Technol 41(2):159–198
3. Website: http://www.h2s.su/index.php-p=ochist.htm
4. Gurbanov MA, Mammadov KhF, Iskenderova ZI, Mustafayev II (1990) The method of hydrogen sulfide purification from methane. Certificate of authorship USSR N1632475
5. Mustafayev II, Mahmudov HM (1988) The kinetics of H_2 generation during the photolysis of gas producsts of caustobiolith semicoking. Azerbaijan Chem J 1:81–85
6. Dzantiev BG, Ermakov AN et al (1975) Power supply during the radiolysis of hydrogen sulfide-ethylen mixture. ACJ (28):175
7. Okabe Kh (1981) Photochemistry of small molecules. Moscow "Mir", pp 243–245
8. Experimental Methods of Chemical kinetics, under the edition of Emmanuel N.M, Kuzmina M.G. Moscow University (1985), pp 252–254
9. Kaloidas V, Papayannakos N (1989) Kinetics of thermal, non-catalytic decomposition of hydrogen sulphide. Chem Eng Sci 44(11):2493–2500
10. Huseynova SA, Mahmudov HM (2010) Photochemical decomposition of hydrogen sulfide/ Institute of radiation problems. Republic conference dedicated to the 60th anniversary of Adil Garibov, Correspondent Member of ANAS, Honoured Scientist. Radiation and environment. 1–2 June 2010, pp 16–17
11. Khriachtchev L, Pettersson M, Isoniemi E, Räsänen M (1998) 193 nm photolysis of H_2S in rare-gas matrices: luminescence spectroscopy of the products. J Chem Phys 108 (14):5747–5754
12. Nunnally T, Gutsol K, Rabinovich A, Fridman A, Starikovsky A, Gutsol A, Potter RW (2009) Dissociation of H2S in non-equilibrium gliding arc "tornado" discharge. Int J Hydrogen Energ 34(18):7618–7625

Chapter 6
Rational Cost-Benefit Analysis for Optimizing Future Energy Resources

Jeremy J. Ramsden

Abstract Securing reliable energy resources is, ultimately, a matter of securing the survival of humanity. In other words, the indefinite prolongation of human activities, all of which require energy, requires sustainable energy resources. The laws of thermodynamics already place some constraints on what is achievable in this respect, but fortunately the Earth is an open system and can afford a certain profligacy. This situation is analysed in this paper to a suffcient level of detail. Nevertheless, such knowledge only gives very general prescriptions for energy policy matters. What is needed is a universal methodology for deciding what resources are affordable. Since the provision of such resources has to compete against other demands, some of which might be less indispensable in the long-term but more urgent, general affordability has to be measured against the actual benefits. The previously developed judgment (J)-value, designed to achieve regulatory consensus on health and safety expenditure, is adapted for this purpose. The purpose of this paper is to introduce the J-value for assessing possible energy supply options.

Keywords Cost-benefit • Optimizing • Energy resources • Reliable • Sustainable • Affordable • Policy matters • Regulatory consensus

6.1 Introduction

There is presently enormous uncertainty about what path, among the many possible ones, to follow in order to achieve an energy-secure future. A good example is provided by the recent debate among members of the University of Cambridge

J.J. Ramsden (✉)
Applied Complexity Research Centre, Collegium Basilea
(Institute of Advanced Study), Ampthill, UK
e-mail: j.ramsden@cantab.net

A. Veziroğlu and M. Tsitskishvili (eds.), *Black Sea Energy Resource Development and Hydrogen Energy Problems*, NATO Science for Peace and Security Series C: Environmental Security, DOI 10.1007/978-94-007-6152-0_6,

concerning the question whether unacceptably vast amounts of land would be required in order to use solar energy to generate electricity and whether the energy used to produce photovoltaic solar cells exceeds their energy output.[1] Clearly, when learned members of the world's leading university dispute even the facts on which the inferences are made, let alone the pathways to those inferences, it can be concluded that the matter is still very unclear and that, in consequence, we lack the basis for making reliable policy decisions. The purpose of this paper is to introduce the use of the judgment (J)-value, previously developed for the purpose of deciding whether expenditure on a safety measure could be justified [1–5], as a general tool for assessing the merits of any new technology.

The J-value analysis is particularly apposite when the objects of the analysis are some human activity subject to regulation. The examples analysed by Thomas et al. include rail traffic, the availability of medicinal drugs, and the control of volatile organic contaminants at petrol stations for motorists [2]. For areas of activity left to their own commercial devices, the J-value analysis might still be useful for internal use by a company seeking to maximize its profitability but cross-industry comparison would appear to have little value since there is no obvious way in which the results could be implemented. In a command economy such as the Soviet Union, it would have been of great utility. Energy is in an interesting hybrid situation. In some countries (e.g., France) energy supply is strictly under state control. In Great Britain the different energy sectors were formerly all nationalized industries (state utilities), on the premiss that they are "natural monopolies" (this did not, however, stop the state gas company from launching expensive advertising campaigns against the state electricity company and vice versa) but today they are privatized and many are in foreign hands. A similar situation prevails in Hungary. In Great Britain, however, government policy is quite interventionist. Thus, the annual road tax for hybrid motor vehicles is about one twentieth the cost for a comparable ordinary vehicle, the installation of photovoltaic cells is heavily subsidized and proprietors can feed surplus electricity into the National Grid at a very favourable price, and so forth. Therefore, at the very least the J-value analysis should be useful to governments to guide them in their interventions.

Section 6.2 of this paper briefly summarizes the energy problem, and the following Sect. 6.3 introduces the J-value. Section 6.4 applies it to the energy problem. Section 6.5 introduces some possible extensions to the J-value concept in order to make it even more powerful. Section 6.6 deals with the following problem: The J-value is designed to produce something akin to a "figure of merit" (e.g., for a proposed safety measure). In other words, are the benefits (valued according to *current* life expectancy and other parameters) greater then the expenditure required *using the present level of technology*? If the J-value is greater than one, the expenditure outweighs the benefits; if it is less than one, it is worth introducing. As, however, especially Kurzweil has emphasized [6], new

[1] As evinced by, for example, the correspondence in the magazine Cam, issue 66 (Easter 2012).

technologies advance exponentially. Therefore a technology that appears unpromising now might acquire merit through technological advance in the future. Hence, a case might still be made for it. Such an early decision can be important where the timescale for full implementation is long. The final Sect. (6.7) states the conclusions, adds some final comments and summarizes the assumptions made.

6.2 The Energy Problem

From a cosmic perspective, the Earth is a very suitable planet for sustaining life as we know it, including human existence. The planet is just the right size (leading to an appropriate gravitational field, with implications for the kind of atmosphere we have and so forth), just the right distance from the Sun, giving the "right" amount of energy daily, the Sun is the "right" kind of star (having a sufficiently stable output to allow life to evolve over many aeons), and so forth; such arguments even reach the assertion that our universe (with its particular choice of fundamental constants) is the "right" one that leads to atoms and condensed matter (cf. the anthropic principle). Be all that as it may, it does not follow that the entire planet is congenial for humanity. It is clearly no accident that civilization began in zones of luxuriant vegetation in which the daily necessities could be procured sufficiently easily to permit mankind to enjoy the leisure needed to develop higher things. Later, the luxuriance turned out to be something of a hindrance and in historical times the greatest powers have been centred in the temperate zones, which have seasons differing more or less markedly in temperature and in which heating is required in the winter. Even on the equator rainfall is seasonal, however, and it was learned that agricultural productivity could be enhanced by managing water supply. While much can be accomplished by human intelligence and muscle alone, such as quarrying and dressing the stones with which to build aqueducts and by excavating reservoirs, and although man is the most intelligent creature on the planet, his capabilities for physical work are relatively puny and by "amplifying" them using power machinery he can enormously increase his control of nature. The Industrial Revolution would have been impossible without abundant energy to power such machinery. All that now contributes to maintaining our civilization (including all that is required for this paper to appear as the typescript before your eyes)—and, unfortunately, a good deal that detracts from it—requires energy. The very fact that we have been able to come together in Batumi to discuss these matters has depended on the consumption of considerable quantities of energy to transport us here from our, in many cases distant, homes.

In other words, energy is absolutely essential for every facet of life as we know it, not only our own life but the lives of other creatures and growing things on which our own depends. Even if these were to be completely substituted by nanofactured sustenance [7], energy would be required (for the nanofacture).

In the past, what kind of energy to use has been principally determined by economic considerations.[2] More recently, the impacts of different kinds of energy on climate change have become a major preoccupation and it is generally accepted that this aspect must also be taken into consideration. This makes what is already a complex problem even more complex [8]. Hitherto, global energy supply solutions have been proposed essentially by looking at a great variety of statistical data and making sensible deductions therefrom [8]. What the present paper is now proposing is that the optimality of energy supply solution can be computed in a straightforward fashion.

6.3 The J-Value

The J-value (J) is the ratio of the actual cost of a safety measure to the maximum reasonable cost [1], which will be elaborated upon below. Hence, if (for example) $J = 3$, three times as much is being spent as is necessary (i.e., there is a net disbenefits). On the other hand, $J = 1/3$ indicates that the measure is excellent value for money: up to three times more could be spent on it was still retaining a net benefit. Generally speaking, the actual expenditure $\hat{a}$ on a measure should be straightforwardly available. The main challenge is to determine the maximum reasonable cost.

A human being is a living creature. The ultimate aim of any living creature is survival (in the language of cybernetics, the creature must ensure that its essential variables are in the ranges corresponding to the living state). The ultimate merit of any proposed action can, therefore, be judged according to its impact on survival. If a proposed action requiring expenditure shortens human lifespan, the J-value will necessarily be negative and, therefore, can be rejected without further computations. Most actions are only proposed on the ultimate basis that they will prolong lifespan.

One can take as an example a measure to prevent leakage of radioactive waste from a nuclear power station into the sea [2, 3]. Expenditure is required to design and construct the antileakage works. The prolongation of life can be assessed on the basis of the avoidance of certain cancers that exposure to the radioactive waste induces. Epidemiological data can be used to determine the number of cancers that are thereby avoided, and combined with similar data establishing the mortality rate in order to end up with the number of premature deaths that are avoided through the introduction of the safety measure.

It only remains to put a value on the human life that is thereby prolonged. This is a well documented actuarial problem (e.g., [9, 10]). Rather than using a fixed value, however, the formula Thomas et al. propose [1] makes use of the *life-quality index* Q, defined as:

[2] Of course, apart from relatively insignificant amounts of geothermal energy, the ultimate source of all available energy is the Sun.

$$Q = G^q X_d \tag{6.1}$$

where G is mean *annual* income of the group of people being considered (which might be an entire nation or, indeed, the whole world), q is a function of the fraction of time w spent working ("work—life balance"):

$$q = w/(1 - w) \tag{6.2}$$

and X_d is the discounted life expectancy of the group. This function has indeed the anticipated properties that quality of life increases with increasing annual income and with increasing life expectancy.[3] Safety measures have to be paid for out of income G, resulting in a decrease $-\Delta G$, but in return (discounted) life expectancy increases by an amount ΔX_d, and the life quality index changes to a new value $Q + \Delta Q$. Expanding Eq. (6.1) and neglecting higher powers and cross product terms (since ΔG and ΔX_d can be assumed to be small) we obtain after rearrangement [1]:

$$\frac{\Delta Q}{Q} = q\frac{\Delta G}{G} + \frac{\Delta X_d}{X_d} \tag{6.3}$$

the right-hand side of which must be equal to or greater than zero in order for there to be a net benefit, implying that:

$$-\Delta G \leq \frac{G}{q}\frac{\Delta X_d}{X_d} \tag{6.4}$$

the total cost of the measure is then $X_d \Delta G$. The annual cost a for a population of size N is $-N\Delta G$, the minus sign signifying the loss of income. Using Eq. (6.4) to eliminate ΔG, we obtain

$$a = \frac{NG}{q}\frac{\Delta X_d}{X_d} \tag{6.5}$$

which is our measure of "maximum reasonable cost". Recalling our original statement of the definition of the J-value,

$$J = \hat{a}/a \tag{6.6}$$

which expands to

$$J = \frac{\hat{a} q X_d}{NG\Delta X_d} \tag{6.7}$$

[3] The literature suggests w ≈ 1/8, implying q ≈ 0.14. Thomas et al. [1] found their results to be insensitive over $0.12 \leq q \leq 0.2$.

Two trade-offs are implicit in the J-value analysis [4, 5]. The first is a trade-off between the (future) free time fraction (work/life balance) and income. One can work more and have more income, or sacrifice income in favour of more leisure time.[4]

Note that the J-value approach uses averages and considers an entire country or supranational entity or indeed the whole world. It does not—at its present level of approximation—consider on which specific sectors the costs fall or on which specific sectors the benefits accrue. National solidarity is assumed even when the costs or benefits are not universal. There is nothing in the principle of the approach to prevent a more detailed consideration of reality, however. Whether to do this is essentially a political decision.[5]

6.4 Application of the J-Value Concept to the Energy Problem

What we need to do is determine the cost of each different kind of energy supply (which affects G) and its effects on life expectancy X. One could take a "blank slate" approach, in which all conceivable options are in principle available, or one can start with the actual situation. The latter is much more realistic, of course, except for a country on the threshold of development. Starting with the actual situation suggests that one should also include the minimalist position of doing nothing (i.e., maintaining the status quo or "business as usual") as a possible energy option, as well as passively diminishing energy use by improving building insulation and the efficiency of motors, and actively diminishing it by "cutting out extravagance" [11]. In this spirit, Table 6.1 sketches out input for computing and comparing J-values for the various energy options presently under consideration.

Here we make some comments on the reasoning behind the entries in Table 6.1. Option 0 is not completely feasible because of appreciable popular resistance based on perceptions of unacceptable global warming. Its feasibility is also affected by possible finiteness of global hydrocarbon reserves.[6] Option 1 refers to the exploitation of oil shale, tar sands etc. Option 2 presumes that construction is feasible on shallow

[4] The definition of "work" is, therefore, any activity which generates income but which is not intrinsically enjoyable. A substantial fraction of the population is, however, are engaged in activities that they find enjoyable, but for which they are also remunerated. Nevertheless, if such activities take place under some kind of involuntary constraint (such as an obligation to be present in a certain place for a certain interval each day), they can still be reckoned as "work" for the purposes of the J-value calculation.

[5] Cf. a policy of compulsory medical insurance that, in effect, gets healthy members of the population to pay for their weaker brethren; and in most developed countries everyone contributes to the costs of state education through taxation, even families without children.

[6] Burning hydrocarbons releases carbon dioxide into the atmosphere. This is refixed, mostly as carbohydrates, via photosynthesis. The timescales for generating fuel hydrocarbons are generally considered to be too long for oil and natural gas to be considered as renewable resources.

Table 6.1 Input for J-value calculation

No	Option	$\mathscr{F}$[a]	Cost (direct)[b]	Cost (indirect)[c]	Benefit[d]	J[e]
0	Business as usual	8	Low	Low	Low	~1
1	Novel gas and other hydrocarbons	6	High	High	High	>1
2	Offshore wind turbines	6	High	Low	Moderate	~1
3	Onshore wind turbines	8	High	High	Moderate	>1
4	Nuclear fission	8	High	High	High	>1
5	Nuclear fusion	1	High	Low	High	<1
6	Photovoltaic cells	6	High	Low	High	<1
7	Solar-powered turbines	10	Moderate	Low	High	$\ll$1
8	Plants	10	Low	Low	Moderate	~1
9	Improving efficiency	10	Moderate	Moderate	Moderate	~1
10	Cutting out extravagance (CoE)	5	Zero	Zero	High	$\ll$1

[a]Estimate of feasibility on a scale of 0 (reckoned to be completely unfeasible) to 10 (technically feasible and could easily be implemented)
[b]Manufacturing and running costs
[c]Includes land requirements, possible health effects, etc
[d]Assessed in terms of how readily the energy produced is available
[e]Indicative estimate of the J-value based on cost/benefit

continental shelves and that amenity loss is low. It is, however, questionable whether manufacturing resources will be sufficient to produce as many turbines as will be required to make an appreciable contribution to energy supply requirements. Although onshore wind turbines (option 3) are easier to construct they are unpopular because of amenity loss. The high indirect costs of nuclear fission (option 4) are mainly due to the problem of disposing of radioactive waste. It must also be kept in mind that uranium (the main fuel) is definitely a finite resource. Nuclear fusion (option 5) is attractive but technically extremely difficult. The technology of photovoltaic cells (option 6) is advancing rapidly and provides a way to make use of otherwise barren desert land. Much hope is presently placed on organic polymer-based photovoltaic cells, which should be much cheaper, with respect to both material and manufacturing costs, than the present silicon-based cells. Their lifetime may, however, be appreciably shorter than that of silicon-based cells, in which case they will need to be frequently renewed. Since the polymers are made from the same hydrocarbon feedstock (oil) as it used to the fuel that the output of the cells is supposed to replace, the relative benefit compared with option 0 is doubtful, although it may be possible to recycle the polymers.

Solar-powered turbines (option 7) represent a well established technology, initially developed prior to the First World War in Egypt, but discontinued due to competition from cheap oil. They represent the most attractive technological solution at the present time. The use of plants (for example, maize stalks) epitomizes renewable energy but the energy density is too low to allow widespread application of option 8, hence its benefit can only be moderate. Besides, crops grown exclusively for use as energy sources ("biofuels") use land that could otherwise be used for food production. Option 9 is attractive because of the

Table 6.2 Costs and impacts on life expectancy for the different energy options

No	Option	R&D	Capital	Running costs	Life expectancy impact
0	Business as usual	None	Infrastructure needs periodical renewal	Fuel supplies need to be mined	Shortened—pollution
1	Novel hydrocarbons	Optimization required	High	Fairly high	Env. degradation
2	Offshore wind turbines	Basic technology developed	Expensive	Almost zero	Minimal
3	Onshore wind turbines	Basic technology developed	Expensive	Almost zero	Low?
4	Nuclear fission	High level of experience	Expensive	Fuel mining, waste disposal	Small risk from endemic leakage and from infrequent catastrophes
5	Nuclear fusion	Still extremely high despite 60 years of effort worldwide	Likely to be very expensive	Fuel continuously required but maybe cheap (e.g., D_2O from sea)	May be minimal
6	Photovoltaic cells	Still intensive	High but falling rapidly	Low	Minimal; occupational hazards of manf?
7	Solar-powered turbines	Mature	Moderate	Low	Minimal
8	Plants	More could be done	Low if land not considered	Considerable processing required	May be positive[a]
9	Improving efficiency	Incremental engineering	Could be high[b]	Lower than predecessors	Probably positive
10	CoE	Zero[c]	Zero	Diminished by definition	Highly positive[d]

[a]For example, if plants effective in eliminating pollution ("green filters") are chosen [12]
[b]Many of the objects of efficiency improvements, e.g., railway locomotives, have long intervals of service; one normally waits for the old ones to wear out, which may take decades, before replacing them
[c]A great deal of research is needed on the problem of how to persuade people to do it
[d]Many people currently develop health problems due to a too sedentary lifestyle or overeating expensive foods, in both cases due to indulgence in extravagance

economic argument—after capital costs have been amortized money is saved. The technical challenges are typically of incremental kind and, hence, it can be considered to be perfectly feasible. In contrast, although the economic arguments in favour of cutting out extravagance are even stronger, there is considerable

psychological resistance against it. In the private sector people are anxious about the possible loss of comfort and convenience or are simply so wedded to a life of material extravagance that they would be extremely reluctant to take the initiative in making cuts. In the public sector venality plays an important role—officials do not wish to forego the perquisites attached to placing contracts for public works with the private sector.

As a next step in sophistication we examine the various costs associated with each option, subdivided into research and development (R& D), capital (construction) and running, and the impacts on life expectancy (Table 6.2).

6.5 Extensions to the J-Value

In its current form the J-value calculation (§3) only looks at overall life expectancy; the actual state of well-being is ignored. Only 11 % of males and a negligible percentage of females maintain good health until death.[7] For the majority, decline sets in for the last two decades of life. For 19 % of males and 12 % of females, decline sets in even earlier and the last two decades of life might be spent on the margins of humanity. Far from being able to enjoy leisure, those two decades are likely to be spent in an institution providing continuous quasimedical care, which has to be paid for. This reality needs to be reflected in the J-value calculation.

6.6 The Exponential Growth of Knowledge

The estimates of technical feasibility in Table 6.1 and, indeed, the very inclusion of the items listed, depends on present-day technology tempered by an assessment of its likely development. In the case of exponentially advancing technology assessment is quite difficult because the individual steps that overall contribute to the exponential advance cannot be predicted, since they often depend on the individual ingenuity of a single inventor. If one simply works by analogy and applies Moore's law-like reasoning to the cost of photovoltaic cells, one is led to the conclusion that they will soon become overwhelmingly advantageous on a purely economic basis. The semiconductor industry, however, to which Moore's law applies, possesses an exceptionally comprehensive roadmap, covering technical developments up to 2025 [13]. No comparable roadmap exists for the solar photovoltaic cell industry.

Furthermore, some commentators believe that worldwide innovation is in decline [14–16], calling into question the assumption of continuing exponential growth. If so, a premium would be placed on the more conservative options (7, 8, 9 and 10 in the Tables), because anything requiring significant novelty, especially

[7] Watanabe, S. et al., unpublished report, p. 13, Figs. 2.4 and 2.5 (2012).

option 4, might become insuperably difficult. One possible explanation for innovation decline is that we are reaching the end of the information technology era; in this worldview all technology-driven eras start with exponential growth, which then flattens off and comes to a halt while the next one starts on its exponential course. There is a quite widely held view that we presently stand on the threshold of a new technology revolution, that of nanotechnology [17], which will re-establish exponential growth. There are certainly grounds for cautious optimism in this regard (Kurzweil relies heavily on nanotechnology to fuel his optimism for future technology growth, for example [6]).

6.7 Conclusions

If innovation continues to grow exponentially, it would be prudent to favour the technology solution with the lowest J-value regardless of apparent technical difficulty. If it does not, the converse is true. The solution requiring no technological innovation at all is cutting out extravagance, which is also likely to have the biggest favourable impact on life expectancy. Since most of the energy options only have a generic impact on life expectancy, a more detailed investigation, looking at wellbeing, will likely be useful in order to differentiate between the options.

References

1. Thomas PJ, Stupples DW, Alghaffar MA (2006) The extent of regulatory consensus on health and safety expenditure. Part 1. Development of the J-value technique and evaluation of the regulators' recommendations. Trans IChemE Part B (Process Saf Environ Prot) 84:329–336
2. Thomas PJ, Stupples DW, Alghaffar MA (2006) The extent of regulatory consensus on health and safety expenditure. Part 2. Applying the J-value technique to case studies across industries. Trans IChemE Part B (Process Saf Environ Prot) 84:337–343
3. Thomas PJ, Stupples DW, Alghaffar MA (2006) The life extension achieved by eliminating a prolonged radiation exposure. Trans IChemE Part B (Process Saf Environ Prot) 84:344–354
4. Thomas PJ, Kearns JO, Jones RD (2010) The trade-offs embodied in J-value safety analysis. Process Saf Environ Prot 88:147–167
5. Thomas P, Jones R, Kearns J (2010) J-value safety assessment: the two trade-offs. Meas Contr 43:142–145
6. Kurzweil R (2006) Nanotechnology dangers and defenses. Nanotechnol Percept 2:7–13, and references therein
7. Freitas RA Jr (2006) Economic impact of the personal nanofactory. Nanotechnol Percept 2:111–126
8. Maltini F (2008) Climate change and the complexity of the energy global security supply solutions: the global energy [r]evolution. In: Ramsden JJ, Kervalishvili PJ (eds) Complexity and security. IOS Press, Amsterdam, pp 185–217
9. de Blaeij A, Floraz RJGM, Rietved P, Verhoef E (2003) The value of statistical life in road safety: a meta-analysis. Accid Anal Prev 35:973–986

10. Miller TR (2000) Variations between countries in values of statistical life. J Transp Econ Policy 34:169–188
11. Ramsden JJ, Kervalishvili PJ (eds) (2008) Complexity and security. IOS Press, Amsterdam
12. Kvesitadze G, Khatisashvili G, Sadunishvili T, Ramsden JJ (2006) Biochemical mechanisms of detoxification in higher plants: the basis of phytoremediation. Springer, Heidelberg
13. International Technology Roadmap for Semiconductors (2009)
14. Huebner J (2005) A possible declining trend for worldwide innovation. Technol Forecast Soc Change 72:980–986
15. Stephenson N (2011) Innovation starvation. World Policy J 28:11–16
16. Ramsden JJ, Feeding man's capacity to innovate (In preparation)
17. Ramsden JJ (2011) Nanotechnology: an introduction. Elsevier, Amsterdam

Chapter 7
Novel Fuels and Materials for Nuclear Energy Generation Technologies

Paata Kervalishvili

Abstract Existing energy generations technologies both electrical and thermal based on the burning of natural energy carriers are dangerous for biosphere of our planet. It became obvious that the further intensive development of modern energetic and transport leads to large-scale ecological crisis.

During last decade attention of worldwide frontier research and technology together with hydropower wind, photovoltaic, earth thermal water, etc. energy generation systems is focusing on the novel nuclear energy production technologies based on the last scientific and engineering achievements. Nuclear power is the principal carbon-free source of electricity, and therefore plays a key role in limiting greenhouse gas emissions. Improving scientific and technical knowledge and competences in the areas of safety, sustainability, security, reliability and cost effectiveness of novel nuclear fuel and materials are one of the main tasks of world science and technology community. The paper represents the analysis of existing level of nuclear materials development. The primary task in this research area is to coordinate the development of concepts and processes that can address the key outstanding issues in elaboration of novel effective technologies for novel technologies of nuclear energy preparation. It is shown that performed theoretical, physica-technical and technological research works clearly indicate the prospects of using new materials, devices and designing schemes for creation of highly effective energy generating technologies also applicable for hydrogen based energy production.

Keywords Energy • Generation • Fuel • Nuclear • Hydrogen • Fission • Fusion • Safety

P. Kervalishvili
Georgian Technical University, Tbilisi 0175, Georgia
e-mail: kerval@global-erty.net

A. Veziroğlu and M. Tsitskishvili (eds.), *Black Sea Energy Resource Development and Hydrogen Energy Problems*, NATO Science for Peace and Security Series C: Environmental Security, DOI 10.1007/978-94-007-6152-0_7,

7.1 Introduction

Current forecasts indicate that the primary energy consumption worldwide by 2050 will probably will doubled in comparison with the year 2000. Energy security is becoming a major global concern. Fossil fuel reserves, particularly for crude oil, are confined to a few areas of the world. Political, economical, and ecological factors often force volatile and high fuel prices [1]. Simultaneously, to combat climate change, a global environmental policy which includes a major reduction in greenhouse gas emissions is required. One of the statements presented in Brundtland Report [2] is underlining: Sustainable development is development that meets the needs of the present without compromising the ability of future generations to meet their own needs. Now it is obvious that nuclear energy both nuclear fission and fusion is a key element for future environment friendly energy generation technologies creation. Nuclear fusion – a very prospective energy generation technology requires the wide research works until it will be consider for transferring to energy production industrial facilities (Fig 7.1).

Nuclear fission energy nowadays can deliver safe, sustainable, competitive and practically carbon-free energy to citizens and industry. It is based on short-, medium- and long-term development of nuclear fission energy technologies, with the aim of achieving a sustainable production of nuclear energy, a significant progress in economic performance, and a continuous improvement of safety levels as well as resistance to proliferation

Following challenges are taking into consideration and performance: Perspective of an important development of nuclear energy in the world relying on III generation of light water reactors; The development of generation IV fast neutron reactors with closed fuel cycle; Elaboration of combined Nuclear – Hydrogen energy generation technologies; elaboration of effective and workable nuclear fusion technologies and reliable ideas of proton based nuclear technologies.

The main problems of nuclear energy generation technologies and facilities are:

- Safety – Necessity of confinement of nuclear radiation substances for prevention from going in to the public's irradiated;
- Waste – Radioactive waste has a very long half-life which compared with whole life history on the Earth. Radioactive wastes will be generated during nuclear energy preparation cycle, and it will be existed over a long period after withdrawal from nuclear energy. The radioactive wastes increase in proportion to the cumulative operation time of nuclear reactor. Therefore this is the difficult problem always accompanying nuclear energy usage;
- Nuclear Proliferation – The problem of civil using of nuclear energy is its similarity with materials and technologies for nuclear weapons preparation. Proliferation problem will not disappear when nuclear reactor stops the operation. It should be controlled to avoid production of nuclear weapons on the basis of developed skills, technologies and materials. The expansion of nuclear power must maintain the highest standards of nuclear safety, security, and nonproliferation.

Fig. 7.1 The vision for future nuclear energy Renaissance and long-term sustainability of nuclear energy: *R* recycling, *T* transmutation, *U* uranium, *Pu*-plutonium, *MA* minor actinides, *DEU* depleted uranium, *FP* fission products (*see color plates*)

There are some key factors to successful construction and operation of nuclear power facilities: Economic competitiveness and financing; Public acceptance; Nuclear fuel (Uranium, etc.) resources; Safety and reliability; Fuel and waste management; Human and industrial resources; Proliferation risk and security; Infrastructures, especially in new nuclear club member countries [3].

In the last years also were elaborated the 19 issues for consideration in each phase of nuclear power development: National position; Legal framework; Regulatory framework; Radiation protection; Financing; Human resource development; Safeguards; Security and physical protection; Emergency planning; Nuclear fuel cycle; Nuclear waste; Environmental protection; Nuclear safety; Sites and supporting facilities; Stakeholder involvement; Electrical grid Management; Industrial involvement; Procurement.

The very important issue for nuclear energy farther development is Social Acceptance which is based on four principle conditions that it takes for co-evolution of science technology and society. (a) Science and technology have formed a healthy evolutionary system; (b) The values of bodies that play a role in science and technology are reflected in the values of modern society; (c) The values created by science and technology are appropriately examined by society, which recognizes them properly; (d) Society has a certain amount of confidence in science and technology, and groups involved with it.

7.2 Nuclear Energy Generation Systems Innovative Development

During last two decades it was established the concept of nuclear power development in the twenty first century, which includes the following stages:

- Near-term (10–20 years):

Evolutionary development of reactor and fuel cycle technologies (light water nuclear reactor – LWR, aqueous reprocessing); development and trial operation of advanced and innovative reactor and fuel cycle technologies (fast reactors, small reactors, dry reprocessing).

- Middle-term (30–40 years):
  Fast growth of nuclear power; demonstration and introduction of innovative technologies; high- temperature reactors; small reactor facilities; hydrogen production and water desalination.
- Long-term (50–100 years):
  Large-scale deployment of the innovative technologies of naturally safe fast reactors and fuel cycle; fuel breeding; closed U-Pl and Th-U cycles; use of valuable isotopes and burning of hazardous nuclides; long-term geological isolation of radioactive waste [4].

For nuclear power systems today we are considering the three fuel cycle alternatives:

- Traditional thermal reactors with an "open" fuel cycle in which fuel is removed from reactors and sent to a disposal site;
- Thermal reactors with a "closed" fuel cycle (France, Russia, Japan) in which plutonium is extracted from the spent fuel and then re-used to fabricate once-through mixed uranium – plutonium oxide (MOX) fuel;
- A two-component system incorporating thermal reactors with an "open" fuel cycle and a properly balanced number of fast reactors burning actinides separated from the spent fuel of thermal reactors. The fast reactors, fuel reprocessing and fabrication facilities should be placed together in safe nuclear "parks".

Following all above mentioned last decades became possible to introduce the new generations of nuclear reactors and relevant nuclear generation facilities: Third generation of nuclear plants meets modern safety and environmental standards and requirements and resolve the current energy problems, but still far from being perfect as regards economics, fuel supply and proliferation resistance; Fourth generation of nuclear plants – new reactors and fuel cycle technologies ensure gradual transfer to safe and competitive heat and electricity generation with unlimited fuel resources relying on inherent production of fissile isotopes.

For current light water nuclear reactors, the spent fuel can be recycled at least once into mixed oxide fuel. This one must be stored, in order to recover the plutonium to be used for a future generation of fast reactors-breeders which can effectively burn this plutonium in a multirecycling uranium-plutonium strategy. Basically, 50 years of operation of one LWR will produce the stock of plutonium needed to start a fast reactor – which could thus form a sustainable source of energy for thousands of years through the use of depleted uranium [5]. The next stage is related to the recycling of minor actinides to reduce the thermal load, the volume and the needed isolation time of the remaining waste requiring geological disposal. Recent R&D results have shown that minor actinides can be separated from spent fuel, thus opening the way for their burning in a fast-neutron system, thereby using their energetic potential, as well as eliminating them as long-lived radioactive material.

Beyond the use of nuclear power for electricity generation, new applications are being developed, based on generation-III or -IV reactor features, in particular through the coupling of (very)-high-temperature reactors with chemical processing plants (BN 350 nuclear reactor based Mangishlack power plant, Kazakhstan). An international conference [6] organized some years ago by the IAEA (International Atomic Energy Agency), in cooperation with the OECD/NEA (Nuclear Energy Agency) and the International Desalination Association, has provided a broad survey of non-electric applications of nuclear energy. These include: processes for producing alternative energy carriers replacing for example the use of oil for transport, including hydrogen and bio-fuel production; processes that require heat and/or electricity, such as desalination.

Generation-III reactors, such as the EPR (European Pressurized-water Reactor), are evolutionary reactors derived from the experience of operating LWRs and developed to optimize their safety and economic performance. These new reactors are designed to be operated for 60 years. In the longer term, generation-IV systems will take over once they have reached technical maturity and met sustainable development criteria, particularly those pertaining to waste management and preservation of energy resources.

In European Union countries, a total of 152 Generation-II light-water reactors are in operation. The average age of these power plants is approaching 25 years for a typical initial design life of 30–40 years.

To meet the growing concerns about security of energy supply and CO_2-emission reductions before LWRs of generation III can be built and operated, a first priority is given to lifetime extension of generation-II LWRs. While maintaining a high degree of operational safety, the already well-proven economic competitiveness of nuclear energy can be further enhanced by research focused on improved availability, fuel performance and safety.

With the European Pressurized-water Reactor (EPR) in Olkiluoto, Finland was the first country in Europe to launch the construction of a new nuclear power plant (NPP) for more than a decade. It was followed by France with the decision to build another EPR plant in Flamanville.

Nuclear market renaissance with the construction of a large number of NPPs will necessarily rely on generation-III LWRs, which offer enhanced safety and reliability and the best available technologies for a responsible management of spent nuclear fuel.

Spent fuel treatment and recycling of uranium and plutonium are already an industrial reality in some countries, such as France, Japan and Russia [7].

The future of nuclear power is trusted now to fast reactors and closed fuel cycle. This implies reprocessing of the spent fuel of nuclear plants and re-use of plutonium produced in power reactors, which may raise the energy potential of nuclear fuel resources ~100 times. Owing to their unique neutronics, fast reactors are capable of burning the most long-lived nuclear wastes.

Fast reactors have been chosen as the baseline in the Strategy of Nuclear Power Development in the First Half of the twenty first Century, and as a promising energy technology in the international programme Generation IV [8]. Spent fuel treatment

Fig. 7.2 Phénix sodium-cooled fast-neutron reactor in Marcoule (France) (*see color plates*)

and multi-recycling is the basis on which future generation-IV reactors will achieve sustainability. Fast neutron reactors with a closed fuel cycle allow: significantly improved usage of natural resources, minimization of volume and heat load of high-level waste.

This option has been selected by several countries, such as Japan (with JSFR, Japan Sodium-cooled Fast Reactor), Russia (with the BN 600 in operation and the BN 800 and BREST 300 reactors), India (with the PBFR prototype), China (with CEFR – China Experimental Fast Reactor) and the United States (with the advanced recycling reactor project). This option was also selected in Europe (with Phénix, PFR, KNKII, and Superphénix). France launched a project to construct a sodium-cooled fast reactor (SFR) prototype by 2020, open to industrial and international partnerships. This could be considered as the first step towards a renewed European initiative. Among the fast reactor systems, the sodium-cooled fast reactor currently has the most comprehensive technological basis, thanks to the experience gained internationally from operating experimental, prototype and commercialized reactors such as the Phénix plant in France, PFR in the UK, and MONJU in Japan (Fig. 7.2).

The technological knowledge gained from these reactors includes key elements of the overall reactor design, fuel types, safety, and fuel recycling. Innovations are sought for a generation-IV sodium-cooled fast reactor in order to reduce costs and to further improve safety. They involve design simplification, improvement of in-service inspection and repair, fuel handling, high-performance materials, and practical exclusion of high-energy release in case of a hypothetical severe accident [9].

Given the maturity of sodium-cooled fast reactors, the next facility to be built in Europe will be a prototype reactor with a power-conversion system of 250–600 MW to demonstrate innovations with respect to existing SFRs and to pave the way for a first-of-a-kind generation-IV commercial reactor.

To face the major worldwide challenges described above, generation-IV fast reactors have to offer a choice of technologies so as to limit the overall technological

risk and be able to satisfy various markets and degrees of public acceptance. While the SFR remains the reference technology, two alternative technologies for fast reactors, namely the gas-cooled fast reactor (GFR) and the lead-cooled fast reactor (LFR) are also elaborating. After selection of an alternative technology, an experimental reactor in the range of 50–100 MW will be needed to gain experience feedback by 2020 on this innovative technology.

Among the attractive features of the GFR, which is a high temperature reactor, the chemically inert and optically transparent coolant (helium) should be mentioned as well as the potential for producing hydrogen, synthetic hydrocarbon fuels and process heat. The most important challenges for this type of reactor are the development of materials resistant to the combined effects of high temperature and high neutron flux (refractory and dense fuel, thermal barrier) and the safety systems.

The LFR is identified as another potentially promising alternative fast-reactor type. Russia has gathered experience in building and operating small lead-alloy-cooled reactors in the 100 MWth range for naval propulsion. The pure lead-cooled LFR system offers the same advantages as the lead-alloy cooled reactors of operating primary systems at atmospheric pressure. As a power reactor, it also offers the potential of being competitive with present-generation LWRs in electricity generation, provided that the designers succeed in simplifying the primary system and eliminating the intermediate cooling system. Current R&D addresses some critical issues associated with using lead as a coolant for reactors in the power range of 1 GWe, such as weight and corrosion. In-service inspection, maintenance and repair remain also a common challenge for both liquid-metal coolants, sodium and lead.

In association with the development of a robust fast-reactor system, a flexible separation and treatment strategy needs to be assessed, aiming towards a closed fuel cycle which better uses the fertile resources by a multi-recycling of uranium and plutonium. This strategy includes the development of actinide chemistry, separation technology and minor actinide bearing fuels with reactor irradiation of such fuel. Such a coherent long-term strategy would allow the transition from the currently practiced mono-recycling of plutonium in light-water reactors (LWRs) to multi-recycling in generation-IV reactors.

Beyond this goal, recycling is also the cornerstone of a strategy for partitioning and transmutation of minor actinides, which would substantially reduce the radioactivity and heat load of the remaining high-level waste. As a result, the isolation time and repository space required in deep geological disposal would also be reduced.

For the incineration of minor actinides, the opportunities offered by accelerator-driven systems (ADS) will be compared to those of fast-neutron critical reactors on a technological and economic basis.

The design of nuclear systems relies on the “defence in depth” principle. It consists in the prevention of accidents and the mitigation of their consequences, and the protection of workers and populations against radiological hazards through the use of multiple barriers and safety systems. For the more recent reactor systems such as generation-III reactors, even extremely improbable accidents are taken into account.

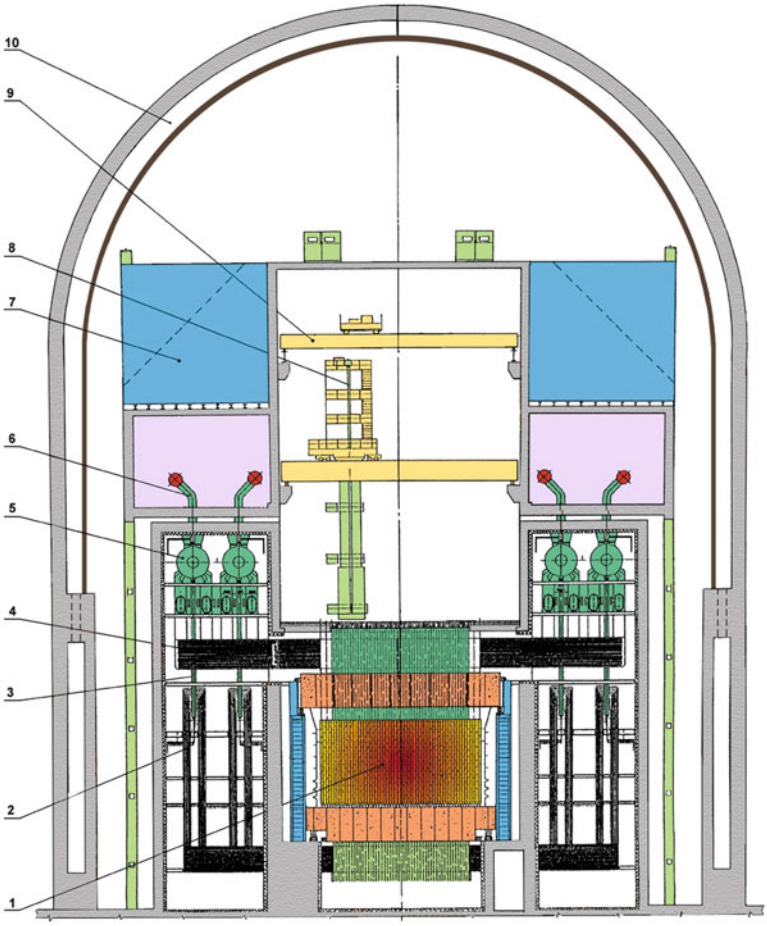

Fig. 7.3 Pressure-Tube power reactor: *1* reactor core, *2* water lines, *3* downcomer, *4* steam-water lines, *5* steam separator, *6* steam line, *7* passive cooling system tank, *8* refuelling machine, *9* bridge crane, *10* containment (*see color plates*)

For example, the European Pressurized-water Reactor (EPR) was designed so that in the very unlikely event of a severe accident, radiological consequences would necessitate only very limited protective countermeasures in a relatively small area and for a limited time for the surrounding population.

The safety analysis of nuclear systems relies on a thorough understanding of the behaviour of the system in normal and accidental conditions, and increasingly on the use of advanced numerical simulation software and its validation through experimental programs. For future reactors design, simplified tools can be developed and applied at first to carry out preliminary analyses of concepts and safety options. Once the design is known, more advanced safety evaluation software tools can be developed and applied. In order to contribute to the harmonization of safety practices in Europe and to better compare the safety aspects of the different reactor systems, the development of common tools and methodologies is favored.

During last decades the nuclear reactors of different novel design were development [10, 11]. And among them it is necessary to underline:

- Simplified vessel-type boiling reactors with natural circulation of coolant;
- Advanced pressure-tube reactors with inherent safety features;
- Pressure-tube reactors with supercritical coolant parameters;
- Transportable nuclear power plants for heat and electricity supply in the far-away and difficult-of-access regions;
- Sodium – cooled loop-type fast reactor;
- Naturally safe fast reactors with heavy liquid metal coolant;
- Small-power reactors.

The novel nuclear reactors have their own advantages which meet the relevant requirements of sustainability and safety. For instant in the pressure-tube power reactors refueling can be done by a refueling machine both off-load and on-load, without power reduction (Fig. 7.3).

The nuclear reactor for small power plant includes: Three interconnected hydraulic circuits, the last of which houses all heating loads (turbo generator set, district heating or process steam boilers) (Fig. 7.4).

The very important safety features has a new designed nuclear reactor −1,200 MWt NPR:

- High-boiling radiation-resistant low-activated lead coolant which does not react with water and air and hence affords low-pressure heat removal while excluding the possibility of fire, chemical and thermal explosions;
- High-density highly heat-conductive mononitride fuel operating at low temperatures (Tmax $<$ 1,150 K, with Tmelt $=$ 3,100 K), which limits the radiation swelling (~1 % per 1 % burnup) and fission gas release under the cladding;
- Core and lead reflector design, the composition and geometry of which affords fuel breeding, provides small and negative power, temperature and void effects of reactivity;
- Small reactivity inventory in the core ($\Delta k/k < \beta eff$) which rules out uncontrollable prompt criticality excursion in the event of inadvertent withdrawal of all control rods in any reactor condition.

Owing to this, it proved possible to abandon some engineered safety features which made this reactor significantly cheaper than other fast reactors recently developed.

7.3 Safety Research for Nuclear Systems

Public acceptance is also an important issue for development of nuclear energy. Therefore research in the field of nuclear installation safety, protection of workers and population against radiation, management of all types of waste is one of the first tasks taking into consideration.

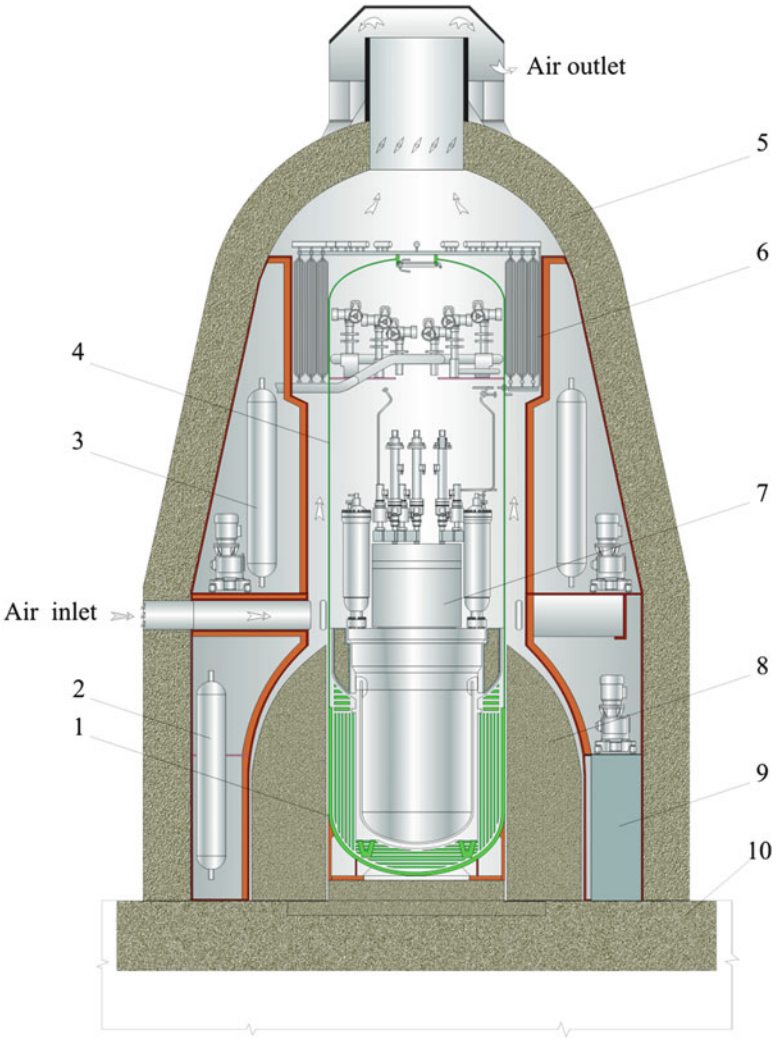

Fig. 7.4 Small power plant. *1* iron-water shielding tank, *2* gaseous waste storage tanks, *3* liquid poison supply system, *4* containment, *5* shock-proof shell, *6* heat exchanger of the cooling system, *7* steam generating unit, *8* biological shielding blocks, *9* liquid and solid radwaste storage facility, *10* foundation (*see color plates*)

One of the main parts for solution of problem of technological safety of nuclear power installations is creation of relevant control system for nuclear reactors of different design [12].

The safety of nuclear reactors operating in prolonged life time conditions in many respects depends on the reliability of control and safety systems (CSS). In this regard, the role of the base of the nuclear reactors' CSS rods – neutron-absorbing

elements (NAE) is being increased more and more, as well as their quality characteristics, which meet new, strict requirements [13].

The more hard operating needs are to be satisfied by rods of CSS for nuclear reactors on fast neutrons, the capacity of which directly depends on CSS [14].

For the practical applications to control systems in nuclear reactors far from all these elements fit this task.

Among neutron absorbing elements the most preferable are based on the isotope B-10 absorbers in terms of efficiency in neutrons' intermediate and fast power spectra. They are distinguished by an optimal absorbing capability and heat-physical and physical-mechanical characteristics from the standpoint of their usability as NAE [15].

The importance of the utilization of boron – containing NAE as well of based on NAE rods of CSS for intermediate and fast neutron power reactors causes a great interest in the technologies of rods' fabrication and investigation of their properties.

Many monographs, articles and inventions are dedicated to nuclear power stations management and control facilities based on boron containing CSS. Alongside with that, it is necessary to be mentioned that at present many issues linked with the principles of technologies for their production as well as with the physics of relevant processes still are to be clarified.

The experience gained since 1970s in the USSR, USA, France and other countries has shown that the development of highly effective CSS requires the realization of complex investigations in the fields of thermo physics and technology, as well as of radiation influence and reactor technology.

Of a highest significance is the definition of materials and mechanical structures for the utilization of different nuclear reactors, as well as the improvement of existing technologies for obtaining items with desired properties (structure, density of the thermal flows, thermo-physical properties). At present, it is well known that the initial properties (phase composition, structure, heat-physical characteristics, etc.) of neutron-absorbing materials and items on their base have a governing influence on the effectiveness of fast reactors' CSS different rods and NAEs.

There was studied the corrosion resistance of items made from B_4C in sodium and its compatibility with stainless steel (NAEs housings' material). It was found out that the boron carbide and stainless steel components actively do not form chemical compounds with the pure sodium below temperature around 950 °C. At the same time, it was shown that the interaction takes place by the materials solving in a liquid metal with their consequent sedimentation upon the stainless steel surface and by diffusion through this surface. As a result, there is observed the boronizing and carbonization of NAEs housings' materials with all subsequent consequences. On the base of computation analysis it also must be mentioned that the corrosive resistance in sodium is strongly influenced by oxygen impurities in the liquid-metallic heat-carrier that rather negatively affects the operational stability of NAEs and CSS rods in total. The behavior and durability of boron-containing elements in high parameters water (increased temperature and impurities concentration) also strongly depend on initial properties of reacting materials, temperatures and time parameters of their operation. In total, the

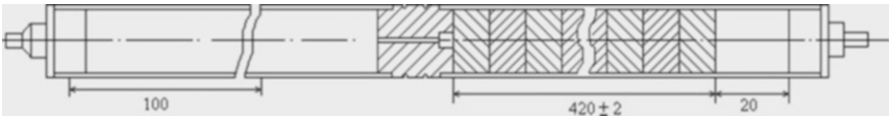

Fig. 7.5 The simple model of neutron absorbing element for fast nuclear reactor regulating rod

corrosion resistance of high dense items made from the boron carbide enriched by the isotope B-10 up to 90 % is very satisfactory in terms of their utilization in CCS rods' NAEs. Structures of neutron-absorbing elements (NAEs) of CSS rods for reactors-breeders basically consist of metallic housings and compact items made from boron-contained materials enriched by the isotope B-10 (Fig. 7.5).

At present, the role of NAEs basically is performed by made from enriched B_4C compacted items of two configurations: cylindrical and annular. NAEs structures and sizes depend on configuration and parameters of the reactor-breeder's active zone. Main problems in terms of NAEs working capacity occur basically because of the temperature field's nonuniformity and also due to gas swelling of their components [16].

One of positive factors of the utilization of neutron-absorbing items made from the boron carbide is their gas swelling's linearity that allows to maintain the structural stability of AE, and hence – of the rod, even in cases of their fast burn-out and heating to high temperature when the emergency stoppage of the nuclear reactor i.e. the rapid insertion of rods into the active zone of the fast reactor take place.

In fast reactors there are used three types of controlling rods. They are rods of fine control, coarse control and emergency rods. Functions of each of them are either the control of nuclear reactivity or stoppage of reactor's operation. Controlling rods serve for reactivity's compensation during the run, temperature increase, burning out and external effects. In particular, from the standpoint of fine adjustment controlling rods' function – reactor's control, the most important parameter of these rods is the control's rapidity. Emergency rods serve specially for emergency stoppage of the nuclear reactor as rapidly as possible.

Rods for compensating the reactivity of the reactor-breeder usually have a structure consisting of seven absorbing elements (NAE) gathered in a cluster inside the housing tube (Fig. 7.6).

Among the CCS rods intended for the emergency stoppage of the reactor-breeder the most optimal is the structure of the emergency guard rod (EG) worked out for the energetic nuclear reactor "BN-600". NAEs of such a rod usually are made from B_4C enriched by the isotope B-10 up to 80 %. The rod is not hermetic; in its upper end component are two inter-perpendicular apertures. The internal volume, through the groove seal between the upper end component and the jacket as well as through special apertures is linked with the heat-carrier. There takes place the initial filling of gaps by the liquid-metallic heat-carrier – sodium as well as the exit of a heat generated during the exploitation.

Last years, according to active zones' parameters of reactors-breeders there are used CCS rods of other structures.

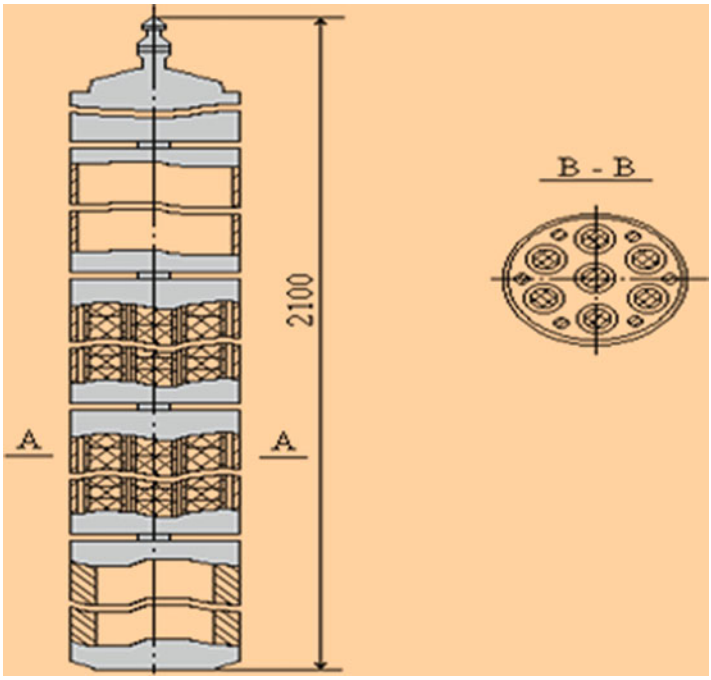

Fig. 7.6 Reactivity compensation rod design (*see color plates*)

The temperature compensation rod (TC) of nuclear reactor's active zone basically is made from NAEs where the composition of europium oxide and metallic molybdenum (Eu_2O_3 + Mo) serves as a neutron-absorbing material. In this rod, inside the absorbing working section there are located 48 absorbing elements. As are encapsulated by end components and welding. They can be of an assorted type (consisting of modules or cylinders) and of a filled type. Rods with filled NAEs are approximately two times cheaper due to the high capacity and absence of any wastes of Eu_2O_3 during the fabrication of their tablets the hot compacting method.

The rods-traps are among the most prospective reactors-breeders' CCS rods. In these rods the role of neutron-absorbing element was performed by tablets made from europium oxide (Eu_2O_3) or ring items from boron carbide (B_4C) enriched by boron-10 up to 92 %.

Experiments carried out for determining comparative effectiveness of rods-traps on the critical assemblages with plutonium fuel have shown that such CCS' rods structures provide the increase of the neutrons absorption effectiveness (working capacity) by up to 10–20 % according to characteristics of neutron field and other parameters of the nuclear reactor's active zone.

In order to increase the effectiveness of CCS rods operating in the high energy neutrons field as well as to improve their reliability some interesting structures were worked out.

For ameliorating NAEs cooling conditions there is developed the rod in which absorbing elements have a form of a disk with central aperture and are bordered from top and bottom by conic surfaces. The angle of a slope of the absorbing elements' lower surface is larger than that of the upper one and between them capillary gaps for the heat-carrier moving.

While the rod operates within the nuclear reactor's active zone there actively circulates in the internal space of rod the liquid-metallic heat-carrier the more cold part of which flows downward and the warmer one – upward. Alongside with that the heat-carrier moves in broadside direction from periphery to centre. Finally, it provides the substantial improvement of the heat transfer from neutron-absorbing NAEs [17].

For ameliorating the evenness of the burning-out process of a neutron-absorbing material there is developed the CCS rod's structure including the container for powder-absorber with permeable walls. While the rod operates within the reactor-breeder's active zone the engendered by the nuclear reaction process of heat liberation continuously takes place in the bulk of the powder-absorber. At the same time, there appear temperature conditions sufficient for organizing the liquid-metallic heat-carrier's boiling process. The liquid-metallic heat-carrier of relatively low temperature penetrates into container trough external walls moving through and cooling the absorbing material. During this process it gets warmed itself, turns into the gas–liquid mixture and enters the rod's central channel. The container's volume and powder-absorber's amount is selected with regard for providing powder's continuous, slow agitation having the mean circulation directivity, the migration results in powder's displacement upward in the central zone. In such agitation conditions the whole neutron-absorbing material will be burnt-out evenly. Such structure of the controlling rod is attractive because of the fact that the absorber's agitation process, hence its even burn-out, runs without using any drive mechanisms, external motor means and engines. All this has a positive effect on the effectiveness and reliability of the nuclear reactor's whole controlling and security system [18]. Last years there is intensively going on an activity focused on creating new highly effective and reliable CCS rods for fast energetic nuclear reactors. Structural particularities of modern rods are determined by new optimizing neutron-absorbing elements as well as by the necessity of providing optimal heat- and thermo-mechanical conditions for their exploitation.

7.4 Nuclear Fusion as Possible Energy Generation Technology

Today the demand of secure and sufficient supply of energy is mainly satisfied by fossil fuels (oil, coal and natural gas), which account for 80 % of the total energy consumption. Secure and sustainable energy sources are required to maintain our standard of living.

Currently researchers from different countries are developing a range of environmentally acceptable, safe and sustainable energy technologies. Fusion is one of

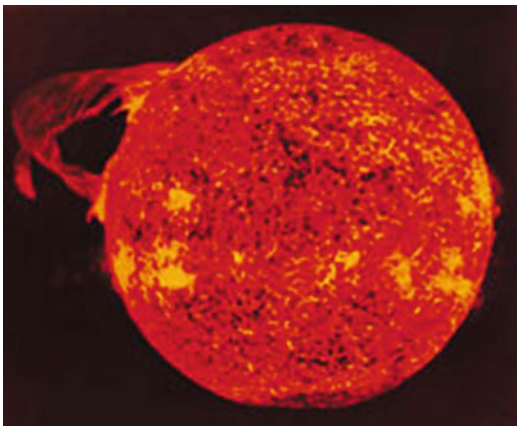

Fig. 7.7 The Sun is a massive fusion power station. It produces around 300 billion watts (3×10^{26}) of power, consuming 600 million tons of hydrogen fuel every second (*see color plates*)

them [19, 20]. For the long term, fusion will provide an option for a large scale energy source that has a low impact on the environment and is safe, with vast and widely distributed fuel reserves.

Fusion power stations will be particularly suited for base load energy generation to serve the needs of densely populated areas and industrial zones. They can also produce hydrogen for a "hydrogen economy". Fusion is the process which powers the sun and other stars. Nuclei of low mass atoms "fuse" together and release energy. In the core of the sun, the huge gravitational pressure allows this to happen at temperatures of around ten million degrees Celsius (Fig. 7.7).

Gas raised to these temperatures becomes "plasma", where the electrons are completely separated from the atomic nuclei (ions). Plasma is the fourth state of matter with its own special properties. The study of these properties is the focus of plasma physics research. Although the plasma state is exotic on Earth, more than 99 % of the universe is made up of plasma. At the much lower pressures (ten billion times less than in the sun) that we can produce on earth, temperatures above 100 million degrees Celsius are required for fusion energy production rates of interest. To reach these temperatures powerful heating of the plasma is required and the thermal losses must be minimized by keeping the hot plasma away from the walls of its container.

This is achieved by placing the plasma in a toroidal "cage", made by strong magnetic fields, which prevent the electrically charged plasma particles from escaping: it is the most advanced technology and forms the basis for the international fusion experiment ITER. It is also the world's biggest energy research project which includes a global scientific and technical collaboration to produce an experimental facility that will demonstrate the potential of fusion power and test many of the components needed for a practical fusion power station. It is being built at Cadarache in the south of France and will be the world's largest tokamak – a toroidal (or doughnut-shaped) device that uses complex magnetic fields to confine and compress the extremely hot fusion plasma.

ITER is designed to study, for the first time, a "burning" plasma. it will be the first man-made fusion device to produce more energy than it consumes to heat the plasma. Fusion reactions in ITER will generate around 500 MW of heat [21].

The fusion reactions between two isotopes of hydrogen – deuterium (D) and tritium (T) – provide the basis for the development of a first generation fusion reactor, as other fusion reactions require even higher temperatures. Deuterium is a naturally occurring, non-radioactive isotope and can be extracted from water (on average 35 g in every cubic meter of water). There is no tritium on Earth, but it will be produced from lithium (a light and abundant metal) inside the fusion reactor. Each fusion reaction produces an alpha particle (i.e. helium) and a high energy neutron.

$$\mathrm{D} + \mathrm{T} \rightarrow {}^{4}\mathrm{He} + \mathrm{n} + 17.6\ \mathrm{MeV} \tag{7.1}$$

The neutrons escape from the plasma and are slowed down in a "blanket" surrounding the plasma. Within this blanket lithium is transformed into tritium, which is recycled back into the vacuum chamber as fuel, and the heat generated by the neutrons can be used to produce steam which drives turbines for electricity generation. To supply a city with a population of about one million with electricity for 1 year, a fusion power plant would require one small truck-load of fuel. A fusion reactor is like a gas burner: the fuel which is injected in the system is burnt. There is very little fuel in the reaction chamber (about 1 g of D-T in a volume of 1,000 m^3) at any moment and, if the fuel supply is interrupted, the fusion reactions last for only a few seconds. Any malfunction of the device would cause the plasma to cool and the reactions to stop.

The basic fusion fuels, deuterium and lithium, as well as the reaction product, helium, are non-radioactive. The radioactive intermediate fuel, tritium, decays reasonably quickly (it has a half-life of 12.6 years) and the decay produces an electron (beta radiation) of very low energy. In air, this electron can travel only a few millimeters and cannot even penetrate a sheet of paper. The energy generated by the fusion reactions will be used in the same way as today, e.g. for the generation of electricity, as heat for industrial use, or possibly for the production of hydrogen.

The fuel consumption of a fusion power station will be extremely low. A 1 GW (electric) fusion plant will need about 100 kg deuterium and 3 tons of natural lithium to operate for a whole year, generating about 7 billion kWh. A coal fired power plant – without carbon sequestration – requires about 1.5 million tons of fuel to generate the same energy.

Fusion reactors do not produce greenhouse gases and other pollutants which can harm the environment and/or cause climate change. The neutrons generated by the fusion reaction activate the materials around the plasma. A careful choice of the materials for these components will allow them to be released from regulatory control (and possibly recycled) about 100 years after the power plant stops operating. For these reasons, waste from fusion plants will not be a burden for future generations.

7.5 Proton – Engine of the Future Energy Generation Method

Proton was discovered in the 20th of Twentieth century during the nuclear experiments with alpha particles. In the 70th by experiments of electron and gamma particles dispersion experiments the inner structure of proton was observed. At the same time up to now there are no information about the nature of proton, its properties and real inner structure (mass of the proton is 1836,1526675 – 39 e mass) [22].

Current research works shown that proton has a fractal structure, and novel model approaches decay of the proton is realized following the fractal algorithm. Ten stages of proton dissociation are following by appearance of simplest charged particles and energy generation [23] (Fig. 7.8).

$$\sum E_i = m_e c^2 \left[\frac{g_e}{2} \left(\sum_{i-2}^{11} 2^{12-i} \left(1 - \left(\sqrt[10]{D_0} \cdot \alpha^2 \right)^i \right) + (2^{10} - 1) \left(1 - \left(\sqrt[10]{D_0} \cdot \alpha^2 \right)^2 \right) \right) \right] \tag{7.2}$$

E energy = 107.7427553 MeV, and it is 11.5 % of proton rest energy. If the volume of outside energy influencing on proton is more then 107.74 MeV proton is becoming unstable

$$P^+ + \sum_{i=1}^{10} E_i \rightarrow 1,046 \text{ MeV} \tag{7.3}$$

It was estimated that energy creating during induced dissociation of Proton is about 938 MeV. For comparison energy generated during nuclear fusion is 17.6 MeV. (Fig. 7.9) [24].

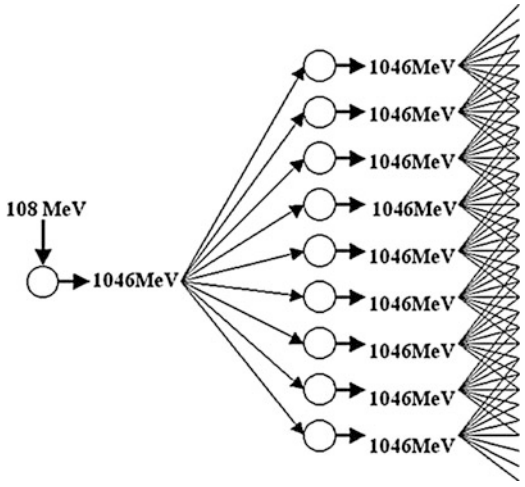

Fig. 7.8 Chain reaction of induced dissociation of proton

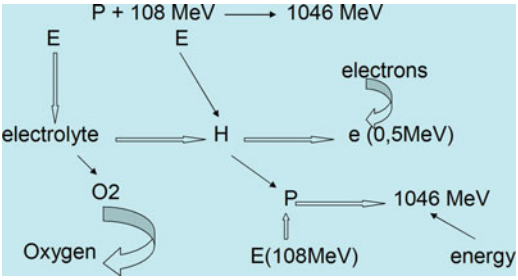

Fig. 7.9 Proton born nuclear-chemical reaction (*see color plates*)

Induced Proton dissociation should be very important nuclear effect, and its end products are not dangerous substances for biosphere.

7.6 Conclusions

At present, in the electricity generation sector: fossil fuels supply around 65 % of world electricity demand; renewable sources just over 18 %; and nuclear generation provides the remaining 17 %. Together these sources currently generate nearly 15, 500 TeraWatt-hours (TWh). However, based on the lowest estimates of future electricity demand, this output must increase to nearly 22, 000 TWh over the next 20 years. Even with growth rates of 10 % in capacity, wind and solar power sources are unlikely to meet more than 1 % of world energy needs by 2020. Among countries with nuclear power generators, in May 2011, total electricity consumption from nuclear energy sources was generated by 441 nuclear power plants (NPPs) ranging from over 80 % in Lithuania to around 1 % in China. New capacity under construction in the Far East suggests that nuclear energy supply in the region will be at least tripled. Further, here in Europe, although the public is not yet convinced, experts believe that geological disposal is technologically feasible, environmentally responsible and ultimately safe. Finland, Sweden and the United States lead in implementing this form of repository technology, and several other countries are actively investigating geological disposal as a viable option, often establishing underground research facilities for this purpose.

The position of nuclear power within the overall global mix of sustainable energy options must be clarified in relation to future commercial efficiency and developmental needs.

A principal milestone which has identified recently is the development of a “new generation of nuclear facilities” that center on innovative reactor design and fuel cycle technologies. In addition to being economically competitive, these new technologies must be inherently safe during operation, produce a minimum of waste and also negate nuclear-proliferation issues. Only through meeting these conditions can public acceptance of nuclear energy be gained.

These new generation technologies will have to be flexible in order to satisfy the energy needs of developing countries, and also adaptable to a broad range of environmental and industrial requirements. In this way, the IAEA foresees the need for small and medium sized reactors, which can produce not only grid based electricity as necessary, but also provide power locally for local needs, such as seawater desalination and domestic heating.

Another major goal is to develop definitive strategies for the disposal of spent fuel and high-level radioactive waste, and in addition to disposal technologies, efforts continue to minimise the radioactive nature of nuclear waste by developing methods that accelerate radioactive decay over time, or convert nuclear waste directly through transmutation techniques.

It is now recognized globally that main new way for nuclear energy technologies is development of novel materials and technologies combined the both effectiveness and safety. These should be done by new scientific approaches to materials technology which will be smart and cost effective.

One of the major obstacles to the future of nuclear power as a readily accepted source of energy is how it is perceived by society at large. In addition to their obvious benefits, all modes of power generation have disadvantages.

Most important tasks are development the nuclear technologies provides the safety and security of nuclear energy generated systems, and among the novel materials and compounds, novel microsystems based nuclear instruments and devices for nuclear reactors control networks.

For instant, investigations focused on the development of novel nuclear materials and technologies for different types of energy generation installations shown that isotopically enriched substances are the most suitable working elements for nuclear energy reactions regulation.

The performed technological, physical-mechanical and radiation tests clearly indicate the prospects of using Boron and Carbon isotopes containing regulating systems. In this respect, particular attention is to be paid to the development of new and upgrading of existing computing models as well as effective technologies for producing the novel generation of items characterized by all physical and strength properties necessary for obtaining desirable operational parameters of novel nuclear materials and tools.

References

1. Kervalishvili P, Utiamyshev I (2006) Some new human friendly energy production technologies. Int Sci J Altern Energy Ecol N 1(33):21–29
2. Brundtland report: our common future, the world commission on environment and development (1987). Oxford University Press, New York
3. European Council 8–9 March 2007, Brussels, Presidency conclusions, 7224/07, Annex I, European Council Action Plan (2007–2009) Energy Policy for Europe (EPE) 10 January 2007
4. Nuclear Illustrative Programme (PINC), COM (2006) 844, published in January 2007, and Annexes 1 and 2, SEC(2006) 1717 and SEC(2006) 1718

5. The WEC Survey of Energy Resources (1995) Estimates that for fast reactors, proven uranium resources allow for more than 3,000 years of energy production. http://www.worldenergy.org/wec-geis/edc/scenario.asp
6. International conference on nonelectric applications of nuclear power: seawater desalination, Hydrogen production and other applications, 16–19 April 2007, Oarai, Japan
7. World Nuclear Association http://www.world-nuclear.org/info/ reactors.html updated on 31 May 2000
8. Generation IV International Forum (2008) www.gen-4.org
9. Gabaraev BA, Cherepnin Yu.S (2009) Innovative designs of nuclear reactors. NATO advanced research workshop "Nuclear safety and energy security", Yerevan, Armenia, 26–29 May 2009
10. Feretic D, Čavlina N, Grgić D (2008) Potential advantages and disadvantages of sequentiaily building smaIl nuclear units instead of a large nuclear plant. Kerntechnik 73:249–253
11. Kervalishvili PJ (2001) Investigations focused on development of control and safety rods for fast nuclear reactors-breeders. In: Proceedings of the XVI PanHellenic conference on physics, 17–20 September 2000, Naphleon, Greece, Ed. Praktika, 2001, Athens, Greece
12. Kokaya MV, Kervalishvili PJ, Kalandadze GI (1987) Cadmium based neutron absorbing materials. J Atomhaya Energya 63:273–275
13. Kochetkov LA, Kazanskey YA, Matveev VI (1985) Investigation on effectivity of rods-traps for fast neutrons nuclear reactors. Report of the Institute for Physics and Energy, Obninsk, N141, 196p
14. Bakhtadze AB, Bairamashvili IA, Kervalishvili PJ (1989) Structural defects influence on boron carbide thermoconductivity. Academy of sciences of USSR. J Neorganicheskie Matereialy 25(10):1652–1665
15. Bakhtadze AB, Shekriladze IG, Kervalishvili PJ (1980) Regulating rod for nuclear reactor. USSR Invention, N 830924
16. Bakhtadze AB, Kervalishvili PJ, Shekriladze IG (1980) Nuclear reactor control rod. USSR Invention, N 936731
17. Kervalishvili P (2010) Some neutron absorbing elements and devices for fast nuclear reactors regulation systems. Nuclear power and energy security, NATO Sci Ser B Phys Biophys , Springer Science + Business Media 147:147–155
18. Kervalishvili PJ (2009) Prospective energy generation technologies. Scientific – Economic Magazin, 2015, Noema, Bergamo, Italy, pp 27–38
19. Robert A, Jean J(2007) Iter: le chemin des etoiles? Edisud
20. Sakharov AD (1967) Violation of invariance; C-symmetry and barion asymmetry. Lett JETF 5:33–35
21. Kosinov NV (2003) Fractal rules in physics of microworld. Physics of consciousness and life, cosmology and astrophysics (4):45–56
22. Jakob M, Landshoff PV (1981) Inner structure of proton. UFN 133(3):14–42
23. International Atomic Energy Agency (IAEA) (2009) A newsletter of the division of nuclear power 6(2), June 2009. http://www.iaea.org/NuclearPower/

Chapter 8
Feasibility of H_2S Production from Black Sea Waters

Hüseyin Murat Çekirge and Rafat Al-Waked

Abstract A model for transporting of seawater with H_2S to shoreline, and possible energy production scheme from H_2S and its feasibility are introduced. In addition to the transport model, various aspects of energy production from H_2S are discussed.

Keywords Black Sea • Hydrogen production • Hydrogen sulfide • Feasibility

8.1 Introduction

Black Sea is a closed basin and more than 100 million people are living around its coastal regions, and 300 million people are connected to this interior water body by various reasons. By geological development, 90 % of this water is anaerobic, under the surface layer of 120–150 m of water body is anoxic and the concentration of H_2S starts from 5 to 6 mg/l and reaches to 9.5 mg/l where the depth becomes around 1,500 m. The H_2S in the water is continuously produced by sulphur reducing bacteria.

There is a constant production of H_2S in Black Sea which is an important threat to the coastal countries. Reduction of H_2S in Black Sea, by converting it to energy, is also a solution to this problem. It is aimed at explaining possible production schemes of H_2S from seawater and energy production from it. It is a great engineering challenge to perform these operations in a feasible way.

H.M. Çekirge (✉) • R. Al-Waked
Department of Mechanical Engineering, College of Engineering, Prince Mohammed University, Al Khobar, Saudi Arabia
e-mail: hmcekirge@usa.net

A. Veziroğlu and M. Tsitskishvili (eds.), *Black Sea Energy Resource Development and Hydrogen Energy Problems*, NATO Science for Peace and Security Series C: Environmental Security, DOI 10.1007/978-94-007-6152-0_8,

The project has two phases, these are:

(a) Transportation of seawater to the power plant and production of H_2S from the seawater, that could be done by transportation of seawater to land, or production of H_2S from a platform, or from a ship sailing in Black Sea.
(b) Production of energy from the transported H_2S could be burning directly, or obtaining hydrogen for fuel cells, or directly using H_2S fuel cells.

In this chapter feasibility of transporting seawater to the coastal installations will be studied; and transportation and an energy production model will be introduced.

8.2 Analysis of Transportation Seawater to Shoreline

The water contains in H_2S starts at the depth of 100–120 m and this distance reaches around 20–25 km from the shores of Black Sea in Turkey. The seawater will be carried by pipes through gravity to a tank below the sea level, where the stripper separates H_2S from the seawater. The intake is more than 25 km distance from the coast, where the seawater starts to contain reasonable amount of H_2S. The best location for such an installation could be in Sinop and Giresun coastal areas in Turkey, where pipelines could be around this length.

The separator unit would be at shoreline and depth of the sprinkler is a design parameter, see Fig. 8.1. The depth of the sprinkler defines flow rate, or volume of the seawater, or indirectly amount of the H_2S carried to the installation. The intake may have a filter, which separates H_2S from seawater (Fig. 8.2).

The head losses through pipeline may be considered as:

$$\Delta H = \sum_{i=0}^{n} h_i \tag{8.1}$$

where;

ΔH = total head loss,
h_i = frictional losses,
i = type of head losses
n = number of head losses; and

the head losses are at entrance, exit, filters and splitters. The energy equation may be written as:

$$H - \Delta H = \lambda(L/D)\left(V^2/2\right) + \left(V^2/2g\right) \tag{8.2}$$

where;

H = depth of the sprinkler,
λ = friction coefficient,

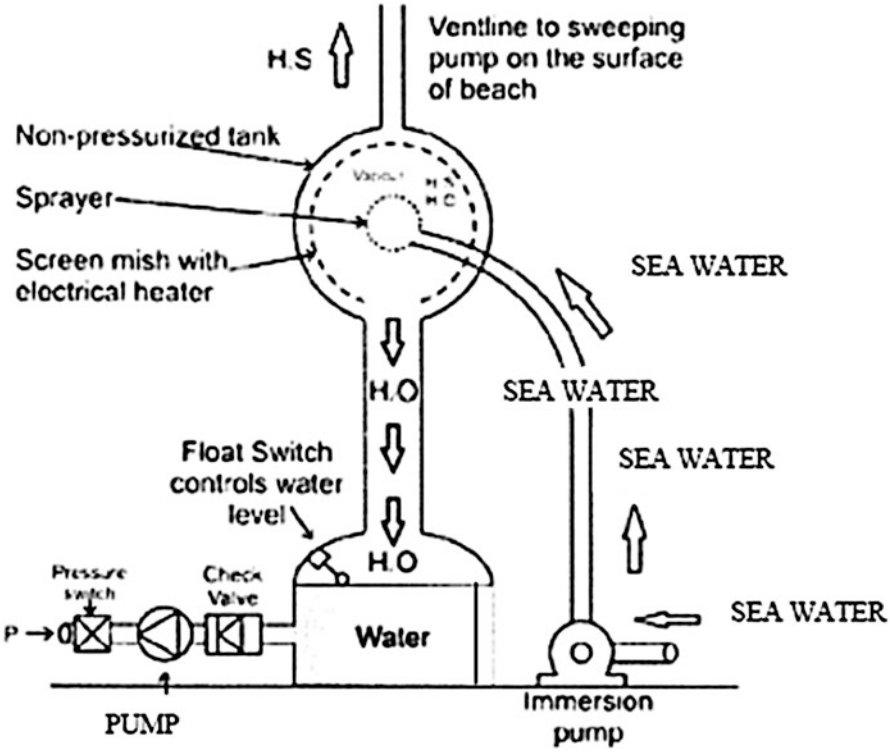

Fig. 8.1 An extraction unit (Naman et al. [1])

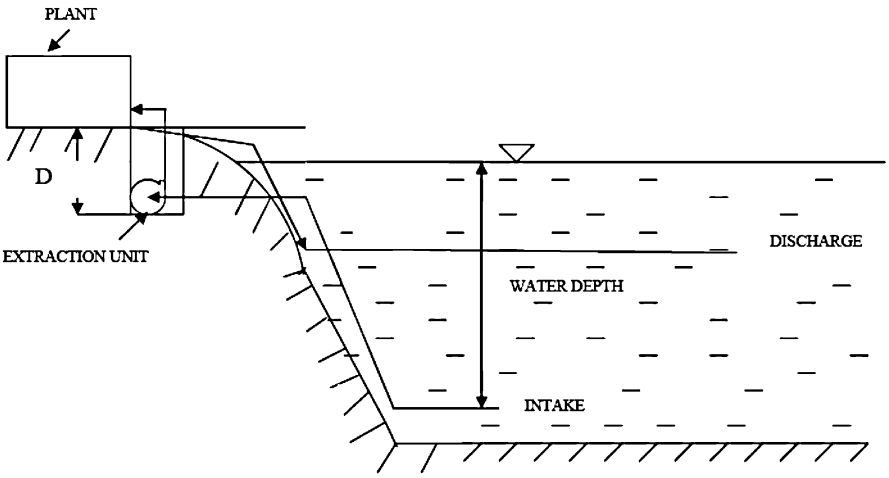

Fig. 8.2 Schematic design of a H_2S power plant (Veziroglu TN, Private Communication 2011)

D = diameter of the pipeline,
L = length of the pipe,
V = velocity of seawater in the pipeline, and
g = gravitational constant.

It is assumed that the accumulated seawater will be evacuated in unit time. The amount of water transported, in unit time or flow rate is, Q:

$$Q = \left(\pi D^2/4\right)V \tag{8.3}$$

where V is obtained from Eq. (8.2). The production of H_2S in unit time is, P, is:

$$P = Q\,c \tag{8.4}$$

where c is the concentration H_2S in the seawater. Total energy production in unit time, E, is:

$$E = \eta\,P\,h_{ev} \tag{8.5}$$

where;

η = energy efficiency of H_2S and
h_{ev} = energy value of H_2S.

If U is the unit price of the energy, then the income from this process in unit time is:

$$\text{Income} = E\,U \tag{8.6}$$

The transported seawater must be returned with the same flow rate to the anoxic zone for completing the cycle. The pump must have the head, ΔH_p:

$$\Delta H_p = \left(V^2/2g\right) + \lambda(L/D)\left(V^2/2\right) + H_r + \sum_{i=0}^{n} h^r{}_i \tag{8.7}$$

where;

H_r = depth of reservoir and
$h^r{}_i$ = losses of returning seawater.

The necessary pump power, P_{pump}, is:

$$P_{pump} = Q\,\Delta H_p \gamma \tag{8.8}$$

where,

Q = flow rate in unit time and
γ = specific weight of the water.

Then, the cost of returning of water in unit time, Cost,

$$\text{Cost} = P_{\text{pump}} \Delta T \, U \tag{8.9}$$

where

ΔT = length of time that the pump is operating.

8.3 Environmental Concerns and Feasibility

Any operation that involves toxic substances is dangerous to the environment in general. In this chapter, the side production of sulphur and its derivatives are not considered, however their economic values must also be considered if a more detailed analysis is taken into account for a feasibility study. The toxic materials can easily be returned into anoxic or dead zone. This discharge into the dead zone is internationally accepted and has no negative considerable effects on the environment. It should also be noted that by production of energy from H_2S may also decrease amount of H_2S in Black Sea waters, and decreases the effects of H_2S pollution in Black Sea indirectly.

The pressure in pipes carrying water are very low respect to crude and natural gas pipelines, and special designed PVC pipes can be used at a lower cost. Considering oil production, H_2S production is quite inexpensive; and the risk for exploration is minimal. The cost of plant operation is at acceptable level for the production of energy in all three cases, namely direct burning, or hydrogen production and using in fuel cells, or using in H_2S fuel cells is considered.

8.4 Numerical Example

Based on the analysis presented in this chapter a numerical model is developed. The results of the model analysis are presented below:

Price of electricity = $ 0.08 kWh (this values may go up to $ 0.22 kWh in many cases)

Energy values of H_2S = 15,000 kJ/kg, half value of methane, Waldheim and Nilsson [2]

Amount of H_2S in the seawater = 10 ppm Naman [1], however 7 ppm is taken for computations as a safety factor for calculations,

Length of pipe = 12,000 m, two pipes are carrying to the shoreline installation and two pipes are returning the seawater,

Diameter = 1.5 m

Depth of the stripper = 4 m

Gravity constant = 9.81 m/s^2
Friction coefficient, $\lambda = 0.008$
Efficiency, $\eta = 0.6$, this is a conservative assumption; it covers possible energy extractions; such as direct burning, or energy through hydrogen extraction, or use H_2S fuel cells.
Minor losses incoming pipes = 1 m
Minor losses returning pipes = 1 m
Radius of the tank = 29.83 m
Height of the tank = 5 m
The pump is located at bottom of tank
Income = $ 349,916.80 yearly
Pumping expenses = $ 28,341.65 yearly
Profit = $ 321,575.15 yearly

The possible incomes from other substances such as S and H_2SO_4 are not considered.

8.5 Conclusion

The analysis is an initial study of the "Front End Engineering Design" for energy production from H_2S of Black Sea waters. With conservative assumptions, it is seen that the project is profitable, and 60 % of this income can be used for operations and the rest can pay the initial investments in acceptable time, that 20 years. It is, of course, these calculations can be made in more detail; and the confidence for producing energy from Black Sea waters can be developed further.

References

1. Naman SA, Ture E, Veziroglu TN (2008) Industrial extraction pilot plant stripping H_2S gas from Black Sea water. Int J Hydrog Energy 33:6577–6585
2. Waldheim L, Nilsson T, Heating value of gases from biomass gasification. Report prepare for: IEA Bioenergy Agreement, Task 30, Thermal Gasification of Biomass, T PS Termiska Preocesseer AB, May 2001, TPS-01/16

Chapter 9
The Low Cost Hydrogen Production from Hydrogen Sulfide in Black Sea

Salah A. Naman and Ayfer Veziroğlu

Abstract Hydrogen sulfide (H_2S) is a polluting gas, smelly, corrosive and highly toxic. Hydrogen sulfide is commonly found in the Petroleum nature gas and Black Sea as follows:

- Petroleum natural gas and refineries contain H_2S especially if the crude oil contains a lot of sulfur compounds (10 %), i.e., Kirkuk Oil Field North of Iraq.
- Black Sea contains H_2S gas which may be produced by microbial sulfur cycle at the equilibrium depth of thousand meters (10 ppm). The total sulfur pool in Black Sea is believed to be 11.38 mg/l (around 4.6×10^9 tons).

The extraction of 10 ppm H_2S from Black Sea at a depth of 1,000 m is the main part of this project, which we believe it is contributing about 90 % of the problem, as it will be very costly if we pump the water from that depth to the surface. Therefore, two pilot plants (Laboratory and Industrial) have been suggested and built by our research group for separation of H_2S gas from water, according to Henry's Law which it is a function of pressure, temperature, pH and salt continent. The results of our laboratory pilot plant gave us good separation efficiency of only H_2S gas from the water condition of the Black Sea.

Therefore, we built another new extraction Industrial pilot plant according to Henry's principle suitable to operate and separate this gas inside the sea at the depth of 1,000 m to transfer this gas to the surface of the Black Sea.

Then with respect to the production of hydrogen from H_2S on the surface of sea, we have built two suitable pilot plants for thermal decomposition and photo thermal decomposition of H_2S to hydrogen and sulfur.

S.A. Naman
Department of Chemistry, Faculty of Science, University of Zakho, Kurdistan Region, Iraq

A. Veziroğlu (✉)
International Association for Hydrogen Energy, Miami, FL, USA
e-mail: ayfer@iahe.org

A. Veziroğlu and M. Tsitskishvili (eds.), *Black Sea Energy Resource Development and Hydrogen Energy Problems*, NATO Science for Peace and Security Series C: Environmental Security, DOI 10.1007/978-94-007-6152-0_9,

We have used these pilot plants to convert our two Clause process plants in Iraq to produce hydrogen and sulfur. We then found that the mixture of H_2S and methane will reduce the cost of production of hydrogen to a very low price due to the production of CS_2. We used in our laboratory pilot plants for the above thermal and photo-decomposition of H_2S gas different catalysts and semiconductors at a temperature range of 450–800 °C instead of 1,500 °C.

Keywords Hydrogen sulfide • Hydrogen • Extraction • Henry's law • Black Sea

9.1 Introduction

The production of hydrogen from hydrogen sulfide in Black Sea faces the following three stages:

1. Low concentration of H_2S gas about 10 ppm in the depth of 1,000 m in the Black Sea [1–4].
2. Extraction of pure H_2S as gas from water of Black Sea at that depth then transfer it to the surface of Black Sea (Baykara et al. Hydrogen from H_2S in Black Sea, Personal communication [5, 6]).
3. Decomposition of H_2S to hydrogen and sulfur on the surface of Black Sea [7–11].

With respect to the first stage, the actual problem of H_2S in the sea is our initial goal. The second stage of the problem is extraction of H_2S gas from water considering all the following physical variables: TDS, minerals salts contains organic molecules and pesticides, suspended particles pH, temperatures and pressure. We believe that stage number two contributes to about 90 % of the problems of production of hydrogen from the Black Sea [8, 12]. Stage number three which is a decomposition of H_2S to hydrogen and sulfur on the surface of the sea, is well established as we can see from different methods on converting Clause processes to hydrogen production instead of water [8, 12–16]. Therefore, this chapter will concentrate on the possible methods for extraction of this H_2S gas.

9.2 Extraction Methods of H_2S from Depth of Black Sea Water

9.2.1 Adsorption Methods

Theories of adsorption indicate that the adsorption of H_2S molecules on the surface of materials may occur as physical or chemical adsorption, depending on the absorbed material particle's size, layers, pH, homogeneous or heterogeneous, and temperature, as well as the adsorbing materials (charcoal, clays, resins, metals oxides, etc.) [17–19].

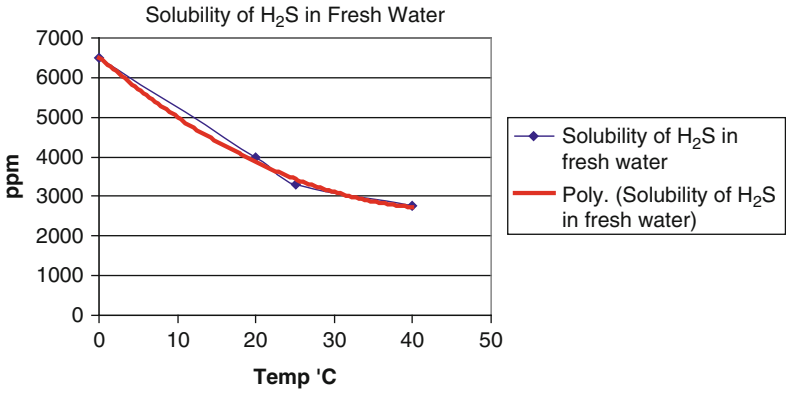

Fig. 9.1 Solubility of H_2S in fresh water at different temperature (*see color plates*)

The process of adsorption and desorption by powder will occurs simply as follows:

$$\text{Powder} + H_2S = \text{Powder} - H_2S = \text{Powder} + H_2S \tag{9.1}$$

The adsorption of H_2S gas in the water and desorption of H_2S from sea water should be selective for only H_2S, because material powder will absorb all other organic molecules, pesticides and suspended particles from the sea water.

In the industrial purification of water and ethanol, charcoal has been used successfully for deodorizing and discoloring of drinking water and ethanol from all contaminant molecules. Literature surveys show that 0.0021 g H_2S will absorb 1 g of charcoal. Other researchers show that 3.8 kg of activated charcoal is needed to absorb 8 ppm H_2S in the Black Sea water, beside the fact that this H_2S will be contaminated with all organic particulars, which will be very bad for hydrogen production from this H_2S [19–21].

Research should be done to find selective material for only H_2S. One of our research groups has used ten different mixed clays to extract H_2S gas from the water at different TDS, pH and temperature, but we couldn't get any good extraction results.

9.2.2 *Phase Separation of H_2S from Black Sea Water*

We found that pure H_2S gas can be separated with high efficiency using Henry's law. This method is well known to separate non-ideal solution of gas–liquid especially separation of natural gas from crude oil. Physical principle of this method is simple, because the solubility of H_2S in fresh water is very high and it is a function of temperature [22]. Figure 9.1 shows this effect, comparing this solubility with the concentration of this gas in the Black Sea, as there are

differences in salinity, pH, temperature, and the chemical and biochemical reactions inside the different depths of the sea [23].

Therefore, a novel method for extraction of H_2S from water is by spraying it on top of a closed tower. This type of extraction of H_2S will be a very useful separation without conversion of the molecules of H_2S, and it can be done through Henry's law. Air strippers are very popular equipment for mass transfer where air and water are contacted, and the contaminants are transferred from water into the air phase [23], but unfortunately some H_2S will be oxidized by air convert to the sulfur or sulfate driving air-stripper. Therefore, exact theoretical and practical extraction of H_2S from Black Sea can be explained by the extensive application of Henry's Law [23–25].

9.3 Application of Henry's Law

The stripping of H_2S from water depends on the properties of H_2S, such as vapor pressure, density and the molecular weight. Henry's Law describes the stripping of various chemicals. It states that the amount of chemical present in air (transferred from water) is directly proportional to its equilibrium concentration in the water. The chemicals that have a low solubility are present in low concentration in water obey Henry's Law [23]. It is also assumed that solution (mixture of H_2S in H_2O) is ideal. Henry's Law constant can be calculated using solubility, molecular weight, density and vapor pressure. Figure 9.2 shows application of Henry's Law for SO_2 gas at temperatures of 50 and 70 [23].

$$y^* = H \cdot x \tag{9.2}$$

Where

y^* – Mole fraction of H_2S in gas phase in equilibrium with liquid
H – Henry's Law constant
x – Mole fraction of H_2S in liquid phase

The error in determining the exact solubility of vapor pressure of H_2S is multiplied in calculating Henry's Law constant H. The other error will come due to the effect of temperature on solubility and non-ideality of solution [23–25], but the value of $H = 515$ (atm) for H_2S.

In Chemistry, Henry's Law is one of the gas laws formulated by William Henry. It states, at a constant temperature, the amount of a given gas dissolved in a given type and volume of liquid is directly proportional to the pressure of that gas in equilibrium with that liquid. Figure 9.2 shows these relations [4]. A formulation of Henry's Law is similar to the previous one, and very similar to Arrhenius equation, for dependence of physical and chemical properties of temperatures:

$$e^p = e^{kc} \tag{9.3}$$

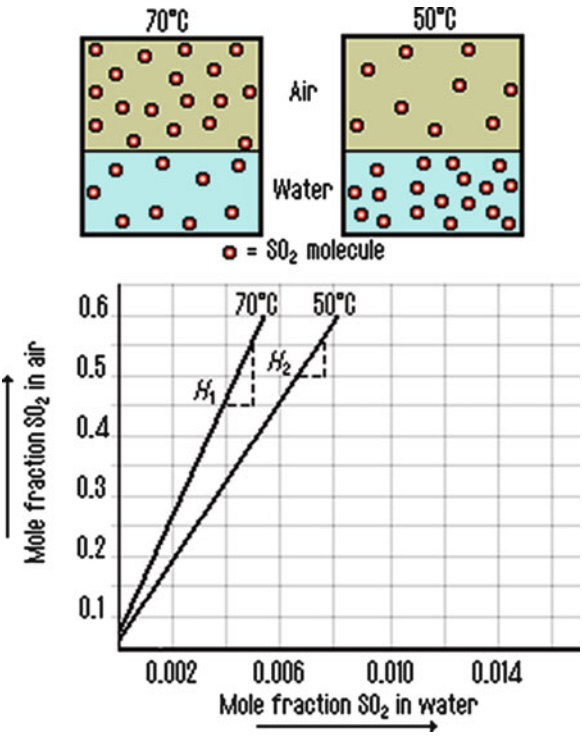

Fig. 9.2 Application of Henry's Law (*see color plates*)

Where

p – The partial pressure of the solute (H_2S) above the solution
c – The concentration of the solute (H_2S) in the solution
k – The Henry's Law constant, which has a unit such as: L.atm/mol; Or atm/mol fraction or Pa m^3/mol

Taking the natural logarithm of the formula gives us as follows:

$$p = k \cdot c \tag{9.4}$$

When H_2S is dissolved in water at 298 K. Note that in the above dimensional units:

L is liter of solution (H_2S + water)
Atm is the pressure of the H_2S gas above the solution (in atmospheres of absolute P)
Mol is the moles of the H_2S gas in the solution

Also, note that Henry's Law constant k varies with the solvent at temperature. There are various other forms of Henry's Law, especially when you change the temperature of the system (Fig. 9.3).

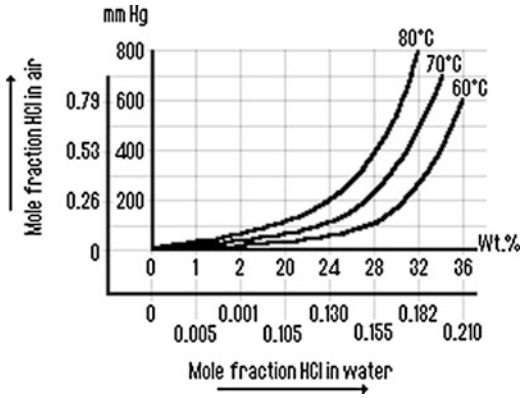

Fig. 9.3 Henry's Law for HCL gas at different temperatures

$$K_H = K_H^0 . \exp\left[-C \cdot \frac{1}{T} - \frac{1}{T_0}\right] \tag{9.5}$$

Where K_H^0 is Henry's standard temperature of 298 K.

It can be seen that the solubility of gases (H_2S) is decreasing with increasing temperature, while heating water (saturated with H_2S) from 25 to 95 °C. The solubility will decrease to about 43 % of its initial value in case of nitrogen. Figure 9.3 shows the effect in temperature.

The constant C may be regarded as:

$$C = \frac{\Delta H_{solvent}}{R} = -\frac{d\ln K_H}{d\left(\frac{1}{T}\right)} \tag{9.6}$$

ΔH is the enthalpy of the solution and R is the gas constant. The value of Henry's Law constant for H_2S varies from different references [23–25]:

515 atm [24]
991 kPa/molal [25]

9.4 Laboratory Extraction Pilot-Plant Unit

Figure 9.4 shows the diagram for this pilot plant which will give us the efficiency of separation of certain amount of H_2S. Hydrogen sulfide should be prepared by Kipp's apparatus as in this reaction $FeS + H_2SO_4 \rightarrow H_2S + FeSO_4$ or it can be purchased as cylinder of H_2S gas [26].

The experiment starts as follows: H_2S gas will pass to the first tank containing water the volume of the gas will be measured as V1. Then, the water will be pumped to the tower and sprayed at a certain temperature, pressure, and at the height of h. The vapor of H_2S will sweep to the separation unit through the condenser, and the

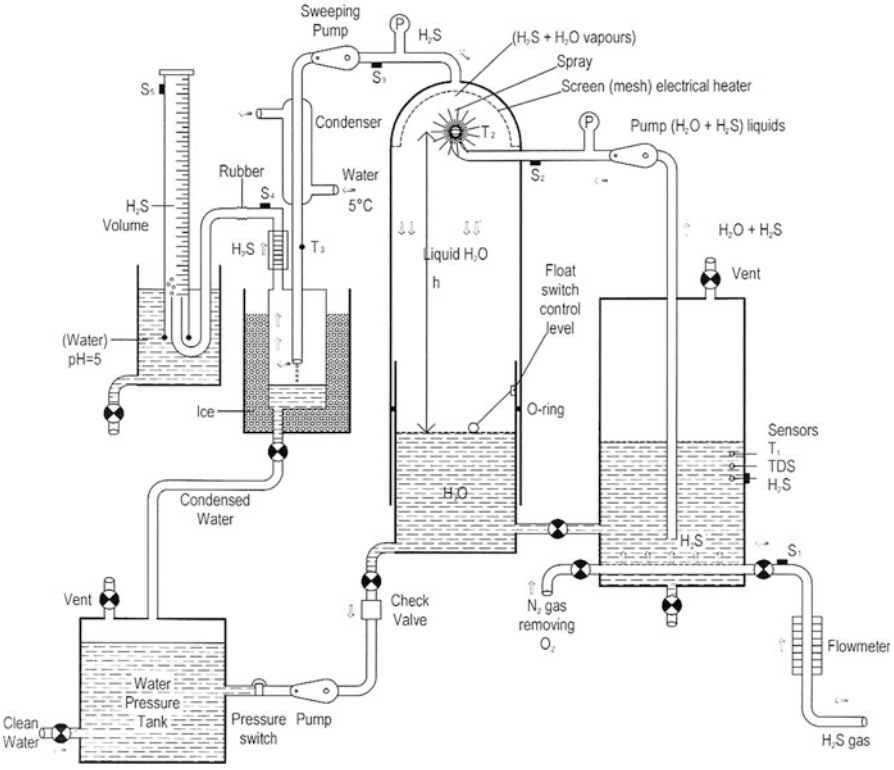

Fig. 9.4 Laboratory extractions of pilot plant

extracted volume of H_2S will measure as V2. Finally, the water vapor and droplet will be collected at the bottom of spraying tower tank. The ratio of V2/V1 will give us the efficiency of separation.

This experiment will be repeated at different variables such as pH, salinity, temperature, and the height of tower pumping pressure. This pilot plant has been built from metal and glass, and it should be in a closed system without any leaks. The spraying tower is semi evacuated in order to strip the H_2S gas. The pilot plant should be in the laboratory's hood, H_2S gas cylinder or Kipp's apparatus should be outside the laboratory. All the experiments will give the efficiency of extraction [26].

Special sensors for measurement of temperature, salinity, H_2S concentration, pressure, etc., have been fixed in different parts of the pilot plant in order to give us accurate results.

This laboratory pilot plant for extraction will work according to Henry's law of gas liquid solution. There are different Henry's law constant H for H_2S gas.

This experiment will separate H_2S gas from non-ideal solution at first tank sweeping pump will transfer H_2S gas to separation unit.

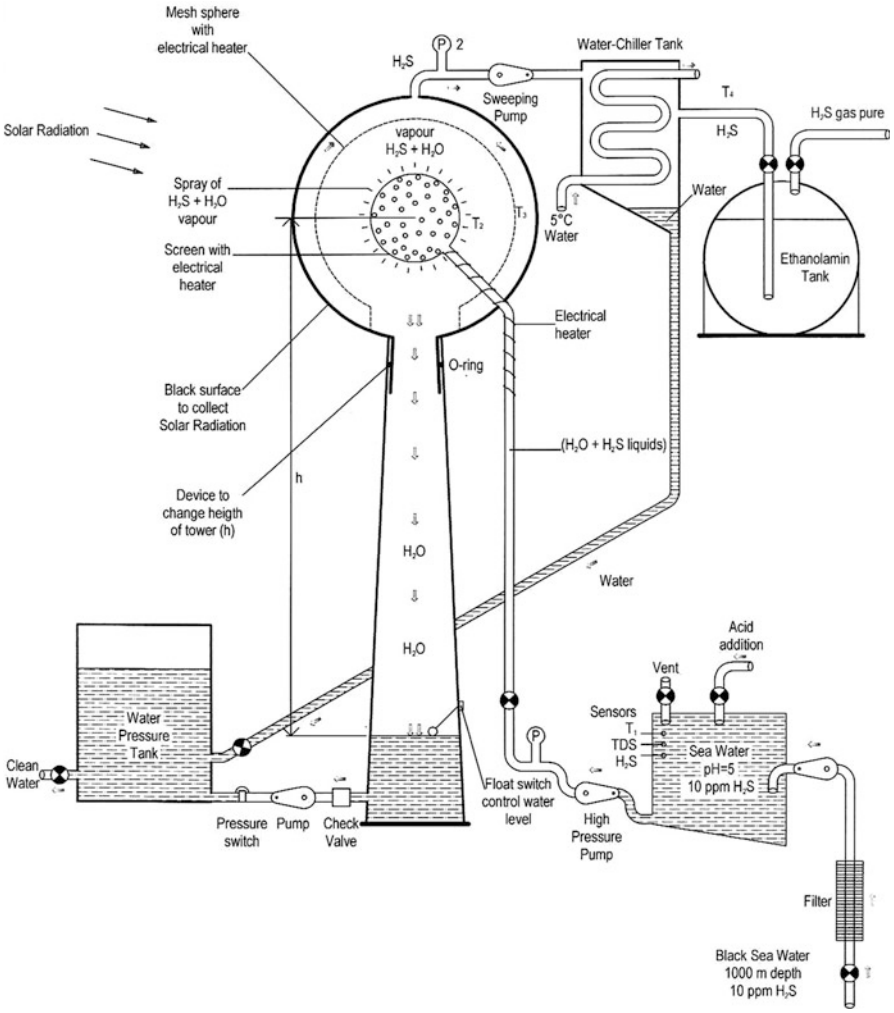

Fig. 9.5 Industrial extraction of H_2S pilot plant

According to Henry's Law equations above:

$$H = \frac{y_{H_2S}\ (\text{gas Phase})}{X_{H_2S}\ (\text{in liquid})}. \tag{9.7}$$

The value for Henry's Law constant can be changed at different parameter of variables. The value has been found equal to 700 atm for a few experiments of the Industrial extraction unit of H_2S gas from water.

9.5 Industrial Extraction of H_2S Pilot Unit

Figure 9.5 shows the pilot plant for extraction of the H_2S from water of the Duhok dam in KRI-Iraq. It is the same principle of Henry's Law, but it can extract large amounts of water containing H_2S. The extracted H_2S will be gradually evaporated to the atmosphere [27].

This pilot plant is in principle similar to the laboratory pilot plant, but it directly pumps from the Duhok dam. It contains screen electrical heater to fix the temperature, water chiller at the top to separate any water vapor, the spraying tower is evacuated by sweeping pump on the top of the tower. Special sensors at different locations of the plant are connected to measure most of the variables. It is also possible to change the height of the tower.

This special tower for industrial extraction has an option to change the height of the tower (h) between 5 and 20 m, in order to separate the H_2S from the droplets of the water by gravity force.

The resulting experimental data will guide us to the best condition for maximum efficiency of separation of H_2S gas from water. Also, the results from laboratories pilot plant will be more helpful to operate the industrial extraction unit.

Another design for this unit has been suggested in this report, which is suitable to operate inside the sea as in Fig. 9.6 and more details in Fig. 9.7 about extraction unit inside the Black Sea water.

9.6 Comparison Between the Extraction of H_2S Inside and Outside Black Sea Water

Table 9.1 with Figs. 9.6 and 9.7 gives the advantages and disadvantages of these two types of extraction.

Advantage of this type of separation can be concluded below:

1. Pumping unit of H_2S in water (10 ppm from depth of 1,000 m) at equilibrium concentration zone. Special pipe with special type of pumps depend on the capacity of plant for the production of 1 ton of hydrogen, which needs pumping of about 10^9 m^3 water.
2. Storage closed tanks for raw water of sea containing H_2S 10 ppm are suitable to the capacity of pumping and extraction. They should be H_2S conversion resistance materials closed on the top of the beach to prevent evaporation of H_2S to the atmosphere.
3. Spraying extraction units separate H_2S from water and concentrated in the ethanolamine tanks unit (4), the unit has different attachments to control temperature and water also to fix the level of water and pressure of spraying.

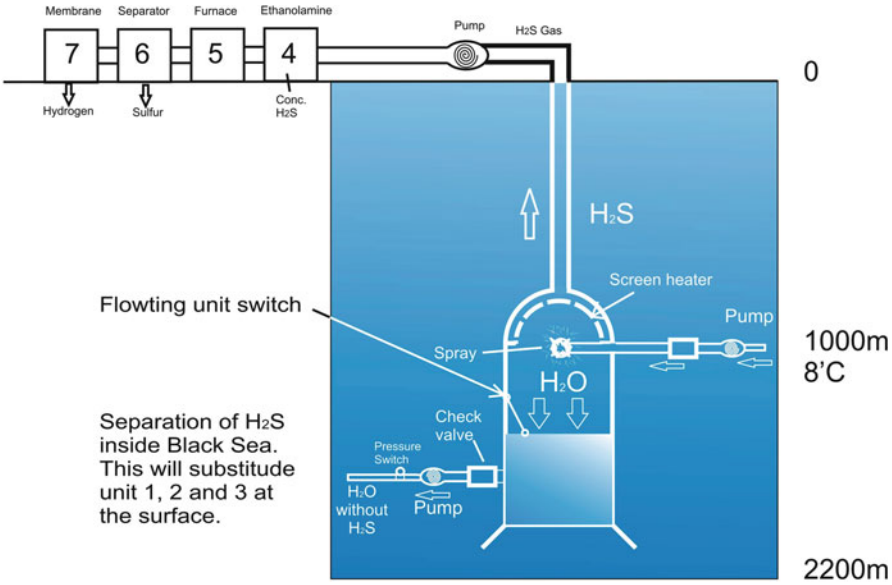

Fig. 9.6 Extraction of H_2S inside the sea (schematic diagram) (*see color plates*)

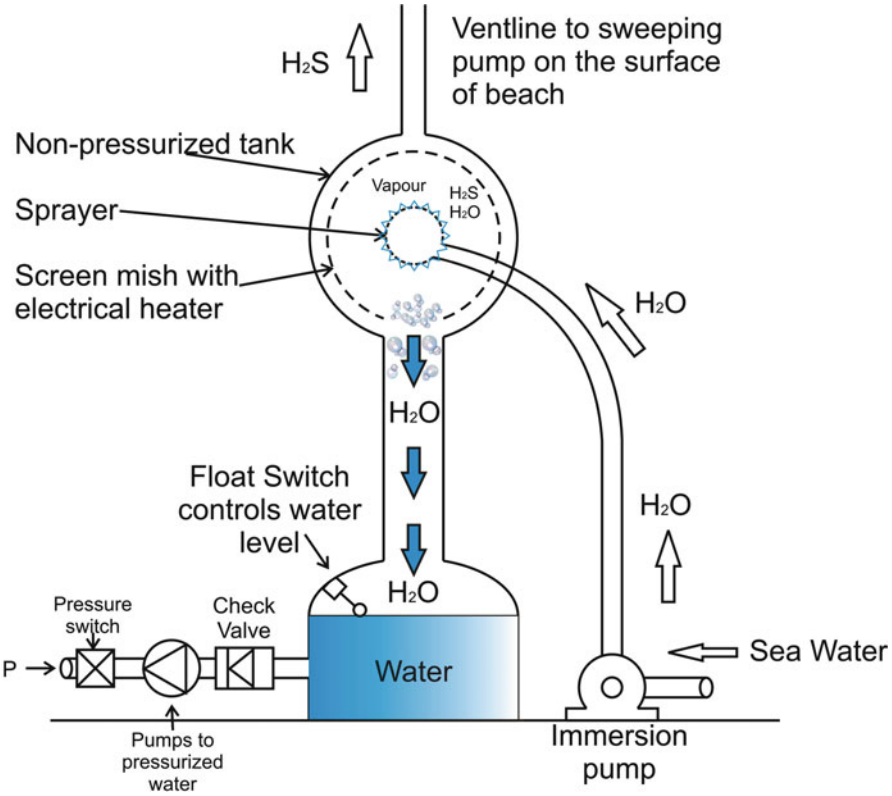

Fig. 9.7 New industrial extraction unit of H_2S designed for inside water (*see color plates*)

Table 9.1 Comparison between outside and inside extraction of H_2S in Black Sea

	Outside water (on beach)	Inside water at 1,000 m depth
1	There is a need of pipes for the transfer of water from the bottom to the surface of the pumping station	No need for pipelines to pump water – only pipe for transporting H_2S gas to the surface
2	Same quantity of water should be pumped to sprayer	Same quantity of water should be pumped to sprayer
3	Pump with certain specification in order to spray water	Immersion pump with same power to spray water inside the sea
4	There is a need for a large closed tank on the beach for water storage	There is no need for tanks for water storage
5	Spraying unit on the surface beach operation at 1 atm	Spraying unit at depth of 1,000 m at pressure of 100 atm (floating unit)
6	There are pumping stations for pumping water to the surface	No need for pumping station to pump water to the surface. Only small pump for pumping H_2S gas from spraying lower to the surface

4. Ethanolamine tanks (30 %) are needed for collection of H_2S gas and concentration. We need two tanks one for dissolving H_2S, and the other for evaporation of H_2S at higher temperatures to decompose units 5, 6 and 7.

   Figure 9.6 shows the schematic diagram for other parts (units) of this flow sheet plant which are units 5, 6 and 7 for thermal decomposition of H_2S.
5. Furnace with certain specifications, superadiabatic certain catalyst and options can be fed partially by H_2S or natural gas. It is well explained in section 9.9 in this project [14–16].
6. Sulfur condensation section for separation, it has been well explained in section 9-1 of this report.
7. Hydrogen separation units by special membrane ceramic or metallic. Details of this separation are in Sect. 9.7, where we explain the thermal decomposition of H_2S to produce hydrogen [14].

9.7 Thermal Decomposition of Hydrogen Sulfide

It has long been recognized that H_2S can be thermally decomposed, yielding hydrogen and sulfur (S) as primary products, however, the equilibrium constant for this thermolysis reaction is unfavorable. The reaction must be conducted to about 700 °C to achieve an even 10 % conversion to hydrogen and sulfur. The complete decomposition of H_2S is achieved only at temperature above 1,500 °C (Fig. 9.8).

Given the high reaction temperature and unfavorable thermodynamic equilibrium constant, it is not practical to achieve complete decomposition of H_2S. Different research groups tried to overcome this problem by:

1. Lowering decomposition temperature of reactors by using catalyst [28–31].
2. Using superadiabatic reactors, by burning some H_2S to increase the temperature of the reactor [13, 14].

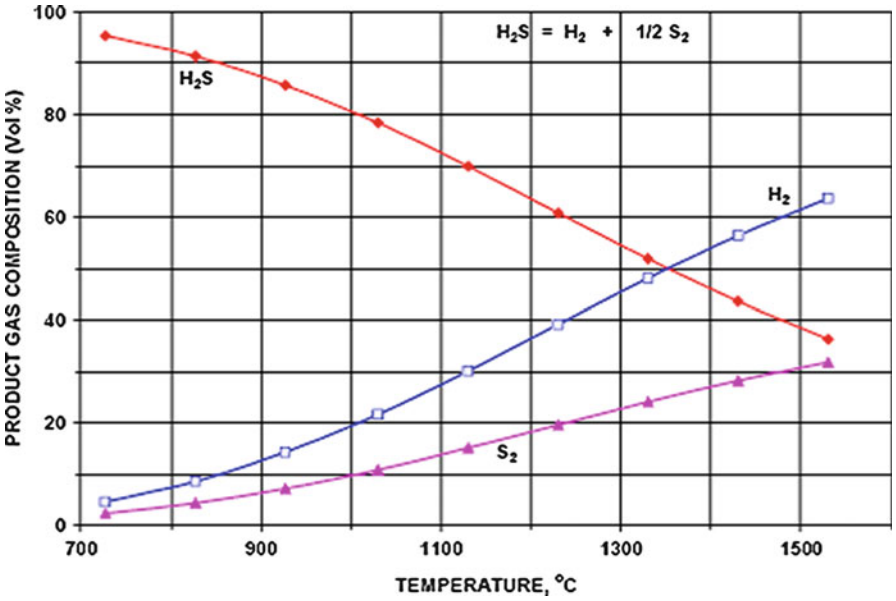

Fig. 9.8 Pure H_2S decomposition reaction as a function of temperature (*see color plates*)

3. By condensing or removing the by-product sulfur from the reaction reactor.
4. Separation of the hydrogen by using ceramic membrane or metallic membranes that tolerate high temperature [15, 16].
5. Thermochemical hydrogen sulfide reformation of methane with or without solar power, and with production of by-products CS_2 beside hydrogen and elemental sulfur [12].

Each research group has suggested special pilot plants for the above methods of decomposition of H_2S. As in Fig. 9.9a, b, all these systems have the ability for the continuous separation of sulfur and/or hydrogen by condensation or membranes. The uses of catalysts are to decrease the temperature of decomposition.

Similar pilot plants have been suggested using quartz reactor with different catalysts and temperatures in flow systems as shown in Fig. 9.9a, b [28].

The Gas Technology Institute, in collaboration with the University of Illinois, has been developing an innovative noncatalytic thermochemical process for the production of hydrogen and elemental sulfur from hydrogen sulfide. The key feature of this process is the superadiabatic reactor, with a partial oxidation of H_2S in the feed gas is carried out in a cylindrical vessel packed with a porous ceramic medium with a high thermal capacity [8, 12, 15, 16].

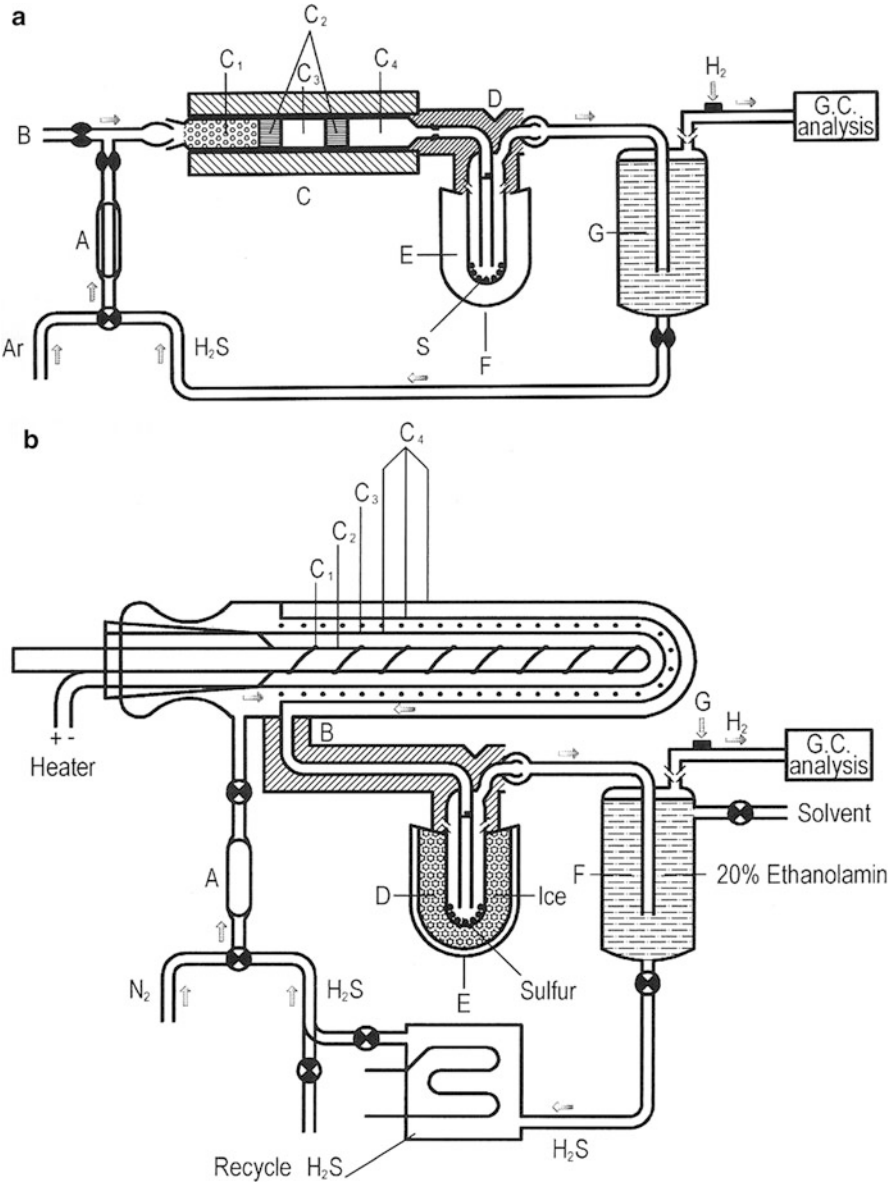

Fig. 9.9 (**a**) Schematic diagram of experimental apparatus for the decomposition of hydrogen sulfide [28]. *A* flowmeter, *B* to vacuum line, *C* tube furnace, *C1* pyrex balls, *C2* glass wool, *C3* catalysts, *C4* tube reactor, *D* heating tape, *E* trap for sulfur separation, *F* sulfur condenser, *G* 30-wt% DEA bath for H_2S separation, *H* gas sampling outlets septum. (**b**) Schematic diagram of experimental apparatus. *A* flowmeter, *B* reactor (thermal diffusion column), *C1* heating wire, *C2* ceramic rod, *C3* catalysts, *C4* quartiz, *D* trap for sulphur separation, *E* sulphur condenser, *F* 30-wt% DEA bath for H_2S separation, *G* septum

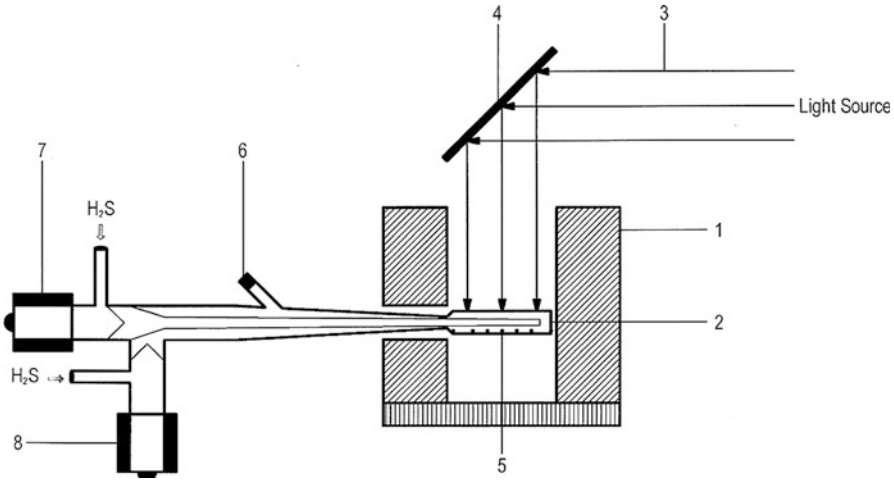

Fig. 9.10 Static reactor [8]. *1* furnace, *2* flate reactor, *3* light, *4* mirror, *5* catalysts on the bottom of reactor, *6* septum, *7* and *8* taps for the admission and withdrawal of gas samples

9.8 Photo Catalytic Recycling of Hydrogen

In this report, a new tail sulfur recovery process is described in which the H_2S having been absorbed into an alkaline solution, is decomposed in an energy-storing solar photochemical scheme to yield not only sulfur, but hydrogen that can be sold or used internally at refineries.

Catalyst-modified semiconductor particulates are employed to facilitate the reaction. Different pilot plants have been suggested. Figure 9.10 shows one schematic diagram for a gas phase decomposition (static reactor) using different semiconductors surfaces for decomposition of H_2S to hydrogen and sulfur on the surface of different semiconductors' powder using quartz cell, comparison have been detected between thermal and photo thermal efficiency of hydrogen production using gas chromatography [8].

9.9 Conclusion

From the results of this study, we can conclude that the main problem of hydrogen production from Black Sea is the extraction system of H_2S molecule at low concentration (10 ppm) at the depth of thousand meters inside the Black Sea water. We also succeeded through our primitive pilot plant that the extraction of H_2S could be performed inside the Black Sea, instead of the surface of the sea, and through Henry's Law of phase separation. Also, we can't extract the H_2S by

adsorption on the charcoal, as the charcoal is not selective for H_2S gas and it will pollute the H_2S gas with other polluted molecules inside the Black Sea.

We believe that control engineers could modify the design of our extraction unit inside the water (Fig. 9.7) to be suitable for different depths of the Black Sea, and be able to inject water continuously with high pressure inside the unit for separation of H_2S gas to surface of the sea and return the clean water back to the sea.

References

1. Naman SA, Project No. 2. Applied to (UNIDO-ICHET) (2005) Production of hydrogen from hydrogen sulfide Black Sea and Kirkuk-Iraq
2. Hydrogen sulfide, microscale gas. file://A:/Hydrogen%20Sulfide%20Microscale%20Gas%20Chemistry%20Experiments.htm
3. Hydrogen sulfide. las-vegas-advisor.info.http://las-vegas.advisor.info/Hydrogen_sulfide
4. Manning Safety Services, Inc. H_2S, what you need to. File://A:\HYDROGEN%20H_2S%what%20you%20need%20to%20know.htm
5. Türe E (2005) Hydrogen energy potential of the Black Sea. In: Proceedings of the International Hydrogen Energy Congress and Exhibition IHEC 2005, Istanbul, Turkey, 13–15 July 2005
6. Midilli A, Murat Ay, Kale A, Veziroğlu TN (2005) Hydrogen energy potential of the Black Sea deep water based on H_2S and importance for the region. In: Proceedings of the International Hydrogen Energy Congress and Exhibition IHEC 2005, Istanbul, Turkey, 13–15 July 2005
7. Haklidir M, Kapkin S (2005) Black Sea, a hydrogen source. In: Proceedings of the International Hydrogen Energy Congress and Exhibition IHEC 2005, Istanbul, Turkey, 13–15 July 2005
8. Al-Shamma LM, Naman SA (1990) Production and separation of hydrogen and sulfur from thermal decomposition of H2S over vanadium oxide/sulfide. Int J Hydrog Energy 15:1–5
9. Bandermann F, Harder KB (1982) Production of hydrogen via thermal decomposition. Int J Hydrog Energy 7:471–475
10. Foord JS, Fitz Gerald ET (2002) The adsorption and thermal decomposition of H_2S. University of Oxford UK. Available online 18 Sep 2002
11. Naman SA (1992) Compression between thermal decomposition and photo splitting of H2S. Int J Hydrog Energy 17:499–504
12. Cox BG, Clark PF, Pruden BB (1998) Economics of thermal dissociation of H2S to produce hydrogen. Int J Hydrog Energy 23(7):531–544
13. Raymont MED (1975) Make hydrogen from hydrogen sulfide. Hydrocarb Process 54 (7):139–142 and Ed Luinsta (2004) Sulfur production by the Claus process, Chemical Process Consultant, Sulfotch Research, Calgary, Alberta, Canada
14. T-Raiss A (2001) Proceedings of the U.S. DOE hydrogen program annual review, Baltimore, 18 Apr 2001, Florida Solar Energy Center, University of Central Florida, 17 Jan 2001
15. Slimane RB, Lau FS, Dihu RJ, Khinkis M (2002) Production of hydrogen by superadiabatic decomposition of hydrogen sulfide. In: Proceedings of the 2002 U.S. hydrogen program review, NREL/CP-610-32405, Golden, Colorado, USA
16. Huang C, T-Raissi A (2003) Analysis of alternative hydrogen production processes liquid hydrogen production via hydrogen sulfide methane reformation, FSEC final report for Task IV-B, 14 Aug 2003
17. Chivers T, Lau C (1987) The thermal decomposition over vanadium oxide. Int J Hydrog Energy 11:235–243

18. Dubinin MM (1989) Fundamentals of the theory of adsorption in micropores of carbon adsorbents: characteristics of their adsorption properties and miroporous structures. Carbon 27(3):457–467
19. Bandosz T, Askew S, Kelly WR, Bagreev A, Adib F, Turk A (2000) Biofiltering action on hydrogen sulfide by unmodified activated carbon. Water Sci Technol 42(1–2):399–401
20. Chiang HL, Tsai JH, Tsai CL, Hsu YC (2000) Adsorption characteristics of alkaline activated carbon exemplified by water vapor. Sep Sci Techol 35(6):903–918
21. Bagereev A, Bandosz TJ (2002) A role of sodium. Ind Eng Chem Res 41(4):672–679
22. Petrov K, Baykara SZ, Ebrasu D, Gulin M, Veziroglu A (2011) An assessment of electrolytic hydrogen production from H_2S in Black Sea waters. Int J Hydrog Energy 36:8936–8942
23. Applying Henry's law to groundwater treatment. http://dbw.eni.edu/Teacher/SNT/log-2/26/2006Ref(2)p-47
24. Carroll JJ. Software for phase equilibric in natural groundwater system. AQV alibrium http://www3.telus.net/public/jcarroll/ION.HTM
25. Who Guidelines for Drinking Water Quality Hydrogen Sulfidein Drinking water 2d. Ed vol. WHO/SDE/WSH/03.04/07 WHO, Geneva 1996
26. "Henry's law" from Wikipedia. http://en.wikipedia.org/wiki/Henry'slaw. 28 Sep 2006
27. Muradov N, Veziroglu TN (2005) From hydrocarbon to hydrogen–carbon to hydrogen economy. Int J Hydrog Energy 30:225–237
28. Naman SA, Al-Mashhadani, Al-Shamma L (1995) Photo catalatic production of hydrogen from H_2S in ethanol amine. Int J Hydrog Energy 20:303–307
29. Naman SA, Al-Omar S, Al-Mosawi I (2005) Production of hydrogen from H2S (New industrial method). In: International Hydrogen Energy Congress and Exhibition, Istanbul, Turkey, 13–15 July 2005
30. Chakarov DV, Ho W (2001) Thermal and photo induced desorption dissection of H2S. Cornel University, Ithaca, USA. Available online 9 July 2001
31. Baykara S, en E (2004) Hydrogen from H2S in Black Sea. In: 15th world hydrogen energy conference, Yokohama, Japan 27 June–2 July 2004

Chapter 10
Traditional and Sustainable Energy Production in Southern Ukraine and Crimea: Current State and Prospects

Igor Winkler, Yarema Tevtul, and Margarita Winkler

Abstract Traditional energy generation technologies cause numerous environmental problems and consume non-renewable resources. Therefore, substitution of traditional energy generation technologies with modern sustainable methods is an important and promising issue.

Current distribution of energy production in Ukraine is: 40–50 % at the nuclear power plants (4 plants); ~40 % at the thermo power plants; ~6–10 % at the hydro power plants and less than 0.5 % at various sustainable power plants (wind power, small hydropower, PV, etc.).

Northern Near-Black Sea steppe region and Crimea possess considerable wind power generation potential. Total estimated wind power potential of the Southern Ukraine and Crimea is about 5,000 MW, which in the long-term outlook can cover about 20 % of the national energy consumption. The Crimean annual wind power energy production can reach about 10 billion kWt-h/year.

Besides, Northern Black Sea steppe is a region of very intense grain production, which produces high-tonnage by-products (hay, non-conditional grains, sunflower wastes, etc.). Most of them can be easily utilized in the biopower energy production (house and water heating, etc.). This would also decrease the need for electricity and other energy consumption required for these purposes.

Detailed estimation proves that total sustainable energy generation potential of the Northern Black Sea region and Crimea is quite considerable and can cover up to 30–40 % of its own energy need.

Keywords Sustainable energy • Energy production • Ukraine • Crimea

I. Winkler (✉) • Y. Tevtul • M. Winkler
Yuriy Fedkovych National University of Chernivtsi, 2 Kotsyubynsky St., Chernitsi 58012, Ukraine
e-mail: igorw@ukrpost.ua

A. Veziroğlu and M. Tsitskishvili (eds.), *Black Sea Energy Resource Development and Hydrogen Energy Problems*, NATO Science for Peace and Security Series C: Environmental Security, DOI 10.1007/978-94-007-6152-0_10,

10.1 Introduction

Traditional energy resources are often deficient and/or irregularly distributed over the globe. Many recent political crises and wars were fuelled by the energy availability/price issues. Since quality of life is improving and urbanization processes are developing in many countries, the need in energy shows strong and long-term tendency to increase. For example, the world electricity generation was steadily rising in 1990–2010 and reached 21,325 TWt-h (2010) [1]. This value has increased in 2010 against 2009 on all continents and in the majority of countries. Similar tendency is reported concerning the natural gas and oil production [1].

However, traditional energy resources distribution over the world is very irregular and many countries, especially in Europe are suffering of shortage of some energy carriers.

Fast depletion of the traditional energy resources is another problem to deal with for many countries. For example, the average daily oil consumption in Romania was **143** thousand barrels (tb) in 1965 while oil production was **266** tb. In 1970, these values were **218** and **284** tb respectively, in 1975 – **279** and **311** tb. Oil consumption reached **333** tb in 1976, while oil production remained at the highest point of **313** tb. In other words, Romania has transformed from the oil exporting country into the oil importer in 1976. Similar tendency can be viewed in Norway, were oil production started in 1971, showed a very strong growth during 1996–2001 and then started to decrease slowly [1]. However, gross national oil consumption in Norway is still much lower than oil production.

There are many possible ways to deal with this problem and substitution of some traditional energy production capacities with the renewable sources can facilitate to compensate the shrinking availability of natural gas, oil and other similar resources and cope with the growing energy needs.

As the traditional energy resources are becoming more and more deficient and expensive, the importance of the renewables promises strong and steady growth.

In this chapter, we analyze the current structure of the energy production in Ukraine and prospects of wider involvement of the renewable energy sources in the Southern area of Ukraine.

10.2 Current Energy Generation Structure of Ukraine

In general, Ukraine is an energy deficient country. The domestic resources can supply about 45 % of the national energy needs, while the rest is covered by the exported energy carriers. Figure 10.1 represents the structure of the energy consumption in Ukraine while some parameters of energy production, export and import are shown in the Table 10.1 [2].

Figure 10.1 and Table 10.1 prove that natural gas, which is one of the most deficient energy carriers, supplies the largest part of the national energy need. This

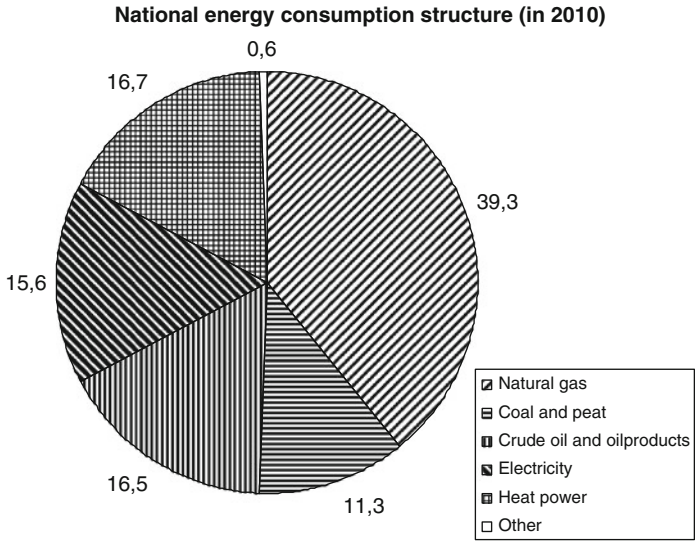

Fig. 10.1 The structure of the national energy consumption of Ukraine in 2010, %

Table 10.1 Energy production, export and import in Ukraine in 2010 (1,000 tons of the oil equivalent)

Energy carrier	Domestic production	Import	Export
Coal and peat	31,019	7,615	4,429
Crude oil and oil products	3,590	13,844	4,066
Natural gas	15,426	30,040	5
Electricity	16,218	2	351
Heat power	14,861	–	–

distribution of the energy carriers is unlikely to change in the nearest future but the dependence on the natural gas import can be lowered through the following options:

- partial substitution of the natural gas consumption in some branches with other energy carriers (mostly domestically-produced electricity and/or shale gas);
- partial substitution of electricity and heat-power consumption with renewable energy sources.

The first option is based on overproduction of the electric power in Ukraine where the total installed electricity generation capacities are higher than the national need for this kind of energy. As a result, Ukraine actively exports electricity to all neighbouring countries. Therefore, the necessity of putting further efforts into substitution of highly deficient and expensive natural gas with cheaper domestic electricity is quite evident.

The second option assumes that even some part of 'traditional' electricity can be substituted with the renewable energy sources and then either used domestically instead of natural gas, or exported.

As seen from Table 10.1, Ukraine only exports about 2 % of the electricity produced domestically and this "potential reserve" seems insufficient for potential widening in the electricity involvement caused by shrinking of the natural gas consumption. Therefore, new resources of electricity should be either produced or substituted with different energy sources, e.g., renewables.

10.3 Prospects of the Sustainable Energy Generation in the Southern Ukraine and Crimea

Near the Black Sea region of Ukraine and Crimea, are densely populated. Agriculture production in these areas is quite intense, while industrial production level is moderate. There are no significant traditional resources of energy in regular exploitation in the region, though quite promising natural gas and some oil deposits have been explored in the region and at the North Black Sea shelf, and extended works on putting the deposits into the regular exploitation are in progress now [3–5].

On the other hand, it is a well known fact that Southern Ukraine and Crimea have significant solar energy production potential. Moreover, the latter region also has serious wind power resources. Intense grain production and cattle farming give a lot of by-products and organic wastes that can be utilized in bioenergy production. All these applications require less financing comparing to putting an oil or gas field in the regular exploitation and can supply this region of Ukraine with energy substituting part of the 'traditional' energy.

Below we provide a more detailed analysis of each branch of renewable energy production in this region.

10.3.1 Solar Energy

North Black Sea shore of Ukraine and especially Crimea are located in the area of economically attractive solar energy production (middle or up-middle solar irradiation efficiency, see Fig. 10.2) [6].

As seen from Fig. 10.2, the solar potential of Ukraine is equal or close to the potential of Romania, Serbia, Bulgaria, Italy and some other countries with highly developed production of this renewable energy.

Preliminary assessment of the repay term for a passive photovoltaic (PV) power plant gives 5–7 years, and first PV project has been started near Simferopol (Crimea). The first PV station project "Rodnikovo" was completed on February 2011. Total installed electric capacity of the station was only 7.5 MW. Next PV station "Ohotnikovo" with total electric capacity of 80 (4×20) MW was completed on October 2011. The world's biggest PV station "Perovo" with the installed electric capacity of 100 MW was completed on December 2011. The fourth PV-park "Mityaevo" with 31 MW capacity was completed on April 2012. Therefore, total peak electric capacity of the Crimean PV projects reached about

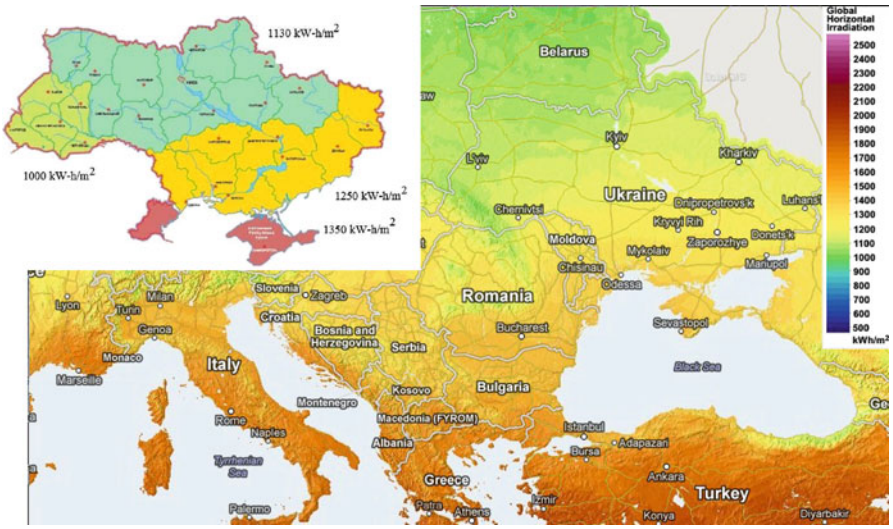

Fig. 10.2 Solar energy potential of Ukraine and neighbouring countries and a more detailed breakdown of the solar energy potential in the regions of Ukraine (*upper left*) (*see color plates*)

Table 10.2 Some technical characteristics of the realized PV projects in Crimea

PV station	Peak electric capacity (MW)	Type	Number of PV modules	Land use (ha)
Rodnikovo	7.5	Passive	32,600	15
Ohotnikovo	80	Passive	347,800	160
Perovo	100	Passive	440,000	200
Mityaevo	31	Passive	134,760	59

215 MW, which facilitates smoother energy supply to this energy deficient region. Other data related to these PV parks [7] are shown in Table 10.2.

Besides, a lot of the small-scale solar modules (PV, water heaters) are used in numerous small enterprises and households in Crimea. Repay period for a fixed passive on-roof solar module is less than 3 years, which promotes fast distribution of such units in the region.

Therefore, both large and small scale solar projects seem to have good prospects in the Southern area of Ukraine. They demand comparatively low construction/maintenance costs, can be installed during a short period of time and provide energy to smooth out the day peak consumption.

On the other hand, the annual estimated reduction in the CO_2 emission by these four PV station is about 225,000 tons. It is less than 0.5 % of CO_2 emitted by all fixed sources in Ukraine in 2010. So current contribution of the solar energy into the energy production is still very low. However, further development of this branch should increase its importance. Together with the wind energy generation, this area is believed to occupy leading positions in the renewable energy generation in

Ukraine with total covering up to 3.5 % in the national need of electricity by 2015. The long-term outlook for the solar and wind power generation reaches about 20 % in the national energy production balance.

10.3.2 Wind Energy

Northern seashore of Black Sea is a region with the highest windpower energy potential in Ukraine. This region is mainly located in the area with average annual wind speed 5 m/s and more. Total assessed wind energy potential of this area is 5,100 kW-h per m^2 year at the attitude 60 m and 6,350 – at 100 m [8]. Technologically functional potential is sufficiently lower and reaches only 975 kW-h per m^2 year (at 100 m).

Five out of six biggest windfarms of Ukraine work in Crimea and have total installed electric capacity of 55 MW (2010) [9]. However, in our opinion, this kind of sustainable power engineering is still underdeveloped in Ukraine. Total national wind energy capacity in Ukraine is only about 90 MW (2010), which is incomparable with capacities of the Czech Republic (215 MW), Poland (1,107 MW) or Austria (1,011 MW) [10]. Spain is one of the world leaders in the solar energy production, also being the second biggest European producer of wind energy (20,676 MW in 2010).

It should be realized that solar and wind powerplants can complement each other and make up for each other's deficiencies. Windfarms can not work stationary and produce predictable amounts of electricity since wind power in every region is significantly changeable, while the character of solar radiation is much more predictable and stable. However, solar stations cannot work in the night time; windfarms, on the contrary, can keep supplying electricity.

Taking into account favourable conditions for development of solar and wind energy in Crimea, we consider this region of Ukraine to be the most promising for the parallel growth of the both branches.

10.3.3 Bioenergy

Consideration of the bioenergy potential of the Southern regions of Ukraine and Crimea can include the following directions:

– biogas production from the cattle-breeding wastes and byproducts;
– utilization of the crops byproducts, non-conditional materials and wastes;
– utilization of the woodworks wastes, byproducts and unconditional materials.

Since timber resources in the region are insignificant and incomparable to those of Central and Western Ukraine, there is no serious timber production facilities working there and woodwork wastes should not be considered as a source of the renewable energy.

Table 10.3 Bioenergy potential of Southern Ukraine regions and the entire country

Region	Cattle wastes biogas potential[a] (MW h/year)	Leguminous plants biomass potential (MW h/year)	Sunflower biomass potential (MW h/year)	Corn biomass potential (MW h/year)	Other vegetables biomass potential (MW h/year)
Odesa	1,773	1,160	4,484	3,560	850
Mykolayiv	1,191	740	3,598	1,470	490
Kherson	1,442	570	2,260	2,300	700
Zaporizhhya	1,773	660	5,720	3,180	580
Crimea	1,470	130	1,102	960	730
Southern Ukraine	7,649	3,260	17,164	11,470	3,350
All Ukraine	38,424	21,110	47,964	49,950	12,070

[a]A coefficient 1 m^3 of biogas = 2.3 kW h is used to recalculate the assessed amounts of biogas into electricity generation units

Table 10.3 represents data related to the potential of some bioenergy resources of the region.

As seen from Table 10.3, sunflower husks and biomass utilization have the most significant bioenergy generation potential in Southern Ukraine. This kind of biomass (35 % of the national sunflower biomass potential) can be easily converted in the wood chips/sunflower husks pellets for heating devices. However, additional transportation stages are expected in this prospective way of utilization since there is no timber production in the region and either biomass or chips transportation is expected from/to the region.

Direct burning of sunflower husks is unsafe ecologically because of the high sulphur content in the husks and emission of significant amounts of the sulphur dioxide while conversion of husks in biogas is too ineffective. On the other hand, the sunflower plants biomass can be utilized without the above precautions.

It should be understood that such serious biomass resources are unlikely to be involved in the electricity generation. Such technologies require specialized equipment and bio-electricity costs becomes too high and uncompetitive even in comparison to other renewable electricity types. However, utilization of the biomass in various heating devices is much easier and well competitive. As stated above, some extra resources of the traditional and other sustainable energy carriers can be released because of the 'heating' biomass applications and used for other purposes.

10.3.4 Geothermal Energy

Crimea is an ancient volcanic region. There are no active volcanoes in the peninsula; but many geothermal basins have been explored at moderate depth in many areas of Crimea. About 82 % of the total geothermal potential of Ukraine is located in Crimea.

Direct energetic utilization of geothermal energy of the Crimean bowels does not look realistic in the nearest future since such technologies are still too ineffective and can be commercially feasible only in the areas with active geysers or highly productive hot wells. So far only recreational/medical utilization of the geothermal energy can be expected and some of these projects are used already.

10.4 Conclusion

Current structure of the energy consumption in Ukraine is weak and ineffective. Traditional high natural gas consumption percentage in the energy usage structure should be lowered because of fast depletion of the available national resources and strong rise in price of the exported gas.

Partially this problem can be resolved through the wider consumption of the inexpensive electricity, which is produced domestically. However, free resources of the domestic electricity are not wide enough (about 2 % of the gross national production) and other solutions should be sought in order to free new resources of energy.

Wider development of the renewable energy generation technologies (mainly wind and solar energy) can be recommended as one of such solutions for the regions of Crimea and Southern Ukraine. Both regions are very rich in both kinds of renewable energy.

In our opinion, renewable energy sources can supply significant part of the local energy consumption in the southern part of Ukraine.

References

1. Available at www.bp.com/liveassets
2. Available at www.ukrstat.gov.ua
3. Blinova VN, Ivanov MK, Bohrmann G (2003) Hydrocarbon gases in deposits from mud volcanoes in the Sorkin Trough, north-eastern Black Sea. Geo-Marine Lett 23(3–4):250–257
4. Kruglyakova RP et al (2004) Natural oil and gas seeps on the Black Sea floor. Geo-Marine Lett 24(3):150–162
5. Herbin JP et al (2008) Oil seeps from the “Boulganack” mud volcano in the Kerch Peninsula (Ukraine – Crimea), study of the mud and the gas: inferences for the petroleum potential. Oil Gas Sci Technol 63(5):609–628
6. Available at www.solargis.info/imaps
7. Available at www.activsolar.com
8. Kudrya SO et al (2010) Atlas of the renewable resources of Ukraine. Institute of Renewable Energy Sources, Kyiv, pp 5–7
9. Available at www.intelcenter.com.ua
10. Powering the energy debate. The European Wind Energy Association annual report 2010

Chapter 11
Evaluation of Biohydrogen Production Potential from Marine Macro Algae

İlknur Şentürk and Hanife Büyükgüngör

Abstract Biomass can also be used as a substrate for energy production, particularly for hydrogen production. By use of microorganisms, hydrogen can effectively be obtained from wood and marine biomass according to purposes. Biomass (i.e., organic matter) such as marine macro algae can be degraded biologically. The use of seaweeds as energy crops have certain advantages: the need for large land areas (which may not be available) is avoided; marine crop yields are expected to be considerably higher than land crop yields although experience from large-scale cultivation is lacking; seaweeds do not contain lignin, which is almost non-degradable under anaerobic conditions; and many valuable extracts, such as alginate, can be extracted from the waste, which is important to environmental protection.

Recent research has shown that the red algae *Gelidium amansii* and the brown algae *Laminaria japonica* are both potential biomass sources for biohydrogen production through anaerobic fermentation. The objective of this review article is to give an overview of marine algae as a prospective source for biohydrogen production.

Keywords Biohydrogen • Marina macro algae • Anaerobic fermentation

11.1 Introduction

Over the past 50 years, the world's population has more than doubled, coupled with an expectation of a higher standard of living and an ever-increasing economic output this has resulted in a large increase in primary energy consumption, particularly the

İ. Şentürk (✉) • H. Büyükgüngör
Department of Environmental Engineering, Faculty of Engineering,
Ondokuz Mayıs University, Atakum, Samsun 55139, Turkey
e-mail: ilknurg@omu.edu.tr; hbuyukg@omu.edu.tr

A. Veziroğlu and M. Tsitskishvili (eds.), *Black Sea Energy Resource Development and Hydrogen Energy Problems*, NATO Science for Peace and Security Series C: Environmental Security, DOI 10.1007/978-94-007-6152-0_11,

use of fossil fuel-derived energy. In 2010, world primary energy consumption grew by 5.6 %, the largest percentage growth in almost 40 years. This growth included an increase in the consumption of all major fossil fuels including oil, natural gas and coal. This trend in increasing energy consumption is expected to continue as the world's population is projected to increase by an additional 1.4 billion people by 2030, and have an increase of 100 % of the world's real income. These increases will put enormous pressure on the finite supply of fossil fuel-based energy, exacerbating global concerns over energy security, fossil fuel-based environmental impacts such as climate change, and the rising cost of energy and food. The utilization of current energy sources has been generating environmental pollution of air, water and soil through the years. These negative effects have increased interest in the development of new technologies to obtain clean energy, mainly through the utilization of renewable energy sources [1]. Currently, the world consumes about 15 TW of energy per year and only 7.8 % of this is derived from renewable energy sources [2].

Hydrogen is seen as a future energy carrier. The recent rise in oil and natural gas prices and global awareness of increasing CO_2 levels in the atmosphere has drawn attention to renewable energy including hydrogen produced from renewable sources [3]. Hydrogen is a clean and renewable energy source that does not produce carbon dioxide as a by-product, when used in fuel cells for electricity generation [4]. Biomass can also be used as a substrate for energy production, particularly for hydrogen production. By use of microorganisms, hydrogen can effectively be obtained from wood and marine biomass according to purposes [5]. Biological hydrogen production from biomass is considered one of the most promising alternatives for sustainable green energy production and important solution to a sustainable power supply and is nowadays being seen as the versatile fuel of the future, with potential to replace fossil fuels [6]. With the development and commercialization of fuel cells, hydrogen production from biomass is being considered as an alternative energy source for decentralized power generation [4]. Hydrogen fermentation of conventional waste, such as food waste and high-strength wastewater, is an environmentally friendly treatment with the additional benefit of hydrogen production. However, the amount of hydrogen production using the leftover biomass is not sufficient for a H_2-based economy [7]. Although hydrogen biogas can be efficiently produced at the laboratory level, there is no known commercially operating hydrogen from biomass production facility in the world today [4]. The feasibility of hydrogen fermentation as a mainstream technology in the near future depends on the utilization of carbohydrate-rich, economical, and sustainable biomass [7].

Till early 2000s, the production of the 1st and 2nd generation biofuels that use edible agricultural crops (sugarcane, sugar beet, wheat, etc.) and lignocellulosic waste biomass (hardwood, softwood, grasses, agricultural residues) as a feedstock, respectively, have been considered an environmentally friendly way [8]. It was estimated that this growth of terrestrial biomass and the replacement of fossil fuels by renewable energy would significantly reduce the greenhouse gases emissions. Global warming has become one of the most serious environmental problems.

To cope with the problem, it is necessary to substitute renewable energy for nonrenewable fossil fuel. Biomass, which is one of the renewable energies, is considered to be carbon-neutral, meaning that the net CO_2 concentration in the atmosphere remains unchanged [9]. Biofuel is a renewable energy source produced from biomass, which can be used as a substitute for petroleum fuels. The benefits of biofuels over traditional fuels include greater energy security, reduced environmental impact, foreign exchange savings, and socioeconomic issues [10].

Owing to its environmentally friendly aspect in producing H_2, biological H_2 production has recently gathered considerable attention. In particular, fermentative hydrogen production is considered a promising method, since it is technically simpler and its H_2 production rate is much faster than other approaches. In addition, organic pollutants could be degraded along with H_2 production [8].

This short review study focuses on the research involved in generating hydrogen using algae as a renewable energy resource. Due to the decline in fossil fuel resource, the energy derived from biomass seems to be the only major source of world's renewable energy. The hydrogen derived from algae is promising due to its sustainability. There are no greenhouse gas emissions during the combustion of hydrogen, and security of its supply even at remote places. The novel approach of generating hydrogen at commercial scale from algae has been a curiosity among many researchers till today. The generation of hydrogen from algae is still at research level. Hence, this review would be an eye opener for researchers who are interested in generating hydrogen from algae. The renewable technology has garnered great importance due to high raise in oil price and global warming. The energy derived from biofuels especially algae in receiving more and more attraction in recent years [11].

11.2 Biohydrogen Production from Marine Macro Algae

Macrophytic marine algae, commonly known as seaweeds, are nonvascular, multicellular, photosynthetic "marine plants" that inhabit the coastal regions of ocean waters, commonly within rocky intertidal or submerged reef-like habitats. Unlike microscopic algae (micro algae), seaweeds generally live attached to rocky substrates on the ocean bottom and can assume considerable anatomical complexity and intricate life histories. The three major divisions of marine macro algae are brown algae, red algae and green algae, which together encompass over 7,000 species. In the rocky intertidal marine environment, competition for light, nutrients, and space is fierce and much marine seaweed have evolved chemical defense mechanisms to ward off predators and enhance survival [12].

The idea of using marine biomass for energy was first conceived by Howard Wilcox in 1968. At that time, the marine biomass energy program was conducted jointly among governmental organizations, universities, and private corporations in the United States until 1990. The program proposed using giant brown kelp (*Macrocystis pyrifera*) as a cultivation species, which is a kind of brown algae

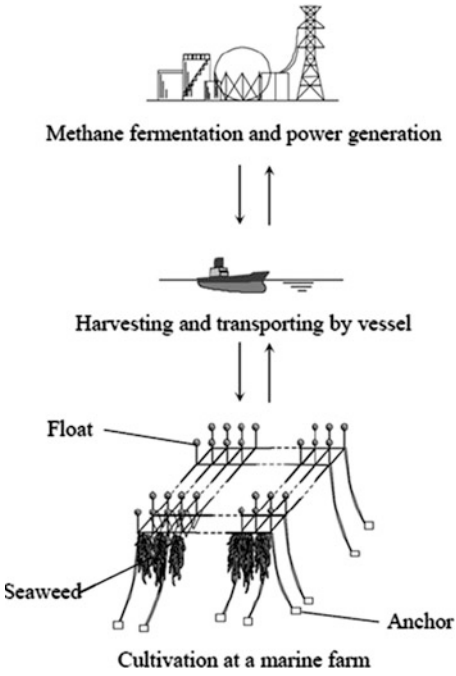

Fig. 11.1 Illustration of energy production from marine biomass

that grows rapidly and may reach up to 43 m long. In Japan, research on energy production from marine biomass was conducted from 1981 to 1983. Figure 11.1 shows of energy production from marine biomass. Seaweeds are cultivated at an offshore farm and then harvested and transported by vessels [9].

If the sea area is utilized efficiently, a vast amount of renewable energy could be produced. In addition, native seaweeds often form submarine forests that serve as habitats for fish and shellfish, and so if a marine biomass energy system is realized, it may boost the production of marine food and promote the marine energy industry leading to CO_2 mitigation. The use of marine biomass energy was investigated in the United States and Japan as an alternative energy in the 1970s after the oil crises, but the studies were discontinued when oil prices stabilized. However, now that global warming has become one of the most serious problems to be solved, we should reconsider the use of marine biomass energy as a means to mitigate CO_2 emissions [9].

Marine biomass has attracted less attention than terrestrial biomass for energy utilization so far, but is now called "the 3rd generation biomass" is paid most attention as the promising alternative renewable sources for biofuel production [8]. Biomass (i.e., organic matter) such as marine macro algae can be degraded biologically. Seaweeds, referred to as marine macro algae, mainly include red, brown, and some green algae. The use of seaweeds as energy crops have certain advantages: the need for large land areas (which may not be available) is avoided; marine crop yields are expected to be considerably higher than land crop yields although experience from large-scale cultivation is lacking [4] seaweed contains almost no non-degradable lignins, which are almost non-degradable under anaerobic

Table 11.1 Comparison of H_2 production using marine seaweed

Feedstock	Inoculum	Culture type	Temperature	pH	H_2 yield	References
Laminaria japonica (do thermal treatment)	Heat treated anaerobic sludge	Batch	35 °C	7.5	28 ml/g dry algae	[4]
Gelidium amansii	The seed sludge from an anaerobic digester	Batch	35 ± 0.1 °C	>5.5	0.518 L H_2/gVSS/d	[7]
Laminaria japonica	The seed sludge from an anaerobic digester	Batch	35 ± 0.1 °C	8 ± 0.1	67.0 mL H_2/g TS	[8]
Laminaria japonica (no pretreatment)	Heat treated anaerobic sludge	Batch	35 ± 0.1 °C	7.5	71.4 mL H_2/g TS	[17]

conditions and thus sugars can be obtained without expensive pretreatment for lignin removal; and many valuable extracts, such as alginate, can be extracted from the waste, which is important to environmental protection [4, 7, 13]. The CO_2 capture rate of marine algae is higher than that of terrestrial biomass. For example, *Laminaria japonica* (4,800 g C/m^2/year) has more than a twofold higher CO_2 utilization rate of tropical rainforests (2,000 g C/m^2/year) [8]. The marine biomass energy system is, therefore, one of the potential countermeasures for global warming mitigation. The use of marine biomass for energy may also have the advantage of providing good fisheries. However, problems still remain to be solved. Example; an economical and energy-saving by-product extraction process should be developed. Cultivation techniques for rapid growth of seaweeds and energy-saving drying process are also important [9]. Due to the complex composition of seaweeds, complete degradation of the material necessitates the presence of microorganisms with a broad substrate range. During anaerobic degradation of organic material, energy carriers such as hydrogen and methane may be produced. This is particularly true for the cell wall of brown algae, which contain cellulose, alginates, sulfated fucans, and protein. As a result of this carbohydrate content, brown seaweeds can be a potential source for the production of hydrogen and methane [4]. The results obtained with other species of algae are given in Table 11.1. So far, however, most of studies were focused on producing bioethanol and biodiesel. Scarce researches has been conducted to use 3rd generation biomass for fermentative hydrogen production [8].

Algae can be classified as either micro algae or macro algae based on morphology and size. Micro algae are microscopic organisms while macro algae are typically composed of multicellular plant-like structure, like giant kelp. Although macro algae can look similar to land plants, these organisms in fact do not have the same lignin crosslinking molecules in their cellulose structures because they grow in aquatic environments where buoyancy allows for upright growth in the absence

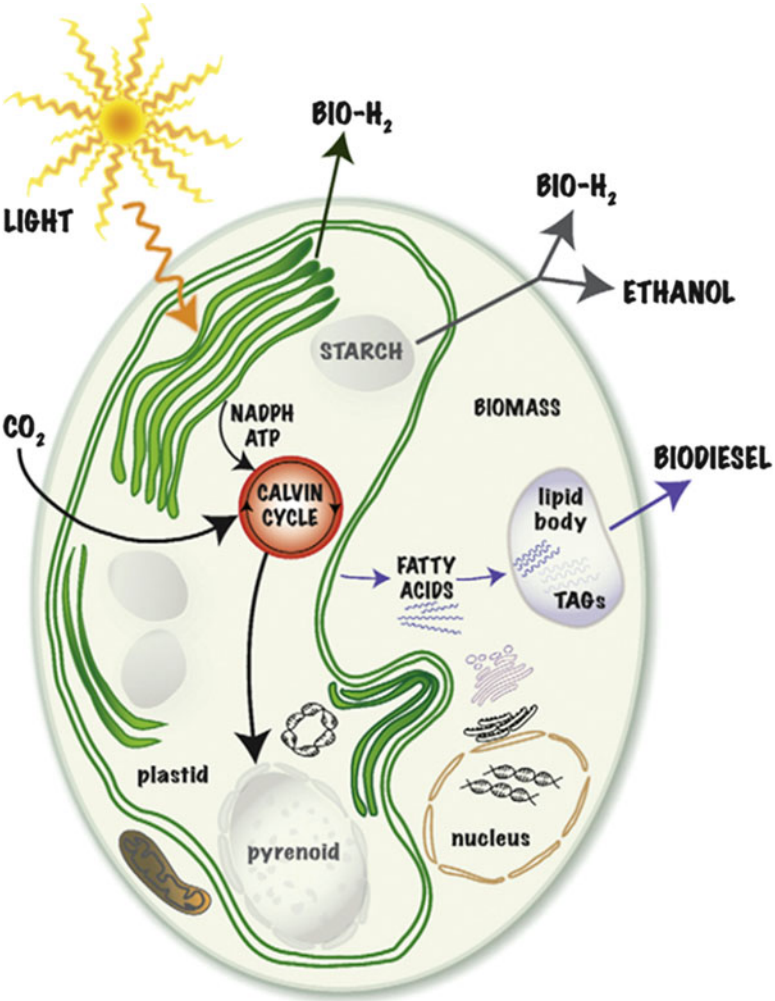

Fig. 11.2 Metabolic pathways in green algae related to biofuel and biohydrogen production [15] (*see color plates*)

of the lignin crosslinking. While having a low lignin content, macro algae contain significant amount of sugars (at least 50 %) [2] that could be used for biofuel and biohydrogen production through anaerobic fermentation. Macro algae or "seaweeds" are multicellular plants growing in salt or fresh water. Macro algae are classified into three broad groups based on their pigmentation: (1) Brown seaweed (*Phaeophyceae*); (2) red seaweed (*Rhodophyceae*) and (3) green seaweed (*Chlorophyceae*) [7, 10, 14]. Some species of red seaweed such as those belonging to the genera *Gelidium, Gracilaria,* and *Euchema* are known for high carbohydrate content [7]. This also allows enormous potential as an excellent source for biohydrogen production. Figure 11.2 shows metabolic pathways in green algae related to biofuel and biohydrogen production [15].

In the past few years, most algae biofuel research has focused on liquid fuels, particularly those that can replace transportation fuels such as biodiesel and bioethanol; however, algae are also a potential source of commercial biohydrogen and biogas (biomethane) used as a gas fuel or for electricity generation [2]. Macro algae are a potential source of biomass for the production of these gases due to their fast growth rates, ability to grow in oceanic environments and their lack of the structural lignin which is typically difficult to digest. Many species of macro algae are known for having high levels of carbohydrate, although in many cases these carbohydrates consist of nonglucose monosaccharides such as galactose [2]. Various seaweeds have been considered to be potential energy crops: *Macrocystis pyrifera*, *Laminaria, Gracilaria, Sargassum, Ulva,* etc. These seaweeds have a high productivity which is required for energy production. Recent research has shown that the red algae *Gelidium amansii* and the brown algae *Laminaria japonica* are both potential biomass sources for biohydrogen production through anaerobic fermentation, but bioprospecting of macro algae for their fermentative future continues. The marine algae are considered an important biomass source; however, their utilization as energy source is still low around the world. The technical feasibility of marine algae utilization as a source of renewable energy was studied to laboratory scale [4]. It will be also necessary to optimize pretreatment methods for maximum biohydrogen production. Many studies have focused on determining the optimal pretreatment conditions (thermal, ultrasonic, acidification, and alkaline pretreatments) for improving the solubilization of algal biomass and waste activated sludge [4, 16]. Although hydrogen production from algae still seems years away from commercial viability, continued progress in this area shows its ultimate potential [2].

11.3 Conclusions

The marine algae are considered as an important biomass source; however, their utilization as energy source is still low around the world. The technical feasibility of marine algae utilization as a source of renewable energy was studied to laboratory scale. Hydrogen can be produced from various marine macro algae quite simply by batch cultures.

Security of abundant, carbohydrate-rich, economical, and sustainable biomass determines the practicability of hydrogen fermentation processes. Seaweeds are regarded as alternative non-food sources for bioenergy production, especially for nations having limited land for energy crop cultivation such as East Asian countries. The renewable technology has also garnered great importance due to high raise in oil price and global warming. The energy derived from biofuels especially algae in receiving more and more attraction in recent years.

References

1. Vergara-Fernandez A, Vargas G, Alarcon N, Velasco A (2008) Evaluation of marine algae as a source of biogas in a two-stage anaerobic reactor system. Biomass Bioenerg 32:338–344
2. Jones CS, Mayfield SP (2011) Algae biofuels: versatility for the future of bioenergy. Curr Opin Biotechnol 23:1–6
3. Bahadir T, Buyukgungor H (2010) Biyokütleden Hidrojen Üretimi. Katı Atık ve Çevre 79:33–40
4. Park J, Lee J, Sim SJ, Lee JH (2009) Production of hydrogen from marine macro-algae biomass using anaerobic sewage sludge microflora. Biotechnol Bioprocess Eng 14:307–315
5. Bahadir T, Buyukgungor H (2010) Hydrogen production with biological methods. In: 5th International Ege Energy Symposium and Exhibition (IEESE-5), Denizli, 27–30 June 2010
6. Guler Senturk I, Buyukgungor H (2010) Biyohidrojen Üretim Yöntemleri ve Kullanılan Farklı Atık Materyallerin İncelenmesi. Sigma Mühendislik ve Fen Bilimleri Dergisi 28(4):369–395
7. Park JH, Yoon JJ, Park HD, Kim YJ, Lim DJ, Kim SH (2011) Feasibility of biohydrogen production from *Gelidium amansii*. Int J Hydrog Energy 36:13997–14003
8. Jung KW, Kim DH, Shin HS (2011) Fermentative hydrogen production from *Laminaria japonica* and optimization of thermal pretreatment conditions. Bioresour Technol 102:2745–2750
9. Yokoyama S, Jonouchi K, Imou K (2007) Energy production from marine biomass: fuel cell power generation driven by methane produced from seaweed. World Acad Sci Eng Technol 28:320–323
10. Demirbas A (2010) Use of algae as biofuel sources. Energy Convers Manag 51:2738–2749
11. Vijayaraghavan K, Karthik R, Kamala Nalini SP (2010) Hydrogen generation from algae: a review. J Plant Sci 5(1):1–19
12. Rorrer GL, Cheney DP (2004) Bioprocess engineering of cell and tissue cultures for marine seaweeds. Aquac Eng 32:11–41
13. Lee JH, Lee DG, Park J, Kim JY (2010) Biohydrogen production from a marine brown algae and its bacterial diversity. Korean J Chem Eng 27(1):187–192
14. Demirbas A, Demirbas MF (2011) Importance of algae oil as a source of biodiesel. Energy Convers Manag 52:163–170
15. Beer LL, Boyd ES, Peters JW, Posewitz MC (2009) Engineering algae for biohydrogen and biofuel production. Curr Opin Biotechnol 20:264–271
16. Guler Senturk I, Buyukgungor H (2010) Atıksu Arıtma Çamurlarından Enerji Eldesi. In: International sustainable water and wastewater management symposium, Konya, 26–28 Oct 2010
17. Shi X, Jung KW, Kim DH, Ahn YT, Shin HS (2011) Direct fermentation of *Laminaria japonica* for biohydrogen production by anaerobic mixed cultures. Int J Hydrog Energy 36:5857–5864

Chapter 12
Approaches to Aquatic Ecosystems Organic Energy Assessment and Modelling

Viktor Moshynsky and Olhga Riabova

Abstract The energetic potential of each water reservoir is formed by main components: solar power, gravitational energy, energy of environmental matter (cosmic, chemical, etc.) and biomass production energy processes. However, the energy contained in biomass producents is an important component of the energy balance of any aquatic ecosystem. Autotrophs production (primary production) is the only process of organic matter formation from inorganic compounds and therefore the energy of the primary products is the only source and indicator of biological energy loading in aquatic ecosystems.

Gathering information about the total annual primary production of biomass and about temporal dynamics of primary biomass is the basis for trophic and energetic process management in freshwater bodies and seas.

We have developed the conceptual approaches and mathematical model for potential energy of organic matters in natural systems assessment which allows the user to calculate on the basis of climatic and hydrochemical monitoring data the total amount of primary biomass within water volume or surface square units. The use of such approaches for energy potential estimation for the Black Sea unconventional power engineering purposes will allow elaborating a new effective management technique for energetic strategy and for environmental protection.

Keywords Mathematical model • Biomass • Primary production • Aquatic ecosystem • Assessment

V. Moshynsky (✉) • O. Riabova
National University of Water Management and Natural Resources Use,
33000, Soborna Str. 11 Rivne, Ukraine
e-mail: v_moshynsky@ukr.net; olha.riab@gmail.com

A. Veziroğlu and M. Tsitskishvili (eds.), *Black Sea Energy Resource Development and Hydrogen Energy Problems*, NATO Science for Peace and Security Series C: Environmental Security, DOI 10.1007/978-94-007-6152-0_12,

12.1 Introduction

Problems of modern power engineering and natural resources disposal put forward the task of designing an exclusive concept and scientific principles for the efficient management of productivity and environmental condition of ecological systems.

The experience of natural and semi-natural ecosystems exploration shows, in general [1–4], that the problem of reliable analysis, evaluation and management can be performed with sufficient reliability only on the basis of simulation modelling by creating the mathematical model (models) of the researched system.

One of the most actual problems of modern nature sciences is the issue of the correct assessment of matter value, features and energy potential of natural systems having different level of anthropological shifts and including aquatic ecosystems. Various researchers proposed different approaches and criteria for such evaluation [5–8].

The energetic potential of water reservoir is formed by such components: solar power, gravitational energy, energy of environment matter (cosmic, chemicals, etc.) and energy of biomass production processes [9]. The energy containing in the biomass producents is an important component of the energy balance of any aquatic ecosystem. Autotrophic products (primary production) are the only process of formation of organic matter from inorganic and therefore the energy of the primary products is the one source of biological energy in aquatic ecosystems.

Getting information on the amount and temporal dynamics of the primary biomass is the basis for the management of trophic and energy processes in freshwater bodies and seas.

Concerning biological, kinetic, biochemical and other types of energy nowadays scientists developed a number of different mathematical models [10–13] most of which use a system of differential equations of motion in three dimensions. As the management practice of the natural systems shows [14, 15], good results can be achieved in case of combining data monitoring analysis via sophisticated functional models with more simple simulation models. We have developed the conceptual principles and a simplified mathematical model for evaluating the biotic potential of natural systems that allows on the basis of climatic and hydro chemical monitoring compute the volume of primary biomass [15]. Using such approaches in evaluating the energy potential of the Black Sea will develop effective management techniques in energy and protection of its natural potential.

12.2 Criteria and Conception of Aquatic Ecosystem Organic Energy Potential Evaluation

For the most objective assessment of aquatic ecosystems it is necessary to establish and justify the criterion of evaluation. Complex analyses showed that in the context of studies the most environmentally and economically justified main criterion of

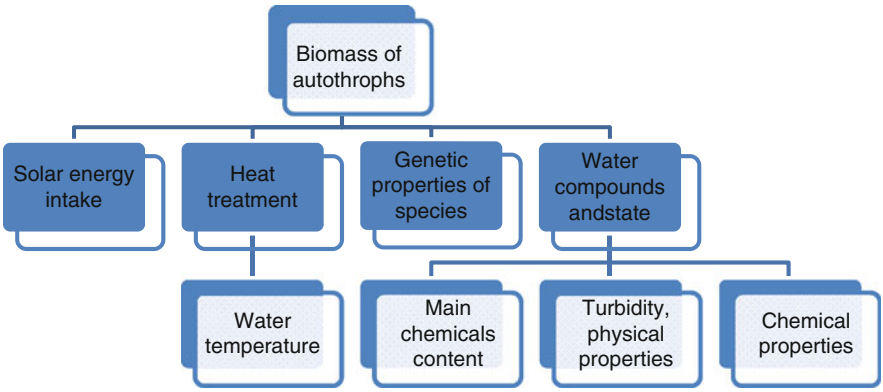

Fig. 12.1 Conceptual chart of water autothrophs biomass production (*see color plates*)

the ecosystem indicator is the intensity of the production of primary producent biomass, in other words, *primary organic potential* of ecosystem.

The most fundamental systematic research of the twentieth century [1–5, 13, 14] was dedicated to the study of energy-entropy aspects of living matter. It was established that the leading role in directing energy flows and its transformation play photosynthetic organisms due to: (1) the transformation of mineral substances into organic production and molecular oxygen by photosynthesis [1, 3], (2) accumulation in phytomass of a lot of potential energy (value of assimilated energy in one order of magnitude is lower on each next trophic level) [1, 4], (3) cyclical growth of energy stock due both to phytomass increase and dead organic matter energy transformation into other forms, and (4) the manifestation of the negentropy effects that in contrast to the second law of thermodynamics provides an increasing ecosystem organization level [2, 5], (5) both environmental status and ecosystem anthropization degree indication.

The primary organic potential of aquatic ecosystems is a meaningful value and depends on many factors of natural and anthropogenic origin and the degree and nature of their interaction in the system: *water – organism – atmosphere- radiation* (short- and long-wave) *and thermal energy* [15]. This approach makes it possible to identify four main factors that consider both elements (components) of the studied system (Fig. 12.1):

1. Water compounds and state (g),
2. Solar energy intake (l),
3. Heat treatment (heat treatment in atmosphere and water) (t),
4. Biological (genetic) properties of species (morphological and biological characteristics of species or group of species) (b).

Then, in general, the model of the specific productivity of individual species or species group has the form:

$$y = f(g, l, t, b) \tag{12.1}$$

12.3 Model Structure

12.3.1 Main Operators

According to (12.1) the following suggestion can be made: different components of the system make various contribution to objective criteria formation – phytomass value. Moreover, it is obvious that the impact of every element on the producents efficiency is the time-varying function for intensity degree (measure) of external influences on each element and the entire system. Therefore, the search for the main operator type was fulfilled taking into account the principal rules and consequences of *measure theory*.

Let's write the function, providing some desired bonds (12.1), as $y = f(x)$ and we remember that it is observed and bounded on the limited interval $[a,\ b]$ so A and B are respectively its lower and upper pointwise limits. By writing Ω^i ensemble of points $[a,\ b]$ of interval x where $y_{i-1}(x) \le y_i$ we can discover two sums called Lebesgue integral sums:

$$\sum_{i=1}^{n} y_{i-1}\mu\left[\Omega^i\right] \quad \text{and} \quad \sum_{i=1}^{n} y_i\mu\left[\Omega^i\right] \tag{12.2}$$

Thus, measure function is a finitely additive set function, from which countably additive finite measure can be calculated [16], i.e., a certain number $\Omega^i \subset \Omega$ can be referred to any subset Ω. Therefore, the whole space measure equals μ_Ω.

It is important to mention that other mathematical spheres also use laws analogous to Lebesgue integral sums [15, 17].

If the whole space measure is equal to one, such kind of measure is called *truth degree* or judgmental probability [16]. This type of measure interpreting is the most comfortable for usage and that is the reason of our putting it into practice. When $\Omega^i \subset \Omega$ take on certain values (become number parameter sets and system variables) the truth degree calculated from them is called *weight*.

In spite of its strong validity and relative simplicity, the above described scheme has an essential fault – it is static. Let's improve it by time introducing.

Supposedly, we'll take solutions set Y $(y_i \in Y)$ of mathematical model. There is a certain two-parameter transformation observed $\varphi_{\tau,t}$ provided introduced measure γ_y is analogous to Ω. If τ and t have been identified with the time points and assumed that $Y = \Omega$, parameters Ω and $\varphi_{\tau,t}$ are considered to be dynaset [16, 17]. If $\Omega^i_\tau \subset \Omega$; $\Omega^i_t \subset \Omega$ then time dependent values should be observed within dynamic measure theory

$$Y^i_t = \Omega^i_t = \Omega^i_\tau \varphi_{\tau,t} \quad \text{i} \quad \mu_{\Omega^i_t} = \mu_{\Omega^i_\tau} U_{\tau,t} \tag{12.3}$$

where $U_{\tau,t}$ is an operator impacting measure.

The above given laws (12.2) and (12.3) are of universal character and can be applied for the mathematical modelling of wide range of issues related to actual and abstract systems formalization and modelling [15–17], and the observed aquatic system consequently.

In consideration of the above mentioned, it has been suggested [17] to use the laws of the type (12.2) and (12.3) as a means of basic modelling operators for the creating ecosystem producing behavior simulated mathematical model.

Therefore, the basic operators of the model can be formulated as the following Lebesgue measure equation for the discrete objective function:

$$y_e = \varsigma_\alpha y_\alpha + \varsigma_s y_s, \tag{12.4}$$

$$y_\alpha = \alpha_l y_l + \alpha_g y_g + \alpha_t y_t + \alpha_b y_b, \quad y_e = \overline{0,\ y_b}, \tag{12.5}$$

where y_e is a specific value of primary biomass, g/m^3;

ς_α and ς_s are weighting coefficients that define involvement degree of cumulative effects in phytoproductivity factors impact, $\varsigma_\alpha + \varsigma_s = 1$;

y_α – weight constituent of productivity item, g/m^3;

y_s – phytoproductivity in the context of cumulative effects of the organism life factors;

$y_f \supset \{y_l,\ y_g,\ y_t,\ y_b\}$ – biomass constituents provided by the light, trophicity and water conditions, heat, biological peculiarities of phytocenosis respectively. $y_b = const$ is defined by the potential (maximum) productivity abilities of phytocenosis, g/m^3.

$\alpha_f \supset \{\alpha_l,\ \alpha_g,\ \alpha_t,\ \alpha_b\}$ – are weighting coefficients (involving degree in the objective function formation) of light, trophicity and water conditions, heat, biological peculiarities of the species or cenosis, $\sum_{f=1}^{4} \alpha_f = 1$.

The component g is a complex subsystem. Phytoproductivity provided by the aquatic environment should also be calculated as Lebesgue measure

$$y_{g\tau} = \sum_{p=1}^{n_p} \gamma_p y_{p\tau}, \tag{12.6}$$

$y_{p\tau}$ – biomass value by p index calculated by Eq. (12.10), $p = \overline{1,\ n_p}$ g/m^3;

γ_p – weight constituent of variables, $\sum_{p=1}^{n_p} \gamma_p = 1$.

12.3.2 Response Operator

We have used logistic equation [18–21] as a universal model basis of species response to the main life factors impact. Considering the assumption that function of increasing intensity within $0 \leq x_i \leq x_i^*$ interval (where x_i is a variable real value, x_i^* is a variable optimal value on i stage of model discretization) is proportional to the phytomass value; accumulated phytomass declines (under the deviation from x_i^*) proportionally to environment resource $S = y_b - y$; for every value of independent variable x there is actual and unique value of dependent variable y. Logistic growth equation can be written as follows

$$y = \frac{y_0 y_b}{y_0 + (y_b - y_0)\, e^{-\mu x}}, \tag{12.7}$$

where y_0 is the characteristic of organism fitness to the variable influences which is explained as some initial phytomass value when $x = 0$, $y_0 = \overline{0,\ y_b}$.

Because of the tolerance (response) submodel requirements, especially the necessity to consider the factor of negative influence excess, we have to improve the formula (12.7), by introducing exponential cofactor which is analogous to Mitscherlich equation [22]:

$$y = \frac{y_0 y_b\, e^{-kx^2}}{y_0 + (y_b - y_0)\, e^{-\mu x}}, \tag{12.8}$$

where k is the characteristic of the function of rate of decay on the interval $x^* \leq x < \infty$, $k = \overline{0,\ 1}$.

Considering that optimum position is different for every variable model and changes in ontogenesis [23–25], the necessity of introducing additionally one more parameter λ, the latest being explained as x's optimum position characteristic ($\lambda = \overline{-x_{\max}, +x_{\max}}$). Moreover, to both simplify model and reduce dependence of parameters y_0 and y_b, we shall change those parameters in the dependence denominator (12.8) into constants. Thus, response operator:

$$y = \frac{y_0 y_b\, e^{-k(x-\lambda)^2}}{1 + (100 - y_0)\, e^{-\mu(x-\lambda)}}. \tag{12.9}$$

Function (12.9) has been testified on the whole interval of its value. The typical curve shapes drawn on the formula (12.9) are shown on Fig. 12.2.

12.3.3 Partial Value Productivity Operator

Since partial phyto-productivity values y_l, y_t, y_p are the quantities that depend not only on instant values of variables l, t and p but also on the previous behavior of

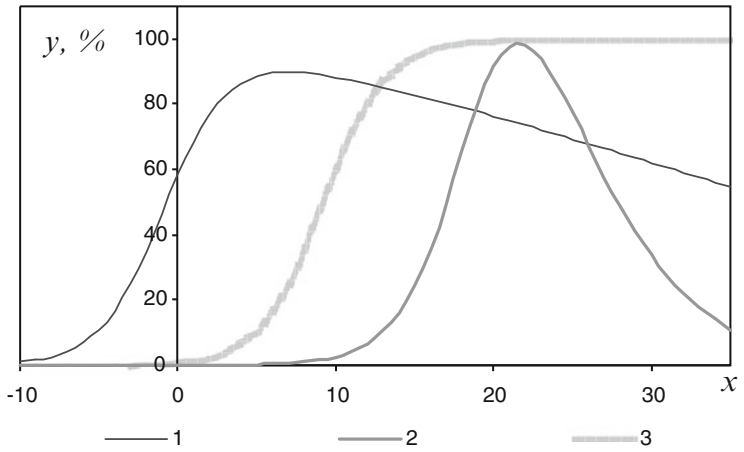

Fig. 12.2 The main types of response curves constructed for dependence (12.9)
1 – curve with parameters: $\mu = 0.5$; $k = 0.0003$; $\lambda = -10$; $y_0 = 1$
2 – curve with parameters: $\mu = 0.5$; $k = 0$; $\lambda = 0$; $y_0 = 1$
3 – curve with parameters: $\mu = 0.5$; $k = 0.0005$; $\lambda = 10$; $y_0 = 2.5$

these variables within the observed system occurred during present period of vegetation and in the past, we shall define these quantities considering growth history and phytocenosis development according to the equation system.

$$y_{ltp} = \frac{\sum_{i=1}^{n} \nu_i y_{ij}}{\sum_{i=1}^{n} \nu_i}, \tag{12.10}$$

where y_{ij} – partial productivity, calculated for j variable on the i stage model discretization;

ν_i – weight coefficients by the i stage of model discretization (provided for every species depending on the phases of organism growth);

n – number of model discretization stages during vegetation;

$$y_{ij} = \frac{y_b y_{0ij} \exp\left(-k_{ij}(x_{ij} - \lambda'_{ij})^2\right)}{1 + (100 - y_{0ij}) \exp\left(-\mu_{ij}(x_{ij} - \lambda'_{ij})\right)}, \tag{12.11}$$

where x_{ij} is the value of j variable at the i stage of model discretization;

μ_{ij}, k_{ij}, y_{0ij} are the characteristics of the response function for j variable (for energetic variables determined at the end of the vegetation);

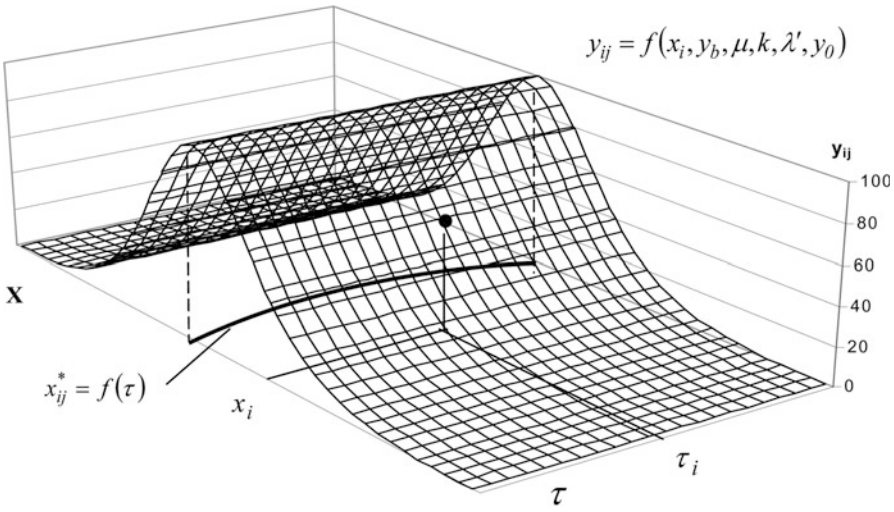

Fig. 12.3 Three dimensional chart of y_{ij} computation

λ'_{ij} – optimum position parameter for j energetic variable at the i stage of model discritization

$$\lambda'_{ij} = \lambda_j - (x^*_j - \widehat{x}^*_{ij}), \tag{12.12}$$

where λ_j is the characteristic of the response curve starting optimum position of j variable (for energy variables);

x^*_j – optimal meaning of j energetic variable at the end of vegetation;

$\widehat{x}^*_{ij}$ – current optimal value of j energetic variable at the i stage of discretization calculated by the spatial submodel of energy variables optimal meaning behavior.

The value y_{ij} determining principle has been shown in Fig. 12.3 as the specification of crossing point of the line with coordinate x_i, τ_i and three-dimensional surface formed by response curve after its moving along the time axis.

12.3.4 Cumulative Effects Modelling

The occurrence of cumulative effect by the producent life aggregate impact [24, 25] is a problem of great concern preventing from production processes modelling in

natural systems. We have developed a special submodel. By means of two operators it is able to simulate a cumulative effect from the influence of infinite number of variables defining ecosystem features. It is all done with the efficient adequate level for practice.

In order to obtain update values of physical and mathematical miscellaneous variables of the observed general model, in the given submodel the values of variables and objective criteria (*primary organic potential*) are given relatively to the optimum meanings of variables and maximum productivity observations (y_b). To describe cumulative effect we have applied *productivity factors interaction relative index* $q = \overline{0,\ 1}$.

The output calculation of cumulative effect is made by the response function which, after parameters value substitution, is as follows:

$$y_s = \frac{y_b\, 0.08 \exp\left(-1.66\,(q-0.24)^2\right)}{0.01 + 0.92 \exp\left(-4.992\,(q-0.24)\right)}, \quad y_s = \overline{0,\ y_b}. \tag{12.13}$$

12.4 Conclusions

The provided mathematical model is not a silver bullet for aquatic ecosystem problems solution but it enables to solve some of following scientific and applied problems:

1. Biomass value of photosynthesizing aquatic organisms, natural and semi-natural aquatic phytocenosises defining and forecasting.
2. Estimating past, present and future condition of the water bodies by calculated and predicted productivity.
3. Defining rational strategies of water body performance management with the help of effective mathematical testing by the on-line data computer processing as well as on long-term basis, in order to obtain optimal organic energetic storage and maximum water body efficiency, to resist reservoir and sea eutrophication processes, algal bloom dynamics control.
4. Explaining the data of hydrochemical, hydrobiological and climatological monitoring correctly.
5. Applying monitoring data for the needs of alternative power industry and Black Sea resources protection.
6. Estimating freshwater body and sea biological power resources stock.
7. Examining engineering construction projects that influence water body power resources.

The above mentioned general statements and the mathematical model structure itself show a high potential of the latter from the aquatic ecosystem ecological condition point of view, predicting and managing their organic energy potential.

The specification (calibration) and verification of the given model for the conditions of certain types of terrestrial ecosystems [15] have provided sufficient convergence of modeling and experimental primary production values.

At this development stage, the model requires modification taking into account sea and fresh water ecosystem features. Especially regarding transition operators from biomass to specific volume within the whole ecosystem and its trophic levels, issues of tolerance operators parameterization for phytoplankton, tasks of input, output dimensional explanation etc.

We hope that international cooperation and joint efforts of researchers from different branches will enable to overcome previously mentioned problems in the nearest future and the given model will be applied in data base creation and receiving new information about natural and semi-natural aquatic ecosystems.

References

1. Odum HT (1996) Environmental accounting: energy and environmental decision making. Wiley, New York, pp 150–300
2. Whittaker RH (1970) Communities and ecosystems. Miscellaneous. Communities and ecosystems, Macmillan, New York, 102–136
3. Hall CAS, Day JW (1977) Ecosystem modeling in theory and practice: an introduction with case histories. Wiley, New York, pp 225–458
4. Reynolds CS (1997) Vegetation processes in the pelagic: a model for ecosystem theory. Ecology Institute, Cumbria, pp 85–102
5. Straskraba M, Gnauck AH (1985) Freshwater ecosystems. Elsevier, New York, pp 98–310
6. Thomas IG, Elliott M (2005) Environmental impact assessment in Australia: theory and practice. Federation Press, Sydney, pp 85–262
7. Moshynsky V (2001) Modern water conditions in the Northwest part of Ukraine: an analysis. Water Eng Manag. Des Plaines IL USA, 148(4):22–26
8. Engel S, Pagiola S (2008) Designing payments for environmental services in theory and practice: an overview of the issues. Ecol Econ 65(4,1):663–674
9. Haase G (1978) Zur Ableitung und Kennzeichnung von Naturpotentialen. In: Petermanns Geographische Mitteilungen 122(2):113–125
10. Беляев ВИ, Совга ЕЕ (1991) Математическая модель экосистемы сероводородной зоны Черного моря. Морской гидрофизический журнал 6:42–53
11. Любарцева СП, Михайлова ЭН, Шапиро НБ (1999) Экологическая трехмерная численная модель Черного моря. Сезонная эволюция экосистемы эвтрофической зоны. Мор. гидрофиз. журн. Севастополь 5:55–80
12. Огуз Т, Дорофеев ВЛ, Коротаев ГК (2007) Моделирование экосистемы Черного моря. Мор. гидрофиз. журн. Севастополь 1:59–72
13. Виноградов МЕ (1989) Динамические модели пелагических экосистем. Модели океанических процессов. Наука М. 252–259
14. Израэль ЮА, Цыбань АВ (1989) Антропогенная экология океана. Флинта Наука М 59–255
15. Мошинський ВС (2005) Методи управління продуктивністю та екологічною стійкістю осушуваних земель: монографія. Рівне НУВГП 42–240
16. Federer H (1996) Geometric measure theory. Springer, New York, pp 88–354
17. Брусиловский Б.Я (1977) Теория систем и система теорий. Вища школа. К. 65–110

18. Maximov VN, Kaitala S (1986) The desirability function in evaluation of the response of phytoplankton communities to toxicants. Tox Assess Int Q 1(1):85–101
19. Potvin C, Lechowicz M, Tardif S (1990) The statistical analysis of the physiological response curves obtained from experiments involving repeated measures. Ecology 71(4):1389–1400
20. Peek MS, Russek-Cohen E, Wait AD, Forseth IN (2002) Physiological response curve analysis using nonlinear mixed models. Ecologia 132(2):175–180
21. Tao L, Granta RF, Flanaganb LB (2004) Climate impact on net ecosystem productivity of a semi-arid natural grassland: modeling and measurement. Agr Forest Meteorol 126 (1–2):99–116
22. Canale RP, Auer MT (1982) Ecological studies and mathematical modeling of *Cladophora* in lake Huron: 5. Model development and calibration. J Gt Lakes Res 8(1):112–125
23. Sakshaug E, Slagstad D, Holm-Hansen O (1991) Factors controlling the development of phytoplankton blooms in the Antarctic Ocean — a mathematical model. Mar Chem 35 (1–4):259–271
24. White MA, Thornton PE, Steven W, Ramakrishna RRN (2000) Parameterization and sensitivity analysis of the BIOME–BGC terrestrial ecosystem model: net primary production controls. Earth Interact 4:1–85
25. Ebenhoh W, Baretta-Bekker JG, Baretta JW (1997) The primary production module in the marine ecosystem model ERSEM II, with emphasis on the light forcing. J Sea Res 38 (3–4):173–193

Chapter 13
H_2 Producing Activity by *Escherichia Coli* During Mixed Carbon Fermentation at Slightly Alkaline and Acidic pHs: Novel Functions of Hydrogenase 4 (hyf) and Hydrogenase 2 (hyb)

Karen Trchounian and Armen Trchounian

Abstract Molecular hydrogen (H_2) production by *Escherichia coli* was studied during mixed carbon (glucose and glycerol) fermentation at slightly alkaline (7.5) and acidic (5.5) pHs. Wild type cells, in the assays with glucose, produced H_2 at pH 7.5 with the same level as cells grown on glucose. Compared to wild type, H_2 production in *fhlA* and *fhlA hyfG* mutants decreased ~6.5 and ~7.9 fold, respectively. In wild type cells H_2 formation at pH 5.5 was lowered ~2 fold, compared to the cells grown on glucose. But in *hyfG* and *hybC* mutants H_2 production was decreased ~2 and ~1.6 fold, respectively. However, at pH 7.5, in the assays with glycerol, H_2 production was low, when compared to the cells grown on glycerol. In contrast to slightly alkaline pH, at pH 5.5 in the assays with glycerol H_2 production was absent. Moreover, H_2 evolution in wild type cells was inhibited by 0.3 mM *N,N′*-dicyclohexylcarbodiimide (DCCD), an inhibitor of the F_0F_1-ATPase, in a pH dependent manner. At pH 7.5 in wild type cells H_2 production was decreased ~3 fold but at pH 5.5 the inhibition was ~1.7 fold. At both pHs in *fhlA* mutant H_2 formation was totally inhibited by DCCD. Taken together, the results indicate that at pH 7.5 in the presence of glucose glycerol also can be fermented. They suggest that Hyd-4 mainly and Hyd-2 to some extent contribute in H_2 production by *E. coli* during mixed carbon fermentation at pH 5.5 whereas Hyd-1 is only responsible for H_2 oxidation.

K. Trchounian
Department of Biophysics, Biology Faculty, Yerevan State University, Yerevan 0025, Armenia

A. Trchounian (✉)
Department of Biophysics, Biology Faculty, Yerevan State University, Yerevan 0025, Armenia

Department of Microbiology & Microbes and Plants Biotechnology, Biology Faculty, Yerevan State University, Yerevan 0025, Armenia
e-mail: Trchounian@ysu.am

A. Veziroğlu and M. Tsitskishvili (eds.), *Black Sea Energy Resource Development and Hydrogen Energy Problems*, NATO Science for Peace and Security Series C: Environmental Security, DOI 10.1007/978-94-007-6152-0_13,

Keywords Hydrogen production • Mixed carbon (glucose and glycerol) fermentation • Hydrogenase • pH • *E. coli*

13.1 Introduction

The present situation of reducing fossil fuels has led to find out alternative and renewable energy sources. Replacement of the existing natural gas and fuel becomes the most important in energy industry. One of the mentioned energy sources is molecular hydrogen (H_2) produced from microbe-mediated biological conversions [1, 2]. H_2 production from sugar-containing industrial, agricultural, water and other wastes has placed renewed interest for finding other substrates or cheap sources which are available in nature and still contained in wastes.

Gonzalez's group [3] has shown that glycerol, like sugars, can be fermented by *E. coli*. Among glycerol fermentation end products H_2 gas can be found [4–9]. That carbon source might be used in energy industry as a cheap source for producing H_2. However, glycerol fermentation studies are undergoing [4, 10–13] but metabolic pathways of glycerol fermentation and their end products, dependence on pH and other factors are still unavailable.

H_2 is known to be produced by *E. coli* via special enzymes – hydrogenases (Hyd), which reversibly oxidize H_2 to $2H^+$: $H_2 <-> 2H^+ + 2e^-$. The important features of these enzymes are their multiplicity and reversibility [13–15]. Indeed, *E. coli* carries four membrane-bound [Ni-Fe]-hydrogenases [10, 13]. Hyd-1 and Hyd-2 are reversible Hyd enzymes dependent on carbon source: during glucose or glycerol fermentation they operate in uptake or producing mode, respectively [7, 9, 13, 15]. Hyd-3 and Hyd-4 are H_2 producing Hyd enzymes upon glucose fermentation [13, 16–19] but they operate in reverse mode during glycerol fermentation [7, 9, 13, 19].

Hyd-1 is encoded by the *hya* operon [20]. The *hya* gene expression is induced under anaerobic conditions at acidic pH [21] and by the presence of formate [22]. Hyd-2 encoded by the *hyb* operon [22, 23] consists of four subunits [24]. The maximal expression of this operon is shown for alkaline pH [21] in cultures grown on hydrogen and fumarate, which is in accordance with pH optimum of this enzyme [25]. Moreover, Hyd-2 activity was observed in a more reduced environment [26] and absent under aerobic conditions [15]. Although physiological role of Hyd-1 is still unclear, it has been proposed to shuttle electrons from formate to fumarate during reduction [27] or to oxidize H_2 ontributing electrons to the quinine pool [28]. On the other hand, Hyd-2 can reversibly oxidize H_2 *in vitro* [15]. But this Hyd enzyme has the potential to function as a "valve" to release excess reducing equivalents in the form of H_2. These observations on Hyd-1 and Hyd-2 might have some role in exploring the exact functions of these enzymes. However, their functions are still not clearly defined.

Hyd-3 and Hyd-4 are encoded by the *hyc* and *hyf* operons, respectively [29–31]. Hyd-3 with the selenocysteine- and molybdenum cofactor-containing formate dehydrogenase (FDH-H) forms the formate hydrogene lyase (FHL-1) complex,

producing H_2 preferably at acidic pH [16, 18]. On the other hand, Hyd-3 was shown to work in reverse H_2 oxidizing mode [14]. Hyd-4 together with FDH-H is suggested to form the second FHL-2 complex [17, 30] which must have functional *hycB* gene product to produce H_2 upon glucose fermentation at alkaline pH [16].

For both FHL complexes the *fhlA* gene is important: it is coding transcriptional activator for *hyc* [32, 33] and probably for *hyf* [34] operons. In addition, a small number of other gene products, namely Hyp proteins are required for the maturation and assembly of Hyd enzymes [13, 35].

It is important to note that some interaction or metabolic cross-talk is suggested for Hyd enzymes in *E. coli* [13, 19] however, the nature of the link is not clear at all. In addition, all four Hyd enzymes are proposed to form H_2 cycling in *E. coli* [13, 26, 36] but their operation and role should be understood.

Previously, it has been shown that during glucose or glycerol fermentation H_2 production by *E. coli* was inhibited by *N,N′*-dicyclohexylcarbodiimide (DCCD), an inhibitor of the H^+-translocating F_0F_1-ATPase [7, 9, 13, 16, 37]. Especially, during glucose fermentation at pH 7.5 a link between Hyd and F_0F_1 could result from Hyd-4 interaction with F_0F_1 to supply reducing equivalents ($H^+ + e^-$) for energy transfer to the secondary transport system [38]. Similar relationship is suggested for H_2-oxidizing Hyd-1 and Hyd-2 where Hyd activity depends on the active F_0F_1 during growth at high and low pHs [37]. Importantly, the relationship between different Hyd enzymes and F_0F_1 or proton motive force generated by F_0F_1 was also demonstrated [7, 16, 37]. Such relationship has been shown recently by Kim et al. [39] for the archaeon *Thermococcus onnuriens*, which generates a proton gradient driven by formate disproportionation via FHL complex. Moreover, an independent investigation of Barrett's group [40] has revealed a relationship between F_0F_1 and FHL complex during thiosulfate reduction by *Salmonella typhimurium*.

Furthermore, it has been shown that *E. coli* Hyd activity is pH dependent [9, 13, 16, 18, 19, 29, 41]. Hyd-2 is mainly active at alkaline pH [25, 38]. Hyd-1 is responsible for overall Hyd activity at acidic pH [38]. Interestingly, Gonzalez's group [3–6] has demonstrated that FHL plays a key role in H_2 production at low pH during glycerol fermentation. Thus, pH dependence seems to be very important in regulating Hyd enzymes to enhance H_2 production efficiency.

Nowadays interest of bacterial H_2 production for developing H_2 bio-production technology is in mixed carbon fermentation since different carbon sources could be found in industrial, agricultural, kitchen, water and other organic substances containing wastes but no data are available on this topics, H_2 metabolic pathways and production as well.

In this paper *E. coli* H_2-producing activity by Hyd enzymes during mixed carbon (glucose and glycerol) fermentation at alkaline and acidic pHs has been investigated. The possibilities of modifying metabolic pathways, coordination of genes and their products and regulatory factors to perform some biochemical functions relating to the production of H_2 could be chosen during mixed carbon source fermentation. Moreover, novel functions of Hyd-4 and in addition of Hyd-2 were revealed.

13.2 Materials and Methods

13.2.1 Bacterial Strains, Their Growth and Preparation for Assays

The *E. coli* wild type and different mutant strains used in this study are listed in Table 13.1.

Bacteria from an overnight growth culture were transferred and grown in glass vessels with plastic press caps under anaerobic conditions at 37 °C in peptone medium (20 g L^{-1} peptone, 15 g L^{-1} K_2HPO_4, 1.08 g L^{-1} KH_2PO_4, 10 g L^{-1} NaCl) with glucose (2 g L^{-1}) or/and glycerol (10 g L^{-1}) at different pHs mentioned in Results and discussion for 20–22 h as described elsewhere [7, 9, 16, 18, 19, 37]. For some mutants, where appropriate (see Table 13.1), overnight growth cultures were supplemented with kanamycin (25 ml L^{-1}). Atmospheric and dissolved O_2 and N_2 were bubbled out of the media by autoclaving, after which the vessels were closed by press caps. The medium pH was measured by a pH-meter with a selective pH-electrode (HJ1131B, Hanna Instruments, Portugal) and adjusted as necessary by means of 0.1 M NaOH or HCl. Bacterial culture absorbance was measured at 600 nm by a Spectro UV-vis Auto spectrophotometer (Labomed, USA).

Preparation of whole cells for the H_2 production assays was done as described before [7, 9, 16, 18, 19, 37]. The assays were performed in a capped vessel placed in

Table 13.1 Characteristics of *E. coli* strains used

Strains	Genotype	Absent subunit or protein	Source and reference
BW25113	*lacI*^{q} *rrnB*$_{T14}$*ΔlacZ*$_{W116}$ *hsdR514 ΔaraBAD*$_{AH33}$ *Δrha BAD*$_{LD78}$	Wild type	Wood (Texas A&M University, College Station, TX, USA)[a] [9, 14]
JW0955 Km^{R} [b]	BW25113 *ΔhyaB*	Large subunit of Hyd-1	Wood [14]
JW2472 Km^{R} [b]	BW25113 *ΔhyfG*	Large subunit of Hyd-4	Wood [14]
JW2701 Km^{R} [b]	BW25113 *ΔfhlA*	FHL activator	Wood [14]
JW2962 Km^{R} [b]	BW 25113 *ΔhybC*	Large subunit of Hyd-2	Wood [14]
MW 1000	BW25113 *ΔhyaB ΔhybC*;	Large subunits of Hyd-1 and Hyd-2	Wood [14]
SW 1001 Km^{R} [b]	BW25113 *ΔfhlA ΔhyfG*	FHL activator and large subunit of Hyd-4	Wood [9]

[a]Present address: Pennsylvania State University, University Park, PA, USA
[b]Resistant to kanamycin

a thermo-stated chamber at 37 °C; bacterial suspension in the vessel was mixed with a magnetic stir bar. In the assays, either glucose or glycerol was supplemented at the same concentration as that added to the growth medium. For DCCD inhibition studies, cells were incubated with the reagent at 0.3 mM for 7–10 min at 37 °C. Dry weight of bacteria was determined as described previously [7, 9].

13.2.2 Redox Potential Determination and Hydrogen Production Assays

The redox potential (E_h) in bacterial suspension was measured with potentiometric method by using a pair of oxidation-reduction, titanium-silicate (Ti-Si) (EO-02, Gomel State Enterprise of Electrometric Equipment (GSEEE), Gomel, Belarus) and platinum (Pt) (EPB-1, GSEEE, or PT42BNC, Hanna Instruments, Portugal) electrodes as described [7, 9, 16, 18, 42, 43].

In contrast to Ti-Si-electrode, which measures the overall E_h, a Pt-electrode is sensitive to H_2 and O_2 [44] and under anaerobic conditions (in the absence of O_2) it can detect H_2 production. Therefore, H_2 production rate (V_{H2}) was calculated as the difference between the initial rates of decrease in Pt- and Ti-Si-electrodes readings per time and expressed as mV of E_h per min per mg dry weight of bacteria as described before [7, 9, 16, 18, 42, 43]. E_h measurement by means of Pt- and Ti-Si-electrodes was done in the assay buffer (150 mM Tris-phosphate, at the appropriate pH, containing 0.4 mM $MgSO_4$, 1 mM NaCl, 1 mM KCl) upon glucose or/and glycerol (the concentration was the same as in the growth medium) addition to bacterial suspension. Pt- and Ti-Si-electrodes standard readings were controlled according to manufacturer's instructions. No significant difference between Pt- and Ti-Si-electrodes readings was detected in bacterial suspension without adding glycerol or/and glucose; bacterial count alteration in the suspension by ~8–10 fold had no marked effect on E_h value [9, 43].

This approach is close to the method with Clark-type electrode employed by Tsygankov and co-workers [45] and Noguchi et al. [41]: a correlation between E_h and H_2 production was shown. Moreover, Piskarev et al. [46] have determined that E_h decrease by H_2 evolution did not depend on salt content in water solution. Also the supplementation of H_2 didn't affect on external pH. Besides, the electrochemical measurement was reviewed to be indirect for H_2 production determination but can give accurate and reproducible data [10, 17].

Using the Durham tube method [16, 40], H_2 production during the growth of *E. coli* was visualized by the appearance of gas bubbles in the test tubes over the bacterial suspension.H_2 production was verified by the chemical assay based on the bleaching of $KMnO_4$ solution in H_2SO_4 with H_2 [16, 18]. This method was suggested for detecting enhanced H_2 production [47].

13.2.3 Reagents and Data Processing

Agar, peptone (Carl Roths GmbH, Germany), DCCD, glucose (Sigma, USA), glycerol (Unichem, China) and the other reagents of analytical grade used were. Each data point represented is averaged from independent triplicate cultures, the standard deviations calculated as described [7, 9, 16, 18, 42, 43] are not more than 5 % if not represented.

13.3 Results and Discussion

13.3.1 *E. coli* Growth During a Mixed Carbon Fermentation, E_h Change and H_2 Production in the Assays Supplemented with Glucose or Glycerol at Different pHs

It is well known that *E. coli* can ferment glucose producing H_2 [10, 13]. Besides glucose, this bacterium can grow under anaerobic conditions on formate, glycerol etc. [3–5, 10, 12, 13, 17, 18, 48]. Anaerobic fermentation of glycerol is shown for *E. coli* cells grown in LB medium at pH 6.3 by Gonzalez's group [3]. *E. coli* couldn't grow under fermentative conditions with glycerol as sole carbon source but this bacterium can grow in the presence of peptone at different pH [7, 9, 19, 37].

The first interesting finding with mixed carbon fermentation was in that at pH 5.5 *E. coli* wild type cells grew worse under anaerobic conditions on glucose or glycerol than at pH 7.5 whereas during mixed carbon fermentation cells grew better at pH 7.5 than 5.5 (data not shown). The effect of mixed carbon, especially glycerol, on *E. coli* cell growth rate at pH 5.5, compared to the cells grown on glucose only, is not known yet and needs further investigation.

Moreover, as it was shown [7, 9, 16, 18, 49], upon glucose or glycerol fermentation E_h measured with a Pt-electrode dropped down to low negative values (~ −600 mV) fast – within 5 min, but during mixed carbon fermentation in the assays supplemented with glucose E_h was obtained to drop down to low negative values (~ −500 mV) slowly – in 10–15 min (data not shown). Simultaneously, the E_h measured with the Ti-Si-electrode at pH 7.5 and 5.5 was not so negative (~ −145 mV and ~ −30 mV, respectively). These differences between the readings of Pt- and Ti-Si-electrodes showed H_2 production by *E. coli* (see Materials and methods). At pH 7.5 for wild type cells in the assays supplemented with glucose V_{H2} was ~5.25 mV E_h/min/mg dry weight (Fig. 13.1). It has, thus, the same value as cells grown on glucose [7, 9, 16, 18, 49]. In the glycerol assays V_{H2} was lower – ~0.52 mV E_h/min/mg dry weight (see Fig. 13.1). This was ~4.3 fold lower than by cells grown on glycerol. At pH 5.5 for wild type cells in the assays supplemented with glucose V_{H2} was ~4.6 mV E_h/min/mg dry weight: this rate was decreased ~2 fold compared to

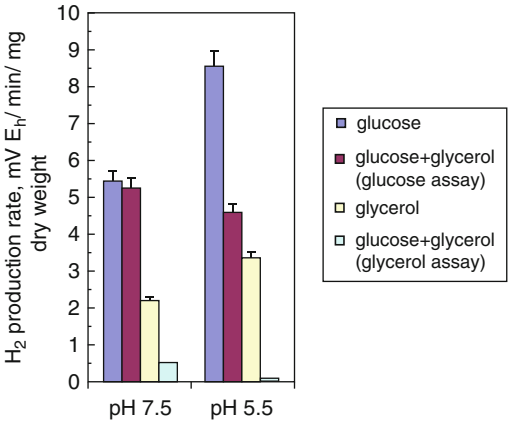

Fig. 13.1 H_2 production rates by *E. coli* wild type BW25113 grown under fermentation conditions at different pHs. Bacteria were grown on glucose, glycerol or mixed carbon sources (glucose and glycerol) and assayed with adding glucose or glycerol as described in Materials and methods. V_{H2} was determined as stated in Materials and methods (*see color plates*)

the cells grown on glucose (see Fig. 13.1). But in the cells with adding glycerol no H_2 production was detected.

H_2 production by *E. coli* during mixed carbon fermentation was confirmed (data not shown) using different methods as mentioned (see Materials and methods).

Thus, H_2 production during mixed carbon fermentation is the second important finding however fermentation pathways and H_2 metabolism under those conditions are still unclear and need further clarification.

13.3.2 H_2 Production by E. coli Mutants with Defects in Hyd-1 and Hyd-2

To understand the role of Hyd enzymes required for H_2 production by *E. coli* during mixed carbon fermentation at slightly alkaline and acidic conditions, mutants with defects in Hyd-1 and Hyd-2 were investigated.

Actually, during mixed carbon fermentation by *E. coli* at pH 7.5 in the assays supplemented with glucose V_{H2} in *hyaB* and *hybC* single mutants was higher than in wild type (Fig. 13.2a), suggesting that Hyd-1 together with Hyd-2 work in H_2 oxidizing mode. On the contrary, during glucose fermentation Hyd-2 was responsible for H_2 oxidation, and Hyd-1 activity was absent [13, 17, 25, 26]. In *hyaB hybC* double mutant V_{H2}, compared to the wild type, wasn't changed significantly (see Fig. 13.2a). This might be due to some pleiotropic effects of *hya* or *hyb* genes on Hyd-3 and Hyd-4 formation and activity suggested [13, 16, 19, 21]. But the effects of glycerol on Hyd-1 and Hyd-2 physiology and appropriate gene expression are not known yet. In contrast to cells grown on glucose, V_{H2} was ~1.5 fold higher than the wild type had (see Fig. 13.2a). However, in the assays supplemented with glycerol, in *hyaB*, *hybC* and *hyaB hybC* mutants V_{H2} was ~2.3 fold higher than in the wild type (see Fig. 13.2a). These data indicate that Hyd-1 and Hyd-2 are working in H_2 uptake mode when glycerol was supplemented as in the assays with glucose.

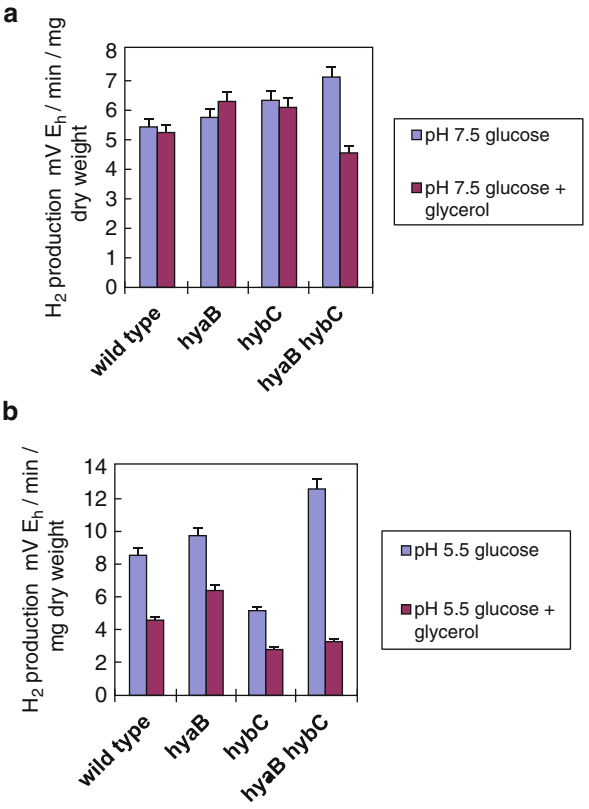

Fig. 13.2 H_2 production rates for *E. coli* wild type and mutants with defects in Hyd-1 (*hyaB*) and Hyd-2 (*hybC*) at pH 7.5 (**a**) and 5.5 (**b**). Whole cells grown were assayed with glucose (22 mol m^{-3}) (For strains, see Table 13.1, for others, see legends to Fig. 13.1) (*see color plates*)

At pH 5.5 during mixed carbon fermentation by *E. coli* the overall situation regarding Hyd activity was quite different compared to glucose or glycerol fermentation. As following the results (Fig. 13.2), in the assays with supplemented glucose Hyd-1 probably had H_2 oxidizing activity which is in conformity with data that *hyaB* mutant is reaching its maximal activity at acidic pH [21]. In *hybC* mutant V_{H2} was decreased ~1.7 fold (see Fig. 13.2b). This is in favor with previously obtained data upon glucose fermentation [9]. The results obtained might be explained due to the different role of Hyd-2 at acidic pH. The latter might be because of interaction with other Hyd enzymes, mainly Hyd-1 and Hyd-3 as suggested [13, 19] and of the pleiotropic effect of *hyb* genes on *hya* expression proposed [13, 16, 19, 21]. Furthermore, in *hyaB hybC* mutant V_{H2} was decreased ~1.5 fold but it was ~1.5 fold higher in cells grown on glucose, compared to the wild type (see Fig. 13.2b). These results had similarity with those obtained during glycerol fermentation [7, 9]. They might be explained by the compensatory uptake functions of Hyd enzymes during H_2 production under different conditions [9]. Then, during *E. coli* growth on mixed carbon in the assays with supplemented glycerol no measurable H_2 production was detected.

13.3.3 Role of *fhlA* Gene Product in H_2 Production by *E. coli*

As it is known a major H_2 producing Hyd enzyme Hyd-3 with FDH-H forms the FHL-1 complex of *E. coli* [10, 13, 16, 28, 30], activated by *fhlA* transcriptional activator [9, 13, 32–34]. However, the key role of *fhlA* gene product is still unknown at different environmental conditions.

During mixed carbon fermentation at pH 7.5 in the assays with added glucose in *E. coli fhlA* single and *hyfG fhlA* double mutants V_{H2} was shown to be lowered significantly ~6.6 fold and ~7.9 fold, respectively (Fig. 13.3a). These results suggest that Hyd-3 with Hyd-4 are responsible for H_2 production. During that mixed growth in the assays supplemented with glycerol in *fhlA* and *hyfG* mutants V_{H2} was higher than in the wild type (see Fig. 13.3a). This could be only when Hyd-3 and Hyd-4 are working in H_2 oxidizing mode. But surprisingly, in *hyfG fhlA* mutant V_{H2} was lowered but less ~3 fold compared to the wild type (see Fig. 13.3a) suggesting that Hyd-3 with Hyd-4 are H_2 producing Hyd enzymes. All these data may be explained if produced H_2 is then recycled by the other two H_2 uptake Hyd enzymes. In single mutants any H_2 production couldn't be detected (V_{H2} was residual) because all produced H_2 is then probably used by the other three Hyd enzymes. This explanation seems to be acceptable since reversibility of Hyd enzymes has been shown and H_2 cycling is probable [7, 9, 13, 26, 36].

At pH 5.5 during mixed carbon fermentation by *E. coli* in the assays with adding glucose in *fhlA* and *hyfG* mutants V_{H2} was decreased ~6.3 and ~2 fold, respectively (Fig. 13.3b). And in *hyfG fhlA* mutant it was decreased ~3.3 fold (see Fig. 13.3b). These are likely to be very important data about Hyd enzymes responsible for H_2 production. It can be ruled out that Hyd-3 and Hyd-4 are responsible for H_2 production. So Hyd-4 has a novel function operating in H_2 producing mode at acidic pH. This could be considered as a new point of view about Hyd-4 physiology and its unusual pH dependent enzyme activity since Hyd-4 has been shown to be major for H_2 production by *E. coli* at alkaline pH [16, 18]. Moreover, it should be noted that in cells grown on glucose at acidic pH Hyd-4 hadn't any H_2 producing activity. So the effect of glycerol on Hyd-4 activity is absolutely novel. On the other side, during mixed carbon growth in the assays with adding glycerol any measurable H_2 production activity could not be detected.

13.3.4 H_2 Production Inhibition by DCCD in *E. coli* Wild Type and Mutant Strains

To establish any relationship between H_2 production and the F_0F_1-ATPase by *E. coli* during mixed carbon fermentation, effect of inhibitors such as DCCD was studied. The latter is known as a non specific inhibitor of F_0F_1 but it becomes specific for *E. coli* during fermentative growth [13, 37, 38, 48].

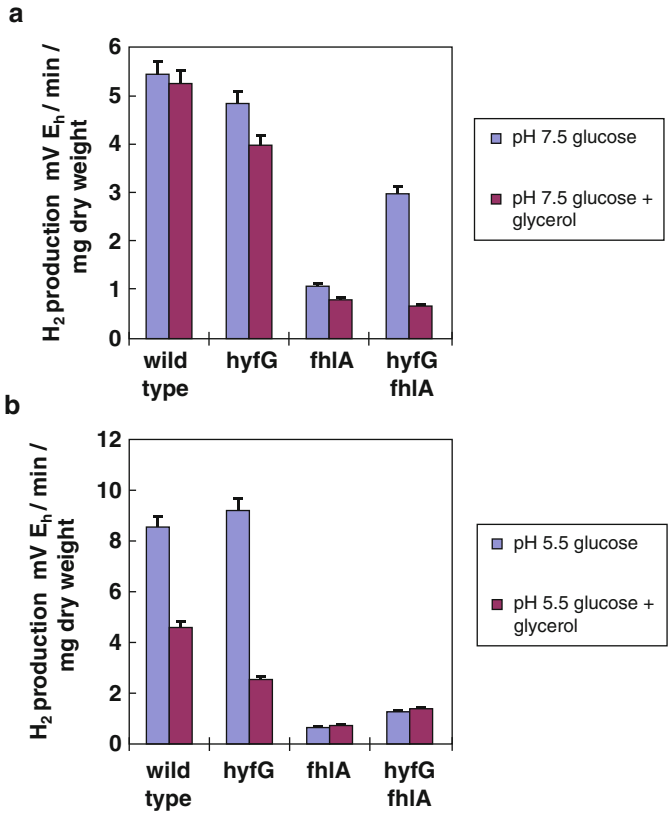

Fig. 13.3 H_2 production rates for *E. coli* wild type and mutants with defects in Hyd-3 (*fhlA*) and Hyd-4 (*fhlA hyfG*) at pH 7.5 (**a**) and 5.5 (**b**) (For others, see legends to Fig. 13.2) (*see color plates*)

At pH 7.5 H_2 production by *E. coli* was shown to be inhibited by DCCD in wild type and mutants in both, glucose and glycerol assays (Fig. 13.4a, b). During mixed carbon growth in the glucose added assays in wild type V_{H2} was lowered by DCCD ~3 fold and in *hyaB* and *hybC* single and double mutants it was inhibited ~5–6 fold (see Fig. 13.4a). The same inhibition was determined in *hyfG* mutant whereas in *fhlA* mutant H_2 production was totally inhibited and in *fhlA hyfG* mutant it was lowered ~1.7 fold (see Fig. 13.4b). Furthermore, in assays supplemented with glycerol V_{H2} was inhibited in the wild type and mutants approximately with the same values but in both cases total inhibition was observed in *fhlA* mutant (see Fig. 13.4b). These findings indicate the relationship of Hyd-3 mainly and Hyd-4 partially to F_0F_1. All the data obtained are in good favor with the previously reported results at pH 7.5 [16, 48].

During mixed carbon growth at pH 5.5 V_{H2} was also inhibited by DCCD in wild type and some Hyd defective mutants (Fig. 13.4a, b). Indeed, in the wild type in the glucose added assays V_{H2} was decreased ~1.7 fold. This is in good correlation with

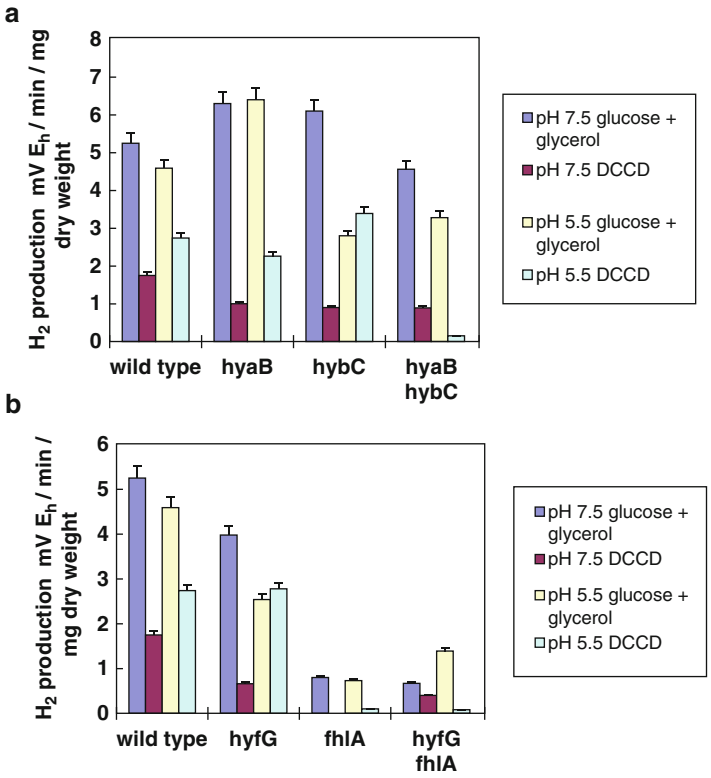

Fig. 13.4 The inhibition by DCCD of H_2 production rates for *E. coli* wild type and mutants with defects in Hyd-1 and Hyd-2 (**a**) and Hyd-3 and Hyd-4 (**b**) at different pHs. 0.3 mM DCCD was used (For others, see legends to Fig. 13.2) (*see color plates*)

previously reported data about DCCD inhibition of H_2 production at acidic pH during glucose fermentation although more effective inhibition was at pH 7.5 [14]. In *hybC* and *hyfG* mutants there weren't any changes compared to that without inhibitor used (see Fig. 13.4a, b). It would be due to less participation of F_0F_1 in H^+ transport and proton-coupled processes. But surprisingly, in *hyaB hybC* mutant V_{H2} was strongly decreased – ~18.3 fold and in *fhlA* mutant total inhibition was obtained (see Fig. 13.4a, b). At this pH also Hyd-3 mainly and Hyd-4 to some extent might be suggested to have some relationship with F_0F_1.

13.4 Concluding Remarks

In this work, *E. coli* Hyd enzyme H_2 producing activity during mixed carbon sources (glucose and glycerol) fermentation was studied using wild type and different mutants at slightly alkaline and acidic pHs. The principal findings at pH 7.5 are that V_{H2} during mixed carbon fermentation in the assays with glucose

supplemented (see Figs. 13.2, 13.3, and 13.4) had similar values compared to that with glucose fermentation reported [7, 9, 16, 18]. Hyd-1 with Hyd-2 formed the overall H_2 oxidizing activity, in contrast to that Hyd-2 was only responsible for H_2 uptake upon growth on glucose. Then, Hyd-3 with Hyd-4 were suggested to be responsible for H_2 production. In assays with adding glycerol H_2 production was low but the Hyd enzymes responsible for H_2 production and uptake are the same as in glucose assays.

At pH 5.5 V_{H2} during mixed carbon fermentation in the assays with adding glucose was shown to be ~2 fold lower, compared with the cells grown on glucose (see Fig. 13.1). Novel role of Hyd-4 has been detected. Analysis of *fhlA* and *fhlA hyfG* mutants done has revealed that not only Hyd-3 but also Hyd-4 was responsible for H_2 production at low pH. On the contrary, Hyd-3 was the only producing Hyd enzyme in the cells grown on glucose. Moreover, the effect of glycerol on the Hyd-1 and Hyd-2 activity is suggested but no clear interpretation could be given. Compensatory effects or interaction of these enzymes with other Hyd enzymes during mixed carbon fermentation have been suggested, further study is required.

Furthermore, H_2 production was inhibited by DCCD, an inhibitor of the F_0F_1-ATPase (see Fig. 13.4). This inhibition is interesting for understanding a relationship of H^+ transport through F_0F_1 to H_2 production. During mixed carbon fermentation the inhibition of H_2 production by DCCD has similarity with the cells grown on glucose. Interestingly, total inhibition of H_2 production in *fhlA* mutant at both pHs was determined and this might be explained if FhlA protein is directly related with F_0F_1 in spite of ATP-dependence of FhlA is suggested [50].

The other important remark is in that glycerol might be fermented in the presence of glucose by *E. coli*. Besides, all data obtained in this work and by other groups [7, 9, 14, 15] confirm the reversibility of Hyd enzymes depending on pH and fermentation substrates and possibly on metabolic pathways [13].

The results could have a general important significance in impact of different carbon sources, especially mixed carbons, in H_2 production technology. They would be also efficient to develop multi-step technology for H_2 and other fuels production. However, detailed mechanisms for activity and regulation of Hyd enzymes and H_2 metabolism by bacteria during mixed carbon fermentation need further investigation.

Acknowledgements The authors thank to Prof. T.K. Wood (Chemical Engineering, Biochemistry and Molecular Biology; Pennsylvania State University, University Park, PA, USA) for supplying mutants and advice, to Drs. A. Poladyan and L. Gabrielyan for useful comments. This study was supported by Research grant (11-F202-2011) from the Ministry of Education and Science of Armenia to AT.

References

1. Hallenbeck PC (2009) Fermentative hydrogen production: principles, progress, and prognosis. Int J Hydrogen Energy 34:7379–7389
2. Mudhoo A, Forsater-Carniero T, Sanchez A (2011) Biohydrogen production and bioprocess enhancement: a review. Crit Rev Biotechnol 31:250–263
3. Dharmadi Y, Murarka A, Gonzalez R (2006) Anaerobic fermentation of glycerol by *Escherichia coli*: a new platform for metabolic engineering. Biotechnol Bioeng 94:821–829
4. Gonzalez R, Murarka A, Dharmadi Y, Yasdani SS (2008) A new model for the anaerobic fermentation of glycerol in enteric bacteria: trunk and auxiliary pathways in *Escherichia coli*. Metab Eng 10:234–245
5. Murarka A, Dharmadi Y, Yazdani SS, Gonzalez R (2008) Fermentative utilization of glycerol by *Escherichia coli* and its implications for the production of fuels and chemicals. Appl Environ Microbiol 74:1124–1135
6. Yasdani SS, Gonzalez R (2008) Engineering *Escherichia coli* for the efficient conversion of glycerol to ethanol and co-products. Metab Eng 10:340–351
7. Trchounian K, Trchounian A (2009) Hydrogenase 2 is most and hydrogenase 1 is less responsible for H_2 production by *Escherichia coli* under glycerol fermentation at neutral and slightly alkaline pH. Int J Hydrog Energ 34:8839–8845
8. Hu H, Wood TK (2010) An evolved *Escherichia coli* strain for producing hydrogen and ethanol from glycerol. Biochem Biophys Res Commun 391:1033–1038
9. Trchounian K, Sanchez-Torres V, Wood TK, Trchounian A (2011) *Escherichia coli* hydrogenase activity and H_2 production under glycerol fermentation at a low pH. Int J Hydrog Energy 36:4323–4331
10. Poladyan A, Trchounian A (2009) Production of molecular hydrogen by mixed-acid fermentation in bacteria and its energetics. In: Trchounian A (ed) Bacterial membranes. Ultrastructure, bioelectrochemsitry, bioenergetics and biophysics. Research Signpost, Kerala
11. Cintolesi A, Comburg JM, Rigou V, Zygourakis K, Gonzalez R (2011) Quantitative analysis of the fermentative metabolism of glycerol in *Escherichia coli*. Biotechnol Bioeng 109:187–198
12. Khanna S, Goyal A, Moholkar VS (2012) Microbial conversion of glycerol: present status and future prospects. Crit Rev Biotechnol 32(3):235–262. doi:10.3109/07388551.2011.604839
13. Trchounian K, Poladyan A, Vassilian A, Trchounian A (2012) Multiple and reversible hydrogenases for hydrogen production by *Escherichia coli*: dependence on fermentation substrate, pH and F_0F_1-ATPase. Crit Rev Biochem Mol Biol 47:236–249
14. Maeda T, Sanchez-Torres V, Wood TK (2007) *Escherichia coli* hydrogenase 3 is a reversible enzyme possessing hydrogen uptake and synthesis activities. Appl Microbiol Biotechnol 76:1036–1042
15. Lukey MJ, Parkin A, Roessler MM, Murphy BJ, Harmer J, Palmer T, Sargent F, Armstrong FA (2010) How *Escherichia coli* is equipped to oxidize hydrogen under different redox conditions. J Biol Chem 285:3928–3938
16. Bagramyan K, Mnatsakanyan N, Poladian A, Vassilian A, Trchounian A (2002) The roles of hydrogenases 3 and 4, and the F_0F_1-ATPase, in H_2 production by *Escherichia coli* at alkaline and acidic pH. FEBS Lett 516:172–178
17. Bagramyan K, Trchounian A (2003) Structure and functioning of formate hydrogen lyase, key enzyme of mixed-acid fermentation. Biochemistry (Moscow) 68:1159–1170
18. Mnatsakanyan N, Bagramyan K, Trchounian A (2004) Hydrogenase 3 but not hydrogenase 4 is major in hydrogen gas production by *Escherichia coli* formate hydrogenlyase ar acidic pH and in the presence of external formate. Cell Biochem Biophys 41:357–366
19. Trchounian K, Pinske C, Sawers G, Trchounian A (2011) Characterization of *Escherichia coli* [NiFe]-hydrogenase distribution during fermentative growth at different pHs. Cell Biochem Biophys 62:433–440

20. Menon NK, Robbins J, Wendt JC, Shanmugan KT, Przybyla AE (1991) Mutational analysis and characterization of the *Escherichia coli hya* operon, which encodes [NiFe] hydrogenase 1. J Bacteriol 173:4851–4861
21. King PW, Przybyla AE (1999) Response of *hya* expression to external pH in *Escherichia coli*. J Bacteriol 181:5250–5256
22. Richard DJ, Sawers G, Sargent F, McWalter L, Boxer DH (1999) Transcriptional regulation in response to oxygen and nitrate of the operons encoding the [NiFe] hydrogenases 1 and 2 of *Escherichia coli*. Microbiology 145:2903–2912
23. Menon NK, Chatelus CY, Dervartanian M, Wendt JC, Shanmugam KT, Peck HD, Przybya AE (1994) Cloning, sequencing, and mutational analysis of the *hyb* operon encoding *Escherichia coli* hydrogenase 2. J Bacteriol 176:4416–4423
24. Dubini A, Pye RL, Jack RL, Palmer T, Sargent F (2002) How bacteria get energy from hydrogen: a genetic analysis of periplasmic hydrogen oxidation in *Escherichia coli*. Int J Hydrog Energy 27:1413–1420
25. Ballantine SP, Boxer DH (1986) Isolation and characterisation of a soluble active fragment of hydrogenase isoenzyme 2 from the membranes of anaerobically grown *Escherichia coli*. Eur J Biochem 156:277–284
26. Redwood MD, Mikheenko IP, Sargent F, Macaskie LE (2008) Dissecting the roles of *Escherichia coli* hydrogenases in biohydrogen production. FEMS Microbiol Lett 278:48–55
27. Francis K, Patel P, Wendt JC, Shanmugam KT (1990) Purification and characterization of two forms of hydrogenase 1 from *Escheriochia coli*. J Bacteriol 172:5750–5757
28. Sawers RG, Ballantine SP, Boxer DH (1985) Differential expression of hydrogenase isoenzymes in *Escherichia coli*: evidence for a third isoenzyme. J Bacteriol 164:324–331
29. Sauter M, Bohm R, Bock A (1992) Mutational analysis of the operon (*hyc*) determing hydrogenase 3 formation in *Escherichia coli*. Mol Microbiol 6:1523–1532
30. Andrews SC, Berks BC, Mcclay J, Ambler A, Quail MA, Golby P, Guest JR (1997) A 12-cistron *Escherichia coli* operon (*hyf*) encoding a putative proton-translocating formate hydrogenlyase system. Microbiology 143:3633–3647
31. Self WT, Hasona A, Shanmugan KT (2004) Expression and regulation of silent operon, *hyf*, coding for hydrogenase 4 isoenzyme in *Escherichia coli*. J Bacteriol 186:580–587
32. Schlensog V, Lutz S, Bock A (1994) Purification and DNA-binding properties of FHLA, the transcriptional activator of the formate hydrogenlyase system from *Escherichia coli*. J Biol Chem 269:19590–19596
33. Self WT, Shanmugam KT (2000) Isolation and characterization of mutated FhlA proteins which activate transcription of the *hyc* operon (formate hydrogenlyase) of *Escherichia coli* in the absence of molybdate. FEMS Microbiol Lett 184:47–52
34. Skibinski DAG, Golby P, Chang Y-S, Sargent F, Hoffman R, Harper R, Guest JR, Attwood MM, Berks BC, Andrews SC (2002) Regulation of the hydrogenase-4 operon of *Escherichia coli* by the σ^{54}-dependent transcriptional activators FhlA and HyfR. J Bacteriol 184:6642–6653
35. Forzi L, Sawers G (2007) Maturation of [Ni-Fe]-hydrogenases in *Escherichia coli*. Biometals 20:567–578
36. Zbell AL, Maier RJ (2009) Role of the Hya hydrogenase in recycling of anaerobically produced H_2 in *Salmonella enterica* serovar *typhimurium*. Appl Environ Microbiol 75:1456–1459
37. Trchounian K, Pinske C, Sawers RG, Trchounian A (2011) Dependence on the F_0F_1-ATP synthase for the activities of the hydrogen-oxidizing hydrogenases 1 and 2 during glucose and glycerol fermentation at high and low pH in *Escherichia coli*. J Bioenerg Biomembr 43:645–650
38. Trchounian A (2004) *Escherichia coli* proton-translocating F_0F_1-ATP synthase and its association with solute secondary transpopters and/or enzymes of anaerobic oxidation-reduction under fermentation. Biochem Biophys Res Commun 315:1051–1057

39. Kim YJ, Lee HS, Kim ES, Bae SS, Lim JK, Matsumi R, Lebedinsky AV, Sokolova TG, Kozhevnikova DA, Cha SS, Kim SJ, Kwon KK, Imanaka T, Atomi H, Bonch-Osmolovskaya EA, Lee JH, Kang SG (2010) Formate-driven growth coupled with H_2 production. Nature 467:352–355
40. Sasahara KC, Heinzinger NK, Barrett E (1997) Hydrogen sulfide production and fermentative gas production by *Salmonella typhimurium* require F_0F_1 ATPase activity. J Bacteriol 179:6736–6740
41. Noguchi K, Riggins DP, Eldahan KC, Kitko RD, Slonczewski JL (2010) Hydrogenase-3 contributes to anaerobic acid resistance of *Escherichia coli*. PLoS One 5:e10132
42. Gabrielyan L, Trchounian A (2009) Relationship between molecular hydrogen production, proton transport and the F_0F_1-ATPase activity in *Rhodobacter sphaeroides* strains from mineral springs. Int J Hydrog Energy 34:2567–2572
43. Gabrielyan L, Trchounian A (2012) Concentration dependent glycine effect on the photosynthetic growth and bio-hydrogen production by *Rhodobacter sphaeroides* from mineral springs. Biomass Bioenerg 36:333–338
44. Beliustin AA, Pisarevsky AM, Lepnev GP, Sergeyev AS, Shultz MM (1992) Glass electrodes: a new generation. Sens Actuators B Chem 10:61–66
45. Eltsova ZA, Vasilieva LG, Tsygankov AA (2010) Hydrogen production by recombinant strains of *Rhodobacter sphaeroides* using a modified photosynthetic apparatus. Appl Biochem Microbiol 46:487–491
46. Piskarev IM, Ushkanov VA, Aristova NA, Likhachev PP, Myslivets TS (2010) Establishment of the redox potential of water saturated with hydrogen. Biophysics 55:13–17
47. Maeda T, Wood TK (2008) Formate detection by potassium permanganate for enhanced hydrogen production in *Escherichia coli*. Int J Hydrog Energy 33:2409–2412
48. Bagramyan K, Mnatsakanyan N, Trchounian A (2003) Formate increases the F_0F_1-ATPase activity in *Escherichia coli* membrane vesicles. Biochem Biophys Res Commun 306:361–365
49. Bagramyan K, Galstyan A, Trchounian A (2000) Redox potential is a determinant in the *Escherichia coli* anaerobic fermentative growth and survival: effects of impermeable oxidant. Bioelectrochemistry 51:151–156
50. Hopper S, Bock A (1995) Effector-mediated stimulation of ATPase activity by the sigma 54-dependent transcriptional activator FHLA from *Escherichia coli*. J Bacteriol 177:1798–1803

Chapter 14
Glycerol Fermentation and Molecular Hydrogen Production by *Escherichia Coli* Batch Cultures Affected by Some Reducing Reagents and Heavy Metal Ions

Anna Poladyan, Karen Trchounian, Mikayel Minasyants, and Armen Trchounian

Abstract Glycerol fermentation redox routes by *E. coli* wild type batch cultures and effects of Ni^{2+}, Fe^{2+} and Fe^{3+} ions of different concentration (0.01–0.3 mM) on cell growth and H_2 production were investigated. Influences of aforementioned metal ions and Cu^{2+}, as well as Fe^{2+} on H_2 production rate *in vitro* assays were also studied in wild type and *hyaB hybC* double mutant (with defective hydrogenase (Hyd) 1 and Hyd -2). Cell growth was shown to be followed by decrease of pH and redox potential (ORP) measured by both titanium-silicate (E_h) and platinum electrodes (E'_h). After 8 h growth, at pH 7.5, E_h dropped down negative value (-120 mV) and H_2 production was observed at the middle log phase. Whereas at the same pH in the presence of 0.05 mM Fe^{2+} both E_h and E_h' electrodes readings dropped to more negative values ~ -170 ± 10 and -450 ± 12 mV, respectively. All ions used at 0.05–0.1 mM concentrations stimulated bacterial growth ~1.2 to ~1.4 fold at different pHs. Ni^{2+} enhanced H_2 formation in a concentration-dependent manner: maximal stimulation, up to 1.5 fold, was observed at 0.2 mM $NiCl_2$ only at pH 7.5. Ni^{2+} also promoted to high H_2 yield at pH 6.5 and 7.5 *in vitro*. In addition, 0.05–0.1 mM Fe^{2+} also affected on H_2 production rate and increased it ~2 fold *in vitro* at pH 6.5 and 7.5 whereas, 0.05–0.1 mM Cu^{2+} had inhibitory effect on H_2 production rate. In *hyaB hybC* mutant H_2 production rate was decreased

A. Poladyan (✉) • K. Trchounian • M. Minasyants
Department of Biophysics, Biology Faculty, Yerevan State University,
1 A. Manoukian Str., 0025, Yerevan, Armenia
e-mail: apoladyan@ysu.am

A. Trchounian
Department of Biophysics, Biology Faculty, Yerevan State University,
1 A. Manoukian Str., 0025, Yerevan, Armenia

Department of Microbiology and Biotechnology Biology Faculty, Yerevan State University,
1 A. Manoukian Str., 0025, Yerevan, Armenia

A. Veziroğlu and M. Tsitskishvili (eds.), *Black Sea Energy Resource Development and Hydrogen Energy Problems*, NATO Science for Peace and Security Series C: Environmental Security, DOI 10.1007/978-94-007-6152-0_14,

compared with wild type and Fe^{2+} had no effect on H_2 production rate and yield both at pH 6.5 and 7.5.

The findings indicate the strengthening of reductive processes by *E. coli* during glycerol fermentation and point out the role of essential heavy metal ions in H_2 production. Furthermore, enhanced H_2 production by heavy metal ions probably depends on operation of Hyd- 1 and Hyd- 2 at pH 6.5 and 7.5.

Keywords Glycerol fermentation • Redox potential • H_2 production • Hydrogenases • Ni^{2+}, Fe^{2+}, Fe^{3}+, Cu^{2}+ • *E. coli*

14.1 Introduction

Biohydrogen is known as ecologically-clean, renewable and abundant alternative energy source for the twenty-first century, because of its safety by-product (during its utilization produces only water) and high energy content (-140 MJ/kg) [1, 2]. Nowadays many projects are focused on investigations of pathways for production and simulation of H_2 during bacterial fermentative processes, besides, the use of cheap carbon sources for H_2 production is more attractive and preferable. Gonzalez's group [3] has discovered that *Escherichia coli* is able to utilize glycerol in a fermentative manner and produce ethanol with different organic acids as well as molecular hydrogen (H_2). Crude glycerol is a main co-product of biodiesel, which is formed during the trans-etherification process of the triacylglycerols [4–6]. Biodiesel is derived from vegetable oil, algae, or animal fat. During the biodiesel production, for every 1 lb of oil converted, there will be approximately 0.1 lb of crude glycerol are produced as well [7]. So, with the increasing demand for biodiesel, the accumulation of glycerol as byproduct, made it cheaper than other carbon source like glucose. On the other hand, *E. coli* is the best-characterized bacterium and promising for glycerol utilization because it is one of the most commonly organisms used for metabolic engineering and industrial applications [6, 8–10].

H_2 is established to be obtained from formate, by formate hydrogen lyase (FHL), with participation of formate dehydrogenase H (FDH-H) and hydrogenases (Hyd) [11]. The genome of *E. coli* encodes four membrane-associated [Ni-Fe]-Hyd enzymes [12]. Hyd-1 and Hyd-2 are thought hydrogen-oxidizing enzymes; on the other hand, Hyd-3 and Hyd-4 reduce protons to H_2 and with the selenocysteine- and molybden cofactor-containing FDH-H and other electron-transferring components form the FHL complex. Participation of different Hyd enyzmes in H_2 metabolism is dependent on medium properties and composition, especially pH and carbon source. Interestingly, H_2 produced at acidic pH has negative impact on cell growth and glycerol fermentation [3, 8]. Recently it has been reported that, depending on medium composition, H_2 could be also evolved at slightly alkaline pH [13, 14]. However the pH dependence of glycerol fermentation and H_2 production is not clear.

Besides, bioenergy is frequently stored and released by means of redox reactions. The ability of bacteria to carry out redox reactions depends on the redox state of the environment, or its redox potential (ORP) [15]. The latter itself depends on rate of redox processes. This simple relationship is hard to understand and to apply in biotechnology. On the other hand, ORP is suggested to be useful for monitoring changes in the metabolic state of bacterial cultures in biotechnology and for optimizing yield of fermentation products [16, 17]. Moreover, ORP has been shown can be applied to discriminate among species of bacteria [18, 19].

No doubt, redox state of environment and growth medium's composition are important factors for bacterial growth and H_2 production: it is known that traces of metal ions such us Fe are Ni are necessary for growth and metabolism of most microorganisms. Moreover, Fe and Ni can stimulate activity of metal-containing enzymes [20, 21]. In some bacteria Fe and Ni are required for a catalyzing Fe-S clusters biogenesis [22]. At the same time, abundance of free Fe and Ni are lethal for bacteria [23, 24].

Interestingly, it is shown that under anaerobic conditions Fe^{2+} is stable and more soluble than Fe^{3+}. The latter is, therefore, inaccessible for living organisms. Thus, bacteria should have many mechanisms to satisfy the requirement of Fe, with the help of various transport systems. Multiple Fe transport system has been identified in *E. coli* under anaerobic conditions [25]. Among them Fe^{2+} uptake system, encoded by three *feoABC* genes, is probably ATP-driven primary transporter. The other ion – Fe^{3+} is also accumulated by *E. coli* but together with siderophore. The latter's complex with Fe^{3+} is bonded to specific proteins to pass through the membrane into the cells; those proteins are components of ABC-type transporters [26].

Although various types of transporters can be involved in Ni uptake under certain conditions, the biosynthesis of Ni-dependent enzymes depends on highly specific transport systems with an affinity of Ni at the very low concentration (nM range). Two major types can be distinguished from each other: an ABC-type Ni transporter has been identified in *E. coli* [20, 23]. The majority of Ni transporters are independent of ATP hydrolysis; they form of novel class – the Ni/Co transporters family [20].

Cu^{2+} are also required for bacterial metabolism in low concentration [27]; but in a considerably higher concentration as an oxidizer they may cause inhibition of bacterial growth, Hyd activity and change H^+ flux through the F_0F_1-ATPase as shown with *E. coli* in our laboratory [28, 29] as well as disrupt the membrane by inducing permeability. Cu^{2+} is found can affect the other bacteria – *Enterococcus hirae* growth through E_h or directly on proteins in bacterial membrane, probably F_0F_1 [30].

In this paper, the effects of Ni^{2+}, Fe^{2+} and Fe^{3+} on growth of bacteria and kinetics of ORP, H_2 production by *E. coli* wild type during glycerol fermentation were studied at different pHs (pH 5.5–7.5). It was shown that 0.05–0.1 mM Fe^{2+} and Ni^{2+} both stimulated bacterial growth at all pHs and enhanced H_2 production rate and yield both at pH 6.5 and 7.5. Inhibitory effect of oxidizer Cu^{2+} on H_2 production was also shown at all pHs. Moreover, Fe^{2+} did not stimulate H_2 production in *hyaB hybC* mutant with defective Hyd-1 and Hyd-2 at pH 6.5 and 7.5.

14.2 Materials and Methods

14.2.1 Bacterial Strain and Growth, pH Determination

The *E. coli* BW25113 (*lacI*^{q} *rrnB*$_{T14}$*ΔlacZ*$_{W116}$ *hsdR514 ΔaraBAD*$_{AH33}$ *Δrha BAD*$_{LD78}$) wild-type and MW1000 (BW25113*ΔhyaB ΔhybC*) mutant with defective Hyd-1 and Hyd-2 [14] were used.

Bacteria were grown in batch culture under anaerobic conditions at 37 °C in peptone medium (20 g/L peptone, 2 g/L K_2HPO_4, 5 g/L NaCl) with glycerol 10 g/L at different pHs. The pH was measured using a pH-meter with selective pH-electrode (ESL-63-07, Gomel State Enterprise of Electrometric Equipment (GSEEE), Gomel, Belarus; or HJ1131B, HANNA Instruments, Portugal) and adjusted by 0.1 M NaOH and 0.1 N HCl. Bacterial growth was monitored by measuring optical density (OD) with a spectrophotometer at the wavelength of 600 nm.

14.2.2 ORP Measurements and H_2 Production Assays

ORP was measured during bacterial growth in peptone medium and in bacterial suspension *in vitro* assays. *In vitro* ORP was measured in the assays mixture, which contained 150 mM Tris-phosphate buffer, 1 mM NaCl and 1 mM KCl, 0.4 mM $MgSO_4$; pH was adjusted by titration of 1 M H_3PO_4.

ORP was determined by use of redox platinum (Pt) (EPB-1, GSEEE; or PT42BNC, HANNA Instruments, Portugal) and titanium-silicate (Ti-Si) electrodes (EO-02, GSEEE); Ag/AgCl (saturated by KCl) electrode was as reference electrode. In contrast to Pt electrode is sensitive to H_2 (or oxygen), Ti-Si electrode measures the overall ORP and is not affected by the presence of H_2 (or oxygen); this is allowing H_2 detection under anaerobic conditions (in the absence of oxygen) [14, 31]. H_2 production rate (V_{H2}) is expressed as difference between Pt (E_h') and Ti-Si (E_h) electrodes readings in mV in time per mg dry weight. The H_2 yield is calculated by the decrease of E_h' to low negative values as described by Piskarev et al. [32]; it is expressed in mol/l. Note E_h' decrease by H_2 evolution did not depend on salt content in water solution; pH was not affected by H_2 supplemented [32].

Before assays ORP of two electrodes were checked in the control solution (the mixture of 0.049 M $K_3[Fe(CN)_6]$ and 0.05 M $K_4[Fe(CN)_6]\cdot 3H_2O$, pH 6.86) according to the manufacturer's instructions. E_h' and E_h at 25 °C were of 245 ± 10 mV. Note no significant differences between E_h' and E_h were detected during H_2 assays in bacterial suspension without carbon source added; bacterial count alteration in the suspension by ~8–10-fold had no marked effect on E_h' and E_h [14]. Moreover, the determination used is closed to the method with Clark-type electrode employed by Noguchi et al. [33].

14.2.3 Others, Reagents and Data Processing

All assays were done at 37 °C. Agar, $K_3[Fe(CN)_6]$, $K_4[Fe(CN)_6]$ were from Sigma (USA), casein peptone, glycerol, Tris were from Carl Roths (Germany), glycerol was from Unichem (China); other reagents used were of analytical grade. Data were averaged from duplicate or triplicate independent measurements, for which the standard errors do not exceed 3 % (if they do not indicated).

14.3 Results and Discussion

14.3.1 Heavy Metal Ions Effects on *E. coli* Growth, ORP Kinetics and H_2 Production

In this study, Ni^{2+}, Fe^{2+} and Fe^{3+} effects on growth and ORP kinetics by *E. coli* BW25113 batch culture during glycerol fermentation at different pHs (5.5–7.5) were investigated. 0.01 up to 0.3 mM concentrations of metal ions were considered; optimal concentrations for bacterial growth were determined. 0.05–0.1 mM Ni^{2+}, Fe^{2+} and Fe^{3+} in the growth medium was shown to stimulate bacterial growth up to ~1.2 to ~1.4 fold at different pHs (Fig. 14.1). These results are valuable, because glycerol fermentation by *E. coli* was relieved for the last years [3, 4] but its metabolism is complicated [34]; and medium composition optimal for bacterial growth are under the study.

The lowering of medium pH and the drop of ORP was observed during bacterial growth with increase of bacterial count (OD). During glycerol fermentation by *E. coli,* E_h' dropped down to −400 ± 12 mV (Fig. 14.2), −450 ± 10 mV and −350 ± 10 mV (not shown) when the culture was of 8 h growth at pH 7.5, 6.5 and 5.5, respectively. E_h with glycerol culture was of −50 to −100 ± 10 mV at pH 5.5–7.5 (not shown). The drop of ORP up to −550–600 mV during anaerobic growth of

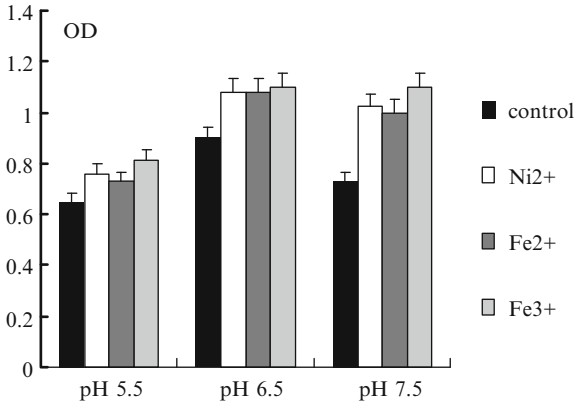

Fig. 14.1 The effects of Fe^{2+}, Fe^{3+}, Ni^{2+}on *E. coli* BW25133 cell growth. Bacteria were grown under glycerol fermentation at pH 5.5–7.5. OD_{600} after 24 h bacterial growth was presented. Control was bacterial growth in the medium without metal ions added. 0.05 mM $FeSO_4$, $FeCl_3$ or $NiCl_2$ were added into the growth medium (For details, see Sect. 2.2)

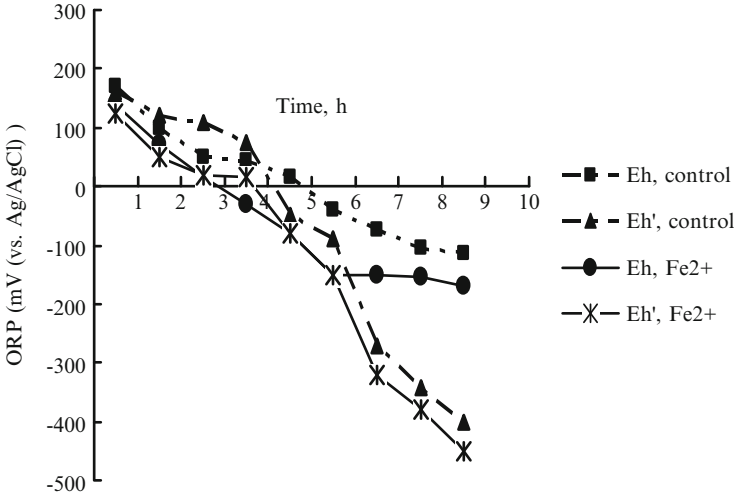

Fig. 14.2 The ORP kinetics by *E. coli* BW25113 during glycerol fermentation at pH 7.5. E_h', measured by platinum and E_h by titanium-silicate electrodes were expressed in mV (vs Ag/AgCl (saturated by KCl)). Control was bacterial growth in the medium without metal ions. 0.05 mM Fe^{2+} was added into the growth medium (For details, see Sect. 2.2)

bacteria in the absence of external electron acceptors has been well demonstrated by many researchers [15, 19, 35–38]. This ORP drop might be a result of the secretion of redox active metabolites into the culture medium, leading to decrease of external pH [36, 37, 39] or might be connected with the processes on (in) the bacterial membranes [15, 40, 41]. Moreover, negative value of ORP with glycerol culture can be regarded by the properties of glycerol having highly reduced carbon and a higher production of reducing equivalents (NADH/NADPH/$FADH_2$) during its fermentation compared to glucose [3, 4]. The reducing equivalents should have a profound effect on the whole metabolic network, when the higher NADH availability significantly changes the end products pattern under anaerobic conditions [4, 42].

Interesting situation was observed with ORP kinetics during *E. coli* growth at pH 7.5 (Fig. 14.2): in the presence of Fe^{2+} both E_h and E_h' dropped to more negative value -170 ± 10 and -450 ± 12 mV, respectively, compared with the control. Probably this effect can be regarded with the reductive properties of Fe^{2+}, which under alkaline pH has specific action: Fe^{2+} may reduce thiol groups on bacterial surface affecting on activity of membrane transport systems or stimulating activity of key enzymes in fermentation metabolism, such as Hyd or proton-transporting F_0F_1-ATPase [29].

Consequently, H_2 production was observed at the middle of log growth phase (Fig. 14.2, Table 14.1). Ni^{2+} stimulated H_2 formation after 24 h growth in a concentration-dependent manner: maximal stimulation (up to ~1.5 fold) was observed at 0.2 mM $NiCl_2$.

Table 14.1 The effects of metal ions on H_2 yield by *E. coli* BW25133 under glycerol fermentation at different pHs *in vitro*

	H_2 yield, mol/L		
Growth pH	Control	Fe^{+2}	Ni^{+2}
5.5	0.80 ± 0.01	0.70 ± 0.02	0.80 ± 0.01
6.5	0.73 ± 0.02	3.50 ± 0.02	2.12 ± 0.01
7.5	1.30 ± 0.02	1.40 ± 0.03	2.10 ± 0.02

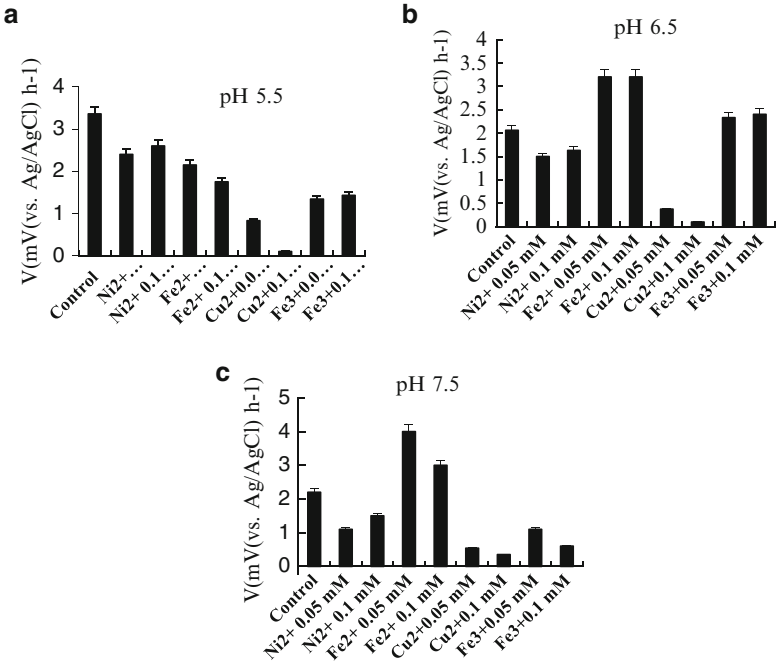

Fig. 14.3 H_2 production rate (V) by *E. coli* BW25113 during glycerol fermentation *in vitro*. Bacteria were grown and V_{H2} was measured *in vitro* at pH 5.5 (**a**), 6.5 (**b**) and 7.5 (**c**) upon glycerol fermentation. Appropriate metal ions at the concentrations mentioned on the figures were added into the assays mixture. Control was H_2 production rate without metal ions added (For details, see Sect. 2.2)

14.3.2 Metal Ions Effects on H_2 Production Rate by E. coli Upon Glycerol Fermentation in vitro

In order to investigate metal ions effects, bacterial culture transferred into the assays mixture (see Materials and methods) was treated 2 min with appropriate compounds; then glycerol was added and ORP kinetics was determined.

In the presence of glycerol E_h and E_h' drops were observed and H_2 production by *E. coli* was detected *in vitro* (Table 14.1). 0.1 and 0.05 mM Fe^{2+} stimulated H_2 production rate ~1.7 and 2 fold at pH 6.5 and 7.5, respectively (Fig. 14.3). Fe^{3+} in 0.05–0.1 mM concentrations had no or opposite, inhibitory effect (Fig. 14.3).

Similar discrimination between Fe^{2+} and Fe^{3+} has been observed with *Rhodobacter sphaeroides*: Fe^{2+} ions affected on ORP stimulating both H_2 formation and bacterial growth, while Fe^{3+} had effect only on bacterial [43]. Moreover, it has been shown that Fe^{3+} increased *Enterococcus hirae* specific growth rate and the F_0F_1-ATPase activity of membrane vesicles, whereas Fe^{2+} had opposite effects [24]. It was supposed that Fe^{2+} may affect directly on Hyd activity or on ORP, which by-turn can regulate F_0F_1 operation. Fe^{2+} and $Fe^{3+}$are reducers and oxidizers, respectively, thus, the opposite effects of these ions are expected.

Furthermore, Ni^{2+} have not affected on H_2 production rate, but both Fe^{2+} and Ni^{2+} stimulated H_2 yield ~5 and ~3 fold at pH 6.5, and ~1.1 and ~1.6 fold at pH 7.5, respectively (Table 14.1). It has been reported by Trchounian's group [31, 44] that during sugar fermentation, *E. coli* possesses membrane protein-protein complex composed from F_0F_1, K^+ transporter TrkA and FHL systems. This complex is responsible for H_2 production; it is formed and operated mainly at slightly alkaline pH. Moreover, the energy within the complex is suggested can be transferred through a dithiol-dosulfide interchange. So reducers could regulate the complex activity as well as H_2 production. The complex is not supposed to operate in *E. coli* during glycerol fermentation although relationship of F_0F_1 with Hyd enzymes has been suggested [14]. Probably, Fe^{2+} and Ni^{2+} could directly affect on Hyd activity, which are [Fe-Ni] containing enzymes, or having reducing properties they may affect on thiol-dithiol interchange and stimulate H_2 production.

As mentioned above Cu^{2+} as oxidizers inhibited Hyd activity in bacteria [28, 45], as well as bacterial growth affecting the lag phase duration and decreasing specific growth rate [30]. Moreover, it has been established [28] that the addition of 0.1 mM to 2 mM Cu^{2+} into the *E. coli* growth medium results in a delayed decrease of E_h although a drop in E_h is less for rather 2 mM than 0.1 mM. All these findings can be taken into consideration to explain oxidizers effects mechanisms on *E. coli*. Thus, it was shown, that 0.05–0.1 mM Cu^{2+} suppressed H_2 production rate at all pHs during glycerol fermentation *in vitro* (Fig 14.3). The obtained effect may be resulted by action of Cu^{2+} on ORP or directly affect on proteins in bacterial membrane, probably on Hyd or the F_0F_1-ATPase as was proposed [29].

It is of interest, that in *hyaB hybC* mutant during glycerol fermentation H_2 production rate was ~2 fold lower (~1.1 mV/min/mg dry weight), compared with wild type, and Fe^{2+} did not stimulate H_2 production rate and yield both *in vitro* at pH 6.5 and 7.5. Thus, it was supposed, that enhanced H_2 formation observed depends on the operation of Hyd-1 and Hyd- 2, which is consistent with the results that during glycerol fermentation at alkaline pH for H_2 formation is responsible Hyd-2 mainly and Hyd-1 [14].

14.4 Conclusions

Ni^{2+}, Fe^{2+} and Fe^{3+} were shown to stimulate bacterial growth on glycerol. Ni^{2+} and Fe^{2+} enhanced H_2 production rate and yield both by *E. coli* during glycerol fermentation especially at pH 6.5 and 7.5. In the presence of Fe^{2+} upon glycerol

fermentation more reductive processes are induced, which by turn may affect on H_2 formation. Increasing H_2 production by heavy metal ions probably is regarded by the action of Hyd-1 or Hyd-2.

The results might be taken into account for optimizing fermentation processes on glycerol and developing H_2 production biotechnology. The coupling of H_2 production to utilization of waste materials containing high concentrations of glycerol may simultaneously provide economic and environmental benefits.

Acknowledgments The authors thank to Prof. T.K. Wood (Department of Chemical Engineering, Texas A & M University, College Station, TX, USA) for supplying strains and advice. This study was done in frame of Research grant to AT (#11-F-202) from Ministry of Education and Sciences of Armenia.

References

1. Momirlan M, Veziroglu TN (2005) The properties of hydrogen as fuel tomorrow in sustainable energy system for a cleaner planet. Int J Hydrog Energy 33:795–802
2. Maeda T, Sanches-Torres V, Wood TK (2008) Metabolic engineering to enhance bacterial hydrogen. Microb Biotechnol 1:30–39
3. Dharmadi Y, Murarka A, Gonzalez R (2006) Anaerobic fermentation of glycerol by *Escherichia coli*: a new platform for metabolic engineering. Biotechnol Bioeng 94:821–828
4. Yazdani S, Gonzalez R (2007) Anaerobic fermentation of glycerol, a path to economic viability for the biofuels industry. Curr Opin Biotechnol 18:213–221
5. da Silva GP, Mack M, Contiero J (2009) Glycerol: a promising and abundant carbon source for industrial microbiology. Biotechnol Adv 27:30–39
6. Khanna S, Goyal A, Moholkar VS (2012) Microbial conversion of glycerol: present status and future prospects. Crit Rev Biotechnol 32(3):235–262. doi:10.3109/07388551.2011. 604839
7. Dasari MA, Kiatsimkul PP, Sutterlin WR, Suppes GJ (2005) Low-pressure hydrogenolysis of glycerol to propylene glycol. Appl Cat Gen 281:225–231
8. Murarka A, Dharmadi Y, Yazmandi S, Gonzalez R (2008) Fermentative utilization of glycerol by *Escherichia coli* and its implications for the production of fuels and chemicals. Appl Environ Microbiol 74:1124–1135
9. Hu H, Wood TK (2010) An evolved *Escherichia coli* strain for producing hydrogen and ethanol from glycerol. Biochem Biophys Res Commun 391:1033–1038
10. Sarma SJ, Brar SK, Sydney EB, Bihan YL, Buelna G, Soccol CR (2012) Microbial hydrogen production by bioconversion of crude glycerol: a review. Int J Hydrog Energy 37:6473–6490
11. Sawers RG (2005) Formate and its role in hydrogen production in *Escherichia coli*. Biochem Soc Transact 33:42–46
12. Trchounian K, Poladyan A, Vassilian A, Trchounian A (2012) Multiple and reversible hydrogenases for hydrogen production by *Escherichia coli*: dependence on fermentation substrate, pH and the F_0F_1-ATPase. Crit Rev Biochem Mol Biol 47:236–249
13. Trchounian K, Trchounian A (2009) Hydrogenase 2 is most and hydrogenase 1 is less responsible for H_2 production by *Escherichia coli* under glycerol fermentation at neutral and slightly alkaline pH. Int J Hydrog Energy 34:8839–8845
14. Trchounian K, Sanchez-Torres V, Wood TK, Trchounian A (2011) *Escherichia coli* hydrogenase activity and H_2 production under glycerol fermentation at low pH. Int J Hydrog Energy 36:4323–4331

15. Vassilian A, Trchounian A (2009) Environment oxidation-reduction potential and redox sensing by bacteria. In: Trchounian A (ed) Bacterial membranes. Ultrastructure, bioelectrochemistry, bioenergetics and biophysics. Research Signpost, Trivandrum, pp 163–195
16. Kwong SCW, Rao G (1992) Effect of reducing agents in anaerobic amino acid fermentation. Biotechnol Bioeng 40:851–857
17. Riondet C, Cachon R, Waché Y, Alcaraz G, Divies C (2000) Extracellular oxidoreduction potential modifies carbon and electron flow in *Escherichia coli*. J Bacteriol 182:620–624
18. Brasca M, Morandi R, Lodi R, Tamburini A (2006) Redox potential to discriminate among species of lactic acid bacteria. J Appl Microbiol 103:1516–1524
19. Soghomonyan D, Akopyan K, Trchounian A (2011) pH and oxidation-reduction potential change of environment during growth of lactic acid bacteria: effect of oxidizers and reducers. Appl Biochem Microbiol 47:33–38
20. Andreini C, Bertini I, Cavallaro G, Holliday GL, Thornton JM (2008) Metal ions in biological catalysis: from enzyme databases to general principles. J Biol Inorg Chem 13:1205–1218
21. Mulrooney SB, Hausinger RP (2003) Nickel uptake and utilization by microorganisms. FEMS Microbiol Rev 27:239–261
22. Touati D (2000) Iron and oxidative stress in bacteria. Arch Biochem Biophys 373:1–6
23. Wu L-F, Navarro C, Pina K, Quenard M, Mandrand M-A (1994) Antagonistic effect of nickel on the fermentative growth of *Escherichia coli* K-12 and comparison of nickel and cobalt toxicity on the aerobic and anaerobic growth. Environ Health Perspect 102:297–300
24. Vardanyan Z, Trchounian A (2012) Fe (III) and Fe (II) ions different effects on *Enterococcus hirae* cell growth and membrane-associated ATPase activity. Biochem Biophys Res Commun 417:541–545
25. Kammler M, Schön C, Hantke K (1993) Characterization of ferrous iron uptake system of *Escherichia coli*. J Bacteriol 175:6212–6219
26. Ouyang Z, Isaacson R (2006) Identification and characterization of a novel ABC iron transport system in *Escherichia coli*. Infect Immun 74:6949–6956
27. Rensing C, Grass G (2003) *Escherichia coli* mechanisms of copper homeostasis in a changing environment. FEMS Microbiol Rev 27:197–213
28. Kirakosyan G, Trchounian A (2007) Redox sensing by *Escherichia coli:* effects of copper ions as oxidizers on proton-coupled membrane transport. Bioelectrochemistry 70:58–63
29. Kirakosyan G, Trchounian K, Vardanyan Z, Trchounian A (2008) Copper (II) ions affect *Escherichia coli* membrane vesicles' SH-groups and a disulfide-dithiol interchange between membrane proteins. Cell Biochem Biophys 51:45–50
30. Vardanyan Z, Trchounian A (2010) The effects of copper (II) ions on *Enterococcus hirae* cell growth and the proton-translocating F_0F_1 ATPase activity. Cell Biochem Biophys 57:19–26
31. Poladyan A, Trchounian A (2009) Production of molecular hydrogen by mixed-acid fermentation in bacteria and its energetic. In: Trchounian A (ed) Bacterial membranes. Ultrastructure, bioelectrochemistry, bioenergetics and biophysics. Research Signpost, Trivandrum, pp 197–231
32. Piskarev M, Ushkanov VA, Aristova NA, Likhachev PP, Myslivets TS (2010) Establishment of the redox potential of water saturated with hydrogen. Biophysics 55:19–24
33. Noguchi K, Riggins DP, Eldahan KG, Kitko RD, Slonczewski JL (2010) Hydrogenase -3 contributes to anaerobic acid resistance of *Escherichia coli*. PLoS One 5:e10132
34. Cintolesi A, Clomburg JM, Rigou V, Zygourakis K, Gonzalez R (2012) Quantitative analysis of the fermentative metabolism of glycerol in *Escherichia coli*. Biotechnol Bioeng 109:187–198
35. Oblinger JL, Kraft AA (1973) Oxidation reduction potential and growth of *Salmonella* and *Pseudomonas fluorescens*. J Food Sci 38:1108–1112
36. Bagramyan K, Galstyan A, Trchounian A (2000) Redox potential is a determinant in the *Escherichia coli* anaerobic fermentative growth and survival: effects of impermeable oxidant. Bioelectrochemistry 51:151–156

37. Bagramyan K, Trchounian A (1997) Decrease of redox potential in the anaerobic growing *Escherichia coli* suspension and proton-potassium exchange. Bioelecrochem Bioenerg 43:129–134
38. Waché Y, Riondet C, Diviès C, Cachon R (2002) Effect of reducing agents on the acidification capacity and the proton motive force of *Lactococcus lactis* ssp. cremoris resting cells. Bioelectrochemistry 57:113–118
39. Oktyabrski ON, Sirnova GV (2012) Redox potentials in bacterial cultures under stress conditions. Microbiology 81:131–142
40. Michelon D, Abraham S, Ebel B, De Coninck J, Husson F, Feron G, Gervais P (2010) Contribution of exofacial thiol groups in the reducing activity of *Lactococcus lactis*. FEBS J 277:2282–2290
41. Kirakosyan G, Bagramyan K, Trchounian A (2004) Redox sensing by *Escherichia coli*: effects of dithiothreitol, a redox reagent reducing disulphides, on bacterial growth. Biochem Biophys Res Commun 325:803–806
42. Berrios-Rivera SJ, Sanchez AM, Bennett GN, San KY (2004) Effect of different levels of NADH availability on metabolite distribution in *Escherichia coli* fermentation in minimal and complex media. Appl Microbiol Biotechnol 65:26–432
43. Hakobyan L, Gabrielyan L, Trchounian A (2012) Discrimination between Fe (II) and Fe (III) effects on redox potential and biohydrogen photoproduction by *Rhodobacter sphaeroides*. ASM 112th General Meeting. San Fransico, USA, Q-2557
44. Trchounian A (2004) *Escherichia coli* proton-translocating F_0F_1-ATP synthase and its association with solute secondary transpopters and/or enzymes of anaerobic oxidation-reduction under fermentation. Biochem Biophys Res Commun 315:1051–1057
45. Sapra R, Bagramyan K, Adams MWW (2003) A simple energy-conserving system: proton reduction coupled to proton translocation. Proc Natl Acad Sci 100:7545–7550

Chapter 15
The Effect of Various Metal Ions on Bio-hydrogen Production and F_0F_1-ATPase Activity of *Rhodobacter Sphaeroides*

Lilit Hakobyan, Lilit Gabrielyan, and Armen Trchounian

Abstract The important aspect in regulation of bio-hydrogen (H_2) production by purple bacteria and its energetics is the requirement of the F_0F_1-ATPase, the main membrane mechanism generating proton motive force. *Rhodobacter sphaeroides* MDC 6521 (isolated from Arzni mineral springs in Armenia) is able to produce H_2 in anaerobic conditions under illumination in the presence of various metal ions. In order to examine the mediatory role of the F_0F_1-ATPase in H_2 production, the effects of various metal ions (Mn^{2+}, Mg^{2+}, Fe^{2+}, Ni^{2+}, and Mo^{6+}) on *N*,*N*′-dicyclohexylcarbodiimide inhibited ATPase activity of *R. sphaeroides* membrane vesicles were investigated. These ions in appropriate concentrations considerably enhanced H_2 production. But the latter was not observed in the absence of Fe^{2+}, indicating the requirement of Fe^{2+}. The *R. sphaeroides* membrane vesicles demonstrated significant ATPase activity. The absence of Fe^{2+} caused to marked inhibition (~80 %) in ATPase activity. In the presence of Fe^{2+} (80 μM) and Mo^{6+} (16 μM) a higher ATPase activity was observed. These results indicate a relationship between H_2 production and the F_0F_1-ATPase activity that might be an important pathway to regulate bacterial activity under anaerobic conditions and provide novel evidence on responsibility of F_0F_1 in H_2 production by *R. sphaeroides*.

Keywords *Rhodobacter sphaeroides* • Heavy metal ion • Redox potential • Bio-hydrogen • F_0F_1-ATPase activity

L. Hakobyan • L. Gabrielyan (✉)
Department of Biophysics, Biology Faculty, Yerevan State University,
1 A. Manoukian Str., 0025 Yerevan, Armenia
e-mail: LGabrielyan@ysu.am

A. Trchounian
Department of Biophysics, Biology Faculty, Yerevan State University,
1 A. Manoukian Str., 0025 Yerevan, Armenia

Department of Microbiology & Microbe and Plant Biotechnology, Biology Faculty, Yerevan State University, 1 A. Manoukian Str., 0025 Yerevan, Armenia

A. Veziroğlu and M. Tsitskishvili (eds.), *Black Sea Energy Resource Development and Hydrogen Energy Problems*, NATO Science for Peace and Security Series C: Environmental Security, DOI 10.1007/978-94-007-6152-0_15,

15.1 Introduction

Rhodobacter sphaeroides grow well in anaerobic conditions under illumination fermenting various organic substrates, which is accompanied by bio-hydrogen (H_2) production and by changes of oxidation-reduction (redox) potential (E_h) and proton motive force [1–5].

The important aspect in regulation of H_2 production by various bacteria and its energetics is the requirement of the F_0F_1-ATPase, the main membrane mechanism generating proton motive force [6–9]. In purple bacteria both the light driven and respiratory electron transfers serve the sole purpose of generating a proton motive force across their inner membrane [6, 7]. The backflow of protons is carried out by the enzyme F_0F_1-ATPase, which producing ATP from ADP and inorganic phosphate (P_i) [6, 7].

Purple non sulfur bacteria *Rhodobacter sphaeroides* produce H_2 under reducing conditions upon the drop in redox potential, which could determine electron transfer within bacterial membrane and generation of proton motive force [4, 5]. A relationship between E_h, ATPase activity and H_2 production is proposed for these bacteria [1, 4, 5].

It is well known that low concentrations of various metals such as iron (Fe), molybdenum (Mo), manganese (Mn), magnesium (Mg), and other are required for the growth of photosynthetic bacteria. Fe, Mo and nickel (Ni) have been shown to be component of several enzymes involved in H_2 metabolism in photosynthetic bacteria such as nitrogenase and membrane-bound uptake hydrogenase [10–14]. Majority of the known hydrogenases are [Fe]- or [Ni-Fe]-hydrogenases [7, 13–15]. Presence of Mo and Fe is necessary since they are found in the nitrogenase structure, and moreover electron carriers of the photosynthetic electron transfer chain such as ferrodoxin and cytochromes also contain Fe [11–13]. Many photosynthetic electron carriers, including cytochromes and protein complexes, contain Mg such as chlorophyll and bacteriochlorophyll [12]. Mn is an essential element in photosynthetic organisms. In purple bacteria it involves in regulation of nitrogenase activity, and participates in the structure of photosynthetic proteins and enzymes [16, 17]. Thus, metal ions play key roles in electron transport and H_2 production by bacteria.

In our previous study, we were shown that purple non sulfur bacterium *Rhodobacter sphaeroides* MDC 6521, isolated from mineral springs Arzni in Armenia, were able to grow and produce H_2 in anaerobic conditions upon illumination in the presence of various concentrations of Ni^{2+} and Mg^{2+} [18]. The obtained results have shown that the 2–6 μM Ni^{2+} and 5–15 mM Mg^{2+} noticeably enhanced H_2 production by *R. sphaeroides*.

In this study, the effect of heavy metal ions on growth properties (specific growth rate, absorption spectra), medium characteristics (pH, and E_h) and H_2 production by *R. sphaeroides* MDC 6521 was investigated. In order to examine the mediatory role of the F_0F_1-ATPase in H_2 production, the effects of various metal ions (Fe^{2+}, Mn^{2+}, Mo^{6+}, Mg^{2+}, and Ni^{2+}) on *N,N'*-dicyclohexylcarbodiimide (DCCD) inhibited ATPase activity of *R. sphaeroides* membrane vesicles were studied. This study was important for understanding the mechanisms of biological effects of heavy metals ions on bacterial growth properties and H_2 production.

15.2 Materials and Methods

15.2.1 Bacterial Strain and Growth Conditions

The purple bacterium *R. sphaeroides* strain MDC 6521 (Microbial Depository Center, Armenia, WDCM803) used in this study was isolated from Arzni mineral springs in Armenia [1–3]. The bacterium was grown in anaerobic conditions in Ormerod medium at 30 ± 2 °C under illumination of approximately 36 W m^{-2} [1, 2]. Succinate (3.54 g L^{-1}) and yeast extract (2 g L^{-1}) were used as sole carbon and nitrogen sources [3]. The concentration of $FeSO_4 \cdot 7H_2O$ in the growth medium ranged from 0, 40, 80 and 120 μM; the concentration of $Na_2MoO_4 \cdot 2H_2O$ ranged from 3, 8, 16 and 32 μM; and the concentration of $MnCl_2$ ranged from 10, 50, 200 and 500 μM. Metal ions free medium was prepared by omitting $FeSO_4 \cdot 7H_2O$, $Na_2MoO_4 \cdot 2H_2O$ and $MnCl_2$ from the Ormerod medium. Fe^{2+} was added to the appropriate concentration from a freshly prepared sterile solution of $FeSO_4 \cdot 7H_2O$. Mn^{2+} or Mo^{6+} was added from sterile solutions ($Na_2MoO_4 \cdot 2H_2O$ or $MnCl_2 \cdot 4H_2O$) to the required concentration into the medium, which contained 40 μM Fe^{2+}.

The medium initial pH was adjusted to 7.0 by means of 0.1 M HCl or NaOH. The pH of growth medium was measured by a pH-potentiometer (HANNA Instruments, Portugal) as described [1–3]. The growth of bacteria was monitored by a Spectro UV-vis Auto spectrophotometer (Labomed, USA) by changes in absorbance of cell suspension at the wavelength of 660 nm [1]. Specific growth rate was calculated over the interval, where the logarithm of absorbance of the culture at 660 nm increased linearly with the time and expressed as 0.693/doubling time (h^{-1}) [2, 3, 18]. The relation of the dry weight to the optical density of the cells was plotted to obtain the growth curves.

In order to test the metal ions effects on the photosynthetic apparatus, the absorption spectra of *R. sphaeroides* suspension were recorded at the wavelength region of 400–1,000 nm on Spectro UV-vis Auto spectrophotometer (Labomed, USA) in cuvette with path length of 10 mm [3, 18]. For obtaining comparable data, the original spectra were subtracted of the scattering and normalized to the same cell concentration.

15.2.2 Determination of Redox Potential and H_2 Production Assays

The external redox potential (E_h) was measured with potentiometric method as described [3, 18, 19]. H_2 production was assayed by using a pair of redox platinum (Pt) and titanium-silicate (Ti-Si) (EO-02, GSEEE) electrodes as described [3, 18, 19]. The H_2 yield was calculated by the decrease of E_h to low negative values as described by Piskarev and co-workers [20] and expressed in mmol g^{-1} dry weight [3].

H_2 production was verified chemically by method based on the bleaching of $KMnO_4$ solution in H_2SO_4 with H_2 [1–3, 19]. This method was suggested for detecting enhanced H_2 production [21].

15.2.3 ATPase Activity Assay

Bacterial membrane vesicles were obtained by the Kaback method as described [1, 5, 8]. ATPase activity in the membrane vesicles was measured by the liberation of inorganic phosphate (P_{in}) in the reaction with ATP by the method of Taussky and Shorr using a spectrophotometer Spectro UV-vis Auto (Labomed, USA) [1, 5, 8, 22]. ATPase activity was expressed in μM P_{in} min^{-1} μg^{-1} protein. The protein content was determined by the method of Lowry [1, 22]. For *N*,*N*′-dicyclohexylcarbodiimide (DCCD) inhibition studies, cells were incubated with the reagent (0.2 mM) for 10 min. For metal ions effects studies, membrane vesicles were pre-incubated with the Mo^{6+} (16 μM), Mn^{2+} (50 μM), Fe^{2+} (80 μM), and Ni^{2+} (4 μM) for 10 min. The choice of used metal ions concentrations is based on the results of our investigations: these concentrations of ions noticeably enhanced H_2 production by *R. sphaeroides*.

15.2.4 Others, Reagents and Data Processing

The electrodes used were immersed into the cultured vessels. The electrodes readings were registered at regular intervals (each 24 h) as shown in the figures. The average data are represented from three independent experiments; the standard errors were calculated as described [23].

Yeast extract, $FeSO_4 \cdot 7H_2O$, $Na_2MoO_4 \cdot 2H_2O$ were from Carl Roths GmbH, Germany; $MgSO_4 \cdot 7H_2O$, $MnCl_2 \cdot 4H_2O$, $NiCl_2$, succinic acid were from Unichem, China; DCCD, ATP were from Sigma, Aldrich, USA, and other reagents of analytical grade were used in this study.

15.3 Results and Discussion

15.3.1 R. sphaeroides Growth Properties in the Presence of Heavy Metal Ions

The purple bacterium *R. sphaeroides* MDC 6521 is known to grow well and produce H_2 in anaerobic conditions under illumination at pH 7.0. The growth and pH changes were monitored during *R. sphaeroides* cultivation at different concentrations of heavy metal ions (Mn^{2+}, Mo^{6+} and Fe^{2+}) containing medium.

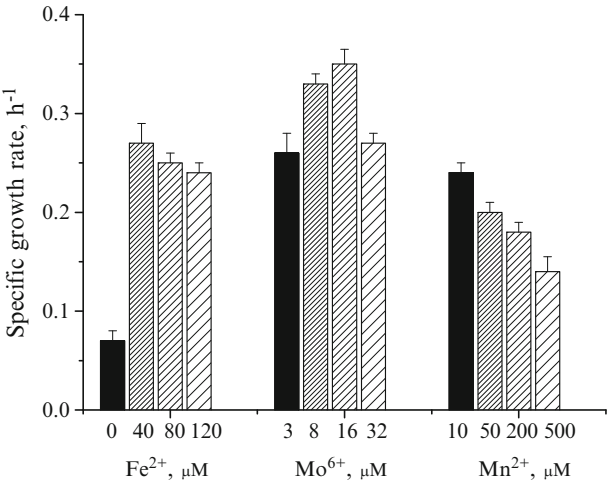

Fig. 15.1 The effect of metal ions various concentrations on *R. sphaeroides* MDC 6521 specific growth rates, which was determined as described in Sect. 15.2

The choice of metal ions concentrations is based on the results of our and other authors investigations [10, 13, 17]. The standard Ormerod medium used contains 40 μM Fe^{2+}, 10 μM Mn^{2+} and 3 μM Mo^{6+} [2].

Interestingly, *R. sphaeroides* MDC 6521 was unable to grow well in medium without Fe^{2+} (Fig. 15.1), which indicated that Fe^{2+} is important for growth of purple bacteria. The addition of Fe^{2+} (40–120 μM) into the growth medium resulted in an increased specific growth rate in comparison with the control (in absence of Fe^{2+}) (Fig. 15.1). The highest growth rate was obtained for *R. sphaeroides* cells in the presence of 8 and 16 μM Mo^{6+}: the latter added gave a stimulated (~1.4-fold) growth rate in comparison with the control (3 μM Mo^{6+}) (Fig. 15.1). Interestingly, this result was similar to the data obtained for bacterial cells with Ni^{2+} and Mg^{2+} [18]. Within Mn^{2+} specific growth rate was lower of control (10 μM Mn^{2+}). The results point out the concentration dependent Mn^{2+} effect: the 500 μM Mn^{2+}added gave a suppressed (~1.7-fold) growth rate. In this medium Fe^{2+} was at a constant concentration of 40 μM.

Growth conditions and medium components have been shown to affect the synthesis of the photosynthetic apparatus of purple bacteria [17, 24]. The photosynthetic apparatus of *R. sphaeroides* is known to consist of two pigment-protein light-harvesting (LH) complexes: LH I or B875 and LH II or B800-850, which are identified by the bacteriochlorophyll *a* (Bchl) absorbance maxima [24, 25].

To reveal the effect of metal ions various concentration on *R. sphaeroides* photosynthetic apparatus formation, the room temperature light absorption spectra was investigated for the cells grown in the presence of Mn^{2+}, Mo^{6+} and Fe^{2+}. The several peaks in wavelength region of 400–500 nm correspond to carotenoids; the LH II Bchl *a* absorption can be seen as a peak at 800 nm and at 850 nm, while the LH I Bchl *a* can be seen as a absorption peak shoulder at 875 nm [18, 24, 25]. In the

presence of Mn^{2+} and Mo^{6+} a decrease in the level of carotenoids and Bchl *a* was observed (Fig. 15.2a, b). The results point out the concentration dependent effect of used ions. In this medium Fe^{2+} was at a constant concentration of 40 μM. As shown in Fig. 15.2c, the presence of Fe^{2+} in the growth medium caused a increasing in the level of both LH complexes.

The obtained results indicate that used metal ions were affecting the level of LH complexes and not pigment content, meanwhile Mn^{2+} and Mo^{6+} have opposite action on the level of the photosynthetic pigments in comparison with Fe^{2+}. These results obtained are similar to the data reported by Horne et al. [17]. Interestingly, this effect of Fe^{2+} on the LH complexes was also opposite to the effect obtained for *R. sphaeroides* in the presence of Ni^{2+} and Mg^{2+} [18].

The obtained results showed that, the final pH in the presence of all metal ions were higher than the initial pH, which is important factor for the bacterial growth. During the growth in the presence of metal ions used pH increased from 7.0 ± 0.1 (initial pH) to ~9.0–9.2 for the first 48 h and then pH followed to ~8.0–8.5 (not shown). It is well known that pH increase was connected with the uptake of organic acids and extrusion of hydroxide anions or with the formation of various products such as polyhydroxybutyrate [11, 13, 18]. Decrease of pH was connected with formation of fermentation end products, which decay with H_2 and CO_2 evolution.

15.3.2 *R. sphaeroides* Suspension E_h Changes and H_2 Production in the Presence of Heavy Metal Ions

The E_h can be considered as the key factor determining bacterial anaerobic growth, which is connected with decreasing of E_h from positive to negative values [2, 26–28]. Lee et al. [29] reported a relationship between the H_2 production and falling of E_h to low negative value: the electron flow can be shifted toward the reduction of proton to H_2 under strong reducing conditions.

All metal ions used affected on E_h of *R. sphaeroides* during the anaerobic growth upon illumination. Interestingly, E_h, measured by a Pt electrode, gradually decreased during the growth (0–96 h) with various concentrations of ions: E_h drop was more intensive in the presence of Mn^{2+} (50 and 200 μM), Mo^{6+} (16 and 32 μM), and Fe^{2+} (80 and 120 μM) (Fig. 15.3). The obtained results pointed out that E_h decreased to more negative value, when Mo^{6+} concentration increased from 3 to 32 μM (Fig. 15.3b). In the presence of 16 μM Mo^{6+} E_h decreased to –735 mV, by addition of 80 μM Fe^{2+} E_h decreased to –720 mV (see Fig. 15.3b, c). Such decrease in redox potential indicate enhanced H_2 production [2, 19, 28–30], which also was confirmed by chemical assay. Lee and co-workers [29] were shown that in the presence of $FeSO_4$ the anaerobic condition was strongly reduced to −545 mV of redox potential, which had the maximum H_2 yield.

In fact, the highest H_2 yields (11.57 and 11.06 mmol g^{-1} dry weights) were obtained for *R. sphaeroides* in medium with 80 μM Fe^{2+} and 16 μM Mo^{6+}, which was ~2 fold higher than that with control (40 μM Fe^{2+} and 3 μM Mo^{6+}) (Table 15.1).

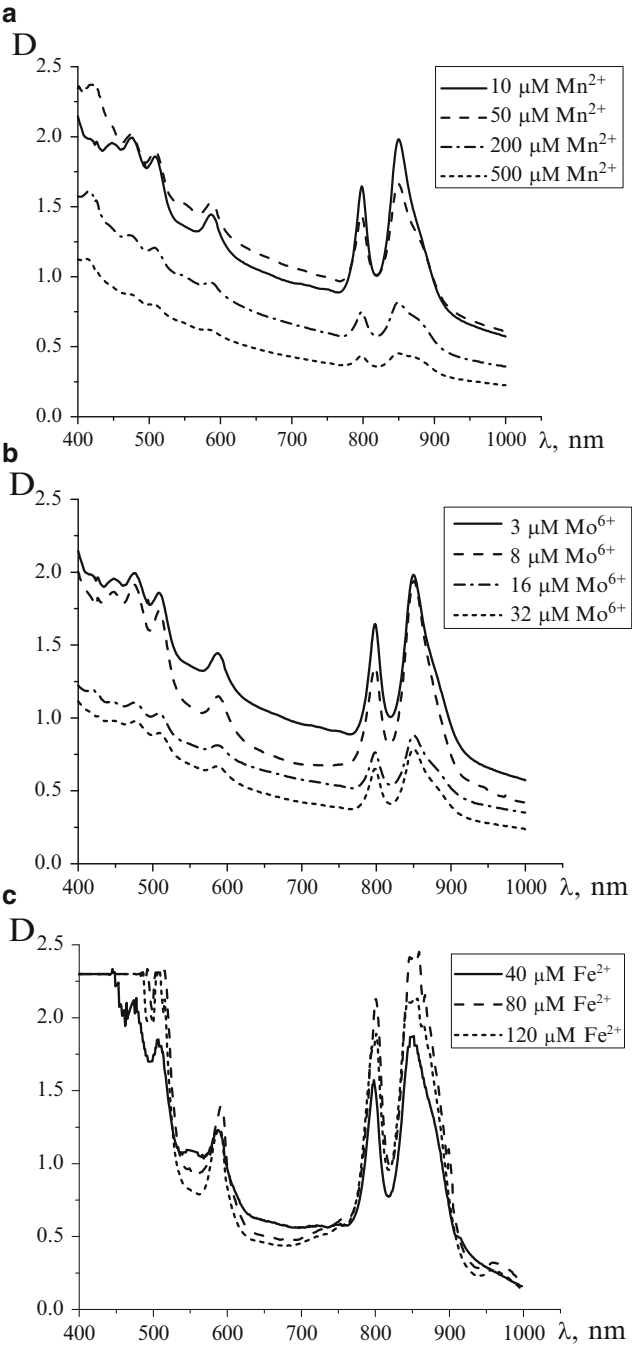

Fig. 15.2 Dependence of the absorption spectra of *R. sphaeroides* strain MDC 6521 suspension on Mn^{2+} (**a**), Mo^{6+} (**b**) and Fe^{2+} (**c**) various concentrations. The absorption spectra were recorded as described in Sect. 15.2. *D* was optical density

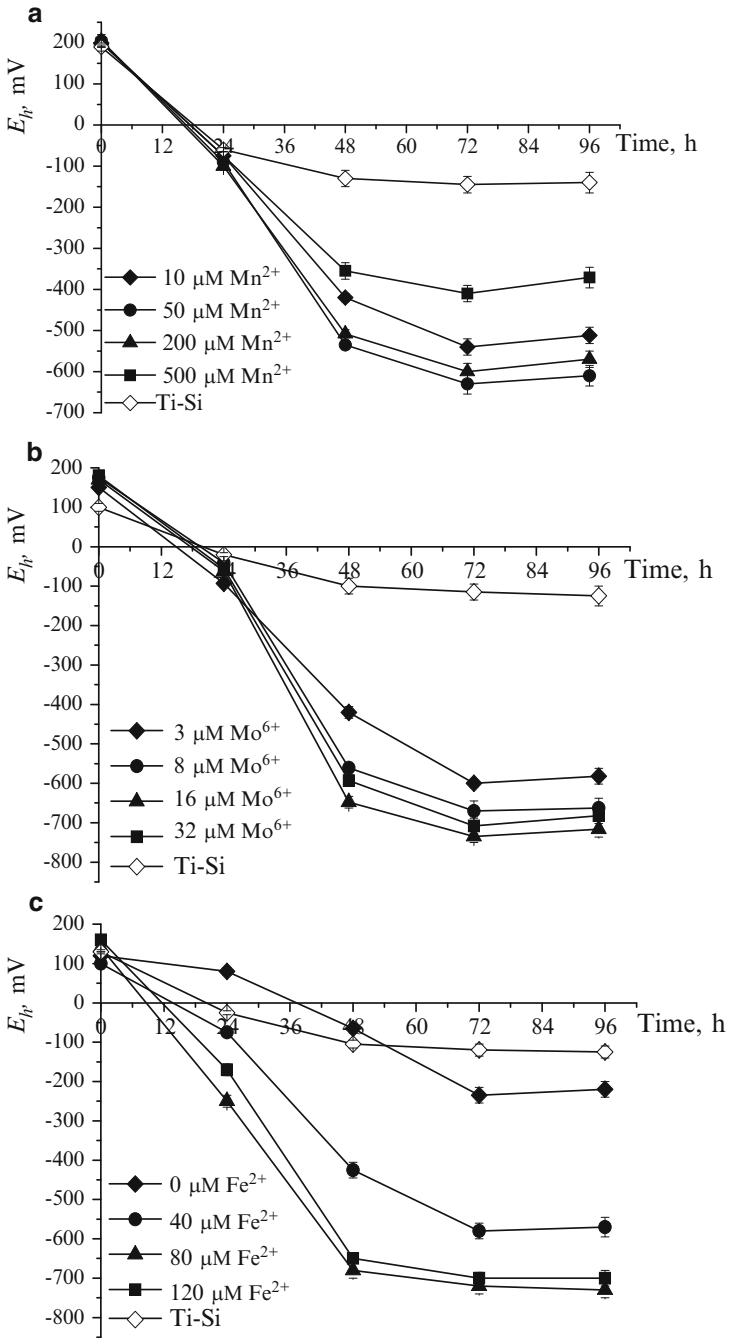

Fig. 15.3 The change of E_h of *R. sphaeroides* strain MDC 6521 during the anaerobic growth at illumination in Mn^{2+} (**a**), Mo^{6+} (**b**) and Fe^{2+} (**c**) various concentration containing medium. E_h of bacterial growth medium was measured at regular intervals using a Pt and Ti-Si electrodes (see Sect. 15.2)

Table 15.1 The effects of metal ions various concentrations on H_2 yield of *R. sphaeroides* MDC 6521 during anaerobic growth and its correlations with E_h

Metal ions	H_2 yield *, mmol g^{-1} dry weight	E_h, mV
No additions	–	−235 ± 20 mV
40 μM Fe^{2+}	5.95	−580 ± 10 mV
80 μM Fe^{2+}	11.57	−720 ± 15 mV
120 μM Fe^{2+}	10.30	−700 ± 15 mV
3 μM Mo^{6+}	5.92	−600 ± 20 мВ
8 μM Mo^{6+}	7.02	−670 ± 25 мВ
16 μM Mo^{6+}	11.06	−735 ± 15 мВ
32 μM Mo^{6+}	9.38	−708 ± 20 мВ
10 μM Mn^{2+}	5.02	−540 ± 20 mV
50 μM Mn^{2+}	7.60	−630 ± 25 mV
200 μM Mn^{2+}	6.84	−600 ± 20 mV
500 μM Mn^{2+}	1.24	−410 ± 20 mV

*The mean values calculated by decrease in E_h (see Sect. 15.2) are represented. Minus (−) sign represented absence of H_2 production

H_2 production was not observed in absence of Fe^{2+}, indicating that Fe^{2+} is necessary for H_2 production. It is suggested that Fe^{2+} can increase nitrogenase or other enzymes expression in suitable concentration. Oxidation of reduced ferredoxin during photo-fermentation could be also proposed to produce more H_2.

The H_2 yield was increased, when Mn^{2+} concentration increased from 10 to 200 μM; but in the presence of 500 μM Mn^{2+} H_2 yield was ~4 fold lower in comparison with 10 μM Mn^{2+} (Table 15.1). The results indicated that Mn^{2+} could enhance or inhibit H_2 production depending on its concentration.

Thus, metal ions used were shown to affect E_h changes in a concentration-dependent manner, and these ions in appropriate concentrations enhanced H_2 production by *R. sphaeroides* during the anaerobic growth upon illumination.

15.3.3 ATPase Activity of R. sphaeroides Membrane Vesicles in the Presence of Heavy Metal Ions

It is well known, that during the photosynthetic electron transport H^+ is pumped through the membrane, proton gradient is developed, which is used by F_0F_1 to generate ATP for the transfer of electrons to the electron acceptor ferredoxin. Under anaerobic conditions these electrons can be used with the energy of ATP by nitrogenase to reduce H^+ into H_2.

In order to determine the mediatory role of F_0F_1 in H_2 production, the effects of metal ions (Mn^{2+}, Mg^{2+}, Fe^{2+}, Ni^{2+}, and Mo^{6+}) on DCCD inhibited ATPase activity of membrane vesicles of *R. sphaeroides*, grown in the presence and absence of Fe^{2+}, were investigated. The *R. sphaeroides* F_0F_1 is a typical F_0F_1-ATPase, which also

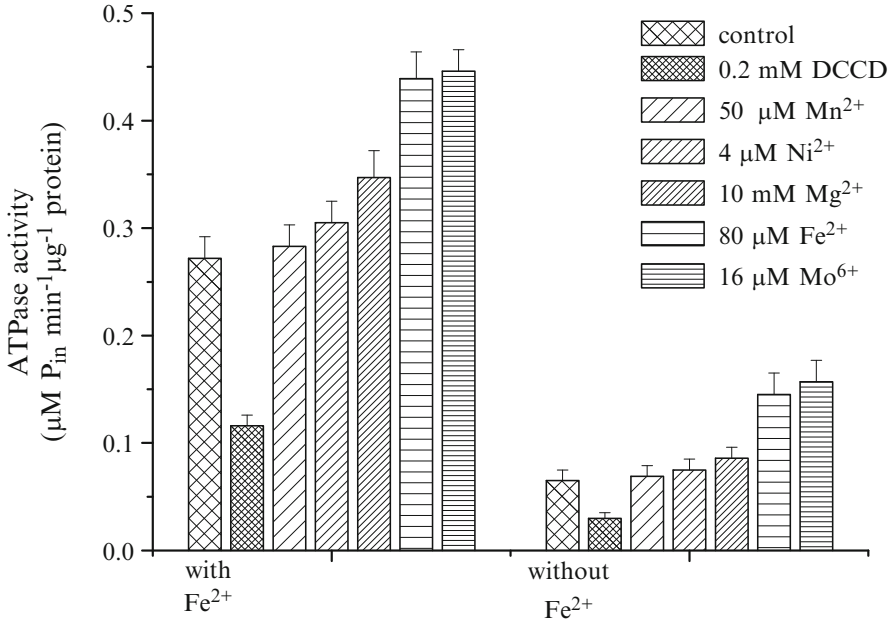

Fig. 15.4 Effects of the heavy metal ions on the ATPase activity of the membrane vesicles of *R. sphaeroides* MDC 6521, grown in the presence and absence of Fe^{2+}. The ATPase activity was calculated by colorimetric determination of liberation of inorganic phosphate (P_{in}) per time and protein upon ATP adding

known as F-type ATPase [6]. By translocating H^+ it derives the free energy for ATP synthesis from the electrochemical potential difference of the proton across the respective coupling membrane [6, 7].

As was shown, metal ions used in appropriate concentrations considerably enhanced H_2 production by *R. sphaeroides*. For metal ions effects studies, membrane vesicles were pre-incubated with the Mo^{6+} (16 μM), Mn^{2+} (50 μM), Mg^{2+} (10 mM), Fe^{2+} (80 μM), and Ni^{2+} (4 μM) for 10 min. The choice of these concentrations is based on the results of our investigations: these concentrations of ions noticeably enhanced H_2 production by *R. sphaeroides* [18].

The membrane vesicles of *R. sphaeroides* grown in the standard Ormerod medium demonstrated significant ATPase activity (Fig. 15.4), which was inhibited by F_0F_1 various inhibitors [1, 4]. The absence of Fe^{2+} caused to marked inhibition (~80 %) in ATPase activity (Fig. 15.4). The incubation of membrane vesicles of this bacterium with F_0F_1 inhibitor DCCD caused to marked inhibition in ATPase activity: the inhibition revealed concentration dependence [4]. In our experiments the inhibition of ATPase activity on ~60 % was detected in the presence of 0.2 mM DCCD (Fig. 15.4). Mn^{2+} (50 μM) did not affect on the ATPase activity, moreover, the value of ATPase activity was almost the same as those of the control (see Fig. 15.4). After treatment of membrane vesicles with Ni^{2+} (4 μM) and Mg^{2+}

(10 mM) the ATPase activity stimulation was observed: the activity was increased by ~15 and 30 %, respectively (Fig. 15.4). In the presence of Fe^{2+} (80 μM) and Mo^{6+}(16 μM) a higher ATPase activity was observed in comparison with control (Fig. 15.4). These ions gave a stimulated (~2.5-fold) ATPase activity of the membrane vesicles of *R. sphaeroides* grown in the absence of Fe^{2+}.

Thus, the appropriate concentrations of the heavy metal ions added gave a stimulated ATPase activity, which indicate a relationship between the F_0F_1-ATPase activity and H_2 production by *R. sphaeroides*.

15.4 Conclusions

The effects of heavy metals ion various concentrations on H_2 production and DCCD inhibited ATPase activity by *R. sphaeroides* was investigated.

All used metal ions increased drop in E_h during the bacterial anaerobic growth. Such decrease in E_h might indicate enhanced H_2 production. These metal ions in appropriate concentrations considerably enhanced H_2 production by *R. sphaeroides*. Actually, the highest H_2 yields were obtained for *R. sphaeroides* in the presence of 16 μM Mo^{6+} and 80 μM Fe^{2+}, those were ~2 fold higher than that of the control. But E_h was not changed much, and H_2 production was not observed in the absence of Fe^{2+}, indicating that Fe^{2+} is required for H_2 production. In phototrophic anaerobic conditions, with the help of energy of ATP electrons derived from ferredoxin then can be used by nitrogenase to reduce H^+ into H_2 [7]. Used heavy metal ions probably stimulate this process.

The obtained results indicate that metal ions were affecting the level of LH complexes and not pigment content during the growth of *R. sphaeroides*, meanwhile Mn^{2+} and Mo^{6+} have opposite action on the level of the photosynthetic pigments in comparison with Fe^{2+}. By addition of Mo^{6+} a decrease in the level of B800-850 complexes was observed, whereas the level of B875 becomes more pronounced. Probably, B875 complex accumulates and transfers the light energy to a reaction centre increasing the H_2 production in comparison with control. The observed results suggest the significant role of these complexes in H_2 production.

To examine the mediatory role of F_0F_1, the main membrane enzyme for bioenergetics responsible for generation of proton motive force, in H_2 production by *R. sphaeroides*, the effects of metal ions on ATPase activity were determined. The absence of Fe^{2+} caused to marked inhibition (~80 %) in ATPase activity of membrane vesicles. After treatment of membrane vesicles with Ni^{2+} (4 μM) and Mg^{2+} (10 mM) the ATPase activity stimulation was observed: the activity was increased by ~15 and 30 %, respectively. A higher ATPase activity was observed by addition of Fe^{2+} (80 μM) and Mo^{6+} (16 μM).

These results obtained indicate a relationship between H_2 production and the F_0F_1-ATPase activity that might be an important pathway to regulate bacterial activity under anaerobic conditions; and provide novel evidence on responsibility of nitrogenase and F_0F_1 in H_2 production by this bacterium.

Acknowledgments This work was supported by the Ministry of Education and Science of the Republic of Armenia, research grant to AT (#11-1 F202) and by a research grant from the Armenian National Science and Education Fund (ANSEF) based in New York, USA to LG (NS-Biotechnology-2704).

References

1. Gabrielyan L, Trchounian A (2009) Relationship between molecular hydrogen production, proton transport and the F_0F_1-ATPase activity in *Rhodobacter sphaeroides* strains from mineral springs. Int J Hydrog Energy 34:2567–2572
2. Gabrielyan L, Torgomyan H, Trchounian A (2010) Growth characteristics and hydrogen production by *Rhodobacter sphaeroides* using various amino acids as nitrogen sources and their combinations with carbon sources. Int J Hydrog Energy 35:12201–12207
3. Hakobyan L, Gabrielyan L, Trchounian A (2012) Yeast extract as an effective nitrogen source stimulating cell growth and enhancing hydrogen photoproduction by *Rhodobacter sphaeroides* strains from mineral springs. Int J Hydrog Energy 37:6519–6526
4. Hakobyan L, Gabrielyan L, Trchounian A (2011) Proton motive force in *Rhodobacter sphaeroides* under anaerobic conditions in the dark. Curr Microbiol 62:415–419
5. Hakobyan L, Gabrielyan L, Trchounian A (2012) Relationship of proton motive force and the F_0F_1-ATPase with bio-hydrogen production activity of *Rhodobacter sphaeroides*: effects of diphenylene iodonium, hydrogenase inhibitor, and its solvent dimethylsulphoxide. J Bioenerg Biomembr 44(4):495–502. doi:10.1007/s10863-012-9450-3
6. Feniouk BA, Junge W (2009) Proton translocation and ATP synthesis by the F_oF_1-ATPase of Purple Bacteria. In: Hunter CN, Daldal F, Thurnauer MC, Beatty JT (eds) The purple phototrophic bacteria. Springer, Dordrecht
7. Gabrielyan L, Trchounian A (2009) Purple bacteria and cyanobacteria as potential producers of molecular hydrogen: an electrochemical and bioenergetic approach. In: Trchounian A (ed) Bacterial membranes. Research Signpost, Kerala, India
8. Trchounian AA, Vassilian AV (1994) Relationship between the F_0F_1 ATPase and K^+ transport system within the membrane the anaerobically growth *Escherichia coli*. *N,N'*-dicyclohexyl-carbodiimide-sensitive ATPase activity in mutants with defects in K^+-transport. J Bioenerg Biomembr 26:563–571
9. Trchounian A (2004) *Escherichia coli* proton-translocating F_0F_1-ATP synthase and its association with solute secondary transporters and/or enzymes of anaerobic oxidation-reduction under fermentation. Biochem Biophys Res Commun 315:1051–1057
10. Kars G, Gündüz U, Yücel M, Türker L, Eroglu I (2006) Hydrogen production and transcriptional analysis of *nif*D, *nif*K and *hup*S genes in *Rhodobacter sphaeroides* O.U.001 grown in media with different concentrations of molybdenum and iron. Int J Hydrog Energy 31:1536–1544
11. Zhu H, Fang HHP, Zhang T, Beaudette LA (2007) Effect of ferrous ion on photo heterotrophic hydrogen production by *Rhodobacter sphaeroides*. Int J Hydrog Energy 32:4112–4118
12. Liu B-F, Ren N-Q, Ding J, Xie G-J, Guo W-Q (2009) The effect of Ni^{2+}, Fe^{2+} and Mg^{2+} concentration on photo-hydrogen production by *Rhodopseudomonas faecalis* RLD-53. Int J Hydrog Energy 34:721–726
13. Eroglu E, Gündüz U, Yücel M, Eroglu I (2011) Effect of iron and molybdenum addition on photofermentative hydrogen production from olive mill wastewater. Int J Hydrog Energy 36:5895–5903
14. Carrieri D, Ananyev G, Garcia Costas AM, Bryant DA, Dismukes GC (2008) Renewable hydrogen production by cyanobacteria: nickel requirements for optimal hydrogenase activity. Int J Hydrog Energy 33:2014–2022

15. Forzi L, Sawers RG (2007) Maturation of [NiFe]-hydrogenases in *Escherichia coli*. Biometals 20:565–578
16. Yoch D (1979) Manganese, an essential trace element for N_2 fixation by *Rhodospirillum rubrum* and *Rhodopseudomonas capsulata*: role in nitrogenase regulation. J Bacteriol 40:987–995
17. Horne IM, Pemberton JM, McEwan AG (1998) Manganous ions suppress photosynthesis gene expression in *Rhodobacter sphaeroides*. Microbiology 144:2255–2261
18. Hakobyan L, Gabrielyan L, Trchounian A (2012) Ni (II) and Mg (II) ions as factors enhancing biohydrogen production by *Rhodobacter sphaeroides* from mineral springs. Int J Hydrog Energy 37:7486–7491
19. Trchounian K, Sanchez-Torres V, Wood KT, Trchounian A (2011) *Escherichia coli* hydrogenase activity and H_2 production under glycerol fermentation at a low pH. Int J Hydrog Energy 36:4323–4331
20. Piskarev IM, Ushkanov VA, Aristova NA, Likhachev PP, Myslivets TS (2010) Establishment of the redox potential of water saturated with hydrogen. Biophysics (Moscow) 55:13–17
21. Maeda T, Wood TK (2008) Formate detection by potassium permanganate for enhanced hydrogen production in *Escherichia coli*. Int J Hydrog Energy 33:2409–2412
22. Vardanyan Z, Trchounian A (2012) Fe(III) and Fe(II) ions different effects on *Enterococcus hirae* cell growth and membrane-associated ATPase activity. Biochem Biophys Res Commun 417:541–545
23. Lakin GF (1992) Biometry. Vishaya shcola, Moscow (in Russian)
24. Kim E-J, Kim J-S, Kim M-S, Lee JK (2006) Effect of changes in the level of light harvesting complexes of *Rhodobacter sphaeroides* on the photoheterotrophic production of hydrogen. Int J Hydrog Energy 31:531–538
25. Hu X, Ritz T, Damjanovic A, Autenrieth F, Schulten K (2002) Photosynthetic apparatus of purple bacteria. Q Rev Biophys 35:1–62
26. Bagramyan K, Galstyan A, Trchounian A (2000) Redox potential is a determinant in the *Escherichia coli* anaerobic growth and survival: effect of impermeable oxidant. Bioelectrochemistry 51:151–156
27. Vassilian A, Trchounian A (2009) Environment oxidation-reduction potential and redox sensing of bacteria. In: Trchounian A (ed) Bacterial membranes. Research Signpost, Kerala, India
28. Trchounian K, Trchounian A (2009) Hydrogenase 2 is most and hydrogenase 1 is less responsible for H_2 production by *Escherichia coli* under glycerol fermentation at neutral and slightly alkaline pH. Int J Hydrog Energy 34:8839–8845
29. Lee D-Y, Li Y-Y, Oh Y-K, Kim M-S, Noike T (2009) Effect of iron concentration on continuous H_2 production using membrane bioreactor. Int J Hydrog Energy 34:1244–1252
30. Noguchi K, Riggins DP, Eldahan KC, Kitko RD, Slonczewski JL (2010) Hidrogenase-3 contributes to anaerobic acid resistance of *Escherichia coli*. PLoS One 5:1–7

Chapter 16
Hydrogen Accumulators for Various Purposes

Dmitry V. Schur, A.F. Savenko, V.A. Bogolepov, Svetlana Yu. Zaginaichenko, Z.A. Matysina, A. Magrez, M. Baibarac, and T. Nejat Veziroğlu

Abstract The hydrogen storage in metal hydrides is the urgent problem of hydrogen power engineering and the demand for metal hydrides as capacitive, safe and convenient in service sources of hydrogen has stimulated the study of hydrogen capacity of multicomponent alloys. In recent years, much attention has been given by scientists to the investigation of hydrogen-sorption and desorption properties of different materials, including nanocarbon structures and composites on their base, the study of peculiarities of the reversible hydrogen interaction with hydride forming metals and alloys, the development of high-pure hydrogen storage and transportation in solids. This chapter deals with the designed hydrogen metal-hydride torches with piezoelectric firing of flame, two models of accumulators/compressors of great capacity on hydrogen, and three modifications of laboratory hydrogen accumulators used in operation of fuel cells. We show the construction of all torches and accumulators, their technical operating characteristics, the special features and advantages of devices developed and produced in our department and their extremely effective applications in conditions of high ecological requirements.

D.V. Schur (✉) • A.F. Savenko • V.A. Bogolepov • S.Yu. Zaginaichenko
Institute for Problems of Materials Science of NAS of Ukraine,
3 Krzhyzhanovsky street, Kiev 03142, Ukraine
e-mail: shurzag@materials.kiev.ua

Z.A. Matysina
Dnepropetrovsk National University, 72 Gagarin street, Dnepropetrovsk 49000, Ukraine

A. Magrez
Ecole Polytechnique Federale Lausanne, Institute of Condensed Matter Physics,
CH-1015 Lausanne, Switzerland

M. Baibarac
National Institute of Materials Physics, Lab. Optical Process in Nanostructured Materials,
P.O. Box MG-7, Bucharest, R077125, Romania

T.N. Veziroğlu
International Association for Hydrogen Energy, 5794 SW 40 street #303, Miami, FL 33155, USA

A. Veziroğlu and M. Tsitskishvili (eds.), *Black Sea Energy Resource Development and Hydrogen Energy Problems*, NATO Science for Peace and Security Series C: Environmental Security, DOI 10.1007/978-94-007-6152-0_16,

Keywords Metal hydride • Hydrogen storage • Oxygen • Compressor • Application • Torch

16.1 Introduction

The world's research society has tried to use the hydrogen-sorption properties of different metals and alloys to solve a great variety of scientific and technical problems for over 50 years [1–18]. The properties of many chemical elements and their hydride alloys and compounds have been studied for this period. Metal hydrides have already found a wide application owing to the peculiarities of thermodynamics of hydrogen sorption and desorption processes that depend on the chemical composition of a solid subjected to the process of hydrogen pickup.

In recent years, much attention has been given to the development of hydrogen absorbing alloys due to their high hydrogen capacity. Under normal conditions, the amount of hydrogen stored in a vessel filled with metal hydride can be larger than that in the same vessel filled with liquid hydrogen. The method of hydrogen storage in solids advantageously differs from that in gas-cylinders and cryogenic. This method is safe and requires lower service costs. Therefore the world-known companies have put in order the serial production of various modifications of metal hydride accumulators of hydrogen.

The application of metal hydride technologies allows the manufacture of compact, safe and technologically flexible hydrogen treatment units. Also, peculiarities of the reversible hydrogen interaction with hydride forming metals and alloys makes it possible to purify hydrogen from gas admixtures in the MH units. The possibility to control the output hydrogen pressure by controlling heat influence on the MH sorbent allows the realization of controlled hydrogen supply to a consumer under the preset pressures. Storage purification, compression/controlled supply can be combined in a single multi-functional unit. This feature makes such applications extremely effective.

At present time, it has found applications both as the energy carrier and as the power source. If the change of electric current by moved hydrogen in pipe-lines is a rather complicated process, its transfering in containers of different construction has been put into operation firmly.

16.2 Hydrogen Accumulators and Compressors

We have developed a series of laboratory MH sources of high-pure hydrogen with hydrogen output under controlled increased pressure (up to 200 bar). The sources use MH placed in a high pressure container equipped with an internal heat exchanger. The hydrogen accumulators have different operating characteristics that can be changed in dependence on requirements of user. The development work has been done for the production of the series of metal hydride storage accumulators for diversified applications (Fig. 16.1).

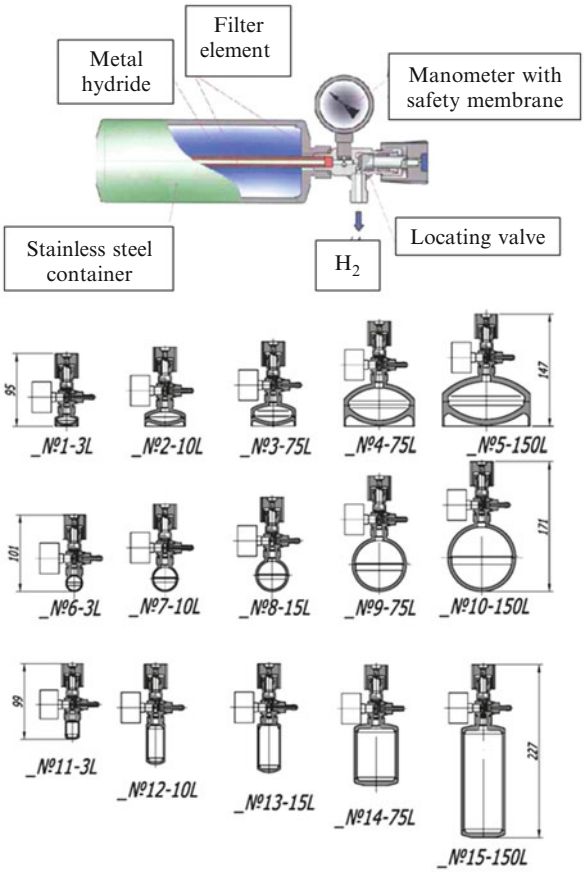

Fig. 16.1 The series of metal hydride storage elements for various applications (*see color plates*)

The metal-hydrogen accumulators have been designed for the laboratory use. Figures 16.1, 16.2, 16.3, and 16.4 show three modifications of the desk hydrogen accumulators of different capacities ("Alsav", "Viachbog", "Dmisch"), which have been designed for operation under laboratory conditions completed with the laboratory fuel cells to perform laboratory training on hydrogen energy.

Intermetallic compounds used in these accumulators were selected on the basis of consumers' individual requirements concerning temperature and hydrogen pressure. Alloys of AB_5 and AB types with different additives are typically used.

The vessels in which the metal hydrides are placed have been designed for pressures from 15 to 20 MPa with a double margin of safety. Hydrogen from the storage units can be provided at the room temperature under a pressure from 0.1 to 3 MPa, and on heating to 100 °C from 4 to 16 MPa. Hydrogen can be produced at 25 MPa on heating to 300 °C. The internal (Fig. 16.3) and external (Fig. 16.4) heat exchangers are used in the accumulators of this modification (Fig. 16.5).

The capacity of hydrogen accumulators can be variable from litres to several thousand of litres. Each accumulator is equipped with a manometer which is simultaneously used as a safety valve.

Fig. 16.2 The high-pressure vessels for hydrogen storage and hydrogen accumulators of "Alsav" modification with a capacity of 3, 10, 15, 75 and 170 l (*see color plates*)

Fig. 16.3 The high-pressure vessels for hydrogen storage and hydrogen accumulators of "Dmisch" modification with a capacity of 3, 10, 15, 75 and 170 l (*see color plates*)

Fig. 16.4 The hydrogen accumulators "Dmisch" supplied with thermostated heat exchangers energized from the constant-current sources of 12 V (*see color plates*)

Fig. 16.5 The high-pressure vessels for hydrogen storage and hydrogen accumulators of "Viachbog" modification with a capacity of 3, 10, 15 and 75 l (*see color plates*)

We also have worked out two models of accumulators of great capacity (2,000–7,000 l) on hydrogen. The model *"VEZAYF"* is designed to be operated for hydrogen delivery at low pressure (up to 0.5 MPa), but has the high hydrogen capacity. The model *"SVETZAG"* has three times smaller capacity on hydrogen, but owing to the presence of the temperature control system it permits to conduct the hydrogen under controlled pressure up to 20.0 MPa.

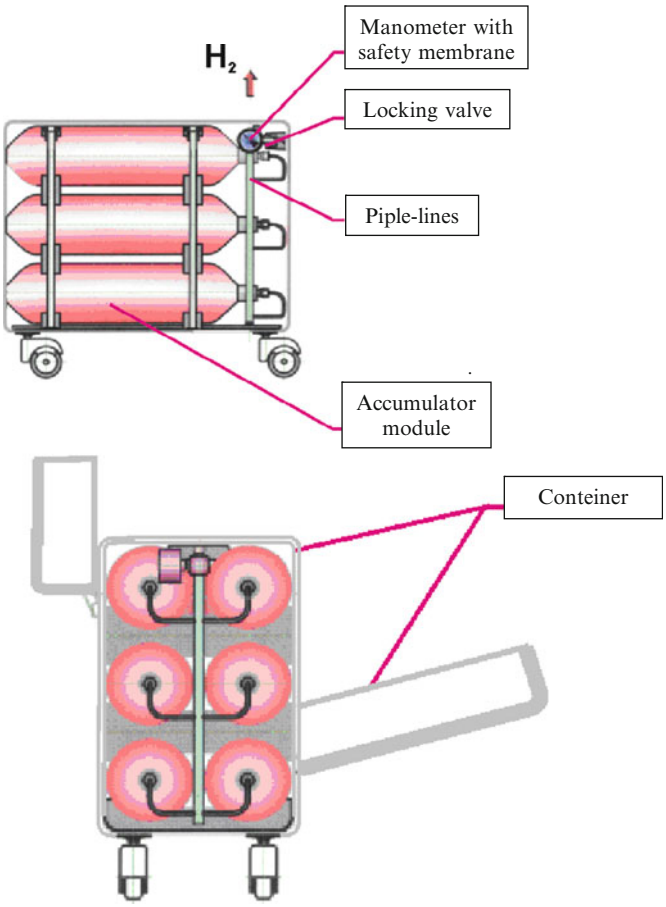

Fig. 16.6 Schematic view of the laboratory metal hydride storage of high-pure hydrogen "*VA – 7000*" (*see color plates*)

16.2.1 VEZAYF

The laboratory metal-hydride storage of high-pure hydrogen is designed for operation in the laboratory setups (Fig. 16.6) in the cases when the high hydrogen demands of low pressure have been in existence.

The RE(Ni,Fe,Al)5 hydrogen storage alloy made on the basis of the commercial cerium ligature (Ce/83 %/La Pr Nd Fe Al), lanthanum and nickel (technical purity grade both) was used in the unit. The composition of the alloy was selected to provide hydrogen equilibrium pressure over the MH of ~0.5 MPa at room temperature.

Specifications for "VEZAYF":
Overall dimensions of *"VA – 7000"*:

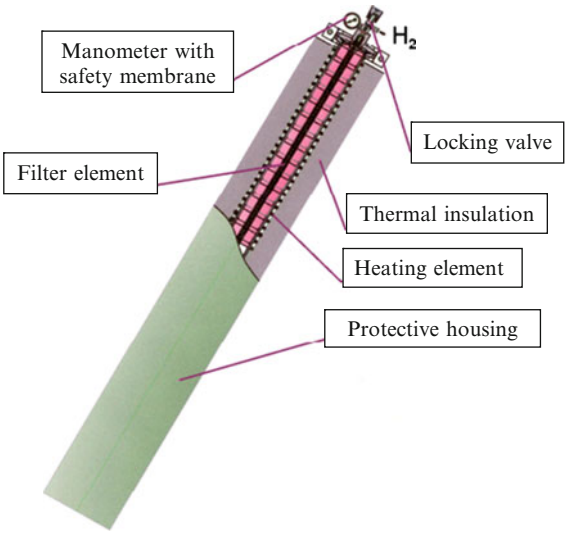

Fig. 16.7 Schematic view of the laboratory metal hydride storage/compressor of high-pure hydrogen "*Svetzag – 2000*" (*see color plates*)

Length: 480 mm
Height : 440 mm
Width : 300 mm

Number of modules: 6 pieces
Mass of a module: 8.8 kg
Mass of metal hydride in a module: 7 kg
Hydrogen capacity of a module: 1,200 l
General hydrogen capacity of a storage element: 7,000 l
Lump of a storage element: 55 kg
Lump of metal hydride: 42 kg
Working pressure: 0.3–0.5 MP (T = 30 °C)

16.2.2 SVETZAG

The laboratory metal hydride storage/compressor of high-pure hydrogen is designed for operation in the laboratory setups.

The performed strength calculations (GOST 14249–89, margin of safety of 1.5 and correction for strength reduction by welding of 0.8) have shown that the allowed working pressure in the MH container can be as high as 400 bar at 300 °C (Fig. 16.7).

The developed metal hydride unit for hydrogen storage and compression is characterized by high compactness and relatively low reheat temperature of MH with the delivery of sufficiently high hydrogen pressure and good dynamic performance:

Specifications for "SVETZAG":
Overall dimensions of *"SVETZAG – 2000"*:

Length: 1,410 mm
Flange diameter: 180 mm Hydrogen capacity: 2,000 l

Diameter of a working reactor: 70 mm Working pressure: 25 MPa (300 °C)
Mass of a storage element: 25.5 kg Working pressure: 0.3 ÷ 0.5 MPa (30 °C)
Mass of metal hydride: 11 kg Chemical composition of metal hydride: AB_5 + X (X = Fe,Al,Mg . . .) alloys

16.3 Hydrogen Torches

In our work, we show the combination in one construction of a container for hydrogen transportation and gaseous torch representing the instrument – demand of hydrogen. The hydrogen metal-hydride torch is the self-contained, compact device and it works without additional sources of energy. This torch is usable in settlements remote from centralized energy supply.

Using the totality of our experience on the creation of hydrogen accumulators with capacity of 1 ÷ 100 l, we have developed and produced the torches with metal-hydride accumulators of hydrogen. The external appearance and schematic view of the created metal-hydride torches are presented in Figs. 16.8, 16.9, and 16.10. The metal-hydride torches are dedicated to the brazing of small-sized parts by high-temperature solders as well as for the cutting of part from foil and in the realization of another specialized works in conditions of high ecological requirements.

Each torch consists of cylindrical container filled with metal hydride, filter element, locking valve, jet orifice, mixing chamber, nozzle and manometer. In addition, the torch "Alsav" (Fig. 16.9) is provided with the device of firing of inflammable mixture on the piezoelectric element.

The torch container has been produced from stainless steel with cylinder wall 1.5 mm thick. The filter element has been made of pipe frame fabricated from stainless steel with external diameter 8 mm and 5 μm filter micron-insert from porous fluoroplastic.

The locking valve, having the centreline channel for hydrogen emission up to the jet orifice, provides the necessary flow of hydrogen in pursuance of specific works.

The main technical characteristics of these torches are:

– inner volume of container – 60 cm^3;
– mass of metal hydride – 0,18 kg;
– hydrogen capacity – 30 *l*;
– total mass – 0,45 kg;
– working pressure at room temperature – 0,2 ÷ 0,5 MPa;
– maximum working pressure – 1 MPa;

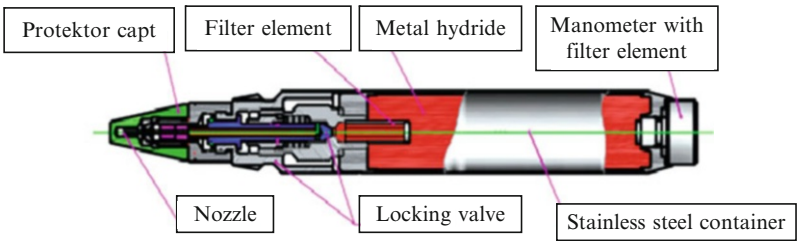

Fig. 16.8 Schematic view of the metal-hydride torch "Viachbog-30" (*see color plates*)

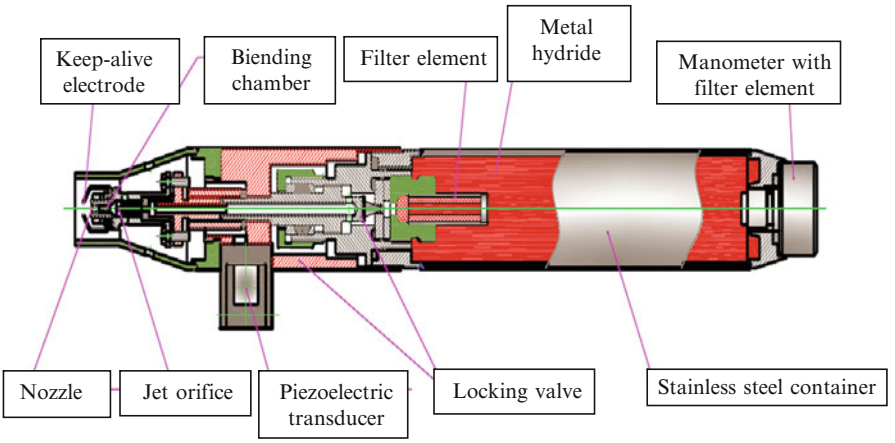

Fig. 16.9 Schematic sketch of the hydrogen self-contained metal-hydride torch "Alsav" with piezoelectric firing of flame (*see color plates*)

Fig. 16.10 Schematic representation of the oxydric metal-hydride torch (*see color plates*)

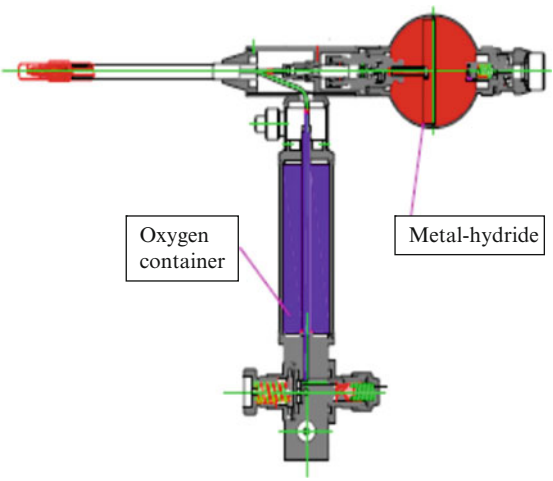

– length – 245 mm;
– diameter – 29 mm.

To increase the temperature of gaseous flame the oxyhydrogen torch has also been developed and manufactured with metal-hydride accumulator of hydrogen, cylinder of high pressure for oxygen and piezoelectric firing of flame.

The main technical characteristics of this oxyhydrogen torch (Fig. 16.10) are:

– capacity of metal-hydride accumulator – 50 l;
– capacity of cylinder for oxygen – 15 l;
– mass – 2.8 kg.

The special features and advantages of the created metal-hydride torches are:

– the high reliability in the work, convenience in operation and maintenance;
– the ease of process of brazing and cutting;
– the possibility of their use in the most severe conditions of surrounding medium;
– the lack of environment pollution.

The work is also underway toward the construction of torches with accumulators of hydrogen of non-permanent application with container from aluminium alloys based on alkali, alkali-earth and another metals.

16.4 Conclusions

At present, method of hydrogen storage in the solids remains rather convenient, efficient and safe as before. Much work was devoted to the development of new hydride materials for hydrogen storage and to the investigation of its physical and chemical characteristics.

The metal-hydride accumulators can be used both for safe and compact hydrogen storage and for the solution of some other problems enumerated below:

– hydrogen purification – scavenging to ppm amounts;
– hydrogen separation – from the mixture containing from 1 to 90 % non-hydrogen atoms and molecules;
– isotope separation – protium, deuterium and tritium;
– hydrogen compression – hydrogen is sorbed at low temperature and desorbed at higher temperature and creates high pressure;
– heat accumulation – the process is based on the use of heat effect (20–60 kJ/mol) of the hydrogenation/dehydrogenation reaction for heat absorption and evolution.

The designed torches, accumulators and compressors are feasible for large-scale industrial applications and for use in the wide areas of man's activities. These devices are needed to fill the gaps in instrumental provision those are bridged by another less suitable devices or are not closed at all at present.

Acknowledgment The work has been done within the framework of SCOPES project "Implementation in East Europe of new methods of synthesis and functionalization of carbon nanotubes for applications in the energy storage and sensors field"

References

1. Ven Mal HH, Bushow KH, Miedema AR (1974) Hydrogen absorption in $LaNi_5$ and related compounds: experimental observation and their explanation. J Less Common Met 35(1):65–76
2. Semenenko KN, Malyshev VP, Petrova LA, Bumasheva VV, Sarynin VK (1977) The interaction of $LaNi_5$ with hydrogen. Izv Akad Nauk SSSR Neorg Mater 13(11):2009–2013
3. Shinar J, Shaltiel D, Davidov D (1978) Hydrogen sorptoin properties of $La_{1-X}Ca_XNi_5$ and $La(Ni_{1-X}Cu_X)_5$ systems. J Less Common Met 60:209–219
4. Lartigue C, Percheron A, Acherd JC (1980) Thermodynamic and structural properties of $LaNi_{5-X}Mn_X$ compounds and their related hydrides. J Less Common Met 75(1):23–29
5. Patrikeev YB, Levenskii YV, Badovskii VV, Filyand YM (1984) Thermodynamics and hydrogen diffusion in $LaCo_5H_X$ alloys. Izv Akad Nauk SSSR Neorg Mater 20(9):1503–1506
6. Percheron-Guegan A, Lartigue C, Achard JC (1985) Correlation between the structural properties, the stability and the hydrogen content of substituted lantanum-nickel ($LaNi_5$) compounds. J Less Common Met 114(2):287–309
7. Colinet C, Pasturel A (1987) Enthalpies of formation and hydrogenation of $La(Ni_{1-X}Co_X)_5$ compounds. J Less Common Met 134:109–122
8. Majer G, Kaess U, Bowman RC Jr (1998) Nuclear magnetic resonance studies of hydrogen diffusion in $LaNi_5H_6$ and $LaNi_{4,8}Sn_{0,2}H_{5,8}$. Phys Rev B 57(21):13599–13603
9. Matysina ZA, Zaginaichenko SYu, Schur DV, Pishuk VK (1997) Hydrogen in lanthan-nickel alloys-accumulators. In: 5th international conference hydrogen materials science and chemistry of metal hydrides, Katsiveli, Crimea, Ukraine, 2–8 September 1997, p 62–63
10. Matysina ZA (1997) Isotherms of hydrogen solubility in hydrogen-storage lanthanum-nickel alloys. Phys Met Metallogr 84(5):495–500
11. Schur DV, Zaginaichenko SY, Matysina ZA, Pishuk VK (2002) Hydrogen in lanthanum-nickel storage alloys. J Alloy Compd 330–332(1):70–75
12. Kadir K, Sakai T, Uehara I (1997) Synthesis and structure determination of a new series of hydrogen storage alloys: RMg_2Ni_9 (R = La, Ce, Pr, Nd, Sm and Gd). J Alloy Compd 257:115–121
13. Koimo T, Yoshida H, Kawashima F, Inada T, Sakai T, Yamamota M, Kanda M (2000) Hydrogen storage properties of new ternary system alloys: La_5MgNi_9, $La_5Mg_2Ni_{23}$, La_3MgNi_{14}. J Alloy Compd 311:L5–L7
14. Chen J, Kuriyama N, Takashita HT, Tanada H, Sakai T, Haruta M (2000) Hydrogen storage alloys with $PuNi_3$ type structure as metal hydride electrodes. Electrochem Solid State Lett 3(6):249–252
15. Liao B, Lei YQ, Chen LX, Lu GL, Pan HG, Wang QD (2004) Effect of the La/Mg ratio on the structure and electrochemical properties of $La_XMg_{3-X}Ni_9$ (x = 1.6–2.2) hydrogen storage electrode alloys for nickel-metal hydride batteries. J Power Source 129:358–367
16. Chen J, Takashita HT, Tanaka H, Kuriyama N, Sakai T, Uehamra I, Haruta M (2004) Hydriding properties of $LaNi_3$ and $CaNi_3$ and their substitutes with $PuNi_3$–type structure. J Alloy Compd 302:304–313
17. Matysina ZA, Chumak VA (2001) Deformational hysteresis and elastic compliance of crystals with H4 structure near Curie point. Ukr Fiz Zhurn 46(9):957–959
18. Matysina ZA, Zaginaichenko SY, Schur DV (2005) Orders of different type in crystals and phase transformations in carbon materials. Nauka i obrazovanie, Dnepropetrovsk, p 524 (in Russian)

Chapter 17
The Peculiarities of Hydrogenation of Fullerene Molecules C_{60} and Their Transformation

Dmitry V. Schur, Svetlana Yu. Zaginaichenko, T. Nejat Veziroğlu, and N.F. Javadov

Abstract This chapter provides an explanation for the kinetic features of C_{60} molecule hydrogenation by analyzing the state and structure of double bonds in the frame of fullerene molecule. The status of these bonds, that changes the chemical activity of C_{60} molecules, and hence the ability of fullerene molecule to accept different number of reagents particles, has been proposed. The special features of fullerene molecule formation and mechanism of structural transformations of fullerene molecule in solutions and fullerite have been considered.

Keywords Peculiarities of hydrogenation • Fullerene molecules • Transformation of fullerene molecules

D.V. Schur (✉)
Institute for Problems of Materials Science of NAS of Ukraine, 3 Krzhyzhanovsky street, Kiev 03142, Ukraine
e-mail: shurzag@materials.kiev.ua

S.Yu. Zaginaichenko
Institute for Problems of Materials Science of NAS of Ukraine, 3 Krzhyzhanovsky street, Kiev 03142, Ukraine

Dnepropetrovsk National University, 72 Gagarin street, Dnepropetrovsk 49000, Ukraine

T.N. Veziroğlu
International Association for Hydrogen Energy, 5794 SW 40 street #303, Miami, FL 33155, USA

N. Javadov
Experimental-industrial plant of Institute for Petroleum Chemical Processes (IPCP) of NAS of Azerbaijan, Baku, Azerbaijan

A. Veziroğlu and M. Tsitskishvili (eds.), *Black Sea Energy Resource Development and Hydrogen Energy Problems*, NATO Science for Peace and Security Series C: Environmental Security, DOI 10.1007/978-94-007-6152-0_17,

17.1 Introduction

The solution of the problem or reverse hydrogenation of each carbon atom in the frame of fullerene molecule will allow to create an effective energy storage. The fullerite properties as volume (8.2510^{22} H atoms/cm^3), weight (7.7 wt.% H) and electrochemical (2,000 mA·h/g) capacities exceed many similar properties of metal hydrides and hydrocarbons.

Over the past two decades many scientific papers have been devoted to solving this particular problem. We have shown that hydrogen in the fcc lattice of fullerite can be found in the lattice (absorbed) and fullerinated (chemisorbed) states [1]. It has also been shown that when T → 0 K up to 18 hydrogen atoms in the absorbed state can be contained per one molecule of C_{60} in the fcc lattice of fullerite. However, under normal conditions, octahedral and tetrahedral interstitial sites should be considered as a possible position of hydrogen atoms arrangement. Theoretical justification for the possibility of hydrogenation of all carbon atoms in the fullerene frame has been given in this paper.

Experiments have shown that the kinetic curve of hydrogen interaction with fullerite C_{60} notes two stage of the process. There are good grounds to believe that the process of physical absorption of hydrogen by crystallites belongs to the first stage (Fig. 17.1) [2]. This stage is determined by the content of the lattice hydrogen corresponding to 0.5 wt.% of hydrogen.

The reaction of chemisorptions of hydrogen atoms by fullerene molecules occurs at the second stage. The experimental curve of hydrogenation of fullerene molecule C_{60} is shown in Fig. 17.2. The fullerinated hydrogen content is marked by an arrow (H_F).

The second stage of reaction of hydrogen atoms chemisorption by fullerene molecules is defined by concentration – 7.7 wt.% of hydrogen (i.e. by formula

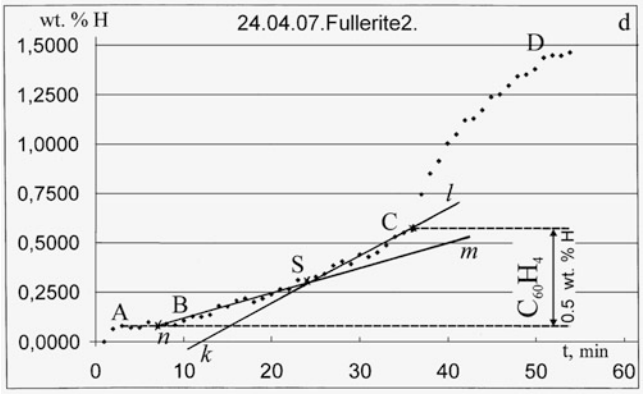

Fig. 17.1 The adsorption of H_2 and two-stage atomic-molecular absorption of hydrogen in fcc lattice of fullerite. *Arrowed line* shows the content of lattice hydrogen (H_L)

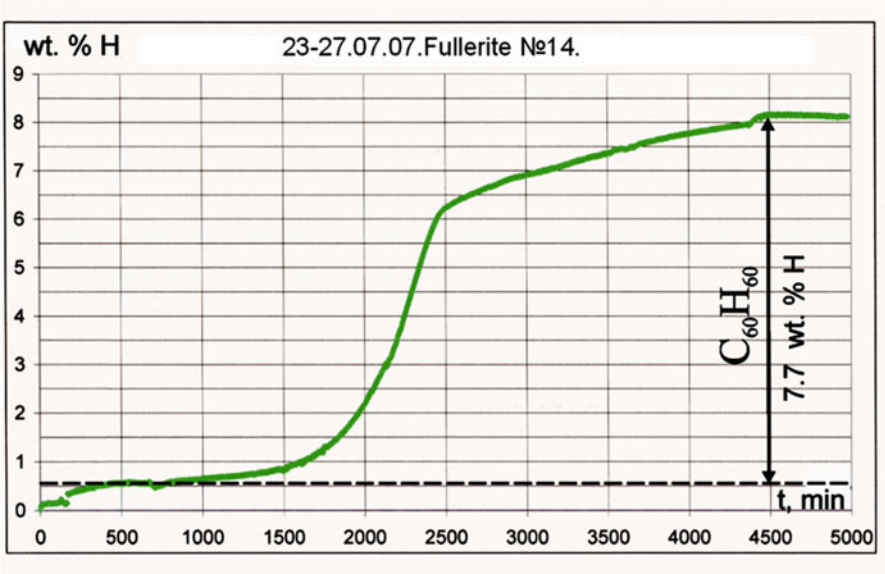

Fig. 17.2 Kinetics of interaction of gaseous hydrogen with fullerite. *Arrowed line* shows the fraction of fullerinated hydrogen (H_F) (*see color plates*)

$C_{60}H_{60}$). However the chemisorption stage has the kinetic features. The kinetic curve has a break at the hydrogen concentration of 6.2 wt.% H. As this takes place, this concentration corresponds to 48 fullerinated hydrogen atoms that are attached to the frame of fullerene molecule, is relevant to the formula $C_{60}H_{48}$ (Fig. 17.2). In this point the energy of process activation has undergone a change and the interaction rate reduces.

In our opinion, the multi-stepwise character of process of fullerene molecule formation in plasma conditions [3] reflects later on the behavior of molecule itself in the crystal lattice and on its interaction with chemical elements and compounds. This multi-step process of fullerene molecule formation, observed on the way of carbon atom from atomic state to the spherical molecule formation, can be presented by the sequence of the following steps: atom – chain of atoms – pentagon (pentatomic molecule) – pentagon pair (pyracyclene unit) – sphere.

The pentagon plays a special role in the structure of C_{60} molecule, it often acts as an independent (separate) energetic centre on the molecule surface. These centers are responsible for the existence of molecule in the free and bound states, as well as for its behavior in solutions and crystals [4–14].

In the present paper through analysis of the state of double bonds structure in the frame of fullerene molecule, an attempt has been made to interpret the kinetic features of C_{60} molecule hydrogenation. The status of these bonds, changing the chemical activity of C_{60} molecule, and hence the ability of fullerene molecule to accept different number of reagent particles, will be considered in this paper.

17.2 Correlation of the Rate of Interaction with the Rate of Temperature Rise

We have pointed out some features of hydrogen interaction with fullerite during the experimental investigations of this interaction process. These peculiarities include the processes occurring both in the crystal lattice of fullerite, and in the frame of fullerene molecule itself.

At the prolonged holding of fullerite in hydrogen, the effect of cross-correlation of the interaction rate and the rate of temperature rise was found (Fig. 17.3) [2]. This effect can be explained by the fact that with sufficient time of interaction of hydrogen atom (sufficient for hydrogen atom diffusion and chemical bond

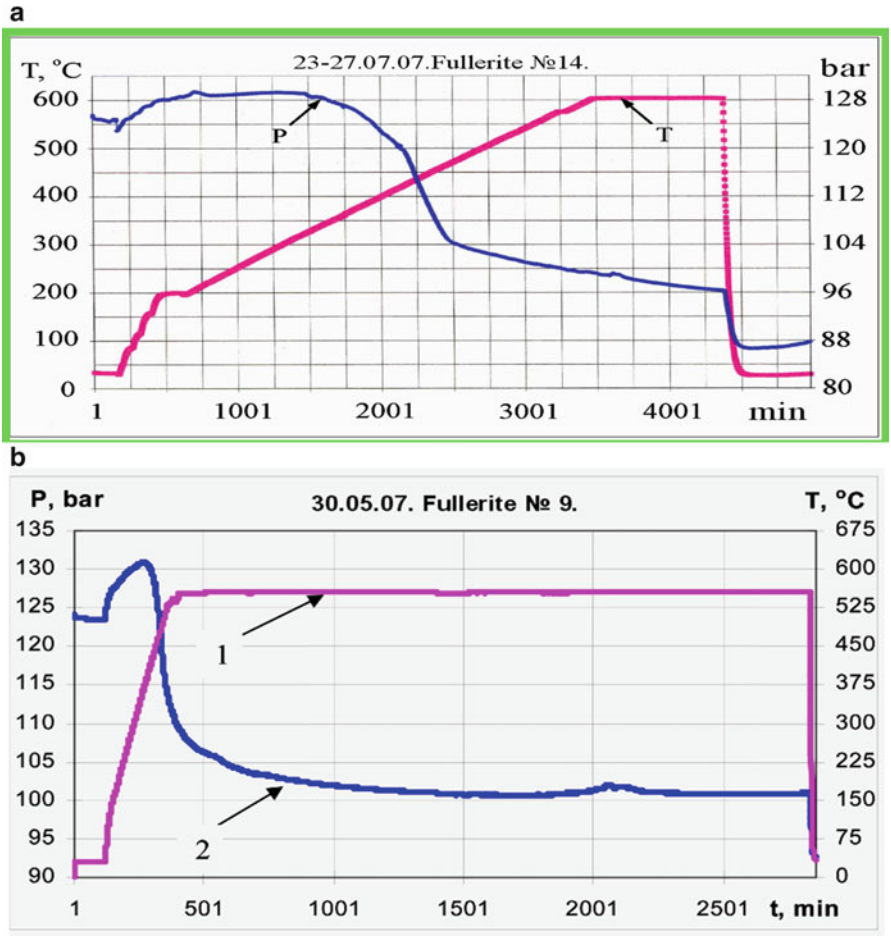

Fig. 17.3 The dependence of the rate of interaction between hydrogen – fullerene (*2*) the rate of temperature rise (*1*) (**a**) 0.2° per hour, and (**b**) 3.2° per minute (*see color plates*)

formation) with carbon atom the energy state (i.e., activation energy of each subsequent elementary act of interaction) of this system is a limiting parameter.

With a rise in temperature, each accepted atom of hydrogen leads to the transformation of the initial compound $C_{60}H_n$ (fullerene molecule with n-attached hydrogen atoms) to the new $C_{60}H_{n+1}$ compound. The newly formed system requires this additional energy for the formation of new C–H bond. The system gets this energy by raising the temperature. A certain temperature range corresponds to a strictly specified number of hydrogen atoms.

Working with metals and alloys, researchers usually have to deal with the metal hydrides where all atoms are energetically equivalent and at the creation of certain thermodynamic conditions it is likely that all atoms interact with the hydrogen atoms. Only surface and diffusion processes in solids interfere with this interaction.

The fact that each molecule C_{60} can be found in 61 (a minimum) energy states (C_{60}, $C_{60}H$, ..., $C_{60}H_n$, where $1 \leq n \leq 60$) must be taking into account when you consider the processes of hydrogenation of fullerene molecule. Each energy state corresponds to a specific chemical compound, which has its own physical and chemical properties. Thus, the benzene molecule changes its properties during the replacement of one, two, etc., hydrogen atoms. During the hydrogenation process the fullerene molecule also changes its electron density, and physical and chemical properties by changing its chemical composition.

According to experimental data, with a rise in temperature the thermodynamic probability of occurrence of all 60 chemical reactions increases. However, at the final stage of interaction due to the increase of the intermolecular electron density, another process occurs, and these processes limit the interaction rate.

We think that the parabolic character of interaction hydrogen-fullerene (after the addition of hydrogen atoms above the amount corresponding to H_{36}) is due not only to the complication of diffusion processes in the fullerite crystal. At the concentrations higher than 48 atoms of hydrogen (H_{48}) this interaction is complicated by the processes of transformation in the fullerene molecule itself. These transformations are primarily determined by the rearrangement of five double bonds in the pentatomic cycles responsible for the association of pentatomic molecules with each other.

Thus, the effect of correlation of interaction rate with the rate of temperature rise can be explained by the fact that the activation energy of each subsequent act of hydrogen atom adding is higher than of the previous act. For this reason an explanation for kinetic features of C_{60} molecule hydrogenation should be found in the structural changes of fullerene molecule itself.

17.3 The Peculiarities of Formation of Fullerene Molecule

Bochvar and Gal'pern [15] performed calculations of the molecule electronic structure, made the quantum-chemical analysis of the stability of fullerene (well before the experimental discovery of fullerene molecule), and predicted the possible existence of stable fullerene molecules C_{20} and C_{60}.

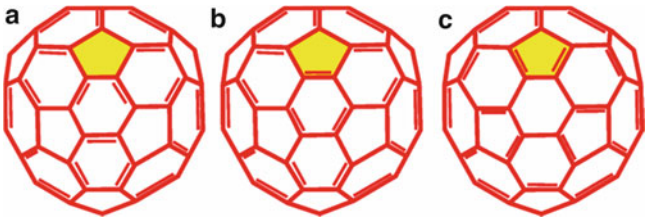

Fig. 17.4 The covalent resonance structures of carbo-s-icosahedron (**a**) – with the axis of fifth order (one structure); (**b**) and (**c**) – with the axis of the third order (Ten equivalent structures in each). All of structures are with 30 double bonds [15] (*see color plates*)

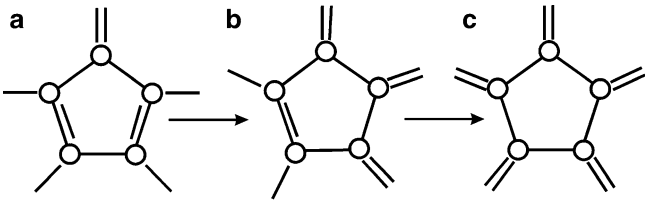

Fig. 17.5 The transformation of the pentadiene molecule into radialene (**a**) pentadiene molecule, (**b**) – pentaene molecule, (**c**) – radialene

In addition, this work made an important conclusion, according to the calculations of electronic structure of fullerene molecule (by the Huckel molecular orbital method (HMO)), and orders of bonds between carbon atoms. It lies in the fact that three basic resonance structures (Fig. 17.4a–c) exist among the large family of fullerene isomers C_{60}.

The structure of (Fig. 17.4a) is the most stable among them. In fact, these structures represent the stepwise graphitization (annealing) of fullerene molecule in the reverse sequence (c → b → *a*) [1, 16, 17]. During the course of graphitization (annealing), there is reorganization of the double intramolecular bonds into the intermolecular for the pentatomic molecules of carbon, forming the fullerene molecule. The cyclopentadiene carbon molecule is transformed into the cyclopentaene molecule and then becomes radialene (Fig. 17.5).

Due to the presence of unpaired electrons, these molecules combined in six pairs in the C_{60} frame can form the stable structures in the form of the pyracyclene units. The existence of such pairs or so-called pyracyclene units distinguishes the fullerene molecule from all other allotropies of carbon and exerts influence on its chemical activity. Figure 17.6 shows the state of the cyclopentadiene molecule at the formation of pairs or the pyracyclene units.

Every fourth electron, in the remaining four electrons, in the 12 pentatomic cyclic molecules in the frame of the C_{60} fullerene molecule is used for the intra- and extramolecular bonds [17] (depending on thermodynamic conditions). All of these π-electrons are 48 ($4 \times 12 = 48$) in each molecule C_{60} and they determine the physical and chemical properties of fullerene molecule C_{60} [18, 19].

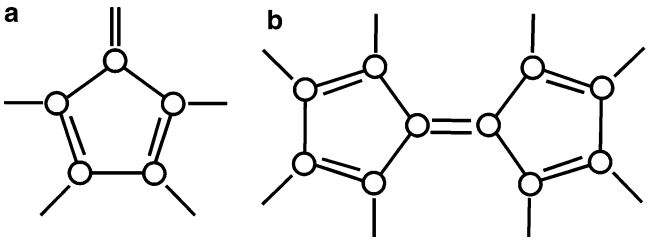

Fig. 17.6 The state of pentatomic molecule at the formation of cyclopentadiene pairs (**a**) – single pentatomic molecule with one double (external) intermolecular bond; (**b**) – pyracyclene-similar unit in the frame of fullerene C_{60} molecule

17.4 The Features of Structural Transformations of Fullerene Molecule and Fullerite

As shown in our previous papers [3, 16–20], the phase transition f.c.c. → s.c. in fullerite the process proceeds through the intermediate stage of the b.c.c. lattice formation. In this case, in the f.c.c. lattice, the pentatomic cyclic molecule in the frame of fullerene molecule exists at high temperatures in the form of radialene, but C_{60} molecule itself is in the γ-state (Fig. 17.7a).

In the frame of fullerene molecule, 12 radialenes interact with radialenes of the 12 nearest fullerene molecules, forming the f.c.c. structure. The radialene is turned into the pentaene molecule (Fig. 17.5) as the temperature decreases below 280 K.

These molecules, interacting with each other, form eight cyclic hexatomic structures in the frame that obey the rule of Huckel. Due to the magnetic interaction, excited by ring currents, these structures attract the eight nearest neighbouring fullerene molecules that form the b.c.c. structure (transitional β-state Fig. 17.8b).

At the temperature below 260 K, the phase transition b.c.c. → s.c. occurs and all extramolecular bonds (except for the pairing) of pentatomic molecule transform into intramolecular bonds. The molecule itself becomes pentadiene (Fig. 17.6a).

In these conditions, the fullerene molecule is formed in the α-state and it has the structure presented in Fig. 17.9b, c. As can be seen from the Shlegel diagram of Fig. 17.9b, this structure has 30 double bonds, 24 of which are intramolecular for the pentadiene molecules, but six other intermolecular bonds combine molecules into six pyracyclene-similar pairs.

In this case, the pairing bonds between the pentatomic molecules become more active and chemically centers in the frame of fullerene molecule. Six pyracyclene units represent aromatic structures and, interacting with the similar structures in the six neighboring fullerene molecules, form the s.c. structure.

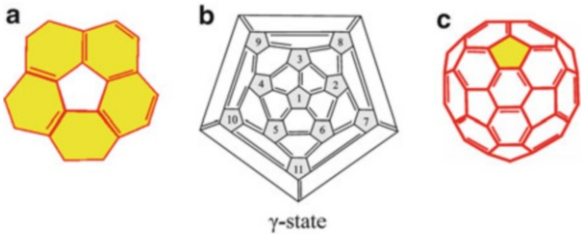

Fig. 17.7 γ-state of the covalent resonance structure of carbo-s-icosahedron with an axis of fifth order, forming the f.c.c. lattice of fullerite (**a**) – pentatomic molecule in the state of radialene; (**b**) – Shlegel diagram; (**c**) – the frame of molecule C_{60} (*see color plates*)

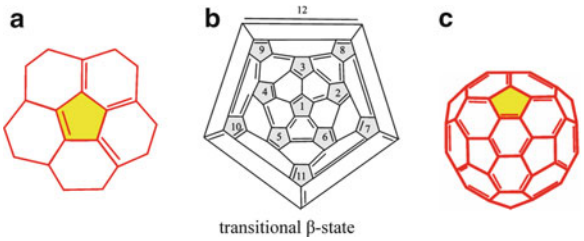

Fig. 17.8 β-state of the covalent resonance structure of carbo-s-icosahedron with an axis of third order, forming the b.c.c. lattice of fullerite (**a**) – pentatomic molecule in the state of pentaene; (**b**) – Shlegel diagram with the marked hexatomic structures (1, 2, 3, 4, 5, 6, 7, 8) that obey the Huckel rule; (**c**) – the frame of molecule C_{60} (*see color plates*)

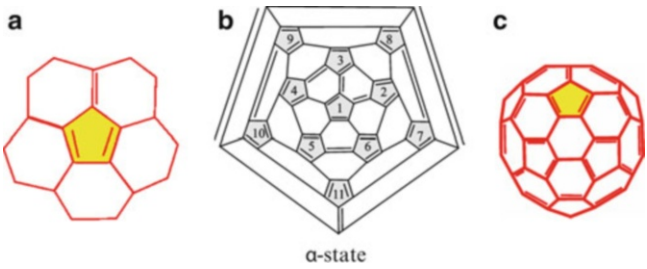

Fig. 17.9 α-state of the covalent resonance structure of carbo-s-icosahedron with an axis of third order, forming the s.c. lattice of fullerite (**a**) – pentadiene molecule; (**b**) – Shlegel diagram with the marked double bonds (1, 2, 3, 4, 5, 6) that combine pentadiene molecules in pyracyclene pairs; (**c**) – the frame of molecule C_{60} (*see color plates*)

17.5 Fullerene Molecule in the Solution

The note on the anomalous solubility of fullerene molecule appeared in 1993, in the journal "Nature" in the section "Letters to Nature" [4]. The experimental results on the solubility of C_{60} molecules were reported in this paper. The anomalous was the fact that C_{60} solubility in the shown organic solvents has a maximum room temperature of 280 K. The revealed dependence did not fit into the existing concepts about solubility of organic bodies in the organic solvents. It is agreed

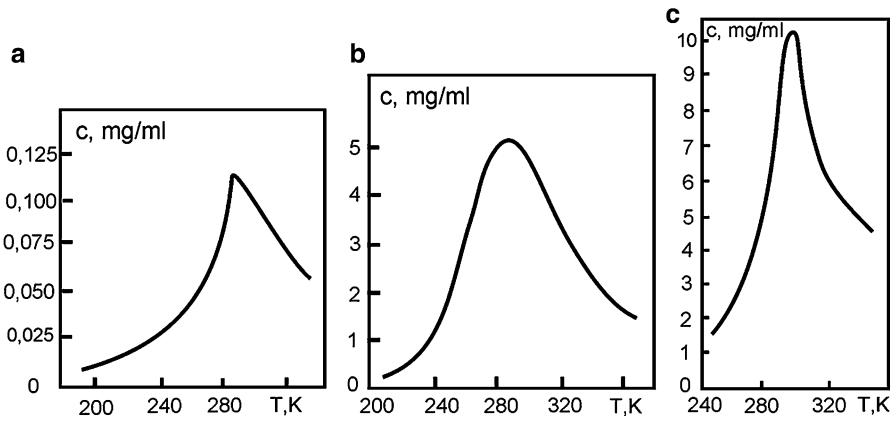

Fig. 17.10 Experimental plots of temperature dependence of fullerite C_{60} solubility in hexane (**a**), toluene (**b**), xylol (**c**)

that the increase in solubility with the increasing temperature is regular. Neither of these presentations or papers of the next 20 years [5–14 and others], did not give an answer to this question.

In our paper [16] in the year 2008, it was demonstrated that the anomalous behavior of fullerene molecule in solutions at the temperature change is determined by the transformations taking place in the frame of fullerene molecule. So it was shown that the fullerene molecule reaches the maximum solubility in the β-modification. Because this β-modification is metastable, the curve of solubility has a maximum at the point where its concentration in the solution reaches 100 % respectively (Fig. 17.10).

The rise in temperature at the fullerene dissolving leads to the transformation of fullerene molecule. Its α-modification is changed into β-modification, and fullerene molecule becomes more chemically active. This is due to the formation of two double external-molecular bonds in each pentatomic molecule in the frame of the C_{60} molecule (Fig. 17.8). These bonds by π – electrons connect X molecules of solvent per each fullerene molecule [21–23] (X – is the number of solvent molecules per one fullerene molecule).

The further increase in temperature transforms β – modification into γ–modification that has two external-molecular bonds more in each pentatomic molecule in the frame of C_{60} molecule (Fig. 17.4). It will double the chemical activity of each fullerene molecule. These bonds, using π-electrons twice as much, connect 2X molecules of solvent per each fullerene molecule. Such situation increases (double) the demands in the solvent molecules that in its turn reduces by one half the fullerene solubility.

The β-modification exists at the temperature of 273 K, with the α-modification at $T \leq 260$ K, and the γ-modification at $T \geq 280$ K. However, these temperatures correspond to the moments in which molecules of one kind exist. In the intervals between these temperatures, the mixtures of two type of fullerene molecules are in existence, the concentration ratio of which changes depending on the temperature (Fig. 17.10).

Thus, the anomalous solubility demonstrates the chemical activity of four of the five external-molecular bonds in the 12 pentatomic cycles ($4 \times 12 = 48$) in the frame of fullerene molecule, that can be the place of priority interaction of fullerene molecule with hydrogen atoms.

17.6 Fullerene Molecule in Crystal

Another confirmation of transformations occurring in the frame of fullerene molecule under changes of temperature can be the transitions in the crystal lattice of fullerite. At the temperature of orientational transition between phases (260 K), the concentration of one or other kind of molecules become more than 50 %. This determines the fullerite structure under these thermodynamic conditions. Thus, the solid-phase transition in the fullerite is possible with the existence of more than 50 % of any modification of fullerene molecule in the system.

When temperature increases the phase transformation s.c. → f.c.c. (α → γ) in the fullerite as well as when temperature decreases takes place through the formation of an intermediate β- phase with b.c.c. lattice (Fig. 17.8). On heating the fullerite higher, the temperature of 260 K and the rearrangement of bonds are found in the frame of fullerene molecule. When fullerene molecules rearrange their frame, causes a change in the structure of the crystal lattice. Fullerene molecule transformations from the α-state (Fig. 17.9) into the intermediate β-state at higher temperatures are replaced by a more stable γ-state (Fig .17.7). In consequence of this, the crystal lattice of fullerite changes the structure (s.c. → b.c.c. → f.c.c. transformation, Fig. 17.11) [24]. In the intervals between these temperatures, the mixtures of two types of fullerene molecules exist, the concentration ratio of which determines the type of crystal lattice in fullerite (Fig. 17.10).

By this means over the long run the density of the inner and outer electron layer of fullerene molecule is changed at the phase transitions α → β → γ in the frame of fullerene molecule, initiating the changes in the crystal lattice. This affects the chemical activity of C_{60} molecule and the ability of fullerene molecule to interact with hydrogen atoms.

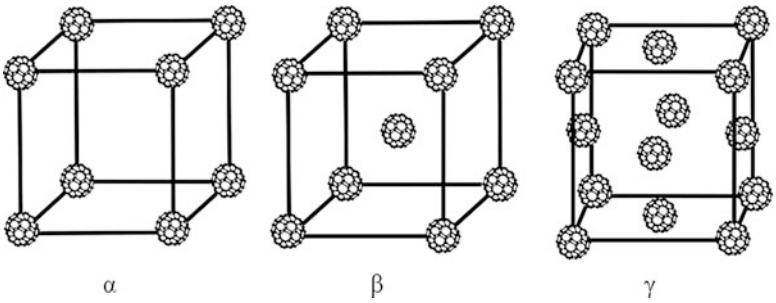

Fig. 17.11 Phase transition s.c. → b.c.c. → f.c.c. in the fullerite lattice with increasing temperature

17.7 Features of Structural Transformations of Fullerene Molecule at Its Interaction with Hydrogen

As mentioned above, each fourth electron of four carbon atoms in the 12 pentatomic cyclic molecules in the frame of C_{60} molecule is used for intra- and extra-molecular bonds (depending on the thermodynamic conditions). In all, there are 48 of these π-electrons ($4 \times 12 = 48$) in each C_{60} molecule and they define the physic-chemical properties of the fullerene molecule. As follows from the consideration of processes in the fullerene frame, all 48 carbon atoms (or their π-electrons) become chemically active for the environment in the γ-modification, which exists at room and high temperatures.

Thus, we can assume that the first stage of chemisorptions process is determined by the interaction of these 48 carbon atoms with hydrogen.

Every fourth electron of fifth carbon atoms (in the 12 pentatomic cyclic molecules in the C_{60} molecule frame) is used for the formation of pyracyclene unit. For pairing each pentatomic molecule uses one π-electron. This leads to the production of the double bond between the pentatomic molecules and formation of the pyracyclene unit. In this way each fifth π-electron (i.e., all 12 π-electrons) in the frame of C_{60} molecule is used for the production of pyracyclene units forming the fullerene molecule frame. Also, this bond contributes to the retention of fullerene molecule in the sites of the fcc lattice of fullerite.

From the above discussion, it follows that the kinetic features of process of fullerene molecule interaction with hydrogen, manifesting itself at hydrogen concentration higher 6,2 wt.% (more than 48 atoms of hydrogen), can be explained by the change in the mechanism of interaction. The change in the activation energy of process and decrease in the interaction rate are due to the expenditure of additional energy on the destruction of pyracyclene units, which are the frame-forming basis for fullerene molecule. As a result, this bond is intra-molecular for pyracyclene unit. In view of the fact that this bond makes contribution to the retention of fullerene molecule in the sites of the fcc fullerite lattice, this gives us grounds to believe that this bond is stronger than the other four in the pentatomic cycle.

Thus, it can be argued that the process of fullerene molecule with hydrogen (at its concentration higher 6.2 wt.%) goes by the way of the breaking of one of two bonds uniting pentagons into the pyracyclene units.

17.8 Conclusions

This chapter presents the study of a multi-step process of the fullerene molecule formation in the plasma conditions that is further reflected on its behavior in the crystal lattice and its interaction with chemical elements and compounds. This multi-step character of the formation process of fullerene molecule, observed in the passing of the carbon atom from the atomic state to the formation of spherical

molecule, can be presented by the following sequence of steps: atom – chain of atoms – pentagon – pentagon pair – sphere.

The pentagon plays an important role in the structure of the C_{60} molecule, acting often as an independent (autonomous) energetic center in the molecule. These energy centers are responsible for the existence of fullerene molecule in the free and bound states.

In our opinion, the kinetic features of the C_{60} molecule hydrogenation can be accounted by the change of structure of the double bonds in the fullerene frame. The status of these bonds modify the chemical activity of the C_{60} molecule, and consequently the ability of this molecule to attach a different number of the reagents particles. The status of the double bonds depends on the state of pentatomic molecules, formed the C_{60} frame, and on the interaction between these molecules.

In cooling the pentatomic molecules in the C_{60} frame transform from the radialene state into pentaene, and then into the pentadiene state. In the course of this process, the double bonds in the C_{60} frame turn from the intermolecular into the intra-molecular bonds for the pentatomic molecules. This conclusion follows from the physical and chemical features of effects observed both in the solid and in the solution at the certain temperature range.

The phase transitions $\alpha \rightarrow \beta \rightarrow \gamma$ in the frame of fullerene molecule demonstrate clearly the dependence of structural transformations in the crystal lattice on the status of the double bonds in the frame of this molecule.

So, at the C_{60} molecule hydrogenation in the fcc lattice of fullerite the activation energy for the reaction of the hydrogen interaction with fullerite changes sharply after the addition of 48 hydrogen atoms to each molecule; in this case there is a decrease in the rate of reaction. By virtue of the fact that each molecule in the fcc lattice has 12 nearest neighbors, it is quite possible that each of 12 electrons is responsible for the bond with each neighbor and in this case these electrons are not yet bonded with hydrogen (12 electrons from 60 π-electrons responsible for the intermolecular bonds of fullerene).

It is obvious that each of the 12 electrons belongs to one of the local energetic centers in the fullerene molecule and 12 pentagons can be such identical energetic centers on the surface of the frame of C_{60} molecule.

After the addition of 48 hydrogen atoms, each of the pentagons has a π-electron paired with the same electron in the neighboring pentagon of the pyracyclene unit. On the breaking of these bonds, the C_{60} molecules loose bonds between each other in the crystal lattice adding the hydrogen atoms to the remaining bonds. As this takes place, the crystal lattice is destroyed and the fullerite transforms into hydrocarbon or hydrofullerene, which is a dense resin-like mass. This stage of hydrogenation process of the fullerene molecule is more energy-intense, because this process is accompanied by the previous processes of destruction of the fcc lattice and of the pyracyclene unit.

Acknowledgment This work has been done within the framework of SCOPES project «Implementation in East Europe of new methods of synthesis and functionalization of carbon nanotubes for applications in the energy storage and sensors field»

References

1. Schur DV, Zaginaichnko S, Veziroglu TN (2008) Peculiarities of hydrogenation of pentatomic carbon molecules in the frame of fullerene molecule C_{60}. Int J Hydrog Energy 33:3330–3345
2. Schur DV, Zaginaichenko SY, Savenko AF, Bogolepov VA, Anikina NS, Zolotarenko AD et al (2011) Experimental evaluation of total hydrogen capacity for fullerite C_{60}. Int J Hydrog Energy 36:1143–1151
3. Schur DV, Zaginaichenko SY, Lysenko EA (2008) The forming peculiarities of C_{60} molecule. In: Carbon nanomaterials in clean energy hydrogen systems, NATO science series. Springer, Dordrecht, pp 53–65
4. Ruoff RS, Malhotra R, Huestis DL, Tse DS, Lorents DC (1993) Anomalous solubility behaviour of C_{60}. Lett Nat 362:140–141
5. Ying Q, Marecek J, Chu B (1994) Slow aggregation of buckminsterfullerene (C_{60}) in benzene solution. Chem Phys Lett 219:214–218
6. Suzuki E et al (1998) Molecular nanostructures. World Scientific, Singapore
7. Sivaraman N, Dhamodaran R, Kaliappan I, Srinivasan TG, Rao PRV (1992) Solubility of C_{60} in organic solvents. J Org Chem 57:6077–6079
8. Doome RJ, Fonseca A, Nagu JB (1999) ^{13}C–MAS–NMR investigation of solutions saturated with fullerenes: study of the anomalous solubility behaviour. Colloids Surf A Physicochem Eng Asp 158(1–2):137–143
9. Beck MT, Mandi G (1996) Fuller Sci Technol 3:32
10. Bezmel'nitsyn VN, Eletskii AV, Okun' MV (1998) Fullerenes in solutions. Uspekhi Fiz Nauk 168(11):1195–1220 (in Russian)
11. Ruof RS, Tse DS, Malhotra R, Lorents DC (1993) Solubility of fullerene (C_{60}) in a variety of solvents. J Phys Chem 97:3379–3383
12. Scrivenns WA, Tour JM (1993) Potent solvents for C_{60} and their utility for the rapid acquisition of ^{13}C NMR data for fullerenes. J Chem Soc Chem Commun, p.1207
13. Beck MT, Mandi G (1996) Fulle Sci Technol 5(2):291–310
14. Letcher TM et al (1993) Solubility buckminsterfullerene, C_{60}, in Benzene and Toluene. S Afr J Chem 46:41
15. Bochvar DA, Gal'pern EG (1973) About hypothetical system: carbododecahedron, s-icosahedron and carbo-s-icosahedron. Dokl Akad Nauk SSSR 209(3):610–612 (in Russian)
16. Schur DV, Zaginaichenko SY, Zolotarenko AD, Veziroglu TN (2008) Solubility and transformation of fullerene C_{60} molecule. In: Carbon nanomaterials in clean energy hydrogen systems, NATO science series. Springer, Dordrecht, pp 85–95
17. Schur DV, Zaginaichenko SY, Matysina ZA (2008) The special features of formation of carbon nanostructures, their classification and site on the state diagram of carbon. In: Carbon nanomaterials in clean energy hydrogen systems, NATO science series. Springer, Dordrecht, pp 67–83
18. Schur DV, Zaginaichenko SYu, Lysenko EA, Golovchenko TN, Vlasenko AYu (2007) The peculiatities of molecule C_{60} formation. In: Proceedings of 10th international conference "hydrogen materials science and chemistry of carbon nanomaterials", Sudak, Crimea, Ukraine, p 716–721
19. Schur DV, Zaginaichenko SY, Matysina ZA (2007) Effects of stimulation of hydrogen solubility in fullerite C_{60}. Nanosyst Nanomater Nanotechnol 5(2):385–409
20. Schur DV, Matysina ZA, Zaginaichenko SY (2007) Carbon nanomaterials and phase transformations in them. Nauka i obrazovanie, Dnepropetrovsk, p 678
21. Zaginaichenko SY, Anikina NS, Zolotarenko AD, Krivushenko OJ, Shur DV (2007) Regularity of C_{60} fullerene dissolving in methyl derivatives of benzene. In: Proceedings of 10th international conference "hydrogen materials science and chemistry of carbon nanomaterials", Sudak, Crimea, Ukraine, p 668–671
22. Anikina NS, Shur DV, Zaginaichenko SYu, Zolotarenko AD, Krivushenko OYa (2008) On the donor-acceptor mechanism of C_{60} fullerene dissolving in aromatic hydrocarbons. Ibid. pp 676–679

23. Anikina NS, Shur DV, Zaginaichenko SYu, Zolotarenko AD, Krivushenko OYa (2008) The role of chemical and physical properties of C_{60} fullerene molecules and benzene derivatives in processes of C_{60} dissolving. Ibid. pp 680–683
24. Matysina ZA, Schur DV, Zaginaichenko SY (2009) The solid-phase transformations in fullerite stimulated by rearrangement of the structure of fullerene molecules. Met Phys Adv Technol 31(2):147–163

Chapter 18
Solubility of Fullerenes in Naftalan

Dmitry V. Schur, N.S. Anikina, O. Ya. Krivuschenko, Svetlana Yu. Zaginaichenko, G.A. Kazimov, A.D. Zolotarenko, M.A. Polischuk, N.F. Javadov, T. Nejat Veziroğlu, and Ayfer Veziroğlu

Abstract From ancient times naftalan is used to treat various diseases both of animals and of humans. The positive use of fullerenes in medicine, pharmacology and perfumery makes them an attractive and promising object of extensive research. The combination of fullerenes and naftalan oil together in one compound, affecting positively on the vital functions of the human body, can bring the unexpected results. The solubility of fullerenes in naftalan oil may be the key moment in the synthesis of products of such kind. A detailed study focused on the elucidation of the fullerenes solubility in naftalans has been presented in this chapter: (1) determination of the solubility of fullerite in naftalan; (2) definition of the regions of naftalan transmission in toluene; (3) measurement of fullerenes solutions spectra in naftalan; and (4) comparison of the measured spectra of fullerene solutions in naftalan and toluene.

Keywords Naftalan • Fullerenes • Solubility • Toluene • Medicine • Pharmacology • Perfumery

D.V. Schur (✉) • N.S. Anikina • O.Ya. Krivuschenko • S.Yu. Zaginaichenko • A.D. Zolotarenko M.A. Polischuk
Institute for Problems of Materials Science of NAS of Ukraine, 3 Krzhyzhanovsky street, 03142 Kiev, Ukraine
e-mail: shurzag@materials.kiev.ua

G.A. Kazimov
Azerbaijani pharmaceuticals firm "BIOOIL", Baku, Azerbaijan

N.F. Javadov
Experimental-industrial plant of Institute for Petroleum Chemical Processes (IPCP) of NAS of Azerbaijan, Baku, Azerbaijan

T.N. Veziroğlu • A. Veziroğlu
International Association for Hydrogen Energy, 5794 SW 40 Street #303, Miami, FL 33155, USA

A. Veziroğlu and M. Tsitskishvili (eds.), *Black Sea Energy Resource Development and Hydrogen Energy Problems*, NATO Science for Peace and Security Series C: Environmental Security, DOI 10.1007/978-94-007-6152-0_18,

18.1 Introduction

Naftalan oil is widely used in medicine in Azerbaijan and abroad. The first written notes about this oil are dated to twelfth and thirteenth centuries. From time immemorial this oil treated medically the skin illnesses, rheumatism and other diseases. The various petroleum jelly, ointments, paraffins are widely used in medicine. The balneological mineral waters having the direct contact with the oil are used for the treatment of various diseases.

In the history of the application of naftalan oil many attempts to determine the chemical composition of its useful component have been made. However, the fundamental systematic study of the naftalan and its physical, chemical and geological properties began after 1920.

It should be noted that the advances of many scientists who purified naftalan from the unwanted components, and have achieved considerable progress in understanding its chemical composition and properties. In the course of the study of naftalan, scientists have made an estimate of the currently available data of the chemical nature, and the biologically active substances included in the naftalan. It was found that the presence of a significant amount of polycyclic hydrocarbons and the absence of light toxic hydrocarbons in the naftalan oil gives it therapeutic properties [1]. In the course of naftalan purification, naftalan changed its colour from the black and brown to yellow, and then turned into the colorless fraction of naftalan hydrocarbons, i.e., the naftalan oil.

Mamedaliev Yu. G. was one of the early investigators who tried to find the solution to the problem of naftalan composition, and first came close to the unraveling of chemical composition of naftalan hydrocarbons in 1953 [2, 3]. His assumption that one of the main active ingredients of naftalan are polycyclic naphthenic hydrocarbons was confirmed by subsequent studies [4–8].

The authors of paper [8] reported that fraction based on cyclopentanoperhydrophenanthrene (cyclopentane – perhydro – phenanthrene) with a short side chain was extracted from naphthenic hydrocarbons. Thus, it has been assumed that compounds, containing the carbon skeleton of cyclopentanoperhydrophenanthrene, form the basis for naphthenic polycyclic hydrocarbons. The cyclopentanoperhydrophenanthrene also known as steranes are class of 4-cyclic compounds derived from steroids or sterols via degradation and separation.

Studies [2, 4, 8] made it possible to draw the analogy between the peculiar kind of four-nuclei system of naftalan hydrocarbons and vital substances as the sterols, bile acids, a series of sex hormones, vitamin D, and others. This points toward possible important biochemical effects of polycyclic naphthenic hydrocarbons on the human body.

Since ancient times, naftalan is used to treat various diseases, both of animals and of humans. Today, Azerbaijan pharmaceutical firm “BIOOIL” successfully develops the technologies for synthesis and purification of naftalan oils and products based on them [9].

The positive use of fullerenes in medicine, pharmacology and perfumery makes them an attractive and promising object of extensive research. The combination of

fullerenes and naftalan oil together in one compound, affecting positively on the vital functions of the human body, can bring unexpected results. The solubility of fullerenes in naftalan oil may be the key moment in the synthesis of products of such kind. The main objectives of this study was to: (1) determine the solubility of fullerite in naftalan; (2) define the regions of naftalan transmission in toluene; (3) measure of fullerenes solutions spectra in naftalan; and (4) compare the measured spectra of fullerene solutions in naftalan and toluene.

18.2 Experimental

Four different specimens of naftalan oil of Azerbaijani production have been used for the experiments:

1. naftalan "1" has been received in the Azerbaijan office of firm «BIOOIL LTD» in Baku;
2. naftalan "2" produced by firm «BIOOIL LTD» was purchased in a chemist's shop in Baku;
3. naftalan "3" has been obtained from the Ukrainian office of the firm «BIOOIL LTD» in Kiev; and
4. naftalan "4" – intermediate product was obtained at the Experimental-industrial Plant of Institute for Petroleum Chemical Processes (IPCP) of NAS of Azerbaijan, Baku, Azerbaijan.

The physico-chemical and pharmaceutical characteristics of naftalan oil "1" of the firm "BIOOIL LTD" production are given in Table 18.1.

This chapter is the result of performed researches on fullerene solutions in the naftalan by the absorption spectrophotometrical method in the region of UV–vis-spectra on the device "Spectrophotometer – 2000".

We have made studies of four samples of naftalan: naftalan 1 and naftalan 2 represent the oily colorless substances; naftalan 3 and naftalan 4 are the similar substances which have the pale colour of lemon.

The fullerites (C_{60} + C_{70}) for our experiments have been produced by the arc method. Fullerites have a C_{60} content of about 85% and C_{70} content of 15%. Fullerites C_{60} and C_{70} have been obtained by the chromatographic fractionation of this mixture.

18.3 Studies of Solutions

18.3.1 Determination of the Fullerite (C_{60} + C_{70}) Solubility in Naftalan

To determine the solubility the fullerite sample has been weighted accurate to ±0.0002 g, placed in a weighing bottle with the precisely defined volume of naftalan and put on the vibrator. The fullerite weighing has been carried out on the

Table 18.1 Physico-chemical and pharmaceutical characteristics of naftalan oil (naphthenic hydrocarbons of naftalan petroleum) [9]

No	Properties	Value
1	Visual appearance	Transparent oily liquid, from white to lemon-yellow colour, with a weak characteristic odor
2	Density at 20°C, g/cm^3	0.8660–0.8790
3	Average molecular weight	290
4	Kinematic viscosity at 20°C, m^2/s (sSt)	14–16
5	Ignition temperature in an open vessel, °C	95
6	Content of aromatic hydrocarbons, wt.%	0
7	Content of resins, wt.%	0.01
8	Content of naphthenic hydrocarbons, wt.%	98.5
9	Acid number, mg KOH	0.05
10	Water content, wt.%	0
11	Mass fraction of water-soluble acids and additives	0
12	Contents isoalkanes, wt. %	1.5
13	Refractive index at 20°C	1.4650–1.4850
14	Content of asphaltenes, wt. %	0
15	Solidification temperature, not higher, °C	1–50
16	Initial boiling point, °C	>200
17	Microbiological purity of 1 g (bacteria)	5×10^3
18	Microbiological purity of 1 g (fungus)	5×10^2

electronic balance. The measurement of naftalan volume has been conducted by pipette with graduation lines with a volume V = 10 ml. The fullerite dissolution has been performed in the weighing bottle with a ground stopper, and protected from sunlight, fixed on the vibrator. After one week of the dissolution the sample was taken regularly from the bottle for the spectrum measurement. The dissolution has been continued up to a full stoppage of the absorption change at

$$\lambda \max = 407 \text{ nm and } \lambda = 472 \text{ nm} \tag{18.1}$$

Following the performed calculations, based on five samples of 0.2 ml solution for spectral analysis, it has been found that the solubility of fullerite (C_{60} + C_{70}) is of 2.50 ± 0.05 g/l.

18.3.2 Determination of Naftalan Passing Regions

To determine the naftalan passing regions, i.e., the areas suitable for identification of the substance dissolved in the present solvent, we have measured naftalan 1 spectra with relation to naftalan 1, as well as analogously for each modification of

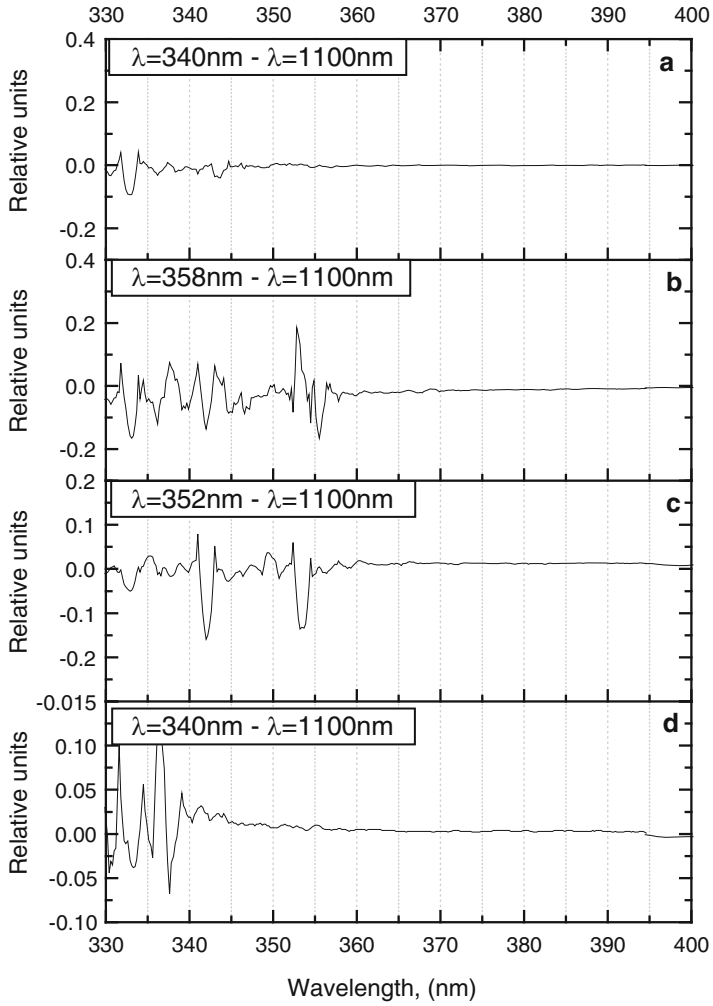

Fig. 18.1 The comparative diagram of spectra of the initial naftalan oils: (**a**) – (spectrum 54) naftalan 1 relatively naftalan 1; (**b**) – (spectrum 113) naftalan 4 relatively naftalan 4; (**c**) – (spectrum 114) naftalan 3 relatively naftalan 3; (**d**) – (spectrum 115) naftalan 2 relatively naftalan 2

naftalan. Figure 18.1a–d illustrates the measured spectra. As can be seen from these figures, naftalan 1 and naftalan 2 are the most suited for identification of fullerenes solution. Their transmission region is somewhat wider than of naftalan 3 and naftalan 4.

18.3.3 The Determination of "Purity" of Studied Naftalans

Since the naftalans 3 and 4 have a yellowish colour, in contrast to the naftalans 1 and 2, it was necessary to establish their difference from each other. For this

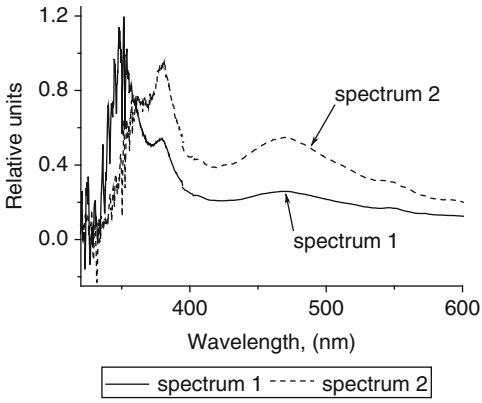

Fig. 18.2 The absorption spectra of fullerene C_{70} solutions in naftalan 2: (**a**) *spectrum 1* (101) – C_{70} in naftalan 2 relatively naftalan 1; (**b**) *spectrum 2* (109) – C_{70} in naftalan 2 relative to naftalan 2

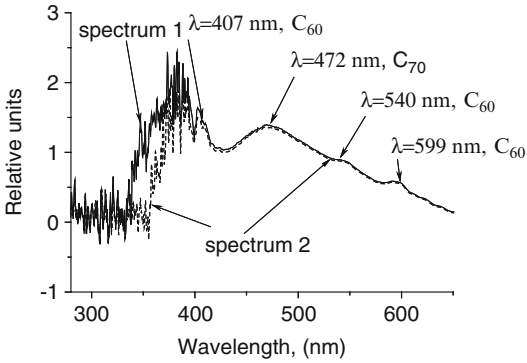

Fig. 18.3 The absorption spectra measured in a solution of fullerenes (C_{60} + C_{70}) mixture in naftalan 1: (**a**) *spectrum 1* has been measured relative naftalan 1; (**b**) *spectrum 2* has been measured relative to naftalan 3

purpose, we have measured the spectra of fullerene C_{70} solutions in the naftalan 2 (Fig. 18.2) relatively the naftalan 1 (spectrum 1) and relatively the naftalan 2 (spectrum 2) and of the solution of a mixture of the fullerenes (C_{60} + C_{70}) in the naftalan 1 (Fig. 18.3) relatively the naftalan 2 (spectrum 1) and relatively the naftalan 1 (spectrum 2). It follows from these figures that, in the region of Vis-spectrum of Fig. 18.2 the position of the absorption bands maxima coincide at $\lambda_{max} = 380$ nm and $\lambda max = 472$ nm, but Fig. 18.3 illustrates that the maxima of the absorption bands spectra of fullerenes (C_{60} and C_{70}) in toluene and naftalan solutions merge together because they are measured in the same solution, but relatively different naftalans. In the range from about 340 to 400 nm the spectra are separated. In this case the spectra divergence in Fig. 18.2 coincides properly with the wavelength of the absorption region for the naftalan 2. In our opinion this fact indicates that the naftalan 2 has a rather broad absorption band in this wavelength region due to the presence of "contamination" of unknown origin in the naftalan 2.

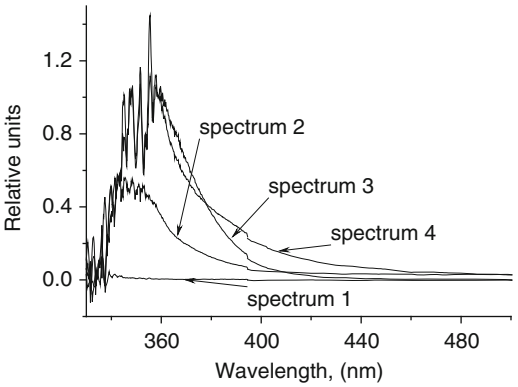

Fig. 18.4 The absorption spectra of naftalan, measured relatively naftalan 1: (**a**) spectrum 1 – naftalan 1 relative to naftalan 1; (**b**) spectrum 2 – naftalan 2 relative to naftalan 1; (**c**) spectrum 3 – naftalan 3 relative to naftalan 1; (**d**) spectrum 4 – naftalan 4 relative to naftalan 1

To check the hypothesis whether there is presence of contamination in naftalan 2, the absorption spectra of each naftalan have been measured relative to the naftalan of another modification:

- naftalan 1 – relatively to naftalans 2, 3, 4;
- naftalan 2 – relatively to naftalans 1, 3, 4;
- naftalan 3 – relatively to naftalans 1, 2, 4;
- naftalan 4 – relatively to naftalans 1, 2, 3.

As a result of this study, it has been found that the purest is naftalan 1 (Fig. 18.4). As evident from this figure, the naftalans 2, 3 and 4 have the broad absorption band in the wavelengths interval from ~330 to 400 nm, which veils the absorption bands of fullerenes C_{70} and fullerenes mixture in this wavelength region. In addition it has been established that the maxima of the absorption bands of solutions of fullerene C_{70} and solutions of fullerenes mixture in toluene and naftalan coincide completely.

18.4 Results and Discussion

This chapter presents the comparison of the absorption spectra of fullerene solutions in toluene and naftalan.

Since the extinction coefficients of fullerenes in naftalan, as well as in toluene, differ greatly depending on the solutions concentration, it is impossible to obtain a well-defined absorption spectrum in one solution. Therefore, the spectra in each wave-length region are presented by the fragmentary pieces.

Figure 18.5 illustrates the absorption spectra of fullerene C_{60} in the naftalan 2 solutions (spectrum 1) and in the toluene solution (spectrum 2). As is obvious from this figure, the spectra of fullerene C_{70} in the both solutions in the range from 355 to 600 nm coincide completely.

At the wavelength of 355 nm, at which the transmission region of naftalan 2 is completed, the spectra 1 and spectra 2 begin to be separated. The spectrum 1 of

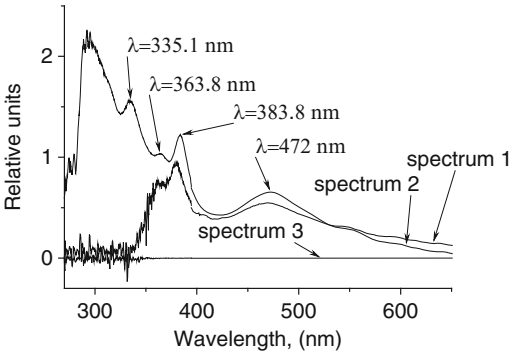

Fig. 18.5 The absorption spectra of solutions of fullerene C_{70}: (**a**) spectrum 1 – fullerene C_{70} in naftalan 2 relative to naftalan 2; (**b**) spectrum 2 – fullerene C_{70} in toluene; (**c**) spectrum 3 – naftalan 2 relative to naftalan 2

solution of fullerene C_{70} in naftalan 2 drops sharply down, whereas the absorption spectrum of C_{70} solution in toluene rises abruptly, but drops sharply at the beginning of transmission region of toluene at the wavelength of $\lambda = 280$ nm.

18.5 Conclusions

A detailed study focused on the elucidation of the fullerenes solubility in naftalans have been presented in this paper. The following conclusions can be drawn:

- As a result of investigation, it has been found that the solubility of fullerite (C_{60} + C_{70}) below than one might be expected, taking into account the concept of sterane structure of molecules constituting the naftalan oil. This can be caused by the high viscosity of naftalan oil or the presence of substituents in the molecules that make up its base, because the fullerene solubility in saturated cyclic hydrocarbons depends on their donor abilities.
- The measured absorption spectra of the fullerenes solutions are unexpectedly similar to the spectra recorded in the fullerene solutions in an aromatic compound as toluene. However, a complete analogy has been observed only at the wavelengths corresponding to the visible part of spectrum. In the UV-part of the spectrum, solutions of the naftalans 2, 3 and 4 contain a substance of unknown origin, veiled the spectra of fullerenes in naftalan.
- The observed analogy between the spectra recorded for the fullerenes solutions in the naftalan and toluene has been observed also in the solutions colour. The both solvents are painted in the same colour at the fullerene dissolution in toluene and naftalan
- The solution's painting is due to the formation of complex with the charge-transfer. This suggests that the fullerene molecules in the naftalan solution form micelles in the form of the charge-transfer complexes. The fullerene molecule itself fulfils the role of an electrons acceptor.

– The fullerene solubility in naftalan and toluene at room temperature fluctuates in a concentration range from 2.5 to 3.0 g/l. From this it follows that, an equal number of fullerene molecules is contained in the equal volumes of a saturated solution of toluene and naftalan. The fullerene molecule is the basis forming the fullerene-naftalan micelle in the naftalan solution. Thus, the equal volumes of saturated solutions of toluene and naftalan contain an equal number of fullerene micelles.

References

1. Karaev AI, Aliev RK, Babaev AZ (1959) Naftalan oil, its biological activity and therapeutic use. Academy of Sciences of the USSR, Moscow
2. Mamedaliev YG (1964) The theory of the mechanism of action of naftalan oil. Bull Acad Sci USSR Div Chem Sci 5:560–562
3. Mamedaliev YG (1953) About chemical composition of the active principle of medical naftalan oil. Bull Acad Sci Azerb SSR 5:9–36
4. Pashayev TG (1950) Results of the study of the Naftalan oil properties.
5. Pashayev TG (1956) Justification of rationalization of methods of medical application of Naftalan oil. In: Proceedings of the Azerbaijan Research Institute of Balneology and Physical Treatments of S.M. Kirov, Baku, Issue 2, pp 180–6
6. Kuliev AM, Baladzhaeva SS, Levshina AM, Mamedov II (1978) Testing for the carcinogenicity of naphthenic hydrocarbons. In: Proceedings of the Azerbaijan Research Institute of Balneology and Physical Treatments of S.M. Kirov, Baku, Issue 16, pp 28–33
7. Kuliev AM, Levshina AM, Kadyrov AA, Polyakova LP (1988) Modern problems of rational use of medical naphthalan oil. Azerb Oil Ind 6:56–61
8. Kuliev AM, Levshina AM, Muradov AN (1968) Researches of hydrocarbon composition of therapeutic naftalan oil. Azerb Oil Ind 7:36–37
9. Kazimov GA (2009) Monography “Chronicle of Naftalan”. ELM, Baku, 584 p

Chapter 19
The Prospects for Use of Hydrogen Accumulators on the Basis of Lanthan-Magnesium-Nickel Store Alloys

Svetlana Yu. Zaginaichenko, Dmitry V. Schur, A.F. Savenko, V.A. Bogolepov, Z.A. Matysina, and Ayfer Veziroğlu

Abstract A theoretical study of hydrogen solubility in alloys with structures of the $L2_2$, D2d, $L6_0$ types and in phase mixtures of these alloys has been developed on the basis of the molecular-kinetic concept. The absorption and desorption isotherms have been investigated, their dependence on the hydrogen activity and the magnesium concentration has been found. It is presented that horizontal plateau appears and is lengthened in the isotherms with increasing concentration of magnesium and with decreasing activity of hydrogen atoms. Considering volume effects, the hysteresis phenomena have been studied and hysteresis constants have been evaluated. A fall in hysteresis constant with reduced activity of hydrogen atoms has been shown. Our calculation results are in agreement with experimental data.

Keywords Hydrogen accumulator • Lanthan-magnesium-nickel alloy • Equilibrium concentration • Hydrogen solubility • Isotherm • P-T-c diagram

19.1 Introduction

Under the joint evaporation of alloy $LaNi_5$ and graphite in the liquid phase the nano-dispersed composite, which contain carbon nanostructures with encapsulated clusters of alloy $LaNi_5$ and spherical particles of alloy $LaNi_5$ of micron size coated

S.Yu. Zaginaichenko (✉) • D.V. Schur • A.F. Savenko • V.A. Bogolepov
Institute for Problems of Materials Science of NAS of Ukraine, 3 Krzhyzhanovsky str, Kiev 03142, Ukraine
e-mail: shurzag@materials.kiev.ua

Z.A. Matysina
Dnepropetrovsk National University, 72 Gagarin str, Dnepropetrovsk 49000, Ukraine

A. Veziroğlu
International Association for Hydrogen Energy, 5794 SW 40 St. #303, Miami, FL 33155, USA

A. Veziroğlu and M. Tsitskishvili (eds.), *Black Sea Energy Resource Development and Hydrogen Energy Problems*, NATO Science for Peace and Security Series C: Environmental Security, DOI 10.1007/978-94-007-6152-0_19,

with carbon nanostructures, is formed. Experiments show that the presence of $LaNi_5$ particles in composite simplifies the kinetics of interaction of carbon nanostructures with hydrogen. The question of studying the interaction peculiarities of alloy with metallic and nonmetallic impurities is of paramount importance, because it will allow to control the catalytic properties of alloy $LaNi_5$ interaction with hydrogen.

It is common knowledge that hydrides are the sources of pure hydrogen necessary for various technologies, engineering and for research purposes. The supplies of hydrogen in the bound state are practically unlimited. The multicomponent composition of hydride systems makes possible the creation of accumulators with controlled content of hydrogen. The systematic study of hydrides could give new practical implementation.

Lanthan-magnesium-nickel alloys attract the attention of scientists in connection with a possibility to use them as accumulators and storage systems of hydrogen and as energy source. Experimentally such alloys were under investigation, for example, in [1–10]. At present, much attention has been given to the study of $LaNi_5$, $LaNi_7$ alloys and multicomponent alloy on their base.

In the last the lanthanum atoms can be partially substituted by atoms of rare-earth elements (R = Er, Gd, Nd, Pr, Sm, Y) and the nickel atoms by atoms of metals and non-metals (M = Al, B, Co, Cu, Fe, Mg, Mn, Si, Sn, C). Such additions can stabilize the structure, increase the hydrogen absorptivity and reduce the material cost. In our papers, we presented the study of $La_{1-X}R_XNi_{5-Y}M_Y$ alloys [11–13], the calculation of hydrogen solubility in these systems.

In recent years the intensive research of lanthan-magnesium-nickel alloys [14–17] was carried out. It has been established that magnesium improves the kinetic characteristics of alloys [17, 18].

In [19], the structure and electrochemical properties of $La_{2-X}Mg_XNi_7$ alloys ($x = 0.3$–0.6) have been investigated regularly. The formation of three phases has been established in the system: (1) $La_{2-X}Mg_xNi_7$, (2) $LaNi_5$, and (3) $La_{1-X}Mg_XNi_3$ in dependence on magnesium concentration x. In this case for different values x the phase mixture of two alloys is formed: at $x = 0.3$–0.5 the test specimens are the mixture of $La_{2-X}Mg_XNi_7$ and $LaNi_5$ alloys, at $x = 0.6$ – the mixture of first alloy with $La_{1-X}Mg_XNi_3$. The content of $La_{2-X}Mg_XNi_7$ alloy in the phase mixture was established as: $X_1 = 81.5$; 93.7; 96.8; 60.7 wt.% respectively at $x = 0.3$; 0.4; 0.5; 0.6. Authors of [19] investigated the hydrogen solubility in these alloys and received the isotherms of absorption-desorption (Fig. 19.1). As can be seen from this figure, the magnesium presence and increase of its concentration modify the course of isotherms of hydrogen solubility in the phase mixtures.

With increasing concentration x of magnesium a plateau (horizontal segment) appears and becomes elongated. The coefficient of hysteresis loops $\ln \frac{P_a}{P_d}$ (P_a, P_d are pressures of absorption and desorption in average points of isotherms) is positive and decreases with increasing concentration x, taking the values of 9.96 at $x = 0.3$; 1.57 at $x = 0.4$; 0.73 at $x = 0.5$; 0.52 at $x = 0.6$, suggesting that reversibility of processes of hydrogen absorption-desorption is improved. Furthermore, as the

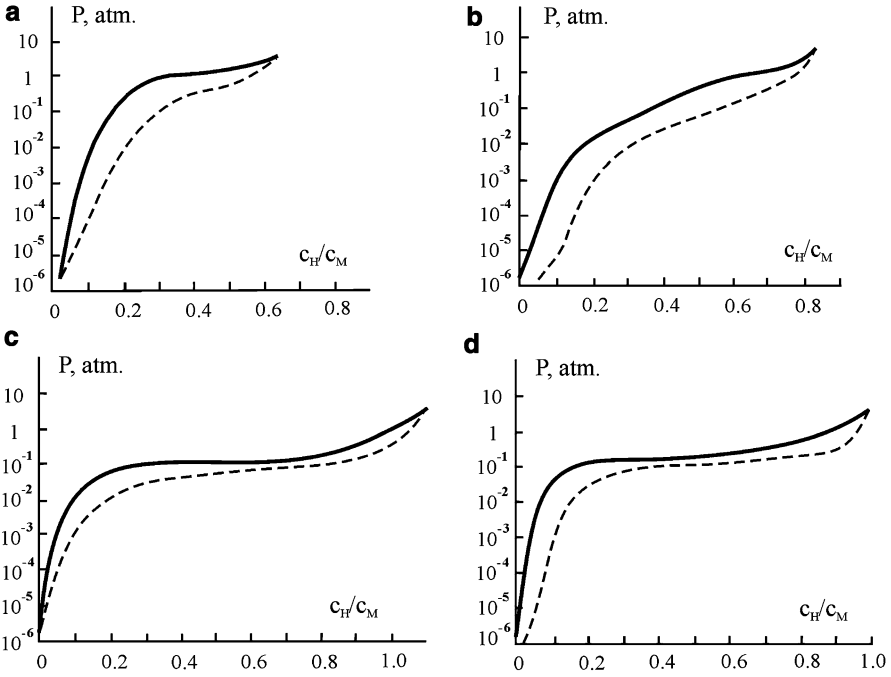

Fig. 19.1 Experimental isothermal curves of hydrogen absorption by phase mixture of $La_{2-X}Mg_XNi_7$ alloy with $LaNi_5$ at $x = 0.3$; 0.4; 0.5 (curves **a**, **b**, **c**) and with $La_{1-X}Mg_XNi_3$ at $x = 0.6$ (*curve* **d**) at the temperature of 293 K and concentrations of first phase equal respectively to $X_1 = 81.5$; 93.7; 96.8; 60.7 in wt.% for cases (**a**–**d**). The *dotted curves* are isotherms of hydrogen desorption

magnesium impurity increases, the hydrogen solubility run at lower pressure (the level of the isotherms is reduced). At first, the hydrogen content in alloys increases $c/c_M = 0.63$; 0.82; 1.09 at $x = 0.3$; 0.4; 0.5 and then decreases moderately up to the value 0.99 at $x = 0.6$ (c, c_M are atomic concentrations of hydrogen and metal).

Therefore, the development of theory of hydrogen solubility in these alloys of $L2_2$, D2d, $L6_0$ structures respectively, the calculation of isotherms of hydrogen solubility in phase mixtures, the evaluation of the influence of magnesium impurity on isotherms run, level, slope, the elucidation of reasons of plateau appearance and the estimation of coefficient of hysteresis loop are of scientific and practical interest.

19.2 Free Energies of Alloys and Hydrogen Solubility

Calculations of the free energies for investigated alloys and their minimization are performed on the basis of the molecular-kinetic concept for solving the raised problems. The method of average energies is used in a model of pair interaction of

nearest atoms, ignoring the correlation in substitution of lattice sites and interstitial sites by atoms. Lattice distortion is not taken into account because, as is well known, the interstitial hydrogen atoms in metals only increase the lattice parameter without changing the lattice.

The free energy of each alloy is calculated by the known formula

$$F_i = E_i - kT \ln W_i - kTN_H \ln \lambda_i, \quad i = 1, 2, 3, \tag{19.1}$$

where E_i is the configuration internal energy of i alloy determined by the sum of energies of pair interactions, k is Boltzmann's constant, T is the absolute temperature, W is the thermodynamic probability of the hydrogen atoms distribution at interstices, which is determined by the combinatorial rule, N_H is the number of hydrogen atoms, λ_i is the activity of hydrogen atoms.

The equilibrium concentrations c_i of hydrogen in each alloy are derivable from the condition of minimum of free energy

$$\partial F_i / \partial c_i = 0, \quad i = 1, 2, 3 \tag{19.2}$$

and then the concentration c_H of hydrogen in the mixture of two phases can be found by formula

$$c_H = X_1 c_1 + X_i c_i, \quad i = 2 \text{ or } 3. \tag{19.3}$$

19.2.1 The $La_{2-X}Mg_XNi_7$ Alloy with a Structure of the $L2_2$ (Ce_2Ni_7) Type

This structure is shown in Fig. 19.2. The La_2Ni_7, $La_{2-X}Mg_XNi_7$ alloys at $x = 0.3$–0.6 and Sb_2Tl_7 alloy are structured so.

Under the assumption that hydrogen atoms occupy positions of one type, we find the free energy of $La_{2-X}Mg_XNi_7$ – H system as follows:

$$\begin{aligned} F_1 = {} & -Nc_1(W_1 + V_1 x) + kTN[c_1 \ln c_1 + (1 - c_1)\ln(1 - c_1)] \\ & - kTNc_1 \ln \lambda_1, \end{aligned} \tag{19.4}$$

where N is the number of lattice sites occupied by metals atoms,

$$\begin{aligned} W_1 &= 2[\nu_1(2\upsilon_{HNi} + \upsilon'_{HNi}) + (2\upsilon_{HLa} + \upsilon'_{HLa})], \\ V_1 &= \nu_2\left(2\upsilon_{HMg} - 2\upsilon_{HLa} + \upsilon'_{HMg} - \upsilon'_{HLa}\right). \end{aligned} \tag{19.5}$$

$$\nu_1 = N_1/(N_1 + N_2) = N_1/N, \quad \nu_2 = N_2/N, \quad \nu_1 + \nu_2 = 1 \tag{19.6}$$

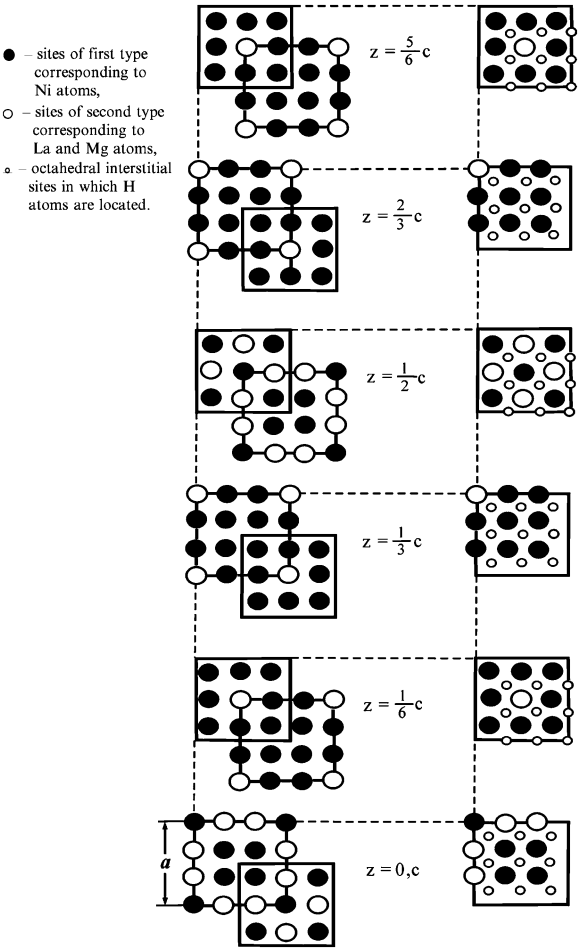

Fig. 19.2 The plan view of tetragonal structure of the $L2_2$ (Ce_2Ni_7) type for the $La_{2-x}Mg_xNi_7$ alloy in projection on equatorial planes. At the *left* the arrangements of sites are shown, to the *right* of figure all 54 sites and 54 octahedral interstitial sites of the crystal elementary cell in these planes are marked off

are concentrations of sites of first and second type, $\upsilon_{HM} = \upsilon_{HM}(r), \upsilon'_{HM} = \upsilon_{HM}(r')$ are energies of the interstitial interaction of MH pairs at different distances r, r′. For examined $L2_2$ structure $r = a\sqrt{2}/6, r' = c/6$. Equation (19.4) defines the free energy F_1 of this alloy based on temperature, hydrogen and magnesium concentrations c, x, hydrogen activity λ_1 and energetic parameters W_1, V_1.

By minimizing the free energy F_1 (19.4) we can calculate the equilibrium concentration of hydrogen atoms:

$$kTln\frac{c_1}{1-c_1} = W_1 + V_1x + kTln\lambda_1. \triangleleft \tag{19.7}$$

Taking into consideration the pressure dependence of energetic parameters W_1, V_1 and activity λ_1 of hydrogen atoms

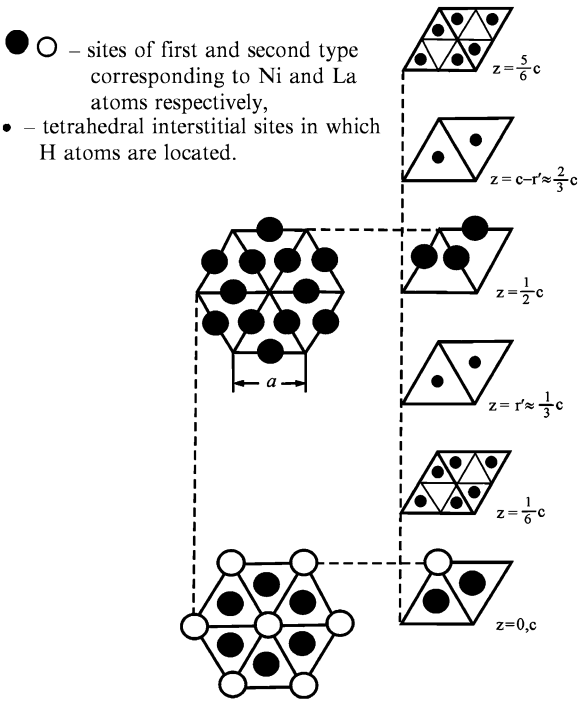

Fig. 19.3 The plan view of hexagonal structure of the D2d ($CaCu_5$) type for $LaNi_5$ alloy. The sites in equatorial planes (at the *left*) and all sites and tetrahedral interstitial sites (6 and 16, respectively) of the lattice elementary cell are presented

$$W_1 + V_1 x \approx W_1^o + V_1^o - \alpha_1 P, \quad \lambda_1 = DP^{1/2} \tag{19.8}$$

the Eq. (19.7) defines the P – T – c_1 diagram of hydrogen solubility in this alloy.

19.2.2 The $LaNi_5$ Alloy with a Structure of the D2d ($CaCu_5$) Type

Figure 19.3 illustrates this system. Examples of such alloys are $CaNi_5$, $CaZn_5$, $CeNi_5$, $CdNi_5$, $LaZn_5$, $PrNi_5$, $ThCo_5$, $ThFe_5$. For studied D2d structure $r = \sqrt{3a^2 + c^2}/6, r' = (c + a^2/3c)/4$. These distances both for the $LaNi_5$ ally (with lattice parameters $a = 0.502$ nm and $c = 0.398$ nm) and for alloys with this structure, differ insignificantly (in the third decimal place: $r - r' = 0.006$ nm). Therefore, we assume $r \approx r'$.

Under the assumption that hydrogen atoms occupy positions of two types, the calculation of free energy F_2 by initial formula (19.1) gives the equation:

$$F_2 = -Nc_2W_2 + kTn_2N\left[\frac{3}{8}c_2 \ln\frac{3c_2}{8} + \left(1 - \frac{3c_2}{8}\right)\ln\left(1 - \frac{3c_2}{8}\right)\right] - kTNc_2 \ln\lambda_2, \tag{19.9}$$

where

$$W_2 = \frac{6}{5}[\nu_1(3\mu_1 + 4\mu_2)\upsilon_{HNi} + 5\mu_1\nu_2\upsilon_{HLa}], \tag{19.10}$$

μ_1, μ_2 are the relative number of interstitial sites of *i*-type in which hydrogen atoms are placed, $\mu_1 + \mu_2 = 1$.

The equilibrium state condition and pressure dependences of W_2 energy and λ_2 activity (of the (19.8) type) enable us to find the hydrogen concentration c_2 in alloy of D2d structure:

$$c_2 = n_2\left[1 + \frac{1}{D_2P^{1/2}}\exp\frac{W_2^o - \alpha_2 P}{kT}\right]^{-1}. \tag{19.11}$$

As in [12], theoretical isotherms, isobars, isopleths of hydrogen solubility in $LaNi_5$ alloys and another system of such structure can be constructed using formula (19.11).

19.2.3 The $La_{1-X}Mg_XNi_3$ Alloy with a Structure of the $L6_0$ ($PuNi_5$) Type

The plan view of face-centered tetragonal structure of $L6_0$ type is presented in Fig. 19.4. The $CuTi_3$, Pd_3Tl, Pt_3In, Pt_3Mg and another alloys have such lattice. The distances r, r′, r″ for the $L6_0$ structure are equal to $r = \sqrt{2a^2 + c^2}$,$r' = a/2$,$r'' = c/2 \approx r$.

The free energy F_3 of $La_{1-X}Mg_XNi_3$ system is calculated by formula (19.1) and we get the formula:

$$F_3 = -Nc_3(W_3 + V_3x) + kTNn_3\left[\frac{c_3}{3}\ln\frac{c_3}{3} + \left(1 - \frac{c_3}{3}\right)\ln\left(1 - \frac{c_3}{3}\right)\right] - kTNc_3\ln\lambda_3, \tag{19.12}$$

minimization of which provides a possibility of estimating the equilibrium concentration c_3 of hydrogen in studied alloy

$$c_3 = n_3\left[1 + \frac{1}{D_3P^{1/2}}\exp\frac{-\left(W_3^o + V_3^o x - \alpha_3 P\right)}{kT}\right]^{-1} \tag{19.13}$$

$$\begin{aligned} W_3 &= 2[(2\mu_1\nu_1 + \mu_2)\upsilon_{HNi} + \mu_2\upsilon'_{HNi} + \nu_2(2\mu_1\nu_2\upsilon_{HLa} + \mu_2\upsilon'_{HLa})], \\ V_3 &= 2\nu_2\left[2\mu_1\nu_2\left(\upsilon_{HMg} + \upsilon_{HLa}\right) + \mu_2\left(\upsilon'_{HMg} + \upsilon'_{HLa}\right)\right]. \end{aligned} \tag{19.14}$$

Formula (19.13) takes into account the dependences of the energetic parameters and hydrogen activity λ_3 on the pressure.

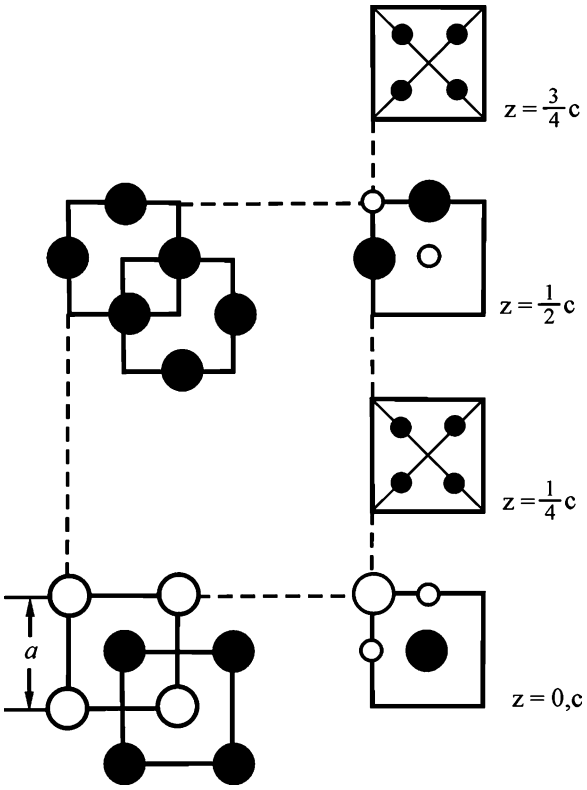

Fig. 19.4 The plan view of face-centered tetragonal structure of the $L6_0$ ($PuNi_3$) type for the $La_{1-x}Mg_xNi_3$ alloy. Designations are the same as in Figs. 19.2 and 19.3

19.3 Discussion of Results and Comparison with Experiment

Let us analyze the results obtained and examine formulas (19.7), (19.11), (19.13). In the case of stoichiometry, full order in distribution of nickel atoms and chaotic distribution of lanthan and magnesium atoms over the sites of second type and hydrogen atoms over all interstices sites the concentration of hydrogen atoms in the ratio to the number of all sites of crystal lattices (the number of matrix atoms) is determined for different systems of examined types (taking into consideration the linear dependence of energies of interatomic interactions of HM pairs on pressure):

$$c_i = n_i\left[1 + \frac{1}{D_i P^{1/2}}\exp\left(-w_i^o - \upsilon_i^o x + \alpha_i P\right)\right]^{-1}, \quad i = 1,2,3, \tag{19.15}$$

where $w_i^o = w_i, \upsilon_i^o = \upsilon_i$ at $P = 0$, coefficients α_i in units of kT are determined by compressibility $æ_i$ ($\alpha_i = æ_i\ d_i^o\left(\frac{\partial U_i}{\partial d_i}\right)_{d_i=d_i^o}$, d_i^o is the diameter corresponding to the

atomic volume of the *i*th structure at P = 0). The formulae defining these energies in kT units and structural parameter for three structures are:

$$\begin{cases} u_1 = -(w_1 + \upsilon_1 x), \\ w_1 = -2[\nu_1(2\upsilon_{HNi} + \upsilon'_{HNi}) + \nu_2(2\upsilon_{HLa} + \upsilon'_{HLa})], \\ \upsilon_1 = -\nu_2\left(2\upsilon_{HMg} - 2\upsilon_{HLa} + \upsilon'_{HMg} + \upsilon'_{HLa}\right), \\ n_1 = 1,\ \nu_1 = \dfrac{7}{9},\ \nu_2 = \dfrac{2}{9},\ \mu_1 = \dfrac{2}{3},\ \mu_2 = \dfrac{1}{3}, \end{cases} \quad \text{for } i = 1 \tag{19.16}$$

$$\begin{cases} u_2 = -w_2 = -\frac{6}{5}[\nu_1(3\mu_1 + 4\mu_2)\upsilon_{HNi} + 5\mu_1\nu_2\upsilon_{HLa}], \\ n_2 = \dfrac{8}{9},\ \nu_1 = \dfrac{5}{6},\ \nu_2 = \dfrac{1}{6},\ \mu_1 = \dfrac{3}{4},\ \mu_2 = \dfrac{1}{4}, \end{cases} \quad \text{for } i = 2 \tag{19.17}$$

$$\begin{cases} u_3 = -(w_3 + \upsilon_3 x), \\ w_3 = -2[(2\mu_1\nu_1 + \mu_2)\upsilon_{HNi} + \mu_2\upsilon'_{HNi} + \nu(2\mu_1\nu_2\upsilon_{HLa} + \mu_2\upsilon'_{HLa})], \\ \upsilon_3 = -2\nu\left[2\mu_1\nu_2\left(\upsilon_{HMg} - \upsilon_{HLa}\right) + \mu_2\left(\upsilon'_{HMg} - \upsilon'_{HLa}\right)\right], \\ n_1 = 3,\ \nu_1 = \dfrac{3}{4},\ \nu_2 = \dfrac{1}{4},\ \mu_1 = \dfrac{2}{3},\ \mu_2 = \dfrac{1}{3}. \end{cases} \quad \text{for } i = 3 \tag{19.18}$$

It follows from formula (19.15) that the hydrogen concentration in the alloys with the structures of the $L2_2$, D2d, $L6_0$ types can vary within the limits:

$$\begin{gathered} 0 \le c_1 \le 1 \text{ at } n_1 = 1, \\ 0 \le c_2 \le 8/3 \text{ at } n_2 = 8/3, \\ 0 \le c_3 \le 3 \text{ at } n_3 = 3. \end{gathered}$$

The hydrogen solubility in the phase mixture of two alloys of X_1 and X_2 (or X_3) concentrations respectively is defined by the formula:

$$c_H = X_1 c_1 + X_2 c_2 \tag{19.19}$$

for the cases (*a*, *b*, *c*) in Fig. 19.1 and

$$c_H = X_1 c_1 + X_3 c_3 \tag{19.20}$$

for the case (*d*) in Fig. 19.1.

Let us carry out the study of the function

$$c = \left[1 + \frac{1}{DP^{1/2}} \exp(u - \alpha P)\right]^{-1}, \tag{19.21}$$

which corresponds to the case of $n_i = n_1 = 1$, i.e. to the alloy with structure of $L2_2$ type.

Taking the temperatures as constant and setting the values for pressure P it is easy to calculate by formula (19.21) the numerical values of hydrogen concentration c for different values of pressure and subsequently to construct the isotherms of hydrogen solubility.

The character of the lnP dependence on $\boldsymbol{c}$ is shown in Fig. 19.5. With decreasing activity of hydrogen atoms and accordingly of coefficient D the plot become more gently sloped and a plateau appears, the length of which increases with decreasing hydrogen atom activity. As this takes place, the hydrogen solubility decreases at each value of pressure as the activity is reduced.

When experimental plots of Fig. 19.1 are compared with that of Fig. 19.5, it can be assumed that appearance and elongation of plateau in moving from plot (*a*) to (*b*) and then to (*c*) and (*d*) is caused by manifestation of two factors: the decrease of hydrogen atoms activity with increasing concentration x of magnesium and the increase of interval of possible hydrogen solubility with increasing amounts of interstitial sites in which hydrogen atoms are distributed.

The qualitative estimates of hysteresis effect of hydrogen absorption-desorption process in the phase mixtures being investigated is of physical interest. Research on ordering of different types (dipole, deformational and another) in solids demonstrated a manifestation of hysteresis phenomena at the expense of volume effects emerging in the dependence of interatomic interactions energies on order parameter and component concentrations [20, 21].

We have made these studies on hysteresis phenomena taking into consideration the quadratic dependence of u energy on hydrogen concentration c. In this case for the $L2_2$ structure, we have (in dimensionless units) the relation

$$\mathrm{lnP} = 2(\mathrm{C} - \alpha \mathrm{P}), \tag{19.22}$$

where

$$\mathrm{C} = \ln\frac{\mathrm{c}}{1-\mathrm{c}} - \gamma \mathrm{c}^2 + \mathrm{u} - \beta \mathrm{x} - \mathrm{lnD}, \quad \gamma = \frac{1}{2\mathrm{c}^2(1-\mathrm{c})}. \tag{19.23}$$

Then, the C value is equal to

$$\mathrm{C} = \ln\frac{\mathrm{c}}{1-\mathrm{c}} - \frac{1}{2(1-\mathrm{c})} + \mathrm{u} - \beta \mathrm{x} - \mathrm{D}. \tag{19.24}$$

The influence of coefficients α, D and magnesium concentration x on hysteresis effects is under investigation and the plots of lnP as a function of hydrogen concentration c at u = 1 and different values of α, D, x are constructed and presented in Fig. 19.6. The hysteresis coefficients $\Delta = lnP_a - lnP_d$ are determined by the difference of the values in extreme points of curves. As evident from Fig. 19.6a, b, the hysteresis constant decreases as the activity of hydrogen atoms (D coefficient) is reduced and the plots of hydrogen solubility isotherms have to be realized at lower values of pressure as magnesium concentration x is increased. Both of these effects qualitatively agree with the experimental data.

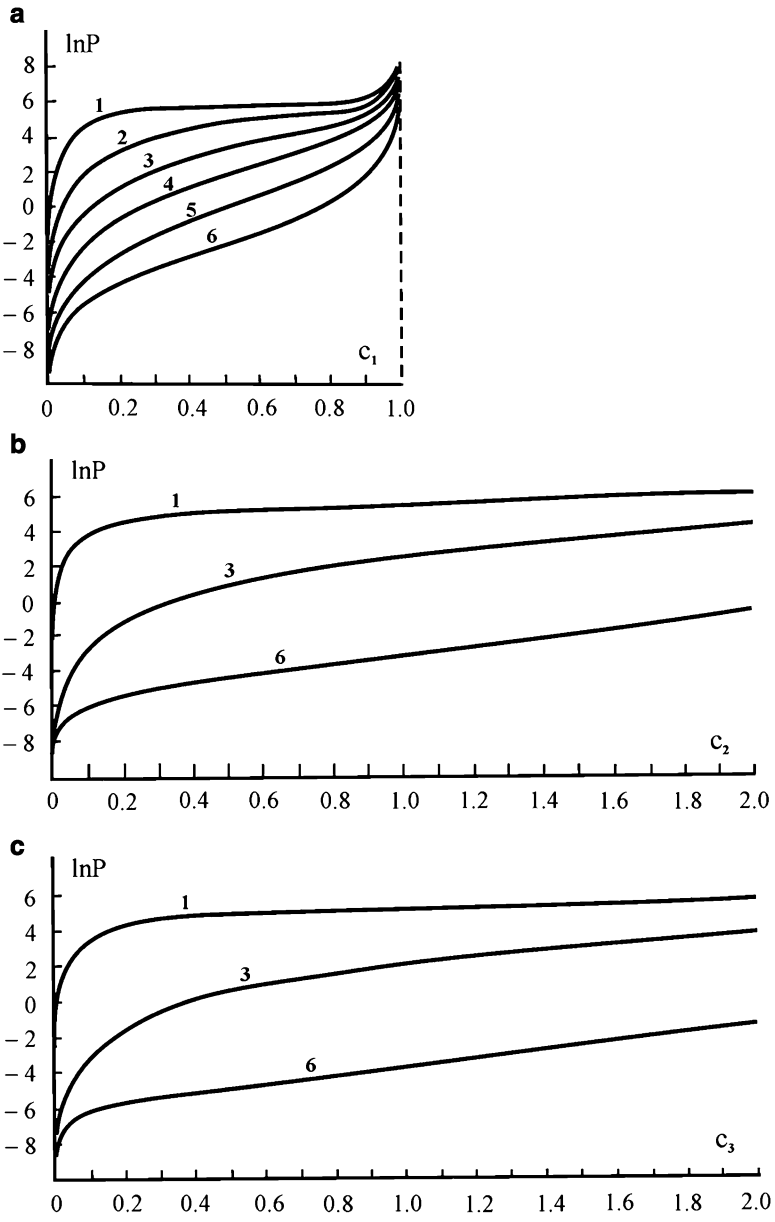

Fig. 19.5 Calculated isotherms of hydrogen solubility in alloys of the $L2_2$ (**a**), D2d (**b**), $L6_0$ (**c**) structures constructed by formula (19.21) for values u = 1, α = 0.02 Pa^{-1} and D_i = 0.01; 0.1; 0.4; 1; 2.5; 10 (*curves 1*, *2*, *3*, *4*, *5*, *6*, respectively)

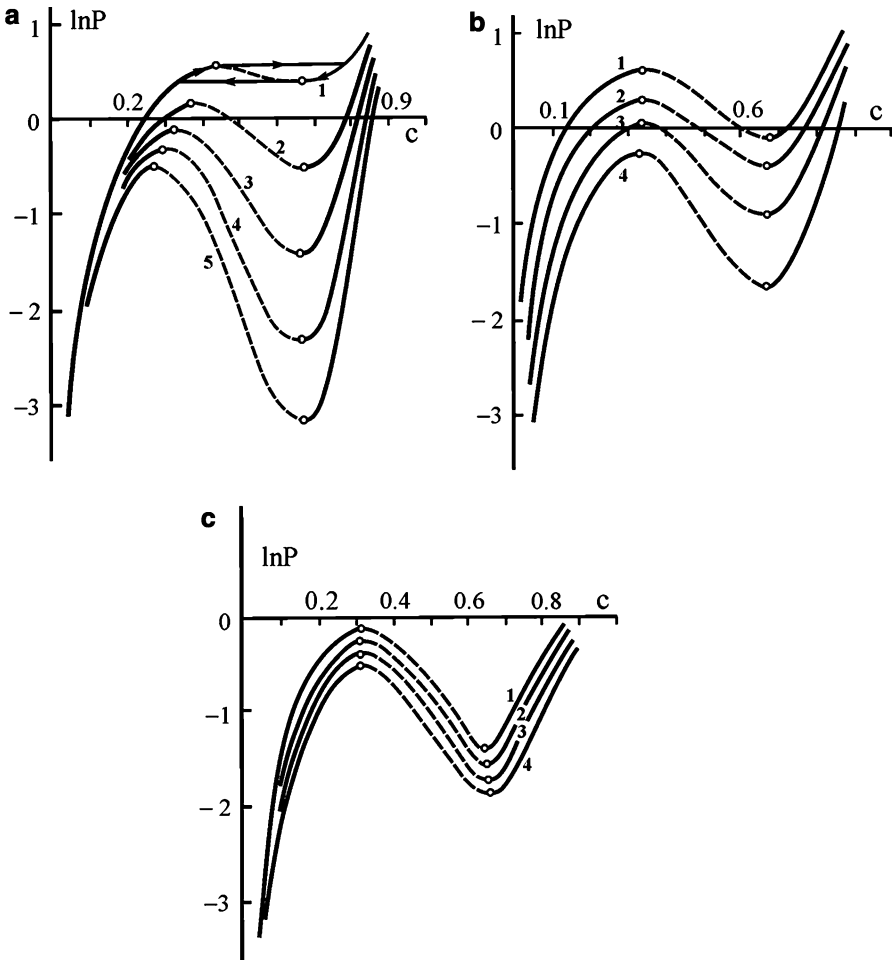

Fig. 19.6 The graphical representations defining the hysteresis phenomenon of hydrogen-solubility isotherms in dependence on the coefficients α (**a**), D (**b**) and magnesium concentration x (**c**) constructed by formulae (19.22), (19.24) for u = 1 and parameters: (**a**) D = 0.4; $x = 0$; α = 0.1; 0.15; 0.2; 0.25; 0.3 (curves 1–5, respectively); (**b**) α = 0.2; $x = 0$; D = 0.21; 0.29; 0.37; 0.45 (curves 1–4, respectively); (**c**) D = 0.4; α = 0.2; β = −0.25; $x = 0$; 0.3; 0.6; 0.9 (curves 1–4, respectively) The extreme points are marked by *circles* on the curves. The *dotted segments* of the curves correspond to non-equilibrium states

19.4 Conclusions

The statistical theory developed for hydrogen solubility in lanthan-magnesium-nickel alloys with the $L2_2$, D2d, $L6_0$ structures makes it possible for us to calculate the free energies of studied alloys, to derive formulae determining the P-T-c diagrams of

hydrogen solubility, to study the isotherms of hydrogen solubility corresponding to different values of hydrogen activity, to investigate the hysteresis phenomena taking into consideration the volume effects, to evaluate the hysteresis constants for different values of theory parameters (α, D) and magnesium concentration x. It has been shown that with a decrease in the activity of hydrogen atoms (of the coefficient D) the hysteresis coefficient decreases, which agrees with the experimental data in the assumption that the presence of magnesium decreases the activity of hydrogen atoms. An increase in the magnesium concentration x should shift the graphs of the hydrogen-solubility isotherms down along the ordinate axis toward lower pressures; the length of the plateau should somewhat increase in this case.

The calculation results have been compared with experimental data for hydrogen solubility in binary $LaNi_5$, $LaCu_5$, $LaCo_5$ alloys and various ternary phases of examined structures. All derived regularities are in qualitative agreement with experimental data.

Acknowledgment The work has been done within the framework of SCOPES project «Implementation in East Europe of new methods of synthesis and functionalization of carbon nanotubes for applications in the energy storage and sensors field.

References

1. Ven Mal HH, Bushow KHJ, Miedema AR (1974) Hydrogen absorption in LaNi5 and related compounds: experimental observation and their explanation. J Less-Common Met 35(1):65–76
2. Semenenko KN, Malyshev VP, Petrova LA, Bumasheva VV, Sarynin VK (1977) The interaction of $LaNi_5$ with hydrogen. Izv Akad Nauk SSSR Neorg Mater 13(11):2009–2013
3. Shinar J, Shaltiel D, Davidov D (1978) Hydrogen sorptoin properties of La1-XCaXNi5 and La (Ni1-XCuX)5 systems. J Less-Common Met 60:209–219
4. Diaz H, Percheron-Guegan A, Achard JC (1979) Thermodynamic and structural properties of $LaNi_{5-y}$ Al_y compounds and their related hydrides. Int J Hydrog Energy 4(5):445–454.
5. Lartigue C, Percheron A, Acherd JC (1980) Thermodynamic and structural properties of $LaNi_{5-X}Mn_X$ compounds and their related hydrides. J Less-Common Met 75(1):23–29
6. Patrikeev YB, Levenskii YV, Badovskii VV, Filyand YM (1984) Thermodynamics and hydrogen diffusion in $LaCo_5H_X$ alloys. Izv Akad Nauk SSSR Neorg Mater 20(9):1503–1506
7. Percheron-Guegan A, Lartigue C, Achard JC (1985) Correlation between the structural properties, the stability and the hydrogen content of substituted lantanum-nickel ($LaNi_5$) compounds. J Less-Common Met 114(2):287–309
8. Colinet C, Pasturel A (1987) Enthalpies of formation and hydrogenation of $La(Ni_{1-X}Co_X)_5$ compounds. J Less-Common Met 134:109–122
9. Kolachev BA, Il'in AA, Lavrenko VA (1992) Gidridnye Sistemy. Spravochnik, Moscow, Metallurgia (in Russian)
10. Majer G, Kaess U, Bowman RC Jr (1998) Nuclear magnetic resonance studies of hydrogen diffusion in $LaNi_5H_6$ and $LaNi_{4,8}Sn_{0,2}H_{5,8}$. Phys Rev B 57(21):13599–13603
11. Matysina ZA, Zaginaichenko SYu, Schur DV, Pishuk VK (1997) Hydrogen in lanthan-nickel alloys-accumulators. In: 5th international conference on hydrogen materials science and chemistry of metal hydrides, Katsiveli, Crimea, Ukraine, 2–8 Sept 1997, pp 62–63
12. Matysina ZA (1997) Isotherms of hydrogen solubility in hydrogen-storage lanthanum-nickel alloys. Phys Met Metallogr 84(5):495–500

13. Schur DV, Zaginaichenko SY, Matysina ZA, Pishuk VK (2002) Hydrogen in lanthanum-nickel storage alloys. J Alloys Compd 330–332(1):70–75
14. Kadir K, Sakai T, Uehara I (1997) Synthesis and structure determination of a new series of hydrogen storage alloys: RMg_2Ni_9 (R = La, Ce, Pr, Nd, Sm and Gd). J Alloys Compd 257:115–121
15. Koimo T, Yoshida H, Kawashima F, Inada T, Sakai T, Yamamota M, Kanda M (2000) Hydrogen storage properties of new ternary system alloys: La_5MgNi_9, $La_5Mg_2Ni_{23}$, La_3MgNi_{14}. J Alloys Compd 311:L5–L7
16. Chen J, Kuriyama N, Takashita HT, Tanada H, Sakai T, Haruta M (2000) Hydrogen storage alloys with $PuNi_3$ type structure as metal hydride electrodes. Electrochem Solid State Lett 3(6):249–252
17. Liao B, Lei YQ, Chen LX, Lu GL, Pan HG, Wang QD (2004) Effect of the La/Mg ratio on the structure and electrochemical properties of $La_XMg_{3-X}Ni_9$ (x = 1.6–2.2) hydrogen storage electrode alloys for nickel-metal hydride batteries. J Power Source 129:358–367
18. Chen J, Takashita HT, Tanaka H, Kuriyama N, Sakai T, Uehamra I, Haruta M (2004) Hydriding properties of $LaNi_3$ and $CaNi_3$ and their substitutes with $PuNi_3$–type structure. J Alloys Compd 302:304–313
19. Zhang F, Luo Y, Wang D, Yan R, Kang L, Chen J (2007) Structure and electrochemical properties of $La_{2-X}Mg_XNi_7$ (x = 0.3–0.6) hydrogen storage alloys. J Alloys Compd 439(1–2):181–189
20. Matysina ZA, Chumak VA (2001) Deformational hysteresis and elastic compliance of crystals with H4 structure near Curie point. Ukr Fiz Zhurn 46(9):957–959
21. Matysina ZA, Zaginaichenko SY, Schur DV (2005) Orders of different type in crystals and phase transformations in carbon materials. Nauka i obrazovanie, Dnepropetrovsk, p 524 (in Russian)

Chapter 20
Polyether Urethane Nanocomposition as a Multi-functional Nanostructured Polymeric Coating for the Future

N.F. Javadov, T.I. Nazimov, E.G. Ismailov, Dmitry V. Schur, Svetlana Yu. Zaginaichenko, A.P. Pomytkin, R.S. Aliev, R.S. Suleimanov, T. Nejat Veziroğlu, and Ayfer Veziroğlu

Abstract Modern science and technology level requires availability of polymeric insulating materials which would have not only high strength, but also the features like adhesion, tensile, impact and erosion resistance. The elaboration of the technology of production of new erosion resistant coating as new generation of materials with high hydrophobic properties is the achieved goal of the presented investigations. This problem has been solved by the development of new primary polyester on the basis of which the polyether urethane composite material containing ferromagnetic nanoparticles has been produced. The synthesis of ferromagnetic superparamagnetic nanoparticles fixed in polymeric matrix of ferromagnetic polymeric nanocomposite has been carried out in special reactor where composition of the polymeric nanocomposite has been controlled.

This nanostructured polymeric nanocomposite will be introduced into the oil production, oil processing (against paraffin and salt deposition processes), petroleum chemistry, aviation, instrument engineering, shipbuilding industry and other sectors. Particularly, application of this nanocomposite in paraffin containing oil production will start a new age in the prevention of paraffin, asphaltic-resinous

N.F. Javadov (✉) • T.I. Nazimov • E.G. Ismailov • R.S. Aliev • R.S. Suleimanov
Experimental-industrial plant of Institute for Petroleum Chemical Processes (IPCP) of NAS of Azerbaijan, Baku, Azerbaijan
e-mail: eip-ipcp@mail.ru

D.V. Schur • S.Yu. Zaginaichenko • A.P. Pomytkin
Institute for Problems of Materials Science of NAS of Ukraine, 3 Krzhyzhanovsky str., Kiev 03142, Ukraine
e-mail: shurzag@ipms.kiev.ua; shurzag@materials.kiev.ua

T.N. Veziroğlu • A. Veziroğlu
International Association for Hydrogen Energy, 5794 SW 40 St. #303, Miami, FL 33155, USA

A. Veziroğlu and M. Tsitskishvili (eds.), *Black Sea Energy Resource Development and Hydrogen Energy Problems*, NATO Science for Peace and Security Series C: Environmental Security, DOI 10.1007/978-94-007-6152-0_20,

components deposits on the inner surface of pipes and also hydrogen sulphide corrosion of pipe material that is a real disaster for oilmen.

It has been proved experimentally that magnetic field was induced in NCT, which accelerate and give special direction of moving for salts ions and paraffin nuclei crystallization centers with the use of polymeric nanocomposite. It has been expected that net cost of the developed polymeric nanocomposite will be 25–30 % lower compare with it for polyether urethane varnish.

Keywords Polyether urethane coating • Polymer nanocomposite • Ferromagnetic nanoparticles • Extraction of oil • Reactor • Varnish

20.1 Introduction

In the recent years, nanoparticles and nanostructures attract much attention of researchers by their unique properties and potential application fields including the new types of very active and selective catalysts, chemical and biological sensors, components of medicines, high-density data mediums, magnetic and optoelectronic devices, etc. [1–3]. Many of unusual properties of nanoparticles depend on their high surface area-volume ratio. The ability to control the value of nanoparticle surface and its chemical composition makes it possible to control properties, and functional peculiarities of materials based on these particles [4–5]. The manufacture of polymeric nanocomposites, making them multifunctional and of special purpose is very essential [6–7]. That's why the problem facing us is to produce the polymer containing nanostructured magnetic material with the regulation of the size and concentration of its particles using electromagnetic resonance in 'insimo' mode.

The nanostructured polymers have unique chemical, physical, biological, mechanical, catalytic, optical and magnetic properties which make possible to apply them in the oil production, oil processing, oil products transportation, informatics, instruments engineering, aviation, military equipment, catalysis, for sensors production, in medicine, biology, etc.

As it has been known, the most serious problems which oilmen encounter are paraffin and salt deposits on the inner surface of pipes, as well as hydrogen sulphide corrosion of pipelines undergoing in a short time. About 35–40 % of oil produced in the world, especially offshore, is paraffin-based and hydrogen sulphide-contained.

The similar situation is typical for the Azerbaijani oils (except for hydrogen sulphide). About the half of all offshore oil wells produce the high-paraffin crude oil, and oil refineries often process the Kazakstani oil which contains 5–7 % hydrogen sulphide.

Therefore, it was necessary to create the multifunctional coating which could be also successfully applied against the paraffin deposits and hydrogen sulphide corrosion.

20.2 Experimental

The goal of our experimental works was to develop the polyether urethane varnish, a new generation of urethane materials. Such varnish has about 40 chemical, mechanical, biological and electrical indices. The positive results were achieved when using the polyether urethane coatings in the paraffin-based oil production.

It is a matter of general experience that deposition of macromolecular paraffins on the inner surface of metallic pipes causes pipe blockage which impedes transportation of hydrocarbon crude inside pipeline. The various methods should be taken for the prevention of paraffin deposits:

- Chemical methods including those using the surface-active agents which promote hydrophilization process of pipe walls and increase in the number of paraffin nuclei crystallization centers in the flow;
- Thermal methods (the pipe is washed with various heat carriers, oil, hot water and steam and is heated by continuous or high-frequency current);
- Magnetic sockets (increase the number of paraffin nuclei crystallization centers in the flow);
- Application of glass enamel polymeric coatings to the inner surface of pipes; and
- Insertion of glass pipes into metallic pipes to the places where paraffin deposition occurs.

Along with the positive effect of the abovementioned methods of paraffin deposit prevention there are also certain negative consequences, for example, the toxicity of chemical agents, problems in delivery and storage, as well as the segregation in the process of refinement and during the oil processing.

Furthermore, the special equipment for pumping chemical agents into the well and physical electrical field generation are required, as well as the maintenance of this equipment. It should be noted that special technology of plating under heating the pipe up to 850 °C is required, when applying glass enamel coating process for the provision of strong adhesion. On the other hand, mechanical admixtures contained in hydrocarbons break the coating structure and reduce the time of these coatings service. At the same time the polymeric coating that would protect both inner and outer surfaces of metallic pipes against hydrogen sulphide corrosion and other aggressive corrosive substances should be developed.

Thus, our challenge is to solve the abovementioned problems by an easier way and with high economic results.

Let us consider the process of transportation and the appropriate structural formula of hydrocarbon molecules in order to find the causes of paraffin deposition process:

$$CH_3\left(CH_2\text{-}CHR\text{-}CH_2\text{-}CH_2R^1\right)n\text{-}CH_3, \tag{20.1}$$

where n = 4-12, R-R^1 are different alkyl radicals in a size not exceeding the size of the main chain.

Two special features of hydrocarbon molecules specified in the formula above should be mentioned, in order to explain the process of macromolecular paraffins deposition during the transportation:

- Positive electric field of nuclei protons of hydrogen atoms bound with carbon atoms; and
- Non-polarity of hydrocarbon molecules.

As it has been known, presence of the large number of free electrons in the crystalline lattice of the pipeline metal generates the negative electric field with static potential. The mutual attraction of fields of opposite polarity creates the favourable conditions for deposition of macromolecular paraffin on the surface of pipeline walls. One of the ways for weakening or elimination of this beneficial influence is the electrical insulation of the inner surface of metallic pipes preventing contact with transported hydrocarbons.

Hence, on the one hand, the insulation material must have high adhesion with the inner surface of metallic pipes, and on the other hand, it must have good electro-insulating properties.

Let us consider the structure of polyether urethane which is the typical effective material of such type:

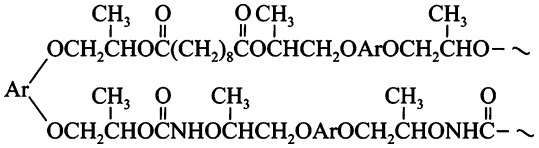

(20.2)

where:

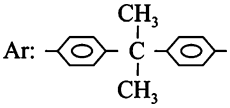

As it's obvious from the formula (20.2), there are also simple ether (-O-), complex ether (-C-O-), as well as urethane-like polar groups

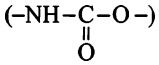

in the macromolecule of polyether urethane along with another groups.

As it has been already mentioned above, hydrocarbons denoted by formula (20.1) consist only of non-polar groups.

20.3 Results and Discussion

Results of the tests conducted in the laboratory conditions show that paraffin doesn't deposit on the walls of pipelines with the inner surface coated with polyether urethane, because of contact between the flow and the pipe surface is

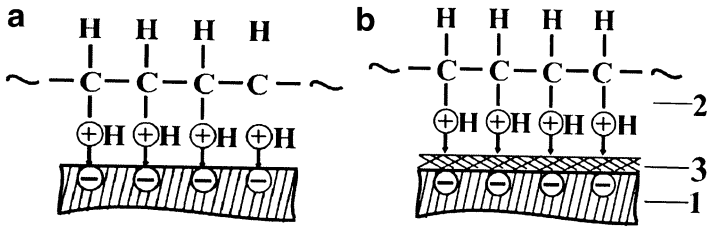

Fig. 20.1 The mutual state of protons of hydrogen atoms in paraffin molecule with free electrons on the inner surface of metallic pipes: (**a**) without coating; (**b**) with polyether urethane coating. *1* a part of metallic pipe surface; *2* paraffin molecules; *3* polyether urethane coating

prevented. Thus, in spite of the fact that the polar groups exist in polyether urethane the paraffin deposition does not occur. This can be explained also by the weak electric field intensity of polar groups.

Figure 20.1 illustrates the scheme of mutual attraction between the protons of the hydrogen atoms in paraffin molecule and free electrons of the pipe metal without coating and with the plated coating.

Table 20.1 contains key physical, mechanical and chemical properties of polyether urethane coating.

One of the main components for fabrication of polymeric nanocomposite structured by magnetic material is ferromagnetic nanoparticles. We have found an appropriate deposit of siderite for generation of ferromagnetic nanoparticles. Siderite supplied from this deposit has been exposed to grinding, burning at the temperature of 800–1,200 °C, milling at the bead mill and reducing down to nanosize particles at the planetary mill. At present, we have organized fabrication of polyether urethane varnish, being a new generation of urethane, and it has been tested in many spheres of science and industry and high results have been achieved.

One of the main directions of the polyether urethane varnish (PU varnish) implementation in oil production is prevention of paraffin deposits. The 433rd offshore paraffin well of the oil-and-gas production department named by N. Narimanov has been selected for the purpose of real testing of PU coating under the contract concluded with Azneft Production Association. In the experimental installation, the polyether urethane coating has been plated to the inner surface of metallic pipes of overall length 1,500 m. On 21 October 2008, these pipes have been sunk into the aforesaid well. As a result, this well was operated till 18 August 2010 without interruption. The key performance indicators before and after application of PU coating are given in Table 20.2.

Taking into account the high economic effectiveness of this method the PU coating has been plated to the inner surface of metallic pipes of total length 14.800 m to the order of Azneft Production Association. Today industrial tests are in progress.

Table 20.1 Main physical, mechanical and chemical indexes for polyether urethane coating

NN	Indexes	Unit of measurement	Value
1.	Density at 20 °C	g/cm^3	0.95
2.	Relative viscosity (VZ-4) at 25 °C	sec.	45–50
3.	Drying time at 20 °C to degree III	hour	6.0
4.	Ignition temperature	°C	370
5.	Working temperature range	°C	−50 ÷ +350
6.	Dielectric permittivity	o/m	1.0–1.5
7.	Adhesion	scores	1.0
8.	Impact resistance	kg/cm^2	50
9.	Chemical resistance in 20 % solution of sulphuric acid in sea water	visually	Indissoluble
10.	Mineral oil resistance	visually	Stable
11.	Hydrocarbons resistance	visually	Stable
12.	Spading resistance	kg/cm^2	17.0
13.	Acoustic speed	m/s	2,000
14.	Specific resistance	o · m	$10^{18} \div 10^{20}$
15.	Pendulum hardness		0.6–0.7
16.	Elasticity	mm	1.0
17.	Gloss	%	80
18.	Stretching resistance	MPa	8
19.	Moisture adsorption	%	0.07
20.	Biological resistance to microorganism impact (according to 6-score system)	score	0
21.	Colour	visually	Light yellow
22.	Volumetric compression at hardening	%	0.05
23.	Usage time after blending with hardener	hour	6
24.	Volumetric compression at hardening	%	0.05
25.	Water solubility	g/m^3	Indissoluble
26.	Guaranteed storage life	month	12

Table 20.2 The basic operational indicators of the well before and after application of polyether urethane coating

No.	Testing time	Performance indicators			
		Well hot treatment (basic well servicing)	Well shut-off for major overhaul	pressure (atm)	Flow rate (t/day)
1.	Till 21.10.2008	In 20 days	In 72–73 days	52–54	9–10
2.	From 21.10.2008 to 18.08.2010	In 42 days	Not interruption	52–54	11–12

20.4 Conclusions

The development of new erosion-resistant polymeric coating is demonstrated in this work. The introduction of such coating in the gas- and -oil producing industry will provide the non-stop operation of wells without major overhaul at least 3–5 years and the wells' hot treatment will be performed within a 50–60 days, instead of 20 days as previously mentioned.

For this purpose, the production technology of polymeric nanocomposite on the basis of polyether urethane varnish and ferromagnetic nanoparticles has been developed.

The synthesis of ferromagnetic superparamagnetic nanoparticles immobilized in a polymer matrix of ferromagnetic polymeric nanocomposite has been carried out in a special reactor with control of the composite composition.

The use of produced polymeric nanocomposite has been provided against paraffin-scaling during the oil extraction and transportation.

Consequently, the introduction of polymeric nanocomposite will provide the following advantages over the polyether urethane coating:

- The cost of polymeric nanocomposite will be lower by 25–30 % (by adding 30 % of magnetic materials) as compared with PU varnish; and
- Experimentally it has been confirmed that the use of polymeric nanocomposite creates a magnetic field that accelerates and gives a special direction to molecules of salts and centers of paraffin deposits.

Acknowledgments This work was supported by the Science Development Foundation under the President of Azerbaijan – Grant № EİF – 2011-1(3)-82/11/1.

References

1. Shashkov AE, Zhdanok SA, Sointsev AP, Buyakov IF, Krauklis AV, Zhukov IA (2005) Carbon nanomaterials production in the electric discharge and their utilization in the polymer composites. In: Symposium H – EMRS 2005 Spring meeting, Strasbourg, France, 31 May – 3 June 2005
2. Pesetsky SS, Zhdanok SA, Krivoguz YuM, Yurkovsky B, Ivanchev SS, Byakov IF, Levitsky IA, Krauklis AV (2005) Peculiarities of the structure and properties of polymeric nanocomposites produced by dispersion of thermoplastic materials. In: Abstracts of international conference "Polymer composites and tribology", Gomel, Belarus, 19–21 July 2005, p 45
3. Zhdanok SA, Buyakov IF, Krauklis AV, Solntsev AP, Zhukova IA (2004) Polymeric composites including carbon nanomaterials. In: Nonequilibrium processes in combustion and plasma based technologies, Minsk, Belarus, 21–26 Aug 2004, pp 210–214
4. Solntsev AP, Valozhyn AI, Zhdanok SA, Buyakov IF, Krauklis AV, Shashkov AE, Zhukova IA (2005) Synthesis of carbon nanomaterials and their utilization for polymer nanokomposites. In: Proceedings of the 7th European technical symposium on polyimides and high performance functional polymers, Monpellier, France, 9–11 May 2005, p 182

5. Shamray YV, Gusev VI, Pokrovsky VA et al (1987) Prevention of deposit of paraffin and asphalt-resinous substances in oil production in the fields with different geological and physical condifions. VNIIOENG, Moscow, 58 p
6. Galonsky PP (1955) Paraffin control in oil production: theory and practice. Gostoptehizdat, Moscow, 148 p
7. Pashayev AM, Mehtiev AS, Aliev PS, Nizamov TI, Mammadov MA, Javadov NF, Isaev EI, Guluzade PK. Sealing compound. Patent ARI 2006 0022

Chapter 21
On the 80-th Brainstorming for Complex Research of Black Sea Ecosystem (The Restoration of the Black Sea Ecosystem: Necessary But Not Sufficient Conditions for Harmonic Existence of the Region)

Strachimir Chterev Mavrodiev and Marat Tsitskishvili

Abstract This chapter describes the efforts of an international scientific group, which worked in the 80-th with aim to explore, quantify and predict the ecosystem variability of the Black Sea on the basis of complex research. We tried to apply the lessons of Nuclear winter model in practice for creating and development of the models which would allow: the descriptions of the past states of the sea, displaying trends and changes, as well the prediction of the future states of the sea.

In fact, we created the first NGO, where participating scientists from Bulgarian, Georgian, Russian and Ukrainian Academy of Sciences Institutes, Hydrographic Services of Bulgaria, Black Sea Soviet Navy, GosGidroMet and other organizations, connected with the Environment and Fishing economy.

Keywords Black Sea's ecosystem dynamics • Pollution distribution • Calculating of self-cleaning capacity • Application of the new knowledge in the practice

21.1 Introduction

We present the list of participants of our group "Clean and Peaceful Black Sea" for the period of 1986–1991: The list of the editorial staff of different levels of reports and books: S.G. Boguslavsky, V. Velev, G. Gergov, S.A. Efremov, A.P. Zhilyaev, I.K. Ivanchenko (Secretary), V.P. Keondjyan (Editor-in-Chief), R.D. Kosyan, A.M. Kudin (Vice-Editor), S. Cht. Mavrodiev (Coordinator), V.I. Mikhailov. M. Ovsienko, I.M. Ovchinnikov, A.G. Pavlova, A.I. Simonov, YU.I. Skurlatov,

S.C. Mavrodiev (✉)
Institute for Nuclear Research and Nuclear Energy, Bulgarian Academy of Sciences, Bul. Tsarigradsko shose 72, 1784 Sofia, Bulgaria
e-mail: schtmavr@yahoo.com

M. Tsitskishvili
Georgian Academy of Ecological Science, Tbilisi, Georgia

A. Veziroğlu and M. Tsitskishvili (eds.), *Black Sea Energy Resource Development and Hydrogen Energy Problems*, NATO Science for Peace and Security Series C: Environmental Security, DOI 10.1007/978-94-007-6152-0_21,

Yu.V. Terehin (Vice-Editor), M.V. Flint, M.S. Tsitskishvili. The list of authors: E.N. Altman, Ph.D., A.A. Bezborodov, Ph.D., YU.I. Bogatova, D.Sc., S.G. Boguslavsky, D.Sc., A.M. Bronfman, D.Sc., Z.P. Burlakova, Ph.D., B.S. Veleva, Ph.D. V. Velev, Ph.D., M.E. Vinogradov, Corresponding member RAS, D.Sc., L. A. Vinogradova, Ph.D., L.V. Vorobyova, Ph.D., G.P. Garkavaya, Ph.D., G. Gergov, Ph.D., I.F. Ertman, Ph.D., Z.A. Golubeva, G.A. Grishin, Ph.D., M.B. Gulin, S.B. Gulin, A. Damyanova, Ph.D., YU.M. Denga, SH.V. Djaoshvili, D.Sc., S.A. Dozenko, V.N. Egorov, D.Sc., V.A. Emelyanov, Ph.D., V.N. Eremeev, D.Sc., L.V. Eremeeva, Ph.D., S.A. Efremov, Ph.D., N.V. Zherko, Ph.D., A.P. Zilyaev, Ph.D., V.A. Zhorov, Ph.D., YU.P. Zaitsev, Corresponding member Ph.D., O.I. Zilberstein, Ph.D., I.K. Ivanshtenko, Ph.D., M.I. Kabanov, Ph.D., V.I. Kalatsky, D.Sc., S Karapeev, V.S. Karpov, Ph.D., T.G. Kasich, V.P. Keondjyan, D.Sc., A.G. Kiknadze, D.Sc., R.D. Kosyan, Ph.D., V.G. Krivosheya, Ph.D., A.M. Kudin, Ph.D., V.S. Kuzhinovski, I.I. Kulakova, Yu.D. Kulev, N.V. Kucheruk, Ph.D., G.E. Lazorenko, Ph.D., S.P. Levikov, Ph.D., O.I. Leonenko, S. Cht. Mavrodiev, Ph.D., O.V. Maksimova, V.I. Medinets, Ph. D., L. Minev, Ph.D., V.I. Mihailov, Ph.D., I.N. Mitskevich, Ph.D., A.I. Nesterov, D. Sc., D.A. Nesterova, Ph.D., L.E. Nizhegorodova, Ph.D., G.G. Nikolaeva, Ph.D., S.N. Ovsienko, Ph.D., I.M. Ovchinnikov, D.Sc., I.G. Orlova, Ph.D., G.G. Polikarpov, Acad.D.Sc., L.N. Polishchuk, Ph.D., V. Popov, R. Rusev, N.I. Ryasintseva, Ph.D., P.T. Savin, Ph.D., A.F. Sazhin, Ph.D., Prof. V.V. Sapozhnikov, A.I. Simonov, D.Sc., I.A. Sinegub, Yu.I. Skurlatov, D.Sc., L.A. Stefantsev, Ph.D., I.N. Suhanova, Ph.D., V. I. Sychev, Ph.D., N.N. Tereshchenko, Ph.D., YU.V. Terehin, Ph.D., V.I. Timoshchuk, Ph.D., V.B. Titov, Ph.D., A. Tomov, A.P. Filipov, M.V. Flint, Ph.D., E.P. Hlebnikov, Ph.D., M.S. Tsitskishvili, Ph.D., V.G. Tsytsugina, T.V. Chudinovskih, Ph.D., E.V. Shtamm, Ph.D., E.A. Shushkina, Ph.D.

Some of them are not between us. So, let us remember their big work for a big aim to have a Clean and Peaceful Black Sea. However, some are still alive and continue their efforts (Figs. 21.1 and 21.2).

21.1.1 Motives

Present civilization faces a serious choice. Nuclear winter is not the only way to self-destruction. The other one is the uncontrolled and non-scientific usage of the planet's resources in the name of "progress". The rates and technologies of development of energetic, industry (especially chemical industry), agriculture and transport in the last 15 years, bringing bad quality of air and drinking water for the next several decades. The warming up of the planet will wash away the lines of seasons.

History teaches that the achievements of science, sometimes find inhuman application. Let us only remind the Nobel invention, the tragedy of Hiroshima and Nagasaki. The power of today's technique is already comparable to the natural processes of our planet. For this reason, the scientifically groundless interference or impact on the processes of nature in later years lead to unforeseen, and as a rule fatal effects of global warming, ozon hole, etc.

Fig. 21.1 The participants of Pomorie, June 1990 seminar, where the book "Applied Ecology of the Sea Regions- Black Sea", 252 pp, Naukova Dumka, Kiev, August,[4] was created

Fig. 21.2 Marat S. Tsitskishvili, participant of Pomorie, June 1990 seminar, now President of the Georgian Academy of Ecological Science

To continue the existence of our civilization, we should learn how to approach nature and exploit its resources on scientific grounds, along with the new attitude in the interstate relations. We should learn how to coordinate the rates and quality of material progress, with the possibilities of the planet. This is an exceptionally difficult scientific task, as almost recently it became possible for ecology and environment science to look for and find solutions with quantitative evaluations on the movement of different elements in nature, the connection among different communities, different geographic regions, forecasting and management of energy and resource industry, due to the impressive development of mathematics, physics, biology and powerful computerization of science.

At the beginning of the 1900s, the Russian Scientist and Academician V.I. Vernadsky foresaw the contemporary ethical, ecological, energy and resource problems of our civilization. He outlined their solution in a qualitative way on the basis of a joint study of biosphere and the discovery that mankind turns into a geological power. However, the knowledge of nature law by scientists still does not mean it is correct in usage and application.

21.1.2 Why Black Sea?

As it is known, the Black Sea is a closed sea. It is a water gathering basin of East and Middle Europe – a region with well developed energy, industry, agriculture, transport and tourism. In the end, all wastes from human activities fall into it. Of course, a part of the substances disintegrate on their way to the sea. After 1970, their volume increased to such an extent that the impact on the Black Sea ecosystems began to be noticed considerably. Also, we cannot forget the undercurrent from the Sea of Marmara through Bosporus, and the rainfalls driven by the Atlantic cyclones and the northeasterly wind that contribute to the pollution. The ecological breakdowns in the northwestern part of the sea, periodic blossoming of plankton, change in quality and quantity of fish catch, decrease of water transparency and appearance of a new settler Mnemiopsis leidyi, all that illustrates qualitatively this fatal influence on the Black Sea's ecosystems.

The quantitative estimation of these phenomena, their interconnection and components of pollution, is an enormous field of interest for mathematicians, physicists, chemists, biologists and engineers of fundamental and applied research.

21.2 The Methodology

The stages of research included:

1. Creation of a data bank containing a huge volume of information about the sea, and its ecosystems collected up to now and periodically enriched.

2. A system for physical, chemical and biological monitoring.
3. Creation of a complex model of Black Sea ecosystems by recording their hierarchy, and thus reliably describing the sea phenomena, as well as their prediction.
4. It is obvious that the ultimate goal may be formulated on such basis only, to "rule" scientifically the Black Sea ecosystem on terms of agreement among the interested countries.

There were scientists who called this a pessimistic prediction for the inevitable ecological breakdown of Black Sea "ecological hysterics". Others believed that the self-cleaning capacity of the sea will develop, and the ecosystems will take in the increasing pollution without much difficulty, and at the same time the quality of the water and air will remain acceptable for people. We know how to KNOW and NOT TO BELIEVE!

All Black Sea countries possess rather powerful science institutions and possibilities for sea investigations. However, all these costly efforts will remain, until now, almost inapplicable and meaningless without functional coordination and a joint unified system for collection and processing of data, information about the results from investigations and predictions given to every citizen of the Black Sea region, control in the measures of the sea's protection and publicity.

It is natural for the citizens of Black Sea towns and other sea users to be most interested in its cleanliness and take good care! There is a saying: "Help yourself alone, so that God will help you". Shortly, mankind is already capable of science-based foreseeing, and ruling its future sustainable development (Harmonic existence) on the basis of complex environmental science, with real time monitoring in the framework of information technologies.

21.2.1 Steps

- Nikolay Ivanovich Vernadsky, from the beginning of the twentieth century: "the contemporary civilization has turned into a geological power";
- The "nuclear winter" model was the first precedent in the history of our civilization, when world leaders used rationally the science achievements, and agreed about the beginning of the nuclear disarmament and the destruction of the chemical, biological and other weapons.

21.2.2 Some Facts from the Black Sea Ecosystem, Burgas Bay

As a result of creating the historical and contemporary data base on the basis of eight special expeditions, satellite data, etc., we arrived to a new knowledge for the Black Sea ecosystem.

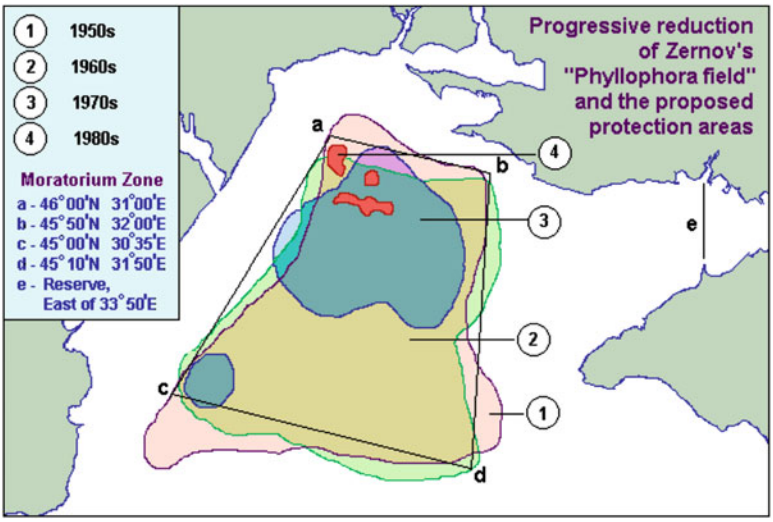

Fig. 21.3 Phyllophora represents a keystone species for the entire NW shelf ecosystem. The proposed protection areas are those referred to: Biolological Diversity in the Black Sea, BSEP Series Vol. 3 (From http://www.grid.unep.ch/hsein/tda/index.htm, Black Sea Transboundary Diagnostic Analysis) (*see color plates*)

After the Santorin catastrophe (The Bible flood) some 6–8 thousand years before the Straits started to work and the heavy Mediterranean water begin to fill the basin, the balance ended about 2–4 thousand years ago. From this time until 1960, the biological diversity of the Black Sea was consistent, depending only on the climate variations.

The strengthened anthropogenic influence after 1960 exceeded the self-cleaning capacity, and the ecosystem parameters started to change:

- 1960–1970: Disappearing of the little eels – Conger and delicacy fish "galya".

Gaidropsarus Mediterranean (Burgas bay):

- 1970–1986: Periodically local increasing plankton blooms;
- 1986: The First everlasting blooms in the west and north- west shelf.
- 1988: The beginning of the Odessa bay slime (Zermov's Phyllophora Field).
- 1989–1995: Decreasing of the commercial fishing.
- 1996: The beginning of the Burgas bay slime process.
- 1997: The first toxic rainfall in Burgas region.
- 2004: First indication of disappearing of the benthos fish (Burgas bay) (Fig. 21.3)

The hydrogen sulphurous level is practically the same as in the twenties, but the width of the layer, where oxygen and hydrogen sulphurous are coexisting, has been increased. This indicates an increased production of oxygen and hydrogen sulphurous in the water column. During the period of 1970–1975, the sea level is raising at the rate of about 1.5 mm/year. This is a result from the general heating of the northern hemisphere, which is a consequence of the total anthropogenic air pollution.

The number and the mean duration of the sea storms, as well as the maximal wind velocities, are decreasing, which in fact reduces the sea self-restoring capacity. The reason is that the energy exchange is going to be not by air streams, but by a translation of all air volume, which explains well the climate exchange in the last 10–15 years.

The coastal shelf is turning into slime, which is already an ecological catastrophe for the region, because the aerobic life is changed with an anaerobic one.

In the surface micro-layer the concentration of pollutants is greater by a factor of 10–100 times. In the coastal regions these concentrations are many times greater than the corresponding ones in the open sea, proportional to the ecological responsibilities of the local pollution sources.

During the 4 years after the Chernobyl catastrophe, the background radioactivity of the seawater has increased by a factor varying from two to three times. Approximately it is the same picture (far from being complete) with respect to the isotopic content, and the concentration in different organs of hydrobionts. According to the latest data, the background radioactivity has been stabilized with respect to both isotopic content and intensity (with light increasing because of the river).

The more intensive investigations after Chernobyl incident and some preliminary results from the modeling of the average anthropogenic radioactivity distribution shows that during the period of 1980–1990, an increase has come by unidentified ways and at a rate exceeding several times the Chernobyl deposits. Concerning the use of artificial black mussels plantations as cleaning stations, it is very promising that the Chernobyl radioactivity was concentrated only in mussels shell, but not in the meat.

The results from the tracing of the radioactivity in the sea depth after the Chernobyl catastrophe gave some reasons to accept that the estimation for the interchange of the water layers in the sea bottom can be decreased in about 50 years.

Although the ecological perspective for the Black sea is darker than for Mediterranean, the tourist and health resort conditions on the Black sea coast are much better. The reason is the high bio-productivity of the Black sea, which leads to short periods for the plankton bloom.

21.2.3 Our 1991 Proposals for Solutions

We do not need "big science" to know what we have to do to stop this catastrophe:

- We have to stop the pollution of the Black Sea, and by catalytically imputes to increase its local and total self- cleaning potential;
- At the same time, the introducing the sea- cultures like artificial black mussels plantation, rapanes, etc., can help catalytically the restoration processes by utilization of the nutrients and by creating new fish's incubator regions.

The high science is needed for the solution of minimizing problems: where, when and how fast and cheap to build the purification installations. This is related to

the introduction of contemporary close-water, energy and resource technologies in industry, agriculture, transport and tourism.

To publish the estimates for the ecological responsibility of the various sources polluting the Black, Azov and Marmara seas and to work out recommendations for appropriate legislative, administrative, managing, economical, scientific and technological solutions.

21.2.3.1 Some Non Solved Science Problems

- The estimation of ecological responsibility for every pollution source.
- The estimation of water exchange of bays, shelf- open sea, vertical exchange.
- The ecological responsibility estimation of atmosphere- sea exchange.
- The local and total correlations between pollution, plankton, fish diversity and fish catchments.

21.2.3.2 Practical Logistic Aims

- Using as catalytically influence the artificial mussels and other plantations.
- Real lime Black Sea monitoring Internet data.
- More effective interaction between different activities: science, application, and control in the framework of sustainable development.
- Joint navy guards for protecting the ecological cleanliness of the Black Sea marine and air environment (first step fulfilled).
- The introduction of new ship traffic rules, compatible with the main Black Sea stream, average wind distributions, capacity and security of the Turkish straits. A new system, analogous to the air's one, for controlling and ruling of the traffic to be created and implemented in the Black Sea region, before the start of the tanker oils' traffic (Burgas Alexandropolis pipe and others), in order the ship and tanker captains to see the situation along his course in a real time via Internet (Fig. 21.4).
- The restoration of the Black sea towns and regions Alliance "Clean and Peaceful Black Sea", founded in Odessa, September 1990, in order to implement the science, technological, business, management recommendations and public control for sustainable existence of the region (Fig. 21.5).

21.2.3.3 The Optimism for Clean and Peaceful Black Sea Future

In the report, presented at the UN Environmental Conference in Rio de Janeiro in 1992 "Black Sea-condition, perspectives and possible solutions", we argued about the possibility for transforming the Black Sea region in a model polygon for science-based transition to democracy and market economy. At the same time

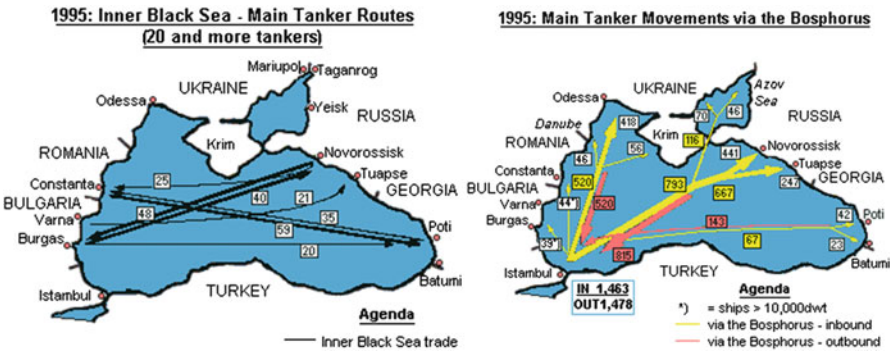

Fig. 21.4 The inner Black sea and main Tanker movements via the Strats (*see color plates*)

Fig. 21.5 The yacht "Chter", with which the author started to convince the Black Sea Mayors for the Alliance "Clean and peaceful Black Sea" (1984–1988)

measures for the protecting of Black Sea ecosystem from ecological catastrophe and restoration of its biological diversity had to be taken.

The optimism for Clean and Peaceful Black Sea future is based on the life logic, the Balkan- Black Sea- Caspian sea region realities and global economic and political development, which enforced objectively in life some of our recommendations:

- The Black Sea Economical Cooperation was created.
- Convention for the preservation and development of the Black Sea ecosystem was accepted.
- Parliamentary Assembly of the Black sea economic cooperation states was created

- Specialized Black Sea economic cooperation Bank was founded.
- The Black Sea Action Plan was accepted.
- A military agreement for the military aspects of the Black Sea ecology safely was signed by the Black Sea Economic Cooperation Countries.
- The new "Black Sea Ecosystem Recovery Program" is now in force.

21.3 Attempt for Formulation of the Necessary and Sufficient Conditions for Sustainable

All international documents, created and legislated with strait or with catalytically efforts of Black Sea Commission can be interpreted as first attempt for formulation of the necessary and sufficient conditions for Sustainable Development (Harmonic existence) of the Black Sea ecosystem:

- The Convention on the Protection of the Black Sea Against Pollution.
- Signed in Bucharest in April 1992, and ratified by all six legislative assemblies of the Black Sea countries-1994.
- The Black Sea Biodiversity and Landscape Conservation Protocol to the Convention on the Protection of the Black Sea against Pollution were signed in Sofia, Bulgaria, in 2003 and it is in force from 1994.
- Strategic Action Plan for the Rehabilitation and Protection of the Black Sea in 1996, and amended in 2002.
- Memorandum of Understanding between the International Commission for the Protection of the Black Sea (ICPBS) and the International Commission for the Protection of the Danube River (ICPDR) on common strategic goals – 1997.
- Memorandum of understanding between the Commission of the Black Sea against pollution and the European Environment Agency (EEA) – 2003.
- Memorandum of Cooperation between the Permanent Secretariat of the Agreement on Conservation of Cetaceans of the Black Sea, the Mediterranean Sea, and the contiguous Atlantic area and the Permanent Secretariat of the Commission for the Protection of the Black Sea Against Pollution concerning the Sub-regional Coordinating Unit for the Black Sea – 2002–2004.

21.3.1 Short Analysis of the Black Sea Scientific Programs 1990–2004

21.3.1.1 Black Sea Transboundary Diagnostic Analysis, 22 June 1996

The Black Sea: A Unique Environment, in Crisis, Need for International Action, A Strategy Development and the Black Sea Environmental Programme is Born, What has been Achieved? What will be done Next?, The Transboundary Diagnostic Analysis, Towards a Sustainable Future

21.3.1.2 NATO SfP Black Sea Project 1998–2002

Project title: Black Sea ecosystem processes and forecasting/operational database management system

The Project was established at the end of 1998 as a co-operation between major marine research institutions in six Black Sea countries, with the support of NATO Science for Peace Sub-Programme.

Major objectives of the Project: To explore, quantify and predict the ecosystem variability of the Black Sea through process studies and development of coupled interdisciplinary models with data assimilation schemes that will allow: prediction of the future states of the sea; descriptions of the present and the past states of the sea and displaying trends and changes.
To develop further the NATO Black Sea Data Base and Management System for management oriented operational marine forecasting and research, requiring transmission to a wide variety of users quality controlled data received from moored buoys, ships, drifting sensor arrays, fixed platforms and satellites, with stringent requirements in DBMS-to-USER transmission in delayed and/or near-real-time modes

Project Description: In relation to its marine ecosystems, the Black Sea deserves increased vigilance and effective environmental management. This is primarily due to the fact that of all the basins of the world ocean, the environmental degradation in the Black Sea is the most severe. Environmental problems of the Black Sea are intimately related to the unique characteristics of the marine environment. The Black Sea is nearly landlocked and the ventilation of the deep waters by lateral influxes is poor. In addition, a strong density stratification effectively inhibits vertical mixing. As a result, permanent anoxia exists within 87 % of the Black Seas volume, making the Black Sea the largest anoxic basin of the global ocean. Its surface area is five times smaller than its catchment basin, covering parts of the neighboring European and Asian continents where human activities impose environmental burdens on this basin. About 162 million people live in the catchment area of the Black Sea [13, 14]. The health and well-being of these people are affected by the environmental degradation in the Black Sea.

Adequate prediction of the environmental variability in the Black Sea is needed to identify, analyze and determine the costs of solutions for better management of the marine environment aimed for sustainable development of the Black Sea resources. Furthermore, the environmental management of the Black Sea and the related scientific and technological developments require an interdisciplinary and easily accessible Data Base Management System (DBMS) with user friendly interfaces for data reception, assembly, quality control, storage, continuous dissemination, and exchange (Fig. 21.6).

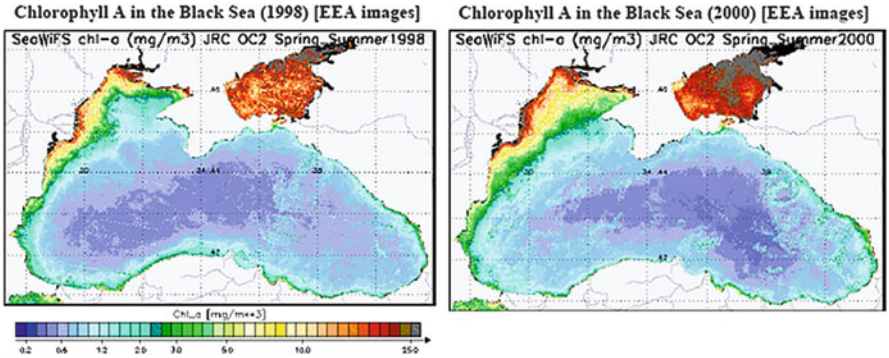

Fig. 21.6 Distribution of Chlorophyll A in 1998 and 2000 (From the Project report) (*see color plates*)

21.3.1.3 State of the Environment of the Black Sea (1996–2000), Commission on the Protection of the Black Sea Against Pollution

The ministers responsible for the protection of the environment of the contracting parties, to the conversion of the Protection of the Black Sea against pollution take note on the report on the environmental status of the Black Sea submitted by the Permanent Secretariat of the Black Sea Commission. Recognizing the fact that some positive trends in the state of the marine ecosystem has been observed during recent years, the Ministers nevertheless remain concern about the fate of this unique water body and call attention to the challenge of sustaining this process in the condition of expected economic recovery of the Black Sea region

The national and international efforts of the Black Sea coastal states shall be directed at two targets:

- Intermediate target: prevent the increase of pressure from human activities when transitional economies of the Black sea states begin to recover.
- Strategic target: to achieve environmental conditions in the Black sea similar to those observed in 1960s.

21.3.1.4 Implementation Proposals for the "Black Sea Ecosystem Recovery Project", Black Sea Commission and the International Commission for the Protection of the Danube River Basin

Project Short Title: Black Sea Ecosystem Recovery Project, Project number: RER/01/G33/A/1G/31, Project name Control and ruling of eutrophication, hazardous substances and related measures for rehabilitating the Black Sea ecosystem, including the using of artificial aquaculture (black mussels) plantations, rifts, islands (Tranche 2), Duration 3 years (July 2004–June 2007), Implementing agency UNDP, Executive agency UNOPS, Requesting countries: Bulgaria, Georgia, Romania, Russian Federation, Turkey and Ukraine, Specific objectives of the BSERP from May 2004–April

2007 are (i) to reinforce regional cooperation under the Black Sea Convention, (ii) to set up institutional and legal instruments and to define priority actions at regional and national levels to assure sustainable coastal zone management, and (iii) to protect of coastal and marine ecosystems and habitats in order to secure sustainable use of coastal and marine resources. To accomplish these objectives, the project will build up on the results achieved during Phase I (Jan 2002–April 2004).

21.4 The Project's Proposal Waiting Their Realization in the Practice with Support of European Commission, NATO, etc

21.4.1 Parallel Production of Black Mussel in Burgas and Egneada Bay

Purpose: The project approbates the possibilities of modern technologies for ecologically conformable and economically profitable combined production of electric power and meat in artificial plantations for black mussel, situated in the reef zone of Burgas bay northeast of the town Pomorie and Engeada bay.

Arguments: The artificial production of 1 kg black mussel means about 1.3 kg less food for plankton, which at bloom means about 1.8 kg less organic sediments production. In the region of the mussel plantation, for a short period of time are created the analogous conditions like in the phyllophora field of Zernov for birth and development of the traditional Black Sea's fishes.

Science: Restoration of the monitoring and estimation of the bloom control possibilities, and development of catalytically helped restoration of the fish species.

Finance: The year productivity is 30–60 kg mussels meat (more than 50 %) from 1 m line for depth 8–15 m.

Business: The 2 years returning of the plantation costs.

21.4.2 The Restoration of Pomorie's Salt Lake

To stabilize the medical utilization of the natural mud resources in the west part of the lake; To restore the systematic discharged salt production; To restore the ecosystem of Liza Salien's annual production (1,000–6,000 t); To restore its role as incubator for artificial newborn turbots, and To study the possibilities for artificial raising of Scomber scombrus, because of the lake salinity and temperature, which are similar to the Marmara Sea (the former born places).

21.4.3 The Implementation of the 1989 Real Time Working Program for Ruling the Oil Accident Consequences in the Local Regions (Ports), Tested for Burgas Bay and Kerch Strait

21.4.4 To Repeat the Black Sea 1989–1990 Film with a New Name "The Burgas Bay Ecosystem After 20 Years" in Order to Illustrate the Slime Process in the Bay

21.4.5 To Restore the NGO of Black Sea Towns and Regions "Clean and Peaceful Black Sea"

The aim of the NGO to support the better Municipality authorities participation for application of the measures, fulfilling the monitoring, getting the statistical data, ecological education of the population, higher person and plants pollution responsibility and control.

21.5 Conclusion

I am sure that if the proposed 1990 measures will be realized, after 10–15 years, like 40–50 years ago, one will catch 5 кг fish for half and hour, and 500 m far away from home at Bulgarian Sea coast.

References

1. Mavrodiev SC (1987) Patent, high speed sail system on the basis of shield effect. IIP, certificate no 1 21 9, Sofia, 16 March 1987
2. Keondjian VP, Kudin AM, Mavrodiev SC et al (1988) Clean and peaceful Black Sea, seminars: "Pomorie 1987", October 1987, "Pomorie 1988", October 1988, program group 435. INRNE, BAS, Sofia, October 1987
3. Mavrodiev SC et al (1989) Report- diagnosis for Burgas Bay condition with science, management and business recommendations, program group 435. INRNE, BAS, Sofia
4. Keondjian VP et al (1990) Applied ecology of the sea regions- Black Sea. Naukova Dumka, Kiev, 252 pp
5. Mavrodiev SC et al (1990) Dynamics and correlations of processes and interactions in Black Sea in real time, Program group 435. INRNE, BAS, Sofia, 450 pp
6. Mavrodiev SC et al (1991) Information Bulletin No 1 of the Black Sea towns and regions alliance "Clean and peaceful Black Sea", Odessa, Jan 1991
7. Mavrodiev SC, Rusev R et al (1991) Background characteristics of sea water in the Bulgarian part of the Black Sea, program group 435. INRNE, BAS, Sofia, 154 pp, July 1991

8. Mavrodiev SC et al (1996) Clean and peaceful Black Sea – applied ecology of the sea- 1990. ECOSEA-BS, Sofia, 105 pp
9. Mavrodiev SC (1998) Applied ecology of the Black Sea. Nova Science Publishers, Inc., Commack, 207 pp. ISBN 1-56072-613- X
10. Mavrodiev SC et al (1999) Black Sea: contemporary status, perspectives and possible solutions – the restoration of the Black Sea ecosystem, World Federation of Scientists, working group on water and pollution, workshop on monitoring Black Sea environmental conditions, Erice, 27 Feb – 4 Mar 1999
11. Mavrodiev SC et al (2002) The restoration of the Black Sea ecosystem. In: Second international conference on marine waste water discharges outfalls and sea lines technologies, Istanbul, Turkey, 16–20 Sept 2002. http://www.mwwd2004.com/Mwwd_Backgrnd_2002.html
12. Mavrodiev SC et al (2003) On the restoration of the Black Sea ecosystem, seminar talk, NATO, METU, IMS, Erdemly, Turkey, Feb 2003
13. Mee LD (1992) The Black Sea in Crisis: a need for concerted international action. Ambio 21:278–286
14. Özsoy E, Ünlüata Ü, Top Z (1993) The mediterranean water evolution, material transport by double diffusive intrusions, and interior mixing in the Black Sea. Prog Oceanogr 31:275–320

Chapter 22
On the FP7 BlackSeaHazNet Project and Its Possible Application for Harmonic Existence of the Regions

Strachimir Chterev Mavrodiev and Lazo Pekevski

Abstract This chapter describes briefly our long journey from the time of working for "Clean and peaceful Black Sea" in the 80-th to the FP7 support of the project "Complex research of Earthquake's Forecasting Possibilities, Seismicity and Climate Change Correlations". The participants are from Slovenia, Macedonia, Greece, Turkey, Bulgaria, Georgia and Armenia. The main aim of the project and the preliminary results were published in the Ohrid, Macedonia (ISBN 978-9989-631-04-7) and Tbilisi, Georgia (UDC 550.348.436 + 551.583.C-73, ISSN 2233–3681), also the proceedings are presented.

Keywords Earthquakes • Geoelectromagnetism • Radon • Geophysics • Sun-earth interaction • Complex interdisciplinary environmental research

22.1 Introduction

The full name of the project is FP7, Marie Curie Actions, People, International Research Staff Exchange Scheme, Scientific panel: Environment, Acronym: BlackSeaHazNet, No 246874, duration of 24 months starting in 2011 (Table 22.1).

S.C. Mavrodiev (✉)
Institute for Nuclear Research and Nuclear Energy, Bulgarian Academy of Sciences, Bul. Tzarigradsko shose 72, 1784 Sofia, Bulgaria
e-mail: schtmavr@yahoo.com

L. Pekevski
Seismological Observatory, Faculty of Natural Sciences and Mathematics, Sts. Cyril and Methodius University, Skopje, Macedonia
e-mail: lazopekevski@hahoo.com

A. Veziroğlu and M. Tsitskishvili (eds.), *Black Sea Energy Resource Development and Hydrogen Energy Problems*, NATO Science for Peace and Security Series C: Environmental Security, DOI 10.1007/978-94-007-6152-0_22,

Table 22.1 List of partner organisations

Partner number	Partner name	Partner short name	Country
1 *Beneficiary* 1	Institute for Nuclear Research and Nuclear Energy, Bulgarian Academy of Sciences	INRNE BAS	Bulgaria
2 *Beneficiary* 2	National Institute for Geophysics, Geodesy and Geography, Bulgarian Academy of Sciences	NIGGG BAS	Bulgaria
3 *Beneficiary* 3	Institute of Oceanography , Hellenic Center for Marine Research	HCMR	Greece
4 *Beneficiary* 4	Josef Stefan Institute	JSI	Slovenia
5 *Beneficiary* 5	Karts Research Institute, Znanstvenoraziskovalni Center Slovenske Akademije Znanosti in Umetnosti	SRC SASA SI	Slovenia
6 *Beneficiary* 6	Geologicheski Institut pri BAN St. Dimitrov	GI BAS	Bulgaria
7 *Beneficiary* 7	Space and Solar-Terrestrial Research Institute	SSTRI BAS	Bulgaria
8 *Beneficiary* 8	Ss. Cyril and Methodius University in Skopje	SORM UKIM	FYRO Macedonia
9 *Beneficiary* 9	Earth and Marine Sciences Institute, TUBITAK Marmara Research Center	TUBITAK MAM	Turkey
10 Partner 1	Western Survey for Seismic Protection SNCO, Ministry of Emergency Situations	WSSP	Armenia
11 Partner 3	Mikheil Nodia Institute of Geophysics, Ministry of Education and Science of Georgia	GI MES	Georgia
12 Partner 4	Ilia State University ILIAUNI	ISU	Georgia
13 Partner 5	Geophysics Institute named after S.I. Subbotin of the National Academy of Sciences in Ukraine	IG NASU	Ukraine
14 Partner 6	National Antarctic Scientific Center	NASC	Ukraine
15 Partner 7	Odessa National Polytechnic University	ONPU	Ukraine
16 Partner 8	Institute for Nuclear Research of NAS of Ukraine	INR NASU	Ukraine

22.2 Project Summary

22.2.1 Balkan, Black Sea, Caucasus, Caspian NETWORK for Complex Research of Earthquake's Forecasting Possibilities, Seismicity and Climate Change Correlations

The purpose of the project, BlackSeaHazNet, is a development of long-term research cooperation through coordinated joint program for exchange of data, know-how and scientists. The partnership in experimental and theoretical aspects

of geophysics will be focused on a creation of fundamentals of a Complex Program for investigation of the possibilities to forecast earthquake's time, hypocenter magnitude, and intensity using reliable precursors. For this aim, a monitoring of the following parameters is envisaged:

- geophysical and seismological variability over South-East Europe;
- water sources and their Radon, Helium, and other gases concentrations;
- crust temperature;
- electromagnetic field variations under, on and above Earth's surface;
- satellite monitoring of meteorological parameters, including earthquake clouds;
- electrical charge distributions and variations in ionospheric parameters.
- near-space monitoring, aimed to detect and exclude the external influences (i.e., those of Sun and Interplanetary medium variations, Cosmic rays) from the meaningful signal of the solid Earth.
- biological precursors.

For many variables, well working global and regional monitoring exists (for example INTERMAGNET monitoring). For others (for example: monitoring of Earth's currents distribution) monitoring have to be created.

The complex monitoring of the broad variety of parameters defines the output of the Program including: (i) estimations of different time scales for more clearer understanding of the Earth's system natural variability, (ii) risk assessment of the appearance of hazards for society events related to earthquakes, climatic changes, etc., and (iii) people's response to an abrupt change in the monitored parameters.

The proposed regional network can be considered as a first step in creation of a wide interdisciplinary scientific consortium capable of formulation of a more adequate paradigm of climate variability and climatic change (distinguishing the differences between them), Earth seismic processes and the actual problem of their forecast. If the hypothesis for Georeactors [15, 17–20] net, as possible reason for Climate change will be confirmed, the surprising new knowledge for Climate variations and its connection with Earth's seismicity can be obtained. Conformation of the hypothesis for existence of new type self-regulated nuclear reactors will enhance the physical understanding of different time scales of Climate – Climate and Climate – Weather transitions and Climate – Seismicity correlations.

The exchange of people, methods for data analysis, different approaches, models, etc., is expected to improve the current knowledge and to build up new concepts, models, etc. Results will be reported and discussed in the workshops and regional training seminars following the principle of brain-storming.

Establishment of such a multidisciplinary program is supported by every partner institutions affording an opportunity to use their own research resources.

22.2.2 Quality of the Exchange Programme

22.2.2.1 Objectives and Relevance of the Joint Exchange Program

The main measurable goals of BlackSeaHazNet programme are:

- To establish real-time closer collaboration between partners for every experimental, theoretical tasks.
- For easier real time exchange of results and for education of the wide public, including authorities, to develop the website Earthquake Forecast Using Reliable Earthquake Precursors (http://theo.inrne.bas.bg/~mavrodi/) to the website named Complex Research of Earthquake's Forecasting Possibilities, Seismicity and Climate Change Correlations, where the project BlackSeaHazNet will be presented task by task, the results of regional monitoring, scientific results, materials from workshops and training seminars;
- To formulate the theoretical need and technical description for new variables monitoring for the production experimental data, for successful work in step by step solutions, the problems from Complex Research of Regional Earthquake's Forecasting Possibilities, Seismicity and Climate Change Correlations and reasons for their variations;
- To summarise exiting regional real time and history data, to analyse their quality through inventory of their acquisition systems for preliminary archiving;
- To compare the existing methods for visualization and analysis of the data, estimation of the risk and forecast of earthquakes (if any), which may be utilized by all participants in the near future;
- To create a regional network for continuous monitoring of the earthquakes' precursors;
- To integrate and synthesise the existing research results related to variations of seismic activity and climatic system on different time scales – for better estimation and predictions of forecasting their future changes;
- To promote the joint research activities on regional and European levels, involving Europe's near neighbour countries into the ad hoc research activities;
- To transfer the "pure scientific" results into a knowledge for the society, facilitating the two-way communication processes with policy and general public for better understanding of the natural hazard risks, and more effective mitigation of its influence on people's life and environment;
- To establish financial support for the realizing of the wide interdisciplinary experimental and theoretical work for solving the imminent when, where and how earthquake's forecast as well as the derived results for different time scale estimations for some natural hazards and risk assessment, and the correlations between human behaviour and electromagnetic, and other geophysical variables variations in the different variants of the real working Complex Research of Regional Earthquake's Forecasting, Seismicity and Climate Change variations.

22.2.2.2 Complementary/Synergies Between Partners

The degree of integration, which BlackSeaHazNet program aims to expand and deeper based on long lasting traditional bi- and multi-lateral collaborations among many of the partners.

A great part of participants are involved in the Balkan-South-Caucasian network for continuous monitoring of solar and geophysical parameters. Moreover, bi-lateral agreements exist between most of countries attending the BlackSeaHazNet program. The national support, provided over the years to the partners, is a proof of interest of their national funding organisations for international cooperative efforts to understand and predict the risk of natural hazardous events. Thus funding of this project, by IRSES scheme of FP7 framework program, will strengthen the existing networks trough provision of new activities, which foster the further integration of the South-East European community. Two types of activities are planned during the duration of the Program:

22.2.2.3 Integrating Activities

International Multi-disciplinary Coordination and Collaboration

The main benefits from this multi-disciplinary networking include: improved efficiency and cost-effectiveness of scientific research, expand the boundaries of existing research for building up a *new cutting-edge knowledge;* the possibility to find a solution of unresolved till now problems due to the limitations of the existing theories, models, etc., as well as enhance the possibility to influence the public policies affecting thus far the quality of life.

Access to Information and Research Infrastructure

All project participants will have the possibility to exchange their own data or to use standardized databases to synchronize the used approaches, to share their research infrastructure, etc. The synergy of research programs between EU countries and near neighbour countries allowing a diffuse of information and different databases may be extremely beneficial for solving such complicated problems.

BlackSeaHazNet Web-Page

BlackSeaHazNet web-page will maintain communications between participants, providing a tribune for exchange of ideas, data, results, as well as including the step by step real time common monitoring data.

Joint Research Activities

Reevaluation of the existing models of Earth's crust conditions, Earth and atmosphere variables, solar and space influences, in order to better understand the physics of Earthquakes; systematization of the earthquake parameters (magnitude, seismic moment, intensity, depth, size of volume and surface fault), and earthquake occurrence by applying different statistical methods, including non-linear and inverse problem methods;

Statistical analysis of empirically determined relations between different geophysical parameters through non-linear inverse problem methods, including special studies of aftershocks activity;

Analysis of the factors influencing climate variability aimed to answer the question: Is the currently observed global warming a manifestation of natural climate fluctuations or it is an indication of an increasing instability of the contemporary climate due to the increased anthropogenic forcing; and investigation of possible relations between climatic variations and seismic activity;

The strong integration within the BlackSeaHazNet program is also demonstrated trough interlinking and interdependence of all tasks and activities of the network. The horizontal link between partners aims to integrate the existing knowledge about the processes governing variations of solid Earth parameters, in order to build a physical model of earthquakes. Most partners are involved in multiple working packages within the project, which favour their effective integration within BlackSeaHazNet program. Most tasks of BlackSeaHazNet project have by their own nature, meaning of integration between the participants illustrated by the common use of data bases, sharing of facilities, exchange of researchers, etc. The organisation of a series of five workshops is aimed to mobilize the interdisciplinary skills and the expertise of the project participants for gathering the optimal conditions for solution of the problems, including complex programming.

BlackSeaHazNet network will make an extensive use of Internet-based techniques to foster communication within scientific community and to implement all BlackSeaHazNet activities. In this context the BlackSeaHazNet web-page (based on http://stardust.inrne.bas.bg/mavrodi/) devoted on complex research of earthquake's forecasting possibilities, seismicity and climate change relations can be considered as the overall integrating toll of the Network.

22.2.2.4 Transfer of Knowledge

Quality and Mutual Benefit of the Transfer of Knowledge

Knowledge Transfer is the two-way flow of ideas, expertise and people between the research base and wide users in society. A special stress is put on the exchange of

knowledge in the BlackSeaHazNet program – demonstrated by the definition of a special work-package devoted on this issue.

One of the main benefits of BlackSeaHazNet realization will increase cohesion between scientists in different branches of geophysics, nuclear physics, etc. It will provide an opportunity for them to develop new skills and collaborations, to capitalise on their research knowledge and findings beyond their narrow areas of high quality expertise.

An interactive transfer of data, ideas, specific approaches in data analysis and modelling between project participants and with international scientific communities – through a direct exchange of people, series of workshops, lectures and trainings for younger staff – is a good prerequisite for building of new knowledge. Jointly executed research has a potential to inspire the experienced scientist to develop strategies for knowledge transfer, as well as and to tailor them to potential users and society.

Adequacy and Role of Staff Exchange with Respect to the Transfer of Knowledge

Effective knowledge transfer strategies rely on the capacity of Universities and Academic institutions to shape their knowledge transfer approaches and activities, in partnership with their various communities, and to respond creatively to the distinctive needs of those communities. From this perspective, a "healthy" system of knowledge transfer should demonstrate considerable diversity in knowledge transfer approaches and activities, both *within and across institutions, and across disciplines and national research priorities*. In this context, the possibility for exchange of scientists within IRSES can be a great step forward in the difficulty of transferring knowledge between project participants. The exchange of ideas during the series of seminars will be extended logically to a two way flow of data, methods and approaches for data monitoring and analysis, for creation of new or improvement of the existed approaches stimulated by the multi-disciplinary brainstorming, for reassessment of the existed models with real possibilities for their improvement via comparison with experiment, and for ability to take advantage of scientific infrastructure of the host country.

As a final accord, it should be reminded that the "innovation does not necessarily require new technologies, existing technologies may be applied in new ways" resulting in a tremendous improvement of the existing or creation of qualitatively new knowledge (FP7, basic ideas).

The effective transfer of knowledge is guaranteed from the visits of exchange programs, attended from seminars and lectures on the topic of the visit, the Programs of workshops and by the fact, that materials will be published in the end of every Workshop, as well as in the Website and will be distributed between authorities.

22.3 History

22.3.1 Hypothesis

The hypothesis for possible correlations between the earthquakes, the magnetic fields, Earth's horizontal and vertical currents in the atmosphere, was born when in early 1988, the historical data on the Black Sea was systemized. The fire pillars, observed during the Crimean earthquake in 1928, could be explained with the dehydration of the biogas condensated at the time of the spread out of the earthquake's waves in the sediments, and the ignition, which follows in the presence of a high degree of ionization of the atmosphere. Such currents can be measured, for example through a precise measurement of the Earth's magnetic fields. A common model for the origin of the attendant Earth's currents before, during and after an earthquake does not exist.

22.3.2 One Projection of Geomagnetic Field Monitoring

In December 1989, a continuous measurement of a projection of the Earth's magnetic field (F) with a magnetometer (know-how of JINR, Dubna, Boris Vasiliev) with absolute precision less than 1 n-T at a sampling rate of 2.5 samples per second. The minute's mean value of F, its error mean value, the minute's standard deviation SDF, and its error were calculated, i.e., every 24 h, 1,440 quartets of data were recorded. Minute standard deviation of F is defined as:

$$SDF_m = (1/N_m) \sum_{i=1}^{N_m} (F_i + F_{mean})^2 \tag{22.1}$$

where

$$F_{mean} = (1/N_m) \sum_{i=1}^{N_m} F_{mean} \tag{22.2}$$

and N_m is the number of samples per minute

22.3.3 The Results: Geomagnetic Quake as Regional Precursor for Increasing Regional Seismicity

The connection between variations of local geomagnetic field and the earth currents was established in INRNE, BAS, Sofia, 2001 seminar [1]. The statistic of earthquakes that occurred in the region (1989–2001), confirmed the Tamrazyan

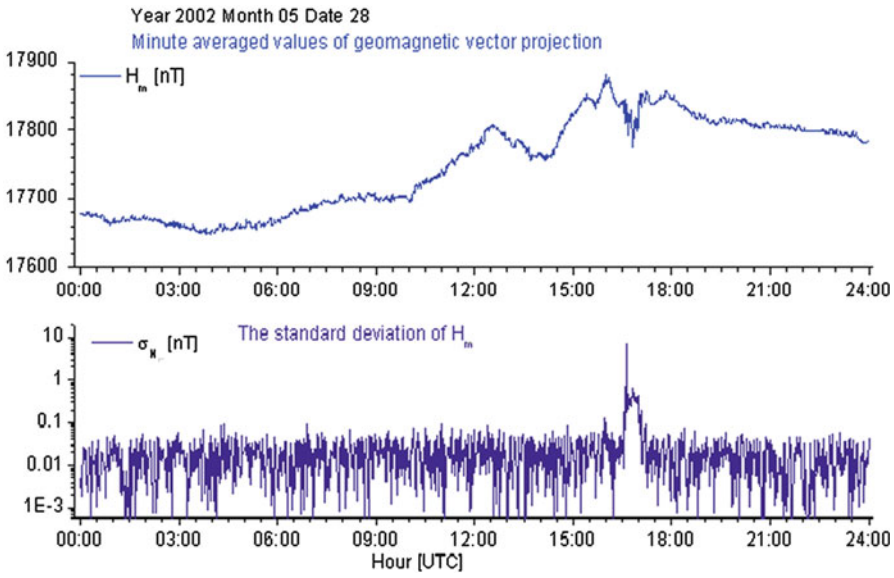

Fig. 22.1 Day with signal (*see color plates*)

notes [2, 3], that the extreme tides are the earthquake's trigger. The Venedikov's code [4, 5] for calculating the regional tide force was used.

The signal for increasing regional seismic activity (incoming earthquake) is the "geomagnetic quake", which is defined as a jump (positive derivative) of daily averaged *SDF*. Such approach permits to compare by numbers the daily behaviour of the geomagnetic field with other days.

The predicted earthquakes can be identified as a maximum of function

$$S_{ChtM} = 10^{1.5M+4.8}/(D + Depth + Distance)^2 \left[\text{energy}/\text{km}^2\right] \tag{22.3}$$

where D = 40 km is fit parameter, calculated for every occurred in the region earthquake.

It is very important to note that the time scale of 1 min, the correlation between the time period of increasing regional seismic activity (incoming earthquake), and tide extrema, recognized of predicted earthquake was established using the Alexandrov's code REGN for solving the over determined nonlinear systems [6–10]. The very big worthiness of Alexandrov's theory and code is possibility to choose between two functions, which describe the experimental data with the same hi-squared, the better one.

The following Figs. 22.1 and 22.2 are illustrations of the day without and with a signal for a "geomagnetic quake", calculated for one geomagnetic component, using *SDF* of Sofia one component geomagnetic monitoring: http://theo.inrne.bas.bg/~mavrodi/ [11].

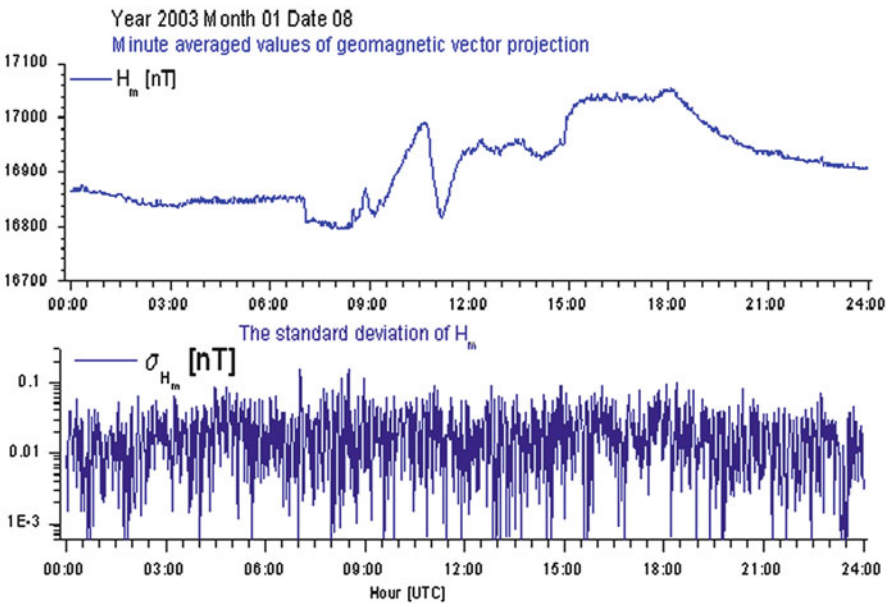

Fig. 22.2 Day without signal (*see color plates*)

22.3.4 The Results of Geomagnetic Vector Monitoring [12–14]

In the following Fig. 22.3 an example of the Skopje daily geomagnetic monitoring is presented:

In the right part of the figure are presented, up to down minute averaged values of *H, D, Z*, and its standard deviation of *SDH, SDD, SDZ* correspondingly, as well as the variable *MinuteSig,* measured with ten samples per second.

$$MinuteSig = \left(SDH^2 + SDD^2 + SDZ^2\right)/\left(H^2 + D^2 + Z^2\right) \tag{22.4}$$

In the left part of the figure, down to up are presented daily averaged values of Middle A indices (http://www.swpc.noaa.gov/alerts/k-index.html). Daily signal graph, where the *GmSig* is

$$GmSig = (1/1440)\sum_{1}^{1440} MinuteSig \tag{22.5}$$

$$PrecursorSig = (1/2)\left(GmSig_{Today} - GmSig_{Yesterday}\right)/\left(A_{Today} - A_{Yesterday}\right) \tag{22.6}$$

In the next upper graph are presented the occurred earthquakes with index, which is the distance (<= 700 km) from the monitoring point. The next graph presents the

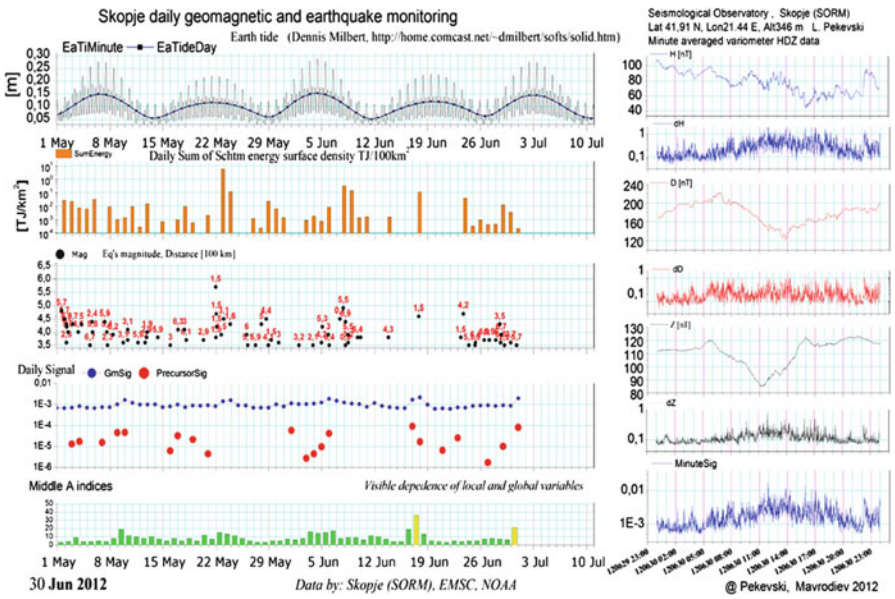

Fig. 22.3 Skopje daily geomagnetic and earthquake monitoring (*see color plates*)

daily sum of function *Schtm*, and the upper graphs presents the behaviour of minutes and daily averaged values of Earth's surface tidal movement, calculated with Dennis Milbert's code http://home.comcast.net/~dmilbert/softs/solid.htm.

In the next Fig. 22.4 is presented an example of the Panagjuriste INTERMAGNET daily geomagnetic monitoring with minute *XYZ* data hour calculations correspondingly.

The above Skopje and Panagjuriste figures illustrate how our approach for Mw 5.6, Pernik earthquakes, May 22, 2012, 00:00 UTC time works, notwithstanding that Skopje data are with ten samples per seconds and difference in distances.

Such posteriori analysis on the basis of INTERMAGNET for England, Alaska, India, Kamchatka, Hokkaido and other regions, where big earthquakes have occurred also confirmed that the geomagnetic quake is a reliable regional precursor for imminent seismic increasing activity.

22.3.5 Some World Earthquake Statistics

The earthquakes' statistic from 1982, presented in the above Figs. 22.5 and 22.6 and occurred big Natural catastrophes illustrates our 2004 statement that our Civilization has some 5–7 years to solve "when, where and how" earthquakes' prediction problem http://theo.inrne.bas.bg/~mavrodi/.

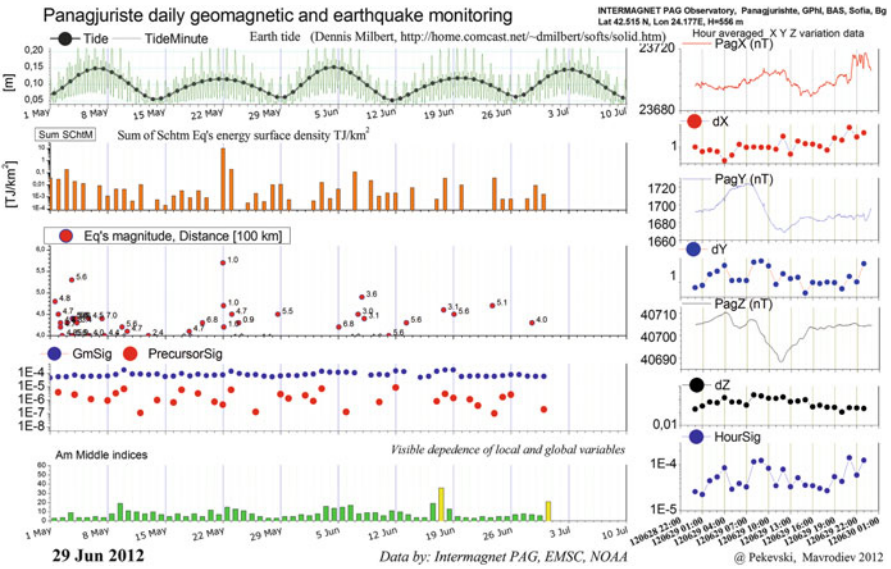

Fig. 22.4 Panagjuriste daily geomagnetic and earthquake monitoring (*see color plates*)

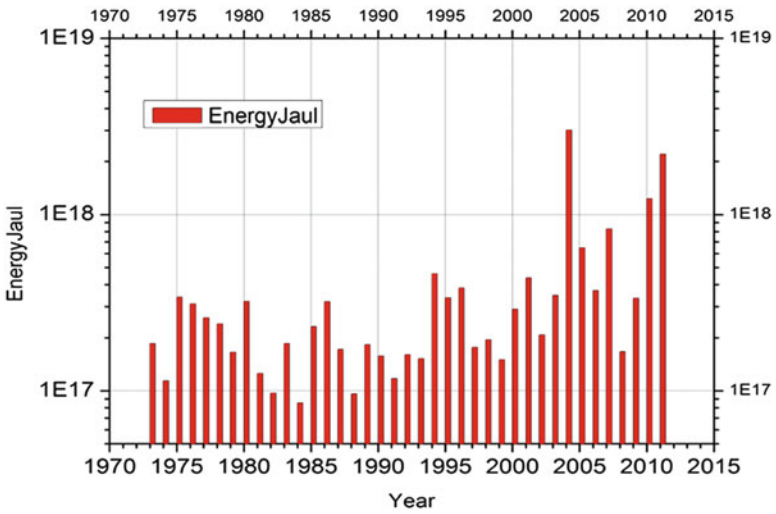

Fig. 22.5 The total world earthquakes energy with magnitude greater than four for the period of 1973–2011 (*see color plates*)

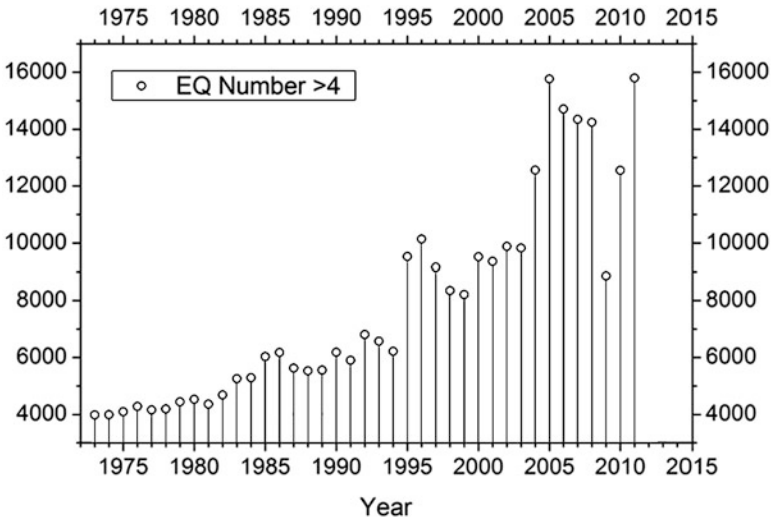

Fig. 22.6 The number of world earthquakes energy with magnitude greater than four for the period of 1973–2011

The next Fig. 22.7 presents the statistical evidence that the daily averaged Earth's local tides extremum are trigger of earthquakes (M > 4).

22.3.6 Deep-Focus Earthquakes Anomalous Statistics, the Axion-Georeactor Hypothesis for Connection Between Seismicity and Climate Change [15]

The NEIC data analysis shows that the dynamics of spatial deep-focus earthquake distribution in the Earth's interior from 1973 to 2008 is characterized by the clearly defined periodical fine discrete structure with $L = 50$ km, which is solely generated by earthquakes with magnitude M∈[3.9; 5.3] and only in the convergent boundary of plates. The explanation is based on an old (1774 year) paper of L. Euler et al. Today authors give estimation of average values of stress in the upper mantle ($\sigma_0 \sim 1.8$ MPa), Young's modulus for the lithosphere ($E_{slab} \sim 55$ MPa) and upper mantle ($E_{mantle} \sim 1$ MPa). Figure 22.8 illustrates the dynamics of peak distribution for the period of 1972–2008. Figure 22.9 illustrates the greater Mag 5.3 earthquake distribution for all periods does not peak, which is in agreement with the understanding of seismic processes concerning the possibility for big earthquake and Earth's core power.

In the next Fig. 22.10, the spatial distributions of deep-focus earthquakes, with magnitude M∈[3.9, 5.3], shows the fine structure of depth distributions in deep-focus earthquakes over the years, 1973–2006. The map is created on the basis of data from http://pubs.usgs.gov/gip/dynamic/world_map.html.

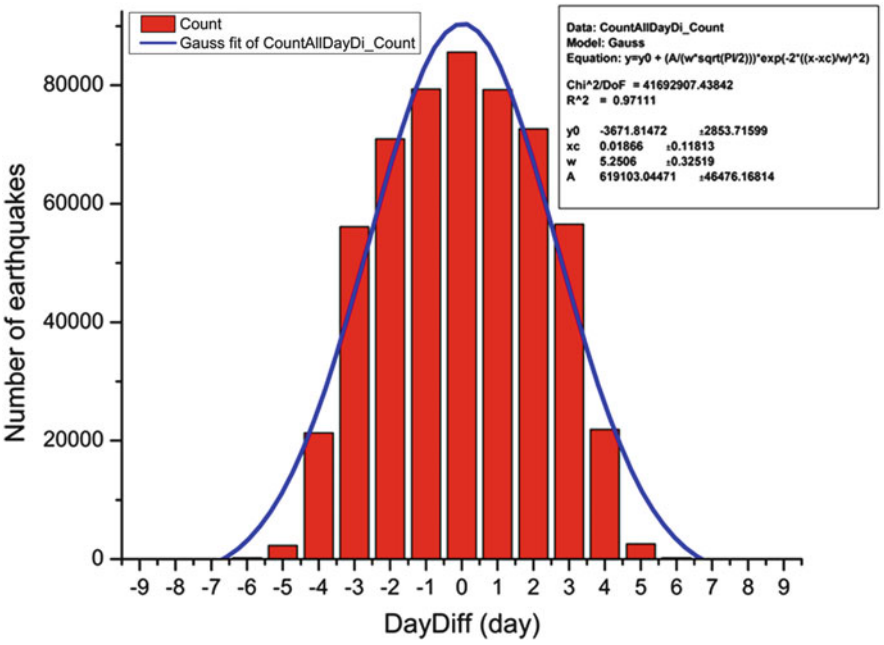

Fig. 22.7 The distribution difference between the time of local extreme tide and the time of occurred earthquake with magnitude greater than four. The http://www.isc.ac.uk/ database was used (*see color plates*)

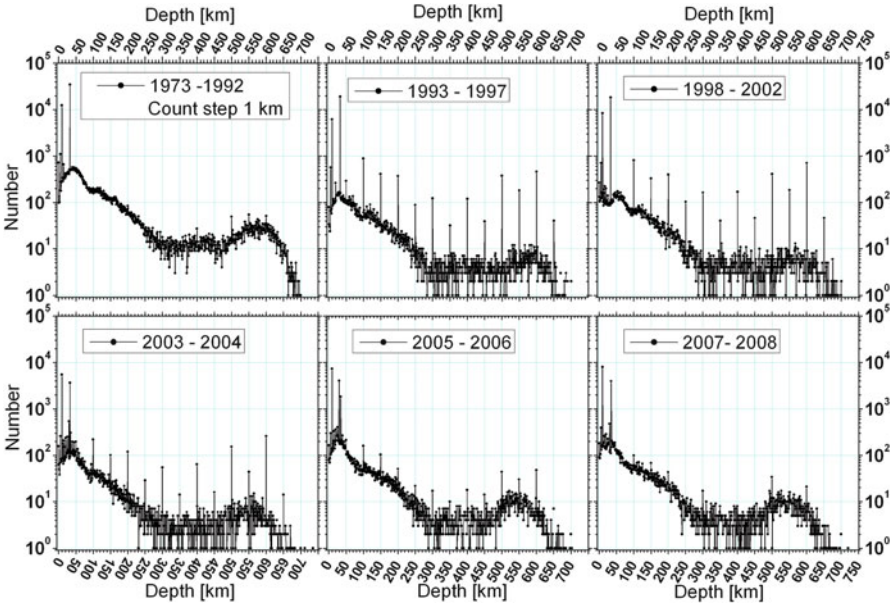

Fig. 22.8 The years' dynamics of depth earthquake's number distributions (*see color plates*)

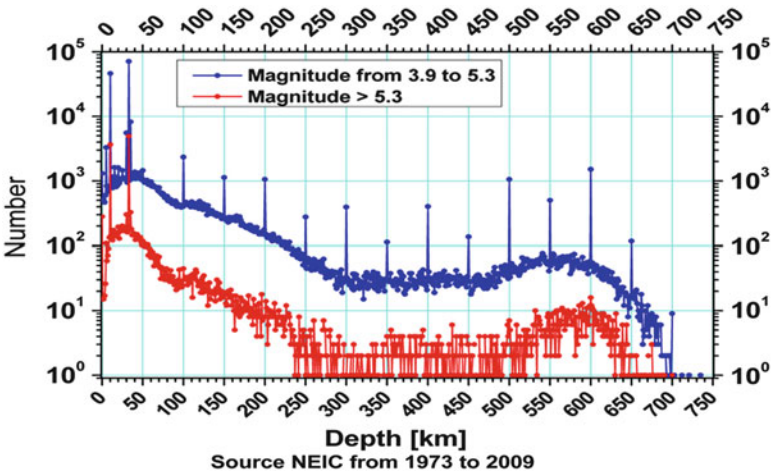

Fig. 22.9 The depth distribution of earthquake numbers for illustration of the fact that the magnitudes of earthquakes which occur in the sleb are limited from sleb's lift (*see color plates*)

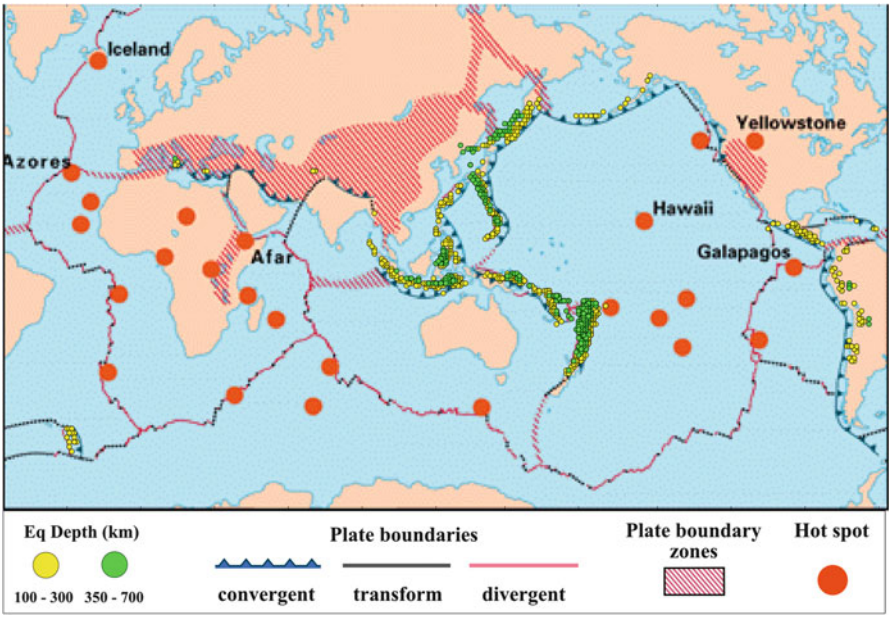

Fig. 22.10 The spatial distributions of deep-focus earthquakes with magnitude M ε [3.9, 5.3] (*see color plates*)

The existence of hot spots and ocean faults can be explained with the Sun-Earth interaction [15, 16] via axion and geo-reactors hypothesis.

One can estimate a strong negative correlation between the temporal variations of magnetic field steroidal component of the solar tachocline (the bottom of the

convective zone) and the Earth's magnetic field (Y-component). Our first hypothesis is the possibility that hypothetical solar axions, which can transform into photons in external electric or magnetic fields (the inverse Primakoff effect), can be the instrument by which the magnetic field of convective zone of the Sun modulates the magnetic field of the Earth. The 57Fe solar axioms, as the main carriers of the solar-terrestrial connection, which by virtue of the inverse coherent Primakoff effect, can be transformed into photons in the iron Earth's core, increasing the temperature, as well as the effectiveness of the nuclear georeactors of Feoktistov type (second hypothesis) depending on the temperature. It is natural to propose that the hot spots and faults are image of Feoktistov's nuclear reactor distribution in the Earth's iron core canyons. In such ways can explain naturally the Vagener movements of continental plates, the seismicity and climate behavior of the Earth.

Of course, creating the balance models, discovering of axions, understanding the processes in the Sun are the fundamental complex interdisciplinary scientific problems with greater significance. This can be compared with the process of Nuclear Disarments in 70-th, which was the consequence of the created Nuclear Winter Model.

22.4 Conclusions

The described above monitoring system now is developing for regional application with hope that in the region will be created a Center for data asquision system with the help of EU and NATO. It is important to stress that the solution of 'when, where, and how' earthquake's prediction problem is connected with meteorological hazards as well as with better step by step understanding the reasons for Earth seismicity and Climate change.

Acknowledgements I would like to note the enormous work of my Colleagues in the time of preparing the project. Of course, we are also very thankful to European Commission for financial support of our Project as well to NATO and organizers of NATO Advanced Research Workshop "The Black Sea: Strategy for Addressing its Energy Resource Development and Hydrogen Energy Problems", 7–10 October 2012, Batumi, Georgia for invitation. We hope that step by step such monitoring system of the Black Sea region will be created, which will help the central and local authorities to organize harmonic existence of the region.

References

1. Mavrodiev SC, Thanassoulas C (2001) Possible correlation between electromagnetic earth fields and future earthquakes. In: Seminar proceedings, INRNE-BAS, Sofia, Bulgaria, 23–27 July 2001, ISBN 954-9820-05-X
2. Knopoff L (1964) Earth tides as a triggering mechanism for earthquakes. Bull Seismol Soc Am 54:1865–1870
3. Tamrazyan GP (1967) Tide-forming forces and earthquakes. ICARUS 7:59–65

4. Tamrazyan GP (1968) Principal ragularities in the distribution of major earthquakes relative to solar and lubar tades and other cosmic forces. ICARUS 9:574–592
5. Venedikov A, Arnoso R (2001) Program VAV/2000 for tidal analysis of unevenly spaced data with irregular drift and colored noise. J Geod Soc Jpn 47(1):281–286
6. Venedikov AP, Arnoso R, Vieira R (2003) A program for tidal data processing. Comput Geosci 29(4):487–502
7. Alexandrov L (1970) Autoregularized Gauss-New-ton-Kantorovich iteration Process. Comm. JINR, P5-5515, Dubna
8. Alexandrov L (1971) Regularized computational process of Newton-Kantorovich type. J Comput Math Math Phys 11(1):36–43
9. Alexandrov L (1973) The program REGN (Regularized Gauss-Newton iteration method) for solving nonlinear systems of equations. Comm. JINR P5-7259, Dubna
10. Alexandrov L (1983) Program code REGN. PSR 165 RSIK ORNL, Oak Ridge, TN, USA
11. Mavrodiev SC (2004) On the reliability of the geomagnetic quake as a short time earthquake's precursor for the Sofia region. Nat Hazard Earth Syst Sci 4:433–447, SRef-ID: 1684-9981/nhess/2004-4-433
12. Mavrodiev SC, Pekevski L (2008) Complex regional network for earthquake researching and imminent prediction. In: Birbal Singh (ed) Electromagnetic phenomena related to earthquakes and volcanoes. Narosa Pub. House, New Delhi, pp 135–146
13. Mavrodiev SC, Pekevski L, Jimseladze T (2008) Geomagnetic-quake as imminent reliable earthquake's precursor: starring point for future complex regional network. In: Birbal Singh (ed) Electromagnetic phenomena related to earthquakes and volcanoes. Narosa Pub. House, New Delhi, pp 116–134
14. Mavrodiev SCht, Pekevski L (2006) On the Balkan- Black Sea- Caspian Complex NETWORK for earthquake's researching and prediction. NATO advanced research workshop management of urban earthquake risk in Central Asian and Caucasus countries, Istanbul, 14–16 May 2006
15. Rusov VD, Vaschenko VN, Linnik EP, Mavrodiev SC, Zelentsova TN, Pintelina L, Smolyar VP, Pekevski L (2010) Mechanism of deep-focus earthquakes anomalous statistics. Europhys Lett 91(2):29001
16. Rusov VD et al (2011) Solar dynamo as host power pacemaker of earth global climate, EU FP7 IRSES 2011 project, complex research of earthquake's forecasting possibilities, seismicity and climate change correlations, ISBN978-9989-631-04-7. Ohrid, Macedonia, BlackSeaHazNet series, vol 1, 2–5 May 2011
17. Rusov VD et al (2009) Global mechanisms in atmospheric models and angular momentum balance of the Earth: P. 1. Atmospheric waveguides, teleconnection, the Gadley cells. Bull Kiev Nat Univ Ser Phys Math 4:556–562
18. Rusov VD et al (2006) One – parameter cascade model of multiple hadrons production in inelastic hh – processes at high energies. Nuclear Phys A764:460–475
19. Feoktistov LP (1998) From the past towards the future: from the hopes of bomb to the safe reactor. Publ. of RFNC-ANRISPh, Snezhinsk, 326 pp
20. Teller E et al (1996) Proceedings of international conference on emerging nuclear energy system (ICENEC'96), Obninsk, Russian Federation, pp 123–127

Chapter 23
Serbian Efforts to Improve Environmental and Overall Security in Black Sea Regional Cooperation

Vesela Radovic and Alexandar Andrejevic

Abstract In recent international relationships, the Black Sea region is recognized as extremely important, especially in the European Union agenda. Energy and overall security, as well as performed activities in creating a favourable political climate for cooperation in the region represent an important aspect of the Black Sea Economic Cooperation (BSEC). At the beginning of the crucial changes in international relations, the Republic of Serbia recognized the importance of the Black Sea region. Many data available from a recent research project gave the author a motive for this article. Applying the appropriate methodology in social science, the article highlights some of Serbian past activities, which lead to significant success in the area of environmental protection of the Black Sea region, mainly through permanent cooperation within the International Commission for the Protection of the Danube river (ICPDR) and other projects financed through the Instrument for Pre-Accession Assistance program (IPA). In the present situation, Serbia is making additional efforts to find a solution for issues raised in the past, although it is suffering from unfavourable macroeconomic conditions and consequences of delayed decision on its candidacy to the EU. Serbian intention to develop cooperation with its neighbouring countries and the countries of the broader region is unquestionable. The visible role of the Republic of Serbia has been shown within the BSEC and was a priority as a current a Chairmanship -in-Office of the Black Sea Economic cooperation (1 January – 30 June 2012). Other parts of the article consist of several best examples of Serbian contribution in the area of developing renewable energy sources, energy efficient technologies in terms of environment protection, decreasing and controlling of industrial and agricultural pollution of the

V. Radovic (✉)
Faculty of Environmental Governance and Corporate Responsibilities, EDUCONS University, Vojvode Putnika 87, Sremska Kamenica 21 208, Vojvodina, Serbia
e-mail: veselaradovic@yahoo.com

A. Andrejevic
EDUCONS University, Vojvode Putnika 87, Sremska Kamenica 21 208, Vojvodina, Serbia

A. Veziroğlu and M. Tsitskishvili (eds.), *Black Sea Energy Resource Development and Hydrogen Energy Problems*, NATO Science for Peace and Security Series C: Environmental Security, DOI 10.1007/978-94-007-6152-0_23,

Danube, as well as its new role in the regional security. The recently established Serbian Russian Humanitarian Centre in the town of Nis should have the significant role in the future intensification and extension of cooperation in the transportation/transiting of energy resources across the BSEC region and other countries. Conclusion remarks of the article present a clear recommendation on how to avoid some obstacles on the path of sustainable governance, and strengthening institutional, organizational and other capacities of Serbia for the purpose of improvement of its future role in BCES.

Keywords Cooperation • Pollution • Environmental protection • Agriculture • Waste water

23.1 Introduction

The twenty first century characterized by the globalization processes has had a profound impact on the international community. The global dynamic environment in which societies have been challenged with different needs and threats (environmental and social problems) searching for the improvements of international cooperation in numerous areas. In recent years, there has been growing international concern about increasing crisis in Global Water Security, and questions how to provide increasing demands for food, energy and water.[1] As a result of this need many regions in the word are influenced by the spirit of regional cooperation. The outstanding importance of the cooperation in the Black Sea Region was recognized two decades ago (in 2012 BSEC celebrated its 20th anniversary in Istanbul, in the Republic of Turkey), and was expressed by the establishment of the Black Sea Economic Cooperation (BSEC).

The influence of BSEC is visible because it presents a platform for political dialogue for its 12 Member States; encompasses an area of approximately 20 million km^2 with 340 million people [1].

The Republic of Serbia (RS) is aware of the two key realities of our planet: rapid diminishing of energy resources and widespread and serious deterioration of environmental conditions. The key issues addressed in the paper include the Serbian efforts in the process of planning adequate response to new challenges and opportunities in the Black Sea region, regional and local environment and enhancing cooperation with other international organizations, including the European Union and focusing on cooperation in the spheres of environmental protection, energy and security.

During its recent 6 month presidency (1 January – 30 June 2012), Serbia has promoted dialogue and cooperation among the member states and atmosphere of trust and respect. Serbia hosted 26th BSEC summit in Belgrade on 11 Jun 2012. At the end of the meeting, a ceremony took place during which the Republic of Serbia handed over the Chairmanship-in-Office of BSEC to the Republic of Turkey [2].

[1] See more in John Beddington book Perfect Storm.

For the future cooperation in the Black Sea region it is important to adopt two important documents in Belgrade: the "BSEC Economic Agenda towards an Enhanced BSEC Partnership", a new BSEC Economic Agenda and a "BSEC Public Communication Strategy".[2] The Declaration of the Ministers of Energy on the Enhancement of the Gas Infrastructure Development gives priority to bilateral and multilateral cooperation of the BSEC Member States in projects related to sustainable exploration and exploitation of shale gas, LNG and CNG terminals and ship-based re-gasification, gas storage facilities and pipelines that further develop interconnections of national gas networks.

The Joint Belgrade Declaration on Climate Change and Green Economy – BSEC contribution to Rio + 20, adopted by the Ministers in Charge of Environmental Protection, addresses the need and possibilities for the future joint action. In the Declaration, the Ministers agreed to identify common approaches on combating climate change and promoting green economy. In this area we need to find an answer to the question: How to provide the rehabilitation of numerous ecological black points and at the same time implement green investments? In which way can we create necessary conditions to attract foreign investments in energy and mining sectors, and implement different ecological instruments to improve environmental protection in our current political and economic situation [3]?

The Republic of Serbia is devoted to the extension of the regional cooperation and coordination in the future in other areas, as well as in the area of the environmental protection. In this process, various activities regarding the fulfilment of European Water Framework Directive (WFD) requirements have an essential role. Multilateral cooperation in the field of waters is implemented through the work of International Commission for Protection of the Danube River (ICPDR), Danube Commission, International Sava River Basin Commission and expert groups within UNECE Convention on the Protection and Use of Transboundary Watercourses and International Lakes (Water convention), Hydrology and Water Resources Programme of World Meteorological Organisation, UNESCO International Hydrological Programme, and especially within Danube countries, cooperation of competent national hydro – meteorological services [4].

Activities of the Republic of Serbia in the area of the environmental protection, renewable energy and regional security are presented in this paper. The paper presents Serbian efforts to adjust its institutional response to those the similar in European Union, and an ongoing battle between current obstacles and incentives to regional cooperation in the time of global financial crisis. Additionally, the paper presents Serbian activities in ICPDR and important projects completed with goal to decrease the Danube pollution and increase capacity in the area of environmental protection and use of renewable energy sources.

Despite Serbia following examples of good practice in Europe, and established integral protection and rescue system, it still has a lot of room for improvement of

[2] The representatives of the Ministers of Energy (Belgrade, 11 April 2012) and Ministers in Charge of Environmental Protection (Belgrade, 23 April 2012) signed those documents.

national capacities. The recently established Serbian Russian Humanitarian Centre in the town of Nis should have the outstanding importance in providing safety during various emergencies. Financial obstacles and international help needed in the future are presented in the last part of this paper, followed by conclusion remarks and references used in preparation of this paper.

23.2 Serbian Role in the Process of Environmental Protection of the Black Sea

The Black Sea region has a universal value for human civilization. Further development of economical potential in this region must be based on ecologically sound modern technologies. This reason raises a need to mobilize the efforts of world scientific communities and to look for new ways of development of clean energy potential of the region [5]. Black Sea is the world's largest and most stable anoxic marine basin. Natural water conditions, as well as the endemic biological communities are unique and extraordinary, and they deserve preservation [6]. Ecological problems of the Black Sea Region and presence of deep hydro sulphuric layer in Black Sea waters initiated "Black Sea Environmental Program (BSEP) working on a policy to protect the Black Sea Region's ecology.

The Black Sea, into which the Danube River flows, is 'at risk' from different kind of pollution (nutrient pollution, organic pollution, pollution from hazardous substances and etc.). With over half of the Sea's waters originating from the Danube, the Danube's waters are bound to have considerable impact. In the 1970s and 1980s, excessive nutrient pollution led to a severe ecological imbalance, and the large-scale eutrophication of tens of thousands of square kilometres of waters in the western Black Sea, as the depletion of oxygen decreased biodiversity and worsened water quality. This was actually one of the main reasons why many influential international organizations became involved in the Danube and Black Sea efforts in the first place. In 1992, the Danube Basin was site of the first 'international waters regional program,' the Danube Regional Project (DRP).

Serbia has extremely important geo-political position in the Balkans. Serbian outflow water counts to 162 billion m^3 annually, since the inflow is 16 billion m^3 annually. Approximately 92 % of all Serbia's accessible water originates from outside its territory. The Danube River flows about 588 km through Serbia. Coming from Hungary it continues at kilometre 1,433 as a border-river with Croatia through Serbia. There are many protected areas along the river banks, two National Parks, numerous heritage sites. The population in cities located directly on the river stream are increasing permanently; in the capital of Belgrade and Novi Sad, as also in a few smaller towns. At the 845, 65 km the Danube leaves Serbia. Serbia shares the Sava River, a tributary of the Danube, with Slovenia, Croatia and Bosnia and Herzegovina; the Tisa River with Ukraine, Romania, Hungary and Slovakia; and the Tamiš River with Romania. The West Morava and Great Morava rivers,

(both parts of the major Morava river system in Serbia), is the only one of the five major rivers not crossing Serbia's borders.

The rivers in Serbia belong to the watersheds of the Black, Adriatic and Aegean seas. In more than 90 % of the Serbian territories there are rivers that join the Danube, and eventually go to the Black Sea. The pollution of transboundary rivers is contributing to the pollution of Black Sea. Serbia is devoted to achieve the goals of sustainable water management on national and regional level, to control the hazards originating from pollution and accidents, and to contribute to reducing the pollution loads of the Black Sea from sources in the Danube catchments area. In the process of environmental and overall security improvement in Black Sea, Serbia cooperates actively with:

- The European Union (EU) in a process of approaching to full membership status Serbia must fulfil all environmental regulations pertaining to environmental protection and the protection and management of water; and
- The Organization of United Nations – as a member of the UN, Serbia is obliged to embed into national legal framework key requests derived from relevant UN conventions, directives, and recommendations.

In the last decade the main strategic documents in the environmental field were developed in accordance with sustainable development principles. The greatest number of strategic documents was developed in 2009 and 2010. The National Environment Strategy [7] identifies the following key environmental problems in Serbia. Serbia belongs to the region with known basic influence of climate changes and that fact needs adequate response on those "new challenges" [8]. Serbia adopted Strategy of Clean production but its implementation is not going so easy.[3]

Institutional framework in Serbia is created in accordance with those similar in the European Union. Environment-related issues are also covered by other ministries in line with their duties as defined by law: Office of Deputy Prime Minister for EU Integration, Ministry of Agriculture, Forestry and Water Management, Ministry of Economy and Regional Development, Ministry of Internal Affairs, Ministry of Energy and Mining, Ministry of Infrastructure, Ministry of Health, etc. Various organizations focus on various environmental topics, from environmental monitoring to statistical data collection, management – Environmental Protection Agency, the Statistical Office, Hydro meteorological Institute, Public Health Institute, and so on [9]. Although Serbia has taken several important steps in formulating and adopting environmental strategies, action plans and legislation, implementation on the ground is a major issue. Those challenges remain according to the reports of the international organizations. In a recent report it is stated that "the level of integration of climate change into development strategies, the level of knowledge, institutional capacities and the availability of technologies are still far from below that necessary for an effective and fast response to combat

[3] Some of the Serbian Strategies are available in English since others are in Serbian language at: www.srbija.gov.rs/vesti/dokumenti_sekcija.php?id=45678

climate change" program [10]. The similar statements have also been given in the First Serbian National Communication to the United Nation Framework Convention on Climate Change (UNFCC) from Ministry of Environmental and Spatial Planning and few other different documents [11].

The global economic crisis has caused a huge impact on world's economic development, and the possible discussion about "the second wave" is on stage [12] and makes economic situations more serious. Crises, as well as different subjective circumstances, generate unfavourable macro economic conditions in Serbia which affect many long term plan in the environmental protection area.

Water protection is one of the most important parts in the Serbian regional activities. Transboundary cooperation on water management is established by the Ministry of Agriculture, Water Management and Forestry (MAFWM) and Republic Water Directorate (RWD) and other stakeholders in this area. In the northern part of Serbia, in the Autonomous Province of Vojvodina (APV), the Article 183 of the Constitution of the RS defines the competences of Vojvodina, empowers the province to organize and provide for environmental protection in its territory in accordance with the Law [13]. Provincial Secretariat for Agriculture, Water Management and Forestry has the jurisdiction over water management at the level of APV based on legislative [14]. Water management activities in APV are performed by Public Water management Company -PWMC "Vojvodina Vode" [15].

A regulated international legal regime in the water sector is extremely important for all neighbouring countries, and consequently for cooperation within the ICPDR. The Development and Aid Coordination Unit (DACU), within the Ministry of Finance, is responsible for overall coordination of international assistance to Serbia. The Division for EU Integration and International Cooperation and Project Management in MESP has overall responsibility for international cooperation in environmental protection and sustainable use of natural resources. Water management and protection falls under the jurisdiction of four ministries: Ministry of Agriculture, Forestry and Water Management (MAFW), (Ministry of Environment, Mining and Spatial Planning (MESP), Ministry of Health (MOH), Ministry of Infrastructure (MOI).

However, in practice, international cooperation in water management and protection is under the jurisdiction of the Republic Water Directorate (RWD). RWD as an administrative body within the MAFW performs duties related to: water management policy. Within the RWD, there is a Group for strategic planning and management and international cooperation in the field of water resources which performs tasks related to: organization, concept of developing and monitoring the Strategy of Water Management in the Republic of Serbia, Danube River Basin Management Plan; conducting the international programs for implementation of EU Water Framework Directive and the World Bank projects within the funds for accession to the European Union and other international projects concerning water management; development and coordination of national accident emergency warning centre, within the international Accident Emergency Warning System (AEWS) of the Danube and Sava river basins and the group also performs other tasks in the related field.

Environmental Protection Agency performs specialized tasks related to development, approximation and management of national information system about the quality and quantity of surface and groundwater, constant updating the cadastre of water polluters, establishment of procedure for processing data about water resources and creating relevant indicators, cooperation with EEA and EIONET in the context of exchange of information about water resources.

23.2.1 Serbian Contribution to the Activities of the International Commission for the Protection of the Danube River (ICPDR)

The water is crucial to our existence, and water is in the centre of every human activity. Serbia wants to protect its water resources and it is starting to accept responsibility in the sustainable management of transboundary watercourses at bilateral and multilateral levels. Serbia has signed bilateral cooperation agreements with Albania, Bulgaria, Hungary and Romania, although the effect of implementing these agreements has varied from country to country. Serbia has not signed bilateral agreements governing the sustainable management of transboundary waters with Bosnia and Herzegovina, Croatia or the Former Yugoslav Republic of Macedonia.

The cooperation which Serbia implements in the ICPDR is recognized to be most successful. The Danube River Protection Convention (DRPC)[4] is the overall legal instrument for transboundary water issues in the Danube River Basin (DRB). The ICPDR is charged with coordinating the conservation, improvement and rational use of Danube waters, and facilitates the implementation of the DRPC. The Danube River Basin is the most international basin in the world and as a complex river system needed one of the most comprehensive water management–one that addresses the needs of the people and nature of the region [16].

The Danube River Basin Management Plan (DRBM) focuses on the main transboundary problems and water management issues that can directly or indirectly affect the quality of rivers and lakes as well as transboundary groundwater bodies, namely pollution by organic substances, pollution by nutrients, pollution by hazardous substances and hydromorphological alterations. In addition to the DRBM Plan, which provides a coordinated strategy for the basin as a whole, detailed National Management Plans have been developed. The EU WFD requires that all waters reach at least good status by 2015 (or at the latest by 2027). Therefore, the European Commission, the Directorate-General for the Environment provided financial support to the ICPDR Secretariat to carry out the "Evaluation of

[4] Conventions on Cooperation for the Protection and Sustainable Use of the River Danube (Danube River Protection Convention) was ratified on 30 January 2003 ("Official Journal of FRY"-International Treaties No. 2/2003). Republic of Serbia became a contracting party of the International Commission for the Protection of the Danube River-ICPDR on 19 August 2003.

Policies, Regulation, and Investment Projects Implemented in the Danube River Basin Countries in Line with EU Directives and Regulations".[5]

Serbia performed many activities in order to decrease pollution of Danube and its tributaries and canal system Danube-Tisa-Danube. Serbia embedded into national policies regulations, and compliance mechanisms on Nitrates Directive, Urban Waste Water Directive, IPPC Directive, Water Framework Directive, etc.

Serbia participated in DABLAS[6] project which aim was to assist the ICPDR in evaluating the accomplishments realized in 11 countries, in the Danube River Basin, in terms of policies, legislation, regulations, and investment projects, which have been implemented in line with the ICPDR Joint Action Programme.[7] The ICPDR-DABLAS database has been revised in 2005 to include municipal, industrial, agro-industrial, wetland restoration, agricultural and land use projects.

Those activities were significant for the implementation of projects for pollution reduction and the rehabilitation of ecosystems in the wider Black Sea region.

23.3 The Main Area in Which Serbia Act to Decrease Negative Environmental Impact on Black Sea

Following the recommendations of different international institutions and decision of policy makers, Serbia performed necessary activities to decrease pollution of the Danube and indirectly of the Black Sea. The most important problems referring to the water quality in Serbia and Vojvodina are the pollution from settlements, industry and agriculture. It is considered that industry is responsible for most of the direct and indirect discharges of hazardous substances into the Danube Basin, mainly due to untreated industrial waters. On the other hand, it is necessary to highlight that Serbian industrial production is at the lowest level in history. It counts only one quarter from those in 1989. For the purpose of this paper authors analysed three main kinds of activities: reducing nitrates and waste water and efforts in increasing the use of renewable energy sources as a tools for decreasing Danube pollution.

[5] ICPDR Secretariat, GRANT Agreement 07.020100/2004/374563/SUB/E1.

[6] The Danube Black Sea Task Force (DABLAS) was set up in 2001 up during the Ministerial Conference on 26 November 2001 in Brussels. The result of conference among others was a joint declaration on the "Protection of Water and Water related ecosystems in the wider Black Sea Region" which is signed.

[7] The Joint Action Programme of the ICPDR outlines the specific steps that were agreed to be taken over the period 2001–2005 to achieve the environmental objectives outlined in the Danube River Protection Convention including many large-scale measures to reduce water pollution, to promote nature conservation, to restore ecosystems, and to safeguard the long-term sustainable management of the environment.

23.3.1 Reducing Nutrient Pollution from Agriculture

Serbian environment is constantly exposed to the different kind of threats [17]. Some of those threats are well known, but unfortunately it happened that in few cases stakeholders failed and faced with great consequences in the society, as well as neighbouring countries. There is an assessment that 40 % of total burden of nitrogen in the Danube originates from agriculture from different countries. The UNDP/GEF Danube Pollution Reduction Programme has identified in 1999, through its Transboundary Analysis (TDA), 130 major manufacturing enterprises (hot spots) within the Danube River Basin of which a significant number of these are contributing to transboundary pollution in the form of nutrients and/or persistent organic pollutants.

Agriculture has long been a major source of income for many people living in the Danube River Basin. The trouble is that in Serbia inappropriate agricultural practices has significantly polluted rivers and ground waters, and reduce standard of living for farmers and local communities in the long run. In the current microeconomic circumstances the modernization of agriculture in Serbia looks like an ideal goal. In the previous form of the country (Serbian and Montenegro), document The National Review on Serbia and Montenegro identified wastewaters from industrial enterprises, notably fertilizers and agro-processors as the largest source of nitrates and phosphates in state part of the Danube Watershed. Presented facts in the report claim that country annually discharges into water flaws 72,000 tonnes of nitrogen and 7,000 tonnes of phosphorus, which counted 13 % of total nitrogen pollution of the Danube and 14 % of its phosphorus pollution. At that time, the country was in the third place due to the total amount of nitrogen and phosphates discharged in Danube water (among 13 Danube countries). In 2004 UNEP announced its report that the main point sources of organic discharge in Serbia are the estimated 130 pig farms with 1.2 million animals. Today those data could be questioned because of enormous decreasing of livestock in Serbia caused by great cost disparities at the market.

One of the first projects which tackled this problem was the Carl Bro project, which was funded by the Washington D.C.- based Global Environmental Facility (GEF). The project was particularly important for the northern part of Serbia, in Vojvodina Province. In Vojvodina the inappropriate agriculture practice put at great risk Begej River, Danube, Tisza and many canals. At that time it was a remarkable example that in a small town of Zitiste which population is about 3,000, one agricultural enterprise slaughtered 30,000 chickens daily (12 million yearly). This project in the end revealed that implementation of the 15 best agriculture practices by the eight farms could annually save the environment from about 14,000 kg of nitrogen, 2,000 kg of phosphorus and 250 kg of pesticides [18].

In Belgrade on 3 March 2011, the Workshop which presented results achieved during 4 year implementation period (2006–2010) of the project Danube River

Enterprise Pollution Reduction in Serbia (DREPR) for Nutrient Reduction in the Black Sea/Danube Basin was organized. The DREPR project can be considered as an initial stage in getting closer to the implementation of the Nitrates Directive in Serbia in the Danube basin and the Black Sea region. The statement during Workshop was that this is one of the most successful agriculture related projects in the Republic of Serbia.

According to the facts presented by the agency IPSOS-Strategic Marketing during realization of the project, public awareness on nutrient containing waste management and water pollution, and their impact on public health, economy and ecosystems rose to 37 % among farmers population, and to 22 % in Serbian overall population. In the ecological framework of the projects piezometers for measurements and control of nutrient pollution on selected farms were installed.

Despite those visible improvements, there are still obstacles in the Republic of Serbia because the Nitrates Directive has not been established yet. A competent institution must define the framework of the Action Programme and to define whether all Serbian territory or just certain parts would be a vulnerable nitrate zone. Additionally, the Water Law, adopted in 2010 does not address the issues about the implementation of the Nitrates Directive [19].

The Code of Good Agricultural Practices which is similar to the Best Agriculture Practices is very important for farmers but Serbia is far from its implementation. Farmers could use in daily work only a brochure about this issue in 2008 which is insufficient. In some areas pollution could be greater, especially because the concern about environmental issues still has low priority on the lists of most farmers. The privatization process brought a lot of problems, which put Serbian agriculture in deep recessions. Farmers have lack of information, education and training support needed to accept best agriculture practices and their daily struggle to survive and response to different risks and threats is enormous. In the last few years state encouraged farmers in organic agriculture, but based on data from inspections Serbia organized organic agriculture production in 2010 only on 9294.61 ha.

Despite all unfavourable evidence, Serbia tries to address the nutrient problem and decrease its part of the nutrient input into the Black Sea. Nitrate concentrations in Vojvodina waters are decreasing. Evaluation the status of river quality is shown using the nitrate indicator. The analysis included 6,497 water samples from 52 measurement sites for the control [20]. Among numerous laws necessary in a process of combat agricultural pollution, the Law on Integrated Pollution Prevention and Control [21] envisages the public participation in the process of issuing the permit for integrated pollution prevention and control.

The Serbian Environmental Agency is in the process of completing an inventory of all relevant point discharges of agriculture, designed to serve as a tool for decision-makers and the local environmental and agricultural authorities to control pollution and improve water quality in the Danube River.

23.3.2 The Reducing Quantity and Quality of Waste Water Discharge in the Danube

One of the most difficult directives for implementation in Serbia is WFD and EU Directive 91/271/EC concerning urban waste water treatment. National Environment Approximation Strategy for the Republic of Serbia started that the future urban waste water treatment (UWW) costs are estimated at EUR 3.204 million and the transition period calculated is to 2030. The worst expectation was stated regarding currently global recession and budget deficit in Serbia. Therefore this period could be extended till 2037. Total administration cost over 2011–2030 in water sector are approximately about EUR 146 million [22]. Most industrial and mining wastewater is discharged into the Sava River and its tributaries, and after that through the Danube into the Black Sea.

Statistical Office data indicate that 365 million m^3 of waste water discharged in 2009, and only 51 million m^3 were treated. In terms of development of facilities for treating waste water according to the data from 2007, from total of 165 units of local self-government in the Republic of Serbia, facilities for municipal wastewater treatment exist in 20 municipalities (15 facilities carried out only mechanical and 5 biological treatment). The largest cities in Serbia: Belgrade, Novi Sad and Nis do not have facilities for treating municipal waste water.

There are a lot of data on the state of sewerage systems in municipalities in Serbia which are used in the field of wastewater. In the Report on the status of environment protection in 2009 (SEPA) [23] specifically highlighted that there was an inconsistence in data on waste waters in Serbia coming from different sources, and because of different reporting methodologies in use.

Pursuant to data of Water Master Plan [24] of the Republic of Serbia it is estimated that the total emission of suspended matters in recipients amounted to 1,549,531 kg/day, i.e. 12,301,223 population equivalent (PE). The total emission of nitrogen was 111,374 kg/day, and total emission of phosphorus was 36,764 kg/day.

In the process of searching for the most appropriate way to solve the wastewater problem it is useful to know that in Vojvodina there are recorded 511 polluters. 447 of them are industrial facilities. Out of them 293 polluters treat wastewaters, 71 treat wastewaters together with municipal waste waters, and 83 polluters treat primarily their waste waters. According to the Strategy of waters supply and water protection in Vojvodina [25] only 44 out of all settlements in Vojvodina have at least some form of sewerage for waste water. The total wastewater quantity in Vojvodina is about 5,250,000 PE, and 40 % of it was generated from settlements. Data show that quantity of wastewater was increasing during the period of 2004–2009 (Table 23.1).

Today, industries within urban areas generally use the municipal wastewater systems to discharge their wastewater, whilst those outside urban areas usually discharge directly into nearest water course, with minimal or no treatment. Some of the existing plants in the cities of the Republic of Serbia stopped working, and some perform only mechanical treatment, but most of them are facing frequent work breaks due to the maintenance problems and lack of financial resources. In a process

Table 23.1 The waste water and purified water from Vojvodina settlements, given in thousands of m^3

Year	Total amount of wastewater	Households waste water	The total amount of treated wastewater	Primary treatment (mechanical-biological)	Secondary treatment (mechanical-biological)	Tertiary treatment (mechanical–chemical-biological)
2004	62.306	39.634	18.201	2.990	15.211	–
2005	59.072	39.964	37.246	3.755	33.491	–
2006	62.197	43.379	32.915	9.107	23.808	–
2007	72.235	44.109	21.417	665	20.752	–
2008	73.386	32.604	21.957	968	20.989	–
2009	73.678	47.752	16.230	770	9.382	6.078

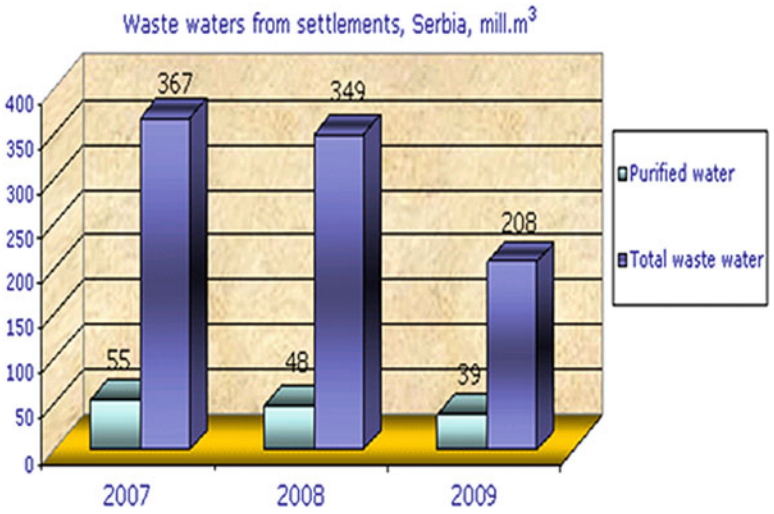

Fig. 23.1 Purified and total waste waters 2007–2009 (million m^3) (Source: Statistical Office of the Republic of Serbia) (*see color plates*)

of privatization Serbian environment was exposed to different kind of ecological and safety risks which affects also a wellbeing of the population [26].

The pollution of the Great Bačka Canal, from which the water flows into Tisa and on to the Danube, is considered as environmental hot spot in Serbia and Europe. The pollution is largely caused by the discharge of untreated industrial and utility waste water. Serbia has also implemented Remediation of the Grand Backa Canal 'project[8] which is to enable waste water treatment and discharge for 120,000 equivalent inhabitants in the municipalities of Vrbas and Kula, collect and treat industrial waste, expand the sewerage system to additional 20,000 inhabitants which will improve water quality in the extremely endangered tributaries of the Danube and the Great Bačka Canal (Fig. 23.1).

23.3.3 Increasing Use of Renewable Energy

Energy sector is a great polluter of the Serbian environment. The majority of energy capacities are built on rivers banks and pollution of water is inevitable. The Government of the Republic of Serbia has adopted the legislation for the promotion of renewable energy sources.[9] The Energy Sector Development Strategy of the

[8] It is a part of UNDP's Western Balkans Environment Programme, UNDP.

[9] In the energy sector Serbia established legal framework in accordance with the provisions of EU Directive on Renewable Energy Sources (Directive 2009/28/EC) and Directive 2001/77/EC on the promotion of electricity produced from renewable sources in the internal electricity market.

Republic of Serbia by 2015 defines five basic energy development priorities of the Republic of Serbia and the third is regarding special priority of use of new renewable energy.[10] Surprisingly, the Law on Renewable Energy Sources does not exist in the legislature of the Republic of Serbia.

Serbia made significant improvement only in the sector of biomass production where the Biomass Action Plan for the Republic of Serbia for the use of biomass as a renewable energy was developed in accordance with requirements of the Treaty Establishing the Energy Community signed by Serbian Government.[11] However, results show increase of the share of electricity produced from renewable energy sources in total energy consumption from 4, 7 % in 1990 on 8, 28 % in 2010, which is an increase of 64 % [27]. In current economic condition the Renewable Energy Sources (RES) Sector is entirely focused on private investors. It is estimated that potential need for investments by 2012 was at a level of EUR 1.58 billion. In Serbia it is hard to estimate any improvement in this area because reliable energy statistics data on the share of renewable energy recourses in total energy consumption are not available. The Statistical Office of the Republic of Serbia has to accept European methodology in the future and provide reliable data.

The most difficult task for Serbia in the future is creation of attractive conditions for future investments in this area. Also the preliminary evaluation of existing procedures for obtaining licenses for renewable energy sources projects confirmed that procedure is very complex. The visible improvement is made only in the area of small hydro power plant where new energy facilities will be built on rivers Ibar and Lim (Italian company SECI energy signed the contract). The main challenges which have to be solved in the future are: lack of experience, transition issues, lack of technical standard and procedures, permits and licenses.

23.4 Serbian New Role: Cooperation Instead a Source of Conflicts

The global community has fully recognized the immense humanitarian, political, and economic problems facing the countries in the region as a result of the various conflicts in which Serbia was involved. Both political and security future of the Balkans highly depend on the conditions of Serbian relations with neighbouring countries. In this moment, Serbia is a country which “promotes cooperation,

[10] The energy policy is implemented through the Energy Sector Development Strategy of the Republic of Serbia by 2015, Programme for Realizing the Energy Sector Development Strategy of the Republic of Serbia by 2015 for the period of 2007–2012 (“Official Gazette of RS”, No.17/07, 73/07, 99/09 and 27/10 of May 6, 2010) and the Energy Balance; The Law on the Ratification of the Statute of the International Renewable Energy Agency (IRENA) (“Official Gazette of the RS” – International Agreements 105/09 of December 24, 2009).

[11] The Treaty Establishing the Energy Community (“Official Gazette of RS”, No. 62/06 of July 27, 2006).

Table 23.2 Republic of Serbia – consolidated energy balance and indicators (Without the data for Kosovo because these data are provided by the competent body)

Energy Source (measured in tons)	Statistics		Forecasts	
	2002	2005	2008	2012
Primary energy production	7,843	8,485	9,411	11,070
Coal	5,975	6,564	7,369	8,480
Oil	667	665	660	1,000
Gas	268	233	201	400
Nuclear energy	0	0	0	0
Renewable energy sources	934	1,023	1,181	1,190
Hydro potential	934	1,023	869	1,010
Bio diesel	0	0	0	180
Firewood	0	0	306	
Wind	0	0	0	
Solar energy	0	0	0	
Geothermal energy	0	0	6	

The Republic Statistical Office

achieves visible progress on the path to the European Union and strives to improve the lives of the people." Serbia showed a willingness to be a "factor for peace, security, and stability in the Balkan region" and in the broader region.

The Republic of Serbia faces enormous economic, social and political problems partly contributed by the civil war and ethnic conflicts in the 1990s and its economic misfortune is further exacerbated by the current global economic recession. Despite all negative circumstances, Serbia creates national security policy which is completely in a function of making good neighbouring relation and cooperation in emergencies with international community.

The best example of that policy could be the final decision of Serbian policy makers in 2009. Instead of the earlier heterogeneous system which existed more than two decades as a communist heritage, Serbia established within the Ministry of Interior a special service, Sector for Emergency Management (SEM), a government institution responsible for the development of a protection and rescue policy. The Serbian National Assembly adopted the Law on Emergency Situations and the Law on Fire Protection [28]. In accordance with the Law on Emergency Situations a number of strategic documents and plans in the field of disaster and emergency management is adopted, such as: the National Strategy for Protection and Rescue in Emergencies, still waiting National Vulnerability Assessment and National Emergency Protection and Rescue Plan (Table 23.2).

The Sector for Emergency Management has been fully functioning since 1 July 2010. It consists of:

(a) In the Headquarters in Belgrade:

1. Department for Prevention
2. Department for Fire and Rescue Units
3. Department for Risk Management
4. Department for Civil Protection
5. National Training Centre

(b) Outside the Headquarters there are 27 units, organized as departments and sections. SEM has four departments for emergency management (Belgrade, Novi Sad, Nis, Kragujevac) and 23 sections for emergency management that monitor and manage emergencies on the district level. Heads of all units of SEM answer directly to the SEM Head, who is also Assistant Minister of Interior.

The Sector for Emergency Management of the Ministry of the Interior actively participates in the initiatives of regional and international organizations in the field of emergency situations and crisis management in activities of various international institutions and organizations, and one of it is the Black Sea Economic Cooperation (BSEC).

The cooperation which attracted the great attention in region, which still bears scars from past events, is those regarding the Russian Ministry of Civil Defence, Emergencies and Elimination of Consequences of Natural Disasters (EMERCOM).[12] In the summer of 2007, EMERCOM assisted Serbia infighting major forest fires and wildfires. Russian EMERCOM sent the Ilyushin 76 fire fighting aircraft, which was deployed in Serbia for a few days. In 2007 emergency services recorded 2021 forest fires, and burnt area was 32,136 ha [29].

The concept of the Emergency Centre in Nis was presented in Serbia and broader public. The Minister of Interior of the Republic of Serbia (MoI) Ivica Dačić, explained: the Centre would operate all year round. It would comprise the warehouses and storage rooms for keeping immediate material reserves, which are necessary for the protective and rescuing activities. Thus equipped the Centre would provide "constant repair and servicing, overhauling and maintenance of the emergency protective and rescuing equipment".

This centre could become a regional centre with the capacity of providing aid to the countries in the region of the Southeast Europe, but also to the countries of the European Union, in various emergencies: forest fires, open air fires, floods, earthquakes, landslides, chemical accidents and other civil emergencies. The Centre should be in charge in organization of various educations and training of fire and rescue units. The training and specialization courses for the protection and rescue forces in emergency situation would be organized for:

- The managers of professional services of defence and rescue.
- professionals in fire fighting and rescue units,
- commanders and members of headquarters for emergency situations,
- members of reserve specialized civil protection units,

[12] That cooperation starts by signed of Letter of Intent for cooperation in prevention of natural disasters and technological disasters and elimination of their effects, signed on 25 June 1996, and after that on 21 October 2009 the Russian EMERCOM and the Serbian Ministry of the Interior signed the Agreement on Cooperation. The President of the Russian Federation Dmitry Medvedev in Belgrade signed an agreement about establishing a common Serbian-Russian Emergency Center in Niš during his last visit.

- managers and persons in charge of institutions trained in defence and rescue, and commanders of territorial and industrial units of civil protection [30].

Serbia was active in the promotion of cooperation within the South East European Cooperation Process (SEECP). During its Chairmanship of SEECP 2011–2012, the RS among numerous goals paid considerable attention to the promotion of the raising the level of regional cooperation in the fields of environmental protection, prevention and elimination of the consequences of all types of disasters [31].

During the meeting of Foreign Affairs Ministers of the South East Europe Cooperation Process (SEECP), held in Belgrade, June 14, 2012) Serbian foreign minister Vuk Jeremic invited all countries in the region to participate in the establishing and operations of the Regional Russian Serbian Humanitarian Centre, which would thus become the "Balkan or Southeast European Emergency Centre".

Serbia has an urgent need to provide security of energy infrastructure, especially during and after the future implementation of the project "South Stream." This centre could be recognized as a valuable source for that "additional security" to the route of the expected gas pipeline. The reason for this is that Serbia does not have a precise legal framework in the area of protecting of "critical infrastructures" and legislative regarding this issue could be marked as confusing and far from many widely accepted approaches [32].

23.5 The Remaining Challenge: How to Move Forward Despite the Current Crises?

Serbia is facing the greatest budget deficit and the cease of negotiation with International Monetary Fund. In the revised Memorandum on budget and economy and fiscal policy for 2010, Serbia projects for environment protection spending about 0.3 % of GDP annually. On the other hand, according to the National Environment Protection Programme, which projected economic growth of 5 % annually, investing to environment protection should grow up to 1.2 % of GNP in 2014 and up to 2.4 % of GNP in 2019. Today when IMF decrease the predicted growth to 0, 1 %, despite Serbian prediction of only half of percent, it is clear that those previous predictions were far from reality.

Even before the global financial crises, Serbia needed a help in the environmental protection area. It is provided by a number of technical assistance projects and projects for strengthening capacities (CARDS, TAIEX, REReP (RENA), twinning projects and through cooperation within the International Commission for the Protection of the Danube River. EU and World Bank experts engaged in these projects usually provide advice and recommendations aimed at improving draft laws etc.

Financial assistance from the EU to Serbia is provided through the Instrument for Pre-accession Assistance (IPA). The IPA was and still is a potential source of funding for urban wastewater management projects, under the condition that a

reform of the public utilities is carried out addressing cost-recovery issues. For the 2007–2009 periods, the EU has supported seven projects totalling 33 M €.

The regional cooperation programmes are implemented through multi-beneficiary IPA (MB IPA), complementary to national IPA programmes for particular countries and its aim is assistance to regional initiatives with the purpose of improvement of collaboration between countries of the region and cooperation with Member States. International Financial Institutions (IFIs) and bilateral assistance amounted to 130 M € in 2005, of which 4.9 M € (or 3.1 %) was for environmental protection. Of this amount, 3.1 M € (or 63 %) went to water-related projects. Japanese government provide preferential loans totalling 400 M € equivalents, for a waste water treatment in Belgrade and several other municipalities in Serbia.

Based on data provided in the document "Technical Assistance for Development of a national Environmental Approximation Strategy – Water sector-draft 2011" the capital investment challenge estimated (in prices actual in that time) in the Serbia was:

- 1.3 billion Euros for Drinking Water Supply
- 3.3 billion Euros for Urban Wastewater Collection and Treatment
- 0.8 billion Euros for Nitrates (agricultural pollution) [33].

The promoted principle of sustainable development in the future will become unrealistic goal if the investors do not recognize Serbia as an area where the things are favourable for their future activities.

23.6 Conclusion

This paper focused on the Serbian efforts to decrease the impact of environmental risks in its territory and broader Black Sea region. Presented data confirmed the need of special attention which should be given to the most visible problems in environmental protection (nitrate pollution, waste water treatment, using renewable energy sources) and rehabilitation of existing environmental hot spots. Moreover, the security challenge rose from the objective to provide environmental and energy security need comprehensive approach to conflict prevention, crisis management and so needed post-conflict reconstruction as a key proponent of effective multilateralism in the Balkan region.

The Serbian policy highlighted the need of cooperation and trust on external relations with neighbouring countries as a prerequisite for full membership in European Union. Among all, Serbia enhances international cooperation on the detection and monitoring of the environmental threats related to the Danube protection, prevention, preparedness, and mitigation and response capacities in broader Black Sea region. Serbia promote the development of regional security scenarios for different levels of presented risk and their implications for regional security ready at the same time to offer all available capacity.

During all these actions it must be noted that Serbia still lacks: financial means, modern governance, responsible natural resource management, technology transfer, trans-boundary environmental cooperation, institutional strengthening and capacity building for crisis management, adequate resource planning, climate-sensitive policy and equality and favourable conditions for foreign investment and has to work on improvement its current state.

The Sector of Emergency Management should be the lighthouse for other stakeholders. It has the capacity to become a modern European service and leading service in the region, with the capacity to assist neighbouring countries in times when they are affected by disaster.

Acknowledgements Kindly support and encouragement of distinguished professor T. Nejat Veziroglu deserves the greatest acknowledgement.

References

1. Black Sea Economic Cooperation (BSEC). Available at: http://www.bsec.organization.org
2. Document Press Release on the 26th meeting of the council of ministers of foreign affairs of the organization of the Black Sea Economic Cooperation (Belgrade, 11 June 2012). Available at: http://www.bsec-organization/bsecnews/PressReleases/PressReleases/Press%20ReleaseEnglish/11%20June%202012.pdf
3. Radovic V, Komatina S (2011) Sanation of ecological black points or green investment-Serbian choice? In: Proceedings of the 2rd international professional conference, Zlatibor, Serbia
4. Response to the EU Questionnaire for the Member States on Experiences (2011) Chapter 27 Environment. Questionnaire on addressing new and emerging challenges. www.serbia.gov.rs/?change_lang=en
5. Invitation on ARW workshop in Batumi. Available at web site http://blackseaenergy2012.ge/index.php?option=com_content&view=article&id=57&Itemid=66
6. Petrov K, Baykara SZ, Ebrasu D, Gulin M, Veziroglu A (2011) An assessment of electrolytic hydrogen production from H2S in Black Sea waters. Int J Hydrog Energy 36:8936–8942
7. The National Sustainable Development Strategy for the period 2009–2017 (hereinafter referred to as: NSDS) was adopted in May 2008 (Official Gazette of RS No. 57/08).
8. Radovic V, Komatina Petrovic S (2012) From failure to success: Serbian approach in mitigation of global climate change and extreme weather events. J Environ Prot Ecol 4(13) (in press)
9. Radovic V (2012) Climate change and adoption strategies: a report from the Republic of Serbia. In: National security and human health implications of climate change, NATO science for peace and security: series C environmental security. Springer, Dordreht, pp 95–102
10. Global risk identification program (GRIP) (2010) Serbia assessment report. For a purpose of regional program on disaster risk reduction (DRR) in South East Europe, sponsored by WMO/UNDP Joint activities. http://www.gripweb.org/~gripwebo/gripweb/sites/default/files/Serbia%20assessment%20report%20from%20government%20input_SRBinput_0.pdf
11. Serbian First National Communication to the UN FCCC
12. Radovic V, Andrejevic A (2011) The unknowns about the role of public-private partnership in disaster management process in the Republic of Serbia. Poslovna ekonomija 9(2):365–381
13. Constitution of the Republic of Serbia, Official Gazette of the RS, No. 98/06
14. The law on determining the jurisdiction of the autonomous province of Vojvodina, Official Gazette of RS, No. 6/02

15. The law on establishing competences of the autonomous province of Vojvodina, Official Gazette RS, No. 99/09
16. Radovic V (2012) Protecting and improving water quality in Vojvodina. In: Vitale K (ed) Environmental and food safety and security for South-East Europe and Ukraine, NATO science for peace and security: series C environmental security. Springer, Dordreht, pp 189–202
17. www.icpdr.org/main
18. Radovic V, Jovanovic L, Hrabovski E (2011) Tomic: Methods for mitigation of environmental risks to the AP Vojvodina environment. Ecologica 18(63):383–390
19. Serbia Danube River enterprise pollution reduction project. Available at http://archive.iwlearn.net/www.drepr.org/
20. The law on waters ("Official Gazette of the Republic of Serbia", No. 30/2010) [in Serbian]
21. The official report of Serbian environment (2011) http://www.unece.org/env/epr/epr_studies/serbiaII.pdf
22. The law on integrated pollution prevention and control (Official Gazette of the Republic of Serbia no. 135/04)
23. National environmental approximation strategy for the Republic of Serbia ("Official Gazette of the Republic of Serbia", No. 80/2011)
24. Serbian Environmental Protection Agency (SEPA) (2009) The official report about environmental state in 2009. Serbian Environmental Protection Agency, Ministry of Environment, Mining and Spatial Planning, Belgrade, Serbia
25. Water master plan for the Republic of Serbia ("Official Gazette of the Republic of Serbia", No. 37/2002)
26. Strategy of water supplying and water protection in APV (2007) The provincial secretary for science and technological development and mathematical faculty, Institute for Chemistry, Novi Sad, Serbia
27. Radović V, Domazet S (2010) Uloga privatizacionog procesa u Republici Srbiji u funkciji ugrožavanja bezbednosti građana i životne sredine – drastični primeri. Poslovna ekonomija. No. 2, Str. 151–169
28. Serbian Environmental Protection Agency (SEPA) (2009) The official report about environmental state in 2009. Serbian Environmental Protection Agency, Ministry of Environment, Mining and Spatial Planning, Belgrade, Serbia
29. Radovic V, Vitale K, Tchounwou PB (2012) Health facilities safety in natural disasters: experiences and challenges from South East Europe. Int J Environ Res Public Health 9(5):1677–1686
30. Radovic V (2010) Forest fires in the Republic of Serbia in 2007 and 2008. Training in disaster planning and management at the Humphrey fellowship program's enhancement activity, New Orleans and Hurricane Katrina: a disaster planning workshop. Tulane University, 31 January to 5 February 2010
31. Karabasil D, Radović V (2010) Is there a need to improve the fire service in the area of emergency management within the Republic of Serbia. Proceedings of international scientific conference, fire engineering; 2010 October 5–6; Zvolen, Slovenia. Zvolen: Technical University in Zvolen, Faculty of Wood Sciences and Technology, Department of fire protection
32. Serbian priorities in the South East European Cooperation Process (SEECP). http://www.mfa.gov.rs/Policy/Priorities/seecp/PRIORITIES.SEECP%202011%2011.07.11.pdf
33. Radovic V, Keković Z (2012) Improving corporate sectors responses to extreme weather events in the Republic of Serbia. In: Čaleta D (ed) Corporate security in dynamic global environment. Institute for Corporative Security Studies –ICS, Ljubljana, pp 215–226

Chapter 24
Numerical Modeling of Spilled Oil Seasonal Transport Processes Into Georgian Coastal Zone of the Black Sea

D.I. Demetrashvili and Teimuraz P. Davitashvili

Abstract In this study, spreading of the oil pollution in the Georgian Black Sea coastal zone on the basis of a 2-D numerical model of distribution of oil pollution is simulated. The model is based on a transfer-diffusion equation with taken into account reduction of oil concentrations because of physical – chemical processes. The splitting method is used for solution of the transfer-diffusion equation. Numerical experiments are carried out for different hypothetical sources of pollution in case of different sea circulation regimes dominated for the four seasons the Georgian Black Sea coastal zone. Some results of numerical experiments are presented.

Keywords Regional circulation • Oil spill • Splitting method

24.1 Introduction

In the last decades, study on regularities of space-temporal distribution of anthropogenic admixtures in the Black Sea have become extremely important and urgent, because of the sharp deterioration of an ecological situation of this unique sea basin. Among different pollutants, oil and oil products present the most widespread and dangerous kind of pollution for World's oceans, including the Black Sea [1–3]. They are able to cause significant negative changes in hydrobiosphere and infringe natural

D.I. Demetrashvili
M. Nodia Institute of Geophysics of I. Javakhishvili, Tbilisi State University,
1, M. Alexidze str., Tbilisi 0171, Georgia
e-mail: demetr_48@yahoo.com

T.P. Davitashvili (✉)
I. Vekua Institute of Applied Mathematics of I. Javakhishvili, Tbilisi State University,
2, University str., Tbilisi 0186, Georgia
e-mail: tedavitashvili@gmail.com

A. Veziroğlu and M. Tsitskishvili (eds.), *Black Sea Energy Resource Development and Hydrogen Energy Problems*, NATO Science for Peace and Security Series C: Environmental Security, DOI 10.1007/978-94-007-6152-0_24,

exchange processes of energies, and substances between the sea and atmosphere. Potentially the most dangerous regions, from the point of view of oil pollution, are coastal zones of the sea, which are exposed to significant anthropogenic loadings [4–9]. Oil and mineral oils spilled into the Black Sea have toxic influence upon the groups of sea organisms, on the coastal area and on the environment. Therefore, it is necessary to define the zone of possible spreading of oil pollution upon the area of sea-water and on shore. The basic mechanisms of distribution of oil spill in water basins are described in [5–9], except for transport and turbulent diffusion processes, evaporation, dispersing, emulsification and dissolution are a concern to main physical and chemical processes during the first several days after spillage. Besides, there is a number of longer biochemical processes: photo and self-oxidation, biodegradation, and sedimentation on a sea bottom, whose contribution to the process of transformation of oil slick are less important in comparison to the above mentioned processes per the first days after oil spillage. Considerable amount of publications are devoted to modeling of oil spill transport in the Black Sea and other seas [4], [7–19]. In [4] a 3-D coupled flow/transport model has been developed to predict the dynamics of the Black Sea and dispersal of oil pollution. The transport module of the model used Lagrangian tracking to predict the motion of individual particles. Currents used in the model have been generated by high resolution, low-dissipative numerical circulation model, DiaCAST [20] implemented for the Black Sea. In [7, 9, 10] the same flow/transport model is used to predict the transport and dispersal of oil spill in coastal waters of the Caspian Sea, but currents and turbulent diffusivities used in the model are generated by the Princeton Ocean Model (POM) implemented for the Caspian Sea [21]. Danish Meteorological Institute (DMI) has developed an improved version of oil drift model based on a 3-D current field [14]. The model is a 3-D oil drift and fate model based on a 3-D ocean circulation model [22]. In [15] the integrated modeling system for weather, currents and wind waves coupled with oil slick transport are developed. The local area weather forecasting model MM5 is used for operational forecasts in the Black Sea region [23], which is coupled with a 3-D hydrodynamics and sediment transport model, and with the third –generation wave model WAVEWATCH III [24]. Météo-France has developed an oil spill response model (MOTHY), designed to simulate the transport of oil in three dimensions [16–18]. Creation of the forecasting system of the Black Sea dynamics for the easternmost part of the Black Sea, which is one of the parts of the basin-scale Black Sea now casting/forecasting system [25, 26] gives real possibility to develop the coupled forecasting system of oil spill transport in the eastern coastal area of the Black Sea.

The main goal of the present chapter is to investigate numerical features of hypothetical oil spill transport under different circulation conditions in the Georgian water area of the Black Sea. With this purpose, a 2-D numerical model of oil spill transport on the sea surface and some results of its implementation for the Georgian coastal area of the Black Sea, under concrete circulation modes are discussed. The circulation modes are predicted from the regional forecasting system using real input data.

24.2 Data and Methodology

The regional domain, which was limited by Caucasus and Turkish shorelines and the western liquid boundary coinciding with a meridian of 39.36 °E was covered with a grid having 193 × 347 points and grid step equal to 1 km spacing. The modeling approach to carry out numerical investigations of oil pollution in the considered water area under typical regional circulation conditions is based on a finite-difference solution of a 2-D nonstationary advection-diffusion equation for a non conservative substance. Flow and turbulence fields were used as simulation of oil spill transport present prognostic fields calculated from the coastal forecasting system of the Black Sea state [25, 26]. The model of oil spill transport takes into account: configuration of the considered sea water area, advection, turbulent diffusion; evaporation and other physical and chemical factors are taken into account parametrically by inclusion in the transfer-diffusion equation of a term containing parameter of non-conservatively.

The numerical model requires the following input data: sea bottom topography (by which configuration of the considered area is defined), coordinates of the location of the pollution source, power and duration of action of the pollution source, flow velocity components and the parameter of non conservatively describing change of oil concentrations due to different factors. The sea surface of the considered regional area was covered with a regular grid having the amount of points of 193 along x axis and 347 points – along y axis (x is directed eastward, y – northward) with the grid step $\Delta x = \Delta \mathrm{y} = 1\mathrm{km}$. In concrete numerical experiments were accepted: $a = 1$, $b = 0$, $\beta = 0$. After formation of oil spill on the sea surface, there is intensive evaporation of light fractions of oil, which is an initial process of removal of oil from the sea surface.

In consideration of the above mentioned, in the numerical experiments described below the parameter of non conservatively $\sigma = 8,023.10^{-6}\mathrm{s}^{-1}$ at $\mathrm{t} \leq 24$ h was accepted, which corresponds to lost of oil mass by 50 % during the first day. It was supposed that on the second and third days of integration reduction of oil concentrations caused by above factors was slowed down and accordingly was accepted $\sigma = 4,011.10^{-6}\mathrm{s}^{-1}$ at $\mathrm{t} > 24$.

24.3 Model Description

After the oil slick is formed under the influence of gravity, viscosity and surface tension forces, it begins migration and changes its sizes and configuration under the effect of hydrodynamic factors – advection and turbulent diffusion. Simultaneously oil slick on the sea surface undergoes physical and biochemical transformations. The oil slick transformation processes may be described by the advection-diffusion

equation. In a two-dimensional bounded area Ω with a lateral surface S the spreading of a substance we will describe by the advection-diffusion equation:

$$\frac{\partial \varphi}{\partial t} + \frac{\partial \mathrm{u}\varphi}{\partial \mathrm{x}} + \frac{\partial \mathrm{v}\varphi}{\partial \mathrm{y}} + \sigma\varphi = \frac{\partial}{\partial x}\mu_\varphi \frac{\partial \varphi}{\partial x} + \frac{\partial}{\partial y}\mu_\varphi \frac{\partial \varphi}{\partial y} + f \tag{24.1}$$

with the following boundary and initial conditions:

$$a\left(\mu_\varphi \frac{\partial \varphi}{\partial n} - \beta\varphi\right) + bQ = 0, \quad \text{on} \quad S \tag{24.2}$$

$$\varphi = \varphi^0, \quad \text{at} \quad t = 0. \tag{24.3}$$

Here φ is the volume concentration of a substance; u and v are the components of the current velocity vector along the axes x and y, respectively; μ_φ is the coefficient of turbulent diffusion; n is the vector of the outer normal to S; $\sigma = ln\ 2/T_0$ is the parameter of non-conservatively, which parametrically describes changeability of concentration, because of physical and biochemical factors; T_0 represents a time interval, during which the initial oil concentrations decrease two times; in general, f describes the space-temporal distribution of a source power, which in case of the point source may be represent by the delta function:

$$f = Q\delta(x - x_0)\delta(y - y_0) \tag{24.4}$$

where x_0 and y_0 are coordinates of a location of the source. a and b are set factors accepting values either unit, or zero; β is parameter of interaction of an impurity with the appropriate lateral surface. Q is power of emission of an impurity from a source. The turbulent diffusion coefficient was calculated by the formula [27]:

$$\mu_\varphi = \mu/c_\varphi, \mu = \Delta x \Delta y \sqrt{2\left(\frac{\partial u}{\partial x}\right)^2 + \left(\frac{\partial u}{\partial y} + \frac{\partial v}{\partial x}\right)^2 + 2\left(\frac{\partial \mathrm{v}}{\partial \mathrm{y}}\right)^2} \tag{24.5}$$

where Δx and Δy are horizontal grid steps along x and y axes, respectively; μ is the coefficient of turbulent viscosity; c_φ is some constant.

24.4 Simulation of Oil Spill Transport

The offered mathematical model (24.1), (24.2), and (24.3) was used to carry out numerical experiments with the purpose of simulating accidental oil spill transport on the Black Sea surface for different real local circulation conditions in the Georgian water area. Simulation and forecast of regional dynamical processes

performed within 2010–1012 on the basis of the regional forecasting system showed that the easternmost part of the Black Sea is dynamically a very active water area, where different types of regional circulation are taking place throughout the year. In performed numerical experiments accidental oil spill in the sea occurred within 2 h in amount of 50 or 80 tones. The oil spill was considered as a point source, which was located in different points of the coastal sea area.

24.4.1 Oil Slick Drifting Under January Circulation

Numerical experiments performed in the case of circulation corresponding to 18 January 2012, showed that at an accidental flood of oil, even on some 10 km in the distance from Batumi or Poti ports, the oil slick can reach to the coast of Georgia for 2–3 days. Figure 24.1 illustrates drifting of oil slick in the case, when accidental oil slick in amount of 50 tones occurred with distance about 40 km from the Georgian shoreline in the water area between Batumi and Poti ports. From Fig. 24.1 it is visible that under the influence of the current oil pollution approaching to the coast of Batumi region, is expanded simultaneously due to turbulent diffusion.

At 48 h after the oil release the area of oil pollution can be observed near Georgian coast. In due course, the oil concentrations decrease as a result of diffusion expansion and physical-biochemical transformation

24.4.2 Oil Slick Drifting Under March Circulation

The presence of jet-like stream, which plays a role of a divider between the near shore zone and other water area, considerably influences the process of distribution of oil pollution in the Georgian water area. A numerical experiment was performed when oil spill points where located in the area of the jet stream. In the first case, the point source was located approximately at latitude 42.5 °E on minimal distance of 33 km from coastline, (the source coordinates: 124 Δx, 166 Δy) and in the other one – location of the point of oil flood was at the same latitude as in the previous numerical experiment with January circulation, but more close to the Georgian coastline – between Batumi and Poti area on distance of 20 km from coastline. Results of calculations have shown that the jet current predetermines trajectory of oil slicks, and in this case the accidental oil spillage does not create danger to the Georgian coast even in that case, when the oil flood has taken place on distance of 20 km from the coast. In the other numerical experiment, the pollution source with coordinates 177 Δx, and 55 Δy was in the right party from the jet current close to the Batumi port with a distance of 15 km from shoreline. Results of calculations have shown that in this case accidental oil spill represents serious danger for trhe Batumi coast region.

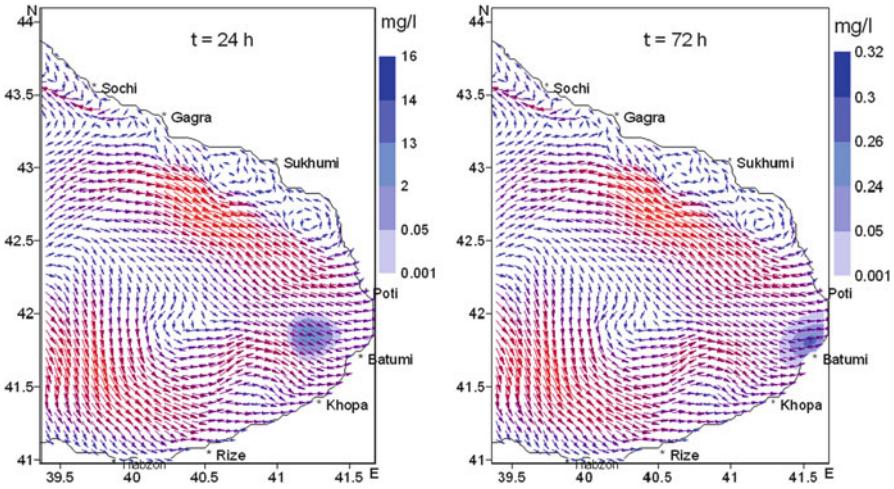

Fig. 24.1 Simulated oil spill at different time moments moving under 18 January 2011 circulation. The source coordinates: 142Δx and 105Δy. 50 tones were released in 2 h (*see color plates*)

24.4.3 Oil Slick Drifting Under August Circulation

In one of the numerical experiments (spreading of oil pollution under circulation corresponding to 7 August 2010) the location of the pollution source was the same as in the numerical experiment under March circulation, where the coordinate of the point source was: 124 Δx and 166 Δy. This point is located in the northeastern part of the Batumi eddy, where peripheral flow is directed to the southeast. Results of calculations for these two cases have shown the different character of pollution distribution. Unlike spring circulation, in the August case oil spillage moves to the south but the stain cannot reach the coast of Georgia. The reason is that peripheral current of the Batumi eddy, which passes approximately on distance of 10–12 km from the coastline. In the other numerical experiment, the accidental oil spill has occurred close to the shoreline in Batumi water area. The point source was located out of the Batumi eddy in the narrow zone of vortex formations. The source coordinates were 177 Δx and 105 Δy. The results of the calculations have shown that the oil slick already reaches the coast of Georgia and pollutes the water.

24.4.4 Oil Slick Drifting Under September Circulation

The specific circulation structure corresponding to 25 September 2011 causes specific character of oil distribution. Figure 24.2 illustrates the penetration of oil pollution to the Poti and Batumi coastal regions, when coordinates of location of pollution sources were: 157 Δx, 142 Δy, respectively. It should be noted that the same numerical experiment with the source coordinates 157 Δx and 105 Δy have been performed under August circulation and results were different.

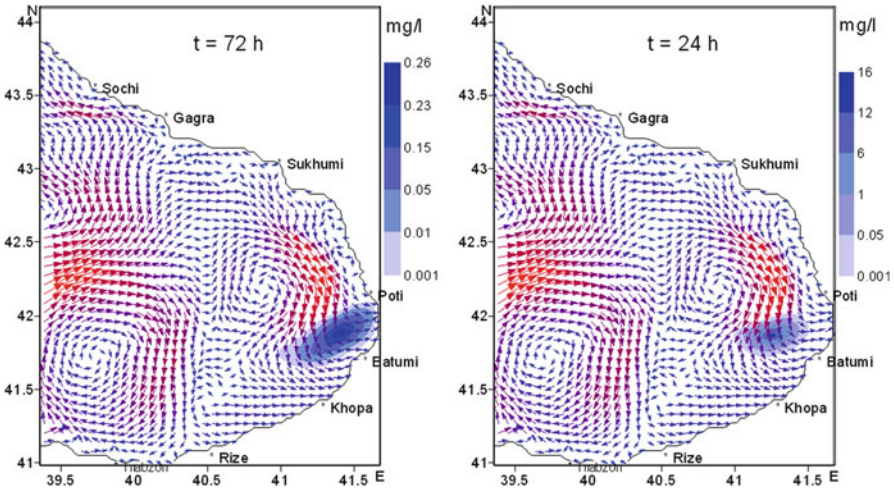

Fig. 24.2 Simulated oil spill at different time moments (after the release) moving under 29 September 2011 circulation. The source coordinates: 157Δx and 105 Δy. 50 t. oil was flooded in 2 h (*see color plates*)

24.5 Conclusions

The analysis of surface flow fields in the easternmost part of the Black Sea shows that in many cases the narrow zone with width of about 20–25 km along the Caucasian shorelines is formed, which is characterized by the clear tendency to vortex formation of very small sizes and nonstationarity. This zone interferes with penetration of waters from area taking place outside this zone, therefore in case of accidental oil spill outside this zone, the danger of pollution of coastal waters decreases. For example, this phenomenon is clearly observed at summer circulation, which is characterized by formation of the Batumi anticyclonic eddy in the considered water area. The formed near shore zone of vortex formation does not let an oil spillage to reach to the coast of Georgia. However, if pollution source is in the area of the Batumi eddy, but if the accident occurred in the narrow near shore zone of vortex formation, it creates danger for the coastal waters, especially, larger danger for the coastal zones, if structure of the regional circulation is characterized by a dominant direction to the Georgian coast (Fig. 24.1). If the accidental release occurred in the central area of the vortex formation, a steady zone of pollution is created, the high concentrations are located in this part, and are not distributed in the next areas.

When computing the distribution of oil pollution at real emergencies, the results will be strongly dependent from of a real circulating mode, which will be formed in the Georgian water area at the moment of the oil flood in the next few days.

Acknowledgements The authors were supported by the Shota Rustaveli National Science Foundation Grant #GNSF/ST09/5-211.

References

1. Osokina NP (2004) Influence of agricultural contamination on ecological safety of coastal and shelf zones (the northwest Black Sea as example). J Ecol Saf Coast Shelf Zones 10:453–458 (in Russian)
2. Dahlin H (2005) Black Sea oil drift forecasting system. Special support actions, EuroGOOS Office, 36 p
3. Mironescu L (2008) The fight against harm to the environment in the Black Sea. Parliamentary Assembly Recommendation 1837, Doc. 11632. http://essembly.coe.int
4. Korotenko KA, Dietrich DE, Bowman MJ (2003) Modeling circulation and oil spill transport in the Black Sea. J Okeanologia 43:367–377 (in Russian)
5. Zhurbas BM (1978) The principle mechanisms of oil distribution in the sea. J Mech fluid Gas 12:144–159 (in Russian)
6. Chemistry of Ocean. T. 1 (1979) In: Bordovski OK, Ivanenkov BN (eds) Moscow, Nauka, 518 p (in Russian)
7. Korotenko K, Mamedov RM, Mooers CN (2001) Prediction of the dispersal of oil transport in the Caspian Sea resulting from a continuous release. J Spill Sci Technol Bull 6:323–339
8. Vragov AV. Methods of detection, estimation and liquidation of emergency floods of oil, Novosibirsk, 224 p (in Russian)
9. Korotenko KA, Mamedov RM, Mooers CN (2002) Prediction of the transport and dispersal of oil in the south Caspian Sea resulting from Blowouts. J Environ Fluid Mech 1:383–414
10. Korotenko KA, Mamedov RM (2001) Modeling of oil slick transport processes in coastal zone of the Caspian Sea. J Oceanol 41:37–48
11. Practical Ecology of Marine Regions (1990) The Black Sea. Naukova dumka, Kiev, 252 p, (in Russian)
12. Reed M, Johansen O, Brandvik PJ, Daling P, Lewis A, Fiocco R, Mackay D, Prentki R (1999) Oil spill modelling toward the close of the 20th century: overview of the state of the art. J Spill Sci Tech Bull 5:3–16
13. Jones B (1999) The use of numerical weather prediction model output in spill modelling. J Spill Sci Tech Bull 5:153–159
14. Christiansen BM (2003) 3D Oil drift and fate forecast at DMI. Technical Report No03-36. Danish Meteorological Institute, Denmark
15. Brovchenko I, Kuschan A, Maderich V, Shliakhtun M, Yuschenko S, Zheleznyak M (2002) The modeling system for simulation of the oil spills in the Black Sea. In: Proceedings of the 3rd EuroGOOS conference, Athens/Greece, 3–6 December 2002
16. Daniel P (1995) Numerical simulation of the Aegean Sea oil spill, pp 894–896. http://www.meteorologie.eu.org/mothy/references/iosc1995.pdf
17. Daniel P, Poitevin J, Tiercelin C, Marchand M (1998) Forecasting accidental marine pollution drift: the French operational plan. Computational Mechanics Publications, WTT Press, p 43–52
18. Chune SL, Drillet Y, Daniel P, Mey PD (2010) Improving operational oceanography for drift applicants. Ocean sciences meeting. AGU, Portland
19. Galabov V (2011) Oil spill drift operational forecasts for Bulgarian coastal area and numerical study of potential oil pollution in the bay of Burgas. Abstracts of 3rd Bi-annual BS scientific conference and UP-GRADE BS-SCENE project joint conference. Odessa, Ukraine, 1–4 November 2011
20. Dietrich DE, Lin CA, Mestas-Nunez A, Ko DS (1997) A high resolution numerical study of Gulf of Mexico fronts and eddies. J Meteorol Atmos Phys 64:187–201
21. Grell G, Dudhia AJ, Stauffer DR (1994) A description of the fifth-generation Penn State/NCAR mesoscale model (MM5). NCAR technical note. NCAR/TN-398 + STR
22. Tolman HL (1999) User manual and system documentation of WAVEWATCH-III version 1.18, NOAA/NWS/NCEP/OMB Technical Note 166

23. Blumberg AF, Mellor GL (1987) A description of a three-dimensional coastal ocean circulation model. AGU, Washington, DC, 4, 1
24. Kordzadze AA, Demetrashvili DI (2010) Some results of forecast of hydrodynamic processes in the easternmost part of the Black Sea. J Georgian Geophys Soc 14b:37–52
25. Kordzadze AA, Demetrashvili DI (2011) Operational forecast of hydrophysical fields in the Georgian Black Sea coastal zone within the ECOOP. J Ocean Sci 7:793–803. www.ocean-sci.net/7/793/2011/
26. Zilitinkevich SS, Monin AS (1971) The turbulence in dynamical models of the atmosphere Leningrad, Nauka, p 44 (in Russian)
27. Marchuk GI (1982) Mathematical modeling in the environmental problem. Moscow, Nauka, p 320 (in Russian)

Chapter 25
The Ecological Evaluation River Basins in West Georgia

Katerina Verbetskaya, N. Klymenko, and N. Voznyuk

Abstract The Black Sea is on the marine arias of the world, most damaged by human activities. The high degree of isolation from the world ocean, the extensive drainage basin and the large number of incoming rivers – all contribute to the unique water balance of the Black Sea. In this work, we have attempted the regulation implementation of the Water Framework Directive of the European Union (2000/60/EU) for Western Georgia area in the framework of implementation of the water management basin principle.

Keywords Black Sea • Hydro morphological assessment • River flow • Water quality • Oil products

25.1 Introduction

The Black Sea region becomes increasingly an important element of economic and geopolitical structure of the international community. Its role will increase in the twenty-first century, especially in the context of international transport corridors development, the absorption of seabed carbonic resources, more efficient use of recreational resources of the seacoast. Obviously, the Black Sea is on the verge of a new stage of intensification of human pressure on its ecosystem. Ecological losses will be accompanied by economical ones, because of sharp decrease of its natural resources potential.

Unsatisfactory ecological state of the Black Sea is based on the polluting substances dilatation over the assimilative capacity of marine ecosystems, which led to sweeping changes in ecosystems of seas and in coastal zone [1–4]. The vast

K. Verbetskaya (✉) • N. Klymenko • N. Voznyuk
National University of Water Management and Nature Resources Use,
Rivne, Ukraine
e-mail: VKU_rovno@ukr.net

A. Veziroğlu and M. Tsitskishvili (eds.), *Black Sea Energy Resource Development and Hydrogen Energy Problems*, NATO Science for Peace and Security Series C: Environmental Security, DOI 10.1007/978-94-007-6152-0_25,

majority of pollutants of the Black Sea (369 km^3/rik) come from a river runoff of the entire basin – the area of almost 20 industrial countries of Europe. River runoff among the Black Sea countries divides in such a way: 1.8 km^3 of river water (1.9 %) comes from the territory of Bulgaria to the Black Sea annually; from Georgia – 46 km^3 (13.2 %), Romania – 0.12 km^3, an average annual flow of the Danube river is 200 km^3/per year (57.5 %), Turkey – 48.0 km^3 (10.9 %); Russia – 6.5 km^3 (1.9 %), Ukraine – 55.5 km^3 (15.9 %), Crimea – 0.32 km^3 (0.08 %) [5–7].

The key point in the development of environmental cooperation in the Black Sea region was the formulation and the adoption of the Convention on the Protection of the Black Sea Against Pollution (Bucharest 1992) and the signing of the Strategic Action Plan (SAP, Istanbul, 1996) based on the Trans boundary Diagnostic Analysis (TDA) [8–11]. According to the list of TDA, the most dangerous types of pollution of the Black Sea waters were marked, which are: oil, nitrogen and phosphorus compounds, pesticides and heavy metals, radioactive wastes, exotic flora and fauna introduction, and solid waste.

The present work represents the first integrated analysis of the anthropogenic factors impact on the environmental condition and the quality of the surface water in the basins of the West Georgia Rivers. The research is aimed at the support of the accomplishment of the internationally important tasks established by the EU Water Framework Directive [12], the Decision of the United Nations Framework Convention on Climate Change (2002), and The Convention on the Protection of the Black Sea Against Pollution (1996).

25.2 River Typology of Western Georgia

In this day and age, Water Framework Directive of the European Union (EU WFD) regulates the necessity of creating the typology (classification) for all water bodies [12]. Typology is one of the first steps for practical implementation of the Directive in the territory of Georgia. The results of determination of ecological status of surface water bodies depend on this aspect. The main purpose of typology is the identification of type-specific conditions, which in its turn, are the first ones in ecological classification.

The typology, created by us, covers the marine facilities only of one category – the river. In general, we dealt with 32 rivers in Western Georgia, 22 of which were classified, catchment basin of the rivers is more than 55 thousand of km^2 [13].

On creating the river typology of Western Georgia, the first step was the selection of Eco region according to geographical area (Annex XI WFD EU, the map A [12]). Bodies of water of investigated area belong to Eco region 24 – the Caucasus.

Bodies of water of West Georgia were divided by us into types using obligatory (height above sea level basin, catchment basin, geology) and one additional descriptor from a number of non-obligatory (type of watercourse), in other words, we used the system B of the Water Framework Directive EU.

After realization of typification according to four selected descriptors within the Western Georgia, we have marked 13 abiotic river types of water bodies [13]. At this stage, performed typology of Western Georgia Rivers is abiotic because it does not contain biotic component. From now on, it requires verification by biotic and chemical factors.

After the typification realization of the Western Georgia Rivers, we have selected five typical rivers, which characterize the state of water bodies of investigated area with account of type-specific conditions, that are usual for each of the selected objects: small lowland river Kubistskali; an average half mountain river Gubistskali; an average mountain river Tkibuli, large mountain river Kvirilia and a very large mountain river Rioni.

25.3 Assessment of Ecological State of Rivers in Western Georgia

During the last 20 years there was the transition to the assessment of ecological state of water bodies in European Union, starting with hydro morphological, chemical and physico-chemical quality elements supporting the biological one. Therefore, we investigated changes of abiotic characteristics of typical river basins of the region, because the Mountain Rivers are specific water bodies, which fall under anthropogenic influence in a strong way, the effects of which appear in the chemical composition of water as well as in overbank complexes.

25.3.1 Hydro Morphological Assessment of Typical River Basins of West Georgia

Hydro morphological river quality assessment is an integral part of WFD EU for the European Union Countries and is a basic component in water bodies' investigation, which determines biotic groups and the whole river ecosystem functioning [12]. Hydro morphological assessment enables us to evaluate changes in overbank complexes of water flows under the influence of human activities, such as agricultural land development, urban development, transport routes of railways and bridges set-up, coast protection etc.

Hydro morphological assessment of basin state is made in five grades according to the European standard CEN 14614 "Water quality – The main assessment standard of hydro morphological river criteria" and methods of Slovakia [13–16], using satellite images Landsat-7, Google Earth maps and topographic maps.

The results of hydro morphological assessment of typical rivers state show, that for most of the areas in uprivers (mountain area) the most common is excellent hydro morphological quality grade, which is close one to the referential conditions.

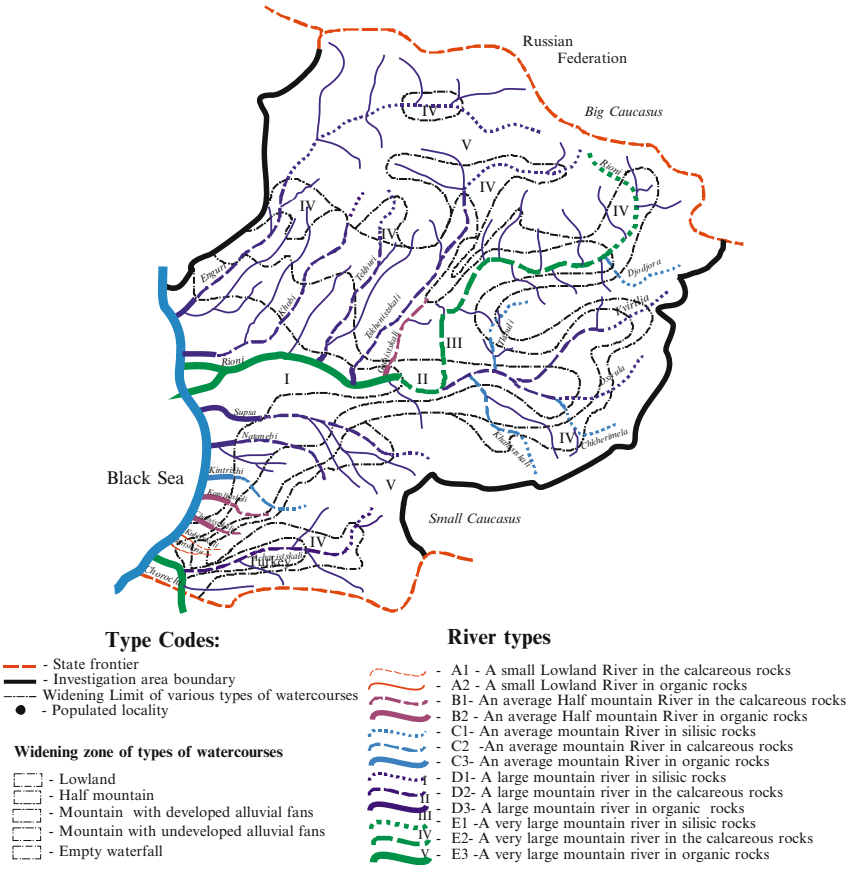

Fig. 25.1 Mapchart of river typology of Western Georgia (*see color plates*)

However, downstream (piedmont and lowland conditions), hydro morphological quality grade worsen to a good and satisfactory (in the areas of urban development, transport routes, coast protection works, and significant agricultural use of basin area) (Figs. 25.1 and 25.2).

25.3.2 Ecological Assessment of Surface Waters Quality of West Georgia Rivers

Assessment of surface water quality of river water bodies is one of the obligatory components determining its ecological state. Since the EU WFD requires ecological assessment of surface water quality with five grades of quality and to assess changes of surface waters quality of West Georgia rivers, we used the technique

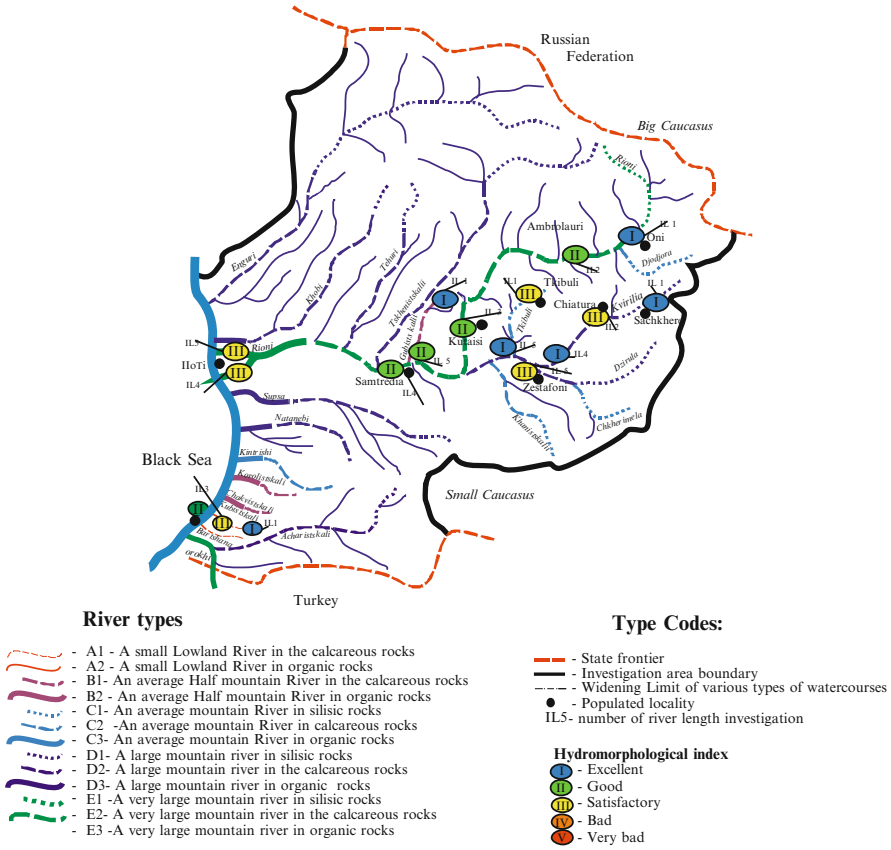

Fig. 25.2 Hydromorphological assessment of typical rivers of Western Georgia (*see color plates*)

of "Simplified ecological assessment of quality of surface waters of dry land and estuaries of Ukraine" (КНД 211.1.4.010-94) [17], which follows these requirements.

Using a detailed ecological assessment of typical rivers quality of Western Georgia, we have analyzed all three blocks of indexes: salt content, trophic-saprobic (ecological – sanitary) and specific indexes of toxic action. Baseline data for ecological quality assessment of surface water basins in Western Georgia are provided by hydro-meteorological services of Georgia.

Analyses of the results of surface water quality assessment make it possible to draw the conclusions, equal for all the five typical rivers of Western Georgia [18–20]:

1. River waters according to content of salt components belong to a category 1 – fresh α-hypohal, carbonate hydrogen grade, magnesium and calcium groups, type 1 – C_{ICaMg}.

2. Analyzing the trophy-saprobic block indexes we found out, that water bodies of the region belong to the α- mesosaprobic and polisaprobic zones and eutrophic, polytrophic and hypertrophic categories.
3. Assessment of toxic action indexes discovered a high content of SAS and oil products in river waters according to which surface waters belong to 4–5th categories of quality.

Formalized ecological assessment of surface water quality of the rivers of the region showed, that in the vast majority of the investigated section lines in the 1980s and early nineteenth century, they belonged to grade 5 (water quality is very bad and too bad) and, in the next years, up to 2008 there was a period of significant improvements to grade 3 (water quality is good and satisfactory) with subsequent worsening of the V-grade quality.

During the selected period, typical indexes of trophy-saprobic block, namely, suspended matters and nitrogen compounds were determinative in water quality formation of the water bodies. Yet, in 1990s, the water quality of rivers Kubistskali and Tkibuli was formed by block of specific substances of toxic action (SAS, oil products, phenols).

Based on the results of ecological assessment of surface water quality during the period of 1985–2010 years we have developed Maps (Fig. 25.3), which show the block and generalized ecological indexes of surface water quality of typical rivers of Western Georgia in the form of circular diagrams.

25.4 The Pollutants Removal into the Black Sea with River Runoff of West Georgia

Georgia is the third of the six Black Sea countries in terms of water supply capacity, that enters the Black Sea. Large and small rivers of Kolhida Lowland, which belong to the Black Sea basin, are carrying with them 74 % of all pollutants from the territory of Georgia. Owing to fact, that 80 % of pollutants enter the sea with river runoff, the calculation of its removal to the Black Sea was made.

The Calculation of pollutants removal to the Rioni River from its inflows to the Black Sea with rivers Rioni, Bartshana and Kubistskali was conducted by a formula based on data on concentrations of pollutants in water bodies in 2009. The calculations were performed for estuaries of rivers alignment Rioni (Poti), Kubistskali and Bartshana rivers (Batumi).

$$G = W\bar{C}, \tag{25.1}$$

Where G – is the number of pollutants per year, thousands of tons; W – is outflow volume for the year km^3; $\bar{C}$ – is the average concentration of a substance per year, or mg/dm^3 or mkg/dm^3.

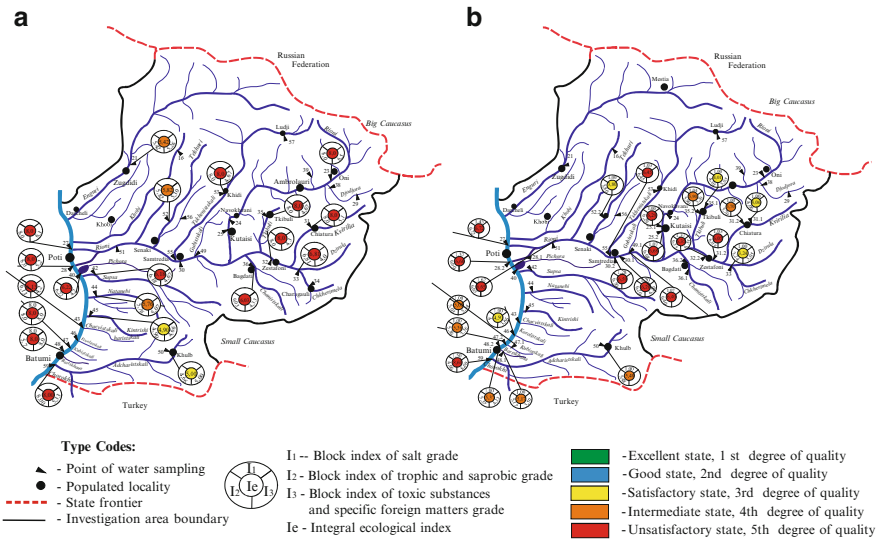

Fig. 25.3 Map-chart of surface water quality of West Georgia. (**a**) 1985, (**b**) 2010 (*see color plates*)

Calculation results are represented in Table 25.1. The list of indexes of calculation includes those ones that have the greatest influence on the water quality in the region.

Pollutants, that enter the Black Sea with river runoff, split up irregular in its volume, localize mainly in the estuary parts of areas. Most of the polluted river flow is concentrated within the most valuable (in terms of biodiversity) north-west area of the Black Sea. Thanks to the peculiar morphology of the bottom and hydrological regime, the north-western part of the sea is out of Oxygen-Free hydrogen sulphide zone and that is why 80 % of the biological potential of the Black Sea is located here.

Significant role in the pollutants diversion, which was brought by river runoff, play surface flows of the Black Sea. These flows are formed in the estuaries of large rivers and in Kerch Strait. River waters, which come into the sea, deviate to the right according to Coriolis force, after that the flow direction is influenced by wind and shoreline [12]. North –west direction flow is dominated around the shores of the Caucasus, which runs from the coast of Georgia along the Russian coast to Crimea and then to the shores of Bulgaria and Romania.

Water flows and the solid load in its structure is connected with geological, soil-forming rocks, biological processes and economic activities (industrial waste, municipal and agricultural origin). Its connection and impact lead to magnification of mineral pollutants in river total run-off of Western Georgia, such as: hydrogen carbonates Ca and Mg, Cu, Fe and others.

Among the list of biogenic substances we also made the calculation of the total nitrogen removal. We didn't define the removal of various compounds of nitrogen (NH^{4+}, NO^{2-}, NO^{3-}) on purpose, since their content in river waters are interconnected.

Table 25.1 The removal of pollutants into the Black Sea with river runoff of West Georgia to the water area of Black Sea, 2009

River	Loss, m^3/s / Flow, km^3	Annual average water composition, mg/dm^3 / Annual average removal, thousands of ton./year										
		∑ N	PO_4^{3-}	SO_4^{2-}	Cl^-	HCO_3^-	Ca^{2+}	Mg^{2+}	$Fe_{зar}$	Cu	SAS[a]	Oil[b]
Rioni	146.833	1.738	0.075	35.88	7.43	148.68	32.827	9.59	0.514	–	0.132	0.198
	4.625	8.040	0.348	165.9	34.35	687.68	151.83	44.37	2.377	–	0.611	0.913
Kvirilia	23.305	1.459	0.058	24.19	5.381	124.70	30.711	6.513	0.347	–	–	–
	0.734	1.071	0.043	17.76	3.950	91.542	22.545	4.781	0.255	–	–	–
Tskhenistskali	29.83	1.41	0.05	25.65	6.92	140.3	32.2	10.07	0.3	–	–	–
	0.94	1.33	0.05	24.10	6.51	131.81	30.25	9.47	0.28	–	–	–
Tekhuti	27.73	0.781	0.032	18.73	3.68	108.66	28.220	5.997	0.200	–	0.031	–
	0.873	0.510	0.215	12.95	16.25	75.220	18.885	4.318	0.171	–	0.024	–
Tkibuli	7.188	0.833	0.043	20.37	4.74	132.92	32.652	7.651	0.255	–	0.046	–
	0.226	0.344	0.015	9.719	2.24	58.648	14.438	4.165	0.142	–	0.022	–
Khanistskali	29.79	0.561	0.020	14.58	3.39	90.896	22.524	5.431	0.151	–	0.025	–
	0.94	0.666	0.021	15.98	3.70	105.41	27.897	5.505	0.152	–	0.021	–
Gubistskali	13.525	1.113	0.042	21.37	6.00	131.15	30.375	10.70	0.215	–	–	–
	0.426	0.474	0.018	9.107	2.56	55.875	12.941	4.559	0.092	–	–	–
Bartskhana	12.8	2.223	0.051	7.417	6.54	105.43	16.998	6.810	0.232	0.005	0.012	0.078
	0.403	0.896	0.020	2.99	2.64	42.511	6.854	2.746	0.093	0.002	0.005	0.031
Kubistskali	11.8	2.280	0.055	11.5	5.8	91.45	11.95	2.4	0.175	0.003	0.015	0.076
	0.372	0.848	0.020	4.27	2.16	33.992	4.442	0.892	0.065	0.001	0.006	0.028

Above the city/below the city

[a]Surface-active substance

[b]Oil products

8.04 tons of nitrogen compounds come per year to the Black Sea from waters of the largest river of Western Georgia – Rioni river. Small lowland rivers Kubistskali and Bartshana carry with its waters almost the same amount of nitrogen compounds, namely 0.896 and 0.848 tons/year, accordingly.

Among the compounds that form the ionic structure of the rivers of Western Georgia, hydrogen carbonates calcium and magnesium is dominant. That is why, the removal of these compounds to Black Sea reach total amount of 883.9 tons/year from Rioni river and 52.11 and 39.33 tons/year from rivers Bartshana and Kubistskali accordingly.

Heavy metals, which are characterized by high toxicity to living organisms in its relatively low concentrations and the ability to bioaccumulation, refer to pollutants priority, examination of which is obligatory for every environment. Rioni River brings iron to the Black Sea 2.377 tons/year, Kubistskali and Bartshana rivers within 0.093–0.065 tons/year.

Cooper is one of the micro-elements that come to the Black Sea from the runoff of small lowland rivers. The quantity of its removal to the sea area is in the range from 0.001 to 0.002 tons/year.

25.4.1 Oil Pollution in the Black Sea

Oil products entry to waters of the Black Sea from Georgia is performed due to river runoff, industrial discharges and ballast waters, loss of oil during the overflow from tankers, unit discharges of wastewaters from industry, utilities and transportation center of the coastal zone.

Analysis of data showed, that the most polluted are the waters of sea port area in Batumi and Poti, where the oil concentrations exceed MPC respectively in 24 and 12 times. Average quantity of oil transportation with shipping ports of Georgia is 11 million tons per year (TDA) [10]. Consequently, maximum oil products concentration: the port city of Batumi – 1.2 mg/dm^3, port of Poti – 0.62 mg/dm^3, in the sea water of port area, was recorded in August 1998.

The most frequent part of oil patch discovering with intensity more than 250 mg/m^2 is typical for the Georgian Part of Black Sea and is 91 % of the total quantity of observation area (based on results of aerial observation of surface pollution by oil port area, oil storage tanks areas and places of unauthorized discharges of wastewaters, performed by State Committee of Ukraine in the 1981–1990) [21]. Most of all, oil patches occur in the Black Sea coast of Caucasus in the area of Batumi-Poti (Fig. 25.4).

Pollution by the oil film of surface layer of the Black Sea during this period reached in average 35.2 mg/m^2, the average amount of oil film −15.4 thousand tons, oil film, the intensity of which is 250–1,250 mg/m^2, was determined in the amount of 1.2 tons. Oil patches average area was 4,100 km^2, with an observation area of 200,000 km^2 [21].

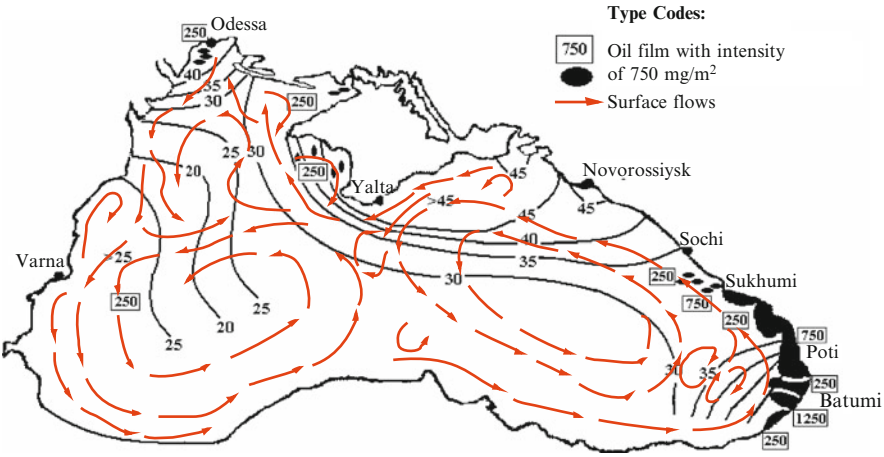

Fig. 25.4 Scheme of surface flows and map chart of oil pollution in the Black Sea (*see color plates*)

Oil products, that enter the Black Sea with river runoff, localize mainly in the estuary parts of areas. The pollution of north-west area of the Black Sea and Crimean peninsula coast is connected with peculiarities of water circulation and pollution substances removal by Black sea flow, which is formed in the estuaries of large rivers and in Kerch Strait. North –west direction flow is dominated around the shores of the Caucasus, which brings oil pollution from the coast of Georgia along the Russian coast to Crimea and then to the shores of Bulgaria and Romania [10, 21].

Waters of Rioni channel bring 0.913 tons of oil products to the sea annually. The largest amount of oil products comes to Rioni river with waters of Tehuri flows (0.024 thousand tons of oil), Tkibuli (0.022 tons) and Hanistskali (0.021 tons).

Small lowland rivers Kubistskali and Bartshana are sewage polluted by Batumi refinery, which contain high content of oil products. 0.028–0.031 tons of oil comes to sea shore land annually.

The maximum oil content in the estuaries of the Bartshana is fixed in September and is 0.22 mg/dm^3, minimum – in December and February and is not more than 2 MAC. The average concentration of oil in the estuaries of the Bartshana river equals 0.146 mg/dm^3.

In the estuaries of the Rioni river, the average concentration of oil products were fixed: the right river branch of the Rioni – 0.216 mg/dm^3, left river branch the Rioni – 0.226 mg/dm^3 (1997). The maximum concentration of oil in the estuaries of the Rioni river was 0.6 mg/dm^3 and the minimum concentration was recorded in winter 0.1–0.12 mg/dm^3. The concentration of oil in water of Rioni river above the city Samtredia was 0.11 mg/dm^3 and Poti – 0.13 mg/dm^3.

In the marine environment, oil pollution is distributed very unevenly. There is a gradual fall in oil concentration with the distance from the oil ports to the open sea (Fig. 25.5). Spatially, the most significant marine pollution occurs the areas of ports and marine transport routes.

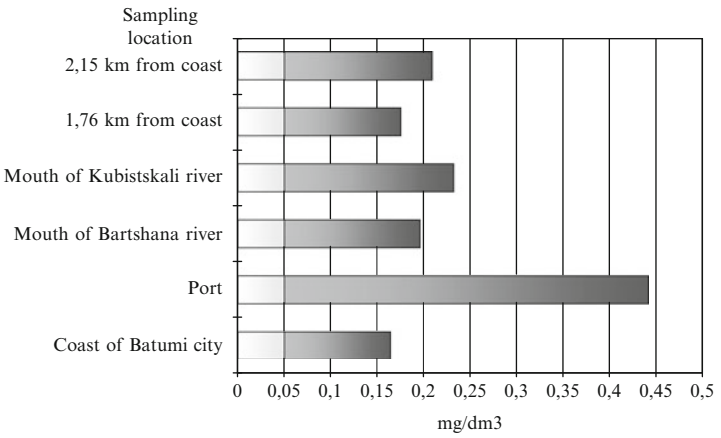

Fig. 25.5 Content of oil products in seawater near Batumi, 1999

According to research of 1997–1999, the average content of oil in the port area of Batumi overestimates MCL in eight times, at the distance of 1.76 miles its concentration reduces to three MAC, but at the distance of 2.15 km from Batumi shore it increases again to 4 MACs.

Analysis of all available monitoring data of Georgian Black Sea oil pollution made it possible for us to find out the most polluted areas in the basins of Batumi –Poti, including port and estuary areas of rivers Rioni, Bartshana and Kubistskali. The quantities of oil concentration in river water confirm the value of river drain as a priority source of marine pollution.

25.5 Conclusions

In summary, in the course of our researches, based on the requirements of the EU WFD according to an assessment of ecological condition of water bodies, we have found that pollution of surface waters of the rivers of Western Georgia, and negative changes in its overbank complex is occurred under the influence of human activities. It impacts negatively on water quality in rivers, degree of quality falls to grade V; hydro morphological characteristics do not correspond to referential requirements, mostly, because of agricultural use of overbanks, construction of hydraulic structures and coastal protection. Therefore, as consequence, we can observe despoliation of ecological state of basins in Georgian Part of Black Sea.

The main stress deals with marine ecosystem of Batumi – Poti area, because of insignificant, on the first sight, local oil outflows and oil products incoming, which are deadly and dangerous for the Sea and its inhabitants.

References

1. Долинський СК (2002) Сучасний екологічний стан Чорного моря//Вода і водоочисні технології —, № 2–3, ст. 30–33
2. Лоєва І (2007) Сучасний екологічний стан Чорного моря.//Рідна природа, Київ, Спецвипуск, — с. 11–15
3. Гидрометеорология и гидрохимия морей СССР. Черное море. Л.: Гидрометеоиздат — Т.4, вып. 1. — с. 429 (1991)
4. Практическая экология морских регионов. Черное море. К. : Наукова Думка — с. 251 (1990)
5. Клименко МО (2009) Нафтове забруднення грузинської частини Чорного моря на ділянці Батумі–Поті/М. О.Клименко, Н. М.Вознюк, К. Ю. Вербецька//Вісник Національного університету водного господарства та природокористування: збірник наукових праць. — Рівне — вип. 3(47). — Ч. І. — С. 16–23
6. Вербецька КЮ (2009) Сучасні екологічні проблеми в басейні Чорного моря/К. Ю. Вербецька, Н. М. Вознюк//Вісник Національного університету водного господарства та природокористування: збірник наукових праць— Рівне — вип. 2(46). — С. 14–19
7. Джоашвили Ш. Реки Черного моря//Технический отчет, № 71, Европейское агентство по охране окружающей среды
8. Verbetska K, The experience of international collaboration the Black Sea basin; Verbetska K, Klymenko N, Voznyuk N (2010) Water management—state and prospects for development. In: Collected articles of young scientists of conference, Rivne, 15–16 April 2010; National University of Water Management and Nature Resources Use — Rivne — Part I. — C. 137–139 (2010)
9. Конвенція про захист Чорного моря від забруднення//Рідна природа, Київ, №4, с.17–24 (2001)
10. Black Sea transboundary diagnostic analysis, GEF, BSEP (1997)
11. Strategic action plan for the rehabilitation and protection of the Black Sea, Istanbul, Turkey (1996)
12. Водна Рамкова Директива ЄС 2000/60/ЄС. Основні терміни та їх визначення. — Київ — 240 с. (2006)
13. Клименко МО (2011) Типізація річок Західної Грузії/М. О. Клименко, Н. М. Вознюк, К. Ю. Вербецька: збірник наукових статей [“ІІІ–й Всеукраїнський з’їзд екологів з міжнародною участю”]. —– Вінниця — С. 193–196
14. CEN №14614 (2004) Water quality—guidance standard for assessing the hydromorfological features of rivers, p 24
15. Pedersen M, Ovesen N, Friberg N, Qausen B, Lehotsky M, Greskova A (2004) Hydromorphological assessment protocol for the Slovak Republic, Bratislava, Slovakia, p 36
16. Lehotsky M, Greskova A (2004) Priprava databazy hydromorfologickych a biologickych ukazovatel’ov pre process vybern a charaktenzacie referertcnych miest podla Smernice 2000/60/EC Report tomSHMI, Bratislava, Slovakia
17. Екологічна оцінка якості поверхневих вод суші та естуаріїв України : Методика : КНД 211.1.4.010-94. — Київ —37 с. (1994)
18. Вербецька КЮ (2011) Порівняльний аналіз методик оцінки якості поверхневих вод (на прикладі типової р. Губісцкалі)/Вербецька К.Ю.//Вісник Національного університету водного господарства та природокористування: збірник наукових праць. — Рівне — Вип. 3 (55): Сільськогосподарські науки. — С. 91–99
19. Вознюк НМ (2011) Дослідження зміни якості поверхневих вод ріки Ріоні/Н. М. Вознюк, К. Ю. Вербецька, О. М. Лимар//Вісник Національного університету водного господарства та природокористування: збірник наукових праць. — Рівне — Вип. 2 (54): Сільськогосподарські науки. — С. 12–22

20. Вербецька КЮ (2011) Оцінка якості поверхневих вод Західної Грузії/К. Ю. Вербецька: Тези Міжнародної науково-практичної конференції ["Актуальні проблеми наук про життя та природокористування"], (Київ, 26-29 жовтня 2011 р.)/Національний університет біоресурсів та природокористування України. —— Київ : НУБіП — С. 5–6
21. Савоськин ВМ, Миньковская РЯ, Демидов АН Уточнение составляющих баланса нефтепродуктов на основе данных мониторинга Черного моря (http//seaway.org.ua)

Chapter 26
Numerical Simulation of the Sea Pollution for the Case of Mine Waters Discharge

Mykola M. Biliaiev, P.S. Kirichenko, and Mykola M. Kharytonov

Abstract Huge quantities of mine waters are discharged to the rivers from Krivoy Rog iron ore mines in the south of Ukraine. At present, the project of these mine waters discharge into the Black Sea is worked out. The problem of this discharge environmental impact assessment is of great interest. One of the branches of this problem is the prediction of the sea pollution in the case of mine waters discharge. Numerical model to calculate the sea point pollution in the case of the mine waters discharge was developed. The model is based on the 3D equations of potential flow and pollutant dispersion. The implicit difference schemes were used for the numerical integration of the governing equations. New type of arrangement for the mine waters discharge into the sea was developed.

Keywords Sea pollution • Numeric forecast • Experiment • Mine waters discharge

26.1 Introduction

The iron ore mining is the leading branch of Ukraine's economy [1]. But this activity results in huge amounts of mine waters. Utilization of mine waters in Ukraine is a problem of great importance. The mineralization of mine waters covers the range 19–36 g/l. The annual total amount of mine waters in Krivoy Rog region (central part of Ukraine) is about $21 \cdot 10^6$ m^3. Now these mine waters are collected in special ponds (Fig. 26.1) and then discharged to the rivers [2, 3]. The ore mining is planned to be increased that is why the problem of utilization of mine waters

M.M. Biliaiev • P.S. Kirichenko
Dnipropetrovsk University of Engineers of Railway Transport,
Dnipropetrovsk, Ukraine

M.M. Kharytonov (✉)
Dnipropetrovsk State Agrarian University, Dnipropetrovsk, Ukraine
e-mail: mykola_kh@yahoo.com

A. Veziroğlu and M. Tsitskishvili (eds.), *Black Sea Energy Resource Development and Hydrogen Energy Problems*, NATO Science for Peace and Security Series C: Environmental Security, DOI 10.1007/978-94-007-6152-0_26,

Fig. 26.1 Mine waters discharge into the pond *Svistunova* (*see color plates*)

attracts attention. In 1988, the project of mine waters discharged in the Black Sea was developed in the USSR, but the ecological study was not carried out at that time. Now this project is under consideration and the problem of the ecological study is appearing again. The engineers working on the correction of the old project to meet the modern demands and the need of tools to predict the sea pollution for the case of mine waters discharge into the Black Sea. The *Regulation Instructions* based on the analytical model and which are used now in Ukraine to predict sea pollution could not provide the solution of the problem considered. This chapter presents a numerical model to simulate the flow field and pollutant dispersion, in vicinity of the discharge pipe opening which is situated in the sea.

26.2 Mathematical Model of Pollutant Dispersion

To simulate the pollutant transport in the sea the gradient transport model is used:

$$\frac{\partial C}{\partial t}+\frac{\partial uC}{\partial x}+\frac{\partial \nu C}{\partial y}+\frac{\partial (w-w_g)C}{\partial z}+\sigma C=\frac{\partial}{\partial x}\left(\mu_x\frac{\partial C}{\partial x}\right)+\frac{\partial}{\partial y}\left(\mu_y\frac{\partial C}{\partial y}\right)+\frac{\partial}{\partial z}\left(\mu_z\frac{\partial C}{\partial z}\right)$$
$$+\sum Q_i(t)\delta(x-x_i)\delta(y-y_i)\delta(z-z_i) \qquad (26.1)$$

where C is concentration; u, v, w are the velocity components; σ is the parameter taking into account the process of pollutant decay; $\mu = (\mu_x , \mu_y , \mu_z)$ are the diffusion coefficients; Q is the intensity of pollutant emission.

Table 26.1 Coefficients to calculate the averaged sea speed and parameters of diffusion

$V \le 6\ m/s$	
a_1	c_1
$a_0 = 3{,}613 \cdot 10^{-2}$	$c_0 = 599 \cdot 10^{-4}$
$a_1 = -2{,}751 \cdot 10^{-3}$	$c_1 = 5{,}347 \cdot 10$
$a_2 = 1{,}108 \cdot 10^{-2}$	$c_2 = -3{,}681 \cdot 10^{-4}$
$a_3 = 1{,}461 \cdot 10^{-3}$	$c_3 = -1{,}469 \cdot 10^{-4}$
$a_4 = 9{,}729 \cdot 10^{-6}$	$c_4 = 5{,}669 \cdot 10^{-6}$
$a_5 = -7{,}189 \cdot 10^{-3}$	$c_5 = 1{,}426 \cdot 10^{-4}$
$a_6 = 9{,}925 \cdot 10^{-4}$	$c_6 = 2{,}276 \cdot 10^{-6}$
$a_7 = -3{,}875 \cdot 10^{-6}$	$c_7 = -2{,}401 \cdot 10^{-6}$

To simulate the mine waters gravity fall as the result of the density difference between them and sea water the parameter w_g is used. This parameter is determined in experimental studies [4].

The transport equation is used with the following boundary conditions:

- at the inlet boundary: $C|_{inlet} = C_E$, where C_E is the known concentration;
- at the outlet boundary: in numerical model the condition $C(i+1,j,k) = C \times (i,j,k)$ is used (this boundary condition means that we neglect the process of diffusion on this plane);
- at the top boundary and the bottom surface : $\dfrac{\partial C}{\partial n} = 0.$

In the numerical model the following approximations for sea averaged speed is used

$$u_M = a_0 + a_1 V + a_2 H + a_3 V^2 + a_4 H^2 + a_5 VH + a_6 V^2 H + a_7 VH^2 \qquad (26.2)$$

where a_I ($i = 1, 2, \ldots, 7$) are the coefficients which are shown in Table 26.1.; H is the sea depth; V is the wind speed.

This approximation is used if the following conditions are fulfilled:

$$2.0 \le V \le 20\ (m/s), \quad 1.5 \le H \le 50\ (m).$$

The diffusion coefficients are calculated using the following approximations:

$$\mu_x = 0.032 + 21.8 u_M^2 \qquad (26.3)$$

$$\mu_z = {}_0 + c_1 V + c_2 H + c_3 V^2 + c_4 H^2 + c_5 VH + c_6 V^2 H + c_7 VH^2 \qquad (26.4)$$

where a_I ($i = 1,2,\ldots, 7$) are the coefficients shown in Table 26.1.

Worthy of note is that these approximations are recommended in the State Regulations, which are used in Ukraine to predict the pollution of the sea, if the problem of waste waters injection into the sea is under consideration. The *State Regulations* do not indicate how the diffusion coefficient along Y axis must be calculated so in the model developed we consider that $\mu_y = \mu_x$.

26.3 Numerical Model

The calculation of pollutant dispersion is carried out on the rectangular grid. Main features of the finite difference scheme for transport equation are presented below.

The time dependent derivative is approximated as following:

$$\frac{\partial C}{\partial t} \approx \frac{C_{ijk}^{n+1} - C_{ijk}^{n}}{\Delta t}. \tag{26.5}$$

At the first step convective derivatives are represented in the following way:

$$\frac{\partial uC}{\partial x} = \frac{\partial u^{+}C}{\partial x} + \frac{\partial u^{-}C}{\partial x}; \tag{26.6}$$

$$\frac{\partial vC}{\partial y} = \frac{\partial v^{+}C}{\partial y} + \frac{\partial v^{-}C}{\partial y}; \tag{26.7}$$

$$\frac{\partial wC}{\partial z} = \frac{\partial w^{+}C}{\partial z} + \frac{\partial w^{-}C}{\partial z}, \tag{26.8}$$

$$\text{where } u^{+} = \frac{u+|u|}{2}; u^{-} = \frac{u-|u|}{2}, \nu^{+} = \frac{\nu+|\nu|}{2}; \nu^{-} = \frac{\nu-|\nu|}{2},$$
$$w^{+} = \frac{w+|w|}{2}; w^{-} = \frac{w-|w|}{2}. \tag{26.9}$$

At the second step the convective derivatives are approximated as following:

$$\frac{\partial u^{+}C}{\partial x} \approx \frac{u_{i+1,j,k}^{+} C_{ijk}^{n+1} - u_{ijk}^{+} C_{i-1,j,k}^{n+1}}{\Delta x} = L_x^{+} C^{n+1}, \tag{26.10}$$

$$\frac{\partial u^{-}C}{\partial x} \approx \frac{u_{i+1,j,k}^{-} C_{i+1,j,k}^{n+1} - u_{ijk}^{-} C_{ijk}^{n+1}}{\Delta x} = L_x^{-} C^{n+1}, \tag{26.11}$$

$$\frac{\partial \nu^{+}C}{\partial y} \approx \frac{\nu_{i,j+1,k}^{+} C_{ijk} - \nu_{ijk}^{+} C_{i,j-1,k}}{\Delta y} = L_y^{+} C^{n+1}; \tag{26.12}$$

$$\frac{\partial \nu^{-}C}{\partial y} \approx \frac{\nu_{i,j+1,k}^{-} C_{i,j+1,k} - \nu_{ijk}^{-} C_{ijk}}{\Delta y} = L_y^{-} C^{n+1}; \tag{26.13}$$

$$\frac{\partial w^{+}C}{\partial z} \approx \frac{w_{i,j,k+1}^{+} C_{ijk} - w_{ijk}^{+} C_{i,j,k-1}}{\Delta z} = L_z^{+} C^{n+1}; \tag{26.14}$$

$$\frac{\partial w^{-}C}{\partial z} \approx \frac{w^{-}_{i,j,k+1}C_{i,j,k+1} - w^{-}_{ijk}C_{i,j,k}}{\Delta z} = L^{-}_{z}C^{\,n+1}. \tag{26.15}$$

The second order derivatives are approximated as:

$$\begin{aligned}\frac{\partial}{\partial x}\left(\mu_{\mathrm{x}}\frac{\partial C}{\partial x}\right) &\approx \tilde{\mu}_{\mathrm{x}}\frac{C^{n+1}_{i+1,j,k} - C^{n+1}_{ijk}}{\Delta x^2} - \tilde{\mu}_{\mathrm{x}}\frac{C^{n+1}_{i,j,k} - C^{n+1}_{i-1,j,k}}{\Delta x^2} \\ &= M^{-}_{xx}C^{\,n+1} + M^{+}_{xx}C^{\,n+1},\end{aligned} \tag{26.16}$$

$$\begin{aligned}\frac{\partial}{\partial y}\left(\mu_{\mathrm{y}}\frac{\partial C}{\partial y}\right) &\approx \tilde{\mu}_{\mathrm{y}}\frac{C^{n+1}_{i,j+1,k} - C^{n+1}_{ijk}}{\Delta y^2} - \tilde{\mu}_{\mathrm{y}}\frac{C^{n+1}_{i,j,k} - C^{n+1}_{i,j-1,k}}{\Delta y^2} \\ &= M^{-}_{yy}C^{\,n+1} + M^{+}_{yy}C^{\,n+1},\end{aligned} \tag{26.17}$$

$$\begin{aligned}\frac{\partial}{\partial z}\left(\mu_{\mathrm{z}}\frac{\partial C}{\partial z}\right) &\approx \tilde{\mu}_{\mathrm{z}}\frac{C^{n+1}_{i,j,k+1} - C^{n+1}_{ijk}}{\Delta z^2} - \tilde{\mu}_{\mathrm{z}}\frac{C^{n+1}_{i,j,k} - C^{n+1}_{ij,k-1}}{\Delta z^2} \\ &= M^{-}_{zz}C^{\,n+1} + M^{+}_{zz}C^{\,n+1}.\end{aligned} \tag{26.18}$$

In these expressions $L^{+}_{x},\ L^{-}_{x}, L^{+}_{y},\ L^{-}_{y},\ L^{+}_{z},\ L^{-}_{y}, M^{+}_{xx},\ M^{-}_{xx}\ldots.$ are the difference operators. Using these expressions the difference scheme for the transport equation can be written as follows:

$$\begin{aligned}&\frac{C^{n+1}_{ijk} - C^{n}_{ijk}}{\Delta t} + L^{+}_{x}C^{\,n+1} + L^{-}_{x}C^{\,n+1} + L^{+}_{y}C^{\,n+1} \\ &\quad + L^{-}_{y}C^{\,n+1} + L^{+}_{z}C^{\,n+1} + L^{-}_{z}C^{\,n+1} + \sigma C^{n+1}_{ijk} \\ &\quad = \left(M^{+}_{xx}C^{\,n+1} + M^{-}_{xx}C^{\,n+1} + M^{+}_{yy}C^{\,n+1}\right. \\ &\quad \left. + M^{-}_{yy}C^{\,n+1} + M^{+}_{zz}C^{\,n+1} + M^{-}_{zz}C^{\,n+1}\right)\end{aligned} \tag{26.19}$$

Solution of the transport equation in finite – difference form is split in four steps during the time step of integration dt:

- at the first step $\left(k = \frac{1}{4}\right)$ the difference equation is:

$$\begin{aligned}&\frac{C^{n+k}_{ij} - C^{n}_{ij}}{\Delta t} + \frac{1}{2}\left(L^{+}_{x}C^{k} + L^{+}_{y}C^{k} + L^{+}_{z}C^{k}\right) + \frac{\sigma}{4}C^{k}_{ijk} \\ &\quad = \frac{1}{4}\left(M^{+}_{xx}C^{k} + M^{-}_{xx}C^{n} + M^{+}_{yy}C^{k} + M^{-}_{yy}C^{n} + M^{+}_{zz}C^{k} + M^{-}_{zz}C^{n}\right)\end{aligned} \tag{26.20}$$

- at the second step $\left(k = n + \frac{1}{2};\ c = n + \frac{1}{4}\right)$: the difference equation is

$$\frac{C_{ijk}^{k} - C_{ijk}^{c}}{\Delta t} + \frac{1}{2}\left(L_x^- C^k + L_y^- C^k + L_z^- C^k\right) + \frac{\sigma}{4} C_{ij}^{k} = \frac{1}{4}\left(M_{xx}^- C^k + M_{xx}^+ C^c + M_{yy}^- C^k + M_{yy}^+ C^c + M_{zz}^- C^k + M_{zz}^+ C^c\right); \tag{26.21}$$

- at the third step $\left(k = n + \frac{3}{4};\quad c = n + \frac{1}{2}\right)$ the expression (26.21) is used;
- at the fourth step $\left(k = n + 1;\quad c = n + \frac{3}{4}\right)$ the expression (26.20) is used.

At the fifth step (if we want to take into account the influence of the source of pollution) the following approximation is used:

$$\frac{\overset{5^{n+1}}{C}_{i,j,k} - \overset{5^{n}}{C}_{i,j,k}}{\Delta t} = \sum_{l=1}^{N} \frac{q_l(t^{n+1/2})}{\Delta x\ \Delta y\ \Delta z}\delta_l. \tag{26.22}$$

Function δ_l is equal to zero in all cells except the cells where the 'l' source of pollution is situated.

This difference scheme is implicit and absolutely steady but the unknown concentration C is calculated using the explicit formulae at each step (so called "method of running calculation").

To simulate the flow field the model of potential flow is used. In this case the governing equation is

$$\frac{\partial^2 P}{\partial x^2} + \frac{\partial^2 P}{\partial y^2} + \frac{\partial^2 P}{\partial z^2} = 0, \tag{26.23}$$

where P is the potential of velocity.

The components of velocity are calculated as follows:

$$u = \frac{\partial P}{\partial x}, \quad v = \frac{\partial P}{\partial y}, \quad w = \frac{\partial P}{\partial z} \tag{26.24}$$

The boundary conditions are as follows:

– at the bottom ant the upper boundary: $\dfrac{\partial P}{\partial n} = 0$, where n – is normal unit vector to the boundary;
– at the entrance boundary: $\dfrac{\partial P}{\partial n} = V_n$, where V_n – is the known speed; and
– at the exit plane $P = P^*(x = \text{const}, y) + \text{const}$.

Instead of Eq. (26.23) the 'time-dependent' equation for the potential of velocity is used in the model:

$$\frac{\partial P}{\partial \eta} = \frac{\partial^2 P}{\partial x^2} + \frac{\partial^2 P}{\partial y^2} + \frac{\partial^2 P}{\partial z^2} \tag{26.25}$$

where η is 'fictitious' time.

For $\eta \to \infty$ the solution of Eq. (26.25) tends to the solution of Eq. (26.23).

To solve Eq. (26.25) A.A. Samarski's change-triangle difference scheme was used [5]. According to this scheme the solution of Eq. (26.23) is split in two steps:

– at the first step the difference equation is:

$$\frac{P_{i,j,k}^{n+1/2} - P_{i,j,k}^{n}}{0.5\Delta\eta} = \frac{P_{i+1,j,k}^{n} - P_{i,j,k}^{n}}{\Delta x^2} + \frac{-P_{i,j,k}^{n+1/2} + P_{i-1,j,k}^{n+1/2}}{\Delta x^2} + \frac{P_{i,j+1,k}^{n} - P_{i,j,k}^{n}}{\Delta y^2} + \frac{-P_{i,j,k}^{n+1/2} + P_{i,j-1,k}^{n+1/2}}{\Delta y^2} + \frac{P_{i,j,k+1}^{n} - P_{i,j,k}^{n}}{\Delta z^2} + \frac{-P_{i,j,k}^{n+1/2} + P_{i,j,k-1}^{n+1/2}}{\Delta z^2}, \tag{26.26}$$

– at the second step the difference equation is

$$\frac{P_{i,j,k}^{n+1} - P_{i,j,k}^{n+1/2}}{0.5\Delta\eta} = \frac{P_{i+1,j,k}^{n+1} - P_{i,j,k}^{n+1}}{\Delta x^2} + \frac{-P_{i,j,k}^{n+1/2} + P_{i-1,j,k}^{n+1/2}}{\Delta x^2} + \frac{P_{i,j+1,k}^{n+1} - P_{i,j,k}^{n+1}}{\Delta y^2} + \frac{-P_{i,j,k}^{n+1/2} + P_{i,j-1,k}^{n+1/2}}{\Delta y^2} + \frac{P_{i,j,k+1}^{n+1} - P_{i,j,k}^{n+1}}{\Delta z^2} + \frac{-P_{i,j,k}^{n+1/2} + P_{i,j,k-1}^{n+1/2}}{\Delta z^2}. \tag{26.27}$$

From these expressions the unknown value P is determined using the explicit formulae at each step ("method of running calculation"). The calculation is completed if the condition:

$$\left| P_{i,j,k}^{n+1} - P_{i,j,k}^{n} \right| \le \varepsilon \tag{26.28}$$

is fulfilled (where ε is a small number, n is the number of iteration). The components of velocity vector are calculated on the sides of computational cell as follows:

$$u_{i,j,k} = \frac{P_{i,j,k} - P_{i-1,j,k}}{\Delta x}, \tag{26.29}$$

$$v_{i,j,k} = \frac{P_{i,j,k} - P_{i,j-1,k}}{\Delta y}, \tag{26.30}$$

$$w_{i,j,k} = \frac{P_{i,j,k} - P_{i,j,k-1}}{\Delta z}. \tag{26.31}$$

A code based on the numerical model was developed. This code was used to predict the sea pollution after mine waters discharge into the Black Sea near settlement Zhelezny Port (Iron Port) which is situated in Kherson region of Ukraine.

26.4 Numerical Experiment

A numerical experiment was carried out for the following initial data. The wind velocity is 3 m/s; the mine waters speed at the pipe opening is 1.27 m/s; the sea depth is 12 m; diameter of pipe is 1 m; the concentration of pollutant in mine waters is 100 units (dimensionless value). The dimensions of the computational region are 12 m $\times$ 16 m $\times$ 12 m. The numerical experiment was carried out for two values of w_g: $w_g = 0.01$ m/s, wg = 0.03 m/s. The results of the numerical experiment are shown in Figs. 26.2, 26.3, 26.4, and 26.5. It's clear that the increase of w_g value causes the decrease of polluted area. So the experiments to estimate this value must be carried out with the needed accuracy. It's obvious that the most intensive polluted area is formed near the opening and is about 11 m long and at this distance the concentration decreases intensively.

The Ukrainian *Environment Protection Law* demands that the concentration of pollutant must not exceed the permitted concentration level at the distance 500 m from the point of discharge. From this point of view the discharge considered meets this demand.

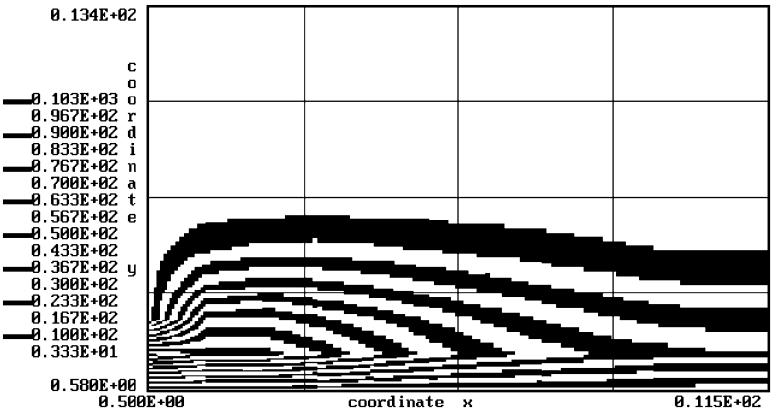

Fig. 26.2 Pollutant concentration near the pipe opening, wg = 0.01 m/s (*Side view*, section y = 5.5 m)

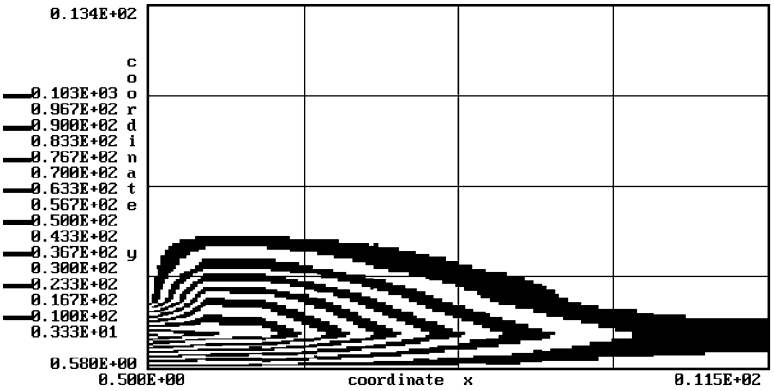

Fig. 26.3 Pollutant concentration near the pipe opening, wg = 0.03 m/s (*Side view*, section y = 5.5 m)

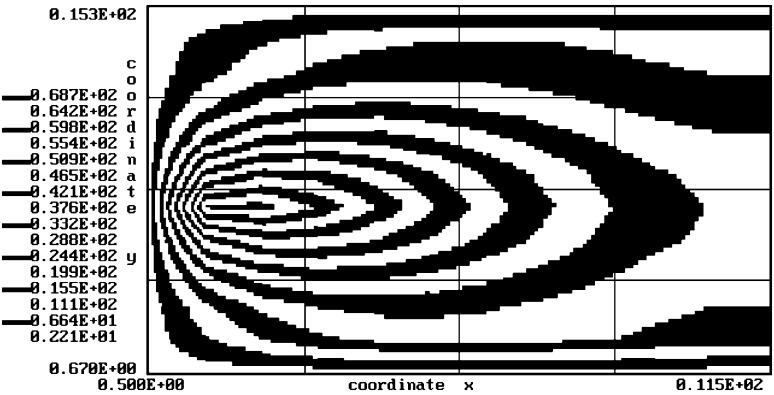

Fig. 26.4 Pollutant concentration near the pipe opening, wg = 0.01 m/s (*Top view*, section z = 1.5 m)

26.5 Conclusion

The numerical model to simulate the flow field and pollutant dispersion in vicinity of the discharge pipe opening which is situated in the sea has been developed. The hydrodynamic model of inviscid flow is used to predict the velocity flow field which is formed as a result of the sea flow and mine waters jet interaction. This model does not consume much of computing time.

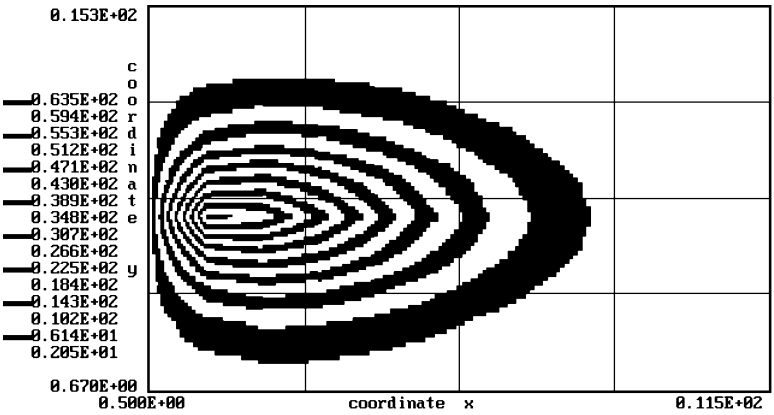

Fig. 26.5 Pollutant concentration near the pipe opening, $w_g = 0.03$ m/s (*Top view*, section $z = 1.5$ m)

References

1. http://www.blackiron.com/
2. Yevgrashkina GP, Rudakov DV, Kharytonov MM (2009) Environmental protection measure assessment in affected area of ponds collecting waste mine-water in Western Donbass. In: Apostol I et al (eds) Optimization of disaster forecasting and prevention measures in the context of human and social dynamics. IOS Press, Amsterdam/Berlin/Tokyo/Washington, DC, pp 122–129
3. Kharytonov MM, Sytnik SA, Vagner AV, Titarenko OV (2012) River pollution risk assessment in the South Eastern part of Ukraine. In: Barry DL, Coldewey WG, Reimer DWG, Rudakov DV (eds) Correlation between human factors and the prevention of disasters. IOS Press, Amsterdam, pp 159–169
4. Biliaiev MM et al (1997) Numerical simulation of the pollutant dispersion in the environment. Naukowa Dumka Publishing House, Kiev, 367 p, (in Russian)
5. Samarskii AA (1983) The theory of difference schemes. Science Publishing House, Moscow, 616 p (in Russian)

Chapter 27
Geomining Site Ecological Assessment and Reclamation Along Coastal Line of the Kerch Peninsula

Mykola M. Kharytonov, O. Mitsik, S. Stankevich, and O. Titarenko

Abstract Kerch district bounded by the sea in the east and by mines in the west was developed along the shore line of the Black Sea due to the free areas located inside city boundary. The territory of the Kerch Peninsula is characterized by open pits, dumps and sludge storages left after opencast mining of iron ores. The assessment of land cover condition on the study area was carried out in the course of time and area. The results of vegetation cover assessment were used to evaluate the changes in normalized difference vegetation index (NDVI) from 1992 to 2010. It was fixed various density of vegetation cover for the same site after two decades of natural restoration. To make research on reclaimed lands fertility more detailed we studied the influence of different thickness of covering layer of soil mass and mining rocks bottom (or their technical mixtures) on the agricultural crops productivity with various adaptive potential. Artificial profiles of creating reclaimed lands to retrieve abandoned ore-mining territories for agricultural use have been proposed.

Keywords Geomining site • Vegetation cover • Land reclamation • Coastal line

27.1 Introduction

Panticapaeum (Kerch) as one of Greek colonies was originally settled by Milesians in the seventh and sixth centuries BCE. During twentieth century, Kerch region has been developed as a big industrial center of the Crimea and Ukraine. Mining, metallurgical, metal working, shipbuilding and ship repairing industries were the

M.M. Kharytonov (✉) • O. Mitsik
Dnepropetrovsk State Agrarian University, Dnepropetrovsk, Ukraine
e-mail: mykola_kh@yahoo.com

S. Stankevich • O. Titarenko
Scientific Centre for Aerospace Research of the Earth, Kiev, Ukraine

A. Veziroğlu and M. Tsitskishvili (eds.), *Black Sea Energy Resource Development and Hydrogen Energy Problems*, NATO Science for Peace and Security Series C: Environmental Security, DOI 10.1007/978-94-007-6152-0_27,

most important objects. Health resort recreation potential of the Kerch Peninsula comprises favorable climatic factors, extended sand beach zones, therapeutic muds, brine, underground mineral waters with a great variety of balneological and tourist resources which make this region as an ecological phenomenon and a perspective area for creating unique resort region on the east of the Crimea Peninsula [1]. Such mineral deposits of ore and non-metallic products as iron ore, fluxing limestone, shell rocks, hydrous sulphate of lime, salt, therapeutic muds, some manifestations of oil and gas are located in the eastern part of the Kerch Peninsula. Oligocene and medium-miocene sands as well as sandstones are oil and gas bearing. Combustible gases have been found in association with oil and in mud volcanic release as well. To obtain borax through mineral waters evaporation combustible gas was used at the plant existing before the period of World War II and located in the region of Bulganak group of mud salse. The fact is that almost all mud volcanoes of Bulganak group are methane bearing while considering the content of salse gases (80–99 % of methane). The deposits of halite, glauber salt and therapeutic muds are concentrated in the lakes of south-eastern part of the Kerch Peninsula: Churbash, Tobechik, Uzunlar, and Lake Chokrak in the north of the Kerch Peninsula. Iron ore deposits are underlied in cut-off synclinal folds and are presented by brown oolitic iron ore (brown clay iron) of Pliocene. Industrial development of iron ore deposits occurred near the city of Kerch dates from 1845. Formed industrial integrated plant comprises three iron ore and one limestone open-pit mines, dressing plants etc. Kamysh-Burun, El'tigen-Ortel and Krasnopartizan deposits are located within the range of Kerch iron ore Basin. The main types of ores are "tobacco" (60 % of deposits) which are overlaid with brown (oxidized) and roe (oxidized redeposited) ores with varieties; oolitic and rarely disseminated ores. The main components of ore are ferrum and manganese, while phosphorus, arsenic, calcium and magnesium oxides and others are adulterants. Opencast mining was used while developing this area. This industrial complex was built in the period of 1932–1939 on the basis of Kamysh-Burun and El'tigen-Ortel deposits of brown iron clay and Krasnopartizan deposit of fluxing limestone located within the Kerch iron ore basin. It is known, that the city of Kerch bounded by the sea in the east and by mines in the west was developed along the shore line of the Black sea due to the free areas located inside city boundary. Poor quality of iron ore and low profitability were the reasons of breaking off iron ore mining and preserving deposits at the beginning of 1990s. About 64 million tons of fine slurry tailings of agglomeration production of former Kamysh-Burun iron ore plant are collected in the waste storage pits and these sludge tailings contain up to 50–55 % of ferric iron. Whereas sludge as well as primary ores of the Kerch deposit contain increased concentrations of arsenic As (0.11 %) and phosphorus (2.15 % P_2O_5) they are practically inadequate for modern metallurgical production. The issue of using ore wastes as correction addition while producing cement and haydite is under consideration nowadays.

One of the urgent regional problems is lack of providing activities aimed to reclamation of damaged soils. However, the activities aimed at land reclamation have been ceased recently. The area of 928, 1,247 ha of soils has been damaged, whereas 10,722 ha are for agricultural purposes [2]. Some pits are used as unregulated sanitary fills of domestic and other wastes.

The aim of this research is to assess the conditions of ore mining areas within the zone of coastal line of the city of Kerch and consider the perspectives of their reclamation.

27.2 Conditions and Methods of Research

Natural conditions of the Kerch Peninsula do not favor forest vegetation development. Sweet briar, black thorn and elder are of frequent occurrence. Speaking about herbage, onion grass, sheep's fescue, sickle alfalfa, germander, milk vetch, thyme, feather grass, spirea and cinquefoil are prevailing [3]. But the area of existing natural reserves within shore line zone is much less than it is required to preserve marine ecosystems. Non-regulated constructions on coastal lines, insufficient quantity of coast protection and landslide works, violation of technical specifications while constructing and operating of industrial objects, removing sand, gravel and shell from the beaches result in regular coast destruction. Previously, in spite of big investments, the effectiveness of shore protection activities was low due to ignoring natural peculiarities of coastal zone. Steppe ecosystems of the Kerch Peninsula are of great demand. Despite considerable percentage of acre large steppe areas still exist and are preserved nowadays.

The assessment of land cover condition on the study area was carried out in the course of time and area. The territory of the Kerch Peninsula is characterized by open pits, dumps and sludge storages left after opencast mining of iron ores. Such relief peculiarities in combination with considerable range of surface exposed mining rocks form the variety of conditions of ecosystem existence. To provide express-assessment of damaged territories located in immediate area of coastal line the method of Earth remote sensing has been used. Due to assessment of spectral reflected surface peculiarities and vegetation cover this method gave the possibility to assess vegetation condition and development dynamics, to carry out mapping and identification of vegetation condition. "Index" images are frequently used to process spectral information. Spectral indexes are estimated due to the combinations of brightness values in defined informative channels and are used to build the images corresponding to the index in each pixel. This affords to separate objects and characterize their condition. Taking into consideration previous research of the areas having been damaged due to ore mining works but still suitable for using as components of ecological line areas of regional ecological network there has been made the assessment of these areas using NDVI and change detection procedure. The results of this assessment were used to evaluate the conditions of their vegetation cover [4, 5]. To display NDVI standard continuous discrete scale with defining NDVI within the range of $-1...1$ in percentage was used. Three Landsat satellite images made in 1992 (May, 5), 1999 (July, 16) and 2010 (September, 22) were involved in the process of vegetation cover assessment and change detection procedure. Kamysh-Burun and El'tigen-Ortel deposits were mined using trenches in the central part of ore fields. Such mining methods as transport and transport-dumped

development with overburden rocks displacement into inner dump have been used. To provide environment protection at Kamysh-Burun and El'tigen-Ortel iron ore plant the sites damaged because of mining works were recultivated for further using as agricultural areas during the period of 1980s of last century. Research work on biological recultivation has been carried out by Dnepropetrovsk State Agrarian University. Kamysh-Burun test station of land reclamation of Dnepropetrovsk State Agrarian University was created on the area of the abandoned quarry "A" of Kamysh-Burun syncline of Kerch iron ore basin. The extraction of iron ore in this quarry was stopped in 1959 and dumps were under natural regeneration till the moment of creating test station of land reclamation which took place in 1977. A bulldozer was used to do the planning of dump surface during the period of preparatory works for creating test site. Vegetation cover was fully destroyed. After completing land planning such activities as dump mapping and additional flattening-out were done. Test site had such extent: the length was equal to 180 m and the width was 100 m with total land of 1.8 ha. Test site was divided into parts comprising artificial profiles of reclaimed land options having loess loam, grey-green clay without cover and soil layer of 50 cm thickness of south black soil which was used to overlay it. Land reclamation was linked with growing field and fruit crops.

27.3 Land Cover Assessment

Natural ecosystems of the peninsula area are represented by steppe, water-swamp and coastal complexes. Ecological line areas are formed along coastal seaboards left unconstructed because of high erosion rates. Due to the analysis of satellite imagery of study area taken in the years of 1992, 1999 and 2010 special differences in relief, area and vegetation cover density were detected. Such objects as limestone and iron ore open pit mines, plant, Churbash ravine, a lake, two slurry pits (northern and southern) are shown in space image (Fig. 27.1).

The area of Churbash ravine is about 5,000 ha. A small river runs along this ravine and flows into Churbash (Kamysh-Burun) lake near the village of Priozerne. The territory is covered with natural and little transformed vegetation. Steppes are dominating and water-swamp associations are prevailing along the ravine thalweg and in ponds formed there. Ancient fortress Ilurat (I–III centuries AD) is situated on the site territory. Olivin open pit located in the ravine serves as a big wildlife reserve. It is necessary to create a landscape reserve of local significance "Churbash ravine" including Olivin open pit mine as well as forming registration of the cultural and historical property site of national significance "Ancient settlement Ilurat with necropolis". Definite perspectives are connected with developing tourist nature trails where some abandoned mines, ancient settlement Ilurat, Tyritake and Nymphaion ruins could be included as places of interest.

It is known that Churbash Lake was divided into two parts by a dam last century. Two slurry depositories were formed in the southern part neighboring to the sea. The millions of tons of iron ore industrial plant wastes were discharged for a long period of time here. The problems arising due to the consequences of mining

Fig. 27.1 Main geomining objects in Kerch district. Legend: *1* iron ore agglomeration plant, *2* iron ore open cast quarry, *3* Churbash ravine, *4* Churbash Lake, *5* and *6* iron ore waste depository, *7* limestone quarry (*see color plates*)

enterprise activities on the territory of the Kerch Peninsula have not been solved yet. Such fact as two big sludge depositories (Lower and Upper Churbash) lie within the boundary of the city Kerch and are immediate close to the zone of city's beach on the coast of the Kerch Strait should be taken into account. Existence of these objects can lead to a real danger of creating large-scale ecological catastrophe for the city and the Strait. The scale of negative influence can greatly extended in the case of destroying alluvial levee due to any anomalous natural situations (lengthy rainfalls etc.). Vegetation cover and change detection data are presented for the same site after 7 and 18 years in 1992, 1999 and 2010 (Figs. 27.2 and 27.3 and Table 27.1).

The comparison of obtained images for the period of 1992, 1999 and 2010 shows differences in vegetation cover of the Kerch Peninsula areas (Table 27.1).

It was connected with decreasing of industrial enterprises and collective farms activity starting from the period of 1990s just after USSR destroying. In particular an industrial activity on iron ore processing in agglomeration plant and hydrotransport for waste keeping has been stopped two decades ago. It led to "dry beaches" forming on the surface of drying out slurry pits. The process of the "dry beaches" forming in iron ore waste depositories was quickly. Up to the half of Lower and Upper Churbash slurry pits surface dried out to 1999 year. Low vegetation covers both depositories surface almost completely to 2010 year. Meantime the industrial activity stopping became a reason for abandoned lands occupation. These areas transformation and development to new residential areas along coastal line led to vegetation cover growth to Mid class (Figs. 27.4 and 27.5).

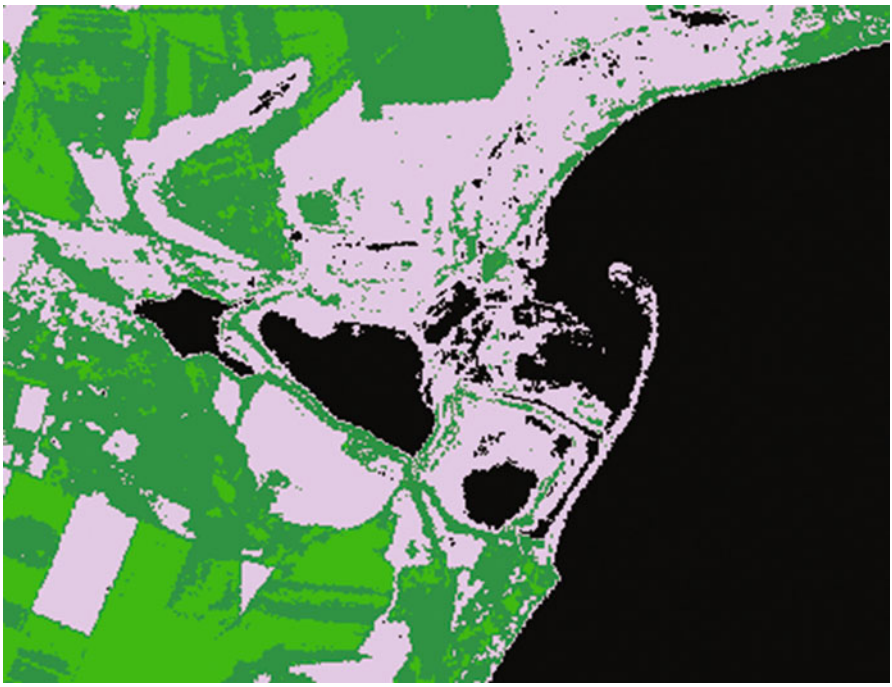

Fig. 27.2 Vegetation cover (1992) (*see color plates*)

Fig. 27.3 Vegetation cover (2010) (*see color plates*)

Table 27.1 Vegetation cover capacity assessment

Code	Vegetation cover class	Percent		
		1992	1999	2010
	Non-vegetation	37.51	30.59	34.70
	Low vegetation	27.73	30.59	54.46
	Mid vegetation	24.09	25.08	10.20
	High vegetation	10.67	1.47	0.64
	Very high vegetation	0.00	0.01	0.00

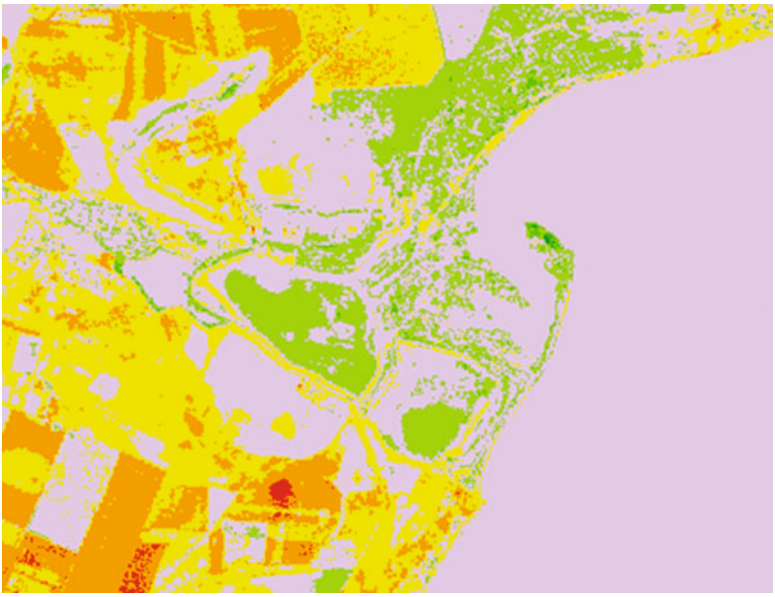

Fig. 27.4 Vegetation cover change (1992–2010) (*see color plates*)

The results of change detection procedure for studied sites for two periods (1992–2010 and 1999–2010) are presented in Table 27.2.

The change detection procedure for three different-time satellite images confirms the tendency on biological self-growing of mining sites – iron ore open cast quarry and waste depositories. The modern technologies of abandoned minelands and Churbash ravine biological conservation application will be challenge to decide current problems of regional environment management.

27.4 Land Restoration and Using Prospects for Abandoned Geosites and Minelands

The territories of abandoned pits as well as non-regulated sites of reclaimed lands can become bench-marks for further development of natural-reserved fund of the Kerch Peninsula. Lands damaged by open pit mining works (with exposure of

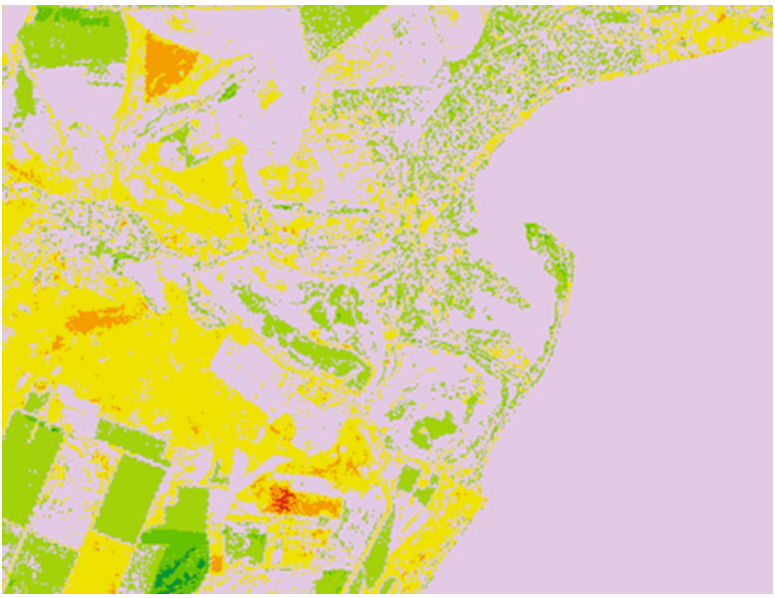

Fig. 27.5 Vegetation cover change (1999–2010) (*see color plates*)

Table 27.2 Vegetation cover change assessment

Code	Vegetation change class	Percent	
		1992–2010	1999–2010
	High degradation	0.30	0.05
	Mid degradation	9.41	1.33
	Low degradation	23.24	20.29
	No change	55.64	64.81
	Low growth	11.01	12.44
	Mid growth	0.39	0.95
	High growth	0.01	0.13

overburden rocks born to the surface) have to pass a very long and complicated process of reclamation without artificial covering by soil mass which was preliminary removed. That is why, in such cases it is necessary to carry out focused reclamation including the activities to preserve upper fertile soil layer. In spite of this they use the technology which does not involve selective extraction of overburden rocks and separate dumping. As the result mechanical blending of above-ore rocks and forming complex technical mixtures take place. Then, flattening-out or reclamation leveling of the surface to serve as an undercoat base for a filling layer of soil mass is carried out.

It is assumed that using reclamation can help create the lands of special target purpose in technogenic landscapes (that can be achieved by varying the thickness of filling layer of black soil mass) crops, feed grains, feeding, reclamative and other directions. The sites dedicated for open pit mining works can have different thickness of artificial profile that defines various thickness of removal and different thickness of damaged soil mass laying. To determine optimal parameters and rational stratigraphy of reclaimed lands detailed study is required.

To solve a set of economic, ecological and biological issues determining optimal thickness of covering soil layer and choosing favorable bottom have a strategic significance while planning the type of reclamation works. To some extent it is connected with the type of damaged landscape as well. Choosing the thickness of a covering fertile layer and a bottom has defining value in the case of planning to use for agricultural purposes the areas being subjected to mining and technical reclamation. The reclamation technology is a perspective one to avoid forming "dry beaches" on the surface of drying out slurry pits. High concentration of water-soluble ferrum in slurries [6] is a risk factor of air pollution of areas close to slurry pits. The thickness of covering slurries by mining rocks (loess loam) or soil can be minimal. As a rule it is within 20–30 cm. To choose vegetation cover is determining. Outside dam cuts are supposed to be fixed by planted land which helps avoid soil erosion and dust removing from cut surface.

First reconnoiter research with covering layer of soil mass in the Kerch iron ore basin were done on the lands of three collective farms of Lenin region of Crimean province. Carried out research demonstrated that harvest volumes of agricultural crops mainly depend on the thickness of covering layer of soil mass rather than utilizing mineral fertilizers. To make research on reclaimed lands fertility more detailed we studied the influence of different thickness of covering layer of soil mass and mining rocks bottom (or their technical mixtures) on the agricultural crops productivity with various adaptive potential. According to the classification of N.I. Gorbunov [7] some of rocks can be characterized as suitable for agricultural utilization owing to qualitative and quantitative composition of secondary minerals. Optimal ratio of clay minerals provides rather high capacity of grey-green clay absorption. It makes possible to consider this mining rock as a potential aquiclude while constructing artificial soil-ecological profile [8]. Obtained experimental data on aquiclude effectiveness while using grey-green clay (GGC) are confirmed by following calculations. It is known, that for the conditions of the Kerch Peninsula mean annual rainfall on Kamish-Burun reclamation station is 397 mm and physical evaporation is 392 mm. Thus, moisture content is 5 mm. Ground water level change is marked as Δh [9]:

$$\Delta h = \frac{\varepsilon \cdot t}{\mu}, \text{m/year}, \tag{27.1}$$

Where
ε is infiltration recharge under natural conditions;
t is time, day;
μ is insufficiency ratio of soil saturation in the zone of aeration.

$$\varepsilon = \frac{5 \cdot 10^{-3} m}{1000 \cdot 365} = 1,37 \cdot 10^{-5}, \text{m/day}. \tag{27.2}$$

For the option of 50 cm Black Soil Filling Layer (BSFL) alteration Δh per annum is:

$$\Delta h = \frac{\varepsilon \cdot t}{\mu} = \frac{1,37 \cdot 10^{-5} \cdot 365}{0.04} = 0.125 \,\text{m/year}. \tag{27.3}$$

In such case underground waters occurrence on the surface takes place in

$$t = \frac{m}{\Delta h} = \frac{0.5}{0.125} = 4 \,\text{years}, \tag{27.4}$$

where m_i is the thickness of specific mining rock layer. Calculation results of time needed for underground waters to reach the surface for options 40 cm GGC + 50 cm BSFL; 40 cm GGC + 100 cm LL; 40 cm GGC + 50 LL + 50 BSFL are given in the Table 27.3.

For comparison of the components of rain precipitation and moisture losses due to evaporation and vegetation transpiration in agroecosystem moisture transpiration velocity formula was applied (V):

$$\mathbf{V} = \frac{P - (E + T)}{1000 \cdot D} \tag{27.5}$$

where P is rain precipitation, mm, E is evaporation, mm, T is transpiration (moisture transfer with corps harvest), D is the amount of days in a year.

Moisture transpiration with crops harvest was calculated by multiplying annual crops harvest to water absorption ratio. Crops yield values for option where grey-green clay is covered with 50 cm of south black soil were taken as calculation values. In average during the period of 3 years the yield of alfalfa, pea and winter wheat grains was 3.49; 16.89 and 2,04 t/ha accordingly. If we take into consideration the fact, that winter wheat will take away 550 m^3/t $\cdot$ 1 $\cdot$ 2.04 t/ha = 112 mm of water per 1 year, and alfalfa (in view of three hay cutting) will take away more, namely 492.1 mm, it will become clear that flood risk is impossible. Thus, using artificial aquiclude under conditions of dry steppe can be considered as a cost-effective water saving technology for irrigation. The results of 2-year field experience of work with the option of using bedding rocks in the form of their mixture, namely loess loam layer and grey-green clay covered with black soil filling layer are given in Table 27.4.

The greatest yield of alfalfa was produced in the case of using grey-green clay layer as a bedding rock. It is greater than it could be produced by using black soil filling layer and could be explained by manifestation of adaptive potential of alfalfa as nitrogen fixing crop.

Table 27.3 Calculation parameters of moisture content forming for reclamation options with artificial clay aquiclude

Option	Thickness of artificial profile, cm	t, year
50 cm BSFL	50	4.0
100 cm LL	100	6.0
50 cm LL + 50 cm BSFL	100	7.0

LL loess loam, *BSFL* black soil filling layer, *GGC* grey-green clay, *t* time durability of moisture content forming, amount of years

Table 27.4 The productivity of alfalfa hay for options with using mining rocks and black soil filling layer, t/ha

Test options	First year	Second year	Mean
Loess loam	4.73	2.96	3.85
LL + 50	3.08	2.89	2.99
Glaucontic clay	8.94	6.03	7.48
GC + 50 BSFL	3.28	3.70	3.49
LSD_{05} mining rocks	0.31	0.18	–
LSD_{05} filling layer	0.26	0.15	–

Table 27.5 Productivity of winter wheat grains for options with using mining rocks and black soil filling layer, t/ha

Test options	First year	Second year	Third year	Mean
Loess loam	1.32	1.03	1.68	1.34
LL + 50 BSFL	2.30	1.65	2.58	2.18
Grey-green clay (GGC)	1.08	1.78	0.88	1.25
GGC + 50 BSFL	1.84	2.29	1.98	2.04
Ore-hosting rock	0.74	0.44	–	0.59
LSD_{05} mining rocks	0.13	0.15	0.26	–
LSD_{05} filling layer	0.13	0.15	0.26	–

To obtain objective assessment of effective fertility of newly created profiles of recultivated lands 3-year field tests with such demanding crop as fall wheat have been made. Account experimental data for 3 year are given in Table 27.5. The greatest yield of winter wheat was produced in options with using subsequent covering technical mixture of mining rocks with grey-green clay and loess loam layers.

Using the calculated data and the results of field tests at Kamysh-Burun station for the zone of arid Steppe as the base the technology of creating reclaimed lands has been determined. Planned surface of industrial waste discharges is covered with waterproof grey-green clay (40 cm) and then with the layers of loess loam (50 cm) and black soil filling (50 cm).

To attract investments into the economics of Kerch the activities on creating the area of priority development and special economic zone on the territory of Eastern Crimea were launched last decade. The creation of the territory of priority development "Kerch" and special economic zone "Port-Crimea" can become an important factor of economy stabilization in this region.

27.5 Conclusions

1. Satellite observations and identification of the conditions of vegetation cover of industrial sites in the eastern part of the Kerch Peninsula was carried out in the course of time and space.
2. Artificial profiles of creating reclaimed lands to retrieve abandoned ore-mining territories for agricultural use have been proposed.
3. It is obvious that reserving natural areas and recovering damaged ones can be achieved in combination with retaining archeological, historical and cultural heritage of the Kerch Peninsula.

References

1. Lebedinsky VI (1988) Geological excursions on Crimea. Tavria, Simpheropol, p 144 (in Russian)
2. Kudrik ID, Oshkader AV, Pytskiy GN (2010) Environmental objects state assessment in the Kerch area. – Kiev: NAS Ukraine: Geology and minerals of world Ocean, №4. – C. 85–89 (in Russian)
3. http://savesteppe.org/ru/archives/7045
4. Rouse JW, Haas RH, Schell JA, Deering DW (1973) Monitoring vegetation systems in the great plains with ERTS. In: Third ERTS symposium, NASA, – SP-351, vol 1, pp 309–317
5. Kriegler FJ, Malila WA, Nalepka RF, Richardson W (1969) Preprocessing transformations and their effects on multispectral recognition. In: Proceedings of the sixth international symposium on remote sensing of environment. University of Michigan, Ann Arbor, pp 97–131
6. Kharytonov M (2007) Geochemical assessment of reclaimed lands in the mining regions of Ukraine. NATO ARW soil chemical pollution, risk assessment, remediation and security. Springer, Dordrecht, pp 57–60
7. Gorbunov NI (1974) Minerology and colloid chemistry of soils. M.: Science, p 316 (in Russian)
8. Kharytonov MM, Yevgrashkina GP (2009) The rocks mass properties and moisture transfer process assessment in the reclaimed lands//sustainable exploitation of natural resources. In: Proceedings of the third international seminar. Ecomining-Europe in 21th Centure, Milos Island, Greece, pp 135–144
9. Zhernov IYe (1971) Meliorative hydrogeology. – K.: High School, p 331 (in Ukrainian)

Chapter 28
Desulphurisation of Karaman-Ermenek Lignites of Turkey at the Accelerated Electrons Impact

Fethullah Chichek, Samira Aliyeva-Chichek, Kamal Yakubov, and Islam I. Mustafayev

Abstract The regularities of desulphurization of lignites from Karaman-Ermenek deposits of Turkey under accelerated electron impact were studied. The absorbed doze in lignites changed within the limits of 1,170–3,120 kGy. As basic indexes of process rate of gas formation, decreasing of initial mass of lignite, the contents of sulfur in the solid have been defined. The gaseous products H_2, CO and CH_4 were identified. The specific features of radiation-chemical decomposition of organic mass of lignite under accelerated electrons impact are discussed.

Keywords Lignites • Accelerated electrons • Desulphurization • Adsorbed dose • Gases

28.1 Introduction

The study of radiation-chemical transformation of coal has great importance for creation of scientific basis of radiation-chemical technology of fossil fuels, establishment of the role of radiation in genesis and metamorphism of fossil fuels as well as determination of radiation stability of carbonaceous materials used in nuclear technology.

Researches on radiation-chemical processes of transformation of fossil fuels have been spent for last 25 years in USA, Japan, Italy, Russia and other countries within the framework of the Programs on atomic-hydrogen power engineering and new methods of processing fossil fuels [1–3]. Radiation-stimulated processes in low-grade lignites of Turkey are not regularly investigated. Istanbul Technical

F. Chichek • S. Aliyeva-Chichek • K. Yakubov • I.I. Mustafayev (✉)
Institute of Radiation Problems, Azerbaijan National Academy of Sciences,
31-a H. Javid ave., AZ1143 Baku, Azerbaijan
e-mail: fcicek49@gmail.com; saliyeva84@gmail.com; imustafayev@mail.ru

A. Veziroğlu and M. Tsitskishvili (eds.), *Black Sea Energy Resource Development and Hydrogen Energy Problems*, NATO Science for Peace and Security Series C: Environmental Security, DOI 10.1007/978-94-007-6152-0_28,

University and Dokuz Eylul University had separate data on radiation-chemical desulphurization and to copyrolysis of lignites of Yatagan, Soma and Yenikoy in 90-d of the last century [3–5].

In this work the regularities of transformation of lignites from Karaman-Ermenek deposits of Turkey under accelerated electrons impact were studied.

28.2 Experimental

The basic characteristics of the investigated samples are: ashes – 19.26 %, moisture – 15.6 %, sulphur – 2.01 %, calorific value – 3,775 kcal/kg. Processes were spent under the impact of accelerated electrons on linear electron accelerator (ELU-6) with power of electron beam P = 12–20 W. The rate of the absorbed doze was determined by combined method-cylinder of Faraday and Calorimeter and equaled to 4,680–7,800 kGy/h. The absorbed dose in lignites changed within the range of 1,170–3,120 kGy. Irradiation was carried out in semiflowing installation, gas products have been collected in gasometer and liquid- in receiver. As basic parameters of process rate of gas formation, losses of initial mass of lignite, the contents of sulfur in solid have been defined. The gases of H_2, CO and CH_4 were identified by chromatography. Decrease of lignite organic weight was determined by gravimetric method. Definition of the contents of sulphur is based on spectroscopic determination of sulphur dioxide-products of oxidation of sulfur.

28.3 Results and Discussion

In Fig. 28.1 kinetics of formation of gases H_2, CO and CH_4 at the radiation-chemical decomposition of lignite sample was illustrated.

The formation rate (W, 10^{15} molec/g s) and radiation–chemical yield (G, molec/100 eV) of gases was determined. In our experiments these parameters are: $W_{(H_2)} = 3.6$, $W_{(CO)} = 5.2$, $W_{(CH_4)} = 0.98$, radiation-chemical yield of these gases are: $G_{(H_2)} = 0.172$, $G_{(CO)} = 0.25$ and $G_{(CH_4)} = 0.047$.

It should be mentioned that these values exceeds radiation-chemical yield of gases in case of γ-radiolysis. In Table 28.1, the values of radiation-chemical yield of gases H_2, CO and CH_4 from lignites of various deposit of Turkey at the γ-radiolysis were given.

The radiation-chemical yield of these gases at the γ-radiolysis are changed: $G_{(H_2)} = 0.019–0.062$, $G_{(CO)} = 0.004$ and $G_{(CH_4)} = 0.001–0.021$ molec/100 eV.

Comparison shows that in case of irradiation by accelerated electrons the radiation-chemical yield of gases three to nine times for hydrogen, 62 times for CO, 2–47 times for CH_4 exceeds the values in case of γ-radiolysis. The observable

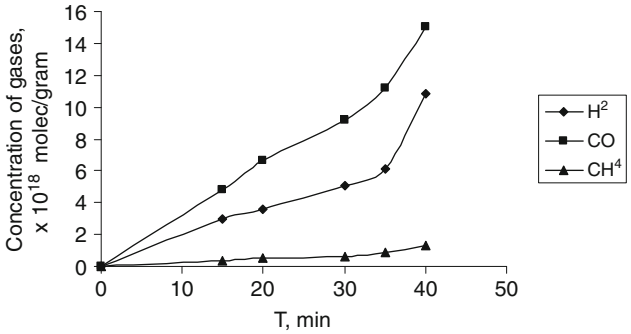

Fig. 28.1 Kinetics of formation of gas H_2, CO, CH_4 at decomposition of lignite under accelerated electron impacts

Table 28.1 Radiation-chemical yields (G × 10^3 molec/100 eV) of gases at the γ-radiolysis of Turkish lignites

Lignite type	H_2	CO	CH_4	C_2H_6	C_2H_4	C_3	C_4	C_5
Karaman–Ermenek, cleaned	24	–	0.7	–	–	–	–	–
Karaman–Ermenek, raw	22	–	1.7	–	–	–	–	–
Nevshehir, raw	24	–	4.9	2	–	–	–	–
Silopi, raw	62		21.7	0.7	0.8	1.0	0.6	0.3
Trakya, mixed	19	4	1.0		–	–	–	–

difference in the yield of gases at the impact of γ-radiation and accelerated electrons can be connected by the influence of high value of dose rate which can lead to qualitatively new processes, or change of physical condition (temperature, pressure, etc.) of reaction zone.

In our early researches [3–6] it has been shown that hydrogen and methane from lignites are formed due to recombination reactions of radiolytic radicals of H, CH_3:

M ® CH_3, H, CO, M^+, M*
H+H ® H_2
CH_3+H ® CH_4 and etc.

Carbon monoxide is formed at radiation splitting of oxygen-containing functional groups. Change of recombination mechanism to reaction of separation in the gas formation demands temperature more 200 °C which in our case is not observed. Small increase in gases yield with activation energy E = 10–15 KJ/mole is possible due to increase of diffusion of particles in reactionary volume. It means that active particles formed at radiolysis can be stabilized in defective structure of lignite mass. Rise in temperature even above 50 °C can lead to simplification of their diffusion and by that increase in recombination rate of radical products with formation H_2 and CH_4. At braking accelerated electrons in the sample volume local rise in temperature and increase in the yield of products may be observed. Such rise in

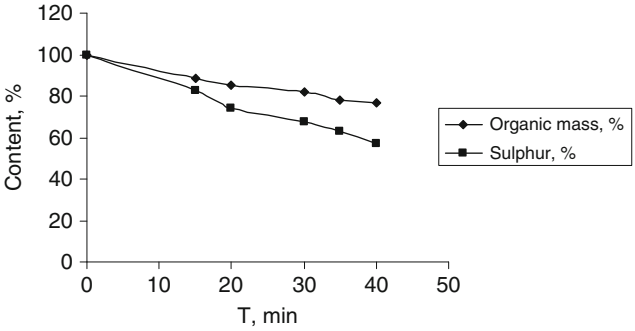

Fig. 28.2 Dependence of relative changes of lignite mass and sulphur content at the irradiation by electron beam

temperature does not happen under the action of γ-radiation and yields of gases considerably decrease under the influence of accelerated electrons. The course of kinetic curves at rather high doses (increase of inclination) also testifies local heating of lignite mass.

The dependence of content of volatile products in structure of lignite at absorbed doze at irradiation in the range of doze D = 1,170–3,120 kGy was illustrated in Fig. 28.2. The lignite mass during irradiation decreases up to 76.5 %. During irradiation volatile products decrease correspondingly from 35 to 11.5 %, so approximately 23.5 % of volatile products are allocated in the form of gases and liquid. In the same figure laws of change of sulphur relative content in solid product, concerning initial value were shown too.

It should be noted that rather deep decomposition of lignites at thermal decomposition below 400 °C temperatures is impossible. The observable phenomenon is connected with destructive effect of ionizing radiation.

Material balance of this process it is resulted in the Table 28.2.

It is evident that in semiflowing installation the products of reactions basically are in liquid phase.

The changes of absolute content of sulphur in lignite sample at absorbed dose of accelerated electrons were adduced in Fig. 28.3. The contents of sulphur in solid decreases from 2.01 up to 1.62 % in the course of irradiation of 40 min in W = 12 W.

If we consider that there is also decomposition of organic mass of lignite a degree of relative reduction the contents of sulfur reaches up to 57.1 % (Figs. 28.2 and 28.3). It shows that in spite of decays up to 23.5 % of organic weight, and thus leaves up to 43 % of sulphur. It testifies about selective desulphurization of lignite mass under electron beam impact. Last circumstance is connected with selective cleaning of sulphur from organic mass of lignites, which is connected with highest electronic density of atoms of sulphur than atoms of carbon and hydrogen. Radiation action on chemical bounds with more density of electrons is more effectively.

Table 28.2 Material balance of process of lignite radiation-thermal decomposition (in mass %)

Initial mass	Solid product	Liquid product	Gases
100	74–78	20–24	1–2

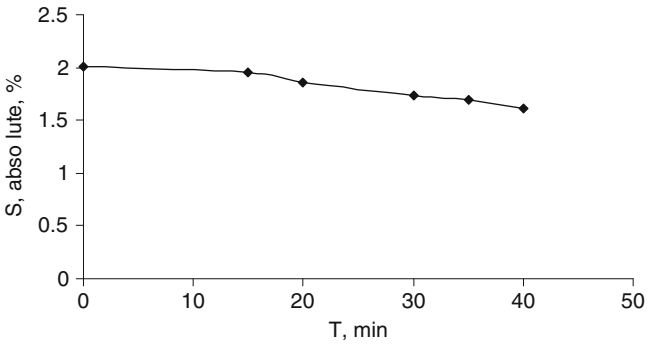

Fig. 28.3 Influence of irradiation (absorbed doze) on absolute content of sulphur in solid product of radiation-chemical decomposition of lignite

28.4 Conclusions

Thus, at radiation-chemical decomposition of lignites under the impact of accelerated electrons a number of the specific features differing influence of γ-radiation was shown:

1. The integrated influence of radiation and temperature can lead to increase of selectivity of radiation desulphurization due to stimulation of separation processes with participation of sulphur-content groups.
2. At braking electron there is local heating of lignite mass, that stimulates diffusion processes in gas formation
3. At pulse impact of accelerated electrons with frequency 50 Hz and duration of the impulse 2.5 s happens high-speed (10^4–10^5degree/s) heating of lignite mass. It leads to deep decomposition of organic mass with formation of liquid products.

These features of influence of accelerated electrons on lignites can be used by development of processes of radiation-chemical technology of processing fossil fuels.

References

1. D'Anjou D, Litman R (1983) Radiation induced transformations of oil shale. Radiochem Radioanal Lett 50(1):37
2. Yermakov A, Popov VN, Dzantiyev V (1988) Radiation-chemical influence of irradiation on thermoradiation processes of coal gasification. Chem High Energy 22:132–136

3. Mustafayev I, Hajiyev H, Yagubov K, Dzantiyev B (1988) Hydrogen and hydrogen-containing gas production from fossil fuels by thermoradiation. In: Proceedings of the 7th world hydrogen energy conference. USSR, Moscow, vol 2, 25–29 Sept 1988, pp 955–965
4. Mustafayev I, Yamik A, Mahmudov H (1994) Coal desulphurization by electron beam. In: Demirel H (ed) 5th international mineral processing symposium Capadociya. Progress in Mineral Processing Technology, Turkey, 6–8 Sept 1994, pp 343–346
5. Mustafayev I, Kemal M, Tolgonay Y, Yamik A (1994) Radiation-stimulated processes of destruction and polycondencation in coals. J Radioanal Nucl Chem Lett 187(5):355–365
6. Mustafayev I, Chichek F (2006) Gas formation at radiation-chemical decomposition of Turkish lignites. In: Proceedings, XXIII International Mineral Processing Congress, vol 3, 3–8 Sept 2006, pp 2554–2558, Promedadvertsing-2006. Istanbul, Turkey

Chapter 29
Influence of Static and Cyclic Tensions on Corrosion – Mechanical Destruction of Steels in Hydrogen Sulfide Environments

Myroslav S. Khoma

Abstract It has been investigated that influence, in terms of loading and composition of hydrogen sulfide environments, are resistant to corrosion-mechanical destruction of typical steels appointed to marine constructions, gas and oil equipment, and pipelines which are exploited on a marine shelf: steel 20, steels 10CrSiNiCu, 28Cr2MoVNbCu, 30CrMo, stainless steel 12Cr21Ni5Ti and steel of 17Mn1Si with the welded joint.

It is discovered that the high resistance of steels to sulphide stress corrosion cracking (SSCC) does not guarantee it high endurance in solution of NACE (5 % NaCl + 0.5 % CH_3COOH + H_2S, sat., pH3. . .4, t = 20 ± 3 °C) at cyclic tensions: at a symmetric cycle endurance the least resistant to SSCC of steel 20 goes down comparatively with air in ~1.4 times, and more resistant steel 30CrMo and 12Cr21Ni5Ti – in ~2.6 and 1.9 times, accordingly. An analogical tendency is observed at an asymmetric cycle at amplitude $\sigma_a = 0.2\sigma_{0.2}$. In presence of the welded joints asymmetric tensions reduce their resistance destruction in a greater measure, than specimen from basic metal. It has also been established that the addition of 3.5 % solution of marine salt 15 mg/l to H_2S does not influence the stress intensity factor of high-strength steel 28Cr2MoVNbCu. At the repeatedly static loading with frequency $f = 1.1 \cdot 10^{-5}$ Hz depending on the level of this steel strength, the value of conditional critical stress intensity factors K_{scc} in this solution goes down on 10–15 %.

Thus at the selection of materials for work in hydrogen sulfide environments, it is necessary, except for the generally accepted approaches, for an estimation of high ability to work to take the influence of alternating tensions.

Keywords Hydrogen sulfide • Steel • Sulphide stress corrosion cracking • Asymmetric tensions • Stress intensity factor • Endurance

M.S. Khoma (✉)
Karpenko Physico-Mechanical Institute of NAS of Ukraine,
Naukova of str., 5, 79601 Lviv, Ukraine
e-mail: khoma@gmail.com

A. Veziroğlu and M. Tsitskishvili (eds.), *Black Sea Energy Resource Development and Hydrogen Energy Problems*, NATO Science for Peace and Security Series C: Environmental Security, DOI 10.1007/978-94-007-6152-0_29,

29.1 Introduction

With development of gas and oil deposits on the shelf of the Black Sea and any use of deep hydrogen sulfide requires the use of materials, which provide a high ability to work with equipment. In relation to that, there is a high-rate of corrosion and hydrogen saturation of metals in hydrogen sulfide environments. This results in their speed-up corrosion-mechanical destruction. The damages of metals in hydrogen sulfide environments carry out mainly at constant deformation or loading. However at planning of construction which will contact with hydrogen sulfide solutions, it is necessary to take into account the possibility of alternating tensions from the choppiness of the sea and wind loading.

29.2 Method of Research

Investigation of steels which are used for the making of construction, and gas and oil equipments appointed for exploitation on a marine shelf: steel 20, steels 10CrSiNiCu, 28Cr2MoVNbCu, 30CrMo and stainless steel 12Cr21Ni5Ti are examined as perspective material for work in such environments. Research also shows steel of 17Mn1Si with the welded joint (electrode UONII-13/55). Research carried out in environments: standard solution of NACE (5 % NaCl + 0.5 % CH_3COOH + H_2S (saturated), pH 3. . .4, 22 ± 3 °C) [1]; 3.5 % solution of marine salt (‰): 10.7 Na^+; 0.39 K^+; 0.45 Ca^{2+}; 1.32 Mg^{2+}; 19.3 Cl^-; 0.07 Br^-; 2.67 SO_4^{2-}; 0.1 HCO_3^-; 0.01 CO_3^{2-} and that solution with 15 mg/l H_2S at a room temperature.

Resistance of steels to sulfide stress corrosion cracking (SSCC) was determinated according to the requirements of the standards of NACE TM0177-90 [1] and methods of MCKP-01-85 [2]. Used cylinder specimens with diameter 6.4 mm which set in cell with working solution and loaded permanent static tensions. During an experiment bubbled H_2S through solution with speed ~0.2 ml/min. Threshold tension σ_{scc} (criterion of steels resistance to SSCC) was determinated at the base of tests of 720 h.

The corrosive crack growth resistance of steels designated on beam specimens with the preliminary created fatigue crack after the stress intensity factors (K_{scc}) and at the cyclic change of tension ($f = 1.2 \cdot 10$–5 Hz) after the maximal conditional stress intensity factors (K_{sccmax}), determinated at the base of 2016 h.

Durability of steels at the compatible action of static and cyclic tensions was studied at frequency 0.5 Hz by asymmetry of cycle of $R = \sigma_{max}/\sigma_{min} > 0$. Base of tests – 720 h The degree of influence of cyclic tensions on the acceleration of destruction of statically tense steels was estimated after a coefficient α ($\alpha = \tau_p/\tau_p'$, where τ_p and τ_p' is time to destruction at the static and asymmetric cyclic loadings, accordingly). On a low-cycle corrosion fatigue round specimens with diameter working part 5.0 mm investigated by deformation a clean bend with a rotation at frequency of loading 1 Hz.

29.2.1 Results of Researches and Their Discussion

It has been established that the threshold tension at SSCC (σ_{scc}) for steel 20 makes 175 MPa ($\sigma_{scc}/\sigma_{0.2} = 0.6$). By the asymmetric cycle of growth of amplitude of loading in 1.2...2.2 times durability of specimens decreases in 1.8...14.0 times and increase of middle tension in 1.2...1.4 – in 1.6...2.4 times (Fig. 29.1, curves 1; 1′). Scilicet, influence of middle tension of cycle on the decline of durability of steel 20 is less than, than his amplitudes (Fig. 29.2, curves 1; 4; p. 5). By middle tension of cycle even $\sigma_m = \sigma_{scc} = 175$ MPa and to amplitude $\sigma_a = 0.2\sigma_{02} = 54$ MPa the cyclic loadings reduce durability specimens in 1.2 times, and at the value of $\sigma_m = 140$ MPa specimens not broke in times of base tests.

For steel 30CrMo threshold tension at SSCC in solution of NACE makes 440 MPa ($\sigma_{scc}/\sigma_{0.2} = 0.8$), thus, it has higher resistance to him, than steel 20. However at the asymmetric cyclic loading ($\sigma_m = \sigma_{scc} = 440$ MPa; $\sigma_a = 0.2\ \sigma_{02} = 96$ MPa) durability of this steel goes down in ~14 times and at the indicated amplitude a value is not obtained at σ_m, at what specimens not broke in times of base. That testifies to the higher sensitivity of 30CrMo steel to the action of cyclic tensions in comparison with steel 20. For low-alloyed steel also there is greater influence on parameter α amplitudes of tensions, than them mean value: for growth σ_a in 1.5...2.0 times α increases in 3.9...13.9 times, and for growth σ_m in 1.4...2.2 times increases in 1.3...5.2 times (Fig. 29.2, curves 2; p. 6; 7).

The results of the investigations of both steels on a low-cycle fatigue confirm this conclusion, in solution of NACE value of fatigue limit for steel 30CrMo goes down in ~2.6 times, and for steel 20 – in ~1.4 times against endurance in the air. Consequently, high resistance of steel under SSCC tension does not determine the same its resistance to the corrosion fatigue.

Ferrite-austenitic stainless steel 12Cr21Ni5Ti also has a high endurance to SSCC: $\sigma_{scc} = 450$ MPa ($\sigma_{scc}/\sigma_{0.2} = 0.8$). It less inclined to low-cycle corrosion fatigue, than steel of 30CrMo, but more than steel 20: its corrosion fatigue limit in solution of NACE in ~1.9 times lower against the value of endurance in air. Under the action of cyclic tensions for amplitude of 98 MPa durability of this steel at middle tension of cycle to even σ_{scc} declined in ~1.5 times (Fig. 29.2, curves 3; p.8). At the indicated amplitude specimens not broke in times of base tests at the value of $\sigma_m = 320$ MPa, that in 1.4 times below from σ_{scc}. The increase of tensions amplitude in 1.7 times ($\sigma_m = 450$ MPa) decreased durability of specimens in ~72 times.

Comparison of resistance of steels 20, 30CrMo and 12Cr21Ni5Ti the actions of asymmetric cyclic and static tensions shows (Fig. 29.2), that more intensive in all cyclic tensions decrease durability of steel 30CrMo, less – steel 20 and least – stainless steel. A tendency shows up also to higher decline of durability of specimens with growth of amplitude of asymmetric cycle, than him middle tension.

All of the steels investigated were in a solution of salt water without any to the hydrogen sulphide and with concentration of 15 mg/l insensitive to stress corrosion cracking: threshold tension σ_{ssc} is not less than $0.9\sigma_{0.2}$, that testifies to its high

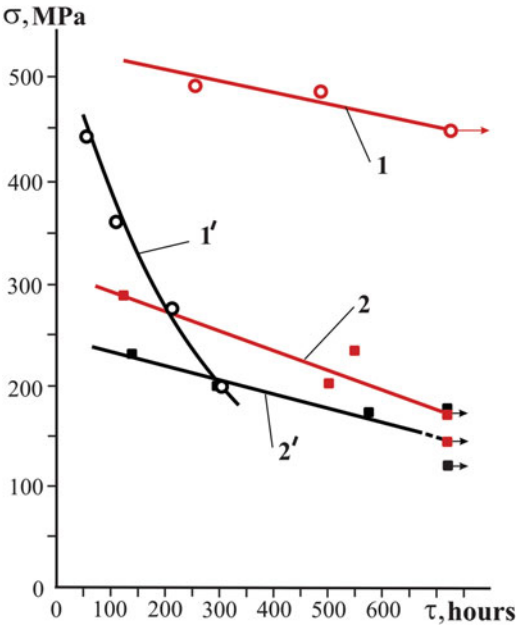

Fig. 29.1 Influence of static (1; 2) and asymmetric cyclic (1′; 2′; f = 0.5 Hz; $\sigma_a = 0.2\sigma_{0.2}$) tensions on durability of steel 30CrMo (1; 1′) and steel 20 (2; 2′) in solution of NACE (*see color plates*)

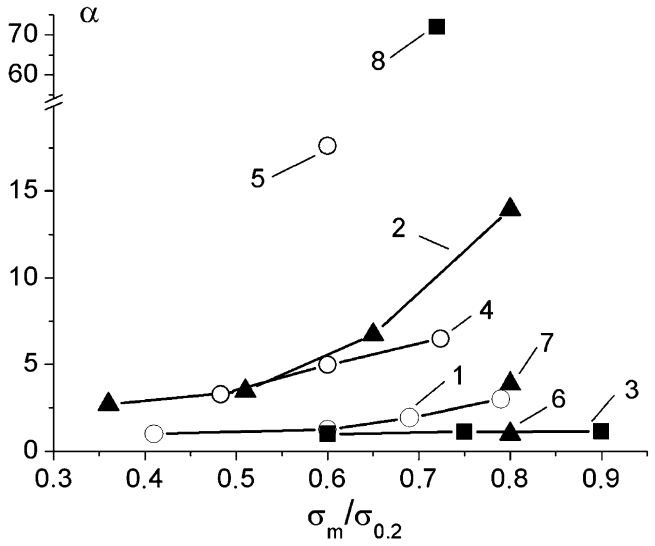

Fig. 29.2 Resistance of steel 20 (1; 4; 5), steels 30CrMo (2; 6; 7) and 12Cr21Ni5Ti (3, 8) to destruction in solution of NACE at asymmetric cyclic tensions: *1* $\sigma_a = 54$ MPa, *2* $\sigma_a = 96$ MPa, *3* $\sigma_a = 98$ MPa, *4* $\sigma_a = 80$ MPa, *5* $\sigma_a = 126$ MPa, *6* $\sigma_a = 40$ MPa, *7* $\sigma_a = 60$ MPa, *8* $\sigma_a = 167$ MPa

resistance the initiation of cracks. Therefore, it was investigated the high-strength 28Cr2MoVNbCu and low-strength 10CrSiNiCu steels on crack growth resistance in these environments.

Maximal crack growth resistance at the short-term loading in air (to 1.5 min) has steel of 28Cr2MoVNbCu after tempering at 620 °C: $K^{air} = 132$ MPa · $m^{1/2}$. An increase of tempering temperature of steel to 680 and 700 °C diminishes this size to the values 107 and 92.5 MPa · $m^{1/2}$, accordingly. In connection with very low speed of development of cracks, the sensitiveness of the steel to stress corrosion cracking judged only on the basis of results of metallography research of tops of cracks in specimens. In 3.5 % solution of marine salt with content of H_2S (15 mg/l) and without him the conditional threshold stress intensity factor K_{scc} for specimens with cracks which are tempered at temperatures 620, 680 and 700 °C, it is 49.6 ($0.38K^{air}$); 79.3 ($0.76K^{air}$) and 74.3 ($0.8K^{air}$) MPa $m^{1/2}$, accordingly. Consequently, an increase of tempering temperature of steel 28Cr2MoVNbCu, that reduces its strength, diminishes the sensitiveness of steel at presence of cracks to corrosion destruction.

A critical stress intensity factor is at short-term loading of specimens from steel of 10CrSiNiCu, which has less strength, than steel of 28Cr2MoVNbCu, in air is 63 MPa · $m^{1/2}$. In 3.5 % solution of marine salt with content of H_2S and without him the conditional threshold stress intensity factor for this steel is 52 MPa · $m^{1/2}$ ($0.8\ K^{air}$). Consequently, the H_2S in such small concentration does not influence on resistant of development of cracks in low strength steel 10CrSiNiCu.

The cyclic change of stress intensity factor creates pre-conditions for local destruction of surface protective films, which assists development of corrosive-mechanical defects in the top of crack. It causes reduction of steels resistance to destruction in corrosive environments. On such conditions, the maximal conditional threshold stress intensity factor K_{sccmax} in this solution for samples of 28Cr2MoVNbCu steel, tempered at 680 and 700 °C, accordingly on 10.8 and 5.8 MPa · $m^{1/2}$ lower from K_{scc} and are 68.5 MPa · $m^{1/2}$. The repeated static loading of specimens from low-strength steel 10CrSiNiCu did not change the value of parameter K_{scc}: it is 52 MPa · $m^{1/2}$.

Decrease of resistance to destruction on 15 and 10 % under the repeated static loading of specimens with cracks from high-strength steel 28Cr2MoVNbCu connected, obviously, with intensification of action of hydrogen factor which is partly accountable for stress corrosion cracking of steels in salt water [3]. For the same reason the repeated static loading do not influence on the parameter K_{scc} for low-strength steel 10CrSiNiCu, the structure of which is little sensitive to the action of hydrogen.

Majority metallic constructions are contained the welded connections which mainly determine their durability. Therefore investigated their influence on endurance of steel 17Mn1Si in hydrogen sulfide environments.

It is set high resistance of steel 17Mn1Si to stress corrosion cracking in solution of NACE (Fig. 29.3, curve 1): threshold tension makes 295 MPa ($\sigma_{scc}/\sigma_{0.2} = 0.67$). At an asymmetric cycle ($\sigma_a = \sigma_{02} = 88$ MPa) specimens not broke in times of base tests only at middle tension of $\sigma_m = 160$ MPa (Fig. 29.3, curve 2).

Threshold tensions are in solution of NACE for the welded specimens of this steel (Fig. 29.4, curve 1), welded the electrodes of UONII-13/55, the same, as well

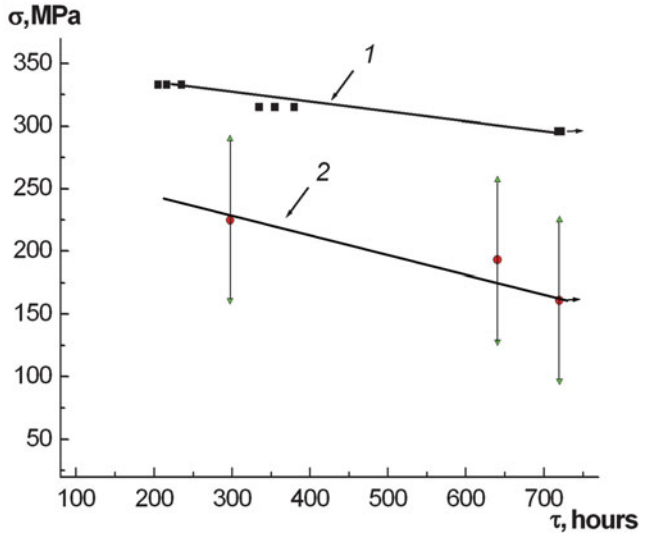

Fig. 29.3 Influence of static (1) and asymmetric cyclic (2; f = 0.5 Hz; $\sigma_a = 0.2\sigma_{0.2}$) tensions on durability of steel 17Mn1Si in solution of NACE (*see color plates*)

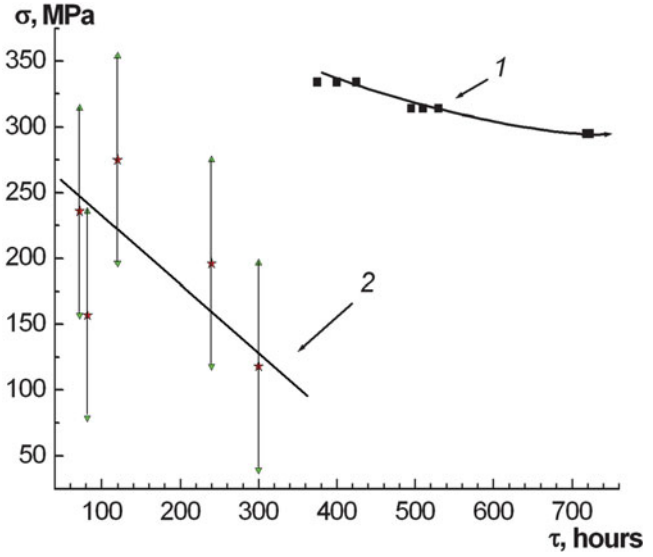

Fig. 29.4 Influence of static (1) and asymmetric cyclic (2; f = 0.5 Hz; $\sigma_a = 0.2\sigma_{0.2}$) tensions on durability of welded specimens from steel 17Mn1Si in solution of NACE (*see color plates*)

as for base metal ($\sigma_{scc} = 295$ MPa). However at higher tensions their durability less than on ~20 %. At asymmetric cyclic tensions for the welded specimens obtain not level middle tensions ($\sigma_a = 0.2\sigma_{02}$) which they do not broke, but their durability in two to three times below, than specimens from a base metal (Fig. 29.4, curve 2).

29.3 Conclusions

It is shown that high resistance steels to sulfide stress corrosion cracking does not guarantee them high resistance to destruction in the saturated hydrogen sulfide environments at the compatible action of static and cyclic tensions: cyclic tensions with different asymmetry and identical amplitude $\sigma_a = 0.2\sigma_{0.2}$ decrease durability of less resistance to SSCC of steel 20 in 1.2...3 times, and more resistance steel of 30XMA – in 2.4...14 times. A tendency shows up also to higher decline of durability of specimens with growth of amplitude of asymmetric cycle, than him middle tension.

It is set that H_2S in a concentration of 15 mg/l does not influence the value of conditional threshold stress intensity factor K_{scc} for high-strength steel 28Cr2MoVNbCu in solution of marine salt. At the repeated static loading with frequency $f = 1.1 \cdot 10^{-5}$ Hz depending on the level of strength of steels values of K_{scc} in solution of marine salt with an admixture H_2S goes down on 10–15 %.

The welded connections of steel of 17Mn1Si, that welded electrodes of UONII-13/55, do not cause the decline of resistance to stress corrosion cracking of metal in solution NACE: the level of threshold tensions is such, as well as for a base metal = 295 MPa. It is showed that cyclic asymmetric tensions ($\sigma_a = 0.2\sigma_{0.2}$) reduce resistance destruction of the welded specimens in solution NACE in a greater measure, than specimens from a base metal: steel of 17Mn1Si does not collapse during 720 h at $\sigma_m = 160$ MPa, in that time as durability of the welded specimens makes only 260 h.

References

1. NACE Standard TM 0177-90 (1990) Standard test method laboratory of metals for resistance to sulfide stress corrosion cracking in H_2S environments. National Association of Corrosion Engineers (NACE), Houston,p 22
2. MCKP-01-85 (1985) Method of test on resistance against to sulphide stress corrosion cracking. Moscow: GKNT of the USSR p 4
3. Pokhmurskii V, Melekhov R, Krutsan G, Zdanovskii V (1995) Corrosion mechanical destruction of weldments. K.: Naukova dumka p 261

Chapter 30
Hydrogen and Hydrogen Containing Gas Formation at the Radiation-Thermal Clean Up of Water from Oil Pollution

Islam I. Mustafayev

Abstract The regularities of hydrogen and hydrogen-containing gas formation at the purification of oil industry sewage by radiation-chemical method have been studied. Radiation-thermal transformations of hydrocarbon admixtures in the water medium have been established. As a model was selected heptane-water system, the received results have been tested on an example of Caspian oil. The experiments have been carried out in the static and thermostable conditions under impact of γ-radiations Co^{60}. The influence of the dose, temperature, medium, initial concentration of components to the radiation-chemical yield of the hydrogen and other gases have been established. It was shown that in the temperatures higher 300 °C as a result of interaction of components and active particles, which are formed from their radiolysis decomposition of hydrocarbons turns into the chain mode and yields of gas products (H_2, CO, CH_4, $\Sigma C_2 - \Sigma C_6$) were higher than additive quantity. It is defined optimal temperature interval T = 400–450 °C and absorbed dose D = 2.5–4.0 kGy for purification of 87–90 % of Caspian oil with initial concentration less than 0.1 % in the water.

The influence of oxygen on radiation-chemical production of hydrogen-containing gases from the water-heptane system was studied. In the water medium proposed four stages, it simplified the kinetic model of the hydrocarbon admixtures radiation-chemical decompositions and hydrogen-containing gas formation. Calculations were carried out according to this model. The mechanism of proceed processes and results of feasibility studies on developed method are discussed.

Keywords Water • Oil admixtures • Radiolysis • Purification • Hydrogen-containing gases

I.I. Mustafayev (✉)
Institute of Radiation Problems, Azerbaijan National Academy of Sciences,
9, B. Vahabzadeh str., AZ1143 Baku, Azerbaijan
e-mail: imustafayev@mail.ru

A. Veziroğlu and M. Tsitskishvili (eds.), *Black Sea Energy Resource Development and Hydrogen Energy Problems*, NATO Science for Peace and Security Series C: Environmental Security, DOI 10.1007/978-94-007-6152-0_30,

30.1 Introduction

The problem of purification of water resources from oil and oil products has great importance as for extraction of additional resources of oil from oil-polluted waters, as well as for environmental protection. In Apsheron peninsula of Azerbaijan as a result of exploitation of oil-fields within 150 years, it was formed more than 250 artificial oil- polluted lakes in which concentration of hydrocarbons sometimes exceeds 25 mg/l. Annually from oil industry are discharged more than 45 million tons (by production of 10 million tons of oil) sewage.

Now it is applied various physical and chemical methods to purification of sewage from oil pollution [1], including radiation-chemical methods [2–6]. In [2] the gamma-radiation of the isotope source of Co-60 and accelerated electrons for decomposition of various fractions of oil in the water medium at the temperature 30–40 °C are used. At the absorbed dose 25–32 kGy is achieved 85–96 % of the cleaning.

Before [7], we established the chain decomposition of hydrocarbons at the radiation-thermal processes. In this work with the purpose of reduction of the absorbed dose and increase of purification degree we used such approach, i.e., the joint action of radiation and temperature on oil polluted waters.

In [8], we have established the dependence of the radiation-chemical yield of the decomposition of n.heptane from its initial concentration. It is shown, that with increase of initial concentration of n.heptane grows radiation-chemical yield of decomposition. At low concentration of heptane ($<10^{-3}$ %) change of its concentration in ten times does not influence the rate of decomposition. Similar result is observed also for the formation of products.

In the present study, we investigated the regularities of production of hydrogen - containing gases in the processes of radiation-chemical decomposition of oil in the water medium. Kinetic calculations on radiation-thermal transformation of hydrocarbons in the water medium are lead also.

30.2 Experimental

The experiments for the study of the kinetics of radiation-thermal process were conducted on mixtures of water with n-heptane as an oil hydrocarbon model. The model mixtures have prepared in vacuum equipment. The water vapor, n-heptane and oxygen sequentially were feed in the glass ampoule of 30 ml volume and were sealed. The total concentration of the mixture in the ampoule was 10^{20} molec/ml, and the components ratio changed in the limits $[C_7H_{16}]/[H_2O] = (1–100) \cdot 10^{-5}$. Irradiation of the ampoule has been carried out in γ-radiation source of Co^{60}, by dose rate 0.7–3.2 kGy/h and adsorbed dose D = 0.5–16.0 kGy. Determination of the dose rate of gamma-radiation was conducted by ethylene and ferrosulphate dosimeters, and results of the measurements were agreed within the limits of 12–15 %.

The concentration of hydrogen-containing gas products of the radiation-thermal decomposition of mixtures of water with n-heptane and oxygen was determined chromatographically.

The numerical modulation of kinetics carried out by the use of Program GEPASI for homogeneous chemical and biochemical systems. As a method of numerical integration, the method of Gere is used.

30.3 Results and Discussion

At the radiolysis of binary mixtures of water-heptane the process of decomposition happens due to transfer of energy from molecules of water to heptane as a result of reaction of recharge. The difference in the potential of ionization −2.7 eV energy is distributed between components. As a neutral active product of recombination of ions are alkyl radical [7]. These radicals play the basic role in formations of the stabile products of radiolysis. The role of medium in course of processes should be essential.

The dependence of the radiation-chemical yield of decomposition of heptane in the water medium on its initial concentration for three temperatures is presented in the Fig. 30.1.

At the concentration above 0.1 % there is sharp increase $G(-C_7H_{16})$ up to 120 molec/100 eV. Under such circumstances grows also the yields of gases. Kinetics of hydrogen and hydrogen-containing gases formation at the $[C_7H_{16}]/[H_2O] = 10^{-4}$ is adduced in Fig. 30.2.

The mechanism of decomposition of initial hydrocarbon and formation of products include the reactions of recombination, separation and dissociation of radicals. Depending on temperature, concentration and dose rate prevail one of the these reactions and changes in rate of gas formation are observed.

At the temperatures above 300 °C besides radiation-stimulated processes thermal processes proceed also. By the rise of temperature the ratio of radiation-thermal and thermal processes (Wrt/Wt) sharply decreases (see Table 30.1).

The influence of oxygen on radiation-chemical decomposition of hydrocarbon admixtures also has been established. If these reasoning lawful at presence of oxygen we should observe reduction of products due to fast reactions of capture of these radicals by oxygen:

$$R + O_2 \rightarrow RO_2,\ ROOH,\ \text{etc.}$$

Probably also direct radiation-chemical oxidation of initial hydrocarbon:

$$RH + O_2 \rightarrow ROOH \tag{30.1}$$

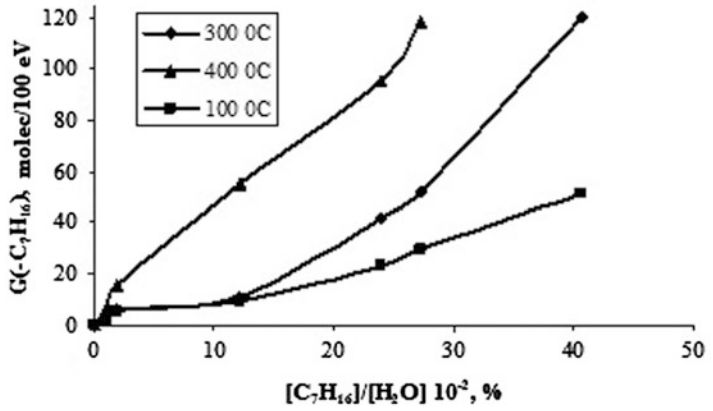

Fig. 30.1 The influence of concentration of heptane in water medium on radiation-chemical yield its decomposition. D = 3.2−16 kGy

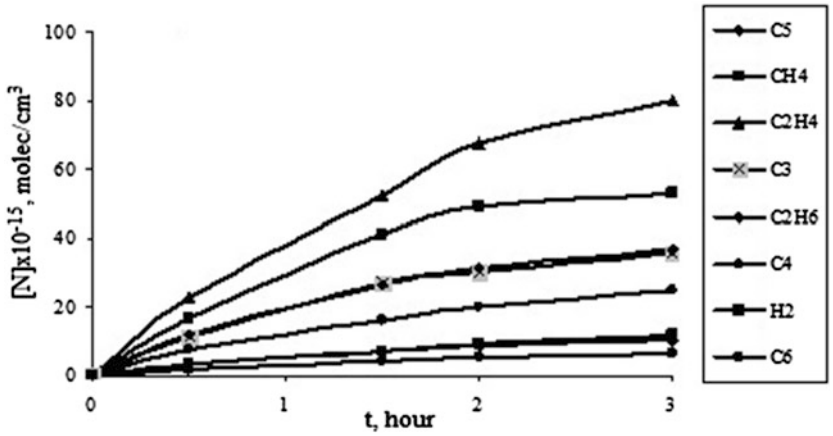

Fig. 30.2 Kinetics of hydrogen-containing gas formation at the radiation-chemical decomposition of heptane admixtures; I = 3.6 kGy/h

Table 30.1 Influence of temperature on ratio of rates of radiation-thermal and thermal processes of gas formation

T°C	300	350	375	400
W_{rt}/W_t	101.2	55.2	26.1	1.9

In order to revise this assumption and establish the correct mechanism of the processes, we studied influence of oxygen addition on yield of stable hydrocarbon products and decomposition of an initial hydrocarbon component.

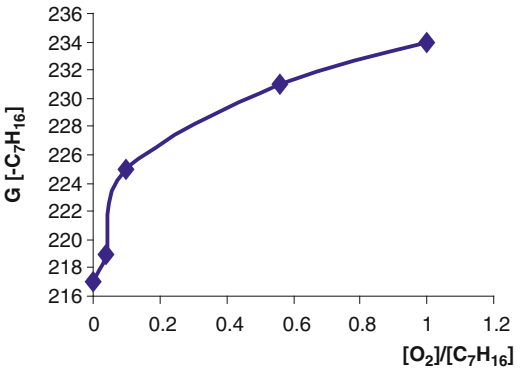

Fig. 30.3 Influence of oxygen on radiation-chemical yield of heptane decomposition in the water medium. $[C_7H_{16}]/[H_2O] = 10^{-4}$ (*see color plates*)

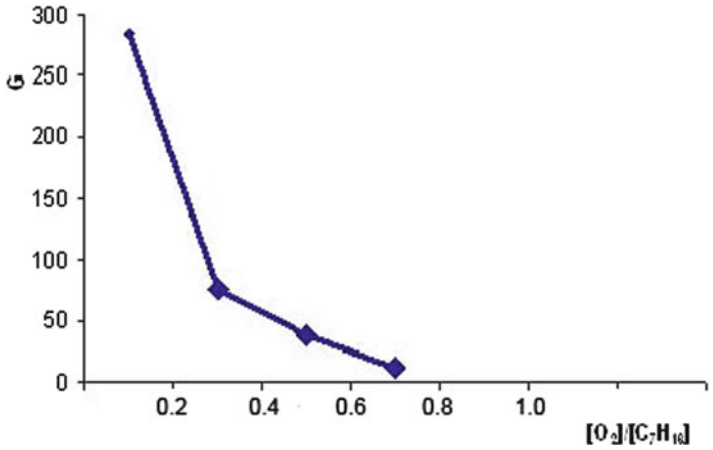

Fig. 30.4 Influence of oxygen on radiation-chemical yield of methane at the decomposition of heptane in water medium (*see color plates*)

The dependence of a radiation-chemical yield of the decomposition of initial hydrocarbon and formation of gases of products on concentration of the entered oxygen results are shown in Figs. 30.3 and 30.4.

It is visible from Fig. 30.3, that at a increase in ratio of concentrations $[O_2]/[C_7H_{16}]$ up to 1 leads to increase $G(-C_7H_{16})$ from 217 up to 234. At the same time the rate of formation of hydrocarbon gases sharply decreases (see Fig. 30.4)

As well as it was supposed at statement of this study due to capture of radicals by oxygen occurs reduction of hydrocarbonic gases yields. The organic oxygen-containing substances are probably formed in this case. In spite of the fact that rate of decay of initial hydrocarbon increases, from the point of view of cleaning this process is non-rational. As a result of such process, oxygen-containing liquid organic compounds (ketons, acids, aldehydes, alcohol, etc.) can be formed and that in the liquid phase can pollute it. Certainly the microadmoxtures of oxygen can give the positive effect as a result of participation of oxygen in destructive process.

Table 30.2 Dependence of G_{gas}/G_{liq} on temperature

T°C		100	200	300	400
G_{gas}/G_{liq}	H_2O—C_7H_{16}	0.07	0.52	5.2	15.8
	H_2O—C_7H_{16}—O_2	0.05	0.1	0.8	2.5

Table 30.3 Reaction scheme of radiation-thermal transformations of heptane admixtures in water medium $[C_7H_{16}]/[H_2O] = 10^{-5} - 10^{-1}$, I = 3.2 kGy/h, D = 3.2 − 16.0 kGy, P = 0.1 MPa, T = 375 − 675 K

No	Reactions	Type of reactions
1	$H_2O \rightarrow H_2O^+ + e$, H_2O^*, H + OH, etc.	Radiolysis
2	$C_7H_{16} \rightarrow C_7H_{16}^+ + e$, $C_7H_{16}^*$, C_7H_{15} + H, etc.	Radiolysis
3	$H_2O^+ + C_7H_{16} \rightarrow C_7H_{16}^+$, $C_7H_{16}^*$, C_7H_{15} + H	Radiolysis
4	$H + C_7H_{16} \rightarrow H_2 + C_7H_{15}$	Separation
5	$OH + C_7H_{16} \rightarrow H_2O + C_7H_{15}$	Separation
6	$C_7H_{15} \rightarrow H + C_7H_{14}$	Dissociation
7	$C_7H_{15} \rightarrow CH_3 + C_6H_{12}$	Dissociation
8	$C_7H_{15} \rightarrow C_2H_5 + C_5H_{10}$	Dissociation
9	$C_7H_{15} \rightarrow C_3H_7 + C_4H_8$	Dissociation
10	$C_7H_{15} \rightarrow C_4H_9 + C_3H_6$	Dissociation
11	$C_7H_{15} \rightarrow C_5H_{11} + C_2H_4$	Dissociation
12	$CH_3 + C_7H_{16} \rightarrow CH_4 + C_7H_{15}$	Separation
13	$C_2H_5 + C_7H_{16} \rightarrow C_2H_6 + C_7H_{15}$	Separation
14	$C_3H_7 + C_7H_{16} \rightarrow C_3H_8 + C_7H_{15}$	Separation
15	$C_4H_9 + C_7H_{16} \rightarrow C_4H_{10} + C_7H_{15}$	Separation
16	$C_5H_{11} + C_7H_{16} \rightarrow C_5H_{12} + C_7H_{15}$	Separation
17	$C_6H_{13} + C_7H_{16} \rightarrow C_6H_{14} + C_7H_{15}$	Separation
18	$C_7H_{15} + C_7H_{15} \rightarrow C_{14}H_{30}$	Recombination
19	$C_7H_{15} + C_7H_{15} \rightarrow C_7H_{16} + C_7H_{14}$	Disproportion

The dependence of the ratio of the yield of products in the liquid and gas phase (G_{gas}/G_{liq}) from temperature of the process is presented at absence of oxygen (1) and its presence (2) adduced in the Table 30.2. The yield of gas products with rise in temperature grows in both cases; in the case of participation of oxygen this growth is slower.

In investigated system except of hydrocarbon gases, it is observed also that carbon monoxide as a product of incomplete oxidation of hydrocarbons.

As a result of the analysis of experimental data, we offer the simplified kinetic scheme of proceeding processes. This scheme is presented in Table 30.3.

It is visible, that in 19 reactions participate about 30 particles. Reactions can be divided into the following groups:

– Processes of generation of active particles (radicals and ions) at influence of radiation on system water-n.heptane (1–3);

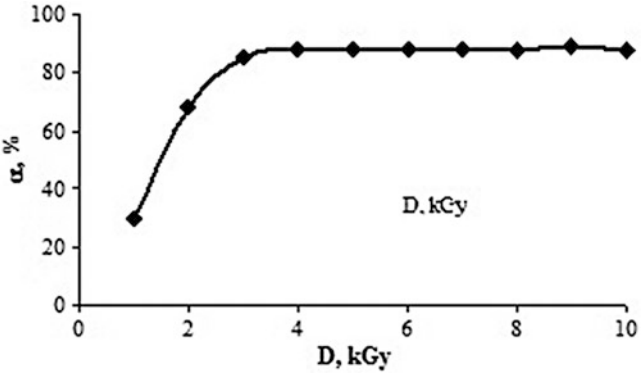

Fig. 30.5 Influence of absorbed dose on degree of decomposition of oil in water medium: initial concentration of oil is 0.1 %

– Recombination reactions of radicals with formation of the saturated hydrocarbons and olefins (18–19);
– Reactions of disintegration of larger alkyl radicals to olefins and small alkyle radicals (6–11); and
– Separation reactions of alkyl radicals with initial heptan (4,5,12–17).

The kinetic regularities of the formation of gases and disintegration of an initial component have been calculated according to this mechanism.

Numerical integration of system of the rigid ordinary differential equations was made with the use of a package of applied programs "Kinetika-90" by Gere's method with a choice of a step and the order of the scheme.

Absorption of radiation by products of radiation-thermal decomposition of heptane at this stage neglected. The rate of constants of monomolecular disintegration stole up so that the calculated yield of products in the best degree corresponded to experimental data. Difference between the results of calculations and experiment results was no more than 15–25 %.

The received results are approved on process of radiation-thermal purification of waste waters from oil pollution. The content of oil is very complex, contains paraffin, naftens, cyclic, etc. the connections having various radiation stability influence of ionizing radiation. Therefore it is possible to expect, that at radiation-thermal influence on such complex systems multistage processes of transformation of oil should precede.

The basic parameters of process were quantity of hydrocarbons in a mix with water, quantity of products of their transformation, and also quantity of residual products of decomposition of oil.

In Fig. 30.5, dependence of a degree of decomposition of oil on the absorbed doze is shown at temperature T = 400 °C.

From Fig. 30.5 it is visible that up to the values of the absorbed doze 3.6 kGy the degree of decomposition of oil makes 88.7 %. The further increase of a dose does not influence a degree of water treating. Other part in quantity about 12 % of oil in

water represents polycyclic aromatic parts that have high radiation stability. For decomposition of this part greater doses are required, that in the practice is not applied because of dearness of radiating energy.

It is shown, that at use of the electron accelerator with power of beam 100 kW can clean up about 70 m^3/h the sewage containing 0.1 % of oil.

30.4 Conclusion

In framework of the offered kinetic scheme of radical reactions the experimental results on radiation-thermal cleaning of oil polluted waters is explained. At the radiation-thermal influence at absorbed doses of radiation 5–6 kGy concentration of hydrocarbon in the water medium decreases from 0.1 to 0.001 %. It shows the perspectives of the processes of radiation-thermal cleaning of water from oil hydrocarbons. At the application of this approach for cleaning of water from natural oil we have a deviation from the results, received on model hydrocarbon up to 30 %. Presence of radiation-resistance polycyclic aromatic hydrocarbons and other compounds in natural oil decreases of process rate.

Acknowledgement This work was supported by the Science Development Foundation under the President of the Republic of Azerbaijan. Grant N EIF-2011-1(3)-82/12/1.

References

1. Muguel M, Norberta DPM (2001) Flocculation /flotation /ultrafiltration integrated processing wastewaters. Environ Sci Technol 35(24):4916–4921
2. Pikaev AK (2001) New environmental application of radiation technology. J Khimiya vysokikh Energiy 35(3):175–187
3. Bao H, Liu Y, Jia H (2002) A study of irradiation in the treatment of wastewater. Radiat Phys Chem 63:633–636
4. Fang XW, Wu JL (1999) Some remarks on applying radiation technique combined with other method to the treatment of industrial wastes. Radiat Phys Chem 55:465–468
5. Getoff N (1999) Radiation chemistry and the environment. Radiat Phys Chem 54:377–384
6. Pikaev AK (2002) The contribution of radiation technology to environmental protection. J Khimiya vysokikh Energiy 36(3):163–175
7. Mustafaev I, Gulieva N (1999) Radiation-thermal transformation of pentadecane. J Khimiya vysokikh Energiy 33(5):354–359
8. Rzayev R, Mustafayev I, Ahmedli G (2008) Calculation of kinetics of radiation-chemical decomposition of heptane admixtures in the water medium. In: The fifth Eurasian conference "Nuclear Science and Its Application", Ankara, Turkey, 14–17 Oct 2008, pp 166–167

Chapter 31
Quantum Effects Based Materials for Nanosensory Systems

Paata J. Kervalishvili and Tamara M. Berberashvili

Abstract Development of sensory elements, devices and novel information technologies based systems is unique for solving organization difficulties of multiparametral and precise measurements of hydrocarbons and related substances. An effective prevention implies sensory system that provides combines and interprets applicable individual information in due time and then takes appropriate measures. Such sensory systems should record data as soon as an action is necessary. Utilization of quantum effects in solid state systems opened a new way for elaboration of novel sensory materials and devices widely using the nanoscience and nanotechnology methods for their preparation.

One of the most suitable examples of nano and quantum effects connection is the process of the spin-polarized transport of charge in -ferromagnetic semiconductor nanolayers with controlled disorder. Operation of a spintronic device requires efficient spin injection into a semiconductor, spin manipulation, control and transport, and spin detection. The relevant role in solution of this problem is shunted to search and investigations of new ferromagnetic materials, which are capable to be reliable spin injectors and effective memory resistors as well.

The execution of researches within the framework of the given chapter will allow studying the quantum effects in ferromagnetic nanolayers with controlled disorder. The most essential mechanisms, responsible for the transport properties, electronic and magnetic structures of these materials were determined. It also served as basis for creation of practical spinelectronics sensory devices having in their structure the interfaces such as ferromagnetic discrete alloy – non-magnetic semiconductor.

Keywords Sensor • Device • Quantum • Nanoscience • Nanotechnology • Material • Spintransport

P.J. Kervalishvili (✉) • T.M. Berberashvili
Georgian Technical University, 77 M. Kostava str., Tbilisi, 0175, Georgia
e-mail: kerval@global-erty.net; tamo.berberashvili@yahoo.com

A. Veziroğlu and M. Tsitskishvili (eds.), *Black Sea Energy Resource Development and Hydrogen Energy Problems*, NATO Science for Peace and Security Series C: Environmental Security, DOI 10.1007/978-94-007-6152-0_31,

31.1 Introduction

Quantum effects in nanostructured magnetic solid state materials open the new ways for preparing the novel electromagnetic devices with unique characteristics. At the same the electron spin based quantum effects are fully determined of formation and growing properties of molecular clusters of these solid state materials which are united in plane and volume structures also according to their quantum (elementary particle interactions) properties.

Molecular nanostructures are small size systems operating on the molecular scale, and therefore they associate with molecular assembling processes. It is proposed approach which involves manipulating single molecules in finely controlled, deterministic ways.

According to classical ideas of small particles formation and growth, atoms being the germs of solid phase unite in aggregates (clusters). These aggregates have a nanometer scale, are very similar to molecular structures of gas and liquid states. The increase of atoms quantity within a molecular cluster results in the increase of atoms aggregate's volume by gradual addition of atoms moving from all sides to the growing cluster (volume growth) and under certain conditions the volume crystallization of the cluster takes place [1–3].

In small molecular clusters the physical effects are totally changed when the scale of the system decreases from micro to nano and pico related to alterations in the electronic band structure of the solid state particle due to its small size and the presence of a high fraction of co-coordinately and electronically unsaturated atoms. They allow building novel molecular (quantum) devices that exploit electron spin, and magnetic storage of the computing machine relies on the magnetic properties created by electron's spin [4, 5].

Within the growing process from atoms to molecule and further to a massive three dimensional (3d) formation there exists the stage when the small (nano) particle looks like a plane formation (2d nano structure) consisting of statistically spread simplest structural elements (molecules), and its width does not exceed the thickness of a single structural element (tetrahedron for Carbon, icosahedron for Boron, etc.) During transition from amorphous state to the crystalline one the putting in order of structural elements within the plane form takes place and then occurs aggregation of these forms into the volume (3d) crystalline formation (fullerenes, nanotubes) [6, 7].

Using the established in last years new approach to the mechanism of cluster's formation it is easy to show that during the formation of small particles (nanoparticles) growth occurs not by joining of separate atoms to their existing aggregate, but by conglomeration of aggregates with stable configuration and preservation of their main individual properties. Such volume molecular clusters consisting of separate clusters of lesser dimensions have much more low density than the matrix substance. Often they are simplest structural elements (tetrahedrons, cubes, bi-pyramids, etc.) one or some surface parts of which are sticker together.

As it is known the formation of nano particles (molecular clusters) actually is carried out by various non equilibrium experimental methods, among which it should be noted: supersonic outflow of vapors into vacuum, thermo-, laser- and plasma-chemical modes of substances reduction from their gas-phase compounds, etc. As to elementary boron and carbon molecules production of which presently is being worked out by dint of various powder and film technologies, the greatest interest is bound with modes of small particles' production providing their high dispersion and purity as well as the possibility to study the processes of molecular clusters formation and growth. It was found that usually small particles consist of one or more nanostructural elements united in molecular cluster of various configurations depending of formation's thermodynamic conditions.

Nano spinelectronics, based on usage of magnetic materials, represents new area of science and engineering. The reason to that is the perspective of creation of principally new devices for information technologies operating as charge, and spin degree of freedom of carriers, free from limitations inherent for metal spinelectronic devices. The main structural property of materials in which we can observe novel nano dimension phenomenas is their imperfection – high concentration of different defects connected with several impurities of metal and non metal chemical elements. So, novel very exiting properties of semiconductors are determined by impurities and their disordered distribution. At the same time the last theoretical and experimental achievements have shown that disorders in semiconductors should be controlled – should have a necessary rules and regulations.

By these approaches it is possible to define the link between matter and information, which is most evidently manifested by the molecular constitution in building molecules connecting in given order. The initial formation directs the synthesis of sequences, which logically are not random; there is an optimization of structure within the system. Such optimization should be expressed in terms of fuzzy entropy and it relates directly to the definition of information. Following novel achievements we could integrate the science and technology of small scale structures (nano, pico structures [8]), quantum size elements based physical effects and information-communication processes, which bring us to novel applied science discipline – quantum information technology (QIT).

31.2 Quantum Effects in Molecular Nanostructures

All approaches treat the nonmagnetic and ferromagnetic metals as free electron materials. Based on the assumption that the elastic scattering time and the inter band scattering times are shorter than the spin flip times the two current model is adequate to describe and explain the observed magnetoresistance effect. However, it is unable to quantify the bulk and interface spin asymmetry parameters and spin relaxation lengths as since Magnetism originates from the spin of the electron, having a much larger magnetic moment than the nucleus of an atom. A net electron spin in an atom results from flexibility of ordering in the electronic arrangement of

the electrons around the nucleus and the requirement for the electron wave function to obey the Pauli exclusion principle, that is: the complete wave function of a two or more electron system has to be antisymmetric with respect to the interchange of any two electrons. Therefore the symmetry (symmetric or antisymmetric) of the spin part of the wave function influences the symmetry of the spatial wave function and hence influences the total Coulomb energy of the electron system. The difference in energy between a two electron system with a symmetric (triplet) or antisymmetric (singlet) spin part of the wave function is referred to as the exchange energy. For example, ferromagnetism exists in some elements due the dependence of the Coulomb energy (the exchange energy) on the particular arrangement of the electrons and their spin in the 3d shell.

The concept of spin injection and accumulation is based on induced magnetization in a nonmagnetic metal. However one this description of spin injection and accumulation is only valid in the situation where a nonmagnetic metal is weakly coupled via tunnel barriers, to its electrical environment.

So-called magnetic discrete alloys todays are of the most prospective materials for solution of the spin injection problem. These alloys involve a periodic system of sub-monolayers of magnetic ions (for example, Mn), placed between semiconducting layers (GaAs, GaSb, InAs) forming a magnetic superlattice. There are as incidentally distributed Mn ions and 2d magnetic islands of MnAs (or MnSb) as well in manganese containing layers. The discrete alloys have high Curie temperatures (above 300 K for the GaSb-system), demonstrate extraordinary Hall Effect at high temperatures and have a relatively high degree of the spin polarization. It is possible in such systems to control not only quality of the border "ferromagnetic metal – non-magnetic semiconductor", but also manage of the current carrier's concentration and change the type of magnetic ordering. The discrete alloys should be considered as random magnet systems owing to hardly inhomogeneous allocation of a magnetic phase in sub-monolayers [9, 10].

Operation of a spintronic device requires efficient spin injection into a semiconductor, spin manipulation, control and transport, and spin detection. The relevant role in solution of this problem is shunted to search and investigations of new ferromagnetic materials, which are capable to be reliable and good spin injectors. Among such objects the magnetic discrete alloys are very promising. They are multilayer systems composed of submonolayers of a ferromagnetic material in the matrix of a non-magnetic semiconductor, for example, Mn/GaAs or Mn/GaSb. It is well known, that these alloys have high Curie temperatures and sufficiently high spin polarization. The circumstance is not less important that it is possible to control and to manage of the "ferromagnetic metal – semiconductor" boundary surface immediately during the synthesis of these materials. As it was investigated recently they should be prepared only by the methods of the MOS hydride epitaxy and mostly by laser epitaxy with usage of pulsed annealing of epitaxial layers (Fig. 31.1).

These technologies are rather simple and, at the same time, allow to perform the doping of layers under the over saturated condition [11, 12].

The significance of spintronics is stipulated by perspectives of development and creation of new types of a non-volatile memory with random access (MRAM),

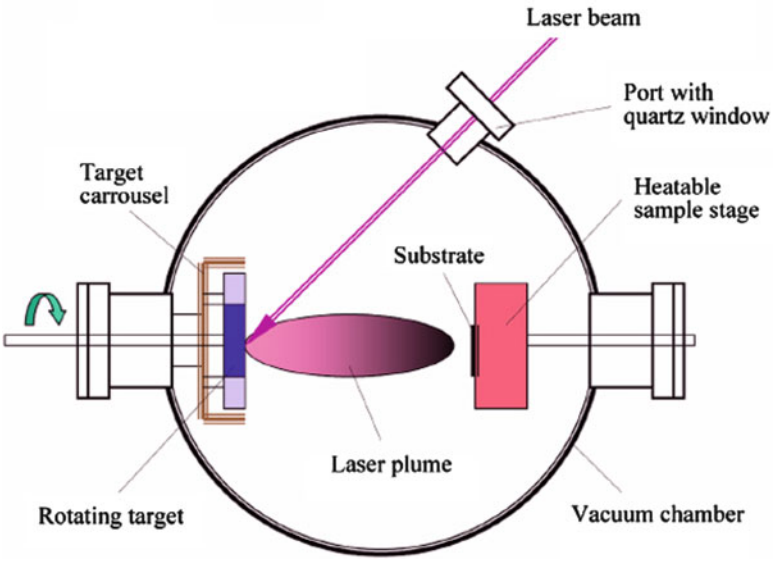

Fig. 31.1 Laser – Plasma deposition process (*see color plates*)

quantum single-electron logical structures and ultra dense information storage media. Thus, elementary information storage unit will be represented by an electron spin. The giant magnetoresistance effect (GMR) brightly has demonstrated, that a spin-polarized electrons can carry magnetic moment through non-magnetic materials with saving spin coherence, this is the meaning of the term "spin transport" nowadays.

The sensors operating with the tunnel magnetic junctions (MTJ) fall into the second class spintronics devices. There ferromagnetic electrodes are divided by very thin dielectric layer, and electrons are tunneling through a nonconducting barrier under influence of applied voltage. The tunnel conductivity depends on relative orientation of the electrode magnetizations, and tunnel magnetoresistance (TMR) it is small for parallel alignment of magnetizations of electrodes and is high in opposite case. In contrast with the GMR of devices, electrodes are magnetic independent in this case and have different critical fields for changing of the magnetic moment orientation. Due to this reason, the third direction of development spintronic devices is based on the development of multilayer nano structures of ferromagnetic semiconductors, which demonstrate properties not available for their metal analogs. In accordance to that the super-giant TMR effect in epitaxial (Ga,Mn)As/GaAs/(Ga,Mn)As structures was observed [13].

Novel very exiting properties of semiconductors are determined by impurities and their disordered distribution. At the same time the last theoretical and experimental achievements have shown that disorders in semiconductors should be controlled – should have the necessary regulations. So it is a very important to know relatively well the properties of materials such as GaSb applicable for spin

Table 31.1 Results of the Hall effect measurements for GaSb/Mn multilayer

d_{Mn}, nm	d_{GaSb}, nm	Measuring Hall effect (HE), presence of a hysteresis	Number of periods
1.9	8.1	AHE at 300K a loop at 77K	16
0.95	9.2	AHE at 300K, a loop at 77K	16
0.5	0.95	AHE with a loop at 300 and 77K	30
0.5	3.8	Ordinary HE	16
0.25	1.2	AHE at 300 and 77K, loops are not present	16
0.25	2.6	AHE at 300 and 77K, loops are not present	46
0.25	4.0	Ordinary HE	16

transport organization in diluted semiconductors. In order to reveal of concentration and ionization energy of thin acceptor centers of undoped p-GaSb we performed the measurement of temperature dependence of Hall coefficient in the temperature range 13–100K [6].

The holes concentration in layers made in this case is ~10^{19} sm^{-3}, the Hall mobility is 20–30 cm^2/Vs. Thus, the Hall effect versus magnetic field curve became anomalous (without a loop) at room temperature and it has shown hysteresis only at 77K.

Typical results of the Hall measurements, obtained in this case, are presented in Table 31.1.

Examinations of structures performed by the method of the X-ray diffraction have shown that in structures with the period $d \geq 10$ nm is detected the periodicity with parameters close to incorporated in the technology of their growth. The depth of manganese penetration in adjacent GaSb layers was near 4 nm. Thus, it is possible to assume that are implemented requirements of the almost complete intermixing of Mn and GaSb in discrete alloys with d < 10 nm, and the behavior of the Hall effect in those samples is similar to its behavior in homogeneously doped GaMnSb layers (Fig. 31.2).

It was shown that the temperature of substrate (T_g) during the laser deposition of Mn is one of most critical parameters for the growth of GaAs/InGaAs heterostructures with δ <Mn> -doped layer. The magnitude of T_g was chosen in such a way to minimize spreading of the δ-shaped Mn profile and simultaneously, to keep high enough quality of the epitaxy for spacer and GaAs cap layers. It was established that $T_g \approx 450$ °C is a good compromise for these goals. Therefore the process of the structure formation was performed in two stages: (1) the growth of the buffer layer, QW and first spacer at 550 °C; (2) deposition of the cap layers beginning with the creation of the δ <Mn> -doped layer after substrate cooling to 450 °C in the same reactor without interruption of the gas flow. At this $T_g \approx 450$ °C a GaAs cap layer retains high crystal quality as observed in X-ray diffraction measurements; the quality was deteriorated at lowering T_g down to 380–400 °C. The role of the δ <Be> -doped layer consists in the conservation of high enough conductivity of structures at low temperatures T_m. In Mn-doped GaAs the freezing of the Mn-acceptor levels takes place at small T_m ($E_a = 104$ meV as distinct from 17 meV for Be). It was established that the quantity of Be in the δ-doped layer may not exceed 4–7 × 10^{12} cm^{-2}, otherwise the effective mobility in those structures is decreasing (Fig. 31.3).

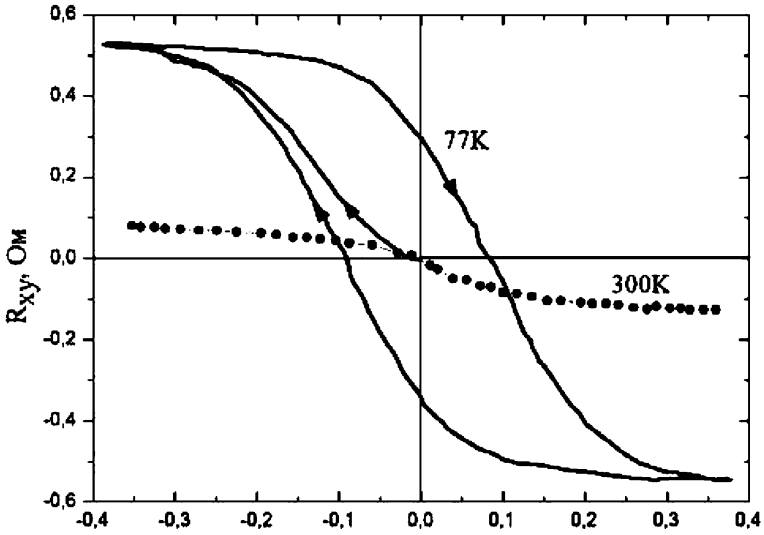

Fig. 31.2 Magnetic field dependences of Hall resistance

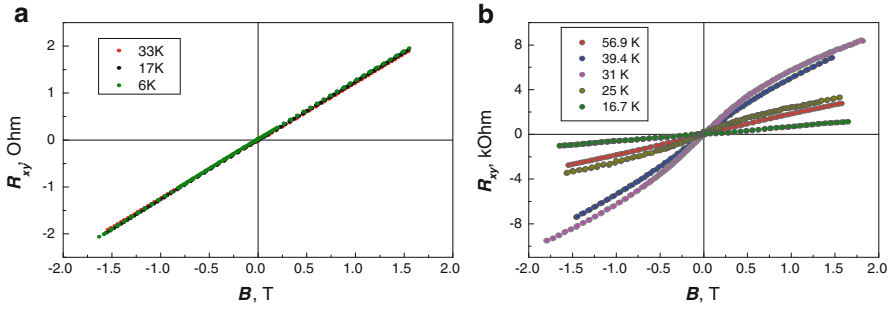

Fig. 31.3 Hall effect in quantum-sized GaAs(δ-Mn)/$In_xGa_{1-x}As$/GaAs structures with metallic (**a**) and activation (**b**) type of conductivity at different temperatures [14] (*see color plates*)

Figure 31.4 shows photoluminescence (PL) spectra for some structures with variation of Mn quantity in δ-doped layers. It was demonstrated that the intensity of the 1.20–1.25 eV peak, related with the transition from the first electron level to the heavy hole level in QW, shows decrease monotonically with the increase of Mn quantity in δ <Mn> -doped layer.

The SEM pictures of the obtained structures had been produced by integrated signal of the secondary and reflected electron beams regime (initial accelerating voltage $E_0 = 20$ KeV). Pictures are shown that: at the crystal surface (substrate) as well as on the surface of deposited layer are observed effects of charge and voltage contrasts. They are connected with the surface contaminations of thin film (Fig. 31.5).

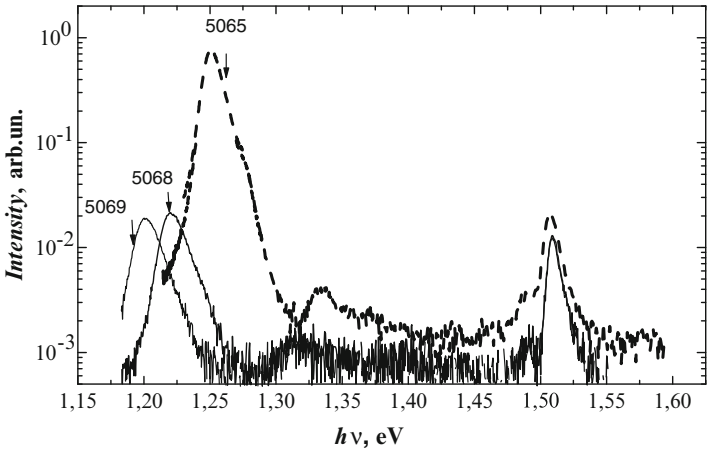

Fig. 31.4 Photoluminescence spectra of the structures at 77 K

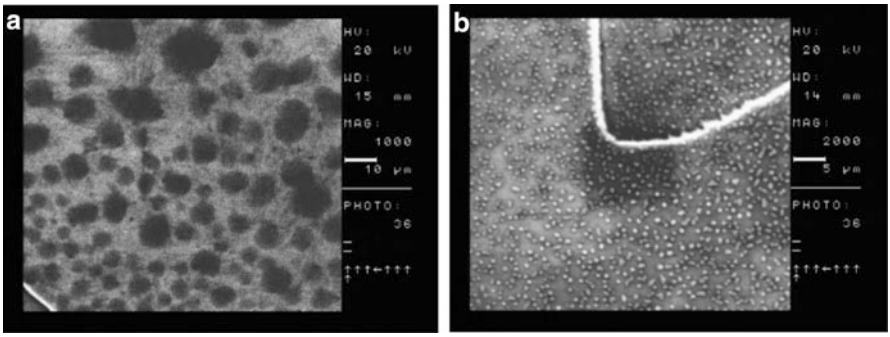

Fig. 31.5 (**a**, **b**) SEM pictures of the prepared sample's surfaces

Novel very exiting properties of semiconductors are determined by impurities and their disordered distribution. At the same time the last theoretical and experimental achievements have shown that disorders in semiconductors should be controlled – should have the necessary regulations. So it is a very important to know relatively well the properties of materials such as GaSb applicable for spin transport organization in diluted semiconductors [12].

In order to reveal of concentration and ionization energy of thin acceptor centers of undoped p-GaSb we performed the measurement of temperature dependence of Hall coefficient in the temperature range 13–100K.

Values of the acceptors and donors concentration as well as the ionization energy were evaluated from the analysis of experimental curves and solution of electro neutrality equation by method of the least squares for two levels model with estimation of compensation. Selection of parameters was performed by using computers which was made searching much easy.

Determination of equation is given the value for activation energy $E_1 = 0{,}013$ eV, acceptors concentration $N_{a1} = 4{,}2\ 10^{15}\ cm^{-3}$, donors $N_d = 3{,}6\ 10^{15}\ cm^{-3}$. Therefore the compensation degree of shallow acceptor level $K = N_d/N_{a1} = 0{,}86$. Obviously because of strong compensation the found value of shallow acceptor level activation energy $E_1 = E_0 + \varepsilon_3$, where E_0 – is energy of isolated acceptor, and ε_3 – activation energy of hopping conductivity. On the basis of energy activation and carriers concentration values it is possible to determine the Bohr radius and the average distance between impurities.

In case of big difference among masses asymptotic character of the wave functions in a long distances determines by the light holes, and because of it $a = a_L = \hbar/(2m_{\text{п}}E)^{1/2}$, where ħ is Plank's constant, $m_L = 0{,}052\ m_0$ – effective mass of the light hole. That means that the average distance between impurities is considerably higher tha in the magnitude of the wave function, which is obligatory condition of the weak doping.

On the Curves of typical dependence of specific resistance from back temperature for undoped p-GaSb in temperature range of 3–77K it is possible to underline two areas: I – in temperature range 3–10K, which is relevant to hopping conductivity, and II – in temperature range 15–77K, which is connecting with zone conductivity and ionization of energy levels $E_1 = 0.013$ eV и $E_2 = 0.034$ eV.

Area I is possible to describe with the formula $\rho = \rho_3 \exp(\varepsilon_3/KT)$, and by the curve inclination to determine activation energy of hopping conductivity ε_3. These values of ε_3 for investigate samples = 3.6 MeV, which is in good connection with activation energy calculated by theoretical formula for a strong compensation. It is obvious that dependence $\ln \rho$ of T^{-1} in low temperatures case is linear which demonstrate existence of hopping conductivity with activation energy of constant. In condition of liner part of dependence extrapolation $\ln \rho = f(1/T)$ into infinity high temperature area ($1/T = 0$), e.g. finding the crossing point of that line with coordinates, when $\rho = \rho_3\ e^{\varepsilon 3/KT}$ it is possible to find out experimental value of $\ln \rho_3$. In Fig. 31.3 this point corresponds to 7.5 Ohmcm. The value of ρ_3 exponentially depends on the impurity concentration and the Bohr orbital parameters – $\rho_3 = \rho_{03} \exp(1.73/N^{1/3}a)$, where $\rho_{03} = 10^{-3}$ Ohmcm and depends on the degree of the impurity concentration and distribution of the energy states. When a = 75 A in above mentioned equation, for the impurity concentration we get that $N_{a1} = 4.2\ 10^{15}\ cm^{-3}$.

In obtained dual phase ferromagnetic GaMnSb films, regardless to the case of previously studied single phase GaMnSb systems (Curie temperatures not exceeding 30K), the anomalous Hall effect (AHE) and the AHE hysteresis character at temperatures up to 300K, as stronger as more the hole concentration, has been observed. The unusual properties of GaMnSb films have been interpreted as interaction of magnetic nanoclusters in a semiconductor matrix, where the matrix has huge concentration of free holes and magnetic ions. The interaction seems to be caused by the potential Shottky barriers at the cluster/semiconductor interface sensitive to the holes concentration in the semiconductor matrix.

One of the most suitable and practical examples of nano and quantum effects connection is the process of the spin-polarized transport of charge in -ferromagnetic semiconductor nanolayers with controlled disorder. Operation of a spintronic

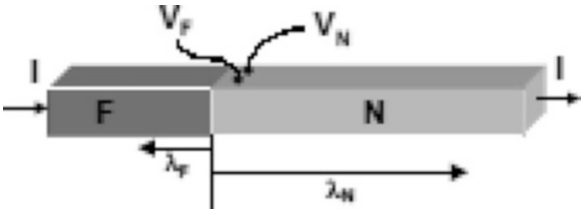

Fig. 31.6 Schematic representation of the experimental layout for electrical spin injection: with λF and λN on either side of the F/N interface represent the distance where the spin accumulation exists in the F and N metal

device requires efficient spin injection into a semiconductor, spin manipulation, control and transport, and spin detection. The relevant role in solution of this problem is shunted to search and investigations of new ferromagnetic materials, which are capable to be reliable and good spin injectors (Fig. 31.6) [14].

Theoretical approaches developed during the last decade present invaluable tools for studying the microscopic origins of ferromagnetism and predicting electronic, magnetic and structural ground state properties of magnetic semiconductors. It is necessary to underline that the local density approximation combined with disorder averaging coherent potential approximation is very useful for studying diluted magnetic semiconductors. The effects of the $As_{Ga} - As_i - V_{Ga}$ transition to the ferromagnetism of (GaMn)As can be explained by the Mulliken orbital populations of the d-shell for both majority and minority spins and the corresponding spin polarization for the ferromagnetic configuration. In this case the ferromagnetic coupling is strengthening considerably by the distortion, and that all together the energy splitting and Mulliken orbital population of As_i V_{Ga} are the very similar to those of defect free (GaMn)As. These suggest that the ferromagnetic order in (GaMn)As is unaffected by the presence of As_i V_{Ga} pairs. This result is in agreement with the hole-mediated picture of ferromagnetism, and can understood by noting that As_i V_{Ga} defects energy levels show minimal splitting in (GaMn)As [15].

Theoretical models of the virtual crystal approximation have been used to study the influence of the impurity disorder on transport and magnetic properties of magnetic semiconductors. The Boltzmann equation with Born approximation for scattering rates provides the estimate of Anisotropic Magnetoresistance Effect up to 12 %. The key for understanding kinetic and magnetic anisotropy effects is a strong spin-orbit coupling in the semiconductor valence band. The most striking feature in off-diagonal conductivity coefficients, in (GaMn)As is the large Anomalous Hall Effect (AHE), which occurs due to the spin-orbit interaction.

For explanation of the ferromagnetism in magnetic semiconductors, such as Ga_{1-x} Mn_x and similar compounds the known RKKY-mechanism of the indirect exchange interaction is recruited. It leads to the correct estimating the Curie temperature in the framework of the traditional mean field theory (MFT). Mn-atoms (with concentration N_μ) substituting for Ga-atoms introduce in the system the own magnetic moments and, in addition, as acceptors deliver free holes (with concentration n). It is precisely those holes become to be carriers responsible for

the interaction. However, the equality of the concentrations $n = N_\mu$ keeps only at low Mn-concentrations ($x \leq 0.05$), so that the carrier concentration is usually less than the concentration of magnetic impurities: $n = \gamma N_\mu$ where the coefficient of the impurity "efficiency" $\gamma < 1$. Nevertheless, the concentration of magnetic impurities, delivering carriers, in actual systems is usually so high that the impurity band is formed which at $x \geq 0.01$ merges into the valence band. Even though, the carrier concentration occurs to be not so high that one could consider them as highly degenerated ones within the whole (being of interest) range of relatively high temperatures. Furthermore, it is important that the carrier concentration is almost independent of the temperature: $n = \gamma N_\mu \approx \text{Const}$.

Using the generalized mean field theory for systems with the indirect interaction of magnetic impurities and taking into account the randomness of their spatial arrangement, by Ising approximation and supposing that the indirect coupling between magnetic moments of impurity atoms is realized by means of RKKY interaction upon system properties are described with the help of the distribution function of local values of the field arising as a result of magnetic ions' coupling with their own surroundings. In real systems, the scattering of those fields proves to be very substantial.

In [15], the expression has been derived for the energy $w(r)$ of indirect RKKY interaction for two parallel spins $\mathbf{S}_1$, $\mathbf{S}_2$ of magnetic ions spaced at the distance r in the two-dimensional system with degenerated carriers:

$$\mathrm{w(r)} = -\frac{\mathrm{m}}{4\pi\hbar^2}\left(\frac{\mathrm{J_{ex}}}{\mathrm{N}}\right)^2 \mathrm{F(r)S_1S_2}, \mathrm{F(r)} = -\int_0^{\mathrm{kF}} \mathrm{kN_0(kr)J_0(kr)dk}, \tag{31.1}$$

where J_{ex} is the exchange energy for interaction of a spin with a free charge carrier of the mass m, N is the concentration of lattice atoms ($N = 1/a^2$ for the square lattice of the period a); J_0, N_0 are Bessel functions. The result generalized to the case of the arbitrary degeneracy (with the Fermi energy ε_F of any value) reads:

$$\mathrm{F(r,T)} = -\frac{1}{\mathrm{r}^2}\int_0^{\infty} \frac{\mathrm{yN_0(y)J_0(y)dy}}{1 + \exp[(\hbar^2\mathrm{y}^2/2\mathrm{mr}^2 - \varepsilon_\mathrm{F})/\mathrm{k_BT}]}. \tag{31.2}$$

The behavior of the function (31.2) is determined not only by the temperature as such but also by the temperature dependence of the Fermi energy.

Let the system consisting of randomly arranged and oriented Ising spins be in the state characterized by the average reduced magnetization $0 \leq j \leq 1$. The total interaction energy $W = \sum_i w_i$ of a given spin $\mathbf{S}_1$ with other spins $\mathbf{S}_i$ ($i = 2,3,\ldots$) is a random value which we shall define by the effective local magnetic field $H = -W/\mu$ ($\mu = \mathrm{g}\mu_\mathrm{B}[\mathrm{S(S+1)}]^{1/2}$) and describe by the distribution function $F(j;H)$ depending on the average concentration N_μ of effective magnetic ions and the reduced system magnetization $j = 2\xi - 1$ where ξ is the average fraction of spins of "magneto-active" ions directed "up". Farther calculations very well described in

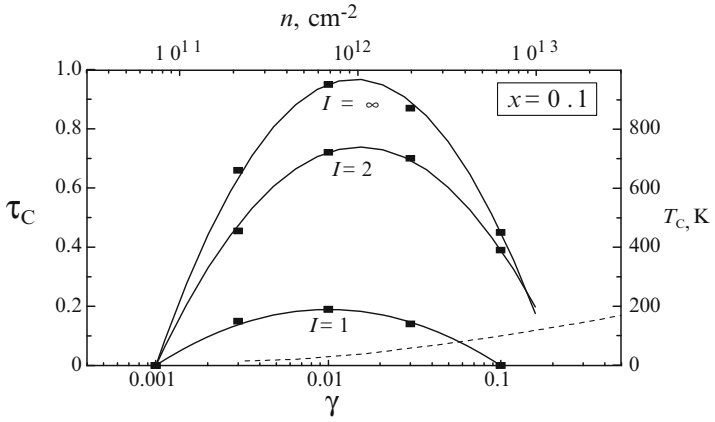

Fig. 31.7 Dependencies of Curie temperature on the carrier concentration for the system with the concentration of magnetic impurities $x = 0.1$ for various interaction strengths I

[16] have shown that prepared final equation predicts the phase diagram of the system, temperature dependencies of its magnetization (in ferromagnetic phase) and susceptibility (in paramagnetic phase), as well as the dependence of Curie temperature on the interaction strength, the relative magnetic ion concentration $x = N_\mu/N$ and the relative free carrier concentration $\gamma = n/N_\mu$.

This equation has the solution corresponding to the ferromagnetic state ($j > 0$) under the condition:

$$\frac{H_j}{\sigma} > \sqrt{\frac{\pi}{2}} \tag{31.3}$$

that means that the effective RKKY-field proportional to H_j has to "overpower" not only the thermal disordering but also the scattering of local fields proportional to σ. The upper boundary $\tau_C{}^{max}$ of the temperature range where the cited condition is satisfied determines the maximum attainable temperature of the ferromagnetic ordering at infinite interaction energy ($I \to \infty$).

Curie temperature at the finite interaction energy could be determined by solving the equation. Relevant non-monotone dependencies $\tau_C(\gamma)$ are displayed in Fig. 31.7.

Theoretical models of the virtual crystal approximation have been used to study the influence of the impurity disorder on transport and magnetic properties of magnetic semiconductors. The Boltzmann equation with Born approximation for scattering rates provides the estimate of Anisotropic Magnetoresistance Effect up to 12 %. The key for understanding kinetic and magnetic anisotropy effects is a strong spin-orbit coupling in the semiconductor valence band. The most striking feature in off-diagonal conductivity coefficients, in (GaMn)As is the large Anomalous Hall Effect (AHE), which occurs due to the spin-orbit interaction. In metals, standard assumption is that AHE arises due to spin-orbit coupling component in the interaction between band quasiparticles and crystal defects, which can lead to

the so called skew scattering with the Hall resistivity contribution proportional to the diagonal resistivity. For diluted magnetic semiconductors, AHE is based on the spin-orbit coupling in the Hamiltonian of the ideal crystal and implies the finite Hall conductivity even without the disorder. More detailed studies of the disorder will combine Kondo description of the spin interactions as well as relevant Monte Carlo techniques applied to both metallic and insulating conditions. The model problem concerning the formation of a ferromagnetic cluster (magnetic polaron) consisting of the free electron bound to a non-magnetic donor impurity in an antiferromagnetic matrix was analyzed. The analysis was performed in the framework of two- and three-dimensional Kondo-lattice models in the double exchange limit. The bound electron forms a ferromagnetic core of the size on the order of the electron localization length. It was shown that the magnetic polaron also produces rather long-range extended spin distortions of the antiferromagnetic background around the core. Such a magnetic polaron state can be favorable in energy in comparison to usually considered one (saturated core without extended distortions).

Conditions of establishing the ferromagnetic state and its parameters in quasi-two dimensional semiconductor systems with magnetic impurities coupled via RKKY interaction have been studied, and two new important factors have been included in the consideration: allowing for the spatial disarray of interacting magnetic impurities, and the temperature dependence of the carrier degeneracy [16]. Both factors complicate transition of the system into ferromagnetic state: disorder of the impurities arrangement reduces the Curie temperature (as compared to the regular system) while lifting the degeneracy of carriers makes the Curie temperature finite even in the extreme case of the infinitely strong interaction. Besides, the concentration dependence of the transition temperature is non-monotone and there is the threshold of the interaction strength to drive the system into ferromagnetic state.

31.3 Conclusions

Quantum effects in novel magnetic materials united distinguish electrical and magnetic properties are very prospective for new very sensitive sensory elements creation. Elaborated laser-plasma technologies are sufficient tools for thin nanolayers preparation in which the electron spin transport effect takes place.

These approaches as well as last achievements in nanostructured devices preparation opened the way for novel nanosensory instruments and systems preparation useful for hydrogen, hydrocarbon and relevant materials precise analyzes.

Acknowledgments This research was performed by international team of distinguish colleagues from: Georgian Technical and Tbilisi State Universities, Russian Research Center “I. Kurchatov Institute” and Nizhni Novgorod University of Russia, National and Kapodastrian University of Athens and Massachusetts Institute of Technology.

References

1. Kervalishvili PJ (1986) Mechanism of boron small particles growth. Solid State Phys USSR 28 (12):3218–3220
2. Kern R (1987) The equilibrium form of a crystal. In: Sunagawa I (ed) Morphology of crystals. Terra, Tokyo, pp 77–206
3. Petrov UT (1982) Small particles physics. Nauka, Moscow
4. Sham LJ, Dery H, Cywinski L, Dalal P (2005) Control of spin-polarized currents for semiconductor spintronics. University of California, San Diego, Research funded by DARPA/ONR and NSF DMR & ITR
5. Cowburn RP, Welland ME (2000) Room temperature magnetic quantum cellular automata. Science 287:1466–1469
6. Colbert DT, Smalley RE (2002) Past, present, and future of fullerene nanotubes: buckytubes. In: Osawa E (ed) Perspectives of fullerene nanotechnology. Kluwer Academic, Dordrecht
7. Shiuh CH, Shou JL (2011) Evaluation of mechanical properties of single-walled carbon nanotubes. Mater Sci Forum 694:12–20
8. Kervalishvili P (2009) Micro – Nano – Pico technologies: the main way of novel materials development. International conference "Material Science Day". CNRS –TSU, Tbilisi, 8–10 July 2009
9. Tyson S, Wicker G, Lowrey T et al (2000) Nonvolatile, high density, high performance phase-change memory. IEEE Aero Conf 5:385
10. Kervalishvili P, Lagutin A (2008) Nanostructures, magnetic semiconductors and spintronics. Microelectr J 39:1060
11. Rylkov VV, Aronzon BA, Granovskii AB (2006) Role of the disorder in transport properties ferromagnetic III-Mn-V semiconductors. The collected papers of XX international school-seminar "New magnetic materials of microelectronics", Moscow, 12–16th June 2006, p 523
12. Aronzon B, Kervalishvili P, Lagutin A (2009) Studies of the carrier spin polarization in ferromagnetic semiconductors. The Sixth Japan-Mediterranean conference on applied electromagnetic engineering and nanomaterials, Bukharest, Romania, July 2009
13. Furdina JK, Dobrowolska M, liu X (2008) Ferromagnetism and spin dynamics in III_{1-x} Mn_x V Alloys. Selected papers of the first international conference in spin electronics: novel physical phenomena and materials (October 2007. Tbiilisi). J Nanotechnol Percept N 2:135
14. Kervalishvili PJ, Khachidze MG (2012) Some size and quantum effects in molecular nanostructures. J Mater Sci Forum 721:71–76
15. Ogarkov SL, Kagan MY, Sboychakov AO et al (2006) Formation of long-range spin distortions by a bound magnetic polaron. Phys Rev B 74:014436
16. Meilikhov EZ, Farzetdinova RM (2006) Quasi-two-dimensional diluted magnetic semiconductors with arbitrary carrier degeneracy. Phys Rev B 74:125204

Chapter 32
Physical Properties of Some Metal Hydrides Applicable for Hydrogen Detectors: Brief Review

Ioseb Ratishvili and Natela Namoradze

Abstract There are briefly reconsidered results of theoretical and experimental investigations performed during the last decade on hydrides of rare-earth and refractory metals in E. Andronikashvili Institute of Physics (I. Javakhishvili Tbilisi State University).

Keywords Properties of metal hydrides: heat capacity • Local mode frequencies • Spin–lattice relaxation processes

32.1 Introduction

The problems of Hydrogen Energetic are usually subdivided into three main parts. These are problems of Hydrogen Production, Safety Storage and Effective Utilization. But there exists the fourth main component of this industry, which is practically of the same significance as the above mentioned. It implies creation of Sensitive Hydrogen Detectors. Low-concentration of hydrogen in air provides formation of a very explosive mixture, and in order to establish a wide application of the hydrogen-fuel installations, we need to accompany them with sensitive hydrogen detectors (indicating existence of free hydrogen in the environment). There exist today a wide number of different detectors based on hydrogen-absorbing materials. We think that those metals, which reversibly absorb hydrogen provide a real basis for creation of

I. Ratishvili (✉)
E. Andronikashvili Institute of Physics, I. Javakhishvili State University,
6 Tamarashvili str., 0177 Tbilisi, Georgia
e-mail: ratisoso@gmail.com

N. Namoradze
V. Chavchanidze Institute of Cybernetics, Georgian Technical University,
5 Sandro Euli str., 0183 Tbilisi, Georgia

A. Veziroğlu and M. Tsitskishvili (eds.), *Black Sea Energy Resource Development and Hydrogen Energy Problems*, NATO Science for Peace and Security Series C: Environmental Security, DOI 10.1007/978-94-007-6152-0_32,

sensitive *renewable* hydrogen detectors. An example of devices of the mentioned type was proposed in E. Andronikashvili Institute of Physics by G. Mamniashvili (see Final Report of the project STCU-3867). It is evident that detectors of this type have to register changes of the physical properties of the absorbent materials caused by the embedded H-atoms.

Thus, easily hydrogen absorbing rare-earth or refractory metals though cannot be considered today as suitable hydrogen-storage containers (due to their high weight), nevertheless retain a wide interest as the basis for creation of hydrogen-indicating renewable devices. In this new role it comes necessary to re-investigate very carefully the hydrogen induced changes of their physical properties in the large temperature and concentration ranges.

Taking into account the above reasons, we have reconsidered analytically the following: first of all, a number of experimental results published some decades ago (but left without description up to today), and on the other hand, we analyzed experiments performed in our Andronikashvili Institute of Physics. Correspondingly, below we shall analyze: (a) the heat capacity of light rare-earth hydrides, (b) temperature dependence of the hydrogen local mode frequencies in vanadium hydrides, and finally, (c) NMR-experiments on rare-earth and refractory metal hydrides.

32.2 Heat Capacity of Hydrides

In the case of rare-earth dihydrides MH_x ($x = 2 + c$) the set of H-atoms inserted in the host metal lattice alters its heat capacity in different ways. First, all inserted H-atoms change the interatomic M-M distances in the lattice and in this way change the spectrum of acoustic modes of the metal lattice. Next, in the heat capacity arises an additional term associated with the local oscillations of H-atoms. (It has to be noted that oscillation frequencies of H-atoms located in tetrahedral and octahedral interstitial positions are, generally, different and provide different input into the total heat capacity. Third, additional term is associated with the hydrogen ordering processes, when the number of inserted H-atoms is lower than the number of interstitial positions of the given type, formation of ordered spatial configurations of H-atoms provides lowering of the total energy). Finally, inserted hydrogen atoms influence on the electronic structure of the host metal and can modify the conduction electron heat capacity term. The energy level of hydrogen 1s-electron can be located over or below of the Fermi-level in conduction band, and respectively H-atoms may be in the H^+ or H^- states, on enriching or depleting the host conduction band.

Thus, generally the heat capacity $C(\mathrm{T})[MH_x]$ of an ordering metal hydride MH_x containing N_t H-atoms in tetra-positions and N_O H-atoms in octa-positions can be presented as:

$$C(\mathrm{T})[MH_x] = C_{\mathrm{ac}}(\mathrm{T}) + C_{\mathrm{op(t)}}(N_t,\ \mathrm{T}) + C_{\mathrm{op(o)}}(N_O, \mathrm{T}) + C_{el}(\mathrm{T}) + C_{ord}(\mathrm{T}) \quad (32.1)$$

In this expression, the first four terms are associated respectively with acoustic waves in the lattice, with local oscillations of N_t H-atoms in tetra-positions and N_O H-atoms in octa-positions, and with conduction electrons. Corresponding analytical expressions are well known (see e.g. [1]) and contain characteristic energy parameters (in temperature units, K): Debye-temperature T_D (for acoustic waves), Einstein-temperatures $T_{E(t)}$ and $T_{E(O)}$ (for local oscillations in the interstitial tetra- and octa-positions, respectively), and constant g (for conduction electrons) which is proportional to the number of free carriers on the Fermi-level. The heat capacity of the ordering process was widely considered by present authors (see e.g. [2, 3]). It was shown, particularly, that development of the ordering process is determined by a pair of energy constants V_1 and V_2 which characterize H-H-interactions in the lattice (see [4, 5]).

32.2.1 The Case of Quasistoichiometric Rare-Earth Dihydrides

It is assumed usually that in an ideal rare-earth dihydride RH_2 2 N hydrogen atoms completely fill 2 N tetrahedral interstitial positions existing in the *fcc* lattice of N metal atoms, while the remained N octa-positions are empty. In this case, the ordering processes are excluded and corresponding part of the heat capacity (associated with formation of ordered configurations of H-atoms) together with the term associated with hydrogen local oscillations in the octa-positions are absent. Thus, the heat capacity of an ideal rare-earth dihydride can be presented as:

$$C(\mathrm{T})[\mathrm{MH}_x] = C_{\mathrm{ac}}(\mathrm{T}) + C_{\mathrm{op(t)}}(N_t, \mathrm{T}) + C_{el}(\mathrm{T}). \tag{32.2}$$

Basing on this expression we have analyzed the results of heat capacity measurements performed by Z. Bieganski with collaborators.

In Figs. 32.1 and 32.2 are presented experimental results for CeH_2 and LaH_2 dihydrides published respectively in [6, 7]. Corresponding calculations were performed basing on expression (32.2) and on following the standard scheme [1]. We see that the selected energy parameters (indicated in the figures) allow us to reproduce the experimental temperature dependences $C(\mathrm{T})[MH_2]$ in a wide temperature range.

One detail retains our attention. Physical and chemical properties of cerium and lanthanum metals are quite similar. But, the heat capacities of their dihydrides in the temperature range 200–300 K differ significantly. It seems that in the lanthanum dihydride some H-atoms have passed from tetra- to octa-positions, but there arise a natural question – why such transfer does not occur in the cerium dihydride. This problem was partly discussed in [8, 9].

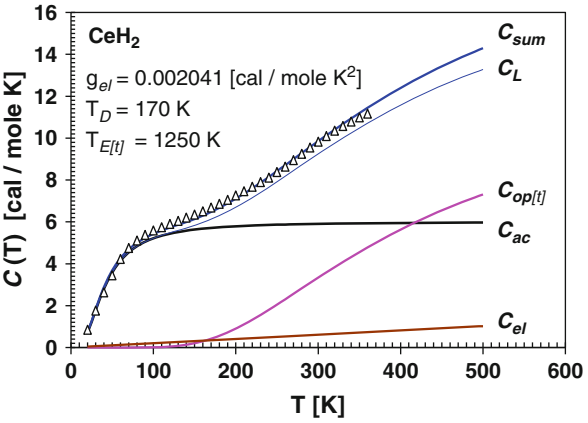

Fig. 32.1 Heat capacity of CeH_2. *Open triangles* – experimental points from [6], notations of calculated dependences: $C_{sum} = C_L + C_{el}$; $C_L \equiv C_{ac} + C_{op[t]}$ (*see color plates*)

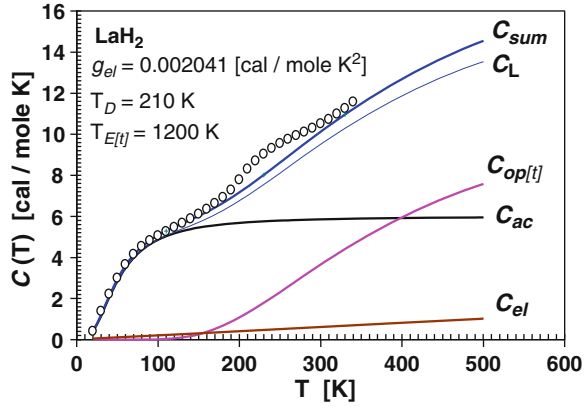

Fig. 32.2 Heat capacity of LaH_2. *Open circles* – experimental points from [7], notations of calculated dependences: $C_{sum} = C_L + C_{el}$; $C_L \equiv C_{ac} + C_{op[t]}$ (*see color plates*)

32.2.2 Ordering Effects in Superstoichiometric Rare-Earth Dihydrides

As it was mentioned above, ordering processes must provide additional term in the heat capacity expression. The corresponding effect was registered in the compound $CeH_{2.86}$ [10]. Description of the heat capacity temperature dependence $C(T)$ was given in [11]. In Fig. 32.3a, b, we present experimental data (open triangles) together with the calculated curve C_{sum} (Fig. 32.3a), and temperature dependences of different ingredients forming C_{sum} (Fig. 32.3b). The relative energy parameter values are indicated in Fig. 32.3a. It was assumed that in the considered system 2 N H-atoms fill 2 N tetrahedral interstitial positions (H_t-atoms), while on the set of N octahedral interstitial positions are distributed 0.86 N H_O-atoms. It was assumed additionally that the ordering substances were not the hydrogen atoms, but *hydrogen vacancies*. Their concentration was equal $c(H_V) = (1–0.86) = 0.14$. The selected set of energy constants provides an excellent coincidence between the theory and experiment.

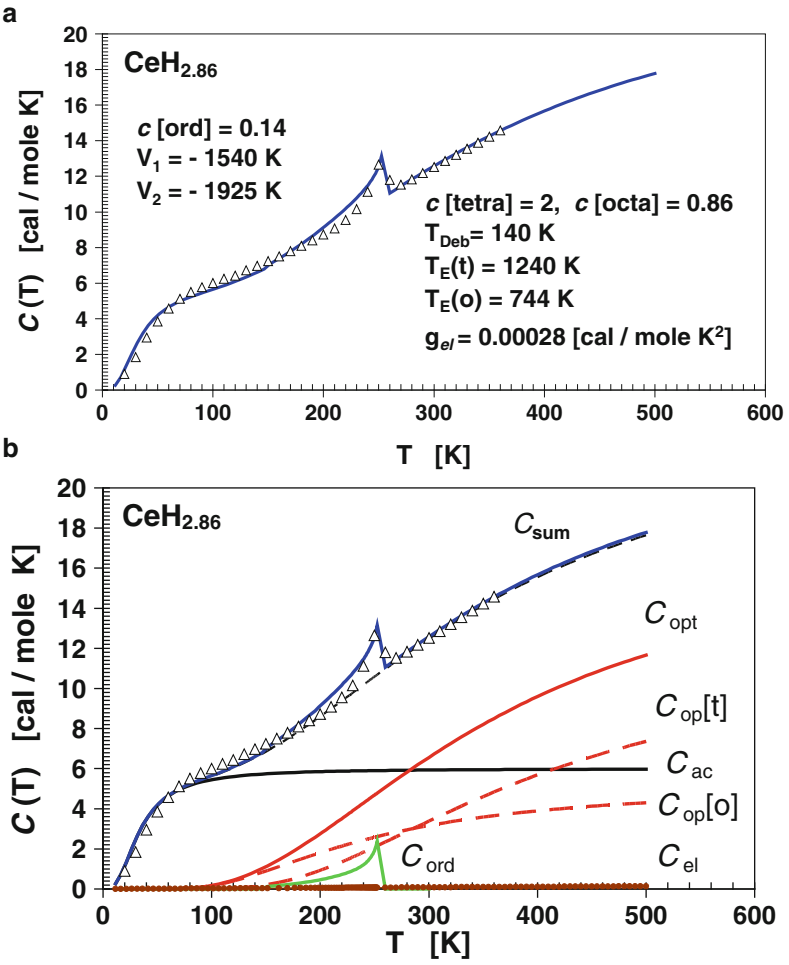

Fig. 32.3 (**a**) Heat capacity of $CeH_{2.86}$. *Open triangles* – experimental points from [10], *thick line* – results of calculation [11], (**b**) ingredients of the total heat capacity of $CeH_{2.86}$. *Open triangles* – experimental points [10], notations of calculated dependences: $C_{sum} = C_{ac} + C_{opt} + C_{el} + C_{ord}$; $C_{opt} = C_{op}[t] + C_{op}[O]$ (*see color plates*)

In the latter two figures, we see that the ordering effect though is remarkable, but is of a limited amount. It was shown [12, 13] that there exist specific conditions when the ordering process plays a dominant role in the heat capacity of metal hydrides. An example is shown in Fig. 32.4. The enormous heat capacity maximum is associated with the established in superstoichiometric ordering rare-earth dihydrides [4, 5, 12, 13] phase transition order change phenomenon.

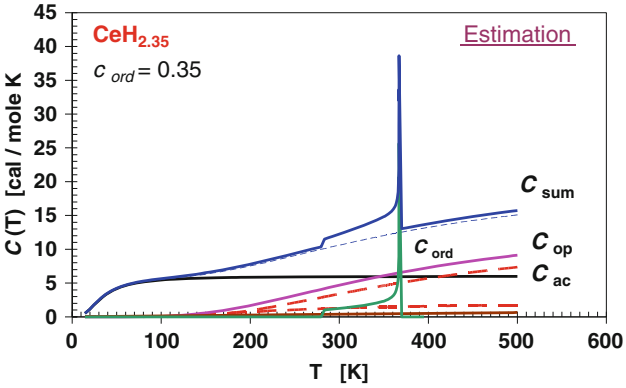

Fig. 32.4 Estimated total heat capacity of $CeH_{2.35}$ (*see color plates*)

32.3 Temperature Dependence of Hydrogen Local Mode Frequencies

We have considered results of inelastic neutron scattering measurements [14] performed on the ordering V_2D compound with a *bcc* lattice, where the embedded hydrogen atoms are located in tetrahedral interstitial positions. It has to be noted that in *bcc* lattices light particles oscillating in tetrahedral interstitial positions are characterized by two different force constants related with displacements along different crystallographic directions. In [14], it was shown that both local frequencies of deuterium interstitials are temperature-dependent, and decreases when temperature is lowered below the disorder–order transition point T_{tr}.

At first glance this effect seems to be a paradox, as in the low temperature region (in presumably energetically more "deep" states) the oscillation frequencies had to be increased. This "anomaly" was explained [15, 16] as a result of an effective "weighting" of hydrogen atoms due to formation of additional H-H bonds in the ordered spatial configurations of D-atoms. The main assumption of this model consists in the statement that H-H (or D-D) interaction potential V_{HH} (which perturbs the eigenvalues of quantum H(D)-oscillators) is proportional to the H-H (D-D) interaction energy E_{HH} providing formation of ordering superstructures in the deuterium subsystem.

The postulated mathematical scheme briefly is as follows [15].

Eigenvalues of the quantum oscillator equation are presented usually as:

$$E_n = \hbar\,\omega_0(n + 1/2). \tag{32.3}$$

If in the oscillator quantum equation we add an additional potential V_{HH}, then its influence can be taken into account by introduction of an effective mass m* and

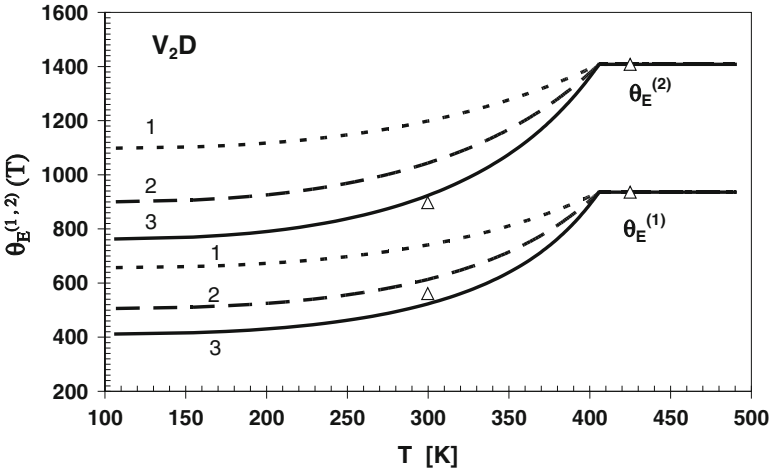

Fig. 32.5 Calculated temperature dependencies of local mode frequencies in vanadium deuteride. *Triangles* denote experimental points [14]

effective force constant K* of the oscillating particle. As a result expression (32.3) will be transformed into the following one:

$$E_n = \hbar\,\omega_H(\mathrm{T})(n + 1/2). \tag{32.4}$$

where

$$\omega_H(\mathrm{T}) \equiv \omega_0\{1 - [\mathrm{V}_{HH}(\mathrm{T})/\hbar\omega_0]\}^{-1}, \tag{32.4a}$$

and $\mathrm{V_{HH}(T)}$ is the potential perturbing hydrogen (deuterium) states. We assume:

$$\mathrm{V_{HH}(T)} \equiv b[\mathrm{E}(\eta(\mathrm{T}), c)/\mathrm{N_H}], \tag{32.4b}$$

where b is a numerical factor and $[\mathrm{E}(\eta(\mathrm{T}), c)/\mathrm{N_H}]$ is the temperature-dependent ordering energy per light particle ($\eta(\mathrm{T})$ being the order parameter of the H(D)-subsystem; c is concentration of H(D)-particles). Rigorous mathematical description of the model is formulated in [16].

In Fig. 32.5, it is presented calculated temperature dependencies of the oscillator energies (given in temperature units, "Einstein temperatures"). Different types of curves are related to different assumed coefficients of proportionality b between V_{HH} and E_{HH}. Experimental results [14] are denoted by triangles. It seems that our interpretation of the mentioned experimental data is physically meaningful.

32.4 Nuclear Magnetic Resonance Results

First of all, we briefly remind the mathematical background of the spin–lattice relaxation phenomenon.

32.4.1 General Relations

As an example of description of the nuclear spin resonance results we analyze proton nuclear spin relaxation processes in the lanthanum superstoichiometric dihydrides LaH_{2+c}, in which the *fcc* lattice of N metal atoms contains $N_t = 2$ N H-atoms in 2 N tetra-positions (H_t-atoms) and $N_O = c$N H-atoms located in N octa-positions (H_O-atoms). When $c < 1$, the subsystem of H_O-atoms undergo an order–disorder transition at some temperature $T = T_{tr}$. It means that at $T > T_{tr}$ occupation numbers $n(i)$ of all octa-sites are equal, $n(i) = c$, while at $T < T_{tr}$ a part of octa-sites become more-occupied ($n(i) > c$), while others become less-occupied ($n(i) < c$). We assume that the given hydride is imposed in a constant field H_0 and in a variable field of frequency ω_0.

In the La-H system, the metal nuclear spin is S and gyromagnetic ratio is γ_S, while the proton spin is I and gyromagnetic ratio is γ_I. In this system with non-magnetic metal ions the spin–lattice relaxation rate of protons R_1 contains only *two components* – that induced by the dipole-dipole interactions between all nuclear spins R_{1d}, and that related to the "conduction electron – nuclear spin" coupling (the so-called "Korringa coupling"), R_{1e}. The following relations are well known [17, 18]:

$$R_1 = R_{1d} + R_{1e,} \tag{32.5a}$$

$$R_1 \equiv (1/T_1), \quad R_{1d} = 1/T_{1d}, \quad R_{1e} = 1/T_{1e} \tag{32.5b}$$

T_1, T_{1d} and T_{1e} are called corresponding relaxation times. Expression for temperature dependence of T_{1e} is very simple:

$$T_{1e}(T) = K_{korr}/T, \quad K_{korr} = \text{const.} \tag{32.6a}$$

In order to calculate the dipole-dipole interaction term $T_{1d}(T)$ on applying the standard expression [17], we have to remind that the subsystem of hydrogen atoms in the superstoichiometric rare-earth dihydrides is subdivided into two sub-groups of particles: H_t-hydrogens which fill all tetrahedral interstitial positions, and H_O-hydrogens distributed on the set of octahedral interstitial positions. We repeat that in the latter subgroup of light particles there are developed the ordering processes: at temperatures below the disorder–order transition point T_{tr} different octahedral interstitial positions i are characterized generally by different occupation numbers $n(i)$ determined by the corresponding distribution function $n(x,y,z)$ [19].

In these conditions we have following expression for the dipole-dipole relaxation rate [17, 19]:

$$[1/T_{1d}] = (2/5)(C_I/\omega_I)y\Big\{\Big[(1/[1+y^2] + (4/[1+(2y)^2])\Big]\Sigma(H) + (C_S/C_I)\big[(1/3)(1/[1+k_1y^2]) + (1/[1+y^2]) + (2/[1+k_2y^2])\big]\Sigma(M)\Big\} \tag{32.6b}$$

Notations used in this expression are as follows:

$$\Sigma(\mathrm{H}) \equiv \Sigma_i^{Ht}\left(1/r_i^H\right)^6 + \Sigma_i^{H_o} n(i)\left(1/r_i^H\right)^6, \quad \Sigma(\mathrm{M}) \equiv \Sigma_i^m\left(1/r_i^m\right)^6 \tag{32.7a}$$

$$C_I = {\gamma_I}^4\,\hbar^2 \mathrm{I}(\mathrm{I}+1), \quad C_S = {\gamma_I}^2{\gamma_S}^2\,\hbar^2\,\mathrm{S}(\mathrm{S}+1); \tag{32.7b}$$

$$\omega_I = \gamma_I H_0, \quad \omega_S = \gamma_S H_0; \tag{32.7c}$$

$$k_1 \equiv (1-(\omega_S/\omega_I))^2, \quad k_2 \equiv (1+(\omega_S/\omega_I))^2; \tag{32.7d}$$

$$y \equiv \omega_I\,\tau. \tag{32.7e}$$

In expressions (32.7a) symbols Σ_i^{Ht}, Σ_i^{Ho} and Σ_i^m denote the sums over the tetrahedral interstitial positions, octahedral interstitial positions and over the sites of the metal lattice.

Also, some words about time parameter τ in the latter expression.

The mobility of hydrogen atoms is usually characterized by the number of jumps in the time unit, ν_{jump} [sec^{-1}]. It can be characterized as well by the "dwell-time" $\tau = (1/\nu_{jump})$ [*sec*] indicating the time spent by the mobile particle at each of the visited sites.

If we consider the temperature range where the "over-barrier jumps" are the dominant channel of motion, then we can write:

$$\tau = \tau_0 \exp(\mathrm{E}_a/\mathrm{k_B T}), \tag{32.8}$$

At temperatures T below the disorder–order transition point T_{tr} there arise a temperature-dependent difference in the occupation probabilities of the octahedral interstitial positions. Correspondingly, the part of the sum $\Sigma(\mathrm{H})$ associated with the octa-hydrogen atoms in (32.7a) becomes temperature dependent. This effect we have considered in [19].

The second effect associated with the hydrogen ordering processes is the mentioned above "weighting" of the jumping particles in the ordered state. This effect was estimated in [20].

This general scheme of consideration is illustrated below by some examples.

32.4.2 Application to $LaH_{2.27}$ Compound

Results of NMR-measurements performed on $\mathrm{LaH}_{2.27}$ were given in [21]. Authors compared the obtained spin–lattice relaxation data with the results of corresponding $\mathrm{T}_1(\mathrm{T})$ calculations and demonstrate an excellent coincidence of both dependences. It has to be stressed that *no one of the mentioned above hydrogen ordering effects had not been taken into account*. There arises a question – what will happen if we

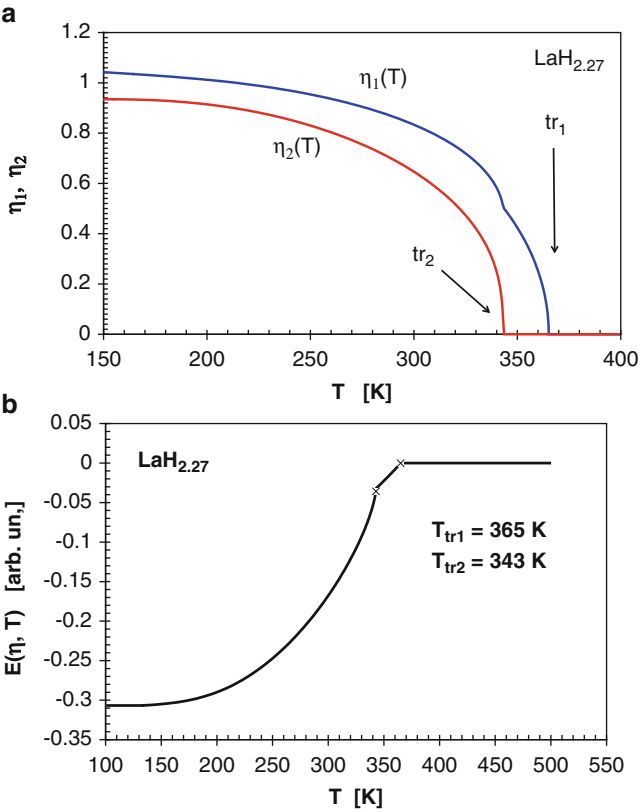

Fig. 32.6 (**a**) Temperature dependence of order parameters η_1 and η_2, (**b**) temperature dependence H-H interaction induced ordering energy (*see color plates*)

include these effects into the calculation scheme. In other words, how must be the selected energy parameters modified [21] in order to retain in these new conditions the already obtained excellent coincidence of measured and calculated data.

The answer seems to be paradoxical at the first glance. Namely, when we take into account both adjustments, no remarkable changes occur and the already selected parameters [21]:

$$K_{korr} = 410\,\text{sec K}, \quad E_a = 0.35\,\text{eV}, \quad \tau_{00}{}^{-1} = 7.4 \times 10^{11}\,\text{sec}^{-1} \tag{32.9}$$

have to be left unchanged.

In order to understand the physical background of this result, we have to consider briefly the ordering process of octa-hydrogens, which is described by *two long range order parameters* η_1 and η_2. Equilibrium states of the ordering LaH_{2+c} system were analyzed in [5]. If we apply the calculation scheme given in [5] to our compound $LaH_{2.27}$, we shall obtain results shown in Fig. 32.6a, b, where there

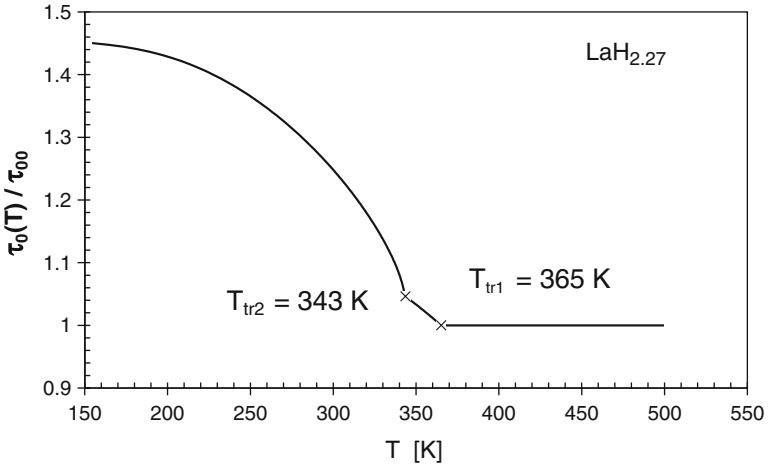

Fig. 32.7 Temperature dependence of the time-parameter factor τ_0

are given temperature dependences of the equilibrium values of order parameters $\eta_1(T)$ and $\eta_2(T)$, and of the ordering energy $E(\eta_1(T), \eta_2(T))$ (denoted as $E(\eta, T)$ in Fig. 32.6b). It is notable that the ordering process contains *two* phase transition points – at $T = T_{tr1} = 365$ K and at $T = T_{tr2} = 342$ K (both continuous, of the second-order-type phase transition).

As it was mentioned above, the mobility of H_O-atoms is characterized by the parameters ν_{jump} [sec^{-1}], or $\tau = (1/\nu_{jump})$ [*sec*]. "Weighting" of the jumping H-atoms can be taken into account by slight modification of time-parameter τ_0 in expression (32.8):

$$\tau_0 \rightarrow \tau_0(T) = \tau_{00}\{1 - b[(E(\eta_1, \eta_2)/N_H)/\hbar\omega_0]\}. \tag{32.10}$$

Here τ_{00} denotes the unperturbed (high-temperature) value of the time-parameter τ_0, and $\hbar\omega_0$ is the "pure local mode" energy, $\hbar\omega_0 \equiv k_B\,\theta_E$ (where θ_E is the corresponding Einstein temperature); $E(\eta_1, \eta_2)$ is the ordering energy of the octa-hydrogen subsystem (shown in Fig. 32.6b), and b is the tentative numerical constant. Temperature dependence of parameter τ_0 is shown in Fig. 32.7.

Both ordering effects – nonuniform distribution of H_O-atoms in the lattice and their temperature-dependent "weighting" – were included in the standard calculations of the $T_{1d}(T)$ dependence. Results are presented in Fig. 32.8. The dashed curve represents the traditional, "high-temperature", result, while the thick line includes both "ordering effects". We see that the difference is very weak. This is caused by the fact that besides the redistributable H_O-atoms there exist a great number of "stably-located" H_t-atoms which are attached to the H_O-atoms with temperature-independent bonds. As a result, both proposed refinements does not really act upon the $T_1(T)$ calculated dependence (see [19, 20]) and coincidence with the experimental curve remains as good as in [21] (see Fig. 32.9).

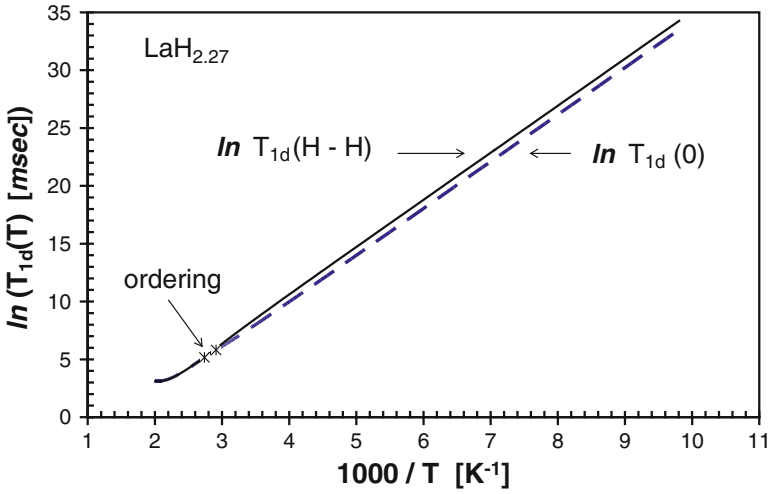

Fig. 32.8 Influence of hydrogen "weighting" on the dipole-dipole part of the spin–lattice relaxation time (*see color plates*)

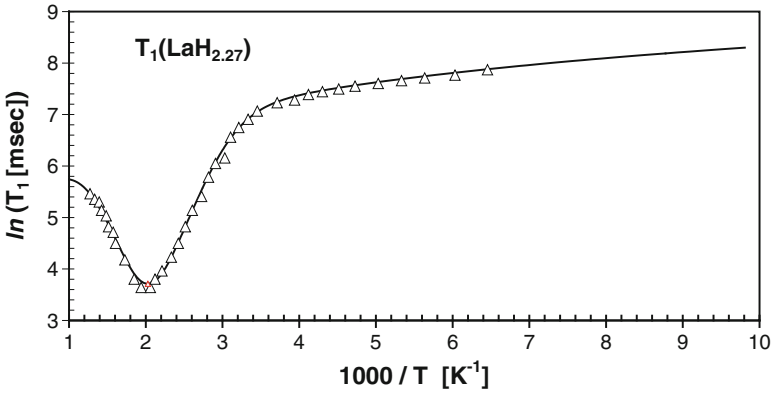

Fig. 32.9 Temperature dependence of the spin–lattice relaxation time T_1 *solid line* – calculated dependence [20], *open triangles* – experimental points [21] (*see color plates*)

32.4.3 Ordering Effects in Refractory Metal Hydrides

We have considered above the case of relaxation process in the system where the ordering process is developed among the minor part of the hydrogen subsystem. In the case of refractory metal hydrides such a "negative background" is absent as the ordering processes involve all H-atoms absorbed by the metal lattice [22]. Corresponding experimental NMR-data were published a few decades ago [23].

In Fig. 32.10, we have reproduced some $T_1(T)$ dependences obtained in [23]. The main qualitative conclusion that can be deduced from the given figure consists

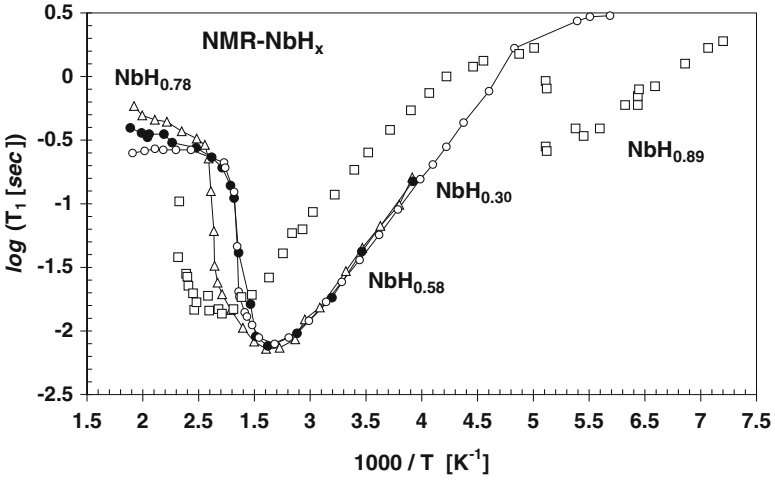

Fig. 32.10 Temperature dependence of the spin–lattice relaxation time T_1 in niobium hydrides NBH_x. *Open triangles* ($x = 0.78$), *open circles* ($x = 0.30$) and *black points* ($x = 0.58$) – results published in [23], *open squares* ($x = 0.89$) – results of Yu. G. Sharimanov [24]

in the statement that the mobility of hydrogen interstitials decreases monotonically at temperature lower than T_{min} (corresponding to the minimum of $T_1(T)$ dependence, provided by the dipole-dipole interaction of nuclear spins). On following [23], this effect seems to be sufficiently general, independent of hydrogen equilibrium state, and, particularly, of hydrogen concentration (at least for $c_H > 0.30$). Such straightforward deductions are incorrect and this conclusion is supported by the experimental results [24] represented in the same Fig. 32.10.

It has to be stressed that indicated discontinuity of the monotonic $T_1(T)$ dependence in $NbH_{0.89}$ (we call it "Sharimanov-effect") occurs in the vicinity of the order-order phase transition point ($T_{tr} \approx 180$ K). In our opinion, it is caused by destroy of the "high-temperature" ($T > T_{tr}$) ordered structure and formation in the hydrogen subsystem a temporal "chaotic" state that destroys the already formed H-H bonds and "liberates" H-particles. Such conception seems to be logically acceptable and qualitatively explains the increase of hydrogen mobility in the vicinity of the phase transition point (before new spatial ordered configuration would be established), but to be finally accepted it needs to be carefully numerically verified. The extreme needfulness of such verification is supported by the existence of another "unusual" effect characteristic for the ordering interstitial alloys, which will be discussed below.

32.4.4 Ordering Influence on Mobility of Hydrogen Atoms

We shall briefly reproduce some examples of our attempts to describe experimental data of spin–lattice relaxation time of protons in metal hydrides obtained in E. Andronikashvili Institute of Physics [25].

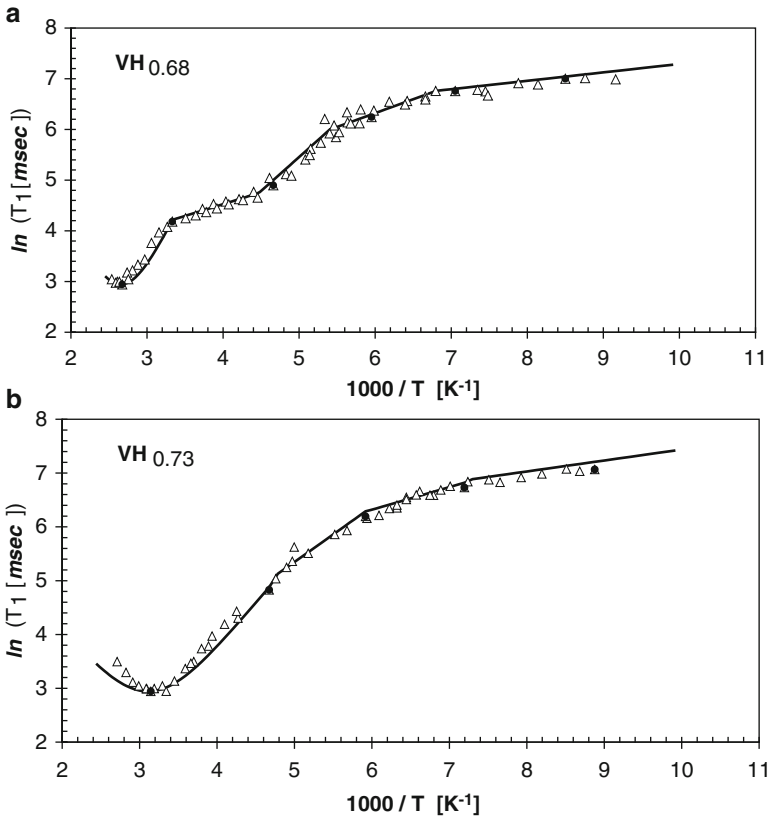

Fig. 32.11 (**a** and **b**) Temperature dependence of spin–lattice relaxation times T_1 in vanadium hydrides [25]

Figure 32.11a, b give experimental dependences $T_1(T)$ for two vanadium hydrides and their description basing on expressions accounting for the dipole-dipole interactions of nuclear spins. In order to obtain physically meaningful coincidence between calculated dependence $T_1(T)$ and experimental points we were obliged to assume that proton jumping activation energy *decreases at increasing of the degree of order*.

This unusual result qualitatively can be "explained" if we assume that on increasing of the role of H-H interactions (with respect to thermal motion) and formation of ordered structures simultaneously increases the possibility of collective motions in the subsystem of light atoms. (I.e. we imply possibility of formation of specific acoustic waves which propagate exclusively in the sublattice of light atoms). This idea seems to be acceptable but has to be verified both analytically and experimentally.

Analogous situation was registered in the case of lanthanum dihydrides. Particularly, for compounds $LaH_{2.36}$ and $LaH_{2.39}$, in order to describe the sequence of experimental points in the low-temperature part of the $T_1(T)$-dependence minimum, we were obliged to assume gradual lowering of the hydrogen jumping activation energy values (Final report of the Project STCU-3867).

32.5 Conclusion

Let us summarize and give some short conclusions:

1. Hydrogen absorbing metals can be considered as the basic work-material for creation of sensitive renewable hydrogen sensors. Such application area should be realized, if different hydrogen contents in the host material provide specific single-valued changes of metal's physical properties. Within the frames of this idea, we have to show up the most significant lattice response on variations of the absorbed hydrogen doses. It follows that we have to compare different physical properties of MH-compounds in different conditions, i.e., at different temperatures, pressures, external fields, fortuitous contaminations, etc.
2. Unfortunately, direct proportionalities between the quantity of absorbed hydrogen atoms and changes of different physical properties are absent. It follows that hydrogen-easily-absorbing metals can be applied only for indicator-type devices, which signalize the existence of free hydrogen in the environment. Nonmonotonic dependences of physical properties on hydrogen concentration are caused, particularly, by existence of H-H interactions in the lattice.
3. Our investigations reviewed in the present report have illustrated the role of H-H interactions in formation of specific properties characteristic for MH-systems. It was shown, particularly, that these interactions provide such effects as "weighting" of light particles (Fig. 32.5), as well as activation energy changes caused by ordering processes (Fig. 32.11a, b). Together with the "phase transition order change" phenomenon (Fig. 32.4) these peculiarities point to the significant role of inter-hydrogen interactions in the metal lattices.
4. Of course, open problems still exist – discrepancy of the heat capacities of lanthanum and cerium dihydrides (compare Figs. 32.1 and 32.2), anomalous temperature dependence of the spin–lattice relaxation rate in $NbH_{0.89}$ ("Sharimanov-effect", Fig. 32.10), absence of similar effects in ordering vanadium hydrides (Fig. 32.11a, b), and some others. These problems need to be considered in the future.
5. From a general point of view, MH-compounds represent an example of a solid with easily variable properties caused by variation of hydrogen content. Hydrogen "contaminations" in the lattice influence on electrical, magnetic, optical, superconducting, thermal properties of the host material. Besides these application-oriented problems, there remain a solid number of fundamental problems, such as energy spectrum of hydrogen subsystem in metal hydrides,

stability of hydrogen associations formed in the metal lattice, the problems of stability of MH-compounds in different external conditions, etc. All these problems have to be solved in order to indicate the specific position of metal-hydrogen systems in the wide range of interstitial alloys and to outline possible technical applications of these systems in the foreseeable future.

Acknowledgement Most of cited theoretical and experimental results were obtained within the frames of two projects: STCU-3867 (2006–2009) and CNSF- ST09-501-4-280 (2010–2012).

One of the authors (I. R.) thanks to the organizers of the NATO Advanced Research Workshop "The Black Sea: Strategy for Addressing its Energy Resource Development and Hydrogen Energy Problems", Batumi, Georgia (October 7–10, 2012) for the possibility to participate at the workshop meetings.

References

1. Keesom PH, Pearlman N (1954) In: Flugge S (ed) Handbuch der Physi, vol XIV. Springer, Berlin, pp 282–337
2. Ratishvili IG, Vajda P, Namoradze NZ (1997) Heat capacity associated with hydrogen ordering in superstoichiometric rare-earth dihydrides: the case of LaH2+x-like systems. J Phys Chem Solid 58:59–62
3. Ratishvili IG, Namoradze NZ (2009) Ordering processes in the systems characterized by two long-range-order parameters. Metallofiz i Nov Tekhnol 31:315–332
4. Ratishvili IG, Vajda P, Boukraa A, Namoradze NZ (1994) Ordering processes in monophase CeH_{2+x}. Phys Rev B 49:15461–15469
5. Ratishvili IG, Vajda P (1996) Hydrogen ordering in superstoichiometric rare-earth hydrides. The case of a system with an energy constants ratio $p = V_2/V_1 < 1$: LaH_{2+x}. Phys Rev B 53:581–587
6. Stalinski B, Bieganski Z (1964) Low-temperature heat capacity of cerium dihydride. Crystal field effects. Bull Acad Polon Sci Ser Sci Chim XII:331–334
7. Bieganski Z (1971) Low temperature specific heats and related thermodynamical functions of lanthanum dihydride $LaH_{2.00}$. Bull Acad Polon Sci Ser Sci Chim XIX(9):581–586
8. Namoradze N, Ratishvili I (2011) Heat capacity of rare-earth quasi-stoichiometric dihydrides. Bull Georgia Nat Acad Sci 5(3):51–54
9. Namoradze N, Ratishvili I (2013) "Anomalous" heat capacity of the stoichiometric lanthanum dihydride. Bull Georgia Nat Acad Sci 7(1):38–45
10. Bieganski Z, Fesenko W, Stalinski B (1965) Low-temperature heat capacity of cerium trihydride. Crystal field effects in rare-earth hydrides. II. Bull Acad Polon Sci Ser Sci Chim XIII(3):227–230
11. Namoradze N, Ratishvili I (2012) Ordering effects in the heat capacity of light rare-earth superstoichiometric dihydrides. $CeH_{2.86}$. Bull Georgia Nat Acad Sci 6(2):51–54
12. Ratishvili IG (1999) Phase transition type change in order-order and order–disorder transformations of LaH2+c-like superstoichiometric dihydrides. Phys Stat Solid B 213:297–315
13. Ratishvili IG, Namoradze NZ (2000) Heat capacity anomalies associated with phase transition type change in CeH2+x-like superstoichiometric rare-earth dihydrides. J Phys Chem Solid 61:1827–1838
14. Rowe JM (1972) A neutron scattering study of the vibrational and diffusional motions of deuterium in the α and β phases of $VD_{0.5}$. Solid State Commun 11:1299–1302
15. Ratishvili I, Namoradze N (2009) Poster presentation at GRC, Barga, Italia

16. Ratishvili IG, Namoradze NZ (2011) Temperature dependence of local mode frequencies in ordering metal hydrides. The case of b.c.c. metal lattices. Metallofiz Noveishie Tekhnol 33:919–938
17. Cotts RM (1978) In: Alefeld G, Völkl J (eds) Hydrogen in metals I. Springer, Berlin, pp 227–288
18. Barnes RG (1995) In: Wipff H (ed) Hydrogen in metals III. Springer, Berlin, pp 93–151
19. Namoradze NZ, Ratishvili IG (2007) In: Veziroglu N et al (eds) Hydrogen materials science and chemistry of carbon nanomaterials. Springer, Dordrecht, pp 87–94
20. Ratishvili IG, Namoradze NZ (2009) Temperature dependence of hydrogen mobility in ordering rare-earth dihydrides. Bull GNAS 3(3):70–75
21. Phua T-T, Beaudry BJ, Peterson DT, Torgeson DR, Barnes RG, Belhoul M, Styles GA, Seymour EFW (1983) Paramagnetic impurity effects in NMR determinations of hydrogen diffusion and electronic structure in metal hydrides Gd^{3+} in YH_2 and $LaH_{2.25}$. Phys Rev B 28 (11):6227
22. Somenkov VA, Shilshtein SSh (1978) Preprint of Kurchatov Institute of AE "Hydrogen in Metals" (in Russian)
23. Lutgemeier H, Arons RR, Bohn HG (1972) Proton spin–lattice relaxation time in the Niobium-Hydrogen system. J Magn Reson 8:74–79
24. Sharimanov YG, Grossescu R (1982) Temperature dependence of proton spin–lattice relaxation time in the Niobium Hydride. Solid State Phys 24(1):310–311 (in Russian)
25. Mamniashvili GI, Namoradze NZ, Ratishvili IG, Sharimanov YG (2005) Proton spin–lattice relaxation time in ordering VH_x-alloys. J Phys Chem Solid 66:1192–1199

Color Plates

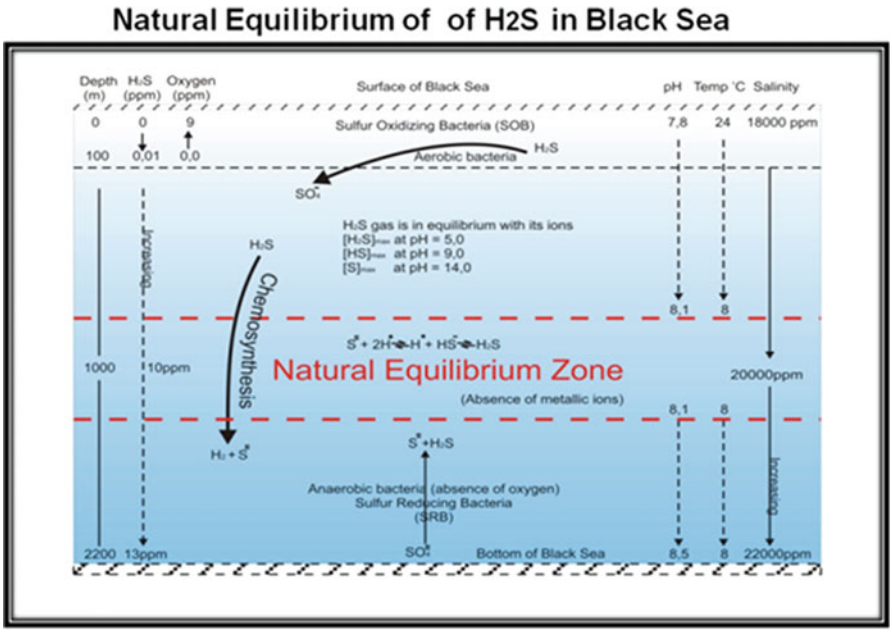

Fig. 2.1 Equilibrium schematics for H_2S in the Black Sea [6]

A. Veziroğlu and M. Tsitskishvili (eds.), *Black Sea Energy Resource Development and Hydrogen Energy Problems*, NATO Science for Peace and Security Series C: Environmental Security, DOI 10.1007/978-94-007-6152-0,

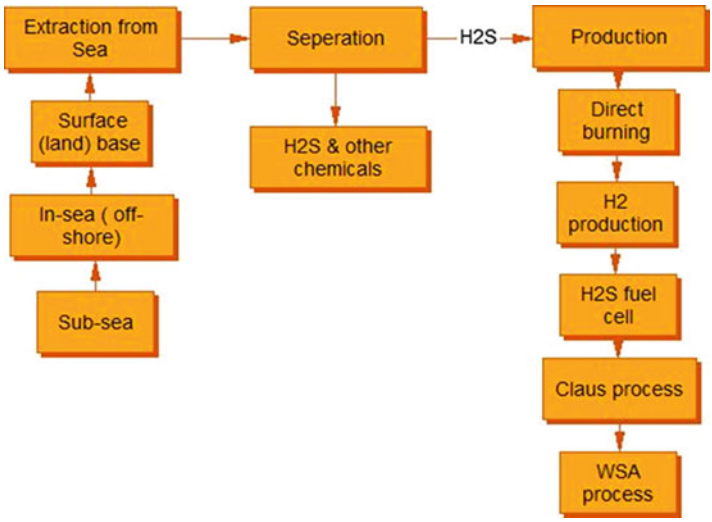

Fig. 2.3 Possible ways to extract and utilize H_2S

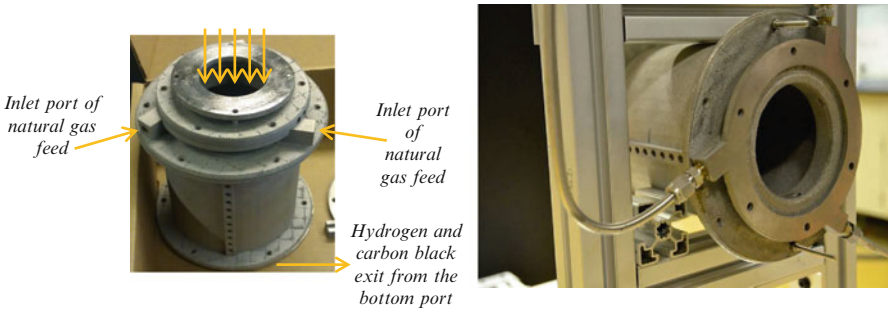

Fig. 3.1 An example solar reactor designed and manufactured at SERL of TAMU-Q

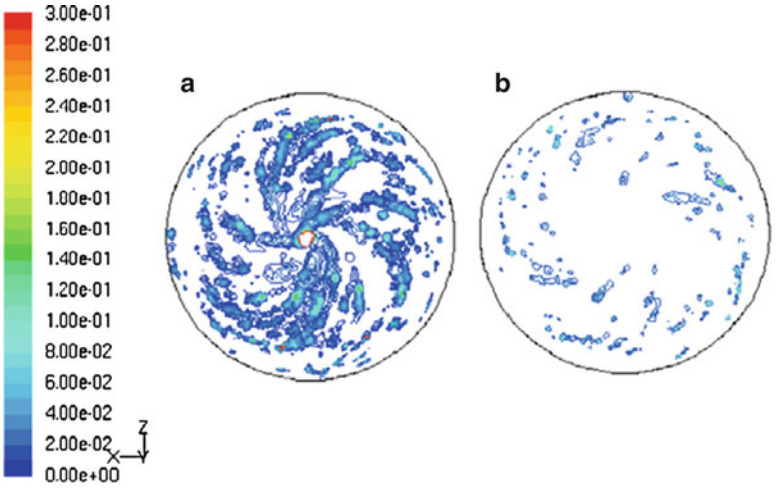

Fig. 3.2 (**a**) Significantly contaminated window, (**b**) Slightly contaminated window [24]

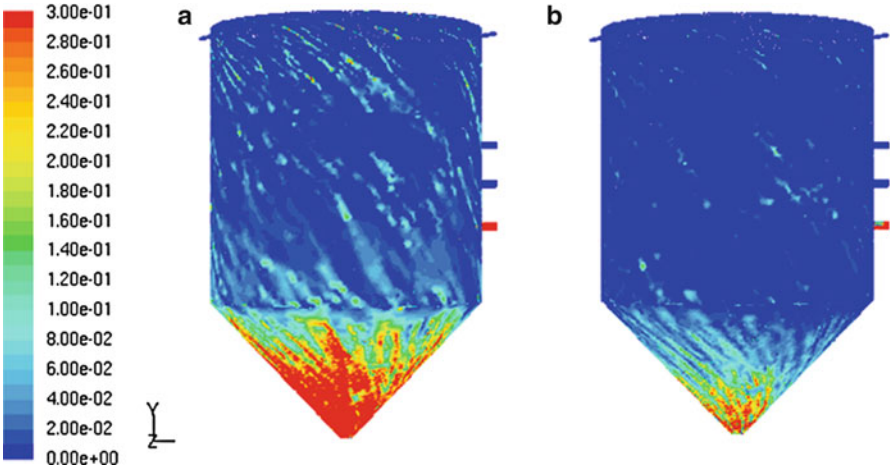

Fig. 3.3 (**a**) Significant carbon deposition at reactor exit, (**b**) Slight carbon deposition at reactor exit [24]

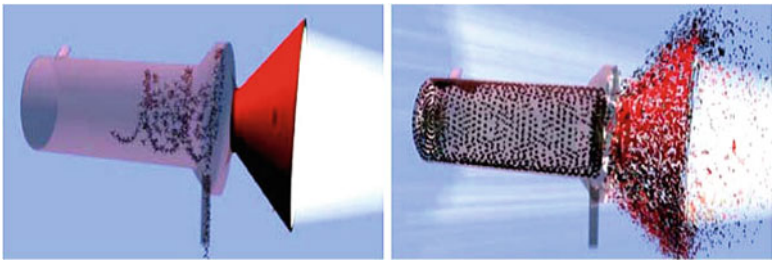

Fig. 3.4 Carbon blockage exploding the solar reactor window

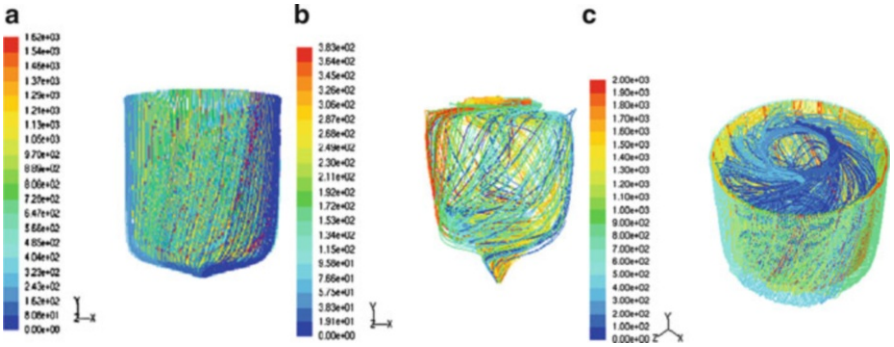

Fig. 3.5 (**a**) Laminar wall screening shield on the walls, (**b**) Cyclone flow in the center, and (**c**) Isometric view of the laminar wall screening and cyclone flow

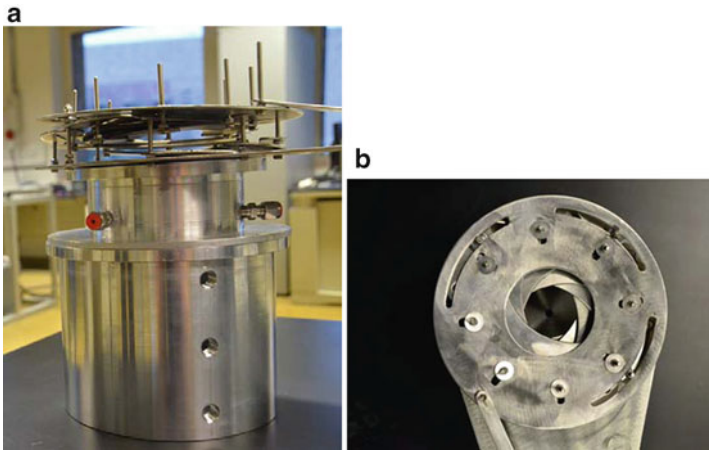

Fig. 3.6 (**a**) Solar reactor with mechanical human-eye like aperture mounted at the solar flux entry, (**b**) Mechanical human-eye like aperture

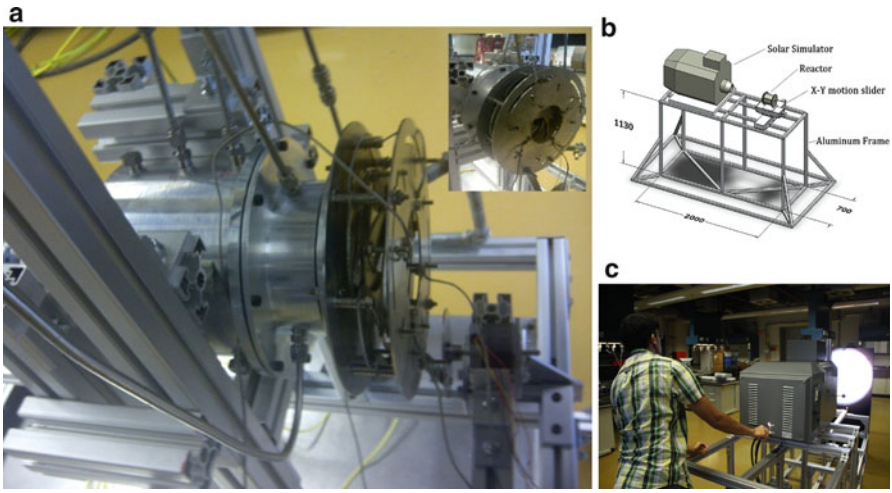

Fig. 3.7 (**a**) Solar reactor with mechanical human-eye like aperture mounted at the solar flux entry, (**b**) Schematic of the experimental setup, (**c**) Optical alignment of the 5 kW solar simulator

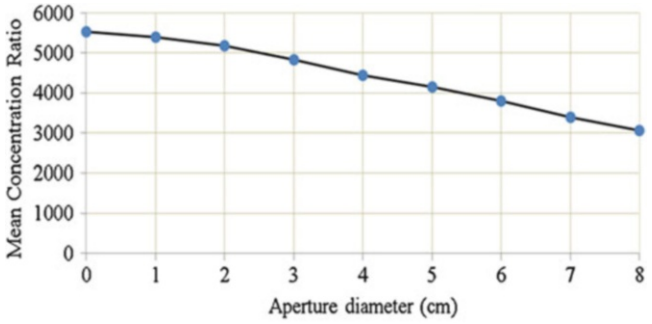

Fig. 3.8 Mean concentration ratio through a circular aperture as a function of its diameter [26]

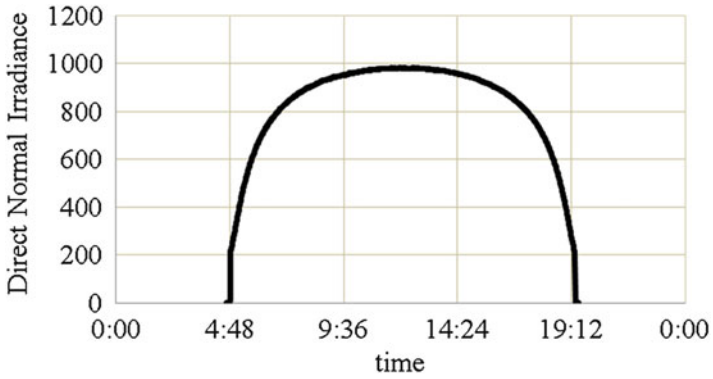

Fig. 3.9 Bird estimated direct normal insolation (*I*) [26]

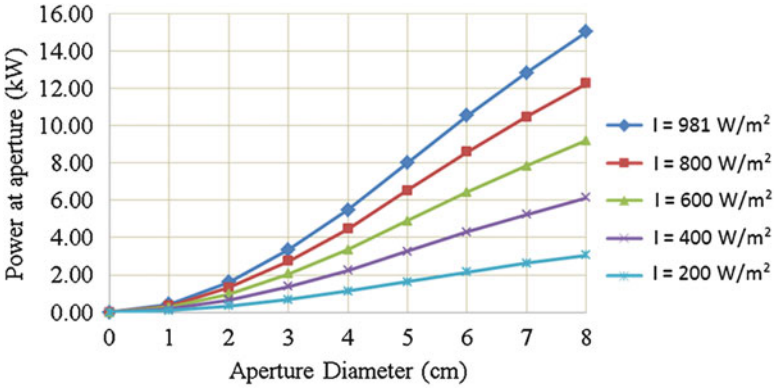

Fig. 3.10 Power intercepted at aperture (P_{ap}) as a function of diameter for different levels of normal insolation [26]

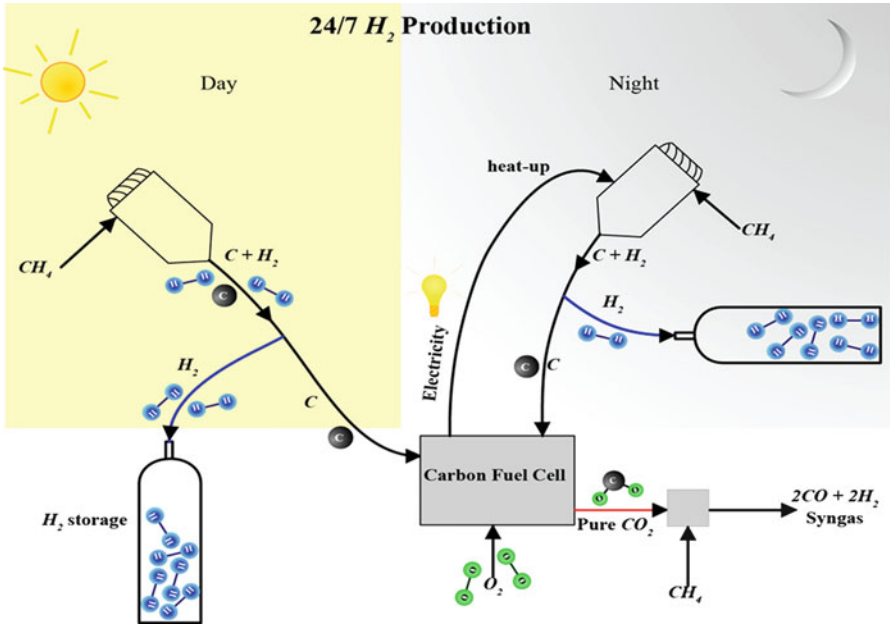

Fig. 3.11 Tri-generation of hydrogen, carbon black, and syngas on 24/7 basis

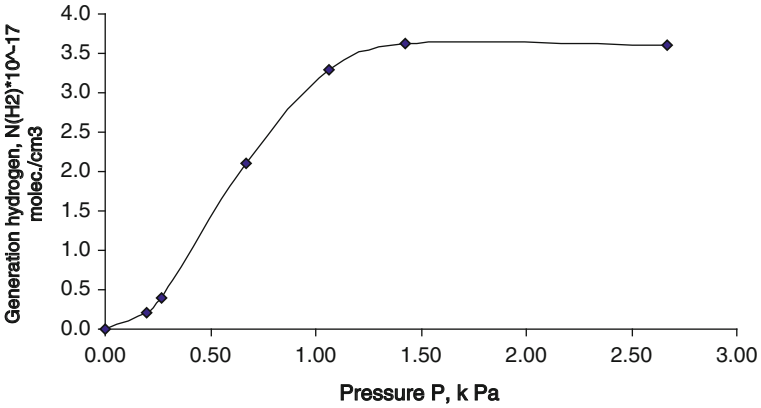

Fig. 5.1 Dependence between hydrogen concentration generated due to photolysis and the pressure of hydrogen sulfide

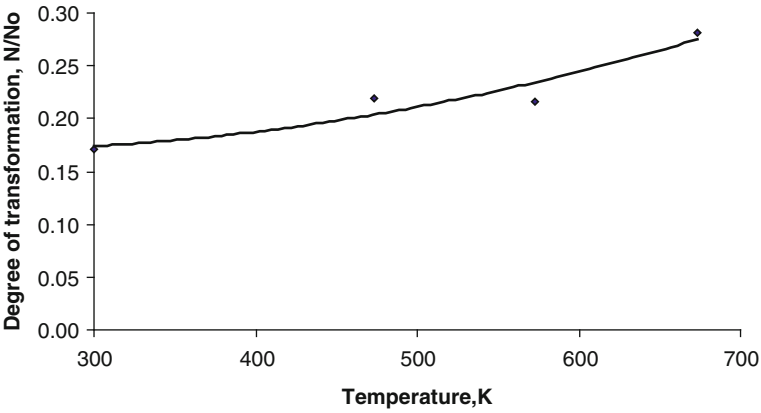

Fig. 5.4 Temperature dependence of hydrogen sulfide photochemical decomposition

Fig. 7.1 The vision for future nuclear energy Renaissance and long-term sustainability of nuclear energy: *R* recycling, *T* transmutation, *U* uranium, *Pu*-plutonium, *MA* minor actinides, *DEU* depleted uranium, *FP* fission products

Fig. 7.2 Phénix sodium-cooled fast-neutron reactor in Marcoule (France)

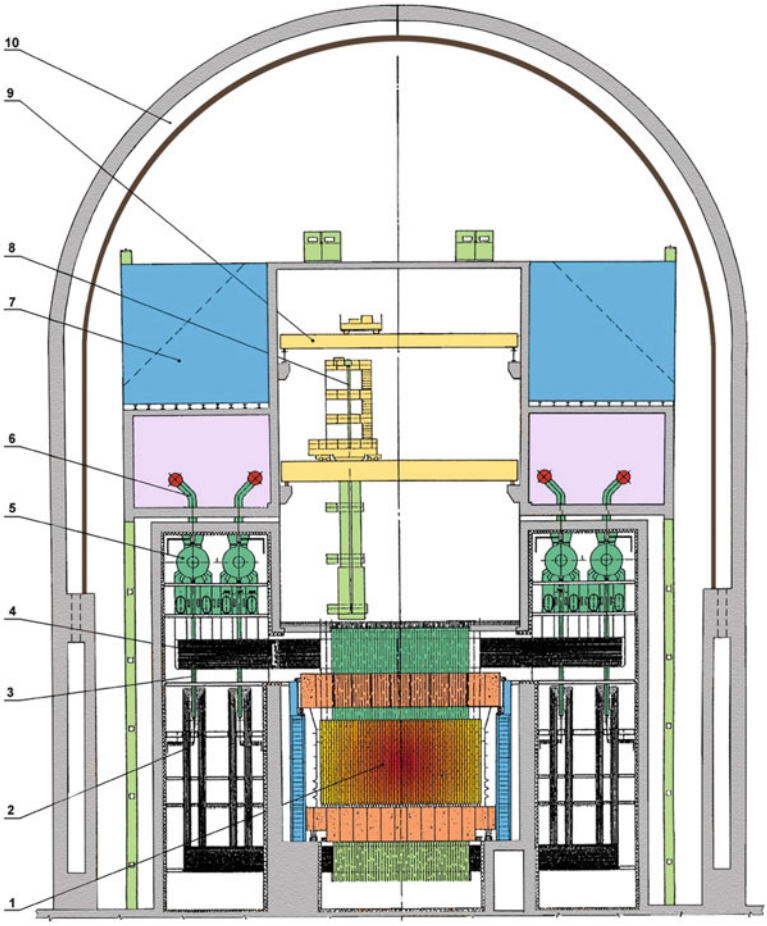

Fig. 7.3 Pressure-Tube power reactor: *1* reactor core, *2* water lines, *3* downcomer, *4* steam-water lines, *5* steam separator, *6* steam line, *7* passive cooling system tank, *8* refuelling machine, *9* bridge crane, *10* containment

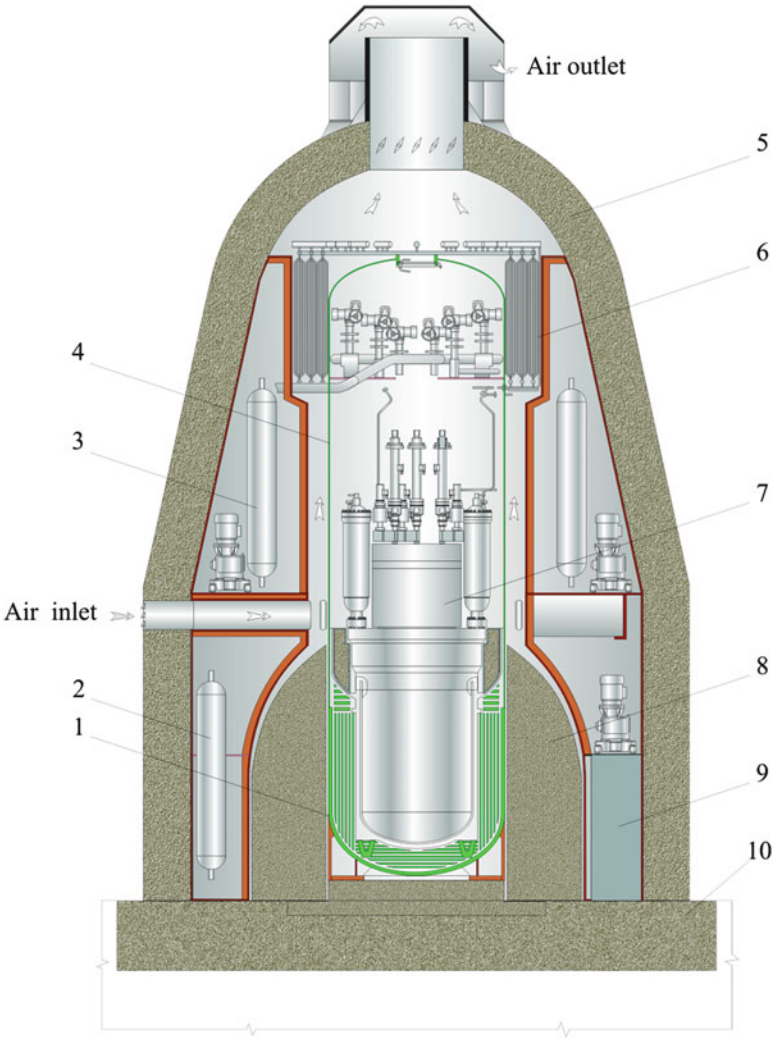

Fig. 7.4 Small power plant. *1* iron-water shielding tank, *2* gaseous waste storage tanks, *3* liquid poison supply system, *4* containment, *5* shock-proof shell, *6* heat exchanger of the cooling system, *7* steam generating unit, *8* biological shielding blocks, *9* liquid and solid radwaste storage facility, *10* foundation

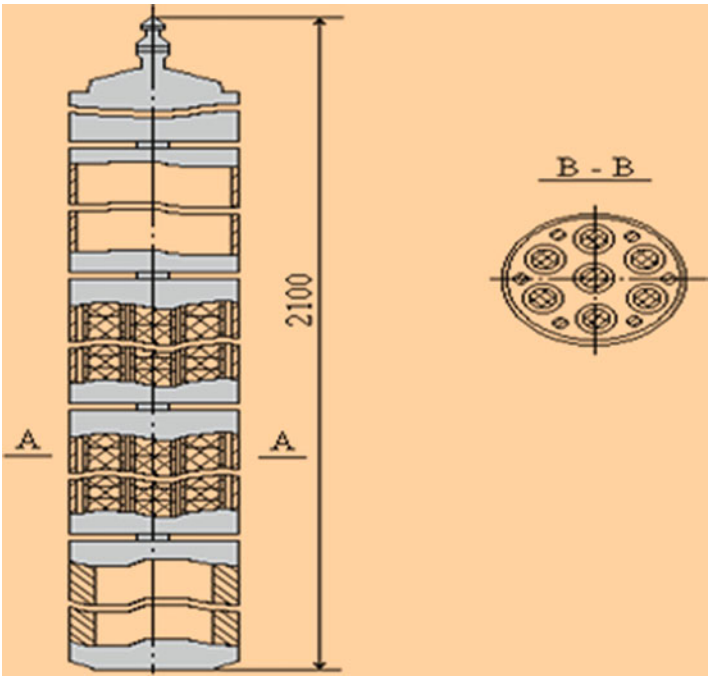

Fig. 7.6 Reactivity compensation rod design

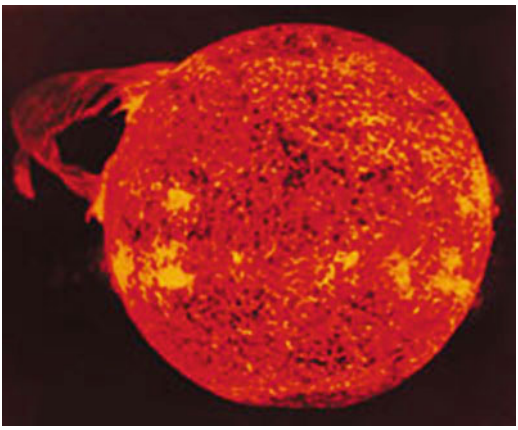

Fig. 7.7 The Sun is a massive fusion power station. It produces around 300 billion watts (3×10^{26}) of power, consuming 600 million tons of hydrogen fuel every second

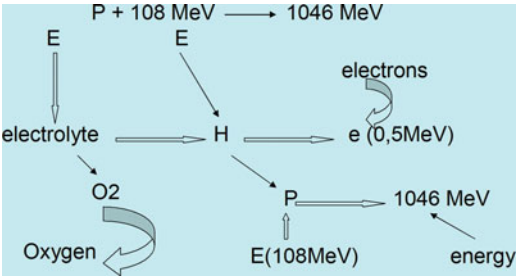

Fig. 7.9 Proton born nuclear-chemical reaction

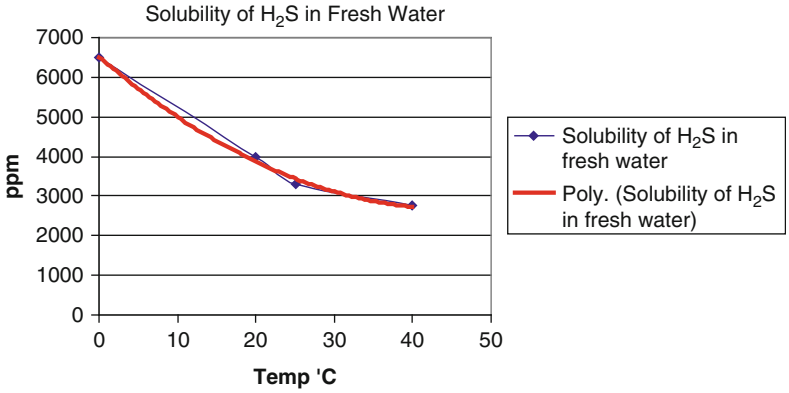

Fig. 9.1 Solubility of H_2S in fresh water at different temperature

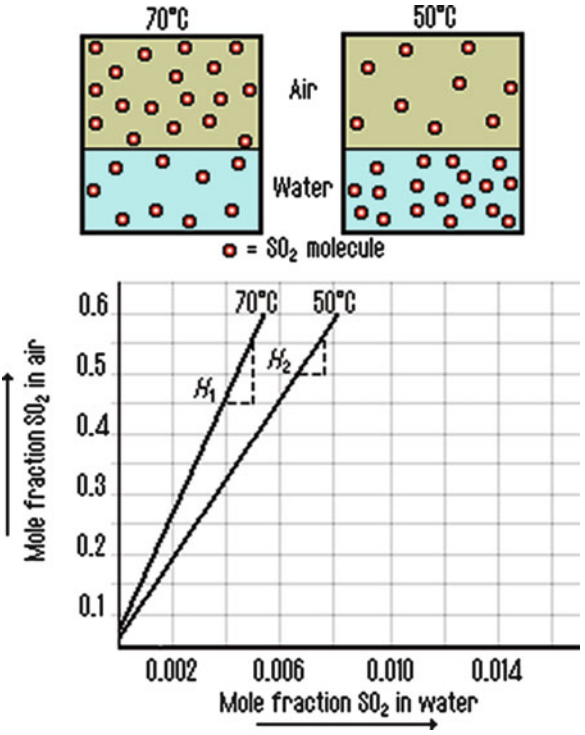

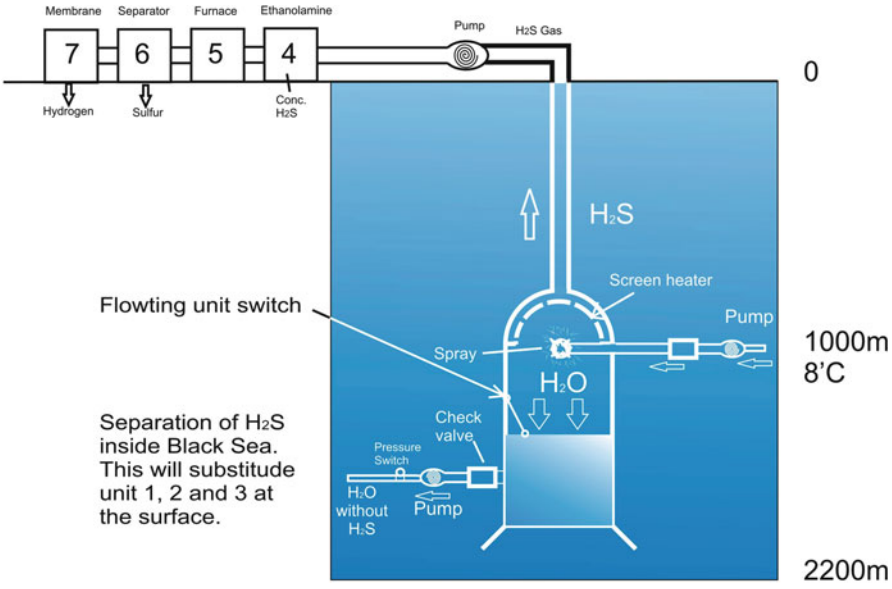

Fig. 9.2 Application of Henry's Law

Fig. 9.6 Extraction of H_2S inside the sea (schematic diagram)

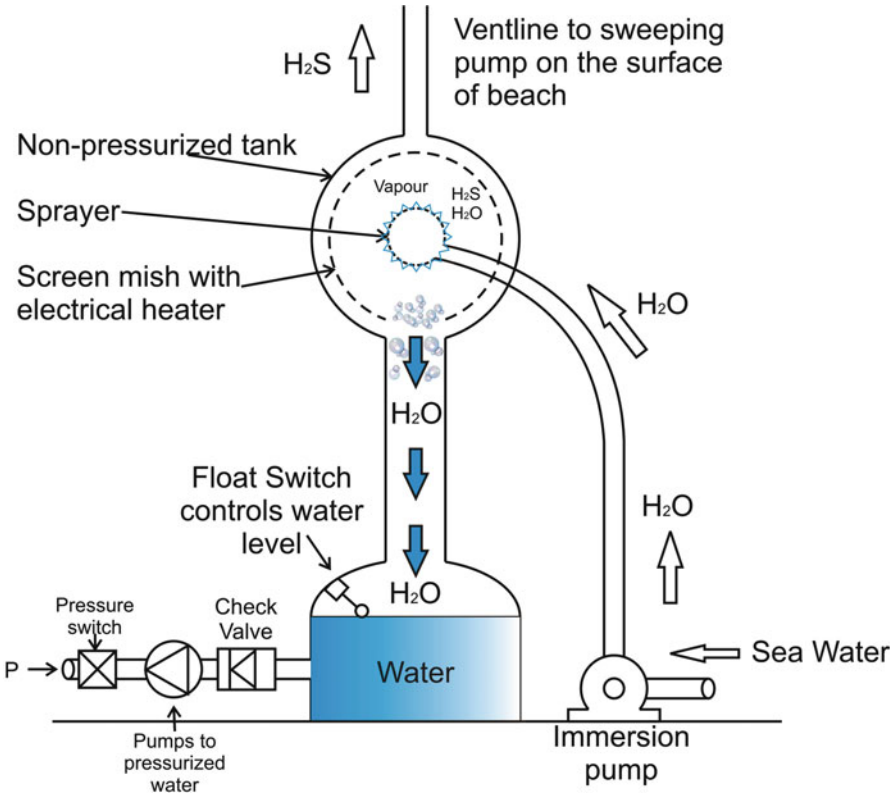

Fig. 9.7 New industrial extraction unit of H_2S designed for inside water

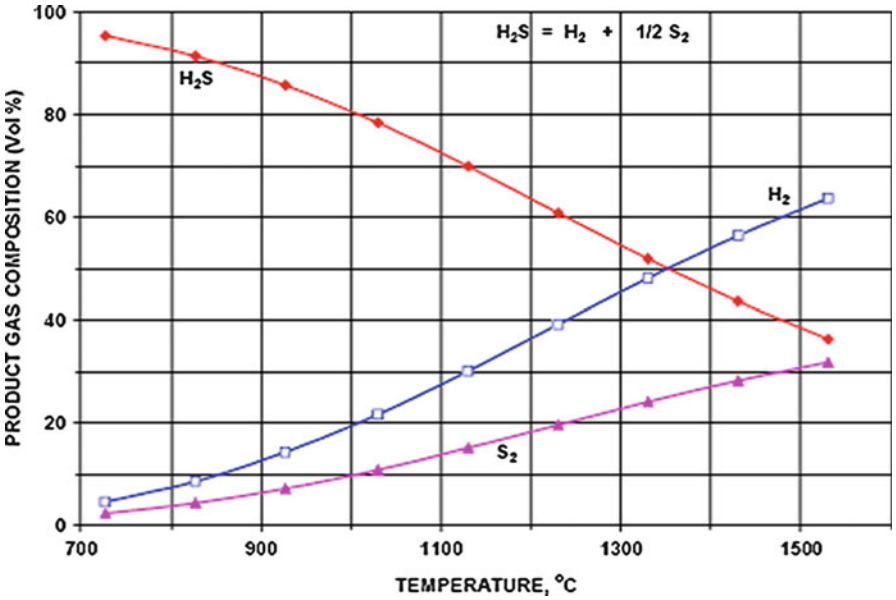

Fig. 9.8 Pure H_2S decomposition reaction as a function of temperature

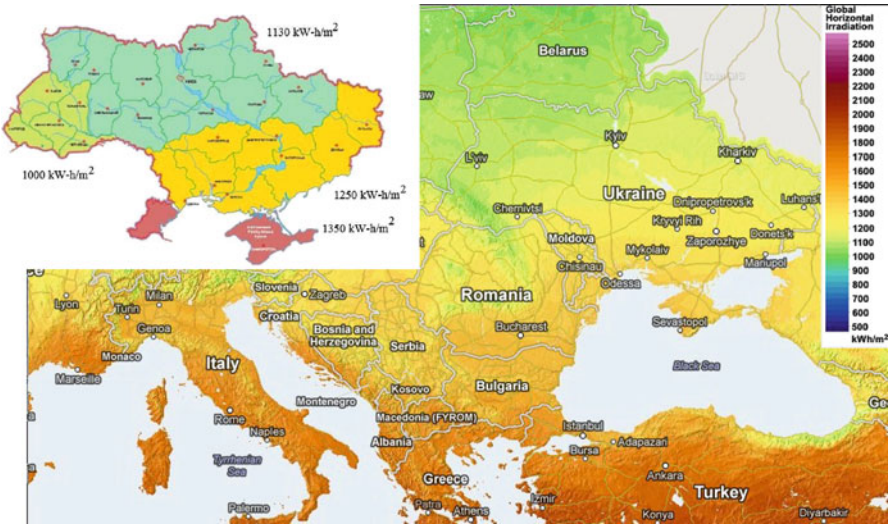

Fig. 10.2 Solar energy potential of Ukraine and neighbouring countries and a more detailed breakdown of the solar energy potential in the regions of Ukraine (*upper left*)

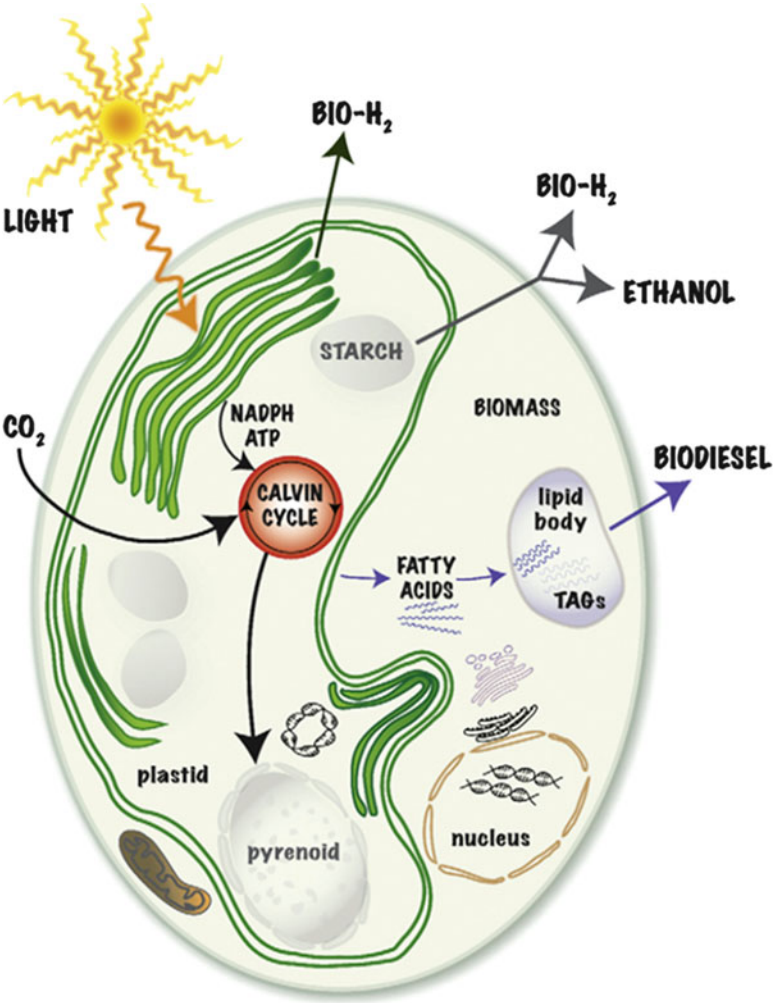

Fig. 11.2 Metabolic pathways in green algae related to biofuel and biohydrogen production [15]

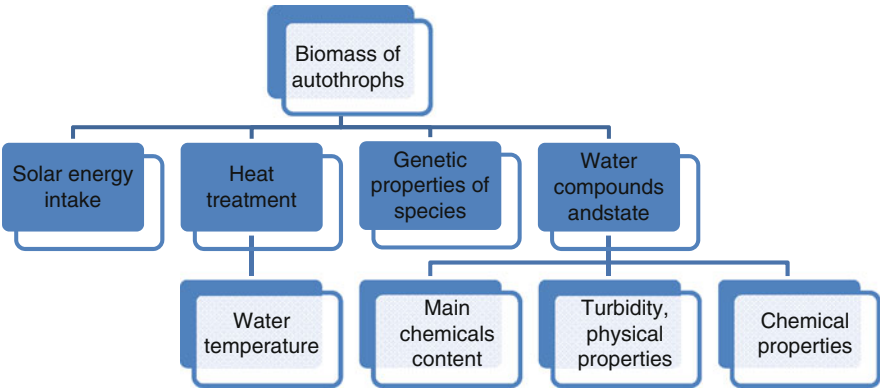

Fig. 12.1 Conceptual chart of water autothrophs biomass production

Fig. 13.1 H_2 production rates by *E. coli* wild type BW25113 grown under fermentation conditions at different pHs. Bacteria were grown on glucose, glycerol or mixed carbon sources (glucose and glycerol) and assayed with adding glucose or glycerol as described in Materials and methods. V_{H2} was determined as stated in Materials and methods

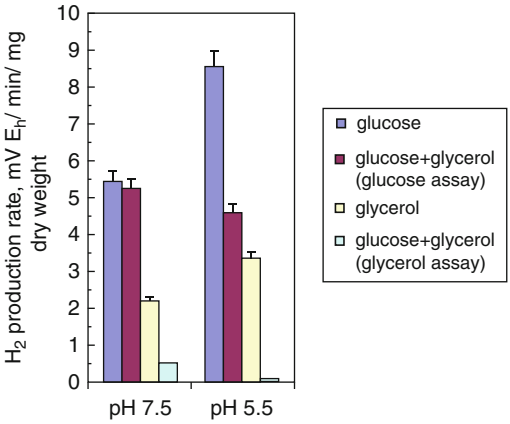

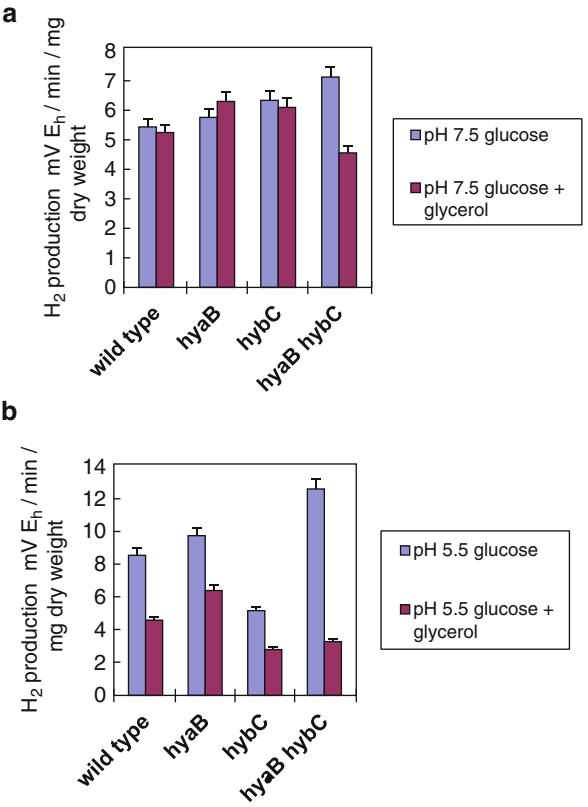

Fig. 13.2 H_2 production rates for *E. coli* wild type and mutants with defects in Hyd-1 (*hyaB*) and Hyd-2 (*hybC*) at pH 7.5 (**a**) and 5.5 (**b**). Whole cells grown were assayed with glucose (22 mol m^{-3}) (For strains, see Table 13.1, for others, see legends to Fig. 13.1)

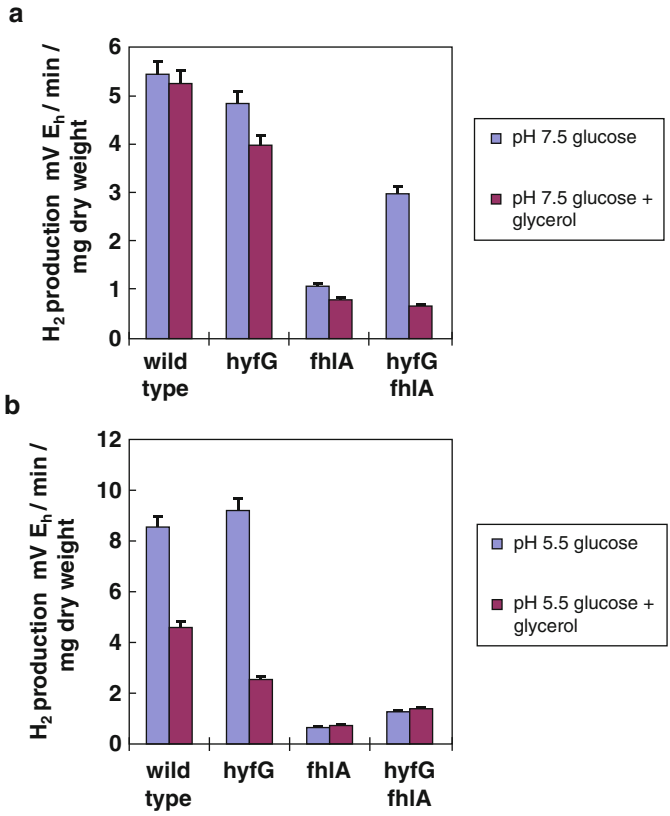

Fig. 13.3 H_2 production rates for *E. coli* wild type and mutants with defects in Hyd-3 (*fhlA*) and Hyd-4 (*fhlA hyfG*) at pH 7.5 (**a**) and 5.5 (**b**) (For others, see legends to Fig. 13.2)

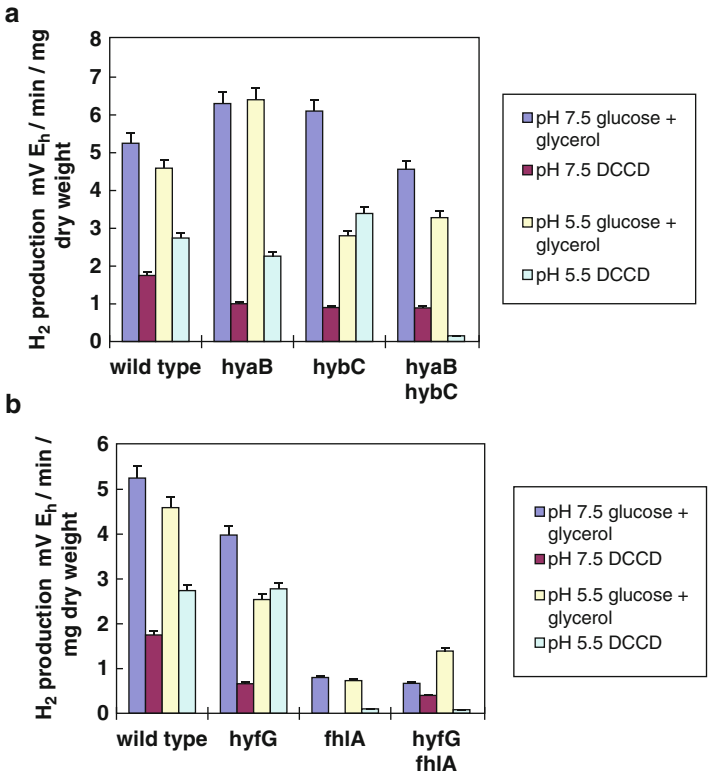

Fig. 13.4 The inhibition by DCCD of H_2 production rates for *E. coli* wild type and mutants with defects in Hyd-1 and Hyd-2 (**a**) and Hyd-3 and Hyd-4 (**b**) at different pHs. 0.3 mM DCCD was used (For others, see legends to Fig. 13.2)

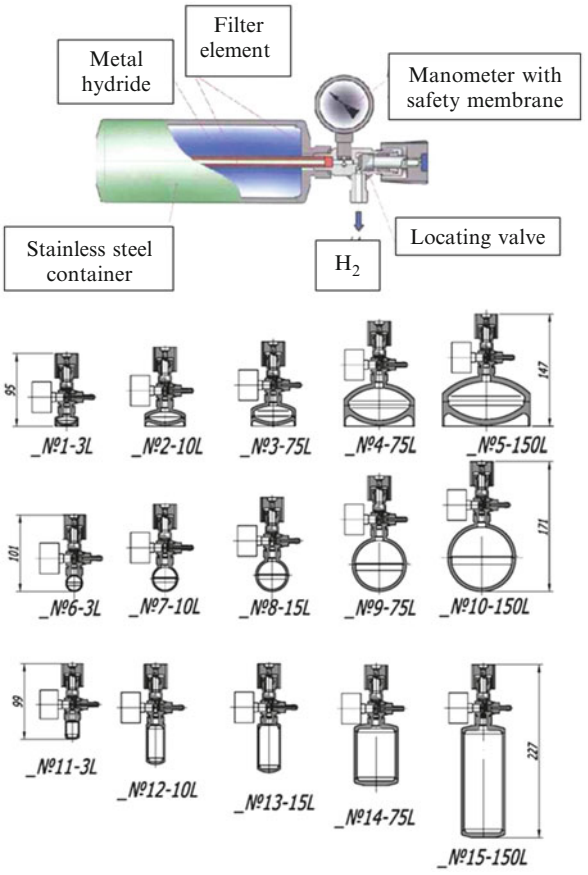

Fig. 16.1 The series of metal hydride storage elements for various applications

Fig. 16.2 The high-pressure vessels for hydrogen storage and hydrogen accumulators of "Alsav" modification with a capacity of 3, 10, 15, 75 and 170 l

Fig. 16.3 The high-pressure vessels for hydrogen storage and hydrogen accumulators of "Dmisch" modification with a capacity of 3, 10, 15, 75 and 170 l

Fig. 16.4 The hydrogen accumulators "Dmisch" supplied with thermostated heat exchangers energized from the constant-current sources of 12 V

Fig. 16.5 The high-pressure vessels for hydrogen storage and hydrogen accumulators of "Viachbog" modification with a capacity of 3, 10, 15 and 75 l

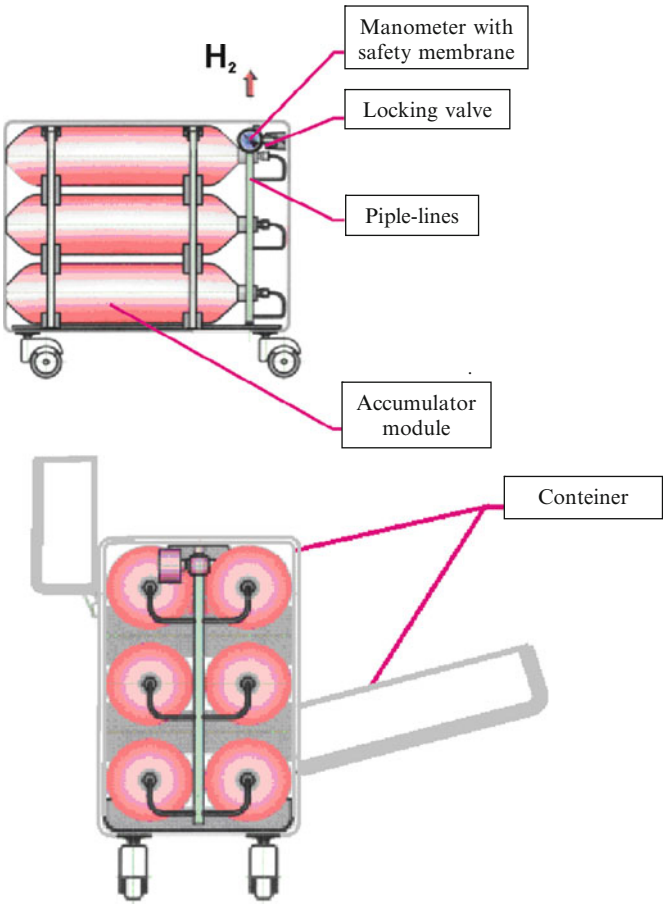

Fig. 16.6 Schematic view of the laboratory metal hydride storage of high-pure hydrogen "*VA – 7000*"

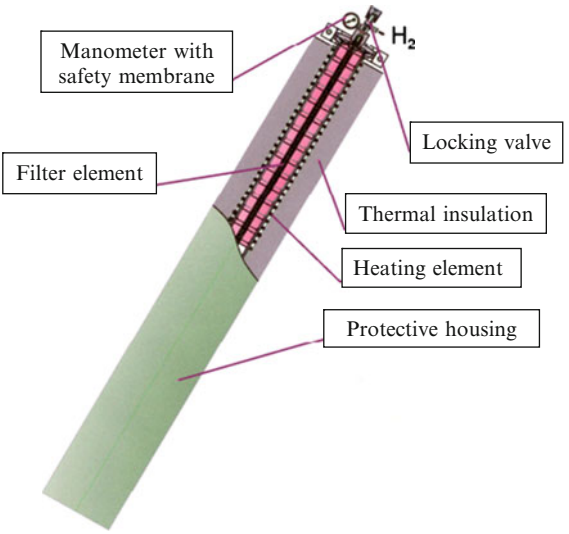

Fig. 16.7 Schematic view of the laboratory metal hydride storage/compressor of high-pure hydrogen "*Svetzag – 2000*"

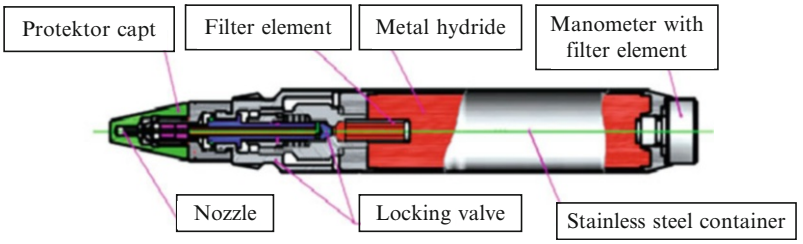

Fig. 16.8 Schematic view of the metal-hydride torch "Viachbog-30"

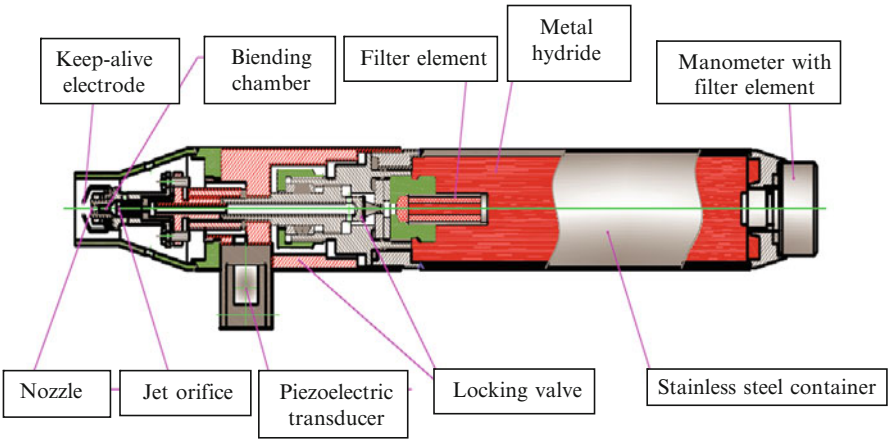

Fig. 16.9 Schematic sketch of the hydrogen self-contained metal-hydride torch "Alsav" with piezoelectric firing of flame

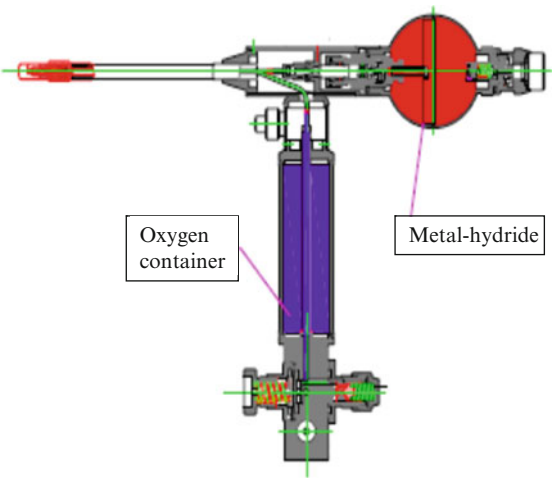

Fig. 16.10 Schematic representation of the oxydric metal-hydride torch

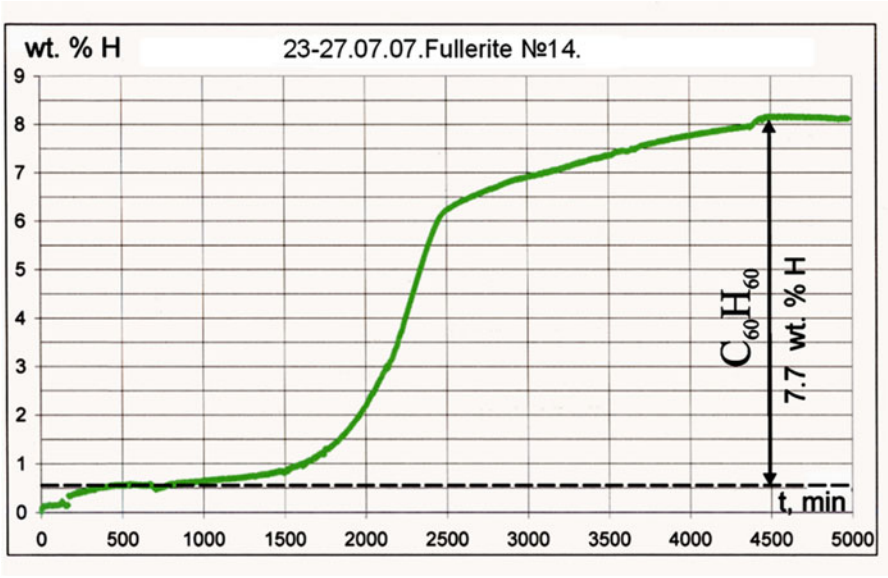

Fig. 17.2 Kinetics of interaction of gaseous hydrogen with fullerite. *Arrowed line* shows the fraction of fullerinated hydrogen (H_F)

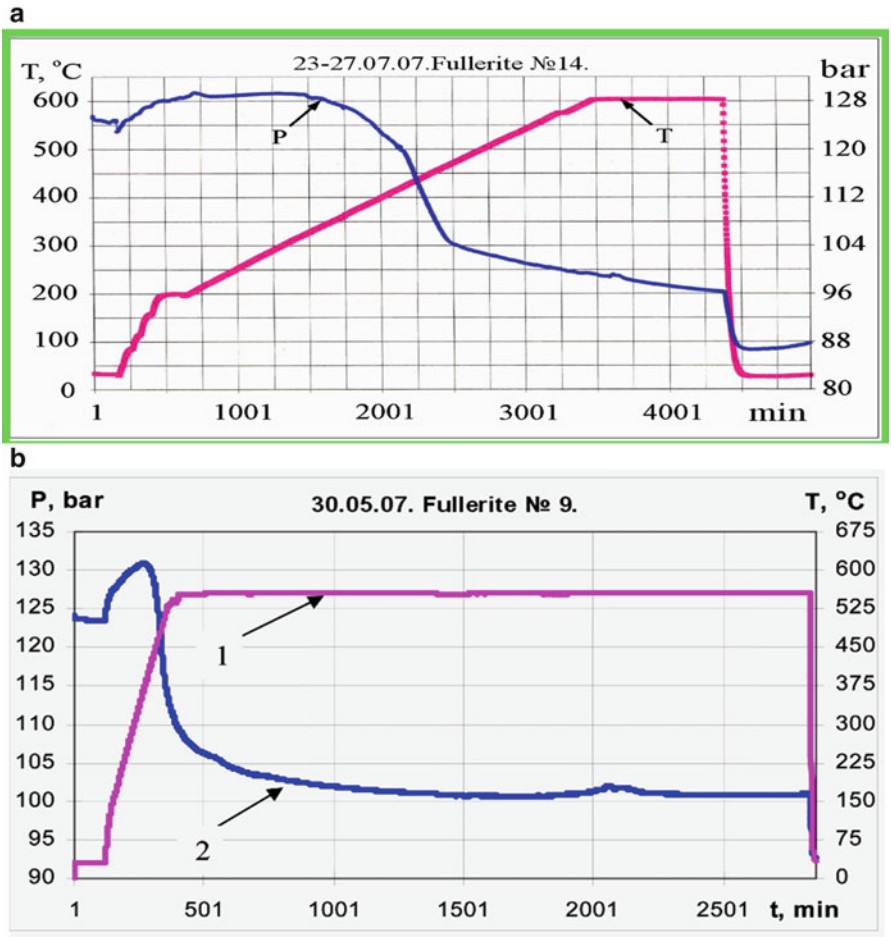

Fig. 17.3 The dependence of the rate of interaction between hydrogen – fullerene (*2*) the rate of temperature rise (*1*) (**a**) 0.2° per hour, and (**b**) 3.2° per minute

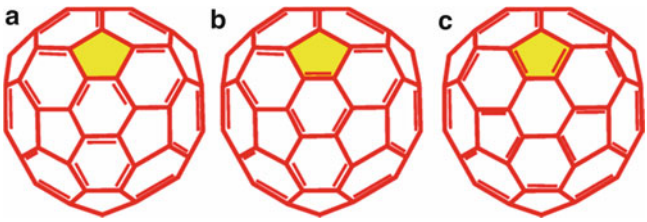

Fig. 17.4 The covalent resonance structures of carbo-s-icosahedron (**a**) – with the axis of fifth order (one structure); (**b**) and (**c**) – with the axis of the third order (Ten equivalent structures in each). All of structures are with 30 double bonds [15]

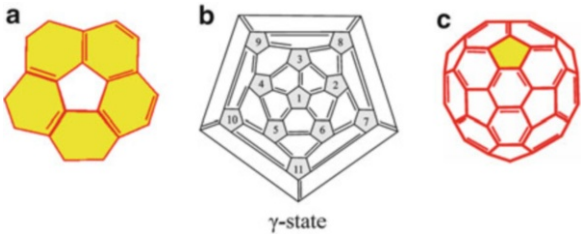

Fig. 17.7 γ-state of the covalent resonance structure of carbo-s-icosahedron with an axis of fifth order, forming the f.c.c. lattice of fullerite (**a**) – pentatomic molecule in the state of radialene; (**b**) – Shlegel diagram; (**c**) – the frame of molecule C_{60}

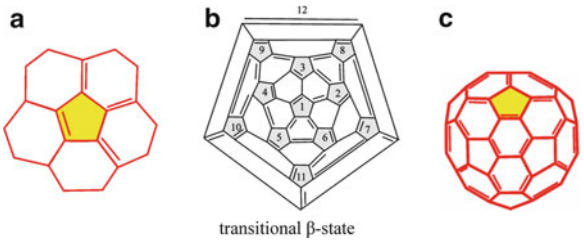

Fig. 17.8 β-state of the covalent resonance structure of carbo-s-icosahedron with an axis of third order, forming the b.c.c. lattice of fullerite (**a**) – pentatomic molecule in the state of pentaene; (**b**) – Shlegel diagram with the marked hexatomic structures (1, 2, 3, 4, 5, 6, 7, 8) that obey the Huckel rule; (**c**) – the frame of molecule C_{60}

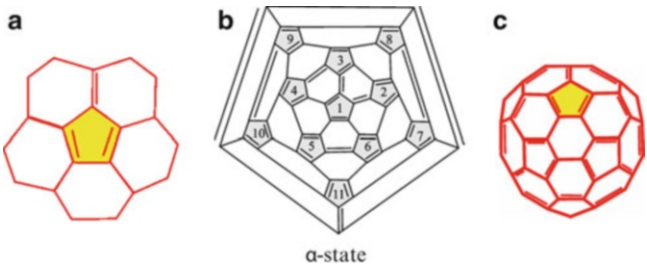

Fig. 17.9 α-state of the covalent resonance structure of carbo-s-icosahedron with an axis of third order, forming the s.c. lattice of fullerite (**a**) – pentadiene molecule; (**b**) – Shlegel diagram with the marked double bonds (1, 2, 3, 4, 5, 6) that combine pentadiene molecules in pyracyclene pairs; (**c**) – the frame of molecule C_{60}

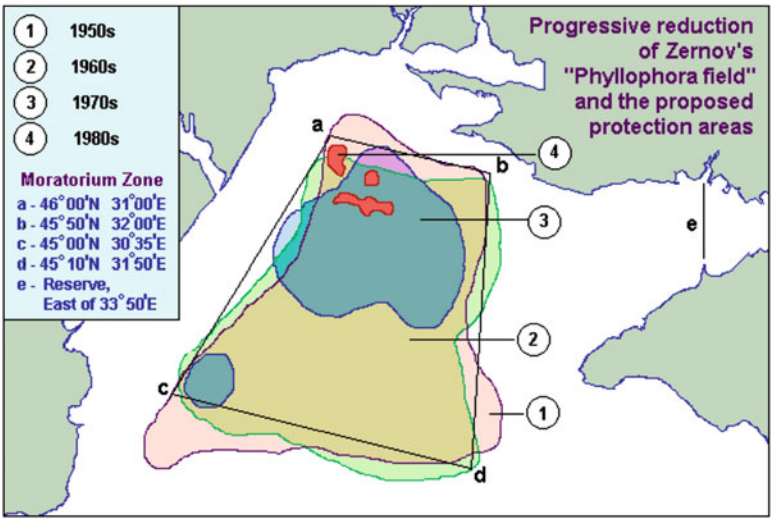

Fig. 21.3 Phyllophora represents a keystone species for the entire NW shelf ecosystem. The proposed protection areas are those referred to: Biolological Diversity in the Black Sea, BSEP Series Vol. 3 (From http://www.grid.unep.ch/hsein/tda/index.htm, Black Sea Transboundary Diagnostic Analysis)

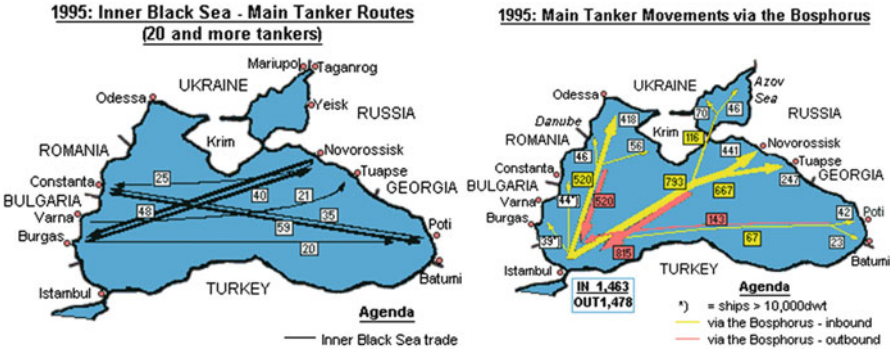

Fig. 21.4 The inner Black sea and main Tanker movements via the Strats

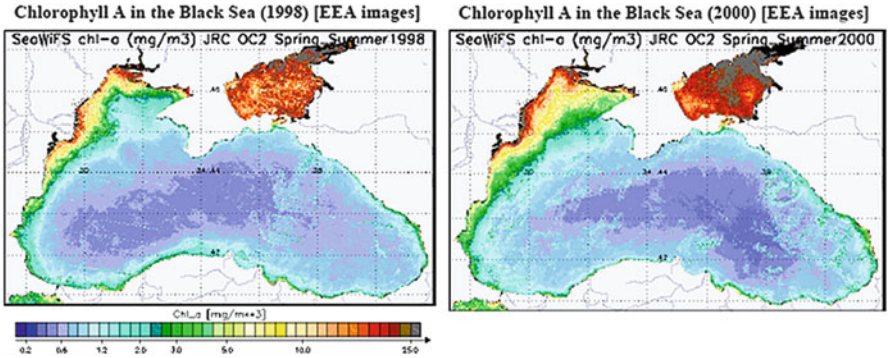

Fig. 21.6 Distribution of Chlorophyll A in 1998 and 2000 (From the Project report)

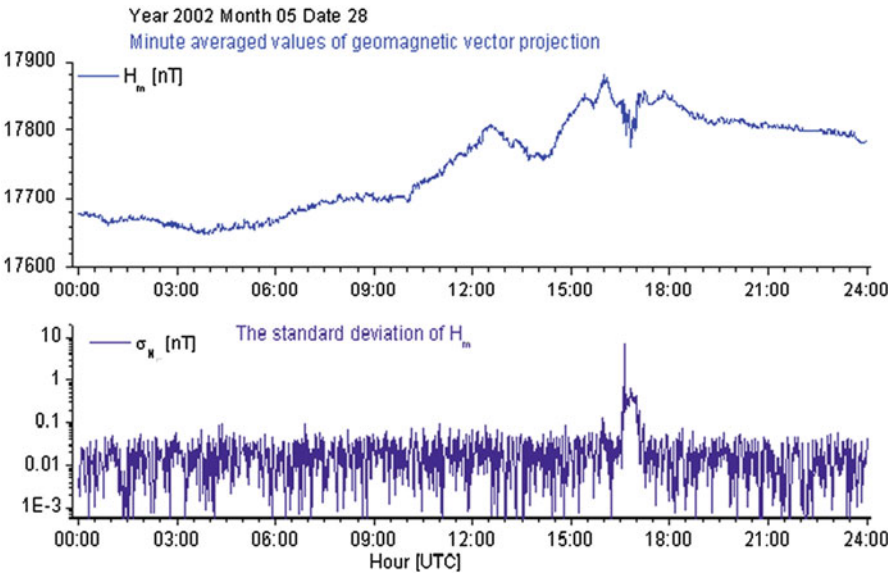

Fig. 22.1 Day with signal

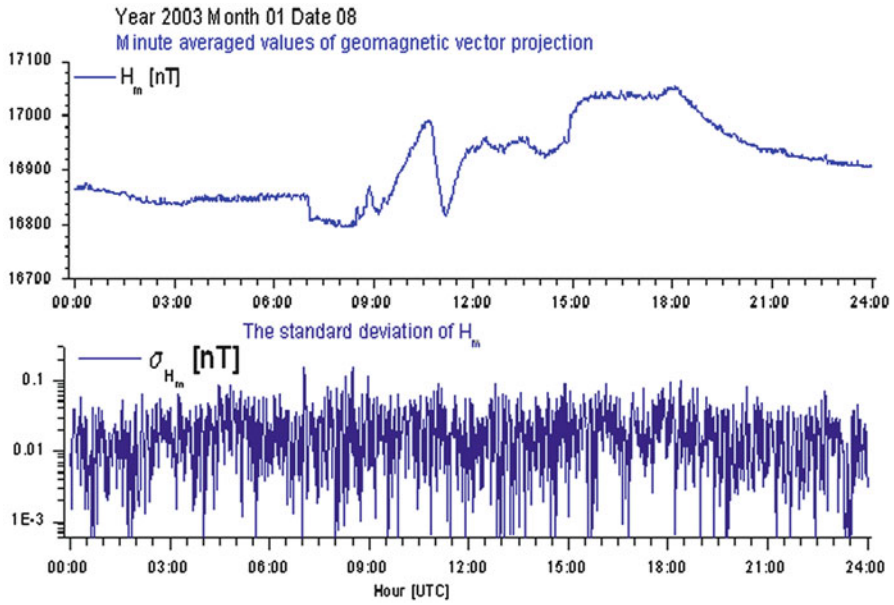

Fig. 22.2 Day without signal

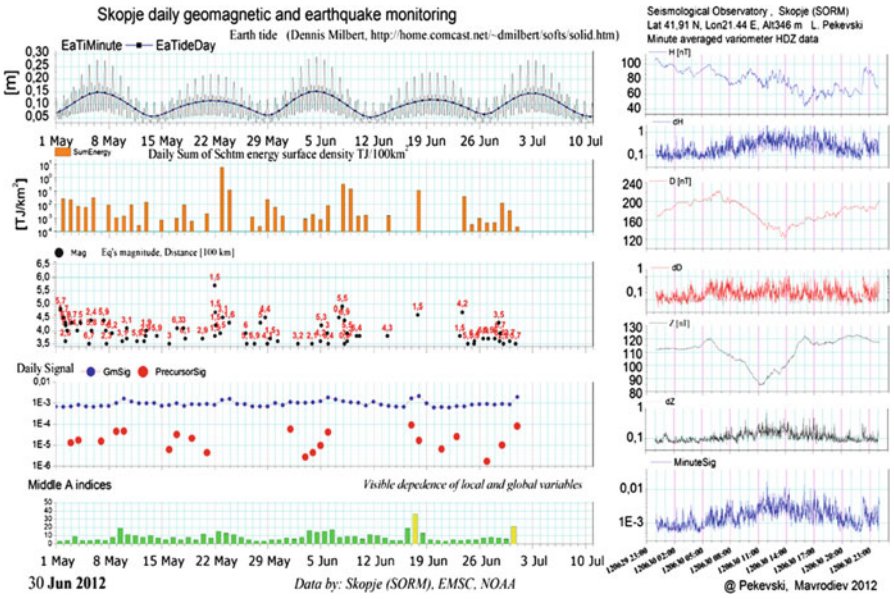

Fig. 22.3 Skopje daily geomagnetic and earthquake monitoring

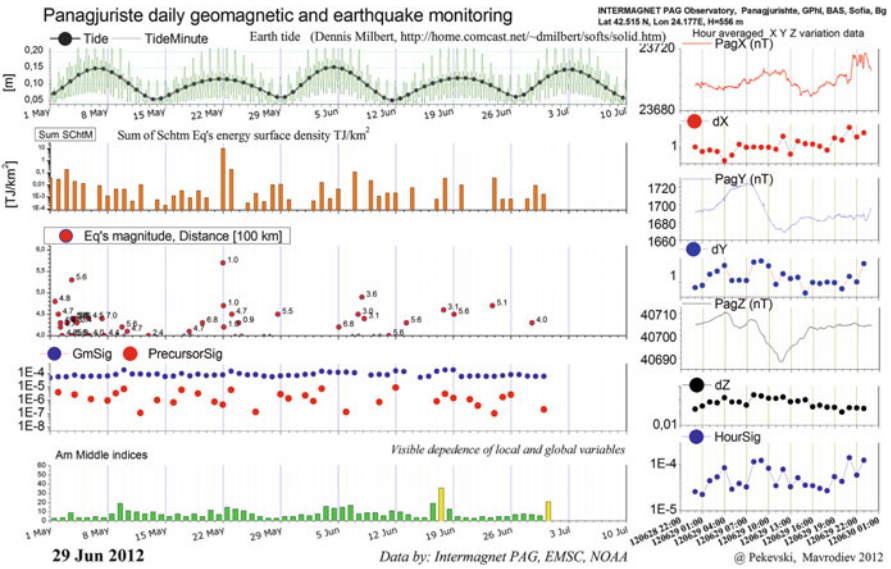

Fig. 22.4 Panagjuriste daily geomagnetic and earthquake monitoring

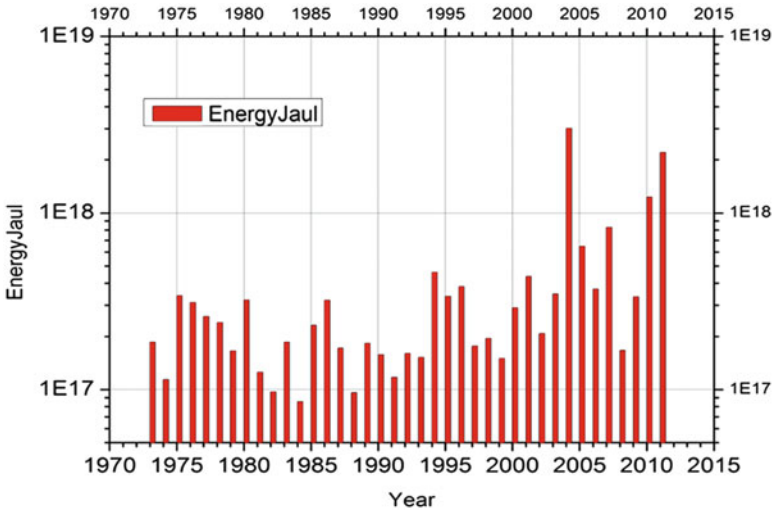

Fig. 22.5 The total world earthquakes energy with magnitude greater than four for the period of 1973–2011

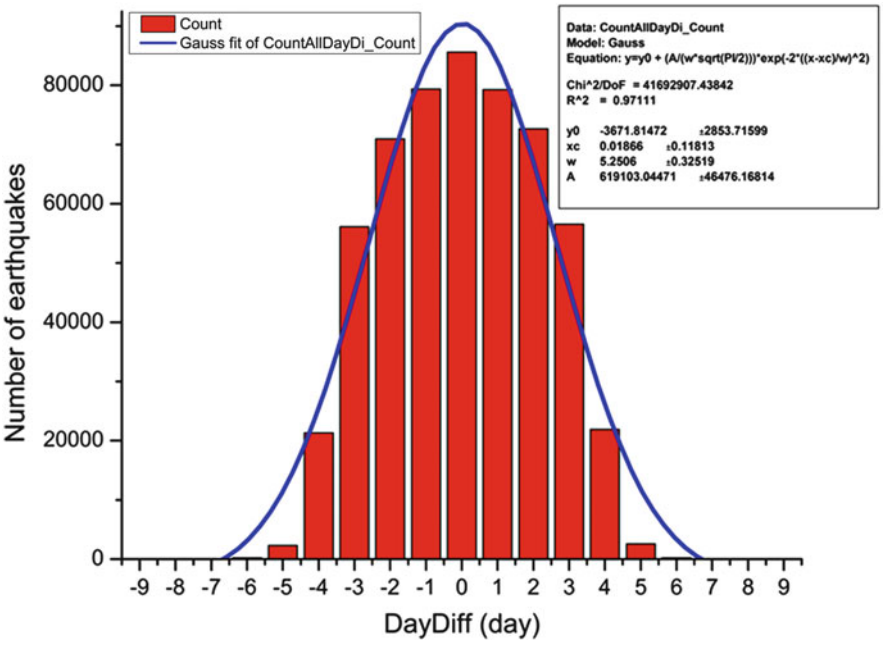

Fig. 22.7 The distribution difference between the time of local extreme tide and the time of occurred earthquake with magnitude greater than four. The http://www.isc.ac.uk/ database was used

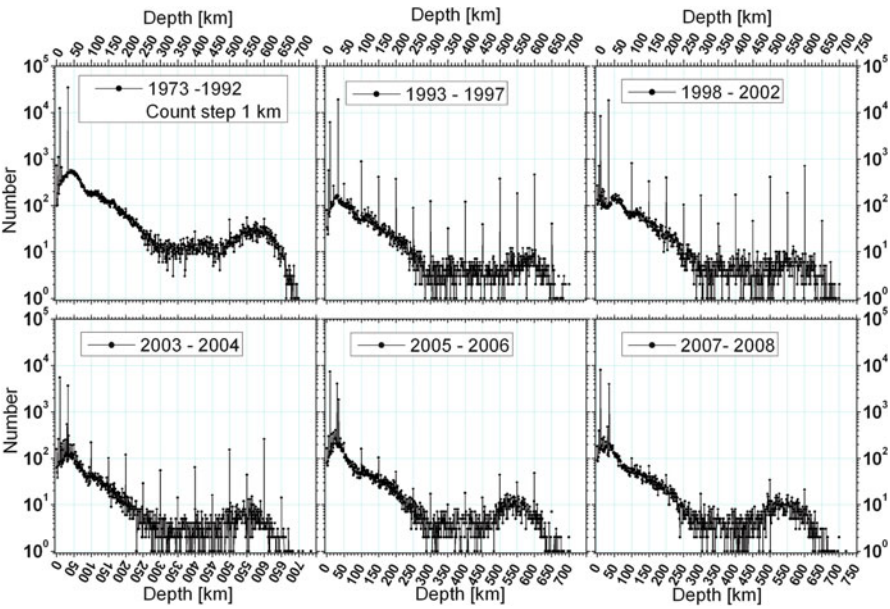

Fig. 22.8 The years' dynamics of depth earthquake's number distributions

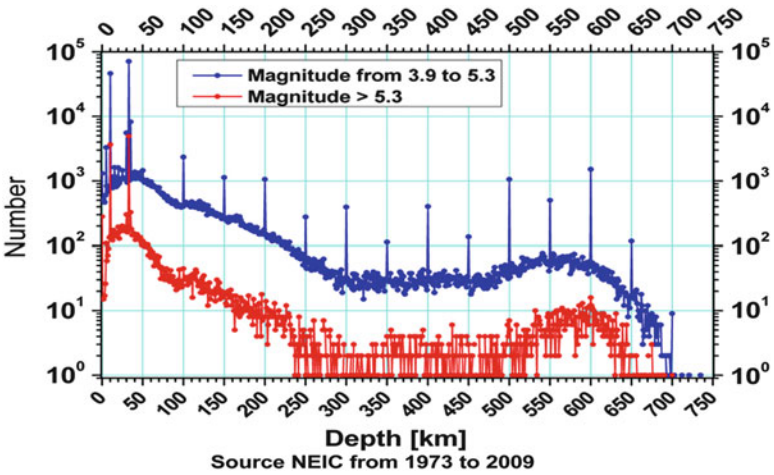

Fig. 22.9 The depth distribution of earthquake numbers for illustration of the fact that the magnitudes of earthquakes which occur in the sleb are limited from sleb's lift

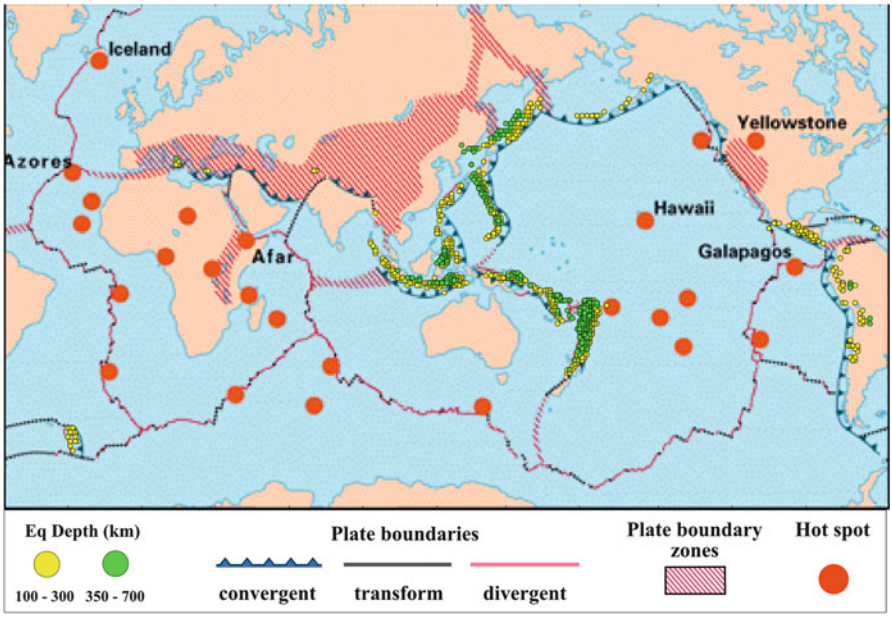

Fig. 22.10 The spatial distributions of deep-focus earthquakes with magnitude M ε [3.9, 5.3]

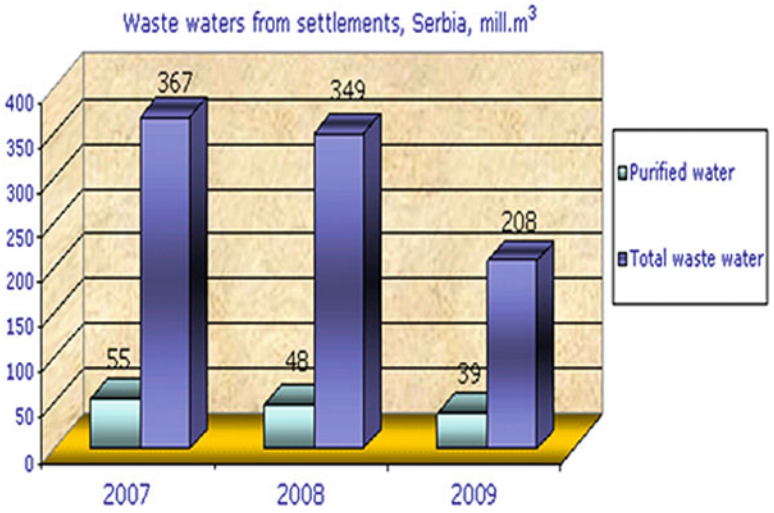

Fig. 23.1 Purified and total waste waters 2007–2009 (million m^3) (Source: Statistical Office of the Republic of Serbia)

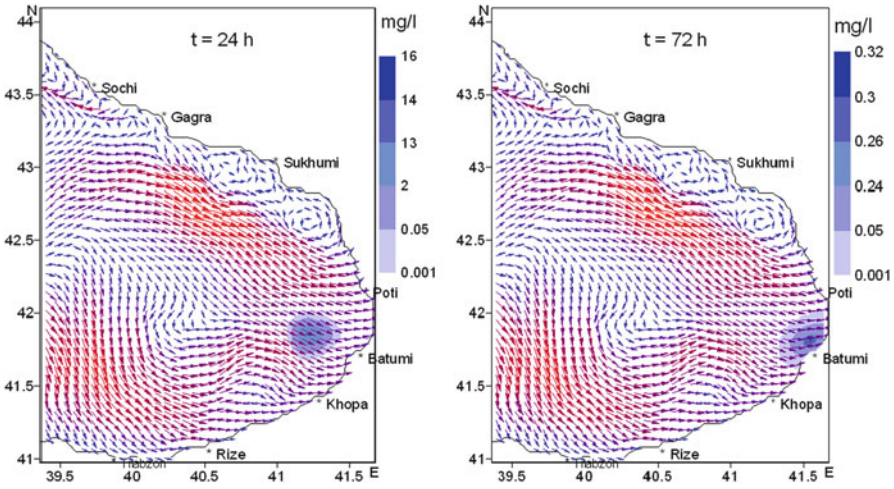

Fig. 24.1 Simulated oil spill at different time moments moving under 18 January 2011 circulation The source coordinates: $142\Delta x$ and $105\Delta y$. 50 tones were released in 2 h

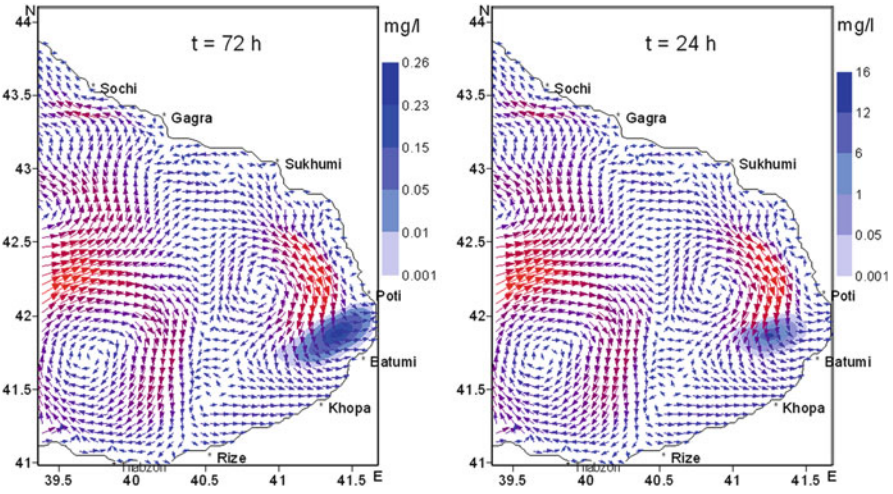

Fig. 24.2 Simulated oil spill at different time moments (after the release) moving under 29 September 2011 circulation. The source coordinates: 157Δx and 105Δy. 50 t. oil was flooded in 2 h

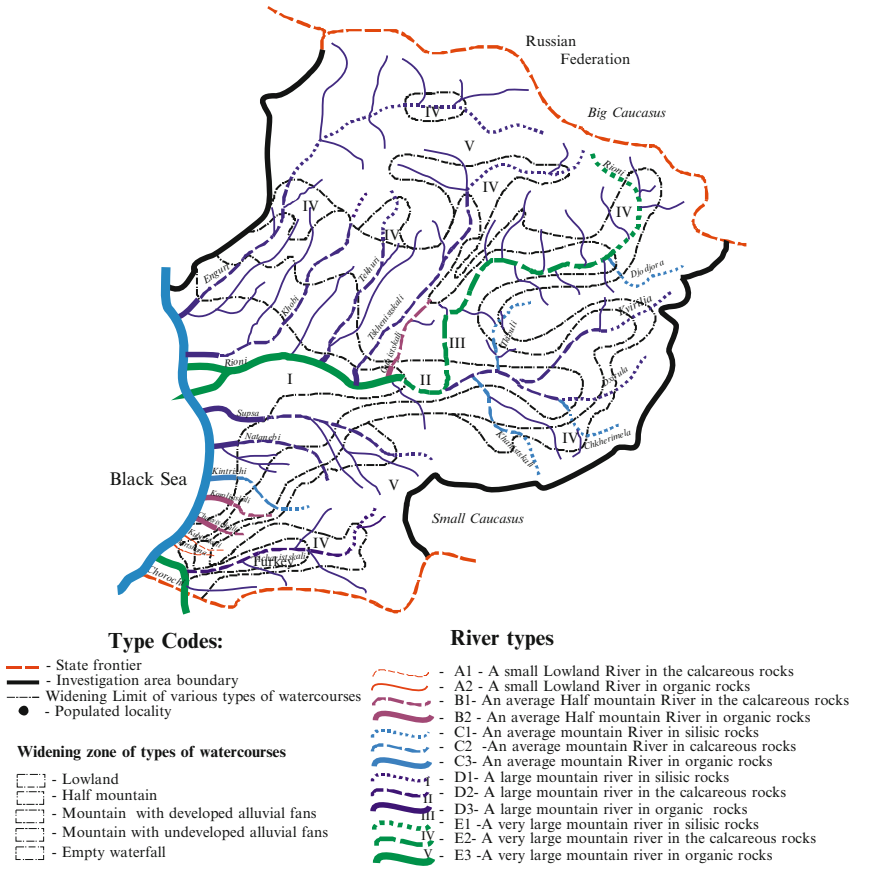

Fig. 25.1 Mapchart of river typology of Western Georgia

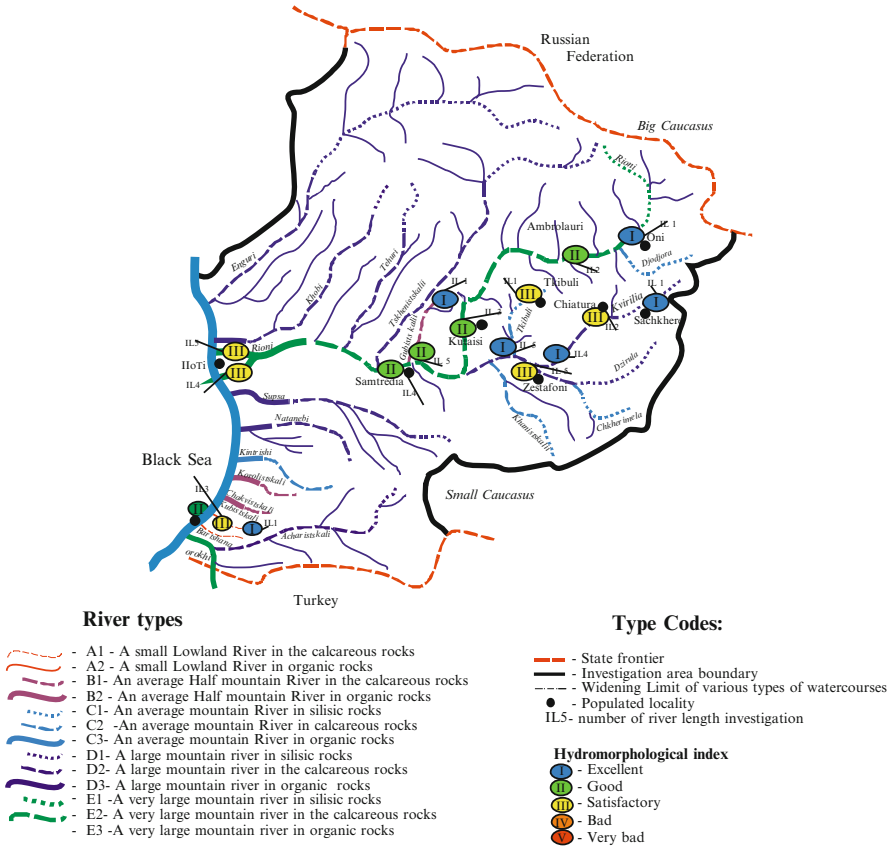

Fig. 25.2 Hydromorphological assessment of typical rivers of Western Georgia

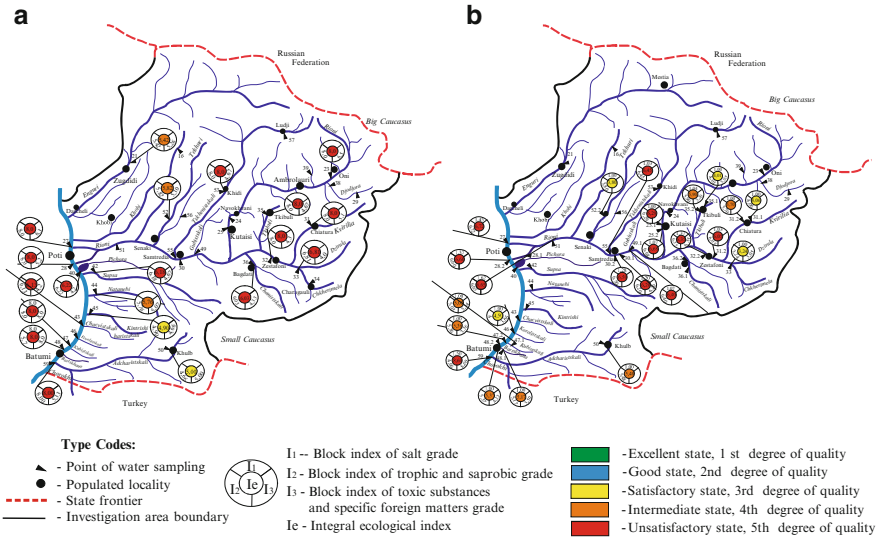

Fig. 25.3 Map-chart of surface water quality of West Georgia. (**a**) 1985, (**b**) 2010

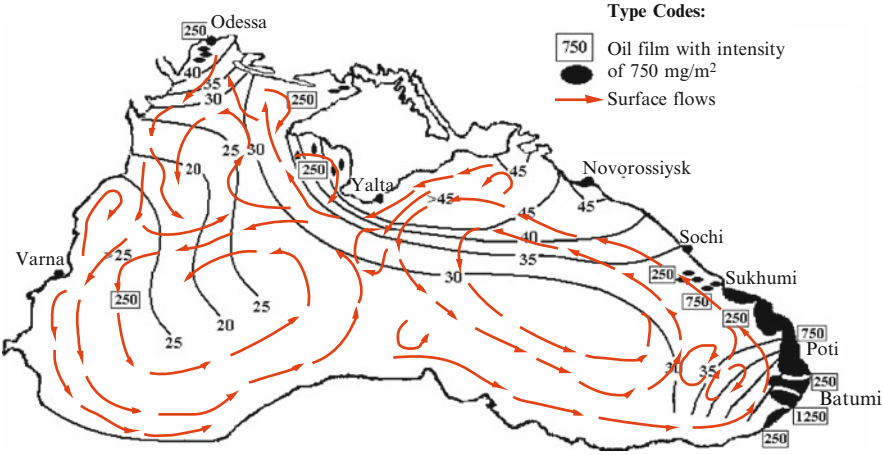

Fig. 25.4 Scheme of surface flows and map chart of oil pollution in the Black Sea

Fig. 26.1 Mine waters discharge into the pond *Svistunova*

Fig. 27.1 Main geomining objects in Kerch district. Legend: *1* iron ore agglomeration plant, *2* iron ore open cast quarry, *3* Churbash ravine, *4* Churbash Lake, *5* and *6* iron ore waste depository, *7* limestone quarry

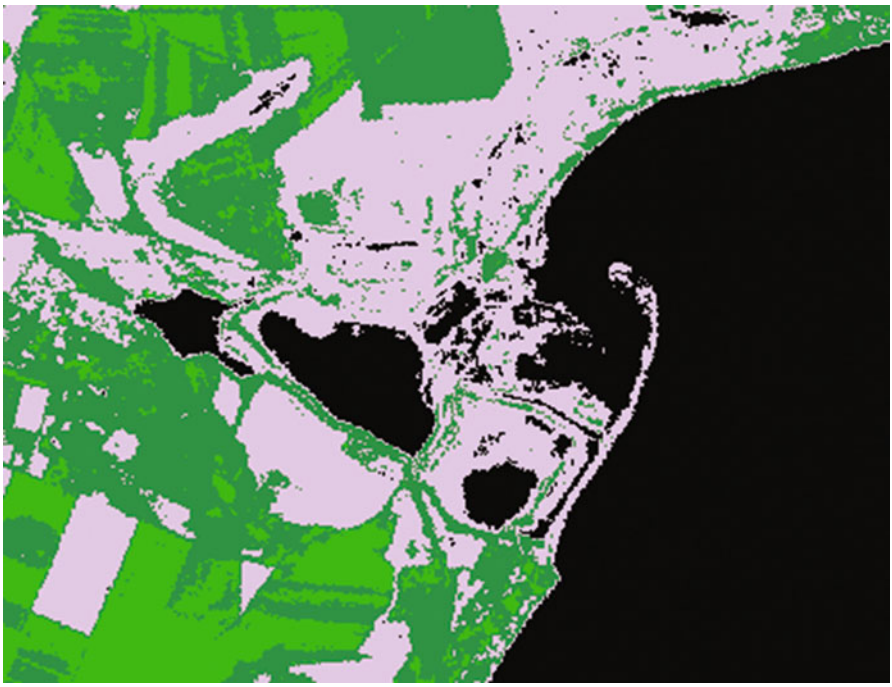

Fig. 27.2 Vegetation cover (1992)

Fig. 27.3 Vegetation cover (2010)

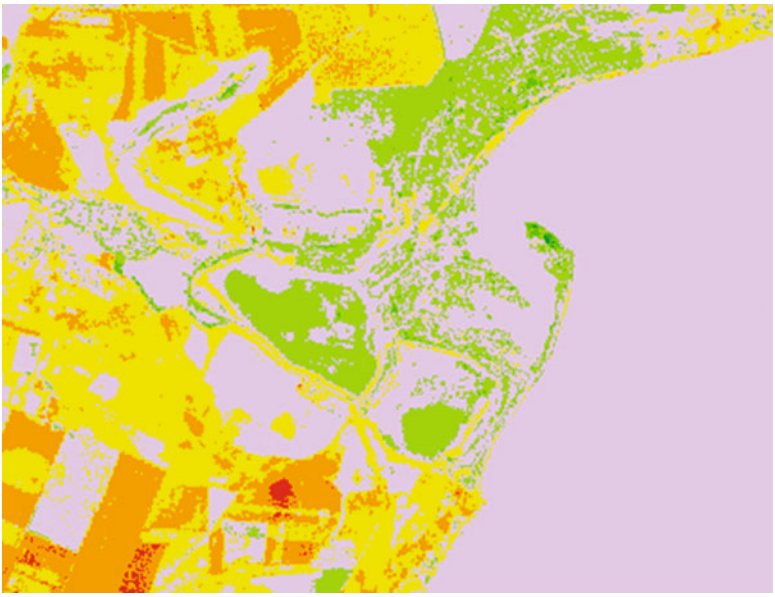

Fig. 27.4 Vegetation cover change (1992–2010)

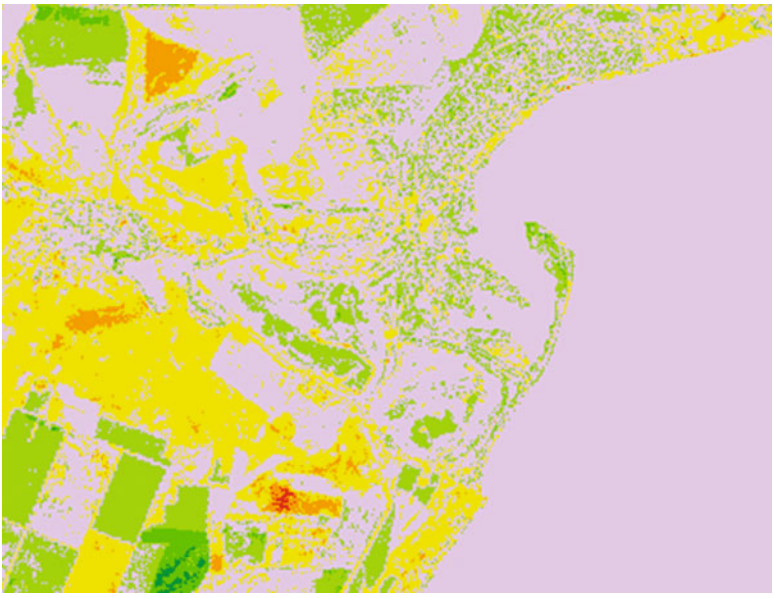

Fig. 27.5 Vegetation cover change (1999–2010)

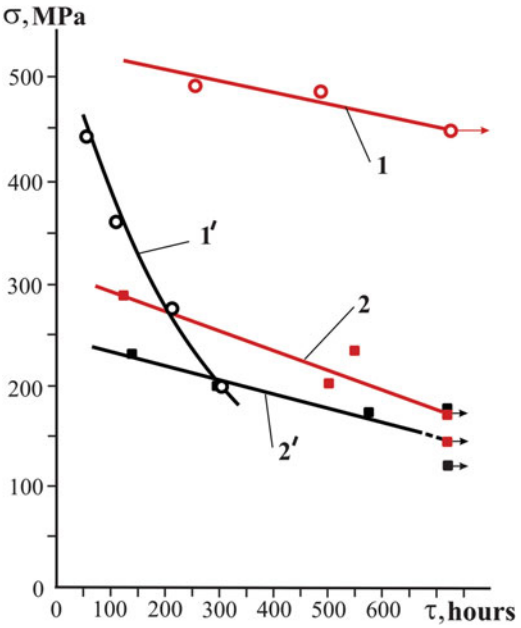

Fig. 29.1 Influence of static (1; 2) and asymmetric cyclic (1′; 2′; f = 0.5 Hz; $\sigma_a = 0.2\sigma_{0.2}$) tensions on durability of steel 30CrMo (1; 1′) and steel 20 (2; 2′) in solution of NACE

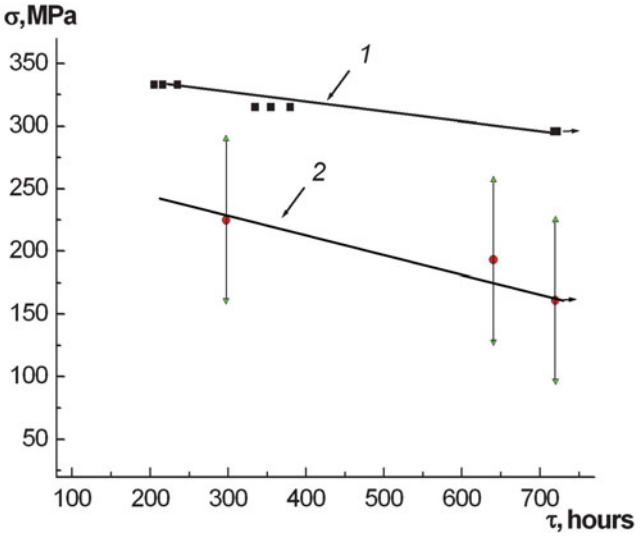

Fig. 29.3 Influence of static (1) and asymmetric cyclic (2; f = 0.5 Hz; $\sigma_a = 0.2\sigma_{0.2}$) tensions on durability of steel 17Mn1Si in solution of NACE

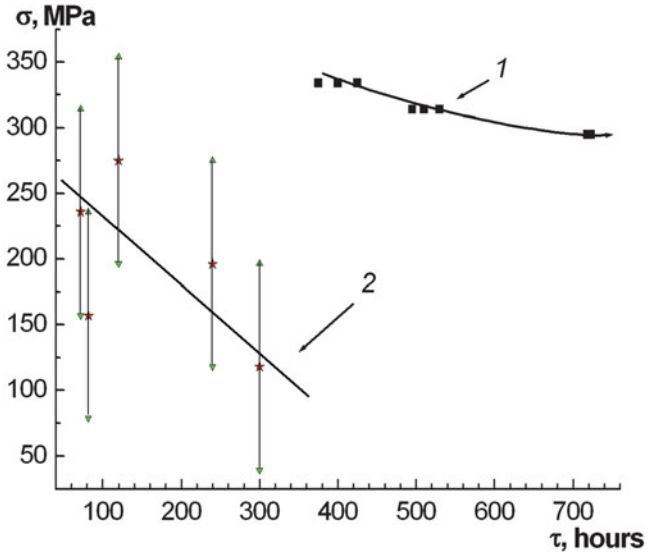

Fig. 29.4 Influence of static (1) and asymmetric cyclic (2; f = 0.5 Hz; $\sigma_a = 0.2\sigma_{0.2}$) tensions on durability of welded specimens from steel 17Mn1Si in solution of NACE

Fig. 30.3 Influence of oxygen on radiation-chemical yield of heptane decomposition in the water medium. $[C_7H_{16}]/[H_2O] = 10^{-4}$

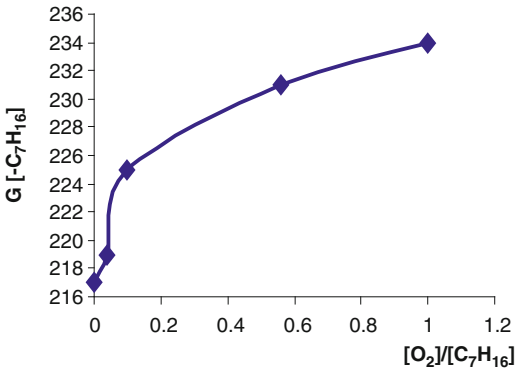

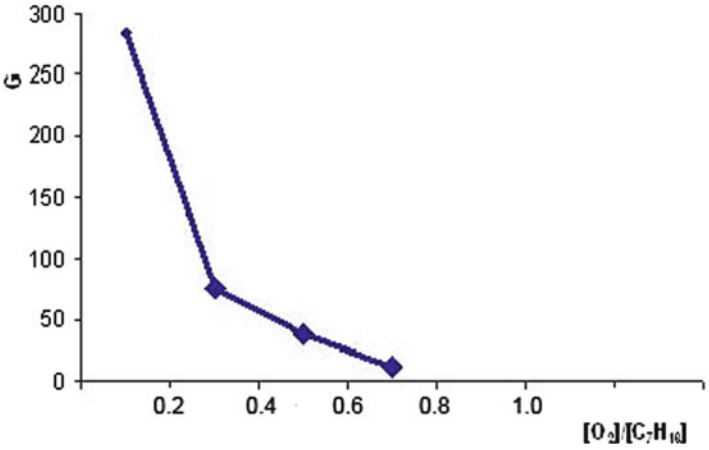

Fig. 30.4 Influence of oxygen on radiation-chemical yield of methane at the decomposition of heptane in water medium

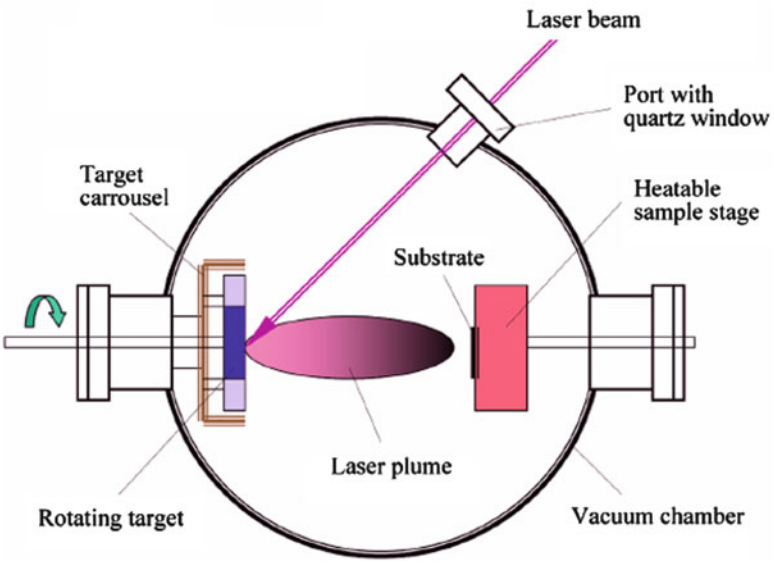

Fig. 31.1 Laser – Plasma deposition process

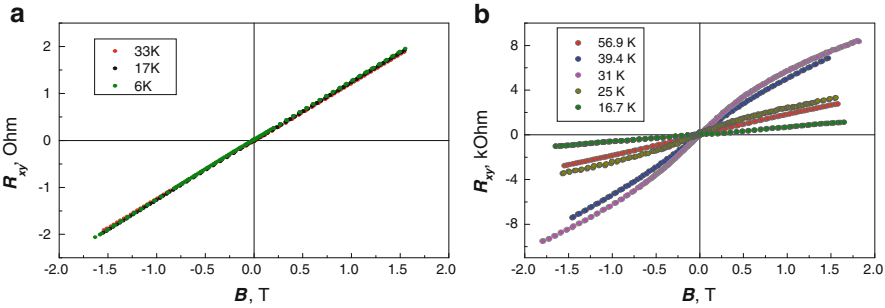

Fig. 31.3 Hall effect in quantum-sized GaAs(δ-Mn)/$In_XGa_{1-x}As$/GaAs structures with metallic (**a**) and activation (**b**) type of conductivity at different temperatures [14]

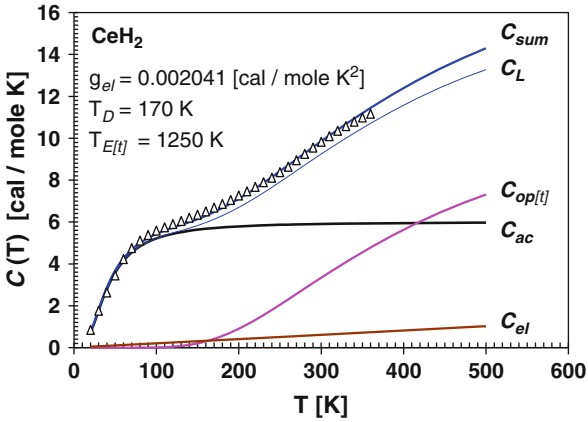

Fig. 32.1 Heat capacity of CeH_2. *Open triangles* – experimental points from [6], notations of calculated dependences: $C_{sum} = C_L + C_{el}$; $C_L \equiv C_{ac} + C_{op[t]}$

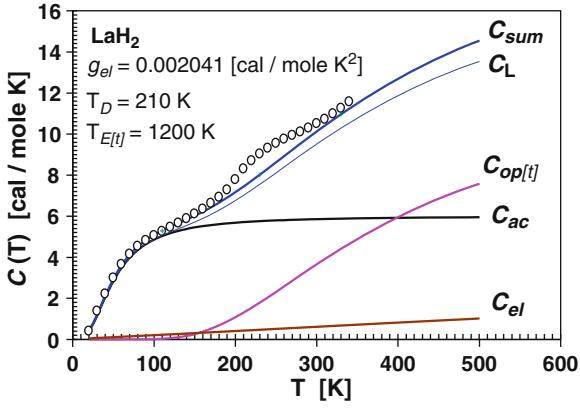

Fig. 32.2 Heat capacity of LaH_2. *Open circles* – experimental points from [7], notations of calculated dependences: $C_{sum} = C_L + C_{el}$; $C_L \equiv C_{ac} + C_{op[t]}$

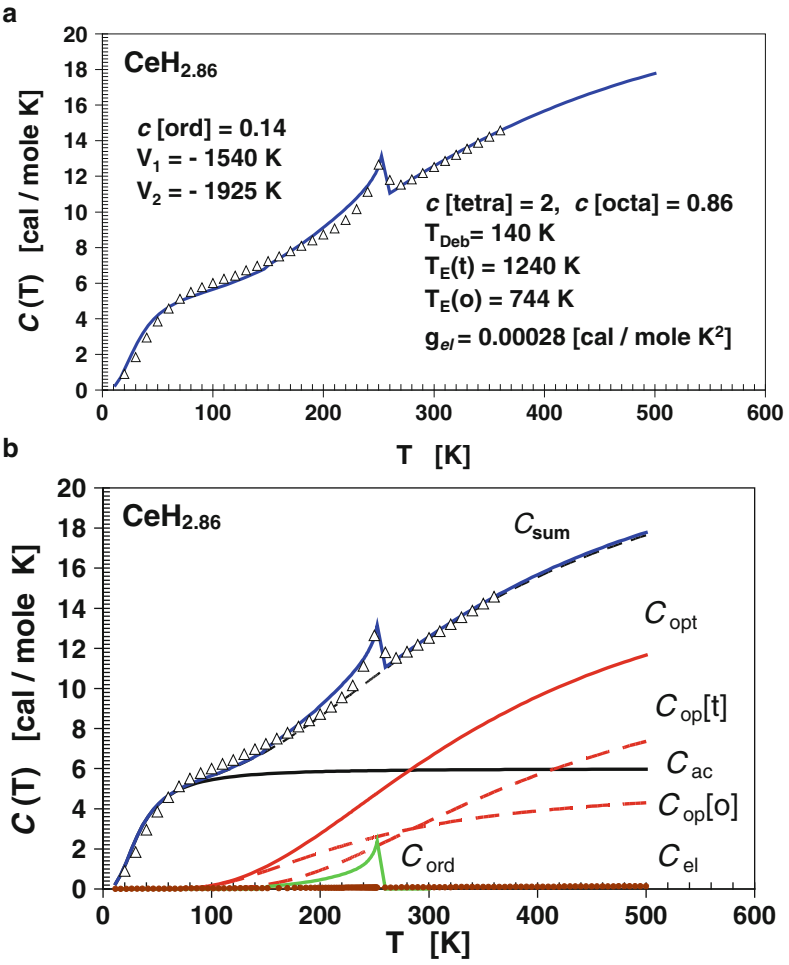

Fig. 32.3 (**a**) Heat capacity of $CeH_{2.86}$. *Open triangles* – experimental points from [10], *thick line* – results of calculation [11], (**b**) ingredients of the total heat capacity of $CeH_{2.86}$. *Open triangles* – experimental points [10], notations of calculated dependences: $C_{sum} = C_{ac} + C_{opt} + C_{el} + C_{ord}$; $C_{opt} = C_{op}[t] + C_{op}[O]$

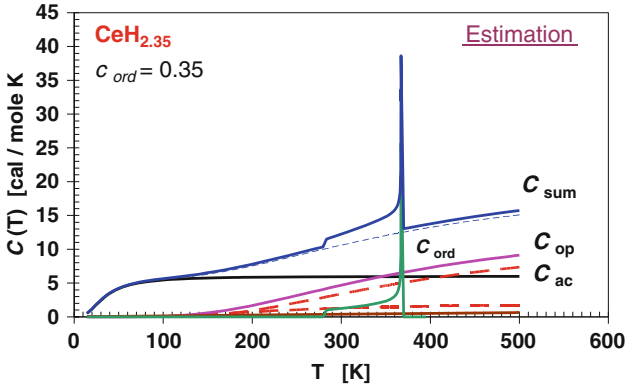

Fig. 32.4 Estimated total heat capacity of $CeH_{2.35}$

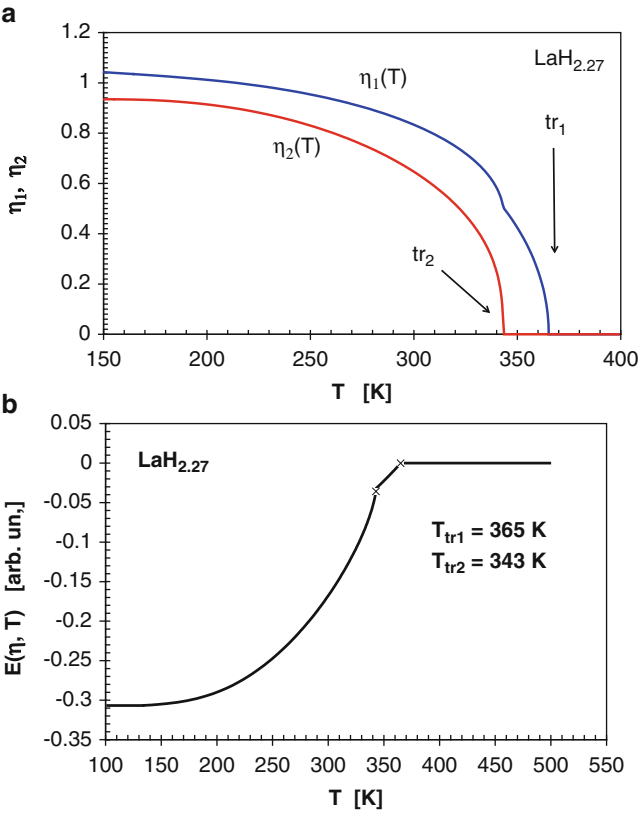

Fig. 32.6 (**a**) Temperature dependence of order parameters η_1 and η_2, (**b**) temperature dependence H-H interaction induced ordering energy

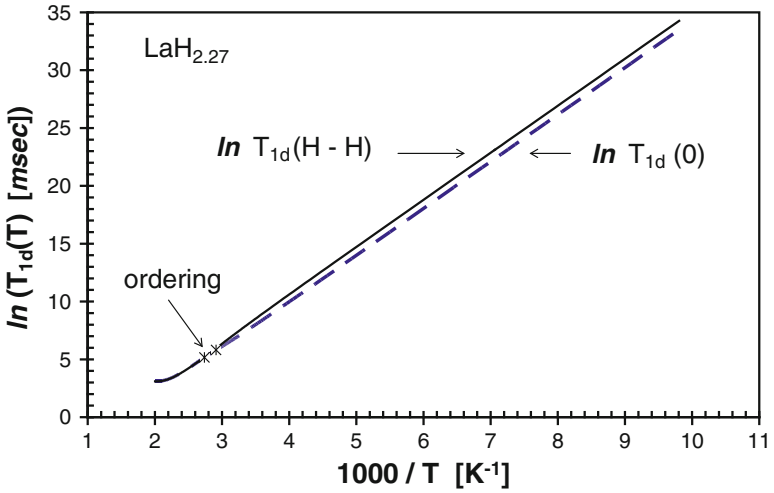

Fig. 32.8 Influence of hydrogen "weighting" on the dipole-dipole part of the spin–lattice relaxation time

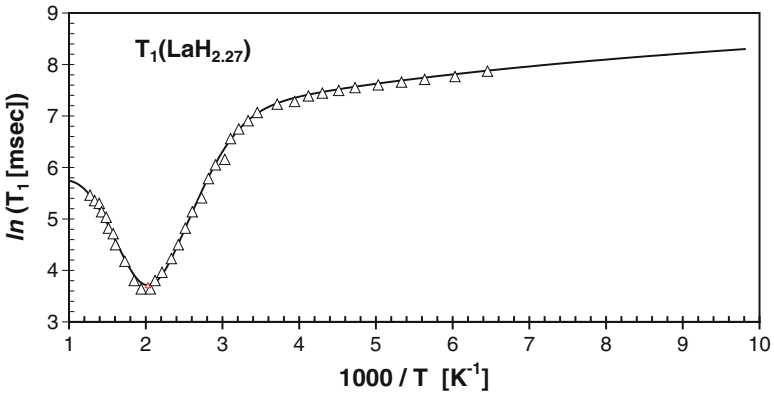

Fig. 32.9 Temperature dependence of the spin–lattice relaxation time T_1 *solid line* – calculated dependence [20], *open triangles* – experimental points [21]